Shear and Compression Behaviour of Undegraded Municipal Solid Waste

By

Ulrich Langer

A Doctoral Thesis

Submitted in partial fulfilment of the requirements for the award of

PhD at Loughborough University

November 2005

Acknowledgements

The research project described in the following was conducted at and funded by Loughborough University Department of Civil and Building Engineering.

First of all, I would like to thank my supervisor Dr Neil Dixon, who provided constant input and support and engaged my work drive in uninspired times by advising and guiding me through the course of this project during these three years abroad. I very much appreciate his openness, honesty, fairness and his ability to open my eyes for details and things, I would have never thought of.

I am also very grateful for the support and advice of Dr Philippe Gotteland from the LIRIGM-Polytech'G, Joseph-Fourier-University, Grenoble, France. During the Franco-British collaboration funded by the French and the British Council, which started in 2003 and is still ongoing, I experienced many fruitful and helpful discussions with Dr Gotteland and Dr Dixon and thus I gained a lot of input from different points of view on my work.

The discussions within the geotechnical "waste" group of the Department of Civil and Building Engineering were another important source of input. Namely, Bo Zhang, Anna Sia and Gary Fowmes provided their opinions and views on problems, which I encountered during the research.

Very important help was brought to me by my French project students Adrian Berthaud and Jean-Marc Pujol. Without their hard work on the shear box, the compression device and also on the sorting of the synthetic waste, the practical part of my project would have hardly been possible. I also would like to thank my colleague Jan Walstra, who accompanied me on a rather sense-challenging job on Narborough Landfill.

Without the technicians of the departmental laboratory my work would not have succeeded. I owe a great deal of gratitude especially to Mark Harrod, Alex Harrison, Barry Carnall and Mike Smeeton, who were always willing to provide, fix, calibrate and adjust technical equipment, and who always solved my technical problems.

Furthermore, thanks are due to REXAM to provide a large part of the synthetic waste components (beverage cans and margarine tubs) and SITA for letting me dig in and analyse their waste.

Last but not least, I am very grateful for all kind of support I experienced from my family and my friends in Britain and in Germany. A special thank you goes out to my parents, who always encouraged and backed me up in every way. Finally, to my fiancé Alex: thank you so much for your patience, and for the greatest present of all still to come.

0 Contents

0.1 Table of Contents

0.2 List of Figures

0.3 List of Tables

0.4 Notation of Parameters

Parameter

Greek Symbol	Description
ε	Strain (horizontal or vertical displacement divided by initial sample length or height)
γ	Unit weight
ϕ	Friction angle
ϕ'	Effective friction angle
ξ	Angle of tensile stress
ρ	Density
σ	Normal stress (anchoring stress)
σ'	Effective normal stress
τ	Shear stress

Alphabetic character	Description
a	Matrix element
c	Cohesion
e	Void ratio
h	Sample height
Δh	Height difference
l	Sample length
m	Mass
m_{ij}	Ratio between individual material group and material sum within the size range i
ms_{ij}	Product of m_{ij} and s_{ij}
mrv	Mass-related volume
n	Number
s	Settlement/compression, in shear testing: horizontal displacement
s_{ij}	Ratio between individual size range and material sum of the particular size range within the material group
t	Time
u	Pore pressure, in shear testing: horizontal displacement

$\dot{u}$	Shear rate
vf	Volumetric factor
Δz	Part of the activated fibre cohesion
A	Area
C_c	Compression index
C'_c	Modified compression index
C_R	Primary compression ratio
C_α	Coefficient of secondary compression
$C_{\alpha\varepsilon}$	Secondary compression index
D	Constrained modulus
E_s	Young's modulus
F	Force
G	Shear modulus
S_T	Total settlement
S_i	Immediate settlement
S_C	Consolidation settlement
S_S	Secondary compression or creep
T	Tensile force
V	Volume

Indices

Symbol	**Description**
0	Initial
1	Before loading
2	Before shearing
α	Angle
a	Apparent
ax	Axial
e	Final
i	Variable
j	Variable
max.	Maximum

min.	Minimum
mob.	Mobilised
s	Shear
t	Time-dependent
v	Vertical
vo	Volumetric
theo.	Theoretical
z	Tensile

0.5 Abstract and Keywords

Keywords: Municipal Solid Waste, Waste Geotechnical Classification, Synthetic Waste, Shear Behaviour, Compression Behaviour

To ensure stability of a construction the physical properties of its components have to be well known. In a landfill, waste presents the largest structural element and controls both the stability and integrity of the lining system. In spite of this critical role there is a dearth of knowledge on behaviour of waste as an engineering material. Waste variability and changes in waste stream aggravate the assessment of waste mechanical properties.

In a literature review the main influences on shear behaviour of municipal solid waste (MSW) were identified. Design values and recommendation for shear parameter were summarised. To assess mechanical behaviour in a systematic way the use of a classification system was deemed crucial for a comparison of different findings from literature and a categorisation of waste in regard to its composition. A framework for a classification system was introduced. Main elements of a comprehensive classification system were identified in a literature review and discussed, and data from literature was applied to the classification framework. For the validation of a classification system, municipal solid waste was examined in an in-situ waste sorting analysis and also applied to the framework.

The findings from the waste sorting and the classification system were also used to develop a family of synthetic waste to gradually examine the influencing factors on waste mechanical behaviour. For this, the materials, size ranges and shapes of waste components identified in the waste sorting analysis were reduced to a minimum but still representative amount. A range of synthetic waste compositions was engineered and tested in a large-scale shear device. Compression tests were also conducted in a large compression cell. The results from the laboratory testing were compared to values from the literature and MSW mechanical behaviour was subsequently discussed in view to potential changes from changing waste streams.

The results from shear and compression tests (constrained and shear modulus) on synthetic waste were linked to the classification system and trends of the mechanical behaviour in relation to the tested synthetic waste compositions were identified.

A framework for classifying MSW and comparing waste mechanical behaviour was presented and demonstrated. A family of synthetic wastes was engineered and tested in shear and compression tests. The results were comparable to values from the literature. Further research is recommended to refine the synthetic waste and the classification.

Contact: Ulrich Langer shearing@online.ms

1 Introduction

To ensure stability of a construction both the properties and mechanical behaviour of its components have to be well known. In a landfill, waste presents the largest structural element and often controls both the stability and integrity of the lining system (Jones and Dixon, 2003). However, in spite of this critical role there is a dearth of knowledge on behaviour of waste as an engineering material.

Fassett *et al.* (1994) describe the necessity of obtaining appropriate waste properties as follows:

> *"The design and permitting of landfills requires performing comprehensive geotechnical analyses to demonstrate that all the landfill systems have been designed to be consistent with long-term performance requirements. Correct selection of geotechnical properties of waste materials for use in these analyses is of paramount importance, as the safety and cost of landfills are sensitive to variations in these properties. Unfortunately, the geotechnical properties of waste materials can vary within broad ranges, change significantly with time, and are not easily amenable to direct measurement, due to heterogeneity and hard inclusions. Furthermore, published data is limited and the conditions under which the properties were measured or back calculated are often unclear."*

This project is concerned with the examination of mechanical properties of MSW and moreover with the detection and assessment of the main factors influencing the mechanical behaviour of MSW within a landfill. The variability of waste and its properties aggravate the understanding of waste behaviour. A uniform basis for comparing data for waste mechanical behaviour is presently not available. Thus a unified framework for waste mechanics that contributes to our ability to design and operate landfills representing a minimal risk to the environment is needed for several reasons. Past experience is a poor guide to future behaviour. Life style changes and the introduction of new legislation (e.g. reductions in biodegradable waste given by the European Community Landfill Directive (1999)) and pre-treatment are resulting in significant changes to waste components and thus to the mechanical behaviour of waste. Knowledge of the properties of waste components is required to evaluate future changes in waste mechanical properties and hence landfill behaviour.

1.1 Municipal Solid Waste

The composition of municipal solid waste (MSW) is subjected to various influences. Hence, waste properties are also influenced and subjected to change. It is therefore crucial to be aware of the variability of MSW and hence the resulting variable mechanical (and also biological) properties. In the following the variability of waste is presented. Waste compositions from different sources worldwide and from the UK are demonstrated and differences are emphasised.

1.1.1 Waste Composition Worldwide

In an attempt to examine the different waste compositions around the world, data from a number of countries was collected. The collection covers 49 data sets from 26 different countries in North- and South-America, Asia, Australia and Europe over the last 12 years. Due to the fact that the components could not be readily identified due to differences in the chosen material groups published by the different authors, there is certain vagueness in this data. Assumption had to be made for a uniform presentation of the composition data. From Figure 1-1 great variability within each material groups of the composition is obvious on the one hand, but on the other hand certain trends are also apparent.

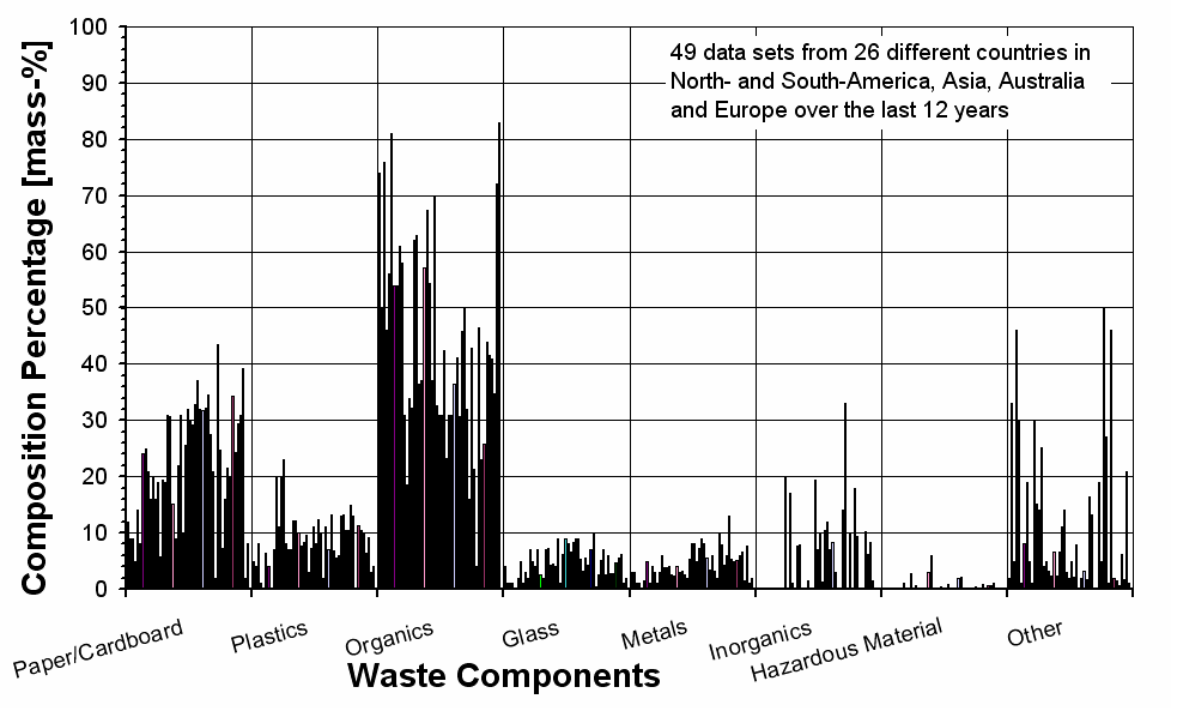

Figure 1-1 Overview of the varying waste compositions[1]

Organic material apparently accounts for the biggest part of the composition, followed by paper/cardboard, glass and minerals. A big scatter is obvious within inorganic and other materials. This is potentially caused by the different definitions of inorganic and other material for each set of data, i.e. the varying allocation of different waste products to the material groups. Groups like inorganic, organic or other material are not explicitly defined in terms of their appropriate components.

Figure 1-2 shows a mean worldwide waste composition with the average deviation to demonstrate the range of possible compositions. As mentioned before, it is hardly possible to specify a certain “overall” composition for waste. The average deviation and the coefficient of variation for the components clearly show the scatter of the mass percentage values within the material groups. While the coefficient of paper/cardboard,

[1] Bouazza *et al.*, 1996; Coumoulos *et al.*, 1995; CSR, 2002; Gabr and Valero, 1995; Gasparini *et al.*, 1995; Hull *et al.*, 2001; Manassero *et al.*,1997; Oweis and Khera, 1998; UNSW, 2003; INGUT, 2003; MoE, 2000; MVRHH, 2003; NSO, 2002, EPA, 1995

plastics, organics, glass and minerals is situated at about 65%, it exceeds 120% up to 260% for inorganic, hazardous and other material. In addition, the variation of distributions among the countries is widely spread, which is due to the various factors influencing the composition of a country and the also poorly defined material groups.

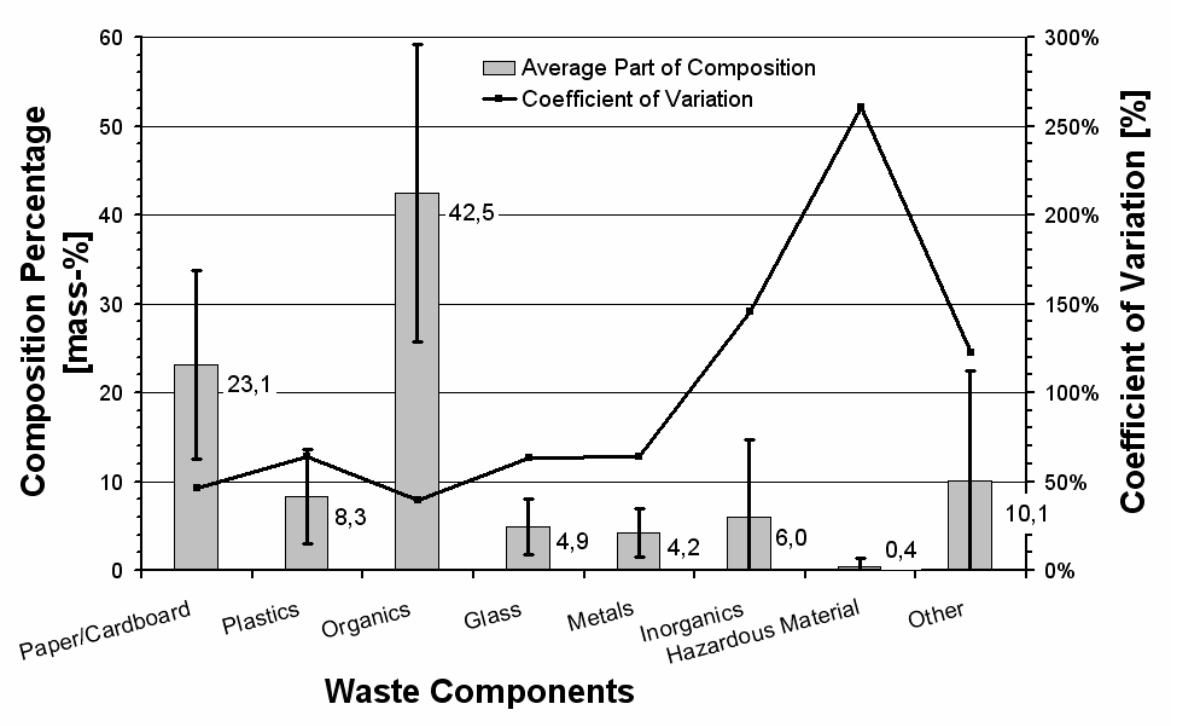

Figure 1-2 Mean worldwide municipal solid waste composition with average deviation and coefficient of variation (Sources as in Figure 1-1)

1.1.2 Waste Composition in the UK

The overview of waste composition for the UK in Figure 1-3 shows less irregularity in comparison to the worldwide data. Figure 1-4 illustrates the average waste composition in the UK. The coefficient of variation is predominantly located in the range of 10-40%. Again, for the material groups inorganic, hazardous and other material the coefficient is very high in a range of 60% to 180%, although this is considerably lower than for the worldwide average composition. Nevertheless, as for the average worldwide composition, there is still much uncertainty associated with UK waste composition and specifically in defining waste groups.

While paper/cardboard and organic material typically account for approximately 30% of the overall sample mass each in UK waste, glass, plastics, mineral and inorganic material amount for less than 10% each. The remaining part is split into hazardous materials (e.g. paint, oil, and batteries) and other material (e.g. electric waste).

The general problem for investigating ranges for waste composition is the definition of different material groups. Some materials fit into more than one group with the result that these materials are not consistently associated to an appropriate group. A unified classification with explicitly defined material groups would simplify the comparison of

waste compositions from different origins and more meaningful statements about influences and differences would be possible.

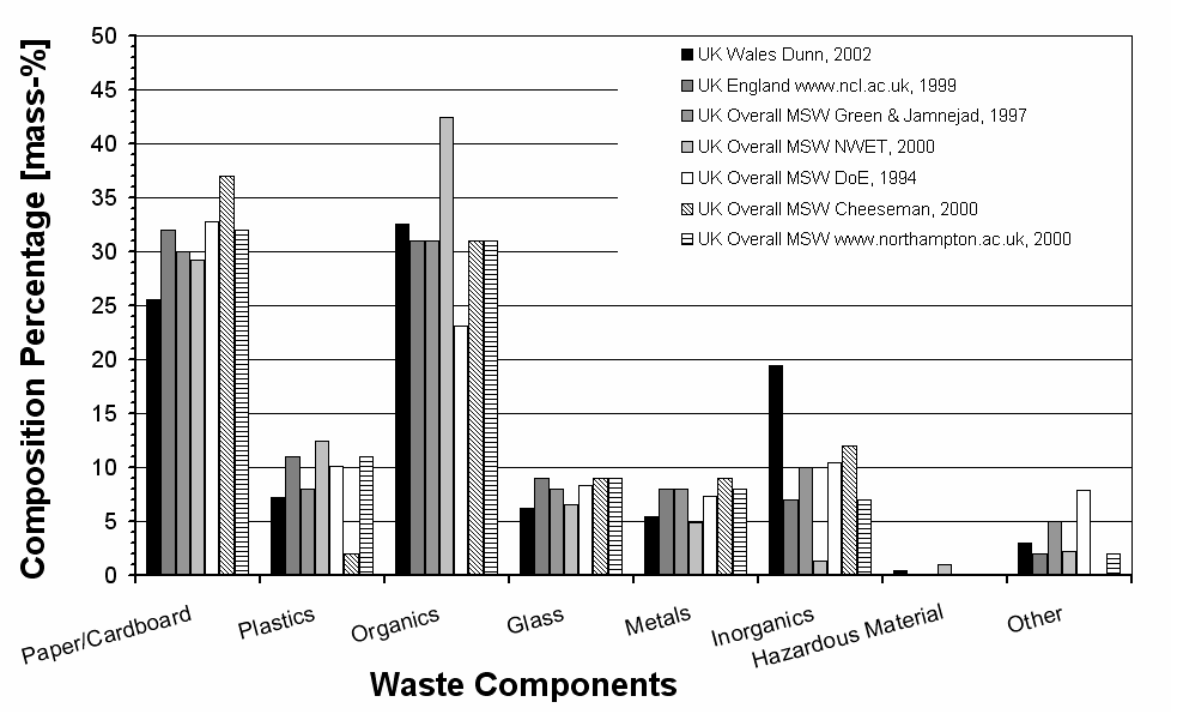

Figure 1-3 Overview of the varying waste compositions in the UK

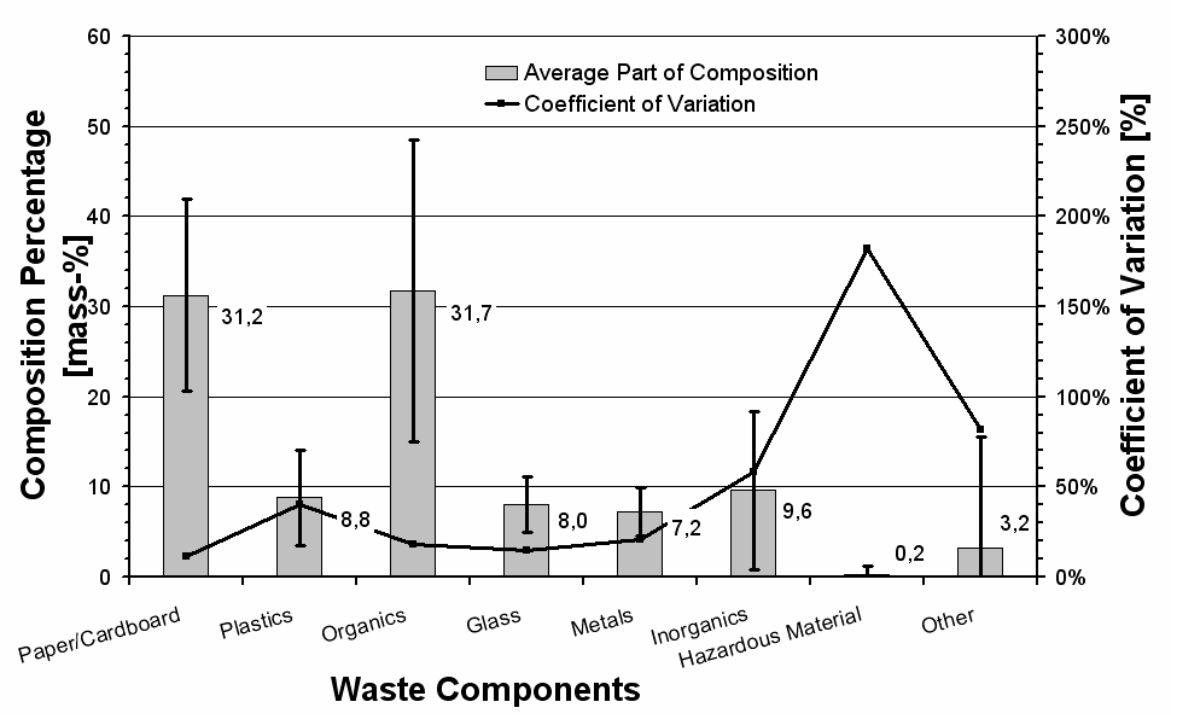

Figure 1-4 Mean UK composition with average deviation and coefficient of variation

1.2 Landfill – An Engineering Structure

Waste bodies are heterogeneous; they have anisotropic physical properties (due to placement in layers) and varying biological properties. To enable the assessment of mechanical behaviour of a waste body it is necessary to investigate the properties of its components. A first step is to develop a classification system that groups components according to their physical and mechanical properties, including an assessment of their potential to influence mechanical behaviour of the waste body. The second step is to describe in-situ waste body structures and hence to evaluate mechanical properties of these volumes of waste (e.g. compressibility, shear strength and stiffness). Structure of waste bodies relates to orientation and particle packing of components. For example, foil type components such as paper and plastic may have sub-horizontal orientations as a result of waste placement and compaction in layers.

The general structure of landfill consists of a lateral and basal lining system, a drainage system for leachate and gas (a leachate re-circulation system in some cases), a top cover and the waste body. Figure 1-5 shows a scheme of the structural elements of a landfill with terms employed in the Landfill Directive and guidance defined (Environment Agency, 2002). As the waste body is the largest structural element of a landfill, changes to its biological, physical and mechanical properties have important impact on the remaining elements. The fact that the waste is a “live” element subjected to constant changes and that is not fully stabilised after years aggravates the need for knowing and controlling its behaviour.

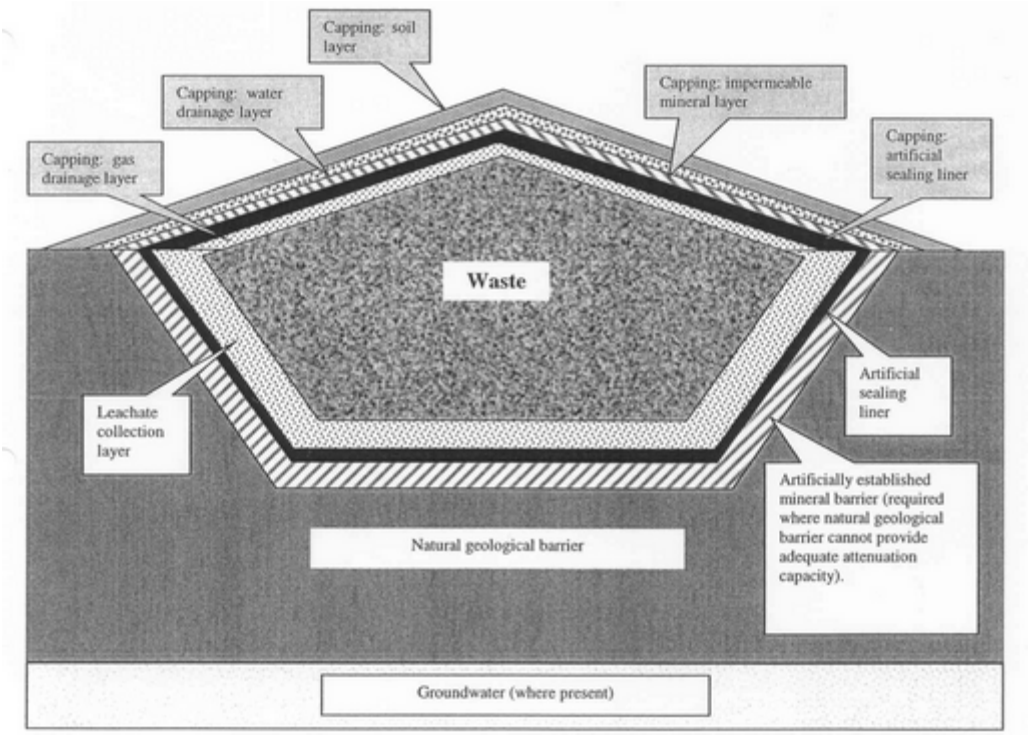

Figure 1-5 Structural elements of a landfill (Environment Agency, 2002)

Changes in waste height due to settlement, increasing lateral and vertical pressure due to surcharge from additional waste layers, weakening the waste material compound due to

pore pressure build-up caused by defective water or gas drainage, rising water tables due to faulty leachate re-circulation or precipitation caused by poor daily cover and waste material shear processes are just a small number of possible events within the waste body, which have impact on the remaining structural elements. They all can result in a loss of stability and integrity of the lining and/or drainage system. To prevent a landfill from these structural damages, it is necessary to know and predict waste mechanical behaviour.

1.3 European Landfill Directive and Implications for Waste Streams

According to Dixon (2003), the original objective of producing the Directive was to ensure that all landfills in the European Union had permits, and to harmonize permitting standards. However, the final document went further and is prescriptive regarding construction and issues of operation, but does not specifically address environmental protection. Each member state was required to implement the Directive in national legislation. In England and Wales, the landfill Directive (LFD) was transposed into legislation and implemented through the Landfill (England and Wales) Regulations 2002.

A short explanation of the EC Landfill Directive and its implications for the UK is given by DEFRA (2003). It is obvious from the demands that major changes in the composition of waste are expected and hence changes in the mechanical behaviour are also likely to occur. According to DEFRA (2003) the Directive comprises the following:

> The Directive's overall aim is
>
> "*to prevent or reduce as far as possible negative effects on the environment, in particular the pollution of surface water, groundwater, soil and air, and on the global environment, including the greenhouse effect, as well as any resulting risk to human health, from the landfilling of waste, during the whole lifecycle of the landfill*".

The Directive sets demanding targets to reduce the amount of biodegradable municipal landfilled in the UK. These targets are:

- By 2010 to reduce biodegradable municipal waste landfilled to 75% of that produced in 1995
- By 2013 to reduce biodegradable municipal waste landfilled to 50% of that produced in 1995
- By 2020 to reduce biodegradable municipal waste landfilled to 35% of that produced in 1995.

These dates include a 4-year derogation from the target years 2006, 2009 and 2016 offered in the Directive to Member States who landfilled more than 80% of their municipal waste in 1995. The UK is adopting this for the first two targets years, and will decide whether to do so for the final target year of 2016 nearer the time.

The main changes that the Directive is bringing are:

- Certain wastes banned from landfill

- All landfill sites must be classified as for inert waste, hazardous waste or non-hazardous waste – this latter category covers most biodegradable waste.
- Requires the pre-treatment of wastes going to landfill (and this treatment can include sorting)
- The UK practice of co-disposal in landfills of hazardous and non-hazardous waste must end by July 2004.

These requirements present major commercial opportunities for the waste management industry. Waste producers will increasingly be looking to the industry for innovative solutions to help them manage their wastes and reduce costs. Investment will be needed to enable the industry to deliver higher value services managing waste higher up the utilisation hierarchy.

For example, the requirement that waste is pre-treated will mean that consideration will need to be given to recycling and recovery of the waste whilst the bans on certain wastes going to landfill will also force operators to look for alternatives. One target is to reduce the amount of commercial and industrial waste going to landfill to 85% of 1998 levels by 2005.

These measures implicate large changes in the mechanical behaviour, e.g. by removal of reinforcing plastics. To become aware of those changes the attention should be centred on waste composition in general, on the development of a generally accepted waste classification system and of course on the mechanical behaviour of MSW itself.

Changing waste streams lead to large uncertainties in the estimation of waste properties. It is generally known that the variability of waste is a huge problem in the assessment of waste properties. With further changes in the waste compositions, experience-based information about waste properties becomes useless. Further use of experience values for the definition of waste properties would result in erratic and dangerous assumptions for design and construction of landfills.

1.4 Aim and Objectives of the Project

To gradually examine waste mechanical (shear and compression) behaviour and to provide a basis for the comparison of information about waste mechanical behaviour from various sources, this project is concerned with

Shear and Compression Behaviour of Undegraded Municipal Solid Waste,

and is accomplished by using recent findings given in the literature and by carrying out a structured set of laboratory shear and compression tests. The main aim is to be fulfilled by processing the following objectives:

1. To identify the factors that control mechanical behaviour of MSW
2. To develop a classification system to categorise waste constituents by their influence on mechanical behaviour
3. To propose a family of synthetic wastes based on mechanical behaviour

4. To investigate the role of compression in development of structure within MSW bodies

5. To investigate factors controlling shear behaviour through the use of synthetic waste materials representing a range of MSW classifications

By achieving these objectives and producing clear conclusions advanced knowledge of MSW mechanical behaviour is expected.

1.5 Contribution to Knowledge

A successful accomplishment of the aim and the objectives would mean a contribution to the general understanding of MSW mechanical behaviour. Providing a classification system that allows comparison of waste mechanical properties on a common base that includes the most important waste component properties of waste for mechanical behaviour would minimise uncertainties derived from comparing values with different boundary conditions. A rigorous classification system is required to help explain mechanical behaviour (e.g. compressibility and stability) of waste bodies, to group wastes with similar mechanical properties and to facilitate the exchange and interpretation of measured properties. Given the significant variation in waste materials, and the limited number of researchers and practitioners engaged in measuring mechanical properties of waste, a classification system is deemed crucial to development of a unified framework for waste mechanics, and hence to our ability to design and operate landfills. Designing a synthetic waste would contribute to the general understanding of waste mechanical behaviour as its influences can be gradually investigated. Conducting shear and compression tests on the synthetic waste provides the possibility to gradually assess the factors influencing the mechanical behaviour of MSW. Testing real waste is always bound to introduce uncertainties, as the composition is often unknown, repeatability is limited due to the variability of MSW, and mostly more than one factor influences waste mechanical behaviour.

Past experience is a poor guide to future behaviour. Life style changes and the introduction of new legislation and pre-treatment are resulting in significant changes to waste composition. Knowledge of waste component properties is required to evaluate future changes in mechanical properties of waste bodies and hence landfill behaviour.

Knowing the element properties of a construction is a necessity in the sector of constructive engineering. Thus knowing and controlling the mechanical properties of waste being the largest structural element of a landfill is crucial to provide safety for human health and for the environment. This is also important for economical reasons, as advantages are derived from a thorough assessment of waste properties, such as the efficient use of landfill space during design and construction, and landfill stability.

This project is therefore concerned with the development of a basic aid to understand waste mechanical behaviour in a structured way. This is accomplished by a geotechnical classification framework, a family of synthetic wastes and a series of large-scale compression and shear tests.

1.6 Outline of Chapters

Chapter 2 presents a literature review on shear and compression behaviour of municipal solid waste. The literature review about shear behaviour is divided into a short presentation of the theoretical background including the most important geotechnical parameters, a section about factors influencing waste shear behaviour, and furthermore, a section about the methods of determination and a summary of design parameters used in the literature. The literature review about compression behaviour of MSW deals with different settlement phases and influences of a waste body. Duration and magnitude of the main settlement phases are presented. The most important geotechnical parameters are given.

Chapter 3 demonstrates the methodology chosen for the accomplishment of the present task of describing and assessing shear and compression behaviour of undegraded MSW. The general approach is presented, followed by detailed explanations of the development of a geotechnical classification system and a family of synthetic wastes. Subsequently, the investigation of compression and shear behaviour is illustrated including sample preparation, test set-up, test procedure and data analysis.

The development of the waste classification system and the synthetic waste are presented in chapter 4. The classification and the synthetic waste are based on the findings of an in-situ waste sorting analysis, which is also presented in chapter 4. The development of the classification system includes the necessary elements and the classification method. The development of the synthetic waste comprises the derivation of the synthetic waste components from a waste sorting analysis. The compositions used for subsequent laboratory work are also introduced.

Results from compression tests on synthetic waste compositions in a large compression cell are presented in chapter 5. Chapter 6 demonstrates results from a performance validation of large-scale shear tests, which includes shear box calibration and large- and small-scale tests on Leighton-Buzzard sand. Moreover, shear behaviour of the synthetic waste is presented.

Chapter 7 contains the discussion of results of the present theoretical (geotechnical classification system and the development of a family of synthetic wastes) and the practical work (compression and shear behaviour). Chapter 8 concludes this work by summarising the results of this project, and further work is recommended.

2 Literature Review

2.1.1 General Introduction

The following chapter is an overview of selected work on MSW mechanical behaviour done by various researchers within the last 25 years. Key issues are shear and compression behaviour. In this respect, shear behaviour and the influencing factors involved are the main focus of this chapter. For the factors in particular, composition, reinforcement, time evolution (i.e. degradation), structure, water content and unit weight are emphasised. Alongside these factors, the determination and interpretation methods play an important role and are also examined.

2.2 Shear Behaviour

2.2.1 Theoretical Background

Shear strength is the maximum value of shear stress before a soil yields. In soils the relationship between stress and strain is non-linear. In waste materials (and organic soils) it is also time-dependent. Volume changes develop from the applied normal and shear stresses. The most commonly used strength theories are those of Coulomb and Mohr. Considering a unit of area, on which a normal effective stress σ' is acting, the failure condition $\tau_f = f(\sigma')$ specifies the shear stress, which can be accommodated by the soil at a given normal stress. According to Coulomb shear strength τ_f, is expressed in terms of cohesion, c and angle of friction, ϕ.

$$\tau_f = c + \sigma * \tan\phi$$ Equation 2-1

Cohesion is defined to be the bonding force between the fine-grained particles of a soil. It is stress-independent. Due to the comparatively large components in waste, cohesion is mostly interpreted as the interlocking of components in waste mechanics. Additionally, this is also often defined as apparent cohesion, which is caused by capillary forces. The friction angle is related to the friction between the particles and is stress-dependent.

According to the Coulomb's failure theory, a critical combination of normal and shearing stress results in failure on a certain plane. A failure envelope is defined by a curve joining the points representing the failure stresses on these planes. It is often difficult to establish the orientation of the failure plane in a test specimen. The failure envelope is then obtained by a curve tangential to the circles representing stress at failure. Frequently, for stresses within a limited range, the Mohr failure envelope is approximated by a straight line, which is then known as the Mohr-Coulomb rupture line. Terzaghi introduced the concept of effective stress and showed that effective stress governs the fracture and deformation behaviour of soil:

$$\tau_f = c' + \sigma' * \tan\phi' \qquad \text{where } \sigma' = \sigma - u$$ Equation 2-2

Oweis (1993) explains the concept as follows. In a saturated soil mass the normal stress on any plane is due to the sum of pressure carried by water in the pore space and effective stress carried by the soil skeleton. The total stress is produced by the

overburden and stresses produced by surface loading. He points out that soils contain water in the void space, which is the reason for any volume change requiring either a decrease or increase in pore water pressure. As an example, he mentions compression on saturated soil, where water would have to be expelled from the voids, whereas expansion would mean a decrease in effective stress and a drawing of water into the soil.

Waste substantially differs from soil considering component/particle size and shape, i.e. waste components are extensively larger than soil particles. Moreover, due to the general heterogeneity of waste (i.e. components of different size, shape and material properties) components are often interlocked and tensile forces can form when exposed to shearing. As waste components are often compressible interlocking is even more advantaged when load is applied with the result that compressible components deform and potentially interlock with other components. Also, components with different material properties (e.g. tensile and shear strength) are involved leading to the possibility of material failure of the weaker component when sheared by an adjacent component with a stronger material, i.e. component crushing is likely to occur. Kölsch (1996) states that shear strength is composed by a shear resistance and moreover, by a tensile resistance caused by fibrous elements. He describes the definition of shear strength as follows:

> *"The resistance, which affects shear stress caused by mechanical stress, is called shear strength. In solid materials the shear strength can be deduced from tensile and compressive strength. In loose materials the shear strength is not a matter of chemical or physical compounds but of friction and adhesion forces. Due to the friction resistance being dependent on surcharge the shear strength of loose materials is dependent on the state of stress. Moreover, at a shear displacement an adhesive resistance (cohesion) is added, which acts in all directions. This resistance is caused by surface tension of water in-between huge particles, electro-static forces (Coulomb) and forces from the bonding force of masses (van der Waal) at a fine particle size (polarisation of the surface; force of attraction and repellence)."*

In terms of bilinear boundary condition, Kölsch (1996) remarks that the results of shear test are often not suitable because with c and ϕ only a straight line is shown. Moreover, in the results the load-dependence of the shear resistance is shown, but not the reason for this. From his opinion, a tensile strength is activated during the shearing process. Physically considered it is a reinforcing effect, which adds to the shear resistance. To take the tensile strength of the fibrous elements into account, Kölsch adds a percentage of fibre cohesion (Δz) and the tensile angle ξ to determine a theoretical shear strength $\tau_{theo.}$:

$$\tau_{theo} = c + \Delta z * \sigma * \tan\xi + \sigma * \tan\Phi \qquad \text{Equation 2-3}$$

The shear modulus G is defined as the ratio of shearing stress τ to shearing strain ε within the proportional limit of a material. The shear modulus is the initial, linear elastic slope of the stress-strain curve in shear.

$$G = \frac{\tau}{\varepsilon_s} \qquad \text{Equation 2-4}$$

2.2.1.1 Determination of Shear Strength

The presentation of the shear parameters cohesion and friction angle in the literature differs considerably, thus the result from the literature review is characterised by the use of both, total and effective parameters. If available, mobilised parameter were also shown.

In laboratory practice for shear strength determination, a test sample is subjected to a constant rate of deformation while the resulting load changes, and volume changes or pore water pressure are measured. The effective stress strength parameters c' and ϕ' can be determined from drained test or tests with pore pressure measurements.

To date there are three common methods for determining shear strength of waste: laboratory tests (direct shear test, simple shear test, triaxial test), in-situ tests including “in-between” in situ tests (i.e. direct shear tests on excavated waste specimen) and back-calculation from failures and observations on waste slopes. Additional possibilities are mentioned by Cowland *et al.* (1993) being an empirical correlation determined between shear strength and index tests, and by Kölsch (1996), who develops shear stresses from tensile test results.

2.2.1.2 Description of Shear Behaviour

Due to the observation that often no peak shear strength occurs, the mobilised friction angle ϕ'_{mob} or cohesion c'_{mob} is used in many cases to describe the shear behaviour of waste. Especially when testing waste in triaxial compression tests a failure, i.e. peak shear strength, is often not measured.

Jessberger (2001), using the Mohr-Coulomb failure criterion, related the shear parameters friction angle ϕ' and the cohesion c' to the failure conditions. He suggests defining a deformation criterion in case a failure cannot be identified up to a pre-determined deformation level, which relates to mobilised shear parameters. Oweis (1993) remarks that unlike soils, waste is not a geological material and the composition varies depending on the type of waste generated. Through experience, he proceeds, the mechanical behaviour of refuse is expressed in terms of an apparent frictional parameter ϕ'_a and cohesion c'_a. The apparent cohesion is a parameter characterising the lateral reinforcement present in waste, which is analogous to the apparent cohesion in reinforced earth. These parameters are empirical and could be defined in laboratory tests at an arbitrary strain level that is considered by the user to be excessive. Alternatively, these parameters could be back calculated from actual cases of failure or cases where large deformations in refuse have occurred, or from slopes that have not failed. He also suggests that the modified Coulomb failure criterion of effective stresses could be used to characterise the shear strength of waste. Considering an apparent friction angle ϕ'_a and apparent cohesion c'_a, the shear strength τ along a given plane is a function of the effective stress σ'_n normal to that plane. Manassero *et al.* (1997) agree in interpreting the tests on waste by means of concepts of shear angle, and "cohesion" intercept, because they are commonly used. On the other hand, he mentions that waste is usually not saturated. Therefore, interpretation of test results in terms of undrained situation with no volume change and $\phi = 0$ may be a very unrealistic approach and an analysis in terms of equivalent c "intercept" - ϕ can be more adequate.

2.2.2 Factors Influencing Shear Behaviour

Fassett *et al.* (1994) provide three main factors affecting the shear strength of MSW:

- The organic and fibre content;
- The age of the waste, and the extent to which it has decomposed; and
- The placement conditions (i.e. the compaction effort, composition, and the amount of daily soil cover).

Amongst these factors the influence of external conditions has to be considered. Figure 2-1 is an overview of the most important factors influencing shear behaviour of MSW. It includes the factors mentioned by Fassett *et al.* (1994) in its sub-divisions, which are complemented by additional factors. Three main influences are to be differentiated being waste composition, operation and external conditions. These factors also have an effect on each other. Due to placement of different waste types (commercial or domestic waste, etc.) there is a possibility of in situ differences in waste composition on the one hand and on the other the waste composition can influence the results of emplacement like compaction. Moreover, operational conditions can influence decomposition (e.g. 'mummifying' of decomposable components due to absence of water as a result of extensive drainage). Dense emplacement or clay layers can influence the effects of external conditions like leachate, precipitation drain or drainage. Weather conditions can influence the operational conditions and the properties of the waste components.

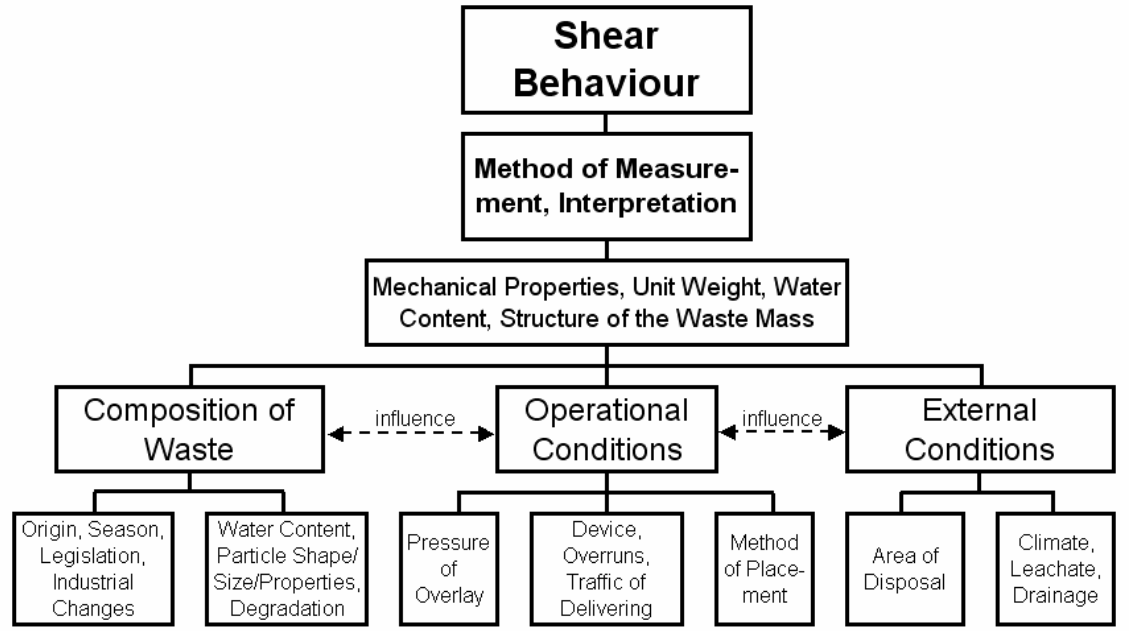

Figure 2-1 Factors influencing shear strength of MSW

In the following chapter selected shear strength values from literature are reported. These values are sorted by different influencing factors to compose ranges for certain influences. Most data relates to a “common” municipal solid waste, as its sources lack further specification. In case additional information is available, it is explicitly mentioned.

2.2.2.1 Heterogeneity

Due to the fact that MSW is composed from various materials of different size, shape and properties the "overall" properties of waste vary significantly within small distances. For example, large differences in assessing the water content can occur just within a depth of a few metres.

Landva and Clark (1990) report on the variety of materials within a landfill. As an aspect of landfill stability the possible existence of local zones of weaker material within the landfill is mentioned. Large collections of plastic sheet waste, for example, if placed in a potentially critical shear zone, could contribute to an overall low factor of safety. Another problem due to the heterogeneity of waste is the sample size for carrying out laboratory tests. Sampling has to be made with great care to achieve a representative amount featuring roughly realistic properties. Here a problem is evolving, as certainly a great amount of waste is necessary for a representative sample, but in many cases the amount has to be reduced to a sample being appropriate for the test device.

Wallace *et al.* (2001) report on this problem, when utilising geotechnical parameters of waste for modelling purposes. Unless waste is placed and compacted under extreme measures of control, it would not exhibit the characteristics of homogeneity, to a great degree, and isotropy, to a lesser degree.

2.2.2.2 Overburden

Extending the waste disposal with additional layers on top of already existing disposed waste causes surcharge. Cowland *et al.* (1993) state that it is possible for strength to either increase or decrease depending on the loading history, the nature of waste, and whether the particles remaining after decomposition interlocked more strongly or not. The surcharge of additional waste layers creates an increase in the unit weight of the lower waste due to migration of smaller particles into void spaces or by changing the physical dimensions and biological and chemical configuration of the waste components, which is a mechanism of settlement.

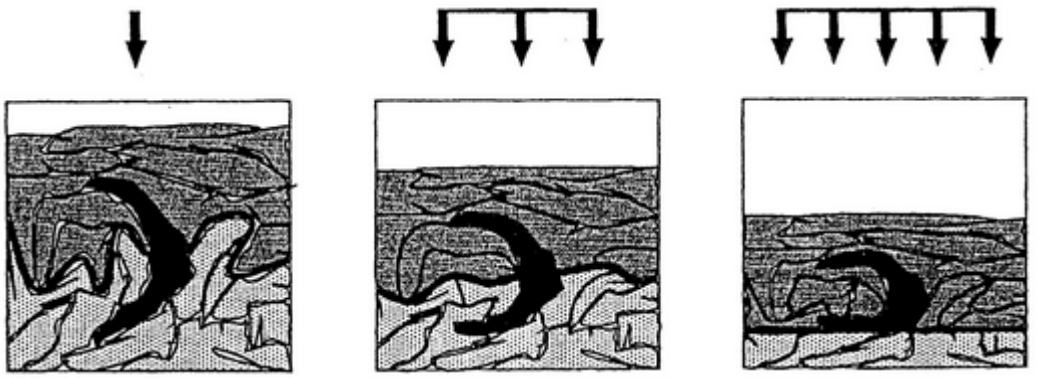

Figure 2-2 Theoretical loss of shear strength due to increasing load (Kölsch, 1996)

Also, the anchoring effect of reinforcing components - if there are any – can be amplified. Moreover, the contact surface between the components is increased due to the increase of the unit weight. As a result the friction and thus the shear stress increases, as well.

Kölsch (1996) shows the opposite effect increasing overburden can have on the interlocking of components (Figure 2-2). Considering a hypothetical shear plane within the waste, an element connecting the areas above and below this plane could be compressed in such a way that a reinforcing effect disappears. The shear strength is potentially decreased.

2.2.2.3 Composition

Mechanical properties vary as a result of different components within the waste body, e.g. with a higher amount of plastic material, reinforcement behaviour is expected to increase. Considering different types of waste (e.g. domestic or commercial waste), various compositions are expected. The origin has a controlling influence on the composition. Waste from areas with an industrial structure show a different kind of waste than from rural areas. Other influences are the social status of the catchment area, seasonal fluctuations, changes in consumer behaviour, legislative actions (e.g. recycling, waste avoidance) and the age of waste.

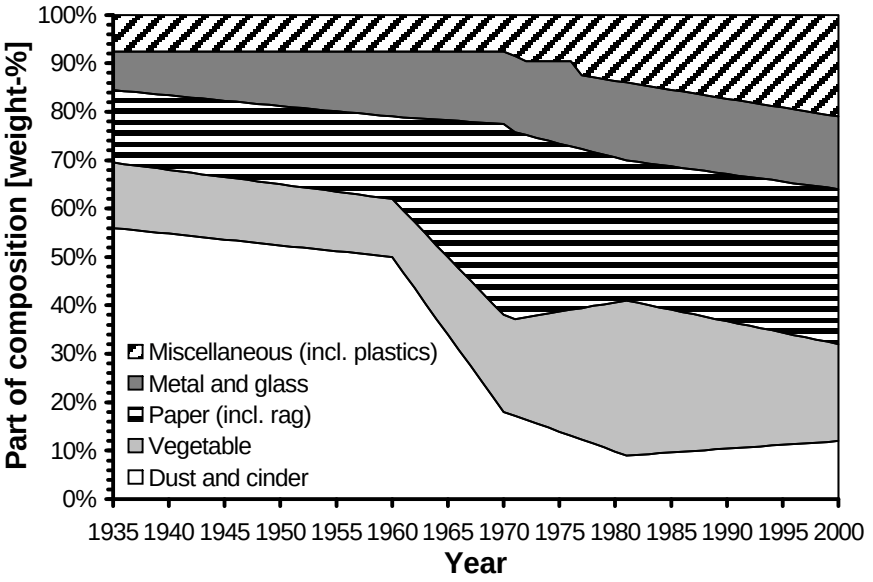

Figure 2-3 Change of the waste composition in the UK (Watts *et al.*, 2002)

The composition worldwide also differs considerably. There are geographical, cultural and social differences between developed, developing and emerging nations and even between countries, which are on the same developing level. This makes it impossible to compare directly overall properties of waste. Even within each country there are compositional changes due to altering consumer behaviour. Looking at the waste composition since 1935 in the UK (Figure 2-3), it is obvious that the amount of dust and cinder is greatly reduced while the amount of miscellaneous material (including plastics) is increasing. Further research is necessary for assessing the influence of composition on shear behaviour. The influence of certain components on mechanical behaviour has to be investigated considering future changes in waste composition. For example, due to the impact of the EC Landfill Directive (1999) the composition of MSW could significantly change due to future recycling or pre-treating actions. This will affect shear behaviour and hence stability of waste bodies.

2.2.2.4 Reinforcement

Waste components with a fibrous or sheet-like character are believed to have a reinforcing effect on waste, especially materials like plastic, paper and textiles. The reinforcing effect consists of two main forces, a bonding resistance due to normal forces acting on the reinforcing element and the actual tensile strength of the material.

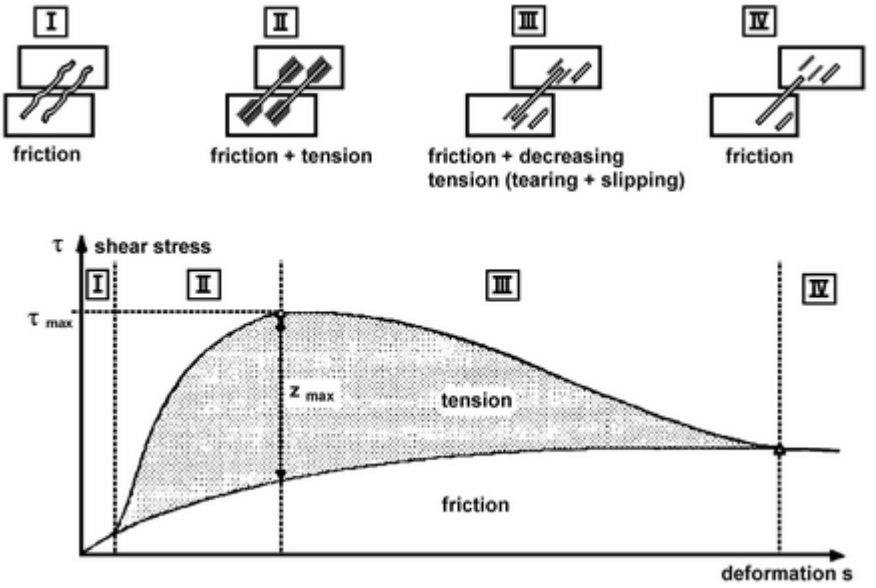

Figure 2-4 MSW Bearing behaviour (Kölsch, 1996)

From results of an on site penetration test in fresh waste, Kölsch (1996) concluded that the reinforcement effect of the fibres was almost completely destroyed after the waste was shredded and a low internal friction angle was determined. Kölsch states that the bearing behaviour of waste can be explained as shown in Figure 2-4. During the deformation only frictional forces arise in the beginning (I), caused by the increase of deformation; the fibres get stressed and the tensile force grows (effect like reinforcement, II). Exceeding the tensile strength or bonding, the fibres tear or slip out (bond failure, III). In this case, the maximum of shear stress is reached. With further deformation the shear stress drops down to that based just on friction (IV). Figure 2-5 shows a potential qualitative distribution of the frictional and tensile forces. The amount of friction is considerably affected by the normal load. It increases linear to the normal stress (friction angle ϕ'). The tensile strength also increases with the normal stress, because the transmission of tensile forces is supposedly improved by a firmer bonding of the fibres. The incorporation of tensile forces into the fibres is restricted to the tensile strength of the fibres, so there is a determined normal stress for a maximum bonding resistance, where the value of tensile forces reaches a maximum level, with the result of various interactions of frictional and tensile forces depending on different normal stress conditions In Figure 2-5, the circles indicate the maximum tensile force, the triangles mark the maximum friction at a determined normal stress. At the lowest normal stress σ_1 only a low tensile force is arising (loose bonding), at higher normal stress the tensile force in the fibres is increasing (firmer bonding), before the tensile force exceed its maximum at the normal stress σ_2. At higher normal stresses ($\sigma \geq \sigma_2$) only the frictional component of total shearing resistance

increases. Depending on the proportions between frictional and tensile forces the total shear resistance is dominated by the tensile forces ($\sigma_1 \leq \sigma \leq \sigma_4$) or by the frictional forces (σ_4). At σ_4, frictional forces are activated and reach their maximum after the tensile force (i.e. no strain compatibility). In that range of normal stress, where the total shear resistance is dominated by tensile force, the shear envelope shows a convexity, which is characteristic for fibrous material. Size and range of the “bulge” depend on the material properties (fibre proportion and strength, friction property).

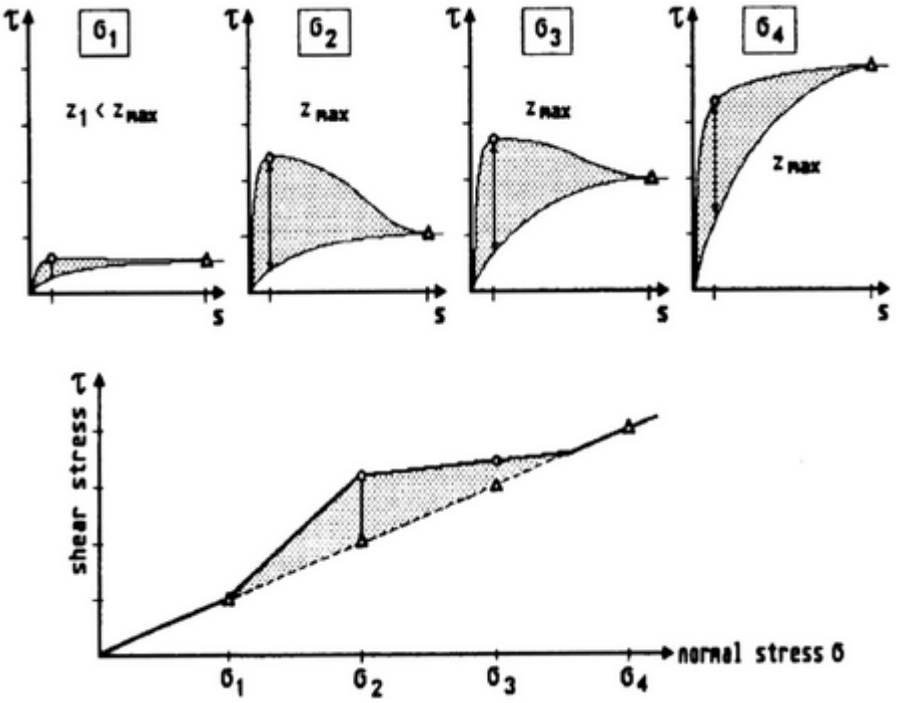

Figure 2-5 Increasing of total shear resistance by tensile force (Kölsch, 1996)

The bearing model considers that fibrous materials are able to incorporate and transmit tensile forces out of the deformation zone. It also considers that the development of tensile forces in the fibres, having the same effect as reinforcement, depends on the bonding of the fibres, i.e. on normal stress, and on the angle between shear plane and fibre orientation. Gotteland *et al.* (2000) carried out shear tests on non-hazardous industrial waste (NHIW) and domestic waste (DW). Some samples of the NHIW showed a large amount of fine components, while the DW contained large amounts of plastics, which are supposed to affect waste by reinforcing. The results confirmed this assumption, as the shear tests on the DW resulted in a higher mobilised friction angle than the tests on the NHIW.

Kölsch (1996) notes that the friction of loose materials is partly based on the friction between the surfaces of particles. In case of shear strain of an element in a loose material a straight shear envelope is assumed. In reality there is not a shear plane but a “toothing” effect on the condition that grains are turned or lifted. There are larger friction forces because the contact area increases. (Figure 2-6)

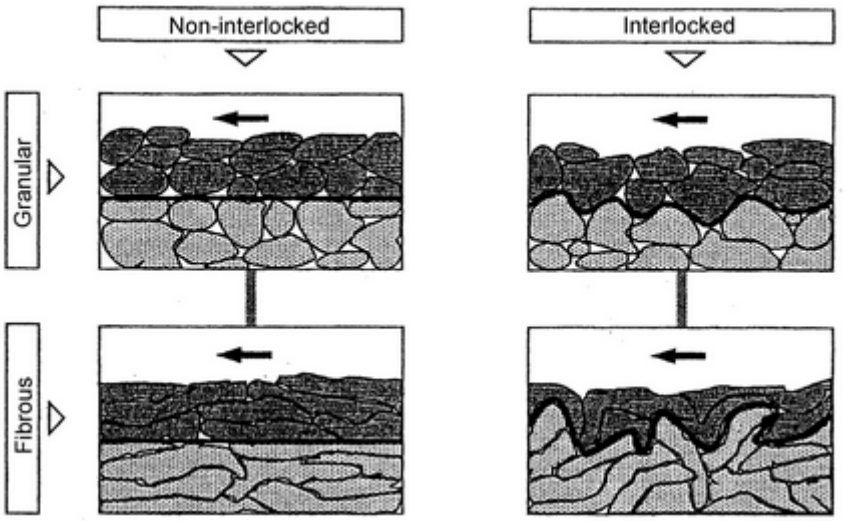

Figure 2-6 Friction increase due to “toothing” effect (Kölsch, 1996)

Until now, loose materials have been measured on the condition that there are no self-deformations of the components in the state of service. This is only true, when the shear force, which acts upon the surface of the components, is lower than the strength of the components. Therefore, low strength and a comparatively high shear force mean the collapse or deformation of the particle in granular compositions, as well as in compositions with fibrous elements like waste. Because of this, friction-independent, additional shear resistance appears due to tensile forces (like reinforcement of soil). In reinforced loose materials, effects of reinforcement contribute to the shear strength. During shearing the deformation of the reinforcing-like constituents generate internal tensile stresses, which raise the shear resistance. If the orientation and location of the reinforcement is known, an analysis can be made separately because the strength of the paste and of the reinforcing elements are known.

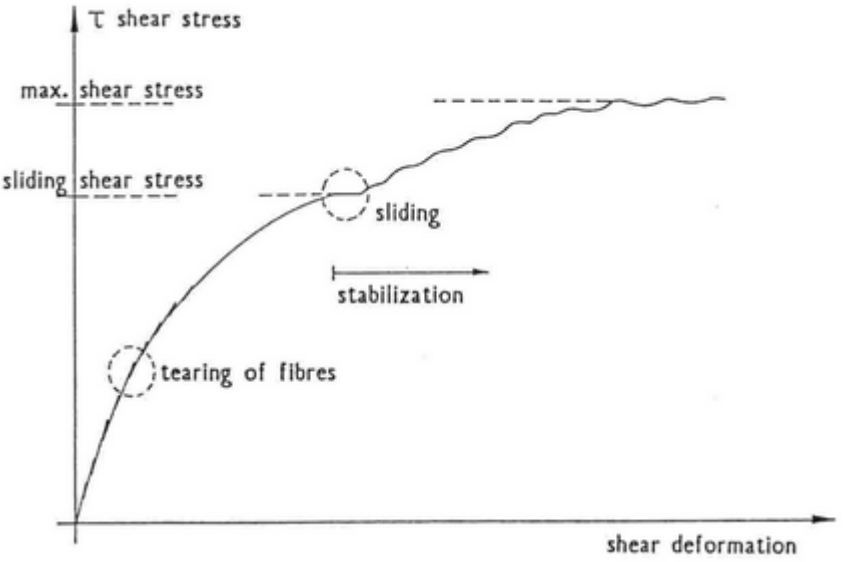

Figure 2-7 Shear test of model waste; characteristic shear behaviour (Kölsch, 1993)

Kölsch (1996) has proven that fibrous, non-cohesive materials are able to incorporate tensile forces, which could be an explanation for the capacity of waste to form steep or even vertical slopes remaining stable for several months. In an earlier publication (Kölsch, 1993) the characteristic shear behaviour of fibrous model waste (Figure 2-7) measured in a shear test is demonstrated. The tearing of the fibres, which is visible as points of discontinuity in the shear-deformation curve and which could even be heard during the shear test, is only detected in a normal stress range exceeding at least 200kPa with the conclusion that the fibres of the simple model waste composition (in mass-%: 28% sand, 62% paper and 10% plastic) incorporate minor tensile forces at lower normal stress, because the fibres seem to be less well-anchored (i.e. bond resistance).

Moreover, it is observed that with increasing shear deformation the sample starts to slide and the shear stress becomes constant for a certain period of time, which is defined as sliding shear stress. Further on, the correlation between sliding shear stress and normal stress (Figure 2-8) of fibrous material is found to be discontinuous (in contrast to granular materials like soil). As the author notices, the straight line shows sharp bends at those normal stress ranges, where tearing of fibres in the shear test was found (at 200kPa paper is supposed to fail, at 500kPa the failure of plastic takes place). For the aged model waste containing plastic fibres only one discontinuity is visible. Tests with shredded model waste samples without large fibres resulted in a linear stress curve without sharp bends. It is therefore inferred that the incorporation of tensile forces in the fibrous solids accounts for an increase of shear stress in determined normal stress ranges; thus leading to the discontinuous normal-shear stress correlation.

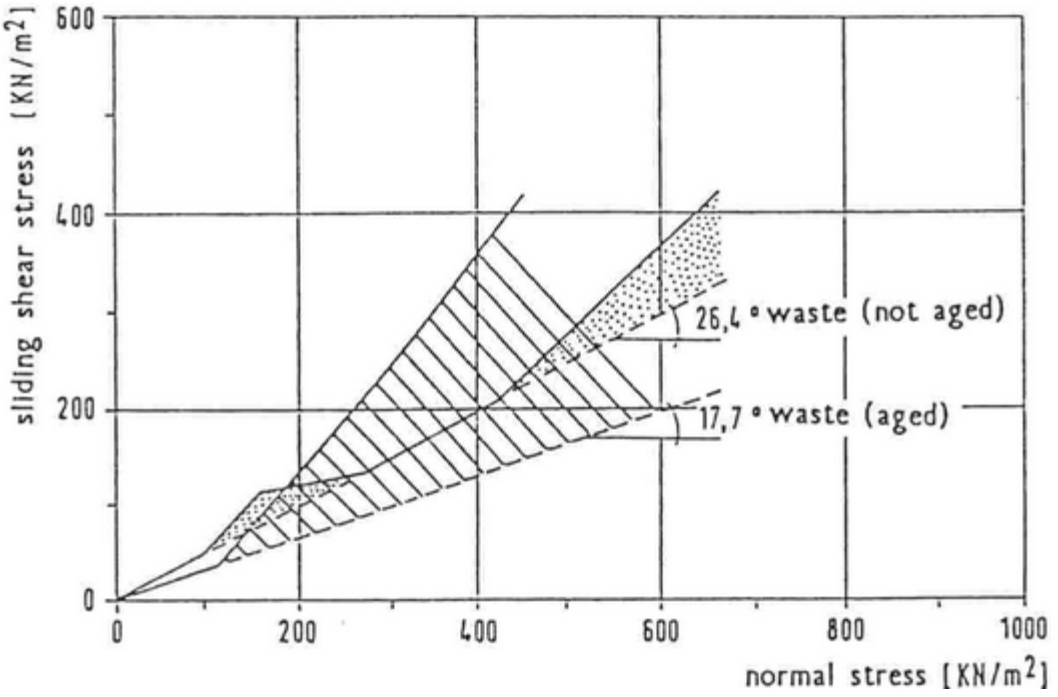

Figure 2-8 Shear test of model waste; shear straight lines (Kölsch, 1993)

Manassero *et al.* (1997) indicate the general assumption of MSW showing a homogenous composition over a certain volume of the waste body (minimum representative volume)

and in most cases reinforced elements are randomly distributed over this area so that the waste can be regarded as isotropic material. They quote Kockel & Jessberger (1995) having shown that the shear strength of the basic matrix is primarily of the friction type with the maximum ϕ_{mob} value of 42° to 45° only activated at very large strains and slightly influenced by the reinforcing plastics. The activation of the intercept cohesion, which depends on the reinforcing matrix and could be defined as "cohesion due to tensile strength" of the reinforcing components, requires, however, large strains and starts at about ε = 20% when ϕ_{mob} is almost fully mobilised. Milled MSW shows a linear failure envelope, which is mainly due to the fact that the mixture of MSW is "reinforced" by plastic with a different length and stress-strain properties. However, this result is assessed to be surprising since the failure envelope of a given material tends to curve down at very low stress.

Jessberger (2001) also assumes that the important amount of the shear strength mobilised with large deformations and observed on municipal solid waste is probably a confirmation of "Reinforced Earth"-like behaviour. It is assumed that fibrous waste components like plastics, textiles, paper or cardboard and wooden branches might act like "reinforcement" of the mixed waste and in this case contribute to the gain in "intercept or fibre cohesion" or strength as seen in reinforced soil. In this respect, waste is regarded as a composite material consisting of two components: a basic matrix comprising the fine and medium grained, mostly soil-like "particles" having a frictional behaviour and the reinforcing matrix, comprising large foil, like fibrous waste components. In that case, the mixed MSW could be modelled similarly to a soil reinforced with randomly oriented fibres.

2.2.2.5 Degradation

Following deposition, waste changes considerably due to biological and chemical degradation and physical change. These changes also affect the mechanical properties and therefore behaviour. Considering bio-degradation, organic components alter their shape and size giving the waste a more soil-like character. Moreover, bio-degradation and/or physical forces can destroy and break up foils and sheets and thus reduce the reinforcement effect. On the other hand the unit weight increases, which could lead to an increase in frictional strength. Oweis (1993) expects the age of refuse to affect the field strength by altering the unit weight. As an argument he brings forward that as the refuse ages, it becomes denser and hence, stronger. On the other hand, decomposition however, might produce the opposite effect, as fibres reinforcing the waste are destroyed.

Siegel *et al.* (1990), who examined wastes with different soil contents, quoted the following results shown in Figure 2-9. With the assumption of zero cohesion the waste with a higher soil content shows a considerably lower friction angle. Since during the degradation process the waste components change their physical appearance (decomposition leads to smaller particle sizes) this could indicate decreasing strength properties for aged and/or degraded waste. Due to the change of the ratio between soil-like and non soil-like materials, it is assumed that there is also a change in the relationship between the cohesion and the friction angle. For instance, Kölsch (1996) assumes the internal friction angle for fresh waste is lower than that for aged waste. This would mean

an increase of the frictional shear resistance over time. Kölsch conducted tensile tests on degraded and fresh waste to investigate the change of reinforcing components with time. As they resulted in better tensile strength properties for fresh than for rotted waste Kölsch suggested that the reason could be the decomposition of organic reinforcing fibres due to the degradation process. Additionally, Siegel *et al.* (1990) quote tests done by Landva and Clark that refuse had a lower strength when retested in direct shear after a year of decomposition. The friction angle that originally ranged from 38 to 42° had decreased to 33°, and the cohesion intercept that had ranged from 16 to 19kPa was 16kPa. Landva and Clark (1990) assume that the strength was indeed lowered because of decomposition, but on the basis of the limited data available it is not possible to quantify the strength after full decomposition. Additionally, there is the influence of the soaking in leachate, which is not assessed and which could also have influenced the shear behaviour.

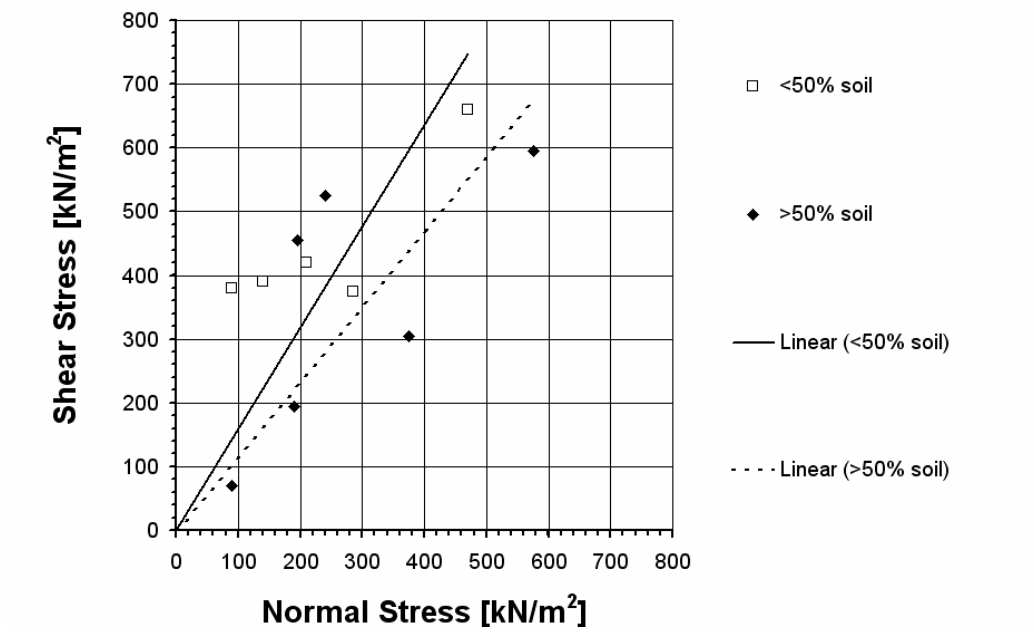

Figure 2-9 Shear strength data (after Siegel *et al.*, 1990)

Jessberger *et al.* (1995) conducted laboratory tests using waste samples of different ages (1 to 20 years old) and composition. They could not demonstrate a clear age dependent effect, e.g. a decreasing friction angle, but they state that the different composition of the material seems to be the important factor. Later, Jessberger (2001) states that the shear strength of MSW and its mobilisation depends on the type and the composition of the waste. They emphasis that a reduction of shear strength with age of deposited waste has not been proven yet. They note that age is not a significant distinctive mark for the waste.

Kavazanjian (2001) mention the sparsity on quantitative information on shear strength of degraded waste. However, from the little information that is available it would be indicated that the drained shear strength of degraded MSW is similar to that of undegraded waste. Figure 2-10 shows the result of large diameter (454mm) direct shear tests performed on waste from OII Landfill. The mass percentage of soil and soil-like material in each specimen is presented there as well. The specimens with over 70 percent soil and soil-like material correspond to areas of the landfill with high liquid content and presumably

represent degraded waste. In Figure 2-11, Kavazanjian (2001) show preliminary results from direct shear testing on bioreactor waste being performed by GeoSyntec Consultants for Waste Management, Inc. Waste recovered from a bioreactor cell was soaked and consolidated to normal pressures of 12.6, 143.6, and 430kPa. The tests were run at a very slow rate to create drained conditions. Results of the tests show ductile stress strain behaviour with a friction angle of approximately 39° for the waste at a shear deformation of 25mm in a 450mm diameter shear box. The drained friction angle indicated by this test is significantly stronger than both the OII waste and the Kavazanjian (2001) lower bound envelope.

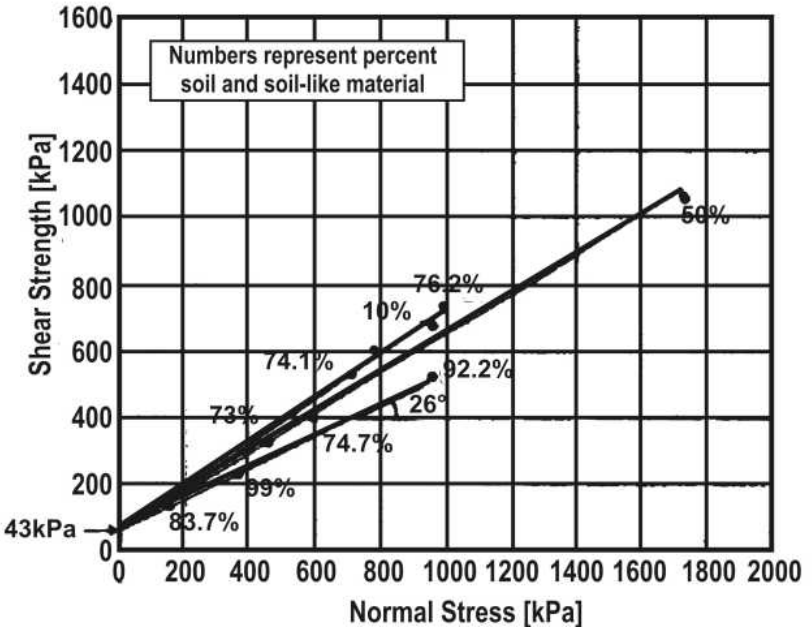

Figure 2-10 Direct shear test results; from Kavazanjian (2001)

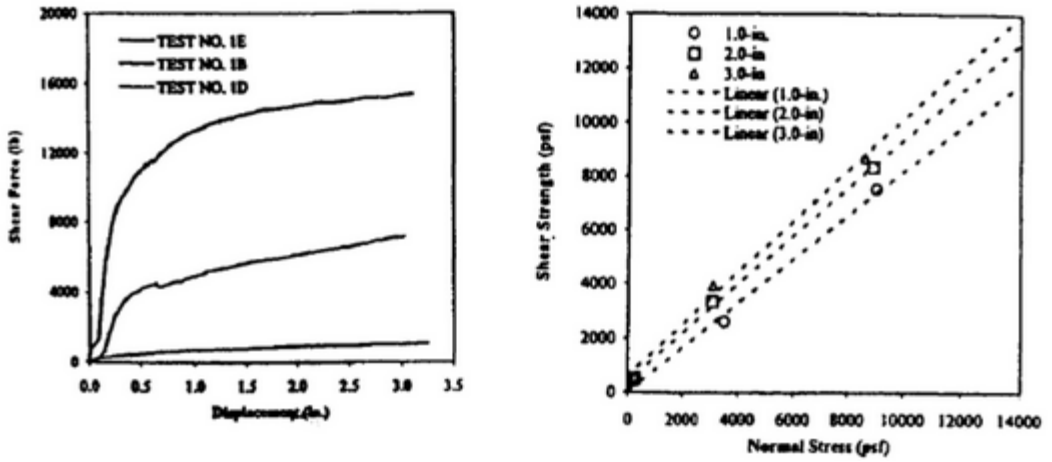

Figure 2-11 Bioreactor direct shear data; from Kavazanjian (2001)

2.2.2.6 Placement

Due to placing the waste in layers often divided by a daily soil cover, an interlocking of the waste constituents (e.g. paper, plastic, etc.) does not take place as it does within the waste layer itself as Brink *et al.* (1999) point out. In their opinion the shear strength between two phases of a landfill can be significantly lower than that of a waste body itself. In particular, it is suspected that the cohesion of the waste is due largely to the reinforcing effect of sinuous particles, as mentioned in Kölsch (1996). This reinforcing effect is discontinuous at the interface and thus considerably reducing the shear strength and creating a plane of potential weakness.

Another aspect of placing the waste is the breaking-up of the waste components due to the wheel texture of the compaction device and its weight as stated in Collins (2001). Reducing the size of the waste's components could reduce the reinforcement effect. On the other hand, by reducing the size of the components void space is reduced as well resulting in an increase of the unit weight, which is also expected to affect the shear strength.

As a passive effect of placement water (precipitation) can infiltrate the waste body during placement, if the waste is not properly covered leading to unwanted wet areas within the landfill, which can endanger the stability by high pore pressure build-ups. The daily soil cover affects the strength in two ways. Firstly, the ratio of soil in the waste affects the shear strength as the waste's character becomes more granular, secondly, the possibility of interlocking effect between to waste layers with a soil layer between is reduced.

The high variability of shear strength depends amongst other things on the type of material examined. Manassero *et al.* (1997) illustrate that, when the domestic solid waste is subjected to higher normal stresses, it is stiffening up leading to higher shear strength parameters, because increased interlocking occurs (Figure 2-12), i.e. the compaction of the material is a crucial parameter for the strength of waste material

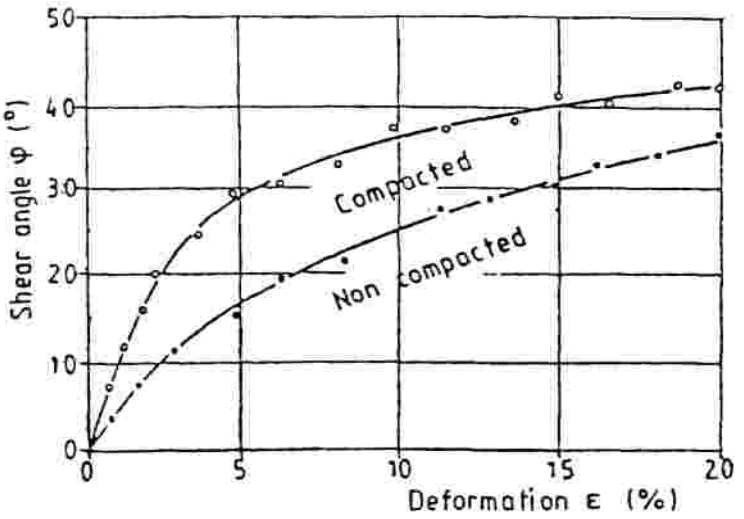

Figure 2-12 Effect of compaction on the mobilised shear angle of municipal solid waste (Manassero *et al.,* 1997)

2.2.2.7 Index Properties

2.2.2.7.1 Water content

Little data is available about the effect of the water content on shear strength. A decrease of strength is expected to occur due to softening of certain components (e.g. paper, wood, etc.). Also, another important point is that an increase in water content means an increase in bulk unit weight.

Pelkey *et al.* (2001) examined waste that had been soaked in leachate, but due to the small amount of data it is difficult to draw any clear conclusions. Compared to waste with the original water content, the wet waste seems to have a lower strength. They also examined shredded paper in a dry and in a wet state (Figure 2-13). Unlike the peak of dry shredded paper mobilised at small displacements wet paper does not reach a peak shear value, even after relatively large displacements. Unfortunately no information is given about the size of the paper particles for a further interpretation of the results.

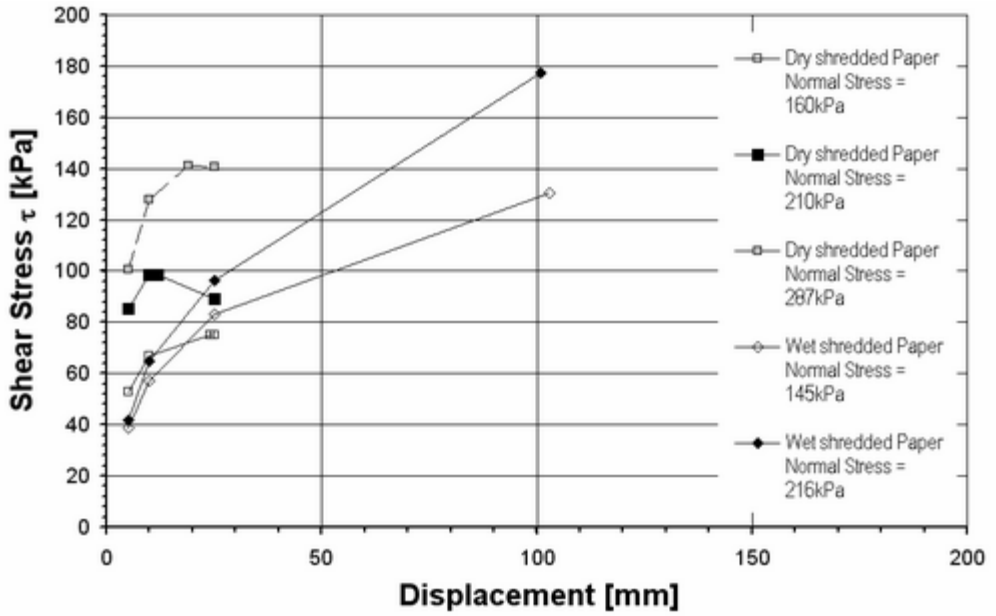

Figure 2-13 Shear stress and displacement of tests on dry and wet paper (after data from Pelkey *et al.*, 2001)

A more global danger is stated in Landva and Clark (1990). They see a source of low strength resulting from seepage along the laminated composite structure made up of horizontal or sloping layers of refuse and less pervious daily covers. Such seepage can cause internal erosion, which eventually leads to slope instability, as high pore pressures result in lower effective normal stress σ', which affects the shear strength (effective stress concept).

Koerner and Soong (1999) similarly stated that concerns regarding leachate masses within the waste body are valid for temporary configurations of steep waste face conditions and for long-term conditions of canyon-type landfills. In both cases, leachate generated hydrostatic forces could lead to possible instability and subsequent waste failure. In addition, recirculation of leachate can affect the stability of a landfill due to the

generation high pore pressures. Considering the effective stress concept, shear strength is proportionally decreased with the decrease of the effective stress due to an increase of pore liquid pressures after leachate injection.

2.2.2.7.2 Organic Content

Howland and Landva (1992) point out the difficulty in assessing shear strength regarding the organic and fibrous content of MSW. On one hand, strength of MSW appears to increase with increasing normal (confining pressures), like a soil. On the other hand, its high organic and fibrous contents when placed make it behave more like a fibrous peat than a mineral soil. Degradation processes will result in a decrease of putrescible organic with time, while the fibrous not degradable elements will remain much the same. Therefore, changes in geotechnical properties must be expected.

2.2.2.7.3 Unit Weight

From data found in the literature, a trend of unit weight influencing pairs of shear strength parameters c and ϕ can be seen in Figure 2-14. To simplify matters, unit weights less and greater than 10kN/m^3 were distinguished. From this distinction it is indicated that for higher unit weights pairs of c and ϕ also tend to be higher. This is visible especially from results of direct shear tests and back-calculations.

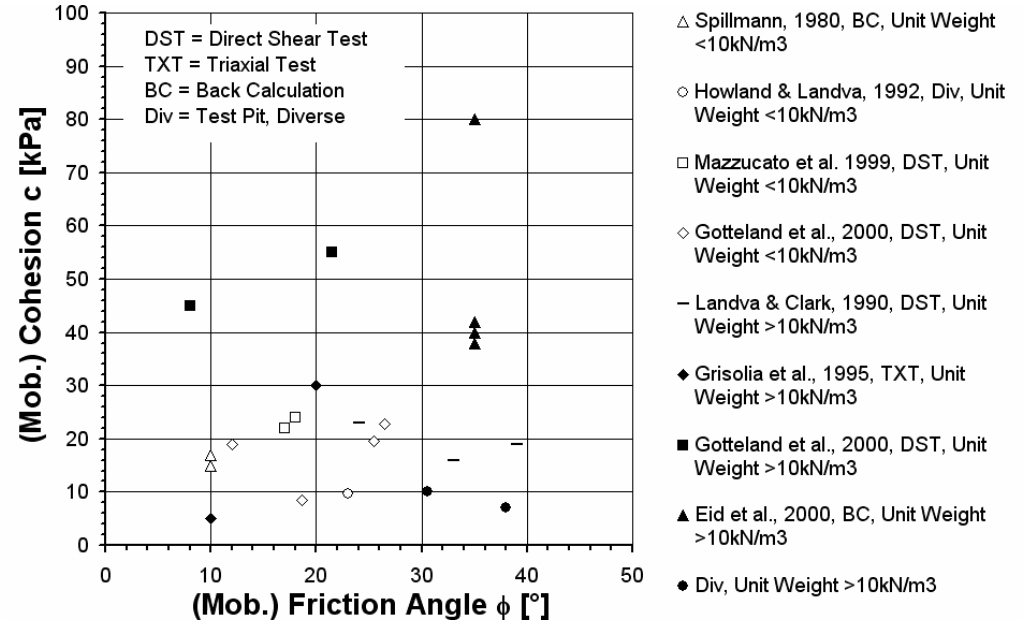

Figure 2-14 Cohesion and friction angle strength parameters in relation to unit weight (Dixon *et al.*, 2004a)

Kavazanjian *et al.* (1999) investigated the effect the reconstitution procedure has on the measured shear strength of the waste. For that purpose, two "identical" samples were reconstituted to different initial unit weights (90% and 70% of the estimated in situ weight), consolidated to the estimated in situ vertical stress, and tested in direct shear. The two samples behaved in a very similar manner independent of the initial reconstituted unit weight. The unit weight of both specimens converged on the field unit weight as the confining pressure increased and the shear strength from the two specimens was

essentially the same. The results of these tests led the authors to the suggestion that the reconstitution procedure (i.e., compaction effort) is not a critical parameter in determining the geotechnical properties of the waste, provided the normal stress is large enough to compress the specimen to the approximate in situ unit weight.

2.2.2.8 Structure

Placement controls waste structure and therefore the anisotropic shear strength behaviour. Considering different kinds of emplacement as shown in Figure 2-15, a horizontal orientation of waste components in the initial state leads to a more or less horizontal alignment after applying load. A preferential horizontal shear plane is easily produced. The possibility of vertical shearing is minimised due to interlocking of the components in a horizontal direction. If the component alignment is initially in a vertical direction, an interlocking and anchoring is possible when overburden load is applied. The structure becomes more variable and a shear plane is not obvious in comparison to the horizontal aligned components resulting in a better compaction.

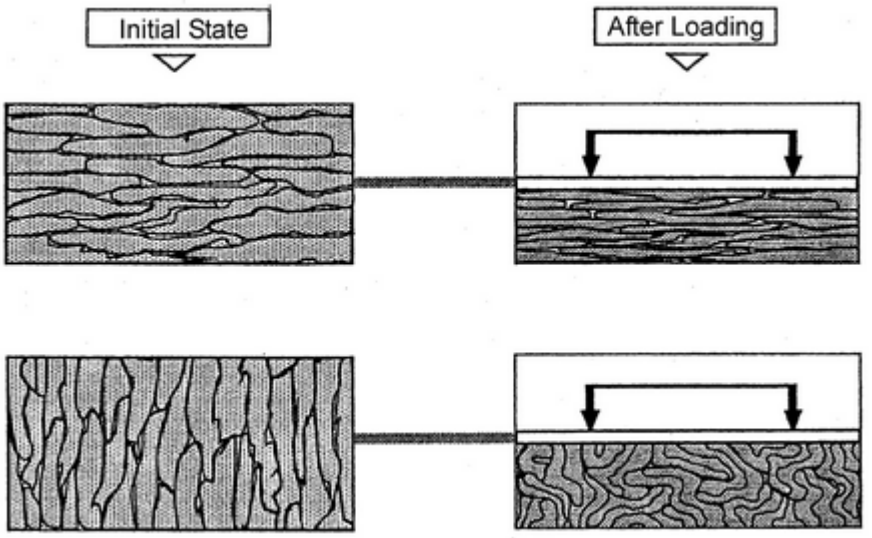

Figure 2-15 Orientation of the waste components in two states (Kölsch, 1996)

Knowledge about waste structure is crucial for understanding both the reinforcing effect and the compression process. Moreover, the interaction between these is important to assess shear behaviour of MSW. The structure is influenced by the waste composition, the size and shape of components, method of placement and layer thickness. For both granular and fibrous materials the increase in friction as a structural effect due to interlocking of components is dependent on the initial structure, which is related to the emplacement method and compaction. Kölsch (1996) discusses the possible loss of reinforcement. Interlocking of particles of waste might reduce due to loading and compression. Fibres, which are orientated orthogonally to the shear plane and therefore contribute to the shear strength, could be deformed during the process of shearing and as a result of the displacement they could align parallel to the shear plane. Consequently the shear resistance would decrease (i.e. strain softening behaviour).

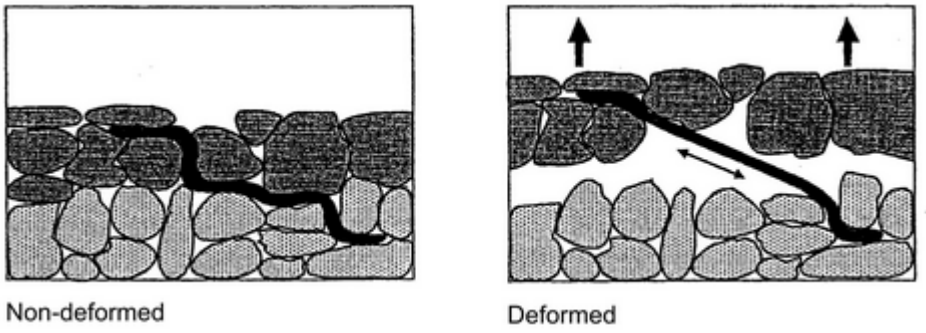

Figure 2-16 Reinforcement effect due to mobilised tensile stress (Kölsch, 1996)

Material failure of waste components is also crucial for assessing the impact of structural changes on shear behaviour. Shear resistance can be weakened due to grain-breakage and deformation of a granular material (loss of friction). This is an important issue for waste due to the large variety of components with different material strength properties in the waste body. Deformation and grain-(component-)breakage can easily occur. Kölsch (1996) further mentions the possibility of a shear plane being formed by destruction of weak components within the structure due to the heterogeneity of waste. Kölsch (1996) highlights the importance of fibre orientation (i.e. reinforcement) for mobilising additional tensile forces in addition to frictional forces. Figure 2-16 shows a schematic of reinforcement tensile stress mobilisation.

2.2.2.9 Component Size

Oweis (1993) states that essentially all tests on refuse are affected by the soil content, and therefore, results can vary over a wide range, especially when small samples are tested. Siegel *et al.* (1990) are quoted, who conducted direct shear tests on 106mm-diameter samples of mixed refuse yielded inferred friction angles from 39° to 81°. Refuse with more granular soil typically exhibits higher friction. Also higher strengths for incinerator residue are reported from literature. A friction angle of 45° from the direct shear test is reported on residues with a unit weight of 15,4kN/m^3. They cite the high angularity of the particles as a probable reason for the high strength. Oweis quotes unconsolidated-undrained triaxial tests to determine the strength of partially saturated residue with about 20% by weight passing No. 200 sieve (0.074mm openings). They report apparent friction angles of 43° to 45° at a maximum dry unit weight of 13,5kN/m^3 and optimum moisture content of 23.5% (60-70% saturation). The author proposed that such apparently high friction angles are partially due to the development of pore water pressures. Therefore tests for stability assessment should be based on saturated samples if ash will eventually become saturated in the landfill.

Manassero *et al.* (1997) show the impact of the grain size distribution on the waste's shear parameters (at a given allowable strain) in Figure 2-17. Data obtained on milled MSW together with typical results obtained for a soil-fibres matrix are plotted in Figure 2-18 from Manassero *et al.* (1997). They note that the MSW does not shows a significant bilinear failure envelope compared to "Reinforced Earth". He explains this behaviour by the fact that the mixture of MSW is "reinforced" by plastics with different length and stress-strain properties. Kockel & Jessberger (1995) report that the rather homogeneous tests results

obtained (at very large deformations) led to the assumption of a linear "failure" envelope to define the mobilisation of shear strength.

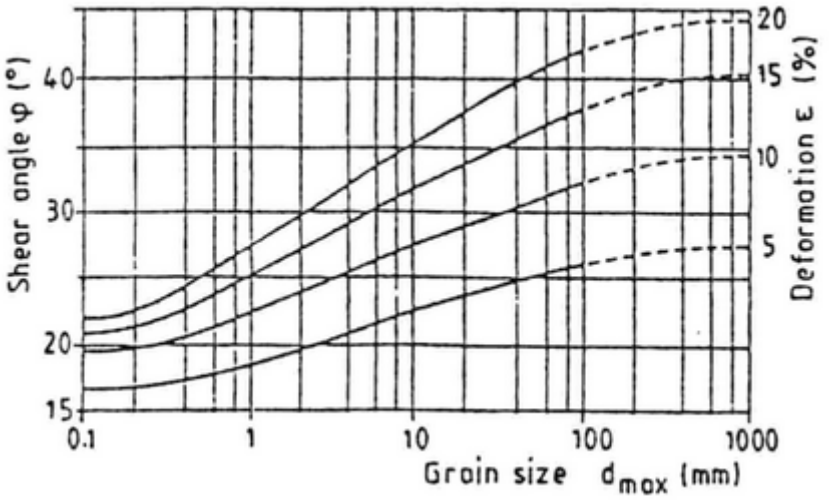

Figure 2-17 Effect of grain size distribution on the shear angle of municipal solid waste (Manassero *et al.,* 1997)

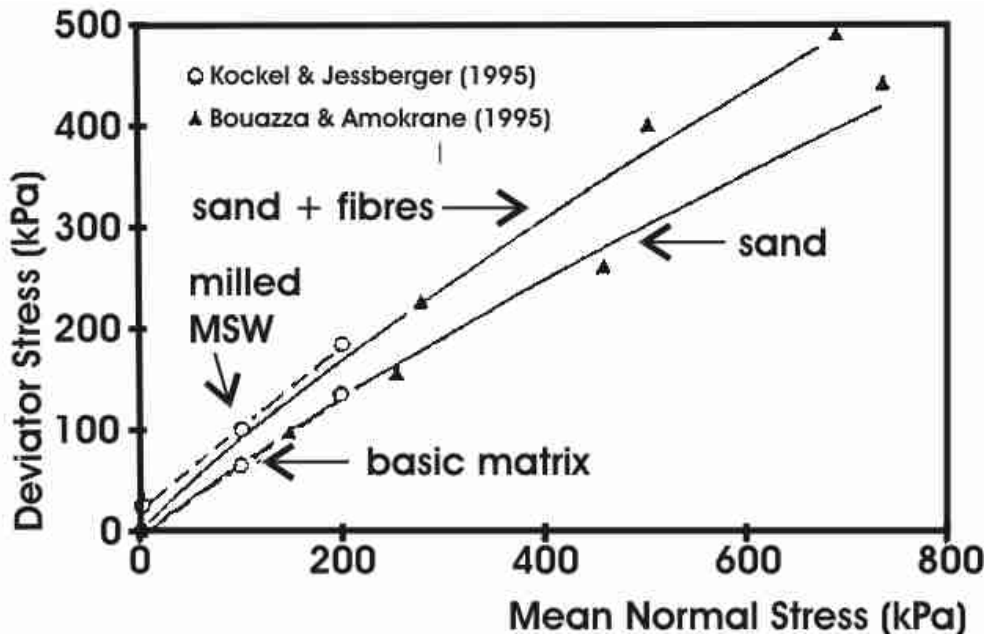

Figure 2-18 Failure strength envelope for different materials; Manassero *et al.* (1997)

Figure 2-18 from Manassero *et al.* (1997) shows that the shear strength envelope of the milled MSW is parallel to the envelope for the basic matrix of MSW. Hence, the authors suggest that the "reinforcement" does not affect the frictional properties of the soil-like material but increases the value of intercept cohesion. The milled MSW exhibits cohesion value unlike the basic matrix, which could be an indication for a cohesive character of the milled and thus small-sized waste.

Scheelhaase *et al.* (2001) examined mechanically-biologically pre-treated (MBP) MSW. Largely due to the mechanical pre-treatment but also due to the biological degradation

process the size of the constituents was widely reduced. The authors expected only a secondary influence of the fibre cohesion on the shear strength due to the smaller maximum grain size. They conclude that the limiting state of the admissible load is obtained when reaching the maximum friction angle because the limit value of the mobilised fibre cohesion will normally appear before that of the friction angle with deformation of the landfill, which is dependent on the compaction of the material. Due to the small particle size of the pre-treated waste components it would be more likely to reach very high landfilling densities with the effect of the shear strength being completely activated after relatively small deformations. Nevertheless, the authors bring out the importance of these deformations and they suggest clarifying for individual cases (e.g. for the proof of static stability the limiting state of the admissible load and/or the limiting state of serviceability becomes decisive).

2.2.2.10 Methods of Measurement

2.2.2.10.1 Size of sample

Dixon and Jones (1998) highlight the problem in acquiring representative results from a very heterogeneous test medium with varying sizes of its constituents. As with all particulate materials, obtaining undisturbed samples for use in laboratory tests is problematic. The heterogeneous nature of waste dictates that large sample sizes should be used in order to be representative. In most cases it is not possible for large undisturbed samples to be obtained, and this has led to the majority of laboratory studies using processed (e. g. milled or sorted) and re-compacted samples. Moreover, Dixon and Jones (1998) evaluate results from these tests to be useful related to general mechanisms of waste behaviour, but they are of limited use and cannot be applied to field problems with any confidence.

The deficiencies of using relatively small laboratory samples has led to the development of a limited number of large scale test facilities for assessing unprocessed wastes, although there are still problems associated with sample disturbance due to the waste having to be re-compacted in the test apparatus. Tests developed include a large shear box and a compression cell. Studies of certain properties have been undertaken using in situ waste. These include trial failures of artificially steepened slopes to obtain shear strength parameters, and compression experiments to obtain stiffness parameters for use in settlement calculations (Dixon and Jones, 1998).

2.2.2.10.2 Methods

Results from different kinds of laboratory tests are generally difficult to compare due to diverse boundary conditions. Amongst waste composition, physical properties like particle size, unit weight or water content, biological properties like organic content, age and degradation progress of the waste, the test setup and test execution (e.g. shear displacement, shear rate) are crucial parameters. As an example for the differences in assessing the shear strength with different methods, Landva and Clark (1990) comment that in triaxial compression tests strength is very high for fibrous material, but decreases considerably with decreasing fibrosity, whereas in direct shear parallel to the bedding

plane the strength is at its minimum. Furthermore they remark that shear strength is not only dependent on the type of waste material but also the mode of deformation and shear.

As for laboratory tests, the same problems have to be considered for field measurements. To relate results to other kinds of testing, the boundary condition should be known. Additionally, depth and waste-to-cover-material ratio should be understood to potentially ensure a correct interpretation of these values. In large-scale field tests a certain area of the landfill is examined by changing the boundary condition in such a way that a failure in the waste could occur. From the measured data the shear strength can be calculated. Standard penetration tests (SPT's), vane shear tests and cone penetrometer tests (CPT's) rank among the field tests. These tests do not seem very reliable regarding realistic results because an even smaller fraction of the heterogeneous waste is described than with laboratory tests. For an “in-between” in situ measurement an undisturbed specimen in its natural condition is examined. As stated in Gotteland *et al.* (1995) a waste specimen is excavated without disturbing its inner structure before building a large shear device around it to conduct a shear test. With this kind of test only the lateral areas of a specimen are disturbed, but again only a limited amount of waste is examined.

Most of the investigations about shear behaviour in the literature have been conducted in the laboratory, i.e. on a small scale. In these tests only a fraction of the waste body’s material can be used to assess shear strength. Therefore, the monitoring of excavated slopes or test embankments seems to be more reliable as proposed by Cowland *et al.* (1993), because a larger amount of the heterogeneous medium is considered. Additionally, an induced failure of landfill slope is interesting since the slip line corresponds to a shear process along a large area, so an average value of shear stress is deduced in case of high strength anisotropy. However, other uncertainties (Gilbert *et al.*, 1998) such as exact geometry of the slope, failure mechanism, and pore water pressure derive from this more global examination. Assumptions have to be made due to the fact that mostly the factors influencing shear behaviour cannot be sufficiently described. Comparing in-situ and laboratory tests, Singh and Murphy (1990) and Howland and Landva (1992) observed that strength parameters assessed in laboratory tests were higher than assessed in field measurements and back-calculations. A reason for the large range of values in literature is according to Kölsch (1996) due to using unsuitable methods of soil mechanics for the investigation of waste. In particular, he discusses problems arising from investigations of waste strength in triaxial tests and states that this test is not suitable for the description of waste’s bearing behaviour, because in these test arrangements the anisotropy of waste is not sufficiently recorded. As a consequence, Kölsch's further investigation of friction and tension are separated by investigating friction in direct shear tests and the tensile forces in a newly developed tension test.

Simple Shear Test

Kavazanjian *et al.* (1999) conducted several simple shear tests on MSW. The age of the tested waste specimens ranged from 15 to 39 years. From a visual classification, it was observed that the waste was predominantly composed of soil and soil-like material. The percentage of the waste composed of soil and soil-like material ranged between 10% and

99% of total refuse composition by weight with a mean value of approximately 81% by weight. Moisture content of the tested specimen ranged from 7.5% to 41.2% with a mean value of 23.5%. The samples were subject to both cyclic and monotonic loading. Cyclic loading to evaluate the dynamic properties of waste at intermediate to large cyclic shear strains was performed first. Thereafter, monotonic loading was used to develop stress-strain curves and the shear strength envelope. Each simple shear test included three to five stages (5-25 cycles of loading) of strain-controlled cyclic loading at double amplitude shear strains increased progressively from approximate 0.25 to 7%. It was observed that the hysteresis loops for cyclic loading at constant strain did not degrade with increasing cycles in any of the tests. In fact, for many of the tests, the shear modulus slightly increased with cyclic loading. This stiffening in shear modulus is likely due to the small volumetric compression that occurred in these drained tests. A significant volumetric compression only began to accumulate when the cyclic shear strain amplitude exceeded 1% and typically equalled 3% to 5% at the end of the test. The monotonic loading reached approximately a shear strain of 25%. To evaluate the shear strength the shear stress at a shear strain of 10% was selected as the appropriate criterion.

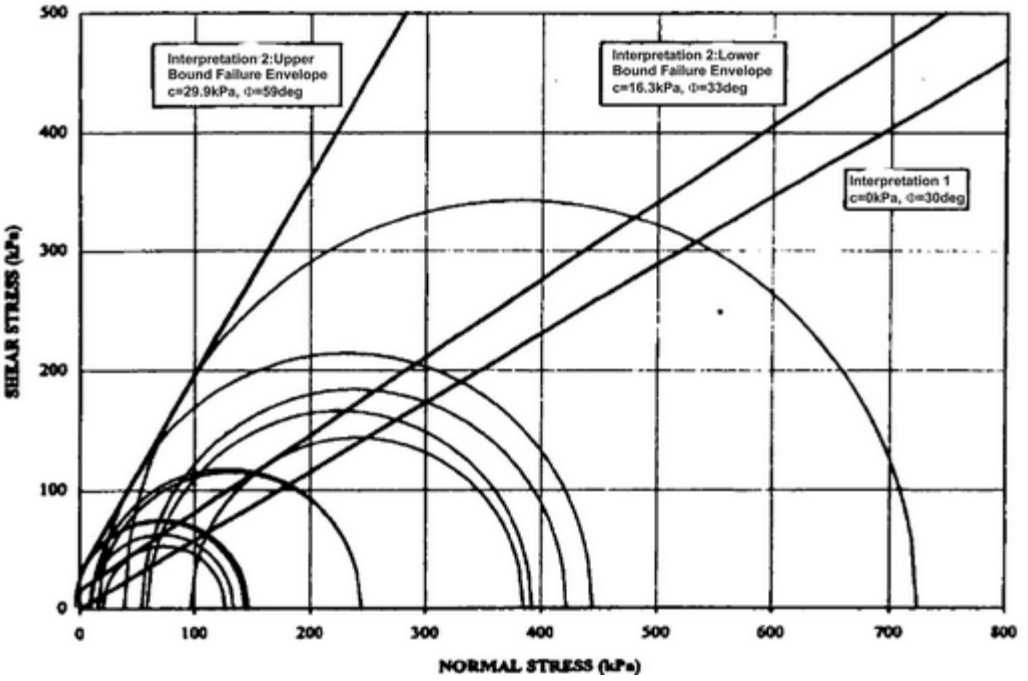

Figure 2-19 Simple shear strength envelopes (Kavazanjian *et al.,* 1999)

To interpret their results, Kavazanjian *et al.* (1999) use two different methods. The first approach is based on the assumption that the shear strength is anisotropic and shear failure occurs on a weak horizontal plane due to the structure of the waste (specimens were compacted in horizontal lifts with the long axis of the particles orientated horizontally). Normal stress was plotted against shear stress at 10% strain. The obtained strength envelope (total parameters) is characterised by zero cohesion and a friction angle of 30°, which is found to be consistent with, but slightly lower than, a direct shear strength envelope in comparison. The second method is based on the assumption that shear failure occurs on the plane within the test specimen with the largest principal stress

ratio (the plane of maximum obliquity). For this interpretation the coefficient of lateral earth pressure at rest, K_0 has to be known, which was estimated to be equal to 0.6. This interpretation method (total parameters) yields a lower bound strength envelope characterised by 16kPa cohesion and a friction angle of 33° (Figure 2-19). The third interpretation (second method) shows the upper bound of the envelope with c = 29.9kPa and ϕ = 59°. As a result, the monotonic loading indicated that the shear strength of the reconstituted specimens on planes not parallel to the placement orientation significantly exceeds shear strength on planes parallel to the waste orientation. Moreover, the stress-strain behaviour during the monotonic loading increments indicated that the shear stress-strain behaviour of the solid waste tested (OII Landfill) follows the same ductile, generally hyperbolic pattern that many soils conform to, contrary to previous data, which indicated strain hardening behaviour.

Pelkey *et al.* (2001) report simple shear tests conducted with a modified large direct shear apparatus. Spikes being attached to the base of the top plate are necessary to transfer the shear load to the sample. The shear force is applied to the lower box and this load is transferred to the sample by bracing the top loading plate with a proving ring, which records the shear load. After consolidation and removing the upper shear box, vertical lines are painted on the test samples to monitor shear strains. The sample is then wrapped in a thin clear plastic, and rectangular metal-retaining frames designed to prevent the sample from bulging during shear is installed. Then the horizontal shearing process is started with the top loading plate being kept horizontal during the test by adjusting the load in the two vertical jacks. The tests are strain-controlled and readings are taken at pre-determined shear strain increments, which were typically 1 to 2%, increasing to as much as 10 to 20% at large strains. For each strain increment, two shear load readings are obtained being firstly recorded upon achieving the desired strain and secondly between 0.5 to 2min, after adjustment of the vertical load to maintain the top plate horizontal. Typically, small shear strains (<0.5%) were noted during this time. The authors calculate the shear strain by dividing the horizontal displacement by the height, which is observed to be the height of the sample above the lower shear box. They assume this definition to be accurate for strains less than about 40% where the arctan (in radians) of the ratio of horizontal displacement to the height is approximately equal to the ratio itself. The shear parameters obtained in the simple shear test were a friction angle of 29.4° and zero cohesion.

Direct Shear Test

Landva and Clark (1990) conducted direct shear tests on MSW (compositions in Table 2-1). The horizontal dimensions of the apparatus used are 434*287mm. The vertical load and the shear load are both applied with hydraulic rams. In cases of wet samples, a rubber membrane is installed prior to sample preparation. A shear rate of about 1.5mm/min was used unless pore pressure measurements indicated that a lower rate was required to maintain drained conditions.

Table 2-1 Description/Classification of MSW samples (Pelkey *et al.*, 2001)

Location	Description/Classification	Water Content [%]	Unit Weight [kN/m^3]
Blackfoot, Calgary	High amount of wood with pieces of metal, crushed cans, some plastics in the form of garbage bags, pieces of hard plastics, odd piece of rubber, broken glass, silt and sand as soil matrix, occasional pebbles	32.5-52.7	13
Edmonton	Fresh shredded garbage, high amounts of plastic and textiles, paper, wood waste trace metal waste, trace glass, dirty gravel, damp to moist	119.0	15.6
Edmunston wood waste	High amount of wood waste (wood chips, fibres, pieces) some cardboard. Small amount of dirty gravel. 80% wood waste. Moist to very moist	126-316	9.1
Hantsport	Wood waste, plastic, metal wire, wool, trace glass, dirty gravel, moist to very moist	57-93	9.8
UNB Art. Refuse (8 years old)	High percentage of fines (12.5mm), some paper, rubber, wood	53.1	11.7

The waste materials in natural and dried conditions showed both a granular and fibrous character. It is concluded that in the direct shear box, it could be expected that friction parameters similar to granular soils would be obtained. As seen from Figure 2-20 and Figure 2-21, this is indeed the case, the friction angle ϕ' varying between 24° and 41°. These materials also have a cohesion parameter c of between zero and 23kPa. Due to a large amount of plastic sheets fresh shredded refuse exhibits a low friction angle of 24°. Fibrous and elongated particles have been found to tend to align themselves in shear direction.

Separate direct shear tests on plastic bags stacked horizontally and allowed to slide along the shear plane gave a friction angle of 9°, as shown in Figure 2-21. Ageing of refuse seems to reduce the shear strength, in this case from c' = 19kPa and ϕ' = 39° to c' = 16kPa and ϕ' = 33° for the old refuse. However, the test results clearly indicate that a large range of shear test parameter is possible in waste fill.

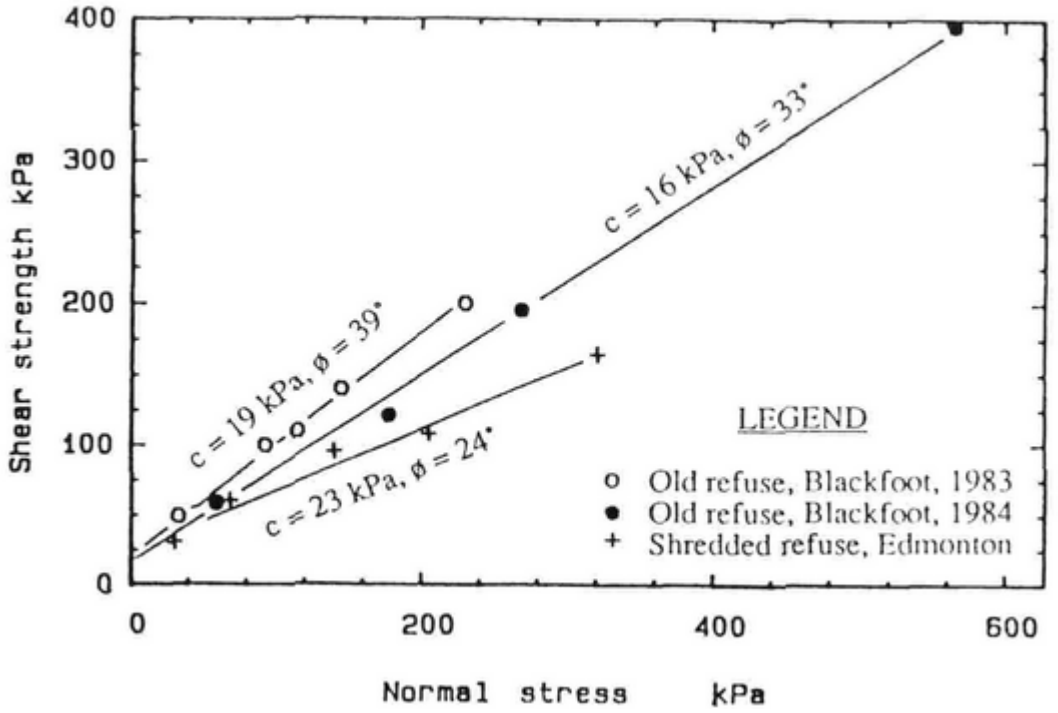

Figure 2-20 Large direct shear tests on aged waste and from fresh shredded waste (Landva and Clark, 1990)

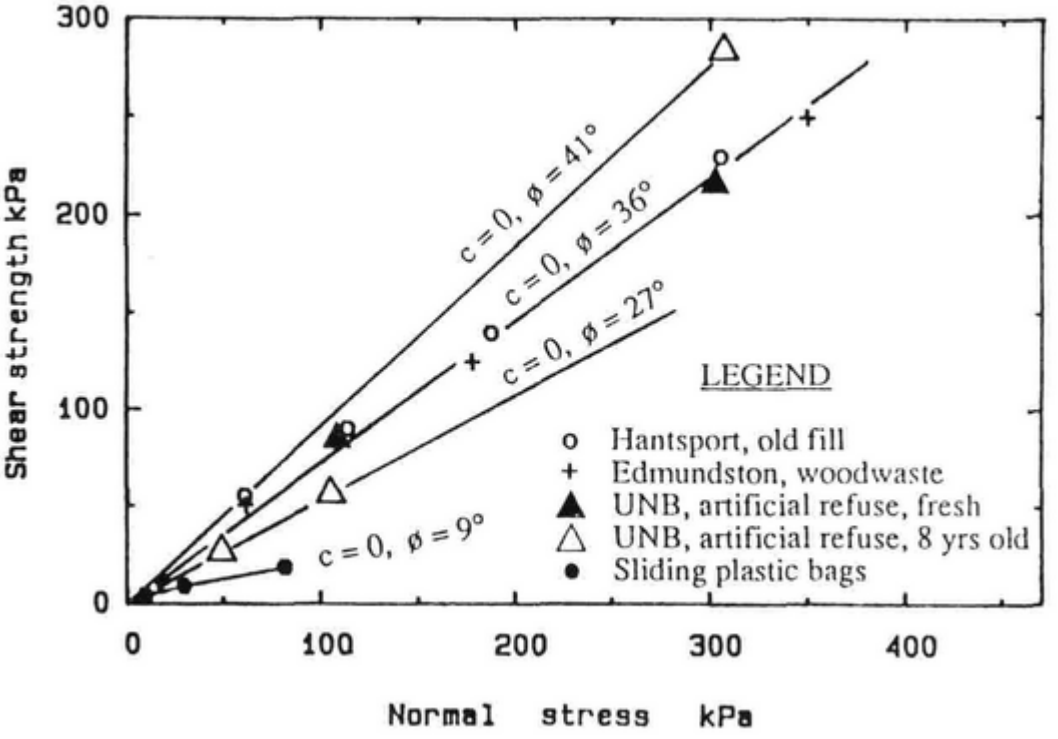

Figure 2-21 Large direct shear tests on samples from aged wood waste/refuse, on artificial waste samples and on plastic bags (Landva and Clark, 1990)

Siegel *et al.* (1990) determined direct shear strength in general accordance with ASTM D 3080-72 under consolidated drained conditions on 76 to 102mm high, 130mm diameter specimens of refuse. The compositional ranges are shown in Table 2-2. The miscellaneous category included canvas, rags, cloth, and decomposed material. Portions

classified as soil also included decomposed material that could not be readily separated from soil. On a volume basis, the percentages of soil were substantially less. Large amounts of paper, wood and rock were found in the samples with smaller amounts of metal, rubber and glass.

Table 2-2 Composition of the examined waste (Siegel *et al.,* 1990)

Miscel-laneous	Paper	Plastic/ rubber	Rock/ brick	Wood	Metal	Glass	Soil
[Mass-%]							
0-13	0-46	0-35	0-15	0-20	0-11	0-5	20-95

All test specimens show a peak or maximum shear strength correspondent to shear displacements substantially exceeding 10% of the sample diameter. In Figure 2-22 the authors show shear stress versus normal stress at 10% shear displacement for each specimen of the five samples tested. Individual test specimens of each sample were dissimilar in both composition and behaviour. Shear stress versus shear displacement curves is found to be grossly different. Given the refuse variability, deriving Mohr-Coulomb friction angles and cohesion intercepts samples is deemed inappropriate by the authors.

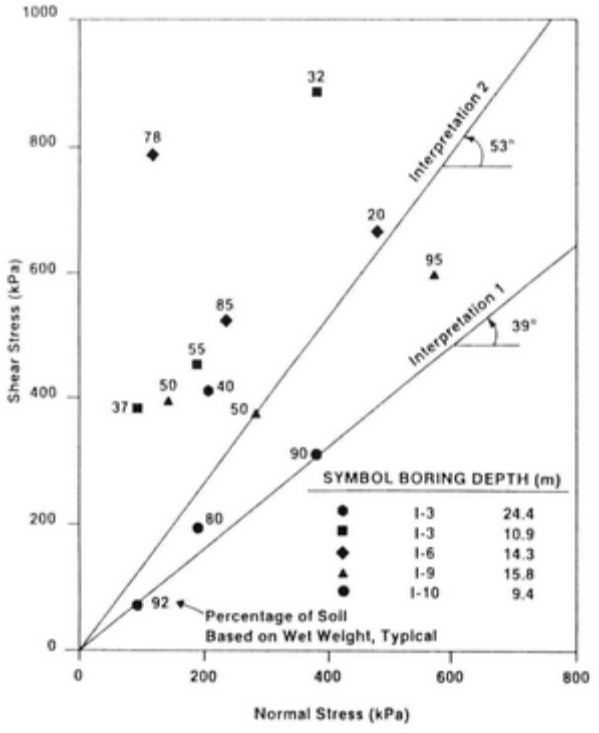

Figure 2-22 Direct shear test results (Siegel *et al.,* 1990)

Direct shear tests conducted on MSW by Siegel *et al.* (1990) produced results for the friction angle of 53° and this was significantly higher than previously published for refuse. For example, Landva and Clark (1990) performed several large-scale, 280 by 430mm; direct shear tests on refuse samples. In these tests friction angles were found to vary from 24 to 42°; cohesion varied from 16 to 23kPa. They interpret these results in two different ways (Figure 2-22). One interpretation of the lower bound considers all test specimens, and the other neglects specimens that contained relatively large soil percentages. In both interpretations they simplistically assume no cohesion.

Gotteland *et al.* (1995) carried out drained direct shear tests on re-compacted and undisturbed samples of MSW. For the tests on re-compacted waste, sample material was placed into the shear box and compacted. As the authors observed a very compressible character of the material, it was necessary to compress the material to obtain a significant thickness of material for shearing. The undisturbed (or rather less re-compacted) samples were excavated to the approximate size of the apparatus (1*1*0.7m). The authors regard this type of test as being difficult to perform and in addition, it needs an interminable preparation of the sample. At the beginning of the test procedure a confining pressure is quickly applied. After obtaining the confining stress the horizontal shear force is applied by means of hydraulic jacks at a constant rate. Pressure build-up and lateral displacement are measured during the test. The authors remark a good correlation between the re-compacted and undisturbed tests, especially for a normal stress of σ = 48 kPa. Up to a lateral displacement of 35% they could not measure a peak value . On this account, the authors confirm other results showing the same phenomenon of large strain without distinct failure. By assuming the limiting criterion of failure at a strain of 20% (displacement u = 0.20m) mentioned by Oweis & Khera (1990) Gotteland *et al*. (1995) report values of c' (0-20kPa) and ϕ' (38-46°) for use in stability calculations (Figure 2-23). The observed high values correspond to those already mentioned by Cowland *et al.* (1993). For the authors it appears more realistic to consider the decreasing shear area for calculating the shear stresses. This correction for the shear stress is defined as τ = F/A with $A = ((l_0-u)/l_0) * A_0$ taking into account the large strains obtained.

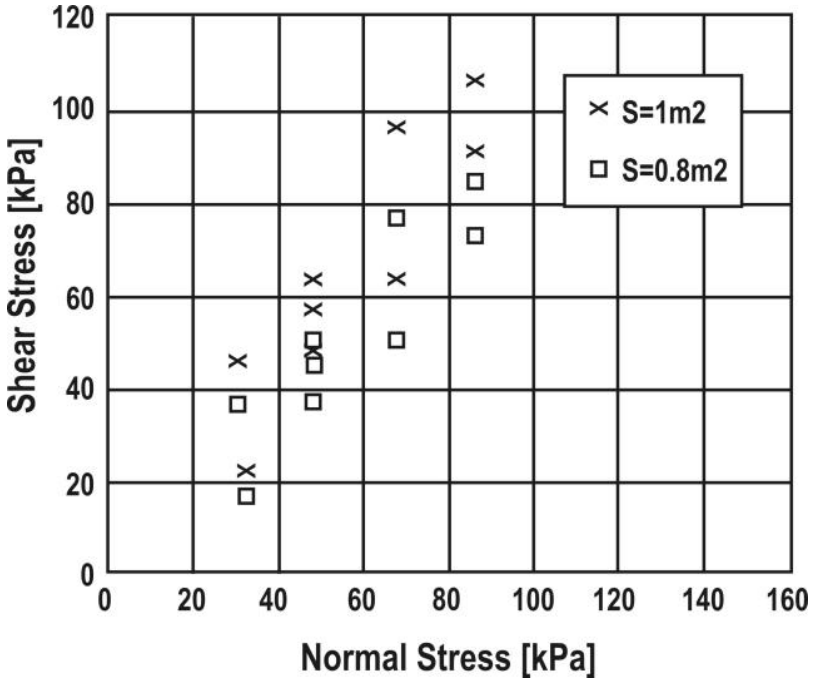

Figure 2-23 Mobilised values for c' and ϕ' at a strain of 20% (Gotteland *et al.,* 1995)

Thomas *et al.* (1999) conducted shear tests on waste from a depth of 6m in the same experimental device as Gotteland *et al.* (1995). The tests were conducted with a normal stress σ ($\leq$150kPa), with a manually controlled shear rate $\dot{u}$ of approximately 3mm/min. The tested compositions are shown and classified in Table 2-3.

Table 2-3 Waste composition and classification (Thomas *et al.,* 1999)

Test	In situ Unit weight	Paper	Plastic	Textiles	Wood	Metal	Inert	Fine
	[kN/m^3]	[mass-%]						
I.2	15.9	17.1	18.4	6.6	4.2	5.0	11.3	37.4
I.3	11.9	25.8	22.4	15.2	7.9	1.8	2.7	24.2
Mechanical Class		Non soil-like: I.2: 42.1% I.3: 63.4%			Soil-like: I.2: 57.9% I.3: 36.6%			

Figure 2-24 and 2–25 show the results of the shear tests. (1), (2a, b, c) and (3) correspond to three different sample locations; (a), (b), (c) correspond to the same waste sample tested three times after new compaction. The authors noticed a good repeatability of results for tests with identical conditions (tests 2-a and 2-c). Apparently, there is an influence of the initial unit weight (test 1 and 2 for σ = 50kPa). No strain softening is observed for lateral displacements up to 200mm. For soils, this behaviour is associated to materials exhibiting continuous decrease of volume during shear test. As the diagrams in Figure 2-24 show, it is consistent with the contraction ΔV increasing (with $\Delta V < 0$) when initial unit weight is decreasing. After selecting a shear displacement value (u) Thomas *et al*. (1999) report the points (σ, τ(u)) obtained in the Mohr plane (Figure 2-25). Using the assumption of the Mohr-Coulomb criterion, they determine cohesion and frictional angle: for instance for u = 100mm (u/l_0 = 10%), c' = 33kPa and ϕ' = 18.2°. These values were comparable to those quoted in literature (Cowland *et al.*, 1993; Jessberger *et al.*, 1995).

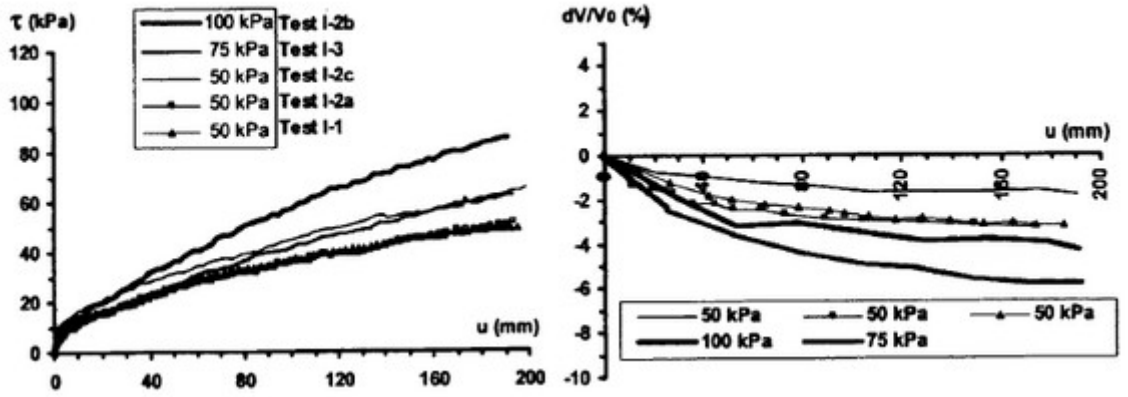

Figure 2-24 Shear stress and volumetric strain curves over horizontal displacement (Thomas *et al.,* 1999)

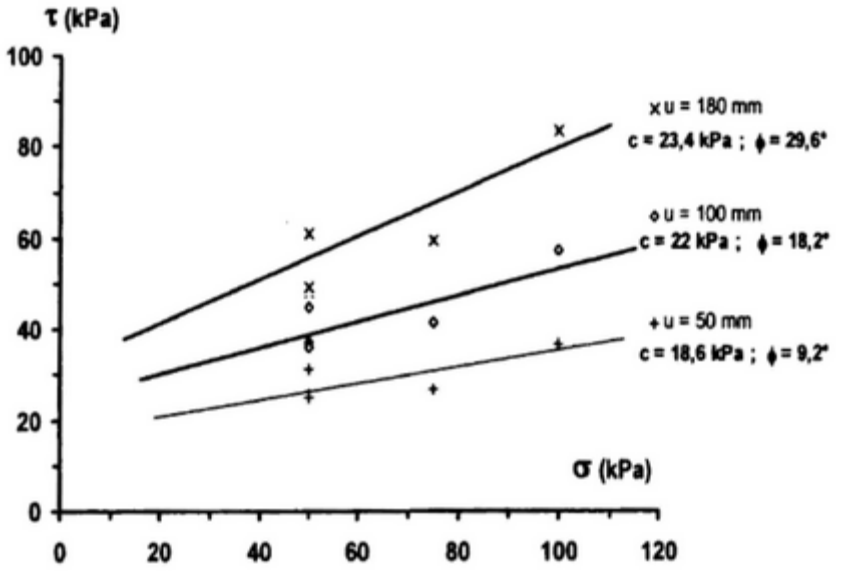

Figure 2-25 Mohr plane presentation (Thomas *et al.,* 1999)

Gotteland *et al.* (2000) conducted another series of tests in the large shear box. Despite the exceptional size of the box, the authors had to sort out various constituents that were of an incompatible size (batteries, metal bars, rolls of carpet, etc.) to prevent any form of disturbance during the test procedure, which comprises two stages. In the first stage the sample is prepared placed in the box and compacted. Preliminary consolidation is accomplished. The unit weight ($\gamma_{in\text{-}situ}$) is determined. Table 2-4 shows the analysed waste compositions.

The material was compacted in successive layers by applying a static load in order to achieve the in-situ unit weight $\gamma_{in\text{-}situ}$ for a sample thickness h_0 of about 0.65m. Then a vertical load of about 125kPa was applied in successive stages of ($\Delta\sigma$) lasting about 2-3 minutes to stabilise the settlement of the compacted waste. Afterwards the normal stress was reduced to the value σ appropriate for shearing. During shearing with a rate of 3mm/min, σ was kept constant. Mentioning the limited range of movement of the moveable part of shear box (150-200mm), the authors necessarily propose to unload in order to continue shearing as far as the final distance (u) required. In a last step the box is emptied and the strained area of the sample is examined.

Again, no shear strength peak value is observed; therefore, the (drained) shear parameters friction angle and cohesion are correlated with the displacement u. The wide scatter of the values obtained by correlating them with the tangential displacement (u/l_0 = 5% and 10%) under the assumption of Coulomb's law is shown in Figure 2-26. As result, Gotteland *et al.* (2000) note that the mobilised friction angle changes linearly as a function of increasing displacement, but there is a deviation of $\pm 5°$ in relation to a mean value, for a fixed displacement u. The cohesion values are very scattered, ranging from 10 to 50kPa, with the mean being situated around 30 kPa; this does not change with the strain level. The values obtained in these tests are compared and integrated in Figure 2-27 in the form of a diagram correlating cohesion and friction angles.

Table 2-4 Waste composition (Gotteland *et al.,* 2000)

Mechanical Classification		Site 1 (Torcy, NHIW)						Site 2 (Montech, DW)					
		Test T-I-2		Test T-I-3		Series T-II		Test M-I-2		Test M-I-3			
	$\gamma_{In\text{-}situ}$	15.9kN/m^3		11.9kN/m^3		10.3kN/m^3		13.2kN/m^3		13.2kN/m^3			
	Volume	2.9m^3		2.0m^3		2.35m^3		3.9m^3		3.9m^3			
	Mass	76kg		66kg		60kg		24.2kg		93kg			
	Components					[mass-%]							
Deformable materials	Plastic	18.4		22.4		11.3		14.9		25.1			
	Cardboard	10.5	42.1	*17.0*	63.4	**5.7**	23.0	**21.5**	37.6	**15.5**	41.7		
	Paper	6.6		25.8									
	Textiles	6.6		15.2		6.0		1.2		1.1			
Inert industrial material	Inert material	11.3		2.7		7.0		5.6		4.9			
	Scrap	5.0	57.9	1.8	36.6	2.6	77.0	7.4	62.4	5.6	58.3		
	Wood	4.2		7.9		3.3		10.5		7.1			
	Fines	37.4		24.2		64.0		38.9		40.8			

Bold values were not available
Italic value is supposed to be erratic

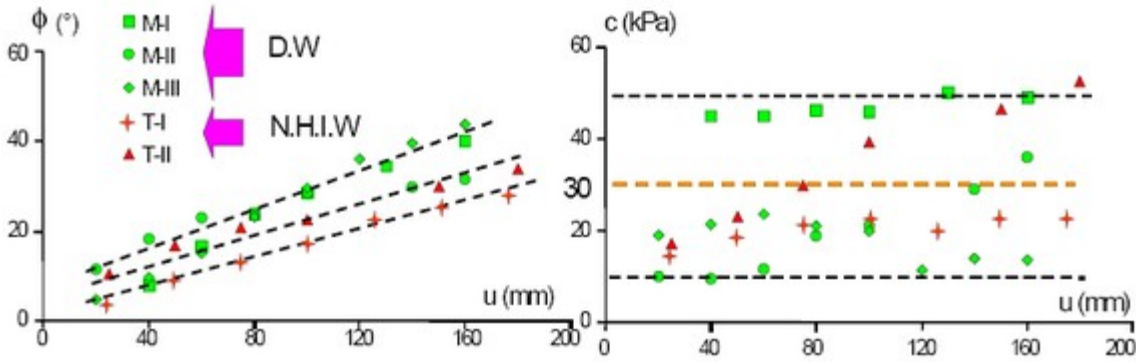

Figure 2-26 Drained shear parameters as a function of tangential displacement u (Gotteland *et al.,* 2000)

From the results of their shear tests the authors draw the following conclusions. The shear stress τ increases as a function of the normal stress applied to the material. No peak or plateau value is obtained for τ. Even with a large relative displacement (≥20%) a failure did not occur. The weight per unit volume variation curves show that the waste material, both NHIW (non-hazardous industrial waste) and DW (domestic waste) always has contracting-type behaviour. Using the same procedure and similar test conditions (shear

rate, weight per volume of the sample γ_0, normal stress, etc.) in tests the authors observed good repeatability.

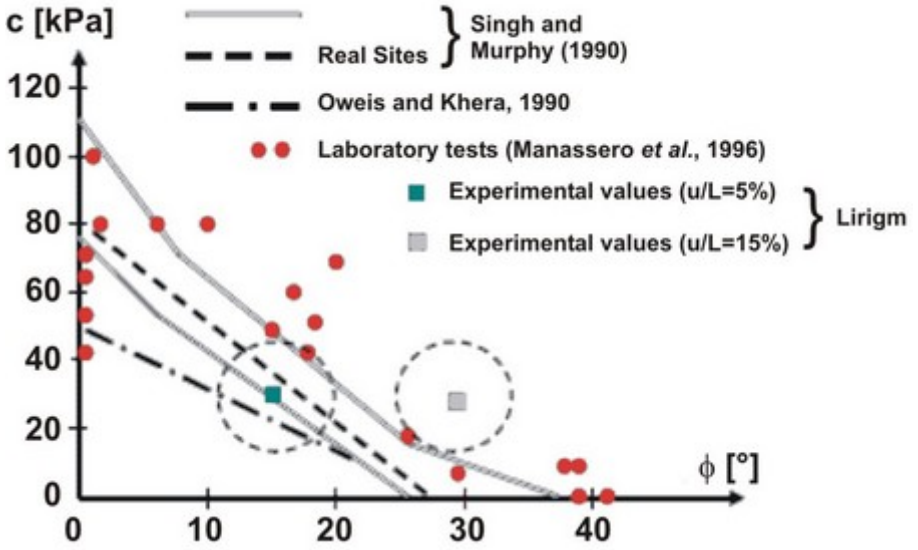

Figure 2-27 Comparison of experimental values for c and ϕ with those given in the literature (modified by Gotteland *et al.,* 2000)

Jones *et al.* (1997) report a series of direct shear tests having been carried out on a 300*300mm apparatus. Disturbed bulk samples of waste (Table 2-5) around three months old with very little degradation were placed into the shear apparatus, with individual components aligned horizontally. Large components, which would not physically fit into the shear apparatus, were removed. Normal stresses of between 50kPa and 400kPa were applied and the waste was consolidated overnight. A shearing rate of 0.5mm/min was used for the series of the tests. Although the mobilised shear stress was increasing, no peak shear strength was observed for maximum displacements of 30mm. Pointing out the difficulty of assessing shear strength in terms of conventional Mohr-Coulomb parameter without having a peak, the maximum shear stress mobilised in the tests are used. The results are shown in Figure 2-28. Values from literature are shown by the shaded portion of the graph, onto which the results of the laboratory testing have been plotted. The scatter of results falls within the central portion of the envelope with the mean line from the laboratory tests giving shear strength parameters of c' = 10.5kPa, ϕ' = 31°.

Table 2-5 Average waste composition (Jones *et al.,* 1997)

Paper	Plastics	Textiles	Demolition rubble	Glass	Garden	Soils	Metals	Kitchen	Animal
[volume-%]									
38	18	17	6	6	5	4	3	2	1

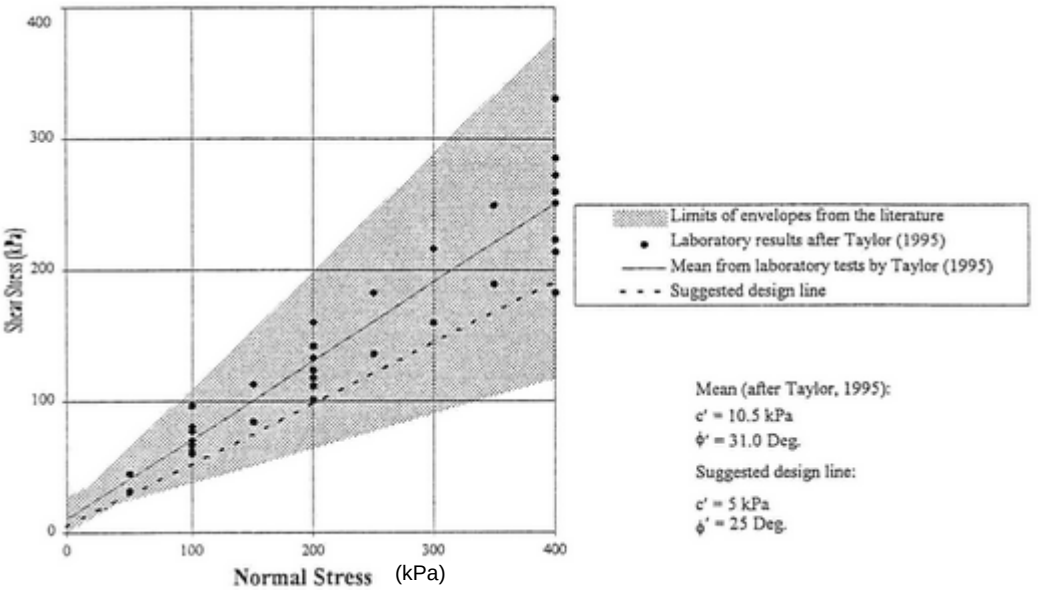

Figure 2-28 Waste shear strength envelopes (Jones *et al.*, 1997)

Figure 2-29 shows an assessment of mobilised friction angles, which was carried out after having observed that no peak was obtained during shearing. The mobilised friction angle increases from around 7° at a displacement of 5mm, to between 27° and 30° at a displacement of 30mm. Having observed this, the authors state that for a failure entirely within the waste mass, strain compatibility would not be an issue and the full shear strength of the waste could be used. But due to the inherent heterogeneity of the waste, a conservative best estimate would be required for design purposes and a suggested design line corresponding to c' = 10kPa and ϕ' = 25° is shown on Figure 2-28.

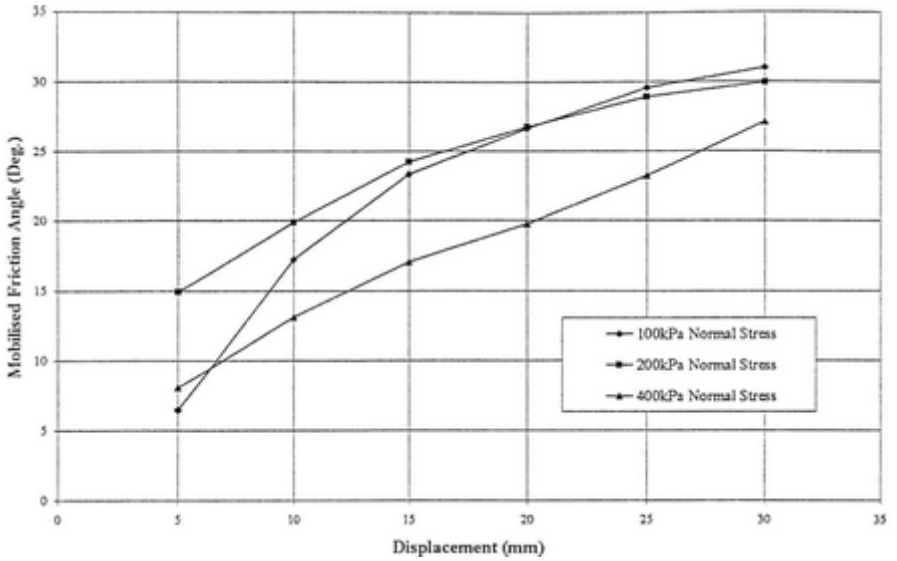

Figure 2-29 Variation of mobilised friction angles with displacement at different normal stresses (Jones *et al.,* 1997)

Manassero *et al.* (1997) examined typical stress-strain curves obtained from various authors. Every specimen exhibited continued strength gain at well excess of 10% strain, but none of the specimen tests reached peak strength.

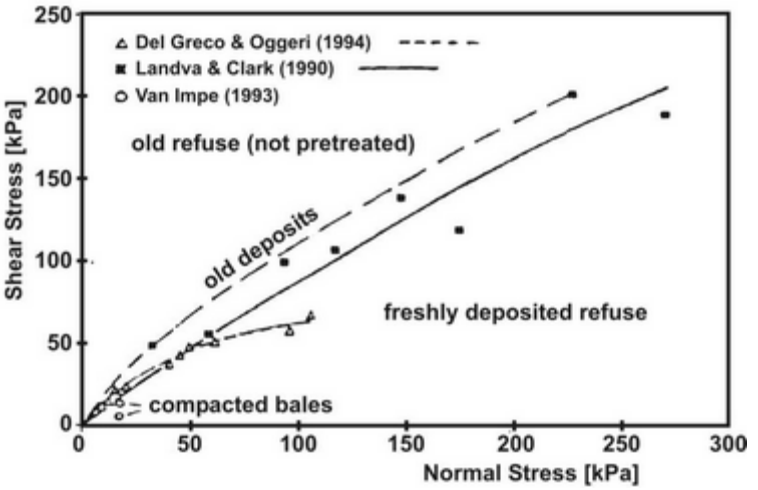

Figure 2-30 τ-σ relationship for MSW (Manassero *et al.,* 1997)

In this case the authors apply the allowable strain concept, where the values of c and ϕ are deduced from the measured data at usually 10% and 15% strain. The striking discrepancy in the results is mainly due to the stress level and more importantly the type and form of waste and its pre-treatment. The variation of the shear stress with normal stress at about 20% strain is shown in Figure 2-30. For the authors it is interesting to note that some aspects are similar to the behaviour of conventional material such as soil. In the case of compacted waste bales, higher values of friction angle are attained at low normal stress levels, whereas the fibres reinforcement is revealed under higher vertical stresses. Mainly because of the large amount of plastic materials, as the authors reckon, the shear angles have a low value. Furthermore, in the case of old refuse, higher friction angles and intercept cohesion are obtained due to the mixed matrix of the material (soil - waste) and also due to the range of stress level.

The setup used for determination of shear strength between two waste bales in the study by Van Impe and Bouazza (1998) is shown in Figure 2-31. The horizontal load is applied by means of 2*2 hydraulic jacks, which are attached to a large concrete block to support the reaction. The normal load is applied by two large concrete blocks (maximum vertical stress of 18kN/m^2). The compacted municipal inorganic solid waste bales were 0.80m high, 1.30m long and 1.00m wide and contained large amounts of plastic materials. After applying the normal stress, the sample was left for half an hour to come to equilibrium before the shearing process took place.

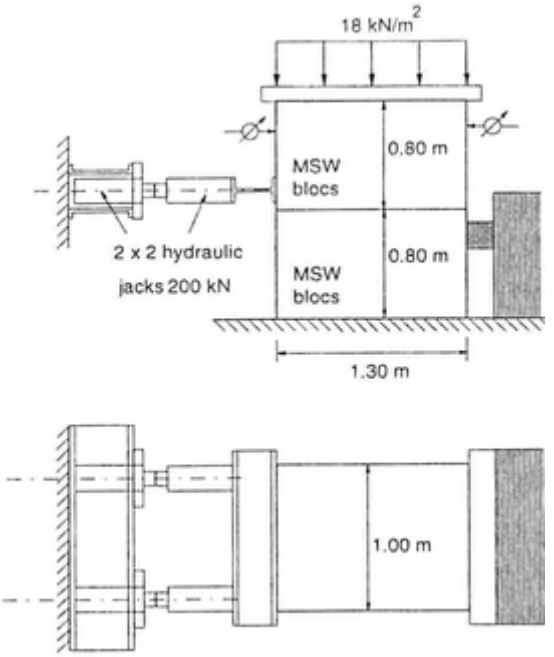

Figure 2-31 Large shear test setup of MSW bales (Van Impe and Bouazza, 1998)

Typical stress-strain curves are shown in Figure 2-32. The authors observed that the stress strain relationship showed no peak data unlike tests with soil materials. They carry on that as matter of fact domestic waste material can sustain very large shear strains without reaching failure. It is not agreed that failure parameters based on the Mohr-Coulomb theory describe satisfactorily the "failure condition". Therefore, they would be more reliably defined on the basis of allowable strain. As an explanation they demonstrate the effect of deformation variation on the friction angle, ϕ, in Figure 2-32, where the application of the allowable strain concept apparently gives values of ϕ varying from 19° for deformation of 5% to 38° for a deformation of 10%. They conclude that whenever shear testing is carried out on municipal solid waste, care should be taken to analyse the results on the basis of allowable strain rather than on the more traditional Mohr-Coulomb theory.

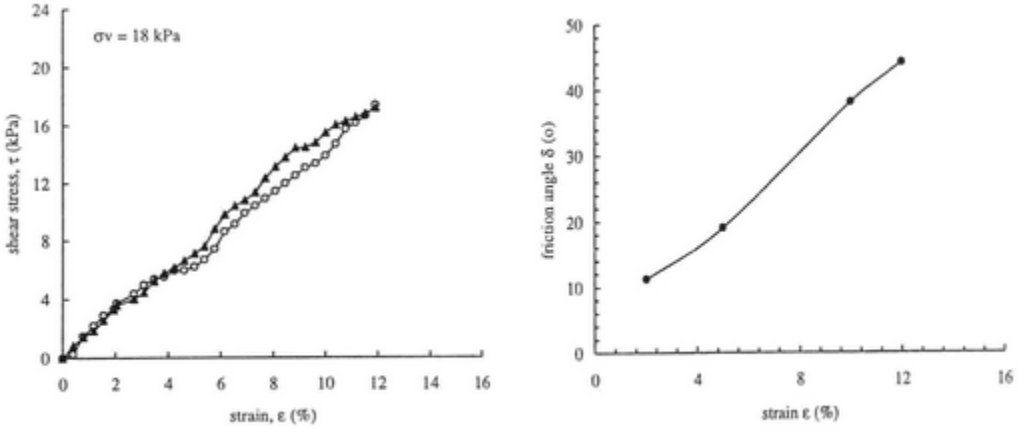

Figure 2-32 Typical stress-strain relationship and variation of the friction angle obtained from large shear test (Van Impe and Bouazza, 1998)

Figure 2-33 shows the stress-strain relationship of shredded rubber under different normal stress levels from Ghaly (2000). While no peak is developed under low normal stress level, a clear peak is obtained at higher normal stress. Ghaly (2000) believes that higher normal stress levels would alter the stress-strain relationship shown in Figure 2-32.

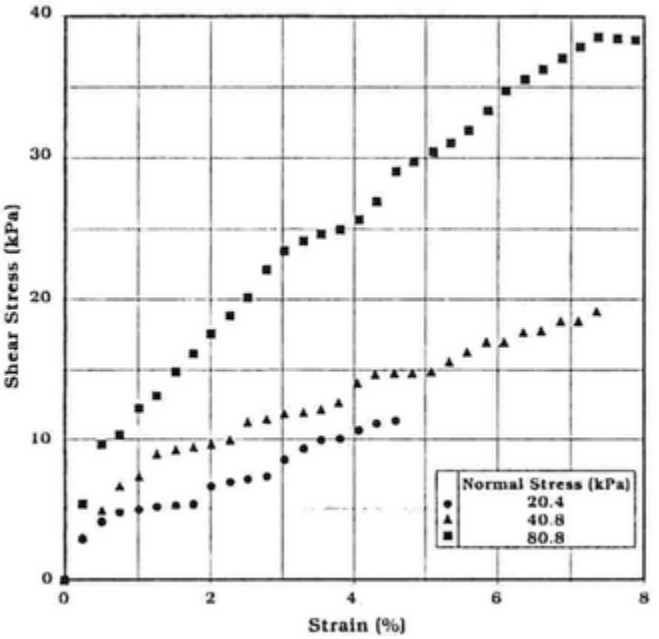

Figure 2-33 Stress-strain relationship of rubber chips (Ghaly, 2000)

Van Impe and Bouazza (2000) do not agree with higher normal stress having effect on the shear curve for MSW (i.e. the curve would have a distinct peak at high normal stress). They quote results obtained on municipal solid wastes at confining pressure of up to 300kPa pointing out the fact that the waste can undergo large deformations without mobilising the maximum shear stress. However, shear strength parameters would indeed depend on the normal stress. They request a better comparison to show results obtained on plastic chips or shredded rubber alone because in the case of a conventional soil randomly reinforced by plastic inclusions, the stress level determines usually the type of failure (frictional or non-frictional).

Pelkey *et al.* (2001) use data from Landva and Clark (1990) and Landva *et al.* (2000). While in those publications cohesion and friction angle were reported for mobilised peak shear stress, Pelkey *et al.* (2001) present the data as mobilised cohesion and/or mobilised angle of internal friction as a function of shear displacement. In addition, new data from the direct shear testing performed on samples of paper, still a major constituent of municipal solid waste, are presented as well. The shear box used is 450mm long by 305mm wide. The lower and upper boxes are each 300mm deep. The upper box is fixed in its position, and the lower box is pushed on specially designed roller bearings using a hydraulic jack. Two hydraulic jacks are used to apply normal load. The samples of waste were first consolidated under a normal and subsequently sheared at a rate of 1.5mm/min. Other details are provided by Landva and Clark (1990). The tests on paper were firstly performed by stacking the sheets horizontally in the box and secondly on shredded computer paper samples placed in the shear box consolidated under a normal load similar to the waste samples. The data for samples (Blackfoot and Hantsport) showing that large shear displacements are necessary to mobilise peak shear stress are found to be representative for MSW. In comparison, shredded fresh refuse (Edmonton) mobilised peak shear stresses at shear displacements, which were 30 to 50% of those required for samples with untreated MSW. Soaking of a waste sample in leachate did not affect the shear displacement required to mobilise maximum shear, as evidenced (Blackfoot). The test on horizontally stacked papers showed very small shear displacements for mobilising maximum shear stress (<3mm for laminated paper and <15mm for computer paper). The samples of wet shredded paper reached maximum shear stress at displacements that are comparable to the samples of municipal solid waste. From these data the authors conclude possible shear displacement compatibility problems within a landfill if there are zones where dry sheets of paper occur in a concentrated fashion.

In Figure 2-34 the bounds to the shear strengths using the peak shear stress values are displayed. For comparison purposes, the authors present the estimated bounds to the strength parameters at 25mm shear displacement in Figure 2-35. From these figures the dependence of mobilised shear strength parameters on shear displacement seems to be evident. It is pointed out that the data presented in Figure 2-34 and Figure 2-35 is for waste samples with different age histories and as such the bounds on shear strength reflect the effects of both the composition and the age. But they constrain this comment that, however, the data from the present testing is not adequate to quantify the effect of age separately.

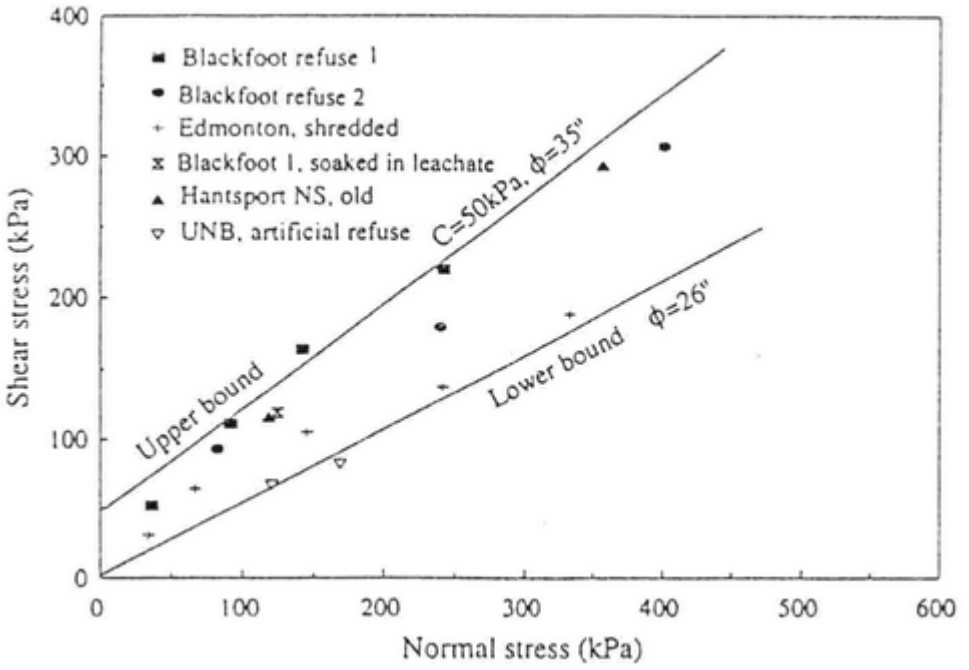

Figure 2-34 Shear strength parameters for peak shear strain (Pelkey *et al.,* 2001)

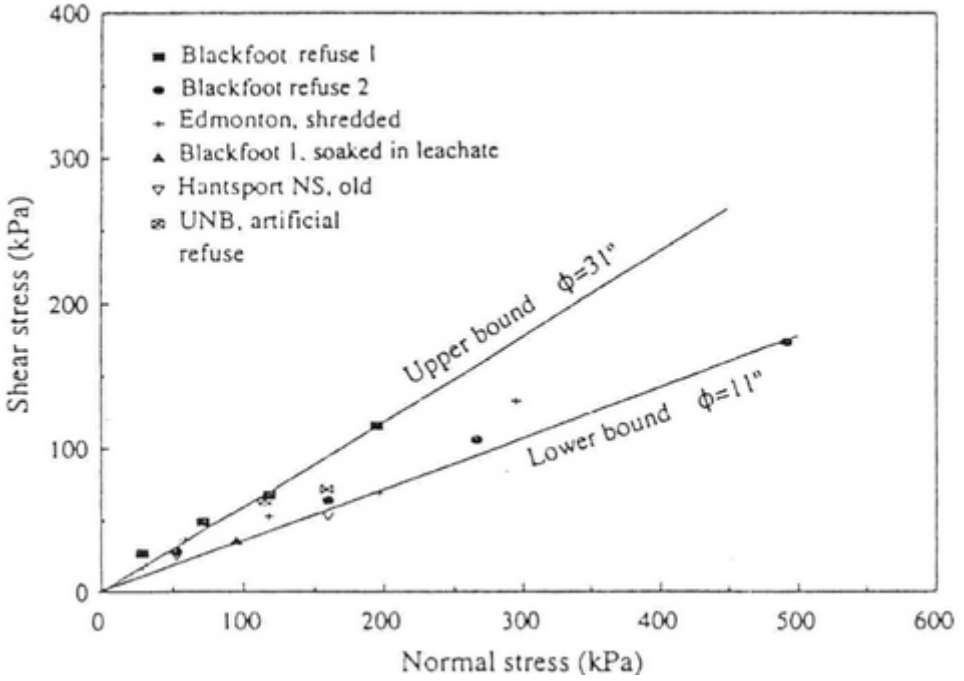

Figure 2-35 Shear strength parameters at 25mm displacement (Pelkey *et al.,* 2001)

Van Impe and Bouazza (1998) is quoted, who reported the effect of age of refuse on its strength properties indicating that old refuse samples had higher shear strength compared to freshly deposited refuse samples. But more data is needed to confirm or contradict this trend reported in literature. Pelkey *et al.* (2001) present data from Jones *et al.* (1997) and a range of mobilised friction angles from their own study in Figure 2-36 as mobilised friction angle versus shear displacement. The dependence of the shear strength of municipal waste on the magnitude of normal stress as well as displacements is clearly visible. The dependence of normal stress results from the curved nature of the Mohr

failure envelope, which is similar to shear strength of granular soils where reduction in mobilised angle of friction with increasing normal stress is well documented.

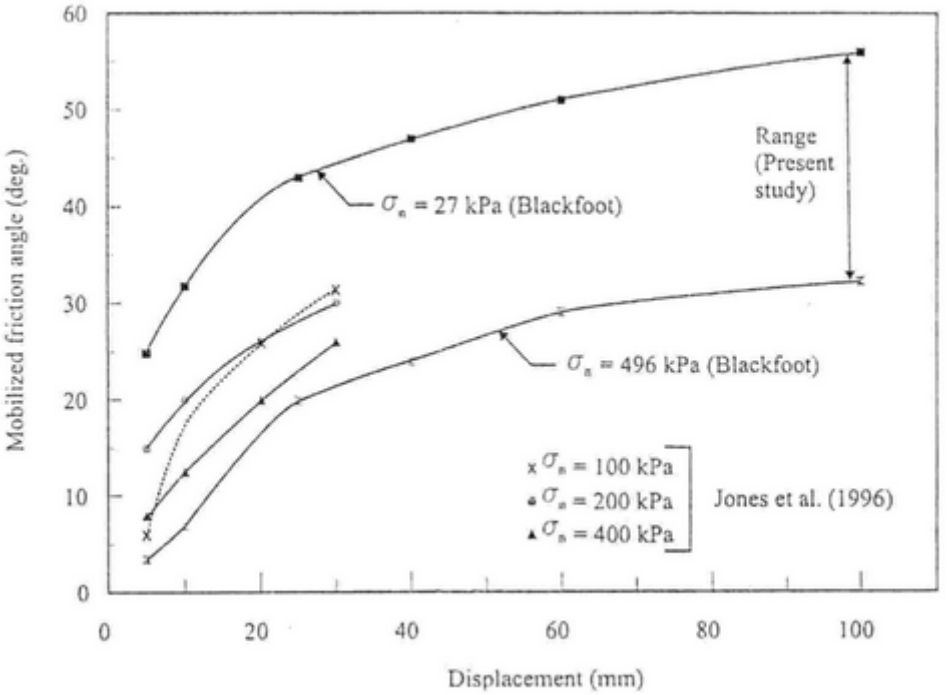

Figure 2-36 Mobilised friction angle (Pelkey *et al.,* 2001)

Scheelhaase *et al.* (2001) conducted tests in a shear device with an area of 300*300mm, a sample height of 200mm, and a maximum displacement of 100mm. To prevent possible interference they removed all solid constituents >60mm. Table 2-6 gives an overview of the test series. Three shear tests on mechanically-biologically pre-treated waste with differing stress rates of 75, 125 and 250kN/m^2 were carried out. The shearing velocity was 0.15mm/min. The material LBG-16w was rotted over a period of 16 weeks, the material MH2-36w over a period of 36 weeks. The MBP materials had soil characteristic; they resembled a bio-compost containing impurities and were largely biologically stabilised. Further details of the examined material are shown in Table 2-7.

Table 2-6 Shear test series (Scheelhaase *et al.,* 2001)

Test series	Designation	LBG-16w		MH2-36w	
		ρ_d [Mg/m^3]	w [%$_{moist}$]	ρ_d [Mg/m^3]	w [%$_{moist}$]
1	Original	0.70	36	0.85	37
2	Dry	0.70	20	0.85	20
3	Very humid[2]	0.70	45	-	-

[2] Moisture content at maximum water-retaining capacity

Table 2-7 Investigation results and other material specific parameters of MBP (Scheelhaase *et al.,* 2001)

Investigation/Parameter	Unit	LBG-16w	MH2-36w
Grain size distribution			
Maximum grain size	[mm]	100	60
Fine grain percentage	[mass-%]	13.2	39.1
Percentage regulation	[-]	13.3	39.1
Curvature	[-]	0.9	0.3
Other solid analysis			
Moisture content	[$\%_{moist}$]	36.0	37.0
Loss on ignition	[$\%_{dry}$]	31.43	22.31
Grain density	[g/cm^3]	2.10	2.30
Respiratory coefficient AT_4	[mgO_2/g_{dry}*4d]	1.81	1.53
Gas formation GB_{21}	[Nl/kg_{dry}*21d]	2.15	2.92

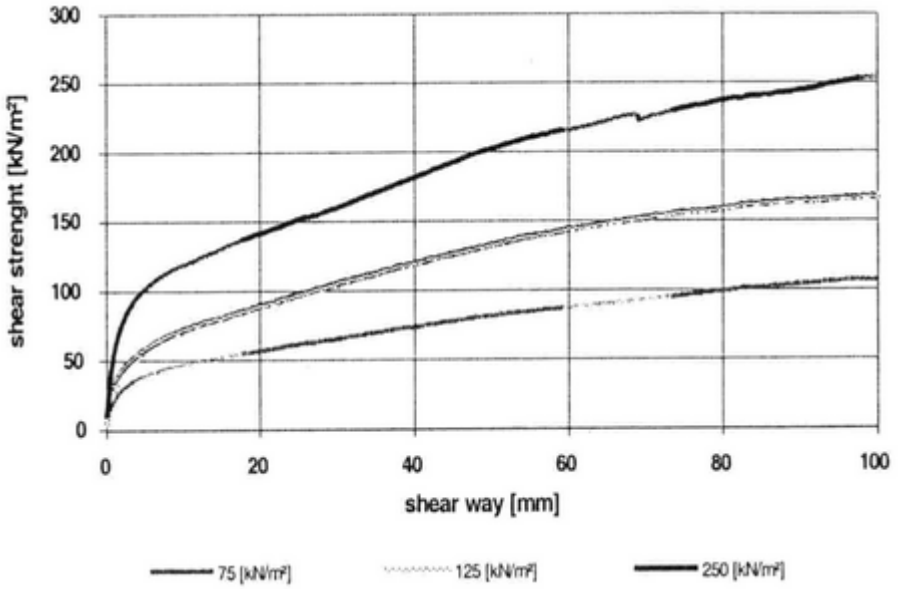

Figure 2-37 Example: shear tests LBG-16w (w = 45%FS; Scheelhaase *et al.,* 2001)

Examining the shear curves in Figure 2-37, a limiting state is not observed. While a peak strength is observed for the material MH2-36w, the mobilisation of the shear strength of the material LBG-16w was not fully mobilised after maximum displacement. No relevant difference concerning the development and the rate of the shear parameters is observed between dry and originally wet material. As closing remark the authors state that the shear parameter of MBP MSW shows higher values and thus higher landfill stability than untreated waste.

Del Greco and Oggeri (1997) performed a study on the subject of shear strength on MSW. They point out the variety of the tests, which have been carried out, partly with unusual equipment. This is accredited to the typology of waste as a material. They describe waste as a loose, and in its composition heterogeneous, but not a granular media. The fact that various elements have different mechanical behaviour and a considerable size dictates a large sample size and equipment that should allow large displacements. Moreover the influence of the water content is pointed out. Particles being able to absorb water are softened. Considering the effective stress concept, increasing water content leads to a decreasing strength.

Triaxial tests

Siegel *et al.* (1990) report triaxial shear strength tests on anisotropically consolidated specimens of 2-year-old milled domestic refuse. The effective friction angle was 44° and zero cohesion. Singh and Murphy (1990) report triaxial testing of MSW performed on "undisturbed" Shelby tube samples. A peak value is not observed, even after undergoing strains greater than 30%, the stress continued to increase. They conducted load tests in California, where a surcharged landfill slope underwent in fact large deformations but no failure plane was apparent. Based on this and other information, Singh and Murphy conclude that a Mohr-Coulomb characterisation of MSW strength might be inappropriate and that slope failure (though the waste material) might not be a critical aspect of landfill design.

Gabr and Valero (1995) used undrained unconsolidated and consolidated undrained triaxial tests and direct shear tests to determine shear strength. The unit weight of the specimens used for consolidated undrained triaxial compression tests varied from 7.4 to 8.2kN/m^3. With the Mohr-Coulomb criterion and the assumption that $\phi = 0$, the cohesion values decreased as a function of the water content (from 100kPa at w = 55% to 10kPa at w = 72%. The water content was measured directly after shearing of the consolidated and undrained tests. They also used data from four consolidated undrained triaxial compression tests with pore water pressure measurements to evaluate apparent effective strength parameters. The tests were conducted on samples with a dry unit weight range of 7.4 to 7.5kN/m^3. Apparent average effective strength parameters evaluated from these tests are a friction angle, ϕ', of 34° and a cohesion, c', of 16.8 kPa. These strength parameters were evaluated at 20% strain level.

Table 2-8 Waste composition at 40% water content (Grisolia *et al.* 1995)

Organic matter	Paper	Plastic	Cloth and wood	Rubble d<20mm	Rubble d>20mm
[mass-%]	[mass-%]	[mass-%]	[mass-%]	[mass-%]	[mass-%]
22	32	8	6	12	20

Strength testing on waste (Table 2-8) was performed by Grisolia *et al.* (1995) using constant cell pressures of 50kPa, 100kPa and 300kPa, which was previously applied for 24 hours. They found the results of the tests being qualitatively in agreement with those obtained from similar tests on other types of waste. Despite the high loads applied and the induced deformation of about 35-45%, failure conditions of the material were never reached. The stress-strain curves display the same trend: the initial section of the curves is practically a straight line and represents the behaviour of the material during a "preliminary phase" characterised by high compressibility. After a transition period, the curve is characterised by a final section ("second phase"), which is also roughly a straight line. The initial consolidation to which the samples were subjected at the beginning has a visible effect on the "preliminary phase" of the process. As the consolidation pressure increases, the initial deformability decreases and the transition towards the "second phase" takes place through smaller deformations. In practical cases, this would mean that attention must be paid to the possible deformations rather than the possibility that failure might actually be reached. In order to apply this condition in practice, the production of excessive deformations has to be prevented. By setting the obtained stress values as limit values, it is possible for the authors to obtain virtual shear stress parameters (apparent cohesion and friction angle) versus measured deformations. They present the mechanical behaviour of waste by means of "friction" and "cohesion" variables in dependence of the variability of the deformations. Similar schematisations have been suggested by other researchers like Jessberger and Kockel (1993) and Cowland *et al.* (1993). Friction angles varied between $\Phi' = 15°\text{-}25°$ for deformation of around 10%-15% of the initial height of the sample and progressively increasing values in the range of 30°-40° for deformations between 20%-35%. Apparent cohesion strongly varied with the deformation degree: it is virtually negligible (c' = 2-3kPa) in the range of deformations up to 10% of the initial sample height, but increases rapidly up to around 10kPa at 10-20% of deformation. They additionally found that in the field of large deformations ($\Delta h/h$ > 30%-35%) slight increases could produce a marked cohesion gain, up to 50kPa for $\Delta h/h$ of the order of 35%. Figure 2-38 presents mobilised friction angle and cohesion.

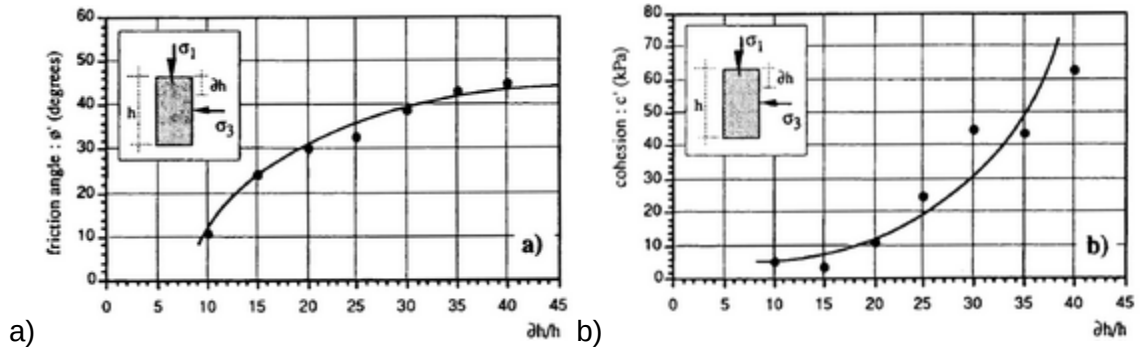

Figure 2-38 Triaxial Test: (a) ϕ and (b) c vs. strain (Grisolia *et al.,* 1995)

The results they obtained confirm data on the stability of shear excavation faces and the corresponding large deformations observed. However, the authors advise against applying the laboratory results directly to practical cases because the deformability of the sample at the laboratory scale cannot be easily related to the actual deformations of the in

situ materials. Grisolia *et al*. (1995) conclude with some remarks. The mechanical characterisation of waste is made exceptionally complex by its composition, by experimental difficulties and above all by the great deformations that the material undergoes when stressed. The shear strength parameters attributed in the literature and obtained by adapting and interpreting the results typically obtained in geotechnical procedures are to be interpreted and adopted with great caution. The mechanical behaviour of waste is strongly dependent on the stress level and on the high deformation induced by the stress level. The mechanical strength tests carried out in the triaxial cell on large reconstructed waste samples proved to be exceptionally useful in highlighting this behaviour. The tests also made it possible to correlate the mechanical behaviour with the unit deformation undergone by the samples. This makes it possible to use the limit geotechnical equilibrium methods in analysing the stability of a landfill by correlating the limit stress levels with a fixed deformation value. In any case, the results obtained cannot be easily transferred from one situation to another. The tests carried out show that the original composition of the waste unquestionably influences the final results. Consequently, Grisolia *et al.* (1995) suggest to develop criteria to technically classify the waste on the basis of simple standardised analyses of the initial composition, pre-treatment processes and ways in which the waste is dumped in the landfill.

Jessberger *et al.* (1995) conducted laboratory tests using untreated waste samples of different ages (1 to 20 years old) and composition in a device with a diameter of 300mm. As result, they not observed a failure but a limit state at very large strains ε_1 of about 40 to 50%. Therefore, the mobilised shear parameter of the three untreated wastes of different age are illustrated dependent of vertical strain ε_1 in Figure 2-39. They could not observe an age depending effect, e.g. a decreasing friction angle. Tests on original and model waste with different fibre content showed similar characteristics. Again, a limit state could only be defined for very large deformations, which was thought to be a critical state and not a shear failure. It was found that shear strength of the basic matrix is primarily defined by the friction, which is activated at comparatively small strains and does not depend on the fibre content. Therefore, the friction angle of the basic matrix should correspond to that of the composite matrix. The authors describe the cohesion being related to fibre cohesion, which is already activated by tensile forces in the basic matrix. Furthermore, they are of the opinion that at vertical strains greater than 20% the cohesive strength is particularly depending on the reinforcing matrix and may be defined as cohesion due to tension strength of the reinforcing components. From these results Jessberger concludes that the reinforcing matrix has no significant influence on the friction properties of the basic matrix. It provides a significant cohesion intercept. It is stated that the shear strength of the tested mixed waste can be approached by a parallel movement of the failure line in the p-q-diagram. The maximum shear strength of the investigated 1 to 3 years old mixed waste is given by ϕ = 42-49° and c = 51-41kPa. It should be borne in mind that the results from laboratory tests consider just mechanical but no decompositional influences. They propose the determination of individual parameters for each landfill or area.

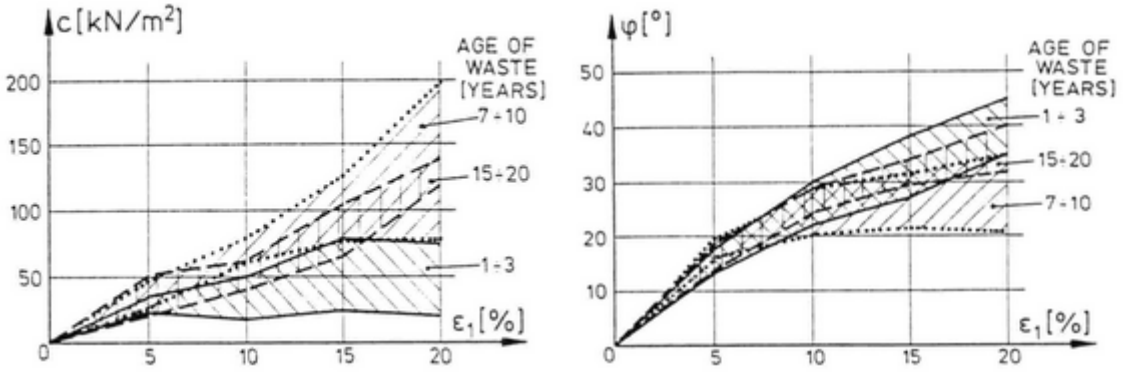

Figure 2-39 Deformation dependent activation of shear strength parameters of variably aged waste (Jessberger *et al.,* 1995)

Reuter and Nolte (1995) examined the results by Jessberger *et al.* (1995). Waste aged between 1-3, 7-10 and 15-20 years were used. The investigation of shear behaviour did not produce any failure in any of the samples, even with the larger distortions of ε = 20%. To display the theoretical or apparent shear parameters ϕ' and c', the distortion criterion is used with ε = 5/10/15/20% being defined as the crucial distortion conditions. On the basis of the results it was stated that all mixtures of refuse displayed a considerable degree of stability, which is not activated until major linear strains have been set up in the material. A qualitatively consistent rise of friction angle and linear strain is shown in all the subsidiary experiments (Figure 2-40 and 2–42). In contrast to the observed behaviour of the friction angle, the calculated values indicate cohesion in the opinion of the authors. Although they do not deny the possibility to observe an increase in the shear parameter at greater linear strains, they could not identify any uniform trend in cohesion with increasing linear strain because of the high degree of scatter in the results.

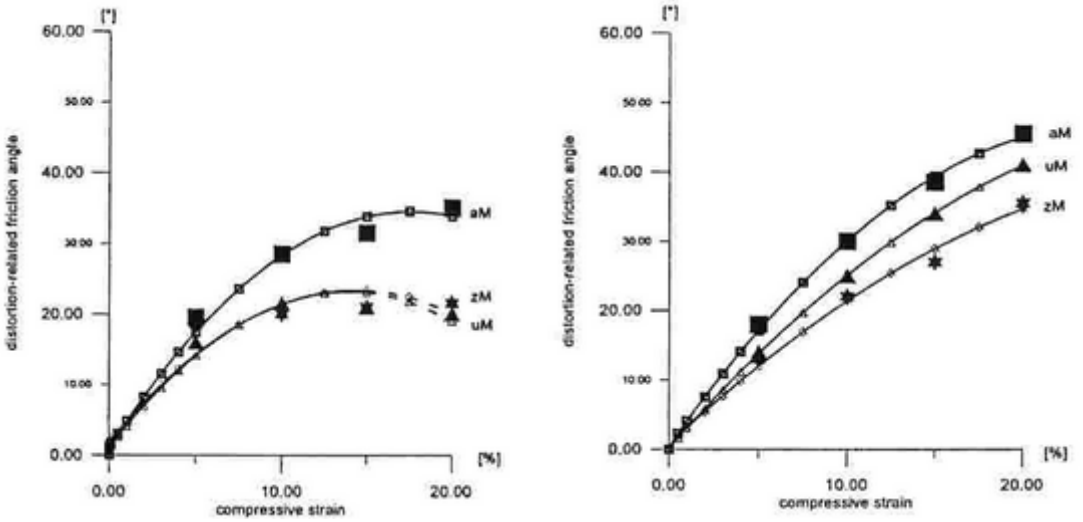

Figure 2-40 Friction angle of 1-3- and 7-10-year-old refuse (Reuter & Nolte, 1995)

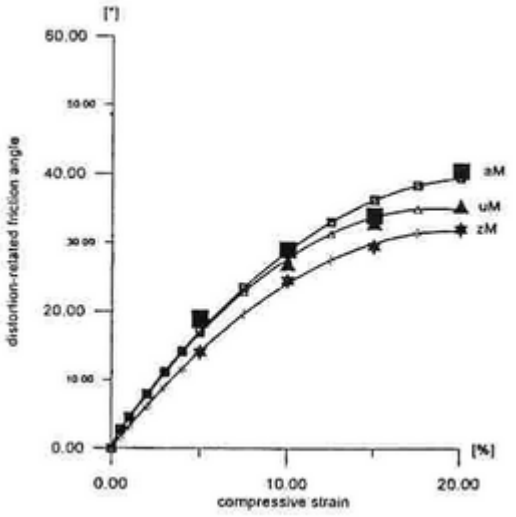

Figure 2-41 Friction angle of 15-20-year-old refuse (Reuter & Nolte, 1995)

Shear stability could only be calculated on the basis of the related critical distortion conditions. An analysis of the existing and permissible or expected distortions and tension conditions therefore has to be carried out in the investigations of static stability. The failure of the system then can be defined as the moment when the permissible distortions are exceeded.

Triaxial compression tests from Machado *et al.* (2002) were carried out using statically compacted specimens (composition in Table 2-9) with nominal unit weights of 10, 12, and 14kN/m^3, diameters of 150 and 200mm and heights of 300 and 400mm. The displacement rate was 0.7mm/min and saturated specimens and specimens remoulded to the natural moisture content were tested using effective confining pressures of 100, 200, and 400kPa. For preparing the sample waste from a borehole was thoroughly mixed and the largest particles were substituted by an equal amount of finer particles so the largest particle size would not surpass 30 or 40mm for the 150 and 200mm diameter specimens, respectively.

Table 2-9 Composition of samples of 15-years-old waste (Machado *et al.,* 2002)

Stone	Rubber	Paper	Plastic	Textiles	Wood	Metal	Glass	Paste
[dry mass-%]								
10	2	2	17	3	4	5	2	55

The paste includes organic matter and a varying proportion of soil

Some assumptions are made regarding the area correction for large deformations, which sometimes exceed 30%. The conventional area correction shown in the following equation is assumed, which takes into account the axial and volumetric strains:

$$A_i = A_0 * \frac{1-\varepsilon_{vo,i}}{1-\varepsilon_{ax,i}} \qquad \text{Equation 2-5}$$

These tests typically show that the deviator stress increased, almost continuously, with axial strain (ε_{ax}), without reaching a well-defined peak or an ultimate value in the stress-strain curve, as found by other authors. In addition, Machado *et al.* (2002) observed another interesting feature, which is the decrease in volumetric strains (ε_{vo}) as the confining stress increases. In comparison to other authors like Grisolia *et al.* (1993) and Jessberger and Kockel (1993) the stress-strain behaviour is typical of urban waste.

Considering Mohr-Coulomb criteria, Machado *et al.* (2002) could only determine the shear strength parameters c and ϕ if they are referred to some value of strain. They note the mobilised shear parameters tending to increase with the deformation in a process that seems to be largely controlled by the reinforcing effect of fibre materials (plastic, textiles, etc.). They illustrate this in Figure 2-42, where the stress path followed in these drained tests and shear strength envelopes for different deformation are shown.

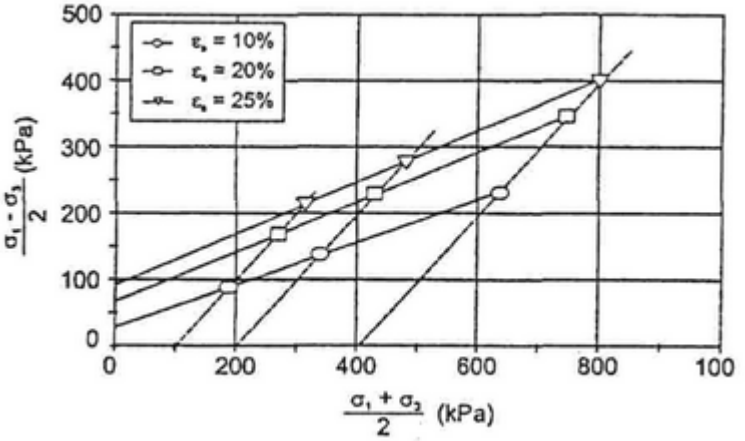

Figure 2-42 Stress path and shear strength envelopes for different strain at natural water content and a unit weight of 10kN/m^3 (Machado *et al.,* 2002)

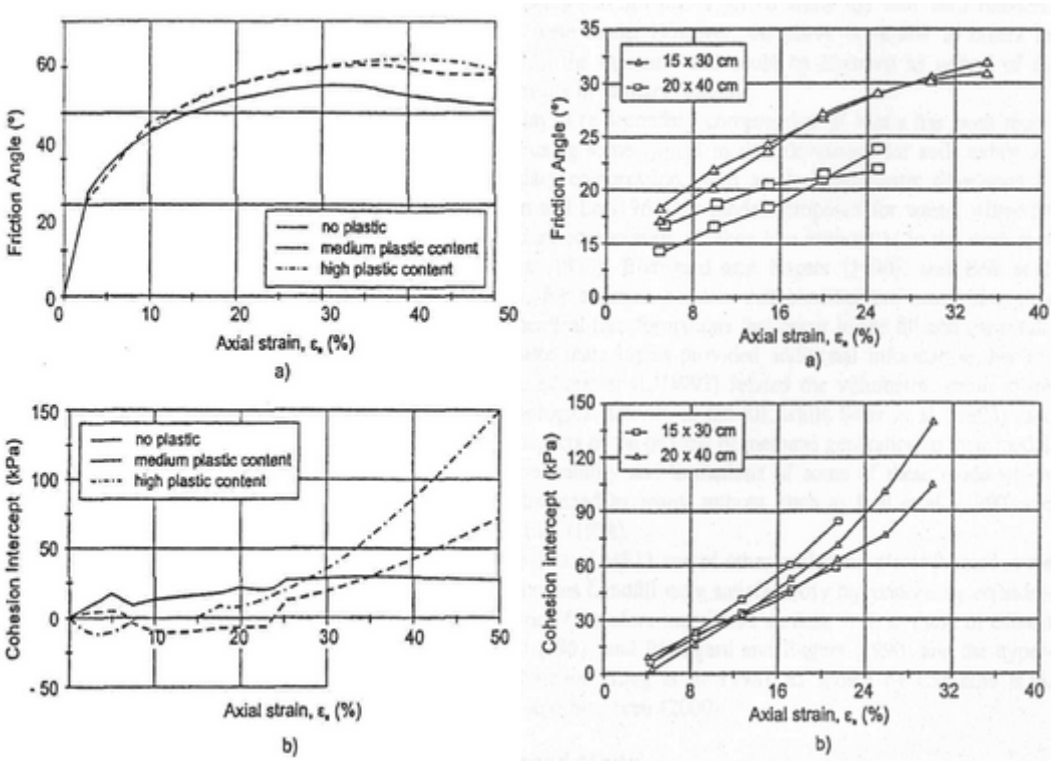

Figure 2-43 Shear strength parameters as a function of axial strain a) Friction angle; b) Cohesion (Kockel and Jessberger, 1995 and Machado *et al.,* 2002)

As described by Jessberger (2001), the friction angle tends to be fully mobilised at large strain values, while the MSW cohesion provided by the fibre starts to become mobilised at strains of 10% or higher, and a limiting value is usually not observed. In Figure 2-43a Machado *et al.* quote results obtained by Kockel and Jessberger (1995) when they tested waste with different amounts of plastic contents where the behaviour mentioned before can be observed. Some typical results related to the waste material described in the publication of Machado *et al.* (2002) are presented in Figure 2-43b. The authors describe the behaviour observed in both tests to be quite similar, although an ultimate value for the friction angle could not clearly be observed in the latter tests, which could be due to the more random distribution of plastics in the sample tested.

Back-calculation

The approach by Singh and Murphy (1990) is chiefly based on the field load test made in Los Angeles. The Los Angeles area landfill was field-tested by loading and monitoring the deformation of the fill. The studies using strength parameters obtained from this test study estimate the back-calculated values in various combinations of cohesion and angle of friction, which are plotted in Figure 2-44. The main justification in using these values by various authors in their studies is that these values represent the lower boundary of the available strength and therefore are conservative. Because these combinations of strength parameters are estimated based on the results of a field test, they may not represent independent estimates of the shear strength properties of the refuse.

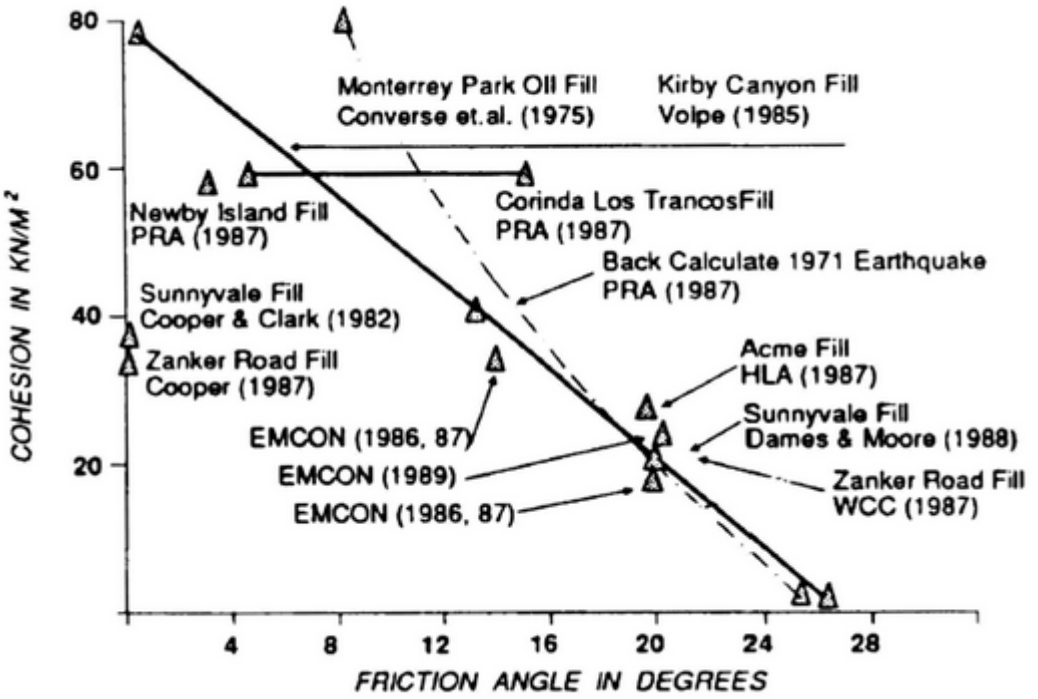

Figure 2-44 Strength parameters estimated by back-calculation from a field load test and from performance records (Singh and Murphy, 1990)

Back-calculated strength data has also been obtained on the basis of the satisfactory performance of the numerous landfill slopes in southern California during earthquakes in 1971 and 1987. Singh and Murphy (1990) quote different authors, who observed the stability of the relatively steep slopes, including nearly vertical cuts. Again, the basis for justifying the use of this approach is that the back-calculated values represent minimum available strength of refuse and are therefore conservative.

Cowland *et al.* (1993) mention back calculations, which have been made on the basis of satisfactory performance of a number of landfills during earthquakes, where no failure occurred emphasising the quite different stress-strain characteristics for the waste and the underlying soils.

In their literature review Fassett *et al.* (1994) report several cases of back-calculation. For example, Howland & Landva (1992) found that the results of back-analyses indicate a lower waste strength than the results of direct measurements. They speculated that this difference might be due to the peat-like fibrosity having a bigger effect on the small-scale direct measurements as opposed to the larger-scale associated with back-calculated values. It is also point out that, since back-calculated values are often obtained from slopes, which did not fail, the resulting values of the Mohr-Coulomb strength parameters are conservative by an unknown amount. Singh and Murphy (1990) recommend that strength parameters chosen for use in stability studies should be "interpreted judgementally in favour of least conservatism" since large, moderately steep landfill slopes are known to exist with few signs of distress. Howland & Landva (1992) mention that no waste index properties have been identified that systematically account for the different strengths observed for different wastes and test methods. They strongly encourage the continued investigation of waste strength data from back-analyses and direct measurements.

In the approach to evaluate shear strengths from back analysis of failed slopes, Gilbert *et al.* (1998) describe the difficulty of obtaining realistic values. They note that slope failures provide a valuable opportunity to estimate the strengths of materials, such as soils or geosynthetics, involved in the failure. They performed stability analyses to back-calculate strengths for the state of failure. Back analyses of strengths have in their opinion advantages over laboratory testing that the scale is much larger and the materials are in their in situ state. However, the authors provide numerous uncertainties in the back analysis approach, which are observed by various authors:

- The exact geometry of the slope, including subsurface stratigraphy and slip surface location, is seldom known.
- Failure mechanisms, such as progressive failure, are difficult to determine.
- Pore water pressure information is typically sparse, if it exists at all.
- There are many different representations of strength, such as different combinations of c and ϕ or linear versus non-linear failure envelopes, that could produce failure.

As a result they suggest combining information from all possible sources including laboratory and field-testing and experience to maximise the potential of back analysis.

In Figure 2-45, Eid *et al.* (2000) present data from large-scale direct shear tests and back-calculation of failed waste slopes. Back-calculated shear strength from plate load tests and test fills is not considered because failure planes were not located, which can result in an inaccurate estimate of shear strength. Back-calculated shear parameters from landfill slopes that had not failed are also not included, as the actual factor of safety is not known, and the back-calculated shear strength is sensitive to the assumed factor of safety.

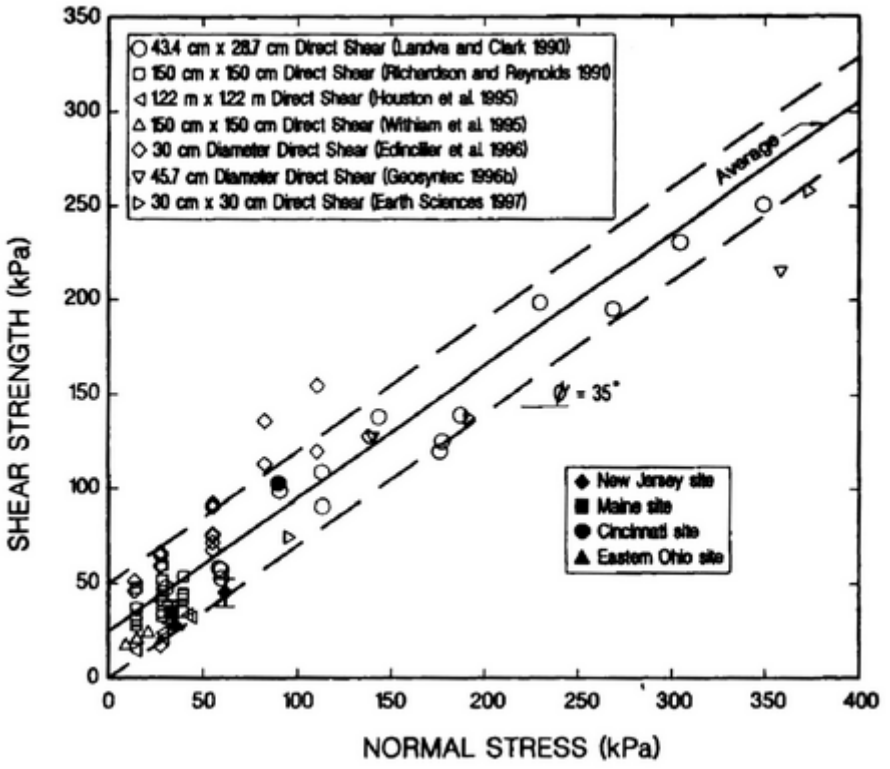

Figure 2-45 Measured and back-calculated data on shear strength (Eid *et al.,* 2000)

Eid *et al.* (2000) assume the Mohr-Coulomb strength criterion to be applicable because of the fact that the shear resistance of MSW increased with increasing normal stress. Using regression analysis of the data the shear strength of MSW is defined by a narrow band with an effective stress friction angle, ϕ', of approximately 35°, and the cohesion, c', that ranges from 0 to 50 kPa. Based on the literature study and back-calculation of field case histories, they propose an average c' and ϕ' of 25 kPa and 35°, respectively, for the design of municipal solid waste containment facilities, which is slightly higher than other published combinations. The lower and upper bounds shown in Figure 2-45 could represent the shear strength of MSW that contains more soil, sludge, and/or other soil-like materials and plastics, respectively. The authors are not clear about the mechanisms that yield high shear strength in MSW, but the interconnection of the plastics and other materials is assumed to be a probably contributing factor.

Tensile tests

Kölsch (1996) explains the estimation of shear strength from tensile loading (Figure 2-46). The left part of Figure 2-46 shows the general relation between reinforcing and the resulting shear stresses. A horizontally reinforced element is loaded by a tensile force T, which is acting axially to the reinforcement orientation. A tensile stress Z is induced in cross section A. Considering an inclined cross section A_α a tensile stress Z_α is induced, which can be expressed through a shear stress τ_z

$$\tau_z = Z_\alpha * \cos\alpha \qquad \text{Equation 2-6}$$

and a normal stress σ_z

$$\sigma_z = Z_\alpha * \sin\alpha. \qquad \text{Equation 2-7}$$

If a shear stress is acting at α defined on the horizontally reinforced element, the friction and the resistance of the reinforcement have to be exceeded to reach a collapse. For exceeding the resistance of the reinforcement a fibre tensile strength is necessary, which results in a shear stress τ_z within the shear plane. As Kölsch (1996) examined the normal stress dependent maximum sustainable tensile stresses Z of the fibres in tensile tests, he directly derives the shear stresses from the Equation 2-7.

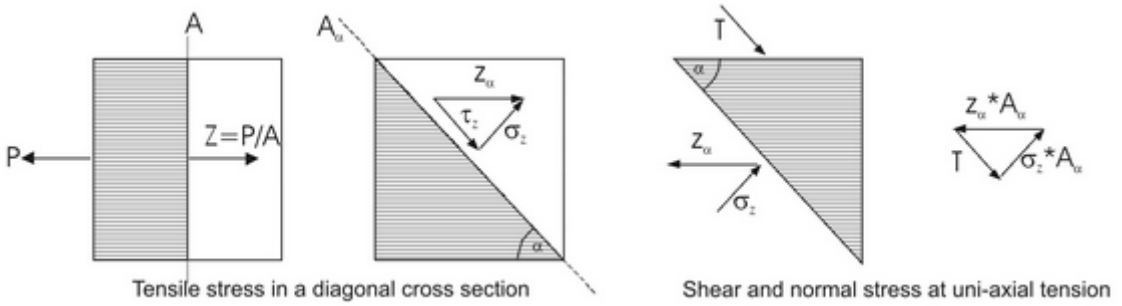

Figure 2-46 Estimation of shear stress from tensile loading (from Kölsch, 1996)

Kölsch (1995) conducted tensile tests in a device with size 3*1*1.5m (l*w*h). It contains a waste sample of about $4m^3$. The waste is compacted in layers with a thickness of 200-300mm. A normal load is applied by means of load plates and load girders with high-pressure pads between. For the tensile tests the sample box is vertically halved in the middle of the box. The front part being connected to a ram is pulled, resulting in a tensile load being applied to the waste sample, which is increased until failure of the sample occurs. For the investigation of the frictional component direct shear tests were accomplished in an apparatus with the size of 2*1*1.5m (l*w*h) and a volume of about $3m^3$. The test procedure does not differ from tests in smaller shear boxes. The results of the tension tests conducted by Kölsch (1995) are shown in Figure 2-47 and Figure 2-48. The deformation behaviour is considerable elastic-plastic. The maximum tensile stress amounts to 230kPa under a normal stress of 284kPa. In Figure 2-48 the relationship between tensile stress and normal load for all samples is shown. The waste composition is shown in Table 2-10 and 2–11. The fresh waste samples generate considerably higher tensile strengths than the other samples, which is probably due to the high number of

bigger sized components. The difference of the results between FRESH and RESIDUAL is attributed to the higher water content of FRESH. The latter is characterised by a water content of near 44%, RESIDUAL only 32%. As a result of the high water content either a pore-water pressure, which reduces the normal stress on the fibres, or a simple sliding effect between the fibres can arise.

Table 2-10 Identification of waste samples - range of dimensions (Kölsch, 1995)

Sample	RESIDUAL	ROTTED 18	SITE	FRESH
[-]		[mass-%]		
DIM 0 (fines)	68.3	26.7	62.5	Not sorted
DIM 1(fibres)	2.8	3.5	3.7	Not sorted
DIM 2	20.3	39.9	18.8	Not sorted
DIM 3	8.6	31.8	15.0	Not sorted

Table 2-11 Identification of waste samples - range of material groups (Kölsch, 1995)

Sample	RESIDUAL	ROTTED 18	SITE	FRESH
		[mass-%]		
<8mm	14.6	27.8	33.3	11.8
8-40mm	9.7	40.3	29.2	25
Organics	2.1	0	0	6.3
Wood	3.5	1.3	6.2	1.3
Minerals	11.1	2.1	11.2	14.6
Metals	4.8	3.5	2.7	5.6
Hard synthetics	6.3	6.9	3.5	8.3
Smooth synthetics	25	12.5	8.3	13.2
Paper	22.9	5.6	5.6	13.9

For the linear relationship between tensile and normal stress Kölsch (1995) defines an angle of internal tensile force ζ shown in Figure 2-48. For fresh waste (RESIDUAL) it increases to 35° and for aged waste (ROTTED18) to 15°. Kölsch relates the part of tensile forces, which is not dependent on normal stress, to cohesion. The tensile angel ζ is utilised to adapt the results of the tensile test to the methods of slope failure calculation. In the same way the tension force could be used like a cohesion, which is increasing with depth.

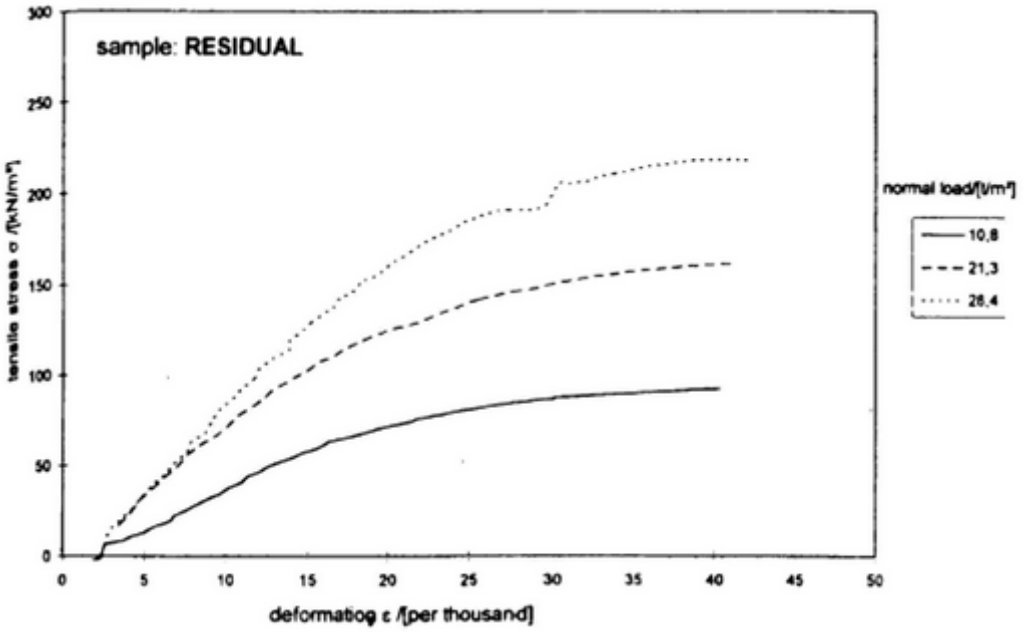

Figure 2-47 Tensile stress-deformation relation (Kölsch, 1995)

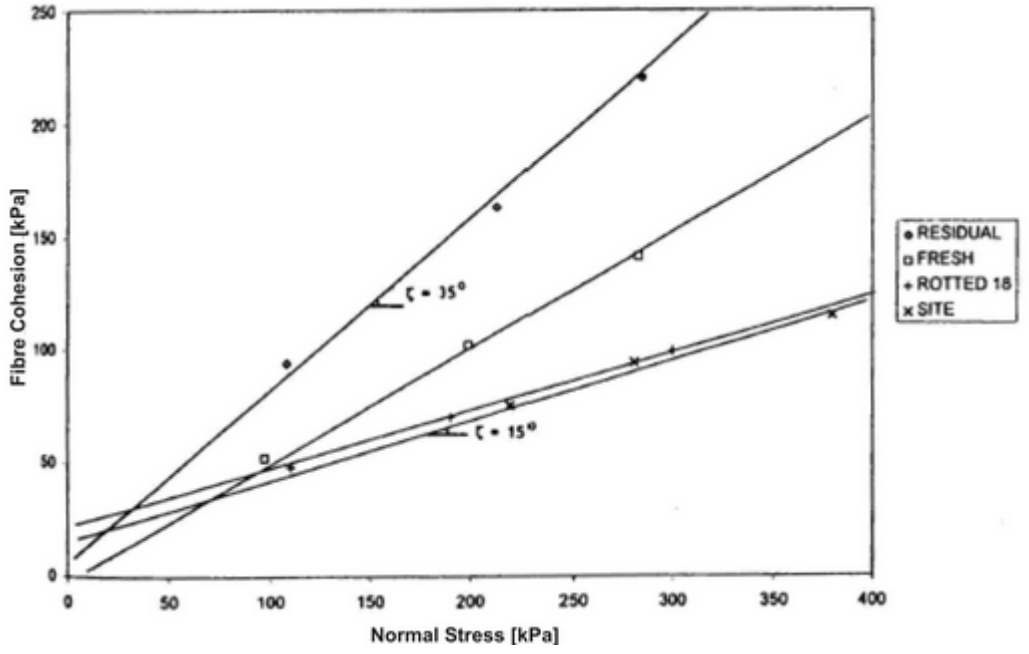

Figure 2-48 Relation between fibre cohesion and normal load (Kölsch, 1995)

2.2.2.10.3 Strain/Displacement

Jessberger and Kockel (1993) presented results of triaxial compression tests on older (i.e. partly degraded) waste. They found that the mobilised friction angle ϕ increased up to a maximum at a certain strain and remained constant with increasing strain thereafter. Only apparent cohesion increased with constant strain and a peak could not be reached. Jessberger *et al.* (1995) conducted laboratory tests using waste samples of different ages and composition, in which they could only observe a limit state at very large strains. Interesting results were also reported by Gotteland *et al.* (2000), in which the mobilised cohesion of the domestic waste (containing large amounts of plastic) was independent of

shear displacement, but only in terms of a best fit line, while the cohesion of fine waste material increased with displacement until it reached a value similar to that for domestic waste. Figure 2-49 shows the mobilised friction angle at different displacements. A clear trend is visible. No big differences between the test methods are identifiable. The upper and lower bounds proposed by Pelkey *et al.* (2001) contain most of the data. The reason for presenting mobilised friction in relation to displacement is because normalising the displacement to percentages in relation to device size (i.e. strain) means a comparison between particle size and displacement is not possible. For example, a strain of 10% means a displacement between 7 to 100mm depending on the size of the shear device. Consideration of the possibility of activating tensile forces due to a given displacement, which accords to the particle size, is not possible. Unfortunately, information about the maximum particle size can seldom be found in the literature. The available data is plotted in Figure 2-50. The biggest increase of the mobilised friction angle occurs up to a displacement of 50mm. In terms of mobilised cohesion, material sized <60mm shows a peak value at about 80mm displacement, while for large-sized material (<100mm) a peak is not visible up to a displacement of 100mm. This could confirm the assumption that component size-related displacements are needed to reach peak values. This trend is confirmed by results of direct shear tests reported by Pelkey *et al.* (2001). Large displacements were necessary to mobilise peak shear stress. In comparison, shredded fresh refuse mobilised peak stresses at shear displacements that were 30 to 50% of those required for samples with untreated MSW. Unfortunately, no information is given on the particle size in these studies.

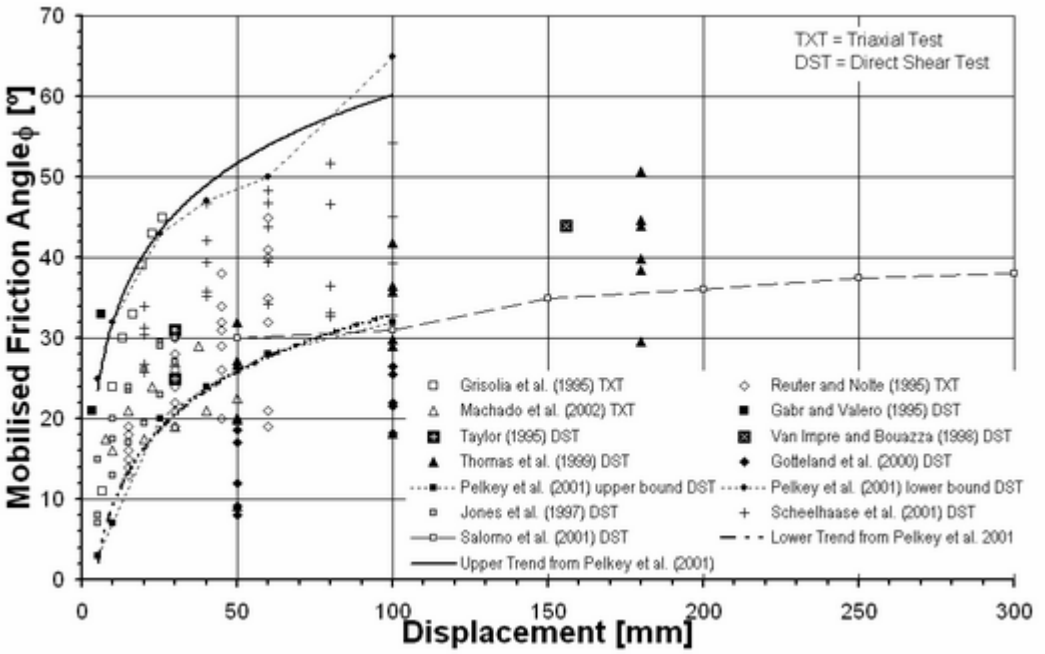

Figure 2-49 Mobilised friction angle and displacement from various authors (summarised in Dixon *et al.*, 2004a)

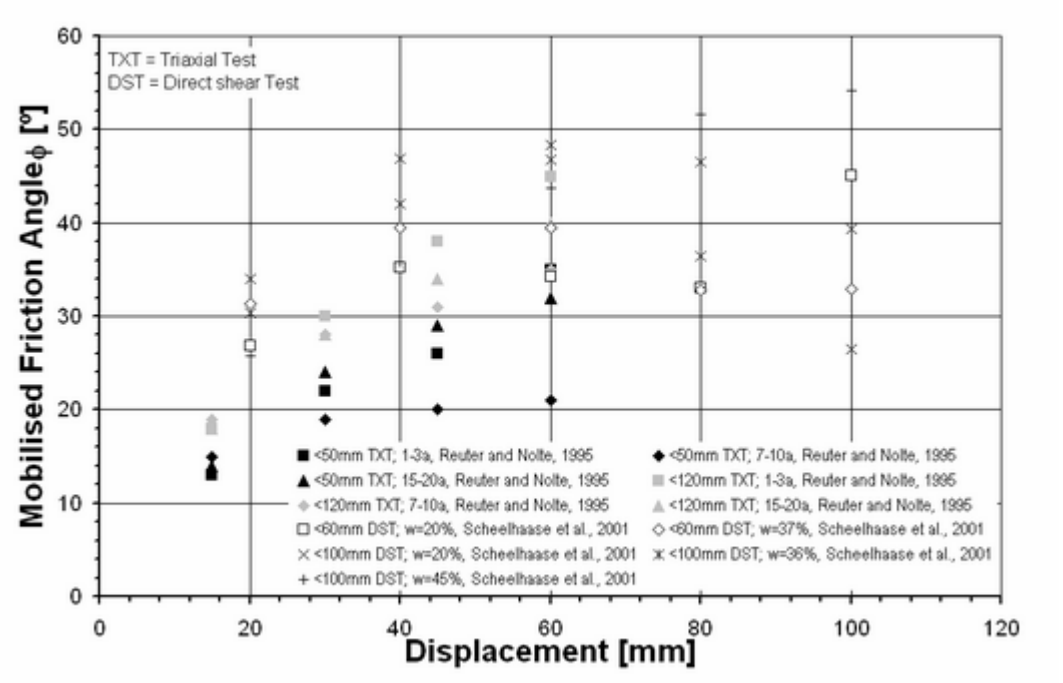

Figure 2-50 Mobilised friction angle and displacement of different component sizes (Dixon *et al.*, 2004a)

Gabr and Valero (1995) suggest that the friction angle increases as a function of increasing horizontal displacement while cohesion remains essentially constant. Thus, they admit that a wide variation in the measured friction angles could result from the inconsistent choice of a horizontal displacement magnitude for data reduction. Gotteland *et al.* (2000) also observed the increase of the friction angle with increasing displacement and the constant cohesion for their tests on domestic and non-hazardous industrial waste. Based on theory of mobilising tensile forces, the maximum displacement has to be related to the length of the fibrous components in order to increase the possibility of fully mobilising tensile forces. If the ratio of maximum displacement and maximum particle-size is <1 the possibility of a peak strength is reduced; if this ratio is bigger or equal to one the possibility of measuring a peak strength is increased.

Sánchez-Alciturri *et al.* (1993) also support the idea of large-scale shear tests. They state that waste does often not show a definite shear failure. But this behaviour has been observed in small or medium scale tests (laboratory or in situ), and it is possible that at larger scales a shear failure is better defined.

2.2.2.11 Design Shear Strength Values and Interpretation Methods

Pairs of Cohesion and Friction Angle

Sánchez-Alciturri *et al.* (1993) present the results of strength parameters of several authors obtained from laboratory test, in situ tests and back analysis of failures in a plot of cohesion vs. friction angle, such as Figure 2-51. Despite a wide scatter in the results of assessing shear strength the authors observe some trends. The results of laboratory tests indicate that a significant friction is mobilised. Most of the values of the friction angle are

between 25°-35°. No value lower than 17° has been measured. The cohesion intercept is very variable, but usually below 30kPa. The lines corresponding to field data diverge in the zone of low friction angle, giving cohesion values from 20kPa to over 100kPa. However, all data converges for $\phi > 15°$. In this zone, the lines of field data fall in the lower bound of the results from the laboratory tests. These trends are shown in Figure 2-52, where a zone has been marked as recommended for design. It corresponds to the interaction between the bands of field and laboratory tests.

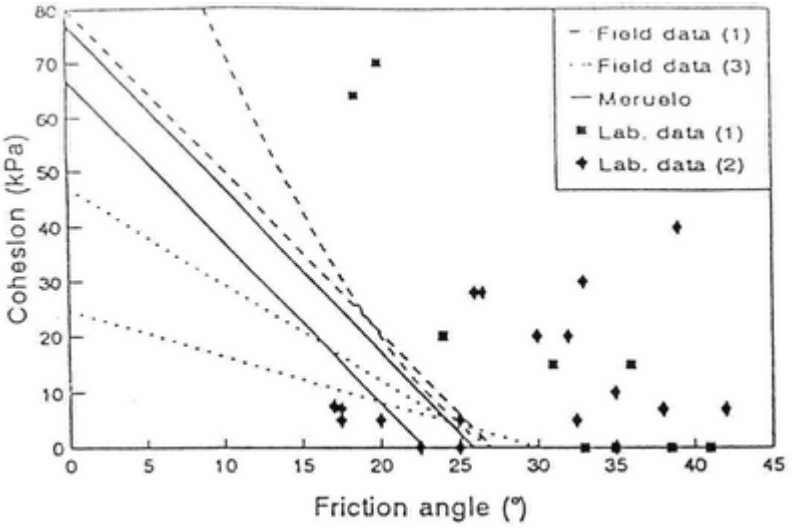

Figure 2-51 Field and laboratory shear parameters (Sánchez-Alciturri et al., 1993)

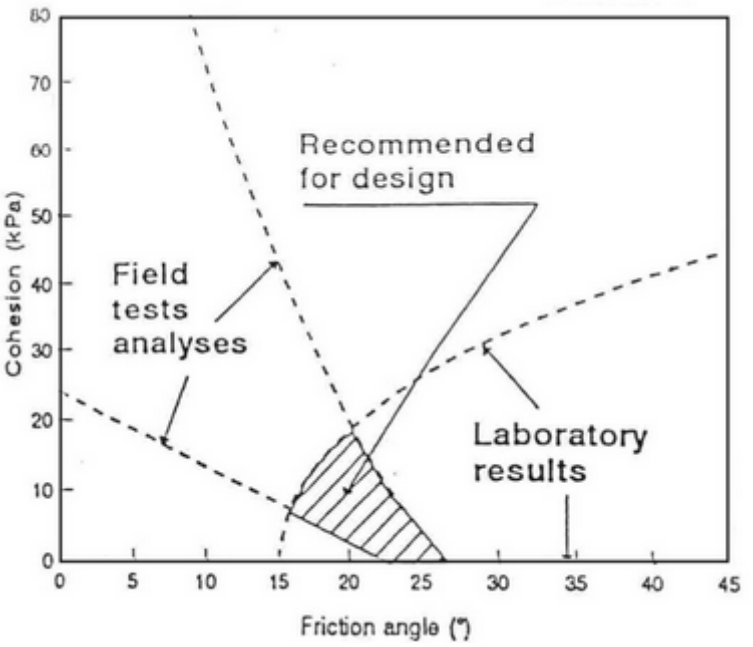

Figure 2-52 Interpretation of Figure 2-51; recommended design shear strength parameters (Sánchez-Alciturri *et al.*, 1993)

As waste is regarded as a very deformable material, which can sustain very large shear strains without reaching a definite failure, the strength parameters are usually defined for a limiting strain condition. But the available evidence from laboratory and in situ tests

show that the shear strength of the wastes is better defined as cohesive-frictional (c-ϕ), and interpretation as undrained behaviour (ϕ = 0) gives unacceptable high values of the shear strength. Regarding laboratory triaxial or shear tests reported in the literature, Sánchez-Alciturri *et al.* (1993) found that a significant friction angle is usually measured, always higher than 15°. For this range, a reasonable agreement is observed between laboratory and field data. This enables the definition of proposed ranges for the strength parameters, which can be taken as preliminary design values (Figure 2-52). As composition or other properties of the examined waste are unknown, it is advised to look at this diagram with care. It is mentioned that the results of laboratory drained triaxial or shear tests provide an envelope in Mohr's plane, and hence the two values of c and ϕ can be determined, however, when in-situ tests or field performance are back analysed, there is only one equation (failure condition or value of ultimate load), and hence the result is a relationship linking the two unknown parameters. The authors describe some assumptions other author made to interpret their results. They mention some cases, where a line is presented as the final result, and they emphasise to bear in mind that only one particular (unknown) point of the line corresponds to the true parameters. Furthermore, they mention other cases, where an additional assumption is made to report individual values of c and ϕ. The most usual assumption they quote, is either that of purely cohesive (ϕ = 0) or purely frictional (c = 0) behaviour. Nevertheless, they consider that this procedure is valid in normal soils, where a basis is given for assuming one of these two types of behaviour, whereas in wastes, a firm basis for this decision does not exist. As a consequence, for field-tests they do not recommend assuming c or ϕ being zero but they add that from the two options, the condition c = 0 seems more realistic.

Manassero *et al.* (1997) also consider presenting shear strengths in terms of Mohr-Coulomb strength parameters, intercept cohesion and shear angle but they also advise to be very careful with interpreting this type of approach.

Gabr and Valero (1995) tested 15-30-years old waste specimens in direct shear tests. These specimens exhibited continued strength gain at horizontal displacements well in excess of 10% of the specimen's diameter. As a consequence, no peak strength was detected. Therefore, the authors evaluated the values of c' and ϕ' at strain of 5 and 10%, respectively. The results by Gabr and Valero (1995) shown in Figure 2-53 and Table 2-12 indicate cohesion values ranging from zero to 27.5 kPa, with the exception of the Siegel *et al.* (1990) data.

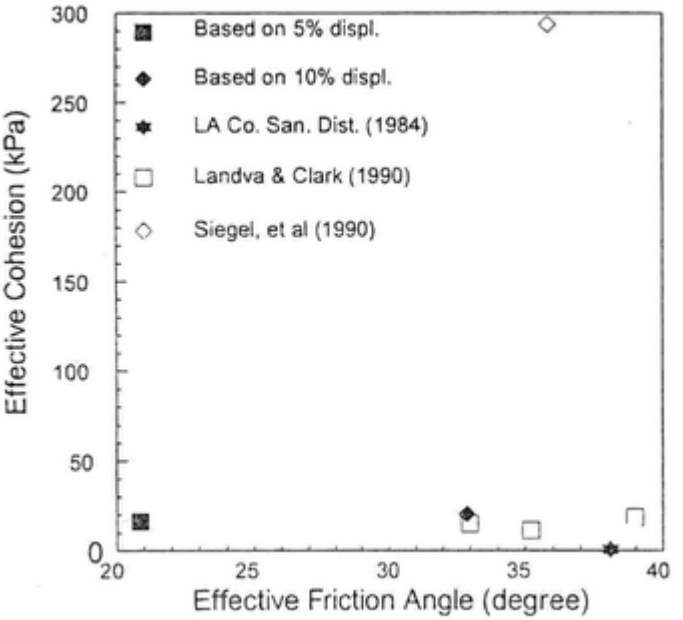

Figure 2-53 Effective strength parameters (Gabr and Valero, 1995)

In this case, the authors speculate that the additional cohesion is the result of component interlocking (i.e. large fibrous material) left intact by the undisturbed sampling techniques. The reported friction angles vary between 20.5° and 39°. From the measured data the authors suggest that the friction angle increases as a function of increasing horizontal displacement while cohesion remains essentially constant. Thus, they admit that a wide variation in the measured friction angles could result from the inconsistent choice of a horizontal displacement magnitude for data reduction.

As an interesting point the authors note that the specimens initially displayed volume change behaviour similar to that of normally consolidated clay. In the later stages of shearing, the volume first decreased, than increased as may be expected in the case of an overconsolidated clay. As the specimens began to dilate after compression a slight dependence of the magnitude of the normal stress was detected, the specimen under a normal stress of 207kPa showed less dilation as compared to the specimen loaded with 138kPa. The authors suppose, as a possible reason for the dilation behaviour the presence of relatively large percentage of granular particles, such as crushed glass, in the waste specimens could cause this. When a critical density is reached, large particles are supposed to roll over each other in a fashion similar to that for the volume change behaviour of dense sand, therefore causing a volume increase.

Gabr and Valero (1995) also summarise other MSW shear strength data shown in Figure 2-54 including their own data, which is an extension of the summary by Singh and Murphy (1990). The effective cohesion is supposed to be derived from the fibrous and organic nature of the waste and may be expected to diminish with the decomposition of the organic materials. Friction angles evaluated from the laboratory data exceeded those evaluated from back calculations by as much as 10°. On the other hand, total cohesion values from laboratory tests tend to be lower than back-calculated values. The reason for this discrepancy is suspected in the difference of the tested material.

Total and apparent effective strength parameters evaluated by Gabr and Valero (1995) are comparable to those reported in the literature. With regard to the water content the cohesion values decreased as a function of the water content from approximately 100kPa at w of 55% to 40kPa at w of 72%. Effective strength parameters were evaluated to be $\phi' = 34°$ and c' = 16.8kPa. The composition of the tested waste is shown in Table 2-12.

Table 2-12 Waste composition (Gabr and Valero, 1995)

Food waste	Garden refuse	Paper products	Plastic and rubber	Textiles	Wood	Metal products	Glass, ceramics	Ash, rock, soil
[mass-%]								
0	0	2	13	23	9	10	10	33

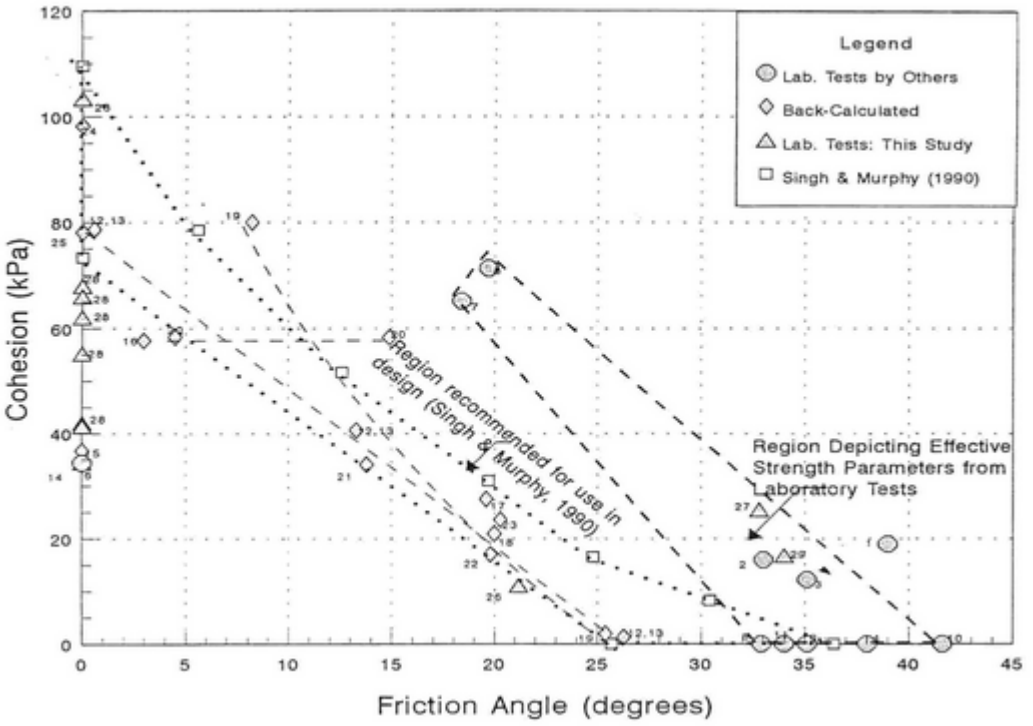

Figure 2-54 Summary of effective and total shear strength parameters cohesion and friction angle (Gabr & Valero, 1995)

Jessberger (2001) reports considerably varying shear strength values from the literature. He gives a range for the friction angle from 10° to 53°, while the range of cohesion varies from 0 to 67kPa. As an important point, he notes that many of the lower values, which have been reported, are contradictory to field observations of stable landfill slopes.

Shear Stress vs. Normal Stress

Fassett *et al.* (1994) conducted a literature review about shear properties, in which they demonstrate ranges of shear strength values used for stability analysis and results from shear strength examinations. They complement a data summary of laboratory tests, back-calculations, and in-situ testing by Singh and Murphy (1990) with data from Jessberger and Kockel (1991), who suggested using $\phi = 32°$, $c = 10 kN/m^2$ for stability analysis of typical MSW landfills. This data is located close to the shaded zone recommended by Singh and Murphy (1990) for stability analysis. They also compare the Jessberger and Kockel (1990) data with back-calculated data determined by Howland and Landva (1992). Figure 2-55 shows the data in terms of a τ-σ-diagram. Included is a line defining the lower bound of the strength envelope used by Fassett *et al.* (1994) in their design.

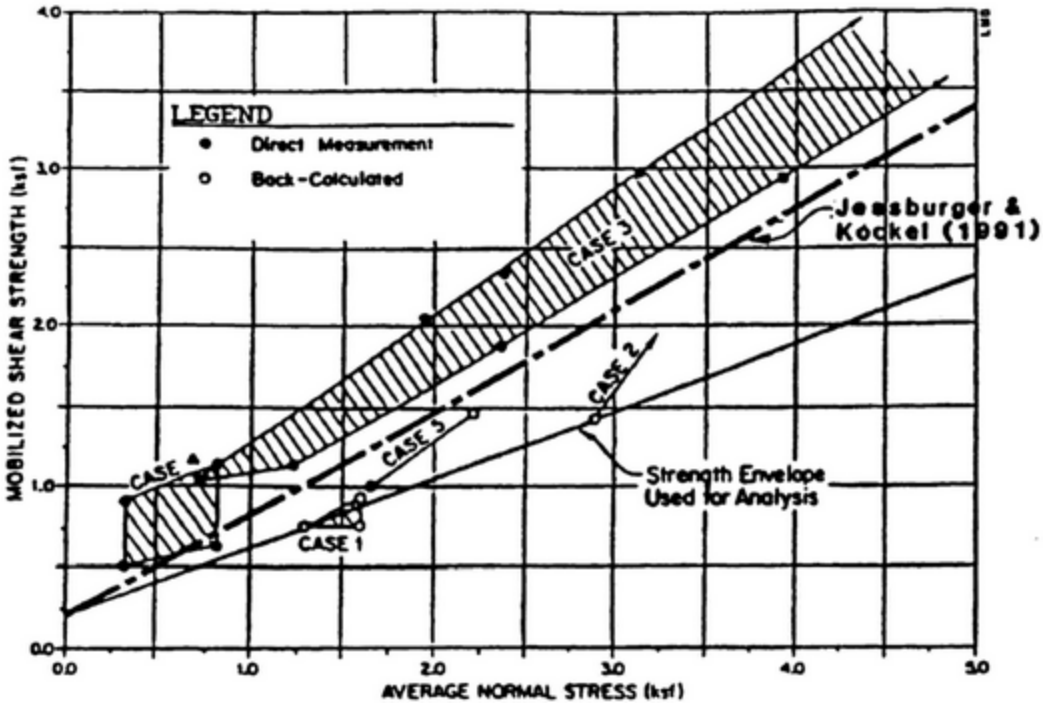

Figure 2-55 Summary of MSW data (modified by Fassett *et al.,* 1994)

Howland and Landva (1992) do not recommend using strength parameters shown in Figure 2-55 for other analyses because various hypothesised factors have not been systematically proved or quantified. But they recommend using the general methodology of comparing available directly measured and back-calculated data. Great care should be exercised in selecting waste strength parameters for use in the stability analysis of high landfills, particularly when the anticipated stresses exceed the stress ranges for which data are available. The general approach used by Howland and Landva (1992) or Fassett *et al.* (1994) to compare the various reported MSW strength data is to plot mobilised shear strength against average normal stress, rather than averaging reported values of Mohr-Coulomb strengths parameters, cohesion (c) and friction angle (ϕ). Howland and Landva (1992) point out the conventional practice to interpret data in terms of shear strength versus normal stress for direct measurements, i.e. laboratory tests, strength back-calculations from failures or load tests are often reported as pairs of c and ϕ that satisfy equilibrium, which is the result of having one known (factor of safety = 1.0) and two unknowns (c and ϕ).

An approach is proposed as described in the following. Back-calculated pairs of c and ϕ that satisfy equilibrium are plotted as shear stress versus normal stress (Figure 2-56). The value of c calculated for ϕ assumed to be equal to zero is the average shear strength mobilised along the failure surface (Point A). For a material with a linear strength envelope, the crossing point of the c-ϕ pairs satisfying equilibrium (Point B) indicates the average normal stress along the failure surface (Point C).

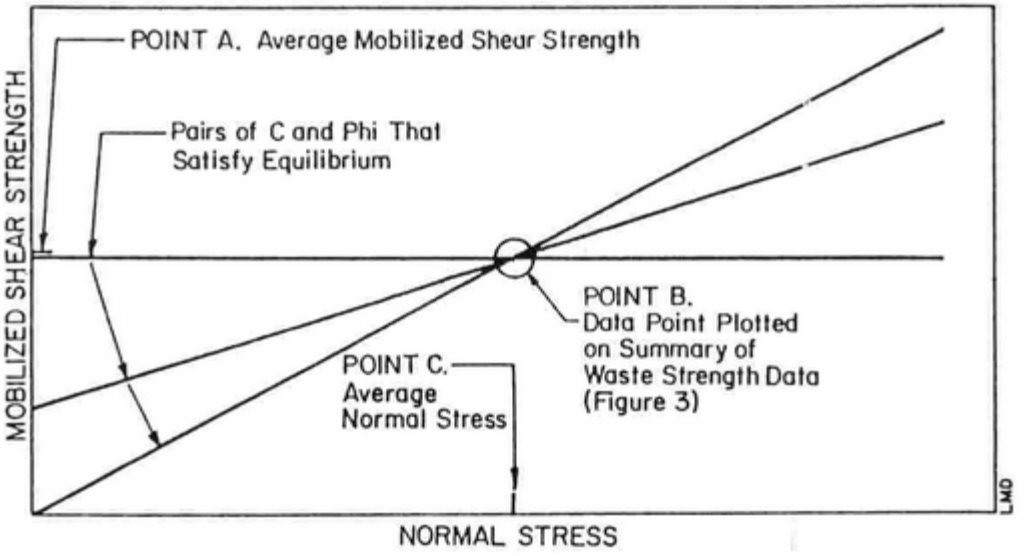

Figure 2-56 Waste strength analysis from case history (Howland and Landva, 1992)

The crossing point is considered to be the one consistent datum derived from an individual case study. The crossing point from each back-analysis case study is transferred to a summary plot of shear stress versus normal stress in order to develop a strength envelope for municipal solid waste. The average normal stress based on the crossing point is checked by estimating the location of the failure surface and calculating the average normal stress based on the reported unit weight of the waste and any applied loads.

Manassero *et al.* (1997) has applied the approach from Howland and Landva (1992) to plot Figure 2-57. It should be borne in mind that compilation of such data is always difficult due to the lack by information and details (especially strain levels) about the case study or test. However, a somewhat curved linear failure envelope can be fitted through the obtained data, a bilinear envelope can be assumed for the sake of simplicity.

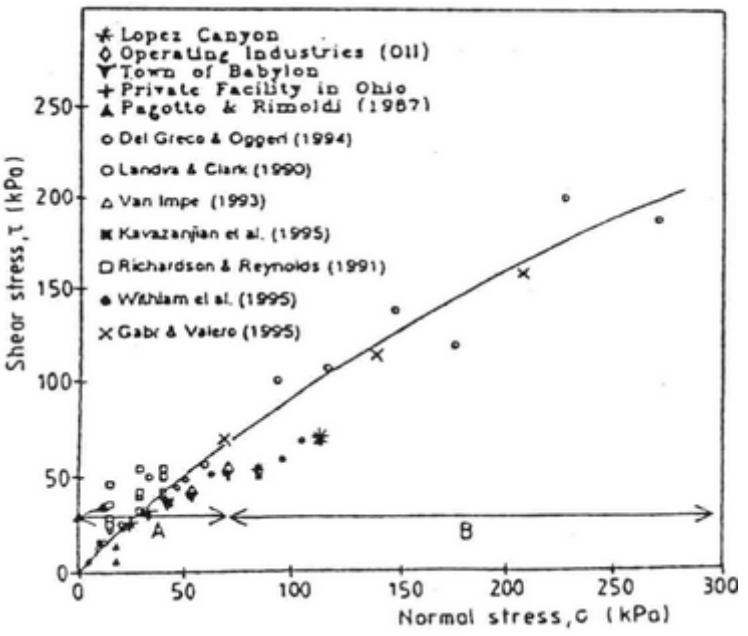

Figure 2-57 MSW strength data from various sources (Manassero *et al.,* 1997)

Two distinct zones can be distinguished: 1) zone A corresponding to low stress levels where the ϕ values are higher and c values are very low. 2) Zone B corresponding to higher stress levels, where the failure is less frictional and c values are higher. The most

usual additional assumptions are either that of purely cohesive (ϕ = 0) or pure frictional behaviour (c = 0) behaviour. For domestic wastes, there is no firm basis for such assumptions. As a consequence, for field tests it is better not to assume c and ϕ to be zero. Manassero's proposal is displayed in Figure 2-58, which should give approximate starting design values of c and ϕ according to three distinct zones:

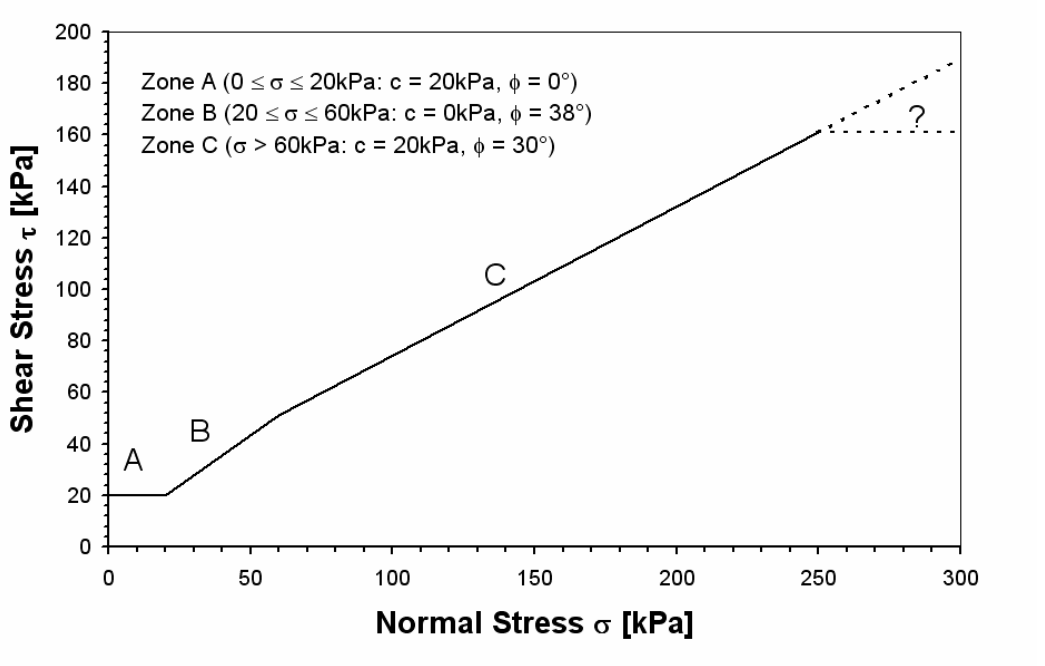

Figure 2-58 MSW strength data design recommendation (Manassero *et al.,* 1997)

- Zone A corresponding to very low stresses (0kPa ≤ σ_v < 20kPa), where the domestic solid waste behaviour can only be cohesive. In this case, c = 20kPa.
- Zone B corresponding to low to moderate stresses (20kPa ≤ σ_v < 60kPa). In this case c = 0kPa and ϕ = 38°.
- Zone C corresponding to higher stresses (σ_v ≥ 60kPa). In this case, c ≥ 20kPa and ϕ = 30°

Kavazanjian *et al.* (2001) regard (drained) shear strength as being the single most important mechanical property of solid waste in landfill engineering. In an earlier paper (Kavazanjian *et al.,* 1995) they proposed the "lower bound" MSW drained bilinear shear strength envelope based upon analysis of available laboratory test data and back analysis of slope stability. They suggest this bilinear shear strength envelope with ϕ = 0 and c = 24kPa, valid for normal stress below 30kPa, and ϕ = 33° and c = 0, for normal stresses larger than 30kPa. This "lower bound" is shown in Figure 2-59. In accordance to this Mitchell (1996) reported strengths back-calculated from the failure of the Rumpke Landfill in Cincinnati, Ohio, USA. In addition, the "mean minus one standard deviation" MSW shear strength envelope of a friction angle of 35° proposed by Eid *et al.* (2000) is mentioned, which is also consistent with the interpretation of Kavazanjian's envelope as a lower bound strength envelope for MSW.

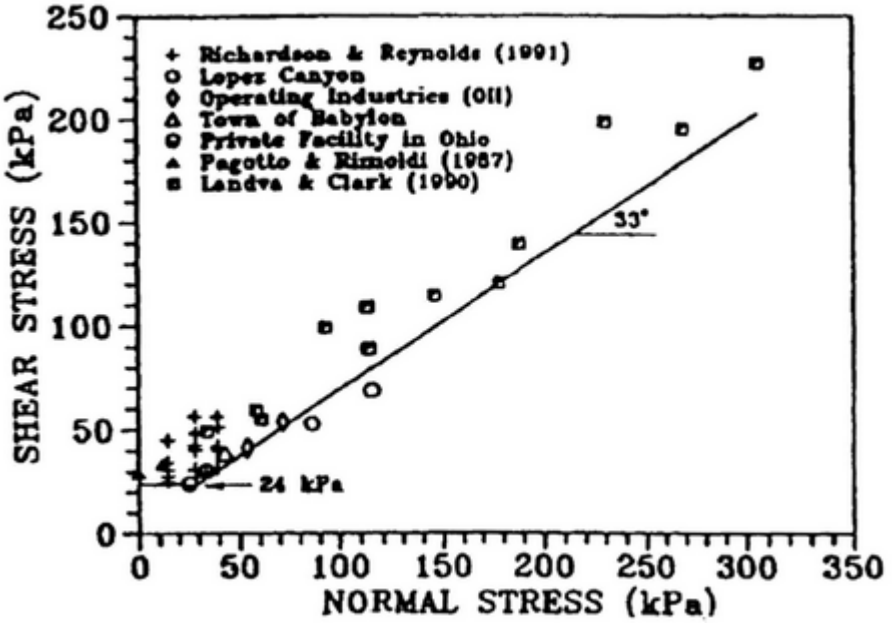

Figure 2-59 Bi-linear MSW strength envelope (Kavazanjian *et al.,* 2001)

2.2.3 Summary of Strength Influencing Factors

Various factors influencing shear behaviour of MSW have been discussed in detail. The main factors were examined and their influences on waste behaviour are demonstrated. However, the individual assessment of these factors has proved to be difficult, because often more than one factor influences waste mechanical behaviour in any given application. For this reason, results obtained from the literature cannot be easily transferred from one situation to another, although they show that various influences unquestionably have an impact on mobilised shear strength.

Waste is a very heterogeneous material. The assessment of its mechanical properties is therefore difficult to accomplish. An appropriately large volume of sampled material has to be examined in order to obtain results, which are representative. Not only the waste material exhibits a heterogeneous character, but also moisture distribution and water tables within the waste mass. This aggravates the overall assessment of landfill stability. Waste also possesses isotropic properties. Isotropy is defined as “having the same magnitude or properties when measured in different directions”. Considering placement and compaction and the horizontal alignment of components, waste seems to have rather the same properties regarding the two horizontal directions. Due to the structure build-up the properties in vertical direction seem to differ, i.e. considering horizontal and vertical direction, the properties of waste also seem to have anisotropic characteristics.

Overburden increases the unit weight. It can have both, positive and negative effects on the interlocking of components. The interlocking can be amplified by an increase of the bonding resistance, i.e. friction, and cohesion due to an increase of contact area between the components, on the other hand the reinforcing effect can be decreased by compressing reinforcing components and thus decreasing the connection between two areas above and below hypothetical shear plane.

The composition of waste differs considerably. Influences like temporal and local origin, waste type, social structure of the catchment area, and legislative pre-treatment actions control the waste and therefore its characteristics. For example, sorting with the purpose of recycling of components as a legislative action reduces the amount of plastic, glass, paper and metal. In terms of plastic and paper, it is expected that pre-treatment has an effect on the reinforcement of waste. Having a separate collection of biological waste (e.g. kitchen waste, food and garden residues) means a decrease of the biological activity, i.e. methane production. As the degradation process is supposed to influence settlement, it also has an impact on the mechanical properties of waste.

Fibrous and sheet-like components can reinforce the waste body by accommodating tensile forces, when loaded. This is due to a bonding resistance, which depends on the applied normal stress, and the actual tensile strength of the reinforcing material, which is the controlling force of the reinforcement. Authors have proved that reinforcement affects the stability of waste similar to reinforced soil. A bearing model for waste has been introduced.

The observed trend in comparing old and fresh refuse seems to show that fresh refuse exhibits higher shear strength than old refuse. If this trend is confirmed it has to be examined what factor (ratio soil-like/non soil-like components, unit weight, etc.) is responsible for the higher strength. A simple distinction of waste components into soil-like and non soil-like seems to be appropriate. For a further analysis of shear behaviour it has to be known, which non soil-like components of the waste's composition will turn into soil-like components (degradation process, physical and chemical destruction) and the rate of this change.

Placing waste in layers results in several effects. If the waste is placed in appropriately thin layers unit weight is increased due to a thorough compaction. As a negative effect, a lack in connection between layers can result, as they are often separated by daily soil covers. But placement also results in a break-up of waste components, i.e. a reduction of size, which could influence the reinforcing effect on the one hand but increase the unit weight on the other. The structure build-up plays an important role in waste mechanics. Waste components tend to align horizontally when they are compacted. Interlocking and bonding between and anchoring of components occur due to surcharge during placement and due to overburden from additional waste layers. With a horizontally aligned structure, the danger of vertical shearing is minimised. The character of the structure is highly related to the applied overburden. In a loose state, the structure differs considerably from a dense state. Interlocking effects like “toothing” in the vertical direction is subject to the applied normal stress, as the interlocking is assumed to lose its impact if the normal stress exceeds a certain threshold.

External influences (e.g. precipitation) have impact on waste properties due to placement methods (i.e. insufficient daily cover). Poorly compacted material show lower shear strength than well-compacted waste, as shear stress dependent on the normal stress.

Little data is available about the effect water content has on shear strength. Certain components and fibres (e.g. paper) are weakened. The high organic content in waste, in

particular the putrescible content result in a composite material with a high alteration potential. A high water content also favours the degradation process and thus has an indirect influence on the altering and destruction of components. With a high water content the overburden is increased, and his can affect layers below as the unit weight of theses layers also increases. A high unit weight tends to result in high pairs of cohesion and friction angle, but high pore pressures are also likely to occur. A global problem is constituted by water accumulation along the interfaces of the lining system resulting in zones of instability. Hydrostatic forces can also lead to possible instability and failure within the waste mass.

The size of the components involved also plays an important role in assessing shear strength. Waste compositions with high soil content typically exhibit a higher friction. Tests on milled MSW generally show that reinforcement effects are destroyed but on the other hand cohesive forces increase.

Not only actively influencing factors but also the way MSW is examined in order to obtain mechanical properties has to be taken into account when considering shear strength results. A method for examining materials has to be chosen carefully to guarantee the appropriate measurement for the highly diverse material. Also the method of interpreting and comparing results has to be considered. The maximum amount of known influencing factors has to be observed for obtaining, comparing and interpreting the results. As a large amount of influences are acting on waste mechanical behaviour, data with similar backgrounds has to be put into groups to highlight a range in which the shear strength behaviour can be found.

Laboratory tests are generally more controlled and manageable than large-scale in-situ tests or back-calculation, but the latter comprise a large amount of sample material, which increases the representativeness of the results. Not only the boundary conditions have to be known, but they also have to be set appropriately for examination of the waste material. For laboratory measurement, the ratio between maximum component size of the material and the size of the test apparatus should be considered in order to obtain meaningful results. The test device should be able to accommodate component sizes as found on a landfill. Often the waste material is sorted before a shear test is conducted in order to fit the sample into the shearing device, which of course falsifies the results. Waste should not be adjusted to the device; the device should be selected by consideration of the size of the waste components. When testing waste in shear devices the displacements has to be large enough in order to activate tensile forces. It is often reported that failure during shearing could not be observed. Considering the theory of activated tensile strength of the reinforcement during the shear process, failure cannot occur unless the displacement exceeds the tensile yield displacement of the reinforcing components provided that the normal stress is high enough to create a bonding of these components. An important point is that waste used in laboratory tests is in a disturbed state. In this state, the original in-situ structure is destroyed. Generally speaking, for both laboratory and in situ examinations it is essential to know as much about waste influencing factors as possible to minimise errors in assessing shear behaviour.

2.3 Compression Behaviour

The highly variable nature of the waste and underlying soft deposits coupled with the variable site formation and ground improvement works, make the prediction of settlement of a landfill extremely difficult, as remarked by Barriera *et al.* (2001). Municipal solid waste has an inherent heterogeneity and anisotropic material properties that are more difficult to characterise than soil. However, it is usually assumed that traditional soil mechanics theories of compressibility also apply to solid waste fill and in general the same parameters are used.

2.3.1 The Importance of Settlement and Compression Analysis

Landfill settlement and compression behaviour of MSW is a well-analysed area of waste mechanical behaviour. Various authors have already described the settlement mechanisms and models have been developed to predict future landfill behaviour for the design of new and the monitoring and general aftercare of existing landfills. In the following, results from literature are summarised and discussed.

For Green and Jamnejad (1997), landfill settlement is a subject that is increasing in importance as the need to understand how landfill sites behave in the long-term is recognised due to redevelopment of closed landfill sites for further uses. The settlement characteristics of a landfill site are individual to the sites' waste composition, rate of filling, volume, depth, age, compaction machinery, etc. They state the importance of investigating and understanding landfill settlement characteristics of waste as excessive or differential settlement can cause a number of problems to a closed landfill site like excessive differential settlement leading to breakage of gas or leachate extraction pipes, which can then lead to a dangerous build-up of landfill gas or can cause saturation of the waste mass. Differential settlement can also cause dramatic changes in the surface profiles of the finished landfill site, which are designed in the landfill licence to allow water run-off. Areas of depression can lead to the formation of permanent water bodies, which results in additional load to the waste and therefore increased differential settlement. With these permanent water bodies, the amount of water percolating into the landfill site is increased, resulting in larger quantities of leachate. They substantiate the need for investigating settlement from an economical perspective. From an economical perspective, there can be additional volume of waste input into the landfill site with a proper management of landfill settlement (i.e. alternating filling of cells; settlement of cell 1, while cell 2 is filled, give the possibility of further use of cell 1). Final surface contours, in theory, settle to the proposed final contours specified in the landfill licence, if this is to occur with more accuracy a better understanding of landfill settlement is needed. This will result in less aftercare and a higher waste input to the site.

Coumoulos and Koryalos (1999) emphasise the importance of predicting the long-term settlement behaviour of landfill cover after closure for the design and performance of the capping system and the successful future development of the site. The time of installation the final capping system and the planning of the development of the site depend on settlement rates rather than total settlement. It is important to know how settlement rates decrease with time. Settlement of municipal solid waste invariably hinders the post-

closure development of landfilled areas as stated by El-Fadel *et al.* (1999). The occurrence of differential settlement is even more critical than total settlement, and is inevitable due primarily to the heterogeneity of solid wastes.

Bowders *et al.* (2000) remark in a similar way that owners of landfills are increasingly making greater efforts to increase the active filling lifetimes of existing facilities by maximising airspace (waste volume) using vertical expansions and in some instances accelerating waste decomposition by operating the landfill as a bioreactor. Both of these practises place greater emphasis on being able to predict the settlement behaviour of landfills. In the case of vertical expansions, it is important to be able to predict the settlement of the underlying waste to assess its effects on any liner system between the original fill and the vertical expansion. The combined settlement of the original waste and new waste in the expansion will impact the performance of the cover system. When operated as a bioreactor, settlements may be accelerated and the magnitude may be increased. It becomes important for the designer, owner or operator to be able to predict or forecast the settlements for purposes of planning landfill cell life and scheduling new construction.

Bowders *et al.* (2000) state a settlement magnitude of about 40% of the original MSW fill thickness under own weight. It is obvious that settlements will vary significantly depending upon the degree of compaction applied to the MSW at the time of waste placement. The use of modern waste compactors with a mass ranging from 10 to 40 metric tons in newly constructed landfills results in considerably higher waste densities than in the past. Consequently, the disposal capacity is maximised, and lower total settlement of MSW is achieved. Total settlements increase with the percentage of decomposable materials in MSW. Conversely, increasing amounts of inert material tends to decrease settlements to lower magnitudes. Decomposition is strongly dependent upon moisture conditions and landfill operating procedure. Accurately predicting waste settlements allows landfill personnel to control or mitigate potential damage to landfill facilities, optimise performance of bioreactor cells, and plan and provide for long-term land use. Existing landfill settlement models are far from reliable. Their predicted total settlements can be significantly in error, they need site-specific calibration and work best when based on total settlement obtained via observations. The ever-changing waste stream and landfill operating techniques will provide significant challenges for all involved in prediction of landfill settlement.

Waste settlement also affects on the side slope lining system as stated by Jones and Dixon (2005). They note that for landfill lining systems using geosynthetics, stability and integrity are both influenced by the shear strength between the various interfaces, i.e. geosynthetic/geosynthetic and geosynthetic/soil. The shear strength developed at a geosynthetics interface is dependent on both the normal stress on the interface, displacement at the interface and the materials' frictional characteristics. For landfill side slopes the waste plays an important role in the magnitude and distribution of the shear strength mobilised at these interfaces. The high compressibility of waste and degradation processes result in large settlements within the waste body and hence significant displacements occur adjacent to the lining system, which could lead to an integrity failure, i.e. a geomembrane failure (Figure 2-60).

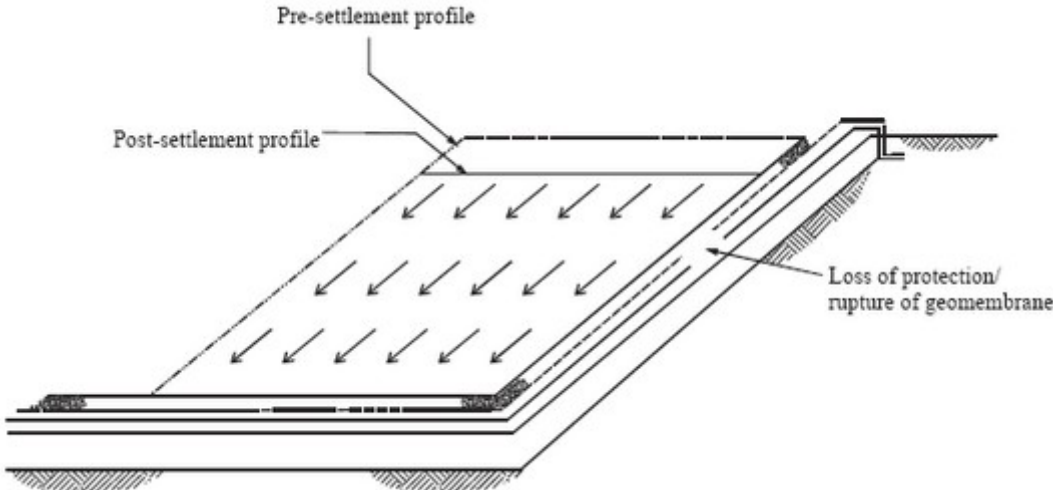

Figure 2-60 Stability and integrity failure of landfill lining systems: Serviceability limit state-integrity failure (Jones and Dixon, 2005).

As McDougall and Pyrah (2001) stated, settlement refers to the overall volume reduction in the most general sense experienced by a particulate material such as soil. It will evidence itself as a general depression of the site surface or, in the case of differential settlement, as pronounced hollows and humps that can be easily measured by simple surveying techniques. In conventional soils, the particles themselves are usually considered to be incompressible so that settlement is due to a reduction in the volume of void space produced by load-induced rearrangement or creep of the particulate structure. With this conceptual model of the settlement process, geotechnical engineers have developed powerful tools for analysing and predicting settlement in conventional soils. These tools have been applied to landfill settlement, with some success.

2.3.2 Settlement Phases and Influences

Edil *et al.* (1990) provide some factors affecting the magnitude of settlement, which are many and are influenced by each other. These factors include:

1. Initial refuse density or void ratio;
2. Content of the decomposable materials in the refuse;
3. Fill height;
4. Stress history;
5. Leachate level and fluctuations thereof; and
6. Environmental factors (such as moisture content, temperature and gases present or generated within the landfill).

It is remarked that refuse settles substantially both under its own self-weight and the weight of a new load (for example, the placement of new refuse over existing refuse). A factor complicating the computation of stress changes due to these weights is the introduction of cover soil to refuse fill. The addition of cover soil makes the measurement and interpretation of unit weight values more difficult. As a result, two types of refuse unit

weight are defined by Edil *et al.* (1990), which are the actual refuse unit weight (weight of refuse per unit volume of refuse) and the effective refuse unit weight (weight of refuse plus cover per unit volume of landfill).

According to Fassett *et al.* (1994), the compressibility of MSW has been studied since the 1940's. The earlier work focussed on the behaviour and suitability of landfills for construction sites; as the practice of sanitary landfilling became widespread, researchers were interested in improving the efficiency of waste placement. The general findings of these reports (earliest works) are:

1. The majority of the settlement occurred quickly;
2. Increased compaction can reduce total settlement; and
3. Settlement under loads decreases with age and depth of MSW.

Gasparini *et al.* (1995) determine different phases of deformation in a theoretical test of compressibility on a waste mass:

1. Initial settlement combined with a quick application of external loads;
2. Discharge of hydraulic over-pressures combined with a loss of liquid parts on the part of waste;
3. Final settlement of the stable section of waste at the end of decomposition processes.

Bowders *et al.* (2000) generally distinguish between load induced mechanical settlements and time dependent settlements such as encountered in MSW. The mechanisms governing domestic waste settlement are numerous and complex. The extreme heterogeneity of the wastes, their own "particle" deformability, the large voids present in the initial refuse fill, and their biodegradation play important roles in this complex process. The settlement behaviour of MSW is often classified as occurring following several distinct phases. These phases quoted by various authors are as follows:

1. Physical compression and creep due to mechanical distortion, bending, crushing and reorientation.
2. Ravelling settlement due to migration of small particles into voids among large particles.
3. Viscous behaviour and consolidation phenomena involving both solid skeleton and single particles or components.
4. Decomposition settlement due to the biodegradation of the organic components.
5. Collapse of components due to physico-chemical changes such as corrosion, oxidation and degradation of inorganic components (residual deformation).

From the findings of a literature review Barriera *et al.* (2001) show that the parameters contributing to settlement of reclamation solid waste landfills are the underlying subsurface conditions beneath the landfill, the method of site formation, the sequence of

landfill development, the waste age, the waste composition, waste compaction and the rate of decomposition. However, trends indicating a correlation between settlement and waste compaction and waste decomposition are inconclusive from the analyses undertaken. Three main stages of settlement have been identified: initial compression, primary compression, and secondary compression. Initial compression is settlement that occurs directly when an external load is applied to a landfill. It is generally associated with the immediate compaction of void space and particles due to a superimposed load. This stage is virtually instantaneous.

Jessberger (2001) cite three modes of MSW settlement:

- Consolidation (effective stress change) refers to settlement resulting from the dewatering of the freshly deposited saturated materials
- Shrinkage (decomposition of organic material) is the process by which organic solids and moisture are gradually decomposed and converted to carbon dioxide and methane, resulting in a corresponding decrease in the volume of the fill.
- Compaction (overburden) is defined as the reorientation of solids into a denser configuration due to gradual loss of rigidity in solids from the creep of solids under overburden or from solid decomposition. It is suggested that such waste solids may initially "build bridges" across voids, but later on collapse, which indeed may be judged to be potentially the most significant feature or settlement of sanitary fills.

Additionally, Jessberger (2001) states that the mechanism within the waste is the one phenomenon that can be most reliably modelled from basic soil mechanics principle and practice. Prediction of the time factors and magnitude of consolidation and its impacts is generally borne out by actual field measurements and data.

Table 2-13 relates the definition of the different settlement phases quoted by Bowders *et al.* (2000), Barriera *et al.* (2001) and Jessberger (2001).

Table 2-13 Settlement modes and phases after different authors

Bowders *et al.* (2000)	Barriera *et al.* (2001)	Jessberger (2001)
Physical compression and creep	Initial, primary and secondary compression	Compaction
Ravelling settlement	Primary and secondary compression	Compaction
Viscous behaviour and consolidation phenomena	Primary and secondary compression	Consolidation, compaction
Decomposition settlement	Secondary compression	Shrinkage
Collapse of components	Secondary compression	Shrinkage, compaction

2.3.3 Duration and Magnitude of the Main Settlement Phases

Edil *et al.* (1990) state the characteristic irregularity of refuse fill settlement. Initially, there is a large settlement within one or two months of completing construction, followed by a substantial amount of secondary compression over an extended period of time. The magnitude of settlements decreases over time and with increasing depth below the surface of the fill. Under its own weight, refuse settlement typically ranges from 5 to 30 percent of the original thickness, with most of the settlement occurring in the first year or two.

For Fassett *et al.* (1994), it is usually assumed that traditional soil mechanics theories of compressibility also apply to MSW; therefore, in general, the same parameters are used. Settlement is generally considered to consist of three components (Holtz & Kovacs, 1981), which immediate and consolidation settlement and creep:

$$S_T = S_i + S_c + S_s \qquad \text{Equation 2-8}$$

S_T = Total settlement
S_i = Immediate settlement
S_C = Consolidation settlement
S_S = Secondary compression or creep

Settlement of MSW resulting from increased loads initially occurs rapidly, typically within the first three months. Waste settlement appears to be similar to that of peat soil in which, after immediate and consolidation settlement, additional settlement is primarily due to long-term secondary compression. Because the consolidation phase is completed so rapidly, it is generally lumped together with the immediate settlement and called "primary settlement". However, unlike peat deposits, the secondary compression of MSW includes important decomposition content.

Gotteland *et al.* (1995) state that the sum of the different settlements: instantaneous, primary and secondary can reach 25% of the initial thickness of a repository. The measurement performed on site cannot lead to precise, quantitative conclusions, but allow qualitative judgements on the material evolution. Green and Jamnejad (1997) conducted laboratory experiment, which show that when a column of domestic waste is subjected to a static load, more than 70% of the total settlement takes place immediately, with 30% of the settlement is over a longer period of time. The magnitude of the waste settlement depends upon the thickness of the waste layer, magnitude of the load and composition of the waste. The extent of the settlement due to a constant load increment decreases as the total applied load and density increases. This is why it is important to know the composition and density of the waste, so that the specific settlement characteristics can be applied to be able to predict it's future settlement.

De Poli *et al.* (1999) stress that the settlement of a landfill has two main effects: the short time deformation of the compressible inerts, and the decomposition of organic matter (paper included), with the production of biogas. The first effect appears in a short time, and is mainly correlated with the compaction of the waste during the disposal, and with the weight of the new layers of waste disposed above. It can occur in 2-12 month. The

decomposition of organic matter reduces the total mass of the waste by 1/3, in a period of 15-20 years. Barriera *et al.* (2001) state that the highly variable nature of the waste and underlying soft deposits, coupled with the variable site formation and ground improvement works, make the prediction of settlement of a reclamation solid waste landfill extremely difficult. The solid waste has an inherent heterogeneity and anisotropic material properties that are more difficult to characterise than soil. However, it is usually assumed that traditional soil mechanics theories of compressibility also apply to solid waste fill and in general the same parameter are used.

Jessberger (2001) quotes settlement measurements carried out in the USA and states different amounts of settlement across the landfill. At this particular landfill it varies from 15 to 20% in the central portions of the fill and decreases rapidly at points along the sides. He concludes that final settlement of waste is characteristically irregular. Initially, there is a settlement within a short time completing construction, followed by a substantial amount of secondary compression over an extended period of time. The rate of settlement decreases over time and with increasing depth below the surface of the fill. Under its own weight, waste settlement typically ranges from 5% to 30% of the original thickness with most of the settlement occurring in the first year or two.

In addition, Richard *et al.* (2001) note that instantaneous settlement is observed even when there is no loading direct of the material column. This settlement is induced by the overload due to the circulation of the trucks on the track of access, the many passages of the compactor to compact the higher layers, with the weight of the layers of waste acting on the lower layers, and also with pushed grounds and waste located at the upstream part of the landfill (site of storage inclined).

2.3.3.1 Primary Settlement (Compression)

McDougall and Pyrah (2001) point out that load induced or primary settlement in landfills, which is considered to be relatively short-lived by comparison to the type of consolidation settlement that occurs in conventional fine-grained soils, has been investigated by many workers, e.g. Jessberger & Kockel (1993), Watts & Charles (1990), Beaven & Powrie (1995). In general, the compressibility of waste varies considerably depending on the composition, age and compaction effort; it also decreases significantly with applied load.

With granular fills (and, indeed, poorly compacted unsaturated fills of all types) primary compression occurs immediately after a load is applied and consequently the major part of compression due to self-weight occurs as the fill is placed (Charles and Burland, 1982). Studies previously conducted indicate that there is usually a large amount of primary consolidation during the initial one to three months after the waste is placed. But due to the fact that the load constantly increases while filling and the filling of landfills can take a couple of years, no unique time of load application exists. The rapid nature of primary consolidation suggests that the initial consolidation settlement occurs during the filling operation and is rarely apparent in operating solid waste landfills as in earth fill projects.

Similar to Charles and Burland (1982), Coumoulos and Koryalos (1999) and El-Fadel *et al.* (1999) observe considerable settlement occurring during the first one or two months

after closure of the landfill. The causing effect is rapid dissipation of pore fluid and gas through the voids because of the high permeability of waste, which is characterised as "primary compression". Initial compression of landfilled MSW in response to self-weight or application of fill or surcharge loads occurs relatively rapidly and is essentially complete in 10 to 90 days as noted by Bowders *et al.* (2000).

An algorithm of settlements calculation was elaborated by Richard *et al.* (2001). A column of waste, height H, is cut in several elementary layers with height h_i, whose history of the stages of implementation of waste is supposed to be known. To each one of these elementary layers, the medium effective overload corresponding to the self-weight of the higher part of the column is applied:

$$\sigma'_{0i} = \frac{\gamma_i * h_i}{2} + \sum_{j=i+1}^{n} \gamma_j * h_j \qquad \text{Equation 2-9}$$

n = number of layers
i = index of the layer considered
γ = unit weight (kN/m^3)
h = height

Primary settlements Δh during the installation of materials and the cover were estimated starting from the formulation (Sowers, 1973), for an overload $\Delta\sigma$ applied to waste.

Primary settlement Δh_1 is given by:

$$\Delta h = \sum_i \Delta h_i = C_R * \sum_i h_i * \log \frac{\sigma'_{0i} + \Delta\sigma'}{\sigma'_{0i}} \qquad \text{Equation 2-10}$$

C_R: primary compression ratio, in conformity with the values usually retained (Gotteland *et al.*, 2001).

2.3.3.2 Secondary Settlement (Consolidation)

Charles and Burland (1982) see significant further movements occurring under conditions of constant stress and moisture content. This can be termed 'creep' settlement. For many waste fills it is found that creep compression shows a linear relationship when plotted against the logarithm of the time that has elapsed since the waste deposit was formed. Fassett *et al.* (1994) state that the most important cause of secondary settlement is generally believed to be volume reduction due to decomposition of organic matter, but this view is largely unsupported at this time. The additional influence of decomposition is regarded to have large impact on secondary compression in terms of duration and magnitude.

According to Powrie *et al.* (1998), there is a considerable uncertainty regarding the secondary compression of waste, which is understandable in view of the various factors that are known to influence its eventual magnitude. These include:

- The composition of the waste, as wastes with a higher proportion of degradable (principally organic) materials will be more susceptible to long-term settlement due to decomposition than wastes containing predominantly inert materials;
- The as-placed dry density of the waste: for a given degradable fraction, a given mass of compacted (i.e. denser) waste would be expected to have less potential for mechanical volume loss and hence long-term settlement - typical dry densities of wastes can be found in Beaven & Powrie (1995);
- The depth of the fill material: for a given waste type and density, the potential loss of volume or mass on degradation is roughly proportional to the original volume or mass of waste, so that in absolute terms deeper landfills would be expected to exhibit greater settlements.

The rate of waste degradation in the long-term depends primarily on the composition of waste, its water content and the rate at which water passes through it. Forced gas extraction may also influence the rate or pattern of degradation, e.g. larger settlements tend to occur around gas extraction wells. Waste already emplaced within a landfill will undergo compression as further refuse is deposited on top. This means that the volume of waste placed will in general be greater than the final volume of the landfill, even allowing for secondary compression due to degradation etc.

For El-Fadel *et al.* (1999), the contribution of biodegradation to settlement can be understood by considering the amount of solid carbon that can biodegrade, the rate at which it degrades and the relation between lost mass and settlement. Since biodegradation occurs mainly during the secondary compression stage, it is suggested that it increases the rate of secondary compression. Thus, if biological processes are enhanced, the time required for stabilisation will be reduced. They define secondary compression as being generally due to creep of the refuse skeleton and biological decay.

Sharma *et al.* (1999) quote Sowers' method estimating secondary compression by using the following equation:

$$S_s = h * C_\alpha * \log\frac{t_2}{t_1}$$ Equation 2-11

S_s = secondary compression occurring in the considered
h = initial thickness of considered waste layer
C_α = secondary compression index
t_1 = starting time for the long-term time period under consideration
t_2 = ending time for the long-term time period under consideration

According to Bowders *et al.* (2000), the phase of secondary compression lasts over an extended period of time and accounts for a substantial amount of the overall settlement. This phase is usually related to the biodegradation process, which takes years to reach completion with the specific rates varying widely depending upon characteristics of landfill site and the MSW it contains. The biodegradation component of long-term (secondary)

compression, or bio-consolidation, is due to a four-stage process by which solid organic particles in the waste are solubilised and converted through methanogenesis to methane and carbon dioxide. It is thought that this reduction in solids directly relates to an increase in the magnitude and rate of secondary settlement. For Barriera *et al.* (2001) also, the secondary compression accounts for the majority of the total solid waste landfill settlement and can take place over many years. Secondary compression of waste is easily observed at a closed or inactive landfill, when the primary consolidation of the waste has been completed and the waste is subjected to a constant load. It is generally believed that the most important cause of secondary settlement is volume reduction due to decomposition of organic matter.

McDougall and Pyrah (2001) define secondary settlement as being predominantly a combination of mechanical creep, physico-chemical corrosion and biodegradation. Mechanical creep can be adequately modelled using 'log-time' methods and physico-chemical corrosion may be considered as mainly time-dependent. It may also be expedient to deal with biodegradation in the same way in a dry entombment installation where the internal environment after capping is relatively stable. However, despite the revision and refinement of conventional geotechnical approaches, there remains a shortcoming in their applicability to waste refuse. The presence of a solid organic fraction and the many factors that control its decomposition are not properly accounted for in existing geotechnical models. Since more than half of the total settlement in landfill can be attributable to secondary settlement, and total settlement ranges between 25% and 50% of initial fill height, this is a potentially costly shortcoming. If the geotechnical analysis of landfill settlement is to be improved, then a more fundamental approach to biodegradation related settlement should be adopted.

Secondary settlement is indicated by Richard *et al.* (2001), as follows:

$$\Delta h = \sum_i \Delta h_i = \int_{t_1/2}^{t_2 - t_1/2} a - b * \log(t) dt \,, \qquad \text{Equation 2-12}$$

where a and b are a function of h_i. Richard *et al.* (2001) remark that the approach suggested remains theoretical and in respect to the complexity of the phenomena of settlement of waste, the observation of the behaviour of the real site and confrontation with estimated calculations appeared suitable.

2.3.4 Parameter Describing Compression and Settlement Behaviour

2.3.4.1 Compression Index C_C

C_C describes the slope of the normal compression line, i.e. the ratio between void ratio increment Δe and logarithmic normal stress ratio σ'_1/σ'_0 = $\log\Delta\sigma'$. The normal compression line is found to be mainly a straight line. The initial curved part is representative of pre-consolidation. The greater the length of the initial part is, the greater is the amount of over-consolidation (Whitlow, 1983).

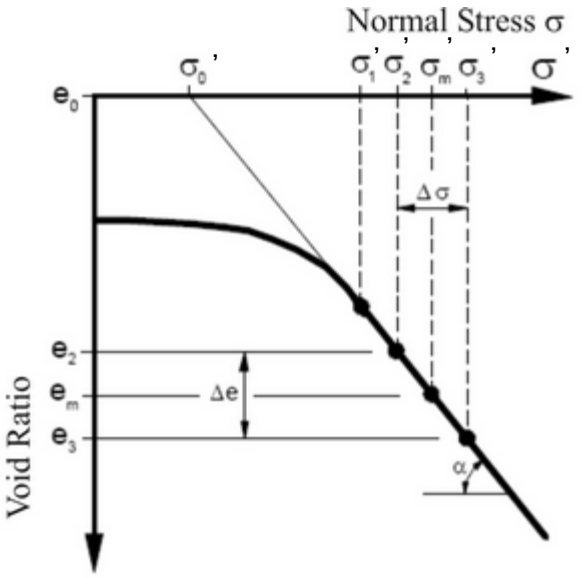

Figure 2-61 Definition of the primary compression index

$$C_c = \frac{\Delta e}{\log \Delta \sigma'}$$ Equation 2-13

Andersland *et al.* (1981) reveal that the compression index C_C varies significantly with stress level and organic content of the soil. Decomposition, in model organic soil, also decreases the compression index and stresses the research on loss of soil solids and the related effect on settlement.

Edil *et al.* (1990) also refer to the compression index. Settlement due to compression of refuse fill under external surface load can be plotted in terms of strain (ratio of settlement to initial fill height) versus the logarithm of effective stress (pressure). Settlement magnitude can be predicted based on the settlement coefficient, the slope of the straight line connecting two selected stresses. The problems with this method include:

1. For older fills, the initial height is usually unknown;
2. Effective stress is a function of refuse density, which usually cannot be determined accurately; and
3. The strain-log stress relationship is not a straight-line relationship;

Therefore, the settlement coefficient, which is proportional to settlement magnitude, varies as the stresses (pressures) within the fill change.

Fassett *et al.* (1994) quote Sowers (1973), who examined settlement of landfills. Sowers (1973) related C_c to the initial void ratio and organic content of waste; his data indicated that C_c falls between the range of $0.15e_0$ for MSW with low organic content and $0.55e_0$ for MSW high in organic matter. Considering organic waste types (e.g. kitchen and garden waste), high organic content can mean high compressibility.

Gabr and Valero (1995) present results from small-scale compression tests (conventional equipment) on old waste samples (15 to 30 years old), yielding values of C_C that ranged from 0.4 to 0.9 for a void ratio of 1.0 to 3.0.

Machado *et al.* (2002) conducted confined compression tests with different MSW samples. From the results, it can be observed that the curves are almost parallel and concave upwards, which suggests that the compression index C_c is void ratio dependent. By adjusting straight curves in the stress interval between 60 and 640kPa it was possible to calculate the primary compression index, which varied between 0.52 and 0.92. C_c is lower for lower MSW void ratios, which confirms the interdependence of C_c and e. Those values for C_c are similar to the ones reported by Sowers (1973) and Gabr and Valero (1995).

2.3.4.2 Primary Compression Ratio C_R or Modified Compression Index (C_c')

When volume change is expressed as vertical strain instead of change in void ratio, the gradient of the virgin compression part of the ε versus log σ' curve is the compression ratio, C_R, defined as:

$$C_c' = C_R = \frac{\Delta h}{h_0 * \log\frac{\sigma_2'}{\sigma_1'}} = \frac{\Delta \varepsilon}{\log\frac{\sigma_2'}{\sigma_1'}} = \frac{C_c}{1+e_0}$$ Equation 2-14

Beaven (1993) draws the following conclusion from results of field tests and preliminary results of large-scale compression cell. Considerable settlement or compression of wastes can occur as a result of surcharging existing wastes with new layers of refuse. A compression ratio (C_R) of 0.2 to 0.25 was determined within a large compression cell for untreated domestic refuse.

Gabr and Valero (1995) note that differences in C_C' values obtained by Landva and Clark (1990) and those measured in this study are not significant despite the difference in the consolidometer sizes. Landva and Clark reported variations of C_C' (the gradient of the compression versus the log time curve) between 0.2 and 3.0% per log cycle of time, while C_C' values measured in this study varied between 0.8 and 0.9% per log cycle of time.

Bowders *et al.* (2001) measured waste settlements in a landfill cell being actively filled. The initial lift (2.6m) of waste settled 0.4m over 18 months while the overburden above the layer increased to 8m. The second lift (5m thick) compressed 0.2m over 9 months while the overburden pressure increased to an equivalent of 3m height. The settlement in the active cell is best correlated to simple compression of the waste due to self-weight and overburden stress. The compression ratios for these two lifts of waste were calculated and found to be 0.22 for the initial lift of waste and 0.05 for the upper lift placing these in the category of highly compressible and slightly compressible media as compared with soil.

Machado *et al.* (2002) report values found for C'_c, which are near the lowest value reported by Landva and Clark (1990) when they tested MSW from Canada in a large compression cell.

Landva and Clark (2000) report values of about 0.17 to 0.24 from laboratory tests on artificial and aged refuse. They also report values from literature in the range of 0.09 to 0,41.

2.3.4.3 Coefficient of Secondary Compression C_α

The coefficient of secondary compression describes the ratio between the increment of the void ratio and the logarithmic increment of time.

$$C_\alpha = \frac{\Delta e}{\Delta \log t}$$ Equation 2-15

Edil *et al.* (1990) quoted Yen and Scanlon (1975) comparing their data with Sowers' field observation and noting that the rate of settlement decreases with time logarithmically. Sowers noted the time-dependent secondary compression of refuse and reported values of the coefficient of secondary compression for some sanitary landfills. Sowers noted that the values for refuse were comparable to those of peat and organic soils and dependent on how favourable the conditions were for decomposition.

This parameter is thought to change during creep and with chemical and biological degradation of the waste. From limited data available at the time, Fassett et al. (1994) quote Sowers, who also developed relationships between C_α and e_0:

$C_\alpha = 0.03e_0$ for conditions unfavourable to decay; and

$C_\alpha = 0.09e_0$ for conditions favourable to decay

Coumoulos and Koryalos (1999) see the accuracy of predicting the attenuation of vertical strain rates depending on the accuracy of the coefficient of secondary compression C_α. If time data are available and the data of closure is known, then C_α can be determined from the secondary compression part of the settlement curve. The Authors developed a method for determining C_α for the cases where the date of closure is not known as it happens with old landfills. Jessberger and Kockel (1993) carried out large-scale consolidation tests on 15-year-old untreated municipal solid waste. A C_α value equal to 0.06 can be derived from their time-settlement curves. The majority of the reported values of C_α under self-weight fluctuate between 0.02 and 0.07. On the basis of the above discussion, it is important to determine the coefficient of secondary compression C_α on the basis of observations of the actual behaviour of waste column under consideration. Published values of C_α should be used with caution. It is of interest to compare C_α values for soils with those associated with the long-term compression of solid waste under self-weight.

Normally consolidated clays C_α = 0.005 to 0.2

Organic soils C_α = 0.03 or higher

Gabr and Valero (1995) present results from the six consolidation tests, yielding values of C_α that ranged from 0.03 to 0.009 for the initial void ratio, e_0, range of approximately 1.0 to 3.0.

Sharma *et al.* (1999) mention values for C_α for refuse having been estimated to be similar to peat. Recommends for C_α are quoted ranging from 0.02 to 0.07 for landfills between 10 and 15 years old. Oweis and Khera (1990) recommend C_α values between 0.01 and 0.04. The secondary compression index (C_α) should be near the lower range of the values cited in the literature as discussed above. A value of C_α = 0.02 would, therefore, be more appropriate for the refuse. Since primary settlement of the waste is completed within one to four months of the fill (either self-weight or superimposed loads) the main source of long-term settlement would be the secondary compression of the waste. Once C_α is known for a refuse, the long-term settlements can be estimated for a particular time interval. Machado *et al.* (2002) found an accentuated secondary compression process (creep) arising just after the beginning of the test (about 15s) and the deformation readings turn out to be linear function of the logarithm of time. The C_α [$C_\alpha = \Delta e/\Delta \log(t)$] values obtained for the MSW range from 0.021 to 0.044, with an average value of 0.032.

2.3.4.4 Secondary Compression Index $C_{\alpha\varepsilon}$

In soil mechanics, the secondary compression index is also called the rate of secondary compression. It is defined as:

$$C_{\alpha\varepsilon} = \frac{\Delta h}{h_0 \log \frac{t_2}{t_1}} = \frac{C_\alpha}{1 + e_\alpha}, \qquad \text{Equation 2-16}$$

where e_α = void ratio at start at the linear portion of the e/log t curve (Whitlow, 1983)

Fassett *et al.* (1994) mention the secondary compression index, which is used to estimate the settlement that occurs after completion of the primary settlement, while the waste is subjected to a constant load. This parameter is thought to change during creep and with chemical and biological degradation of the waste. The most widely reported compressibility parameter is the modified secondary compression index, $C_{\alpha\varepsilon}$. Therefore the discussion will focus on this parameter. The reported values of $C_{\alpha\varepsilon}$ range from 0.001 to 0.59. The lowest value represents the compressibility of a landfill, which had been subjected to dynamic compaction. For typical landfills the lower limits of $C_{\alpha\varepsilon}$ is generally around 0.01 to 0.03. This compares to 0.005 to 0.02 for common clays. The typical upper limit of $C_{\alpha\varepsilon}$ appears to be approximately 0.1.

In an earlier publication Fassett published an attempt to examine what effect various parameters (including unit weight, waste thickness, and compaction effort) have on $C_{\alpha\varepsilon}$. The findings of this endeavour include the following:

- Little correlation was evident between $C_{\alpha\varepsilon}$ and unit weight;
- A rough correlation was found to exist between waste thickness and $C_{\alpha\varepsilon}$; and
- The available data showed no relationship between compactive effort and $C_{\alpha\varepsilon}$.

$C_{\alpha\varepsilon}$ would be expected to decrease with increasing unit weight, provided the higher unit weights were achieved by compaction. The fact that little correlation was obtained

between $C_{\alpha\varepsilon}$ and unit weight suggests that settlements also contributed to increases in unit weights.

According to Yen & Scanlon (1975), the settlement rate of waste increases with depth, hence larger values of $C_{\alpha\varepsilon}$ should be associated with thicker fills. Yen & Scanlon's observations indicated that this effect levelled off at about 27m. It was suggested that below this depth condition within the landfill limited the biological activity to anaerobic decomposition, which is much slower than the aerobic decomposition believed to occur in shallower fills. However, evidence suggests that anaerobic decomposition may be the dominant reaction even at shallow depths. Long-term compressibility of MSW would be expected to decrease with increasing compaction effort. However, as mentioned above, no such trend is evident with the available data. This is due to the limited number of data points available and the unclear relationship between reported values of $C_{\alpha\varepsilon}$ and the actual settlement rate.

For Fassett *et al.* (1994), values of $C_{\alpha\varepsilon}$ are dependent on the values used for e_0 or h_0. $C_{\alpha\varepsilon}$ is also dependent on stress level, time, and how the origin of time is selected. The filling period of landfills is often long and should be taken into consideration for settlement rate analyses (Yen & Scanlon, 1975). Watts and Charles (1990) show time settlement curves developed for two sites using different criteria for selection of the zero time. The zero time selection is seen to have a large impact on $C_{\alpha\varepsilon}$ particularly during the earlier times. An additional problem with determining $C_{\alpha\varepsilon}$ is the fact that it is not generally constant. Bjarngard and Edgers (1990) cited by Fassett *et al.* (1994) present settlement log-time data from 24 case histories. The majority of the curves show a relatively flat slope (i.e. low $C_{\alpha\varepsilon}$ values) at small times, but at larger times the slope greatly increases. They attributed the higher slopes in the later stages of compression to increasing decomposition, but it may simply be an artefact of the log-time scale. It is certain that decomposition of MSW will affect its compressibility. However, to date, the relative contribution of mechanical compression, thermal effects, and biological decomposition to the total settlement has not been adequately addressed.

Green and Jamnejad (1997) found the internal stresses of the waste displaying linear trends with increased surface stress, with the compaction occurring throughout the whole column of waste. The secondary settlement gradients varied from 0.01 to 0.08, which confirms the result of Oweis and Khera (1990) that the secondary compression gradients for waste that varied from 0.02 to 0.072. El-Fadel *et al.* (1999) mention that the secondary compression index ($C_{\alpha\varepsilon}$) is proportional to initial void ratio and favourable decomposition conditions. Bowders *et al.* (2001) measured settlements in two different old cells (21m of overburden), which can best be correlated with degradation of organics in the waste. The modified secondary compression index (secondary compression ratio) was determined to be 0.0025. Machado *et al.* (2002) report values varying between 0.012 and 0.016 for the modified compression index, with an average of 0.013. These values are lower than those found by Sowers (1973) and by Gabr and Valero (1995), and conform more to the data published by Landva and Clark (1990).

2.3.4.5 Modulus of Elasticity (Young's Modulus)

"*The relationship between the stress and the strain that it causes is termed the stiffness of the material. A material is said to be elastic when the same amount of strain is caused at the same level of stress regardless of whether or not the material has been loaded or unloaded beyond this point. The slope of the stress/strain curve is termed* […] *Young's modulus.*" (Whitlow, 1983)

$$E_s = \frac{\Delta\sigma}{\Delta\varepsilon}$$ Equation 2-17

Soil stiffness modulus as measured in a one-dimensional compression test under static load and with radial support is named odometric modulus or constrained modulus D or M. It is a tangent modulus and represents the volumetric stiffness of the soil that varies with density and stress level. Moreover, values from first loading and values differ considerably.

According to Jessberger *et al.* (1990) the modulus of elasticity is varying between 0.3-3.0MPa in literature. From their test results values between 1MPa and 4MPa were calculated. Green and Jamnejad (1997) determined modulus of elasticity for household waste of 0.7MPa; this confirms Watts and Charles' (1990) suggestion that E_s for waste is generally just smaller than 1MPa.

The geotechnical recommendations for landfills and contaminated land (GDA) of the German Geotechnical Society (DGGT, 1997) give an approximate equation for the modulus of elasticity (Equation 2-18). From 21 large-scale odometer tests a linear relationship between stress σ>50kPa and E_s was deduced. The parameters a and b have been determined. Parameter "a" is varying between -294kPa and -106kPa and "b" between 10.9 and 12.5.

$$E_s = a + b * \sigma \quad [kPa]$$ Equation 2-18

Jessberger (2001) notes that the modulus E_s is derived from the virgin compression and therefore only yields information on settlements of waste that never before has been subjected to loads higher than of those applied in the tests.

Dixon *et al.* (2004b) conducted field measurements resulting in values between 0.3 and 2.0MPa. Similar values of 0.2 to 2.5MPa are reported by Landva *et al.* (2000), Beaven and Powrie (1995) and Powrie and Beaven (1999), who conducted large-scale test in the Pitsea compression chamber resulting in modulus of 0.3 to 4.5MPa.

2.3.5 Methods of Measurement

To measure the compressibility resulting from an increase in load, Fassett *et al.* (1994) and Manassero *et al.* (1997) advice researchers having to use plate load tests, which are usually performed on top of landfills after closure once the final sealing cover has been installed, pressuremeters, and odometers. To measure the rate of settlement under constant load, surveying methods are most widely used. The settlements could be measured at different landfill levels so that the compression of the interlayered strata

would be analysed separately as Manassero mentions. This would already be an important improvement to the general settlement follow-up. Techniques include comparing aerial photos over time, surveying benchmarks on the landfill surface, and settlement platforms placed below earth embankments constructed on landfills. An additional technique is telescoping inclinometers. These devices allow measurements of settlement at various depths under both increases in load and constant load. Frequent readings during landfilling are needed to back-calculate separate values of C_c and C_α. Manassero *et al.* (1997) additionally mention more advanced techniques like spectral analysis of surface waves. The usual aim is to evaluate the bearing capacity for potential "constructional" use of the landfill area. In some cases, tests have been run during landfill operations, in order to analyse the mechanical behaviour of the waste material. To be meaningful, some tests have to be located on the weakest and some on the strongest areas of the fill.

Jessberger (2001) noted that it is important to draw attention to the fact that most of the results describe only the mechanical (effective stress change and overburden) settlement, degradation of the waste is not or only partly considered. One alternative to evaluate compression tests is the ε-σ-diagram and the determination of the compression index C_c from the inclination of the curves in half-logarithmic scale. These results of Landva & Clark (1990) on compressed old waste (age unknown) from different sites in a 0.5m diameter consolidometer show the high compressibility of the waste. Jessberger & Kockel (1993) used a large-scale (= 1m) compression cell to test a 15 years old, untreated municipal solid waste. The investigation of time dependent settlements seems to be very difficult under laboratory conditions. More representative and closer to reality are field measurements. These measurements include all factors and interactions dominating the settlement behaviour. But the transfer of the behaviour observed on one special landfill to other landfills or to general statements has to be carefully discussed.

2.3.6 Summary of Compression Behaviour

Settlement of landfills is a well-analysed area of waste mechanics. Especially for volume management of landfills research about compression behaviour of MSW is of high interest, as settlement means the reduction of volume and thus new space for waste deposits is generated. Various researchers have examined the behaviour of waste bodies in a landfill and in laboratory tests, respectively, under surcharge. Two general types of settlement processes are distinguished, which is the primary settlement (compression) mainly depending on applied stress and the secondary settlement (consolidation) mostly caused by time-dependent processes, e.g. degradation.

The specific values for describing settlement behaviour have been summarised. For primary settlement, primary compression index C_c and the modified coefficient of compression C_c' (C_R) are often used, for the secondary settlement the parameters C_α (coefficient of secondary compression) and $C_{\alpha\varepsilon}$ (secondary compression index) are frequently found. As a general parameter for stiffness the modulus of elasticity E_s and the constrained Modulus D is common.

In regard to determination of those parameters, load plate tests, back-calculation and oedometer tests rank amongst others. Generally, similar problems as for shear tests arise for waste as a testing medium. Its heterogeneity in terms of physical, mechanical and biological properties aggravate the assessment of commonly useable results. Factors such as composition, degradability, size, etc. influence compression behaviour and have to be known when acquiring and comparing data.

2.4 Classifications of Waste

2.4.1 Existing Waste Classification Systems for Mechanical Behaviour

Waste is often classified in terms of type, hazard perception or biologically active content but a geotechnical classification, i.e. a classification towards its mechanical properties is hardly found. A number of the existing classification systems are simply based on material groups (e.g., paper, plastic, metal, etc., Siegel *et al.*, 1990) or on the distinction between soil-like and non soil-like, or fibrous, appearance (Manassero *et al.*, 1997; Thomas *et al.*, 1999). These existing classification systems do not fulfil the requirements of a rigorous classification framework. Table 2-14 provides a summary of existing classification systems including the parameters defined. Key elements of these classification systems are considered further.

Table 2-14 Overview of existing classification systems

Author	**Basis for Differentiation**	**Parameters Used for Differentiation**
Turczynski (1988)	Waste type	Density, shear parameters, liquid/plastic limit, permeability
Siegel *et al.* (1990)	Material groups	Part of composition
Landva and Clark (1990)	Organic, inorganic materials	Degradability (easily, slowly, non) Shape (hollow, platy, elongated, bulky)
Grisolia *et al.* (1995)	Degradable, inert, deformable material groups	Strength, deformability, degradability
Kölsch (1996)	Material groups	Size, dimension
Manassero *et al.* (1997)	Soil-like, other	Index properties
Thomas *et al.* (1999)	Soil-like, non soil-like	Material groups

Landva and Clark (1990) proposed a classification system that differentiates between organic and inorganic components. They subdivided these into putrescible and non-putrescible within the organic components, and degradable (corrodible) and non-degradable within the inorganic components (Figure 2-62). Additionally, void-forming

constituents within each subdivision, excluding the putrescible group, are highlighted. This system provides detailed information on degradation and compressibility potential of components but does not consider component shape or material properties (e.g. tensile strength of components).

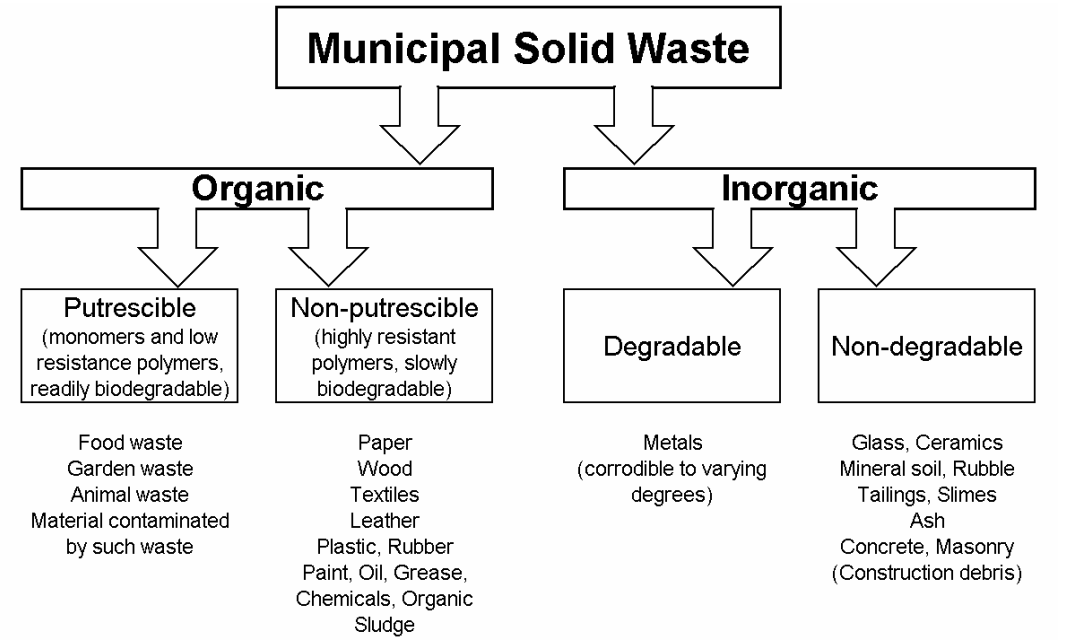

Figure 2-62 Waste classification (after Landva and Clark, 1990)

Grisolia *et al.* (1995) defined degradable, inert and deformable component groups and classified wastes by plotting the percentages of each group in a ternary diagram. This allows comparison of the composition of different wastes. A strength of this system is that it provides information about compressibility and degradability of components. However, it is possible for a component to fit into more than one group (e.g. food residues are biodegradable and highly deformable) and again particle shape is not considered.

Kölsch's (1996) classification system includes material groups, size and dimension of components. The advantage of this system is the possibility for a more detailed examination of component properties, which is consistent with the known large variability of waste component form and properties. The disadvantage is the large amount of data required and the omission of information on degradation potential. Such a detailed system is more appropriate for research purposes than regular practical use.

2.4.2 Findings from Existing Classification Systems

None of the existing systems fulfil the requirements for a rigorous waste mechanics classification. However, they provide useful criteria. The information required to classify waste components can be summarised as:

- A distinction is required between the material groups (i.e. based on typical component material properties), with dominant groupings established. Information is then required on the proportion (e.g. by weight) of different size components in each material group.

- Knowledge of component shape is required to distinguish between soil-like (three-dimensional e.g. granular) and non soil-like (two-dimensional e.g. sheet) components. This allows classification of components in relation to their potential for influencing mechanical behaviour of the waste mass (e.g. compressibility, shear and tensile strength).
- Grading by size is required for each group of components (size assessment of each component).
- An assessment of component compressibility and hence the potential for components to change shape during placement and/or burial.
- An assessment of degradation potential for both organic and inorganic components.

2.5 Findings of the Literature Review

Various researchers have examined the shear and compression behaviour of MSW. Generally, a large amount of data about shear strength and compression behaviour is available in literature, but due to the high number of parameters influencing mechanical behaviour of MSW and due to the fact that often more than one of these influences are present, a structured assessment of MSW mechanical behaviour from the literature is not possible.

For the comparison of data from shear tests, a uniform basis is not given, aggravating the problems arising from the variability of waste and its influences. Often, crucial information about boundary conditions of the test and the character of the tested material is not provided, leaving a comparison of data from different sources incomplete, and thus often dissatisfactory statements about waste mechanical behaviour are derived.

A structured analysis of real waste behaviour is not possible, as too many factors influence the mechanical character of MSW. For example, the composition of MSW is constantly changing, not only due to legislative and consumer-related factors, but also due to general heterogeneous character of waste. Repeatability results of tests on different samples from the same source are subject to fluctuation, producing a range in which possible behaviour can be found. It is still questionable whether this range of results is due to small compositional differences or other factors affecting waste mechanical behaviour.

It is therefore crucial to:

1. Find a uniform basis for the ability to compare data from different sources and incorporate the main influencing factors like waste composition, particle size, particle shape and degradability; and
2. Assess the mechanical behaviour of MSW in a structured way, i.e. examine preferably each influence individually to be able to identify their impact on waste mechanical behaviour.

A uniform basis could be provided by a waste classification as suggested by many authors. But to be able to compare data for mechanical behaviour a waste classification should be comprehensive to evaluate waste characteristics that are causing the mechanical behaviour. For the development of a geotechnical classification the findings in section 2.4.2 can be utilised.

To assess mechanical behaviour in shear and compression tests, there are generally two possibilities. The first possibility is testing real waste, which is meaningful for the simulation of real waste behaviour (provided that the sample amount is large enough to be representative). However, as mentioned before, due to the variability of waste, a thoroughly controlled testing programme is unrealistic, as a vast amount of factors influence the outcome. The second possibility could be a family of synthetic wastes with components, which reflect the mechanical properties of real waste components. The synthetic waste family has to be related to real waste and its properties. With the design of an engineered waste, thoroughly controlled tests are possible. In particular, the main factor, being the composition of waste, is controlled as the composition of the tested sample can be defined. For example, with the structured exchange of components, influences like reinforcement and compressibility could be examined individually. By altering the sample amount, the influence of unit weight could be defined. The influence of decomposition, and therefore of altering the size of components, could be assessed by adjusting the size ratios of the components involved.

In the following chapters an attempt is presented to implement a geotechnical classification and develop a family of synthetic wastes. Moreover, shear and compression tests on the synthetic waste were conducted and the results are presented and discussed.

3 Methodology

3.1 General Approach

For the implementation of the aims and objectives introduced in section 1.4, six work steps had to be fulfilled, which were interdependent to a certain degree. The literature review (factors influencing mechanical properties of MSW, waste composition and classification) and the sorting analysis created the cornerstones of the research, from which the waste classification resulted. In a next step the synthetic waste was derived from waste sorting, classification and literature review, before laboratory tests were conducted. Using the element tests, the synthetic waste and also the waste classification were validated.

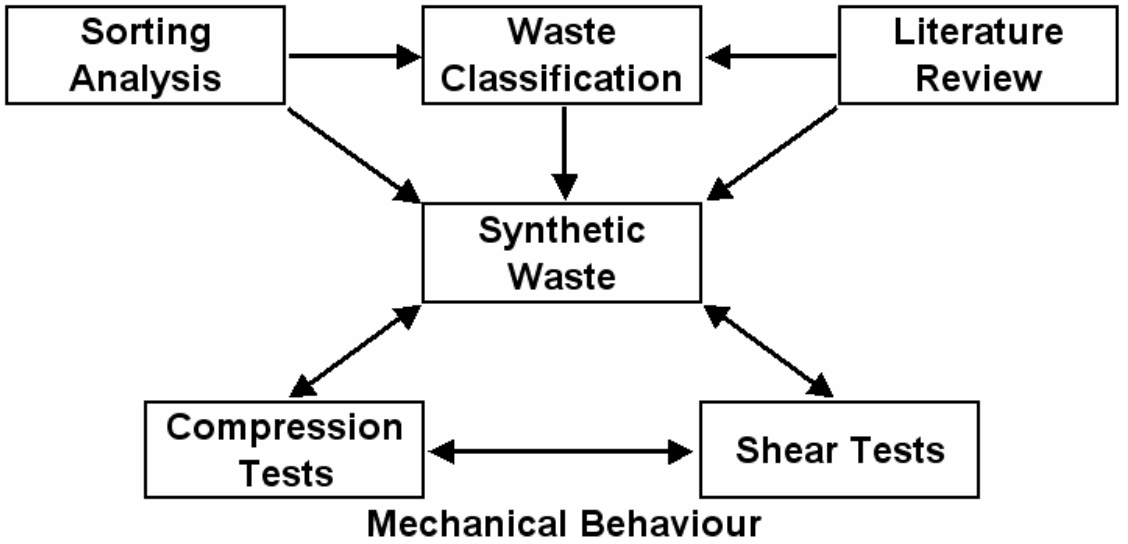

Figure 3-1 Interaction of work steps

3.2 Identification of Factors Influencing the Mechanical Behaviour of MSW

Literature published in journals and conference proceedings constitute a good source of knowledge. There is a variety of journals and conferences in the field of geotechnical and environmental engineering, all of which are easily accessible and thus very appropriate for finding answers to questions emerging from the subject processed in this work, due to the wide and comprehensive range of research.

To identify the factors influencing the mechanical behaviour of MSW literature provides a broad range of direct information from examinations conducted on waste, in particular tests done with focus on stability issues like shear strength and compressibility. But also other work was found, mainly on composition, pre-treatment, degradation processes, hydraulic properties, case studies of failures, legislation-related discussions, biogas evolution, modelling and statistic analysis, which often provided indirect information about waste mechanical behaviour. As obviously a variety of parameters an have effect on mechanical behaviour ten key issues were chosen for a structured and focussed review. These issues were:

1. Heterogeneity
2. Overburden
3. Composition
4. Reinforcement
5. Degradation
6. Placement
7. Index Properties
8. Structure
9. Component Size
10. Methods of Measurement

It is often not possible to isolate one factor to examine its direct impact on waste. Therefore, the main aspect emphasised in a scientific paper is considered.

3.3 Development of a Geotechnical Classification System

As the results from the literature review in section 2.2.3 show, a common basis for comparing results from different tests and various boundary conditions is not existent. It was therefore crucial to find a framework for a geotechnical classification, which comprises the key aspects for a waste classification, i.e. the key factors influencing mechanical behaviour and the characteristic properties of MSW. In a following stage, key classification issues had to be defined to complete the system. For the justification of the system, laboratory shear and compression tests had to be conducted with synthetic waste, which is based on the classification system in association with the study on composition of waste, and the results derived from these tests had to be evaluated by means of existing results for real waste with comparable composition.

An aim of the classification system is the adaptability to cover all types of solid wastes. Assumptions had to be made about the compressibility and about the degradability of waste components. These assumptions had to be proven by data. In case they are inaccurate or wrong they had to be corrected and adapted. The system has to be able to reveal the class of waste in every stage of its degradation or mechanical process. The classification system should be able to not only classify the components, but also the behaviour of the waste mass. The choice of the parameters of the system also had to be verified. They had to be checked whether they were really meaningful in practice. Existing frameworks were not applicable for practical purposes. For easy access, a practical classification strategy had to be developed.

3.4 Development of a Family of Synthetic Wastes

3.4.1 Waste Sorting Analysis

3.4.1.1 Aim of the Waste Sorting Analysis

To explicitly assess physical properties like shape, size and material of waste components a sorting analysis was necessary. Although information about the specific waste composition in terms of percentage of mass or volume is available in literature, less information was given about size and shape of those components at the same time. A waste survey was contributing to the project by providing a set of data with all details necessary to build a stable framework for all subsequent work.

For classification of waste, detailed information about the physical properties of waste components was necessary. To validate a classification framework, it was advantageous to work with self-assessed data, which would minimise uncertainties. In a first step, the proposed classification framework was based on a data set from literature, which was bound to contain uncertainties due to the fact that some detailed facts about the character of waste were missing. As a result, assumptions had to be made, which contributed to the lack of clarity of results and conclusions drawn from the data. For the implementation of compositional parameters, fresh waste was examined in a first step. A waste survey opened up the chance to collect data needed as a basis for the ongoing and future work, which was the development of synthetic waste. This was used to simulate real waste by combining and composing its components to systematically investigate the engineering properties of real waste. Knowledge on composition, size and shape of the components was also useful for assessment of the structure within waste bodies. Structure influences the mechanical behaviour of the waste body. The waste composition survey included:

1. Mass- and volume-based composition
2. Material groups of the components
3. Size ranges of the components
4. Shape of the components (shape-related groupings)

Moreover, the visual impression of the materials could provide important information, if assumptions have to be made in a later stage of the research. Knowledge on composition, size and shape of the components were also useful for the assessment of structure within waste bodies, which has a crucial influence on mechanical behaviour of the waste body. Kavazanjian (2003) provides information about the GeoSyntec classification system to describe MSW. Part of it is the definition of the degradation (none = no refuse discolouration, slight = discolouration, moderate = highly discoloured, high = grey to black), of the compaction (slight = waste easily falls out of bucket auger, moderate = waste falls upon impact, heavy = waste falls after being struck several times). In terms of describing the structure five different kinds of structure are mentioned.

1. Layered: waste constituents orientated with long axis in a preferred direction (e.g. horizontal)
2. Encapsulated: waste constituents encapsulated in a soil matrix
3. Fibrous: waste constituents intertwined
4. Interlocked: waste constituents interlocked (“compact”, “granular” type structure)
5. Indistinguishable

Biological properties, like degradability, were estimated from literature values. With this, statements about the long-term behaviour of the components were made, which could clarify the mechanical changes of waste due to biodegradation. Moreover, the water content of the examined components is also an interesting issue for the degradation.

3.4.1.2 Work Procedure

The work procedure of the sorting analysis consisted of four subsequent steps:

1. Sorting the components into material groups
2. Sorting of each material group into shape groups
3. Sorting of each shape-group into sizes and re-sorting the shape-groups, if necessary
4. Weighing of the sorted groups in order to accomplish the mass relations of material groups, shape or size groups and total sample weight.

After delivering to a defined working area as shown in Figure 3-2, which was unaffected by delivery and depositing traffic, the waste sample was sorted into material groups. For that, the following ten material groups were chosen:

1. Paper/Cardboard
2. Flexible plastic
3. Rigid plastic
4. Rubber
5. Textiles
6. Wood/Leather
7. Glass
8. Metal
9. Putrescible organics
10. Miscellaneous

Figure 3-2 Defined working area

The shape-groups were preliminarily chosen according to their mechanical functions being reinforcing, compressible and incompressible. In terms of the compressible components a sub-differentiation was introduced, which were groups of high and low compressible components. For the size distribution, a scheme used by Kölsch (1996) was

utilised and modified, which differentiates between six size ranges: <10mm (instead of >8mm), 10-40mm (instead of 8-40mm), 40-120mm, 120-500mm, 500-1000mm, >1000mm. For achieving a fraction <10mm the material was sieved.

For the assessment of composition the sorted waste material groups were subsequently weighed. According to the proposed classification system, the sorted material groups was sub-divided into shape-related subdivisions of compressible, incompressible and reinforcing components. This was done by consideration of the shape. The first main distinction feature was the shape of the components, as there is “three-dimensionally” shaped, i.e. bulky components, and “one- and two-dimensionally” shaped components, which are foils and fibres. Moreover the component size was also considered for two reasons. The first reason was the practicability of sorting, i.e. the smaller the components size the more difficult and laborious it would get to sort the material. The second reason comprised the mechanical function of the components. A rough distinction of three- and one/two-dimensional components into (in-)compressible and reinforcing components, respectively, neglects the size of the components. Especially in terms of reinforcing components, the size is of crucial importance. The components with a reinforcing function should exceed the diameter of the surrounding components (three-dimensional) in order to ensure a bonding of the foil or fibre, which is a premise of the reinforcing effect. Therefore, component size less than 40mm were not included in the group of reinforcing components but reassigned to incompressible components. They were assumed to not exhibiting reinforcing effect.

Incompressible components were solid components, like small pieces of glass, soil-like materials and pieces of metals. Rigid plastic blocks and firm rubber, which did not seem to compress, were also defined as incompressible components. Generally, solid three-dimensional components were sorted to this group, but also two-dimensional components, which were not assumed to reinforce the waste body due to their size, were put into this category.

Within each of the shape-related groups a size analysis of the materials was conducted. For this, not the whole sample was sorted into size ranges, but random tests were conducted in every material group. In practise, several kilograms of the sorted sample were analysed in regard to the components’ size and shape. The sub-divided samples were weighted in order to accomplish the mass relations of material groups, shape or size groups and total sample weight.

Due to the size of the components, a sample for the analysis of the water content was not taken, i.e. to get a representative sample amount it would have been necessary to analyse at least one bag (3-12kg/bag) of each sorted material group (10 groups) and the sorted shape-related subdivisions and size ranges, respectively (3 shape-related subdivisions, 6 size ranges and 10 material groups mean about 180 samples), which would have exceeded the practicality of the survey.

3.4.2 Derivation of a Family of Synthetic Waste

The creation of synthetic waste provided a basis for all subsequent practical laboratory tests. After establishment of a “typical” waste composition in the composition study, synthetic components were chosen, which adapted to and simulated the physical and mechanical properties of real waste. Another advantage over the examination of real waste was the cleanliness of synthetic waste, if appropriate, well-defined, and slow- to non-degradable components are chosen. The process of degradation was simulated by changing the waste composition to reflect the way the physical and mechanical properties change in time. The cognition about the effect of decomposition should derive from the research about biological properties of waste components. Knowledge of the physical, mechanical and biological properties would simplify the process of choosing appropriate components for a synthetic waste, which should simulate the engineering behaviour of real waste in a laboratory scale. The more is known about the properties of real waste, the better synthetic waste can be selected for simulation.

As there is great variety of factors influencing the mechanical behaviour of MSW a big uncertainty is in validating results of experiments. For this reason, the factors had to be reduced in order to minimise the number of variables influencing the findings. The waste survey provided information about a random composition of fresh waste. In connection with findings from literature about fresh waste compositions, key waste materials and components were identified. The waste survey resulted in a large number of variables, i.e. ten material groups, three shape-related subdivisions and six size ranges. But as one of the synthetic waste objectives is to be representative but also simple and easy to reproduce, the amounts of variables had to be reduced. The material groups were reduced to a minimum for the synthetic waste to decrease the factors leading to ambiguous results by creating groups based on similar material properties. With the information about size and shape of the component an unknown parameter of waste components was indeed covered, but as the synthetic waste was designed to be simple, only the most important size ranges were considered. In a first step, the number is automatically decreased as not every size range and shape group was represented in each material group. In a second step, the remaining information was reduced further by assessing and comparing the relevance of each fraction to result in a simple composition of an engineered waste (Figure 3-3).

The choice of components for the synthetic waste should result in a simulated composition for real waste only. Moreover, some limiting combinations of components should be found, which are able to describe the borders of the range in which the composition for MSW is located.

It was advantageous to start the laboratory tests with examining extreme kinds of composition, like a composition of just reinforcing, compressible or incompressible components. These composition resulted in extreme mechanical behaviour and thus set the range for real waste mechanical behaviour. By combining components from those groups step by step an approximation towards typical behaviour could be achieved. It was expected that the results from the laboratory experiments described in the next section would affect and possibly change the choice of components for the synthetic waste. To

come to a final and realistic synthetic waste composition, iteration between experiments and the choice of synthetic components was likely to occur.

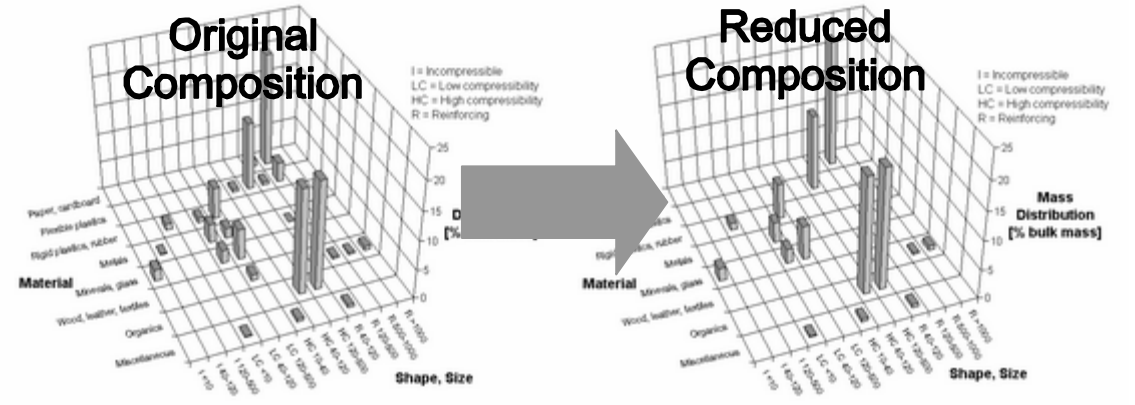

Figure 3-3 Example for reducing the waste fractions

For the implementation of synthetic waste different materials were required to replace the real components. Main material groups had already been introduced. Nevertheless, for an exact simulation of real waste they have to be reviewed and defined. If appropriate material groups were found both in terms of definition and replacements, the synthetic waste would be a matter of composition in order to reflect the “natural” physical, mechanical and biological real waste properties.

3.5 Investigation of Compression Behaviour

3.5.1 Aim of the Compression Tests

The main target for conducting compression tests was to investigate the impact of changing waste component shape and size, and the structure within the waste body on waste mechanical behaviour. Another goal was to verify the synthetic waste behaviour in comparison to real waste compression behaviour. Finally, from the findings of the compression tests, conclusions were drawn to aid the design of subsequent shear tests.

The testing program covered the following issues:

- Validation of the synthetic waste by testing different compositions including a composition that is based on real waste
- The influence of the composition on the structural changes (with emphasis on the expected change due to the European Landfill Directive)
- Structure changes after placement
- Structure changes in long-term consideration

3.5.2 Compression Box

For investigating the compression behaviour a large box was utilised, which was previously used for large-scale compression tests of Leighton-Buzzard-sand. It consists of a steel frame with horizontal and vertical stiffening (Figure 3-4a). To the back and the

sides of the inside frame metal plates are welded; the front is equipped with a thick (35mm) glass plate, which allows monitoring of the compression process (Figure 3-4b). The outer dimensions of the box are length/width/height = 1.88m/1.37m/1.55m, the effective inner dimensions are 1.54m/1.05m/1.39m. The overall volume of the compression cell is about 2.25m^3.

a)  b) 

Figure 3-4 a) Large compression cell; b) Detail of the monitoring area

a) 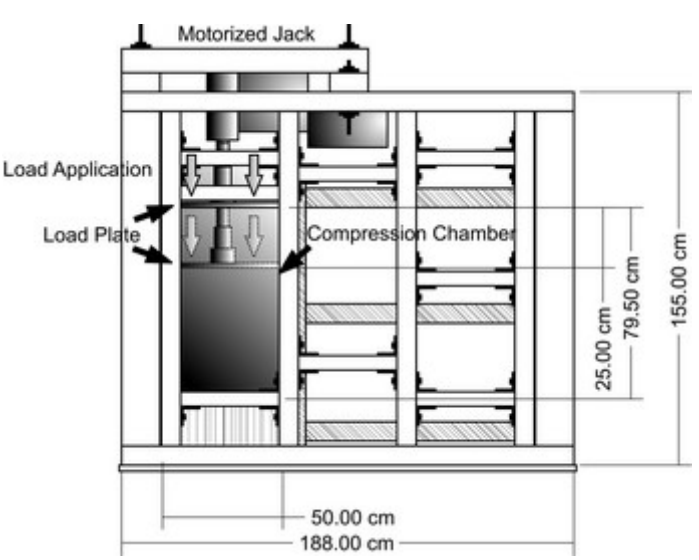

b) 

Figure 3-5 a) Scheme of the large compression cell front with jack; b) Partition from above without jack

To minimise the amount of sample used to a manageable size, the volume was reduced to approximately 0,2m^3 by placing a wooden partition into the front left corner of the box. The dimensions of the partition for length/width/height are 0,50m/0,50m/0.75m with an area of 0.25m^2 inside the box (Figure 3-5b). A motorised jack was mounted onto two square section beams on top of the box to apply the normal load. The jack has a capacity

of 200kPa at 0.25m^2 and a maximum displacement of about 300mm. The tests were conducted with a constant compression strain rate.

The waste sample was placed into the partition between two wooden plates, which were located at the bottom of the partition and on top of the sample, and which were connected by nylon ropes at each corner to allow the sample to be vertically pulled out of the partition in one step on completion of testing

For measuring displacement, two linear variable displacement transducers (LVDTs) with a range of 150mm each were used and a load cell was used to measure the applied normal stress.

3.5.3 Sample Preparation

Plastic foils and textiles were cut into appropriate sizes according to chosen composition basing on the definition of the synthetic waste components and classification, respectively. They were thoroughly mixed with the remaining components of the chosen composition in a compartment as shown in Figure 3-6 before they were carefully filled into the compression apparatus. Fine-sized material (i.e. sand) was added during the filling process to ensure an “even” distribution and to avoid agglomeration at the bottom.

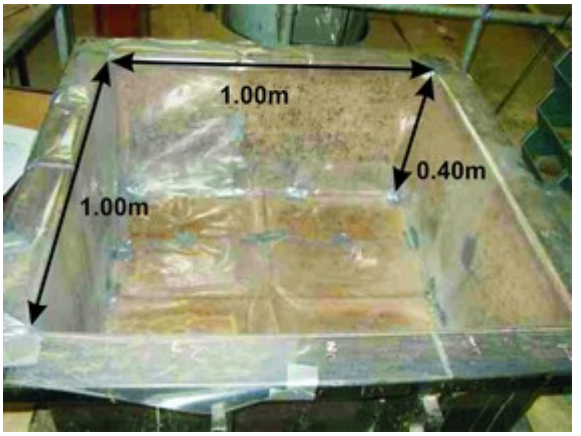

Figure 3-6 Mixing compartment

3.5.4 Compression Test Setup

The bottom plate was placed into the partition of the compression box. The nylon ropes attached to the bottom plate were positioned in each corner of the partition to avoid interfering with the process of filling and pre-compacting of the sample. On top of the bottom plate the thoroughly mixed sample was placed. To achieve a certain sample height/unit weight the volume of the sample had to be decreased, as required. This was done by pre-compacting the sample to the desired sample height. To monitor the compression processes during the test the starting sample height should coincide with the bottom edge of the upper horizontal stiffening of the metal frame. This was also necessary, as the initial position of the jack did not allow this sample height to be exceeded, bearing in mind that a load cell, a ball bearing and the load plate had to be positioned between jack and sample. The load plate was put on top of the sample after the nylon ropes were inserted into locating holes in the load plate. If a high unit weight was desired, the sample was placed in layers, which were manually compacted. This could be achieved by trampling down the sample, provided that the applied force for the pre-compaction is known (e.g. weight of the executing person, amount of steps).

After pre-compaction, the load plate stayed in place. On top of it, if necessary, appropriate spacers were placed. The weight of the spacers had to be known and considered as additional load. A ball bearing and the load cell were placed on top of the spacers. The ball bearing established an even force transmission between the jack and sample in case the load plate started tilting.

Thereafter, the screw jack was lifted on top of the compression box frame by means of a crane. It was bolted to its position onto two square section metal beams. The linear variable displacement transducers were put in position on opposite sides of the load plate, e.g. at the front and the back. It was made sure that all load cell and LVDTs were connected to the data-logging unit (computer) and a test measurement to assure correct data logging was made. For the compression test, the logging intervals were set to 10sec as the compression rate of 0.1-0.2mm/sec (4-10mm/min) did not require a higher data resolution than one measurement per millimetre.

3.5.5 Test Procedure

Samples were compressed to a maximum normal stress depending on the material and the initial unit weight. The test was displacement-controlled. The stages of the compression test were as follows:

1. Loading and compressing of the sample within the range of the LVDTs (<150mm)
2. Unloading (but confining the sample height to its last loaded position) and driving back the jack
3. Adding spacers and re-locating LVDTs, i.e. lowering their position
4. Re-loading
5. Repeating of 1. to 4. until desired compression is reached
6. Unloading (without confining, i.e. relaxation of the material)

After filling the partition, mounting and bolting the jack on top of the box and placing LVDTs and load cell, a normal load was applied. The normal load and the displacement was measured and logged constantly in 10-second intervals. If a maximum displacement (<150mm) was reached, the test was stopped. Wedges were inserted into the gaps between load plate and sides of the partition and pinned down to maintain the load plate in its final position, i.e. the sample was hindered from relaxing. The jack was driven back to its initial position. Thereafter, an appropriate amount of spacers matching the gap between the ball-bearing/load cell and the jack was placed. The spacers were put below the ball bearing. The additional weight of the spacers had to be considered in the analysis of the test result. The LVDTs had to be re-positioned. They were adjusted to the position of the load plate in order to log further displacement. This interval (1. - 4.) was repeated until the aspired compression was reached. At the end of a test, the jack was driven back without keeping the load plate in its final position. After no further relaxation of the sample is visible, the data logger was stopped. The jack was dismantled and lifted off the compression box. The LVDTs, load cell, ball bearing and spacer were removed before the

sample was removed by lifting the sample in its “sandwich”-position out of the wooden partition. The sample was carefully disintegrated and special attention was paid to the structure, which had been developed during compression. The components were examined for signs of damage, stretching and so forth.

The examination of the structure build-up was supported by documenting the compression process by means of digital imaging, i.e. digital pictures were regularly taken. For this purpose, a digital cameral was placed in front of the lower left segment of the compression box. This segment showed the sample during compression (Figure 3-4b and Figure 3-7). During the compression process, pictures were taken at constant intervals (e.g. every 2-5 minutes, which is equal to 1% to maximum 8% strain). The amount of pictures was sufficient to be able to analyse the compression process visually.

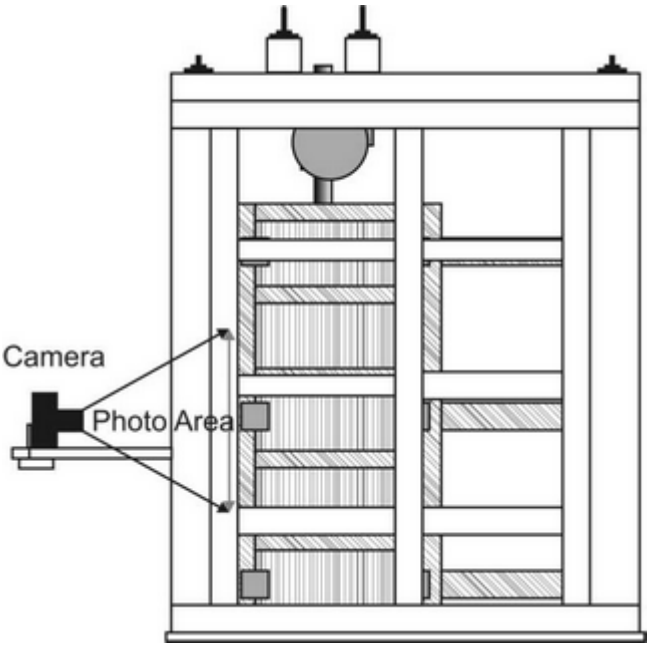

Figure 3-7 Side view with camera of the compression apparatus

3.5.6 Analysis and Presentation of Compression Data

During the compression the test time and the voltage output for vertical displacement and normal load were logged. With the sample area, the normal stress was calculated:

$$\sigma_{v,t} = \frac{F_{v,t}}{A_{Sample}}$$ Equation 3-1

The initial height was used to calculate the vertical strain:

$$\varepsilon_{v,t} = \frac{h_0 - h_t}{h_0}$$ Equation 3-2

As the area of the sample was constant, the volume change could be calculated and the resulting increasing unit weight could be derived.

$$\gamma_t = \frac{m_0 * g}{h_t * A_{Sample}}$$ Equation 3-3

Assumptions about the overall material density of a composition led to the void ratio e:

$$e_t = \frac{\frac{\sum_{i=1}^{n} \rho_i * m_i}{\sum_{i=1}^{n} m_i}}{\rho_t} - 1$$

Equation 3-4

The constrained modulus was calculated as stated in Equation 2-17 for Young's modulus. The compression index C_c is stated in Equation 2-13. Both specific geotechnical values were displayed in dependence of the normal stress level (Chapter 5). For trends and best-fit-lines the features of Microsoft® Excel were utilised.

Digital photographs were related to the stress level and the vertical displacement. It was focussed on the deformation of the compressible components and the structure formation in regard to the applied normal stress. From a series of photographs taken during compression a set of ten pictures at stress levels with concise effect on the components and structure were chosen and compared.

After compression, the components of sample was examined and sorted according to the classification system (section 4.2) into material groups, shape-related subdivision and size ranges.

3.6 Investigation of Shear Behaviour

3.6.1 Aim of the Large Shear Tests

Main objective of conducting large direct shear tests was to understand shear behaviour of MSW. A range of compositions was planned to be examined, from which different impacts on MSW shear behaviour were expected. Additionally, the engineered synthetic waste had to be validated by comparing the results to real waste tests. Furthermore, shear tests were set up using the findings of the compression tests to examine the impact of structure on the shear behaviour.

The testing program covered the following issues:

- Calibration tests
    - Tests to assess the friction of the box
    - Large-scale tests on sand
    - Small-scale tests on sand in a 100*100mm direct shear tests
- Validation of the synthetic waste by testing compositions based on real waste
- Structure-related shear tests
- The influence of the composition on the changes in structure

The small-scale direct shear tests on Leighton-Buzzard sand are described in section 6.2.2.2. A comparison between large- and small-scale test results is provided in section 6.2.2.3.

3.6.2 Large Direct Shear Device

To keep the boundary conditions near to reality, the synthetic waste components examined in shear tests should not be downscaled. For instance, it would be of great interest and importance to examine in-situ size ranges in a shear device, which provides a maximum displacement to assess the influence of reinforcing components. For an even more realistic examination of waste, which does not have to be processed in any way before placing in a shear device, the latter should be able to accommodate even large particles with a size up to more than 1000mm, which are typical for UK waste. For that the measurements of the whole device should exceed the usual 300*300mm used for tests on soils.

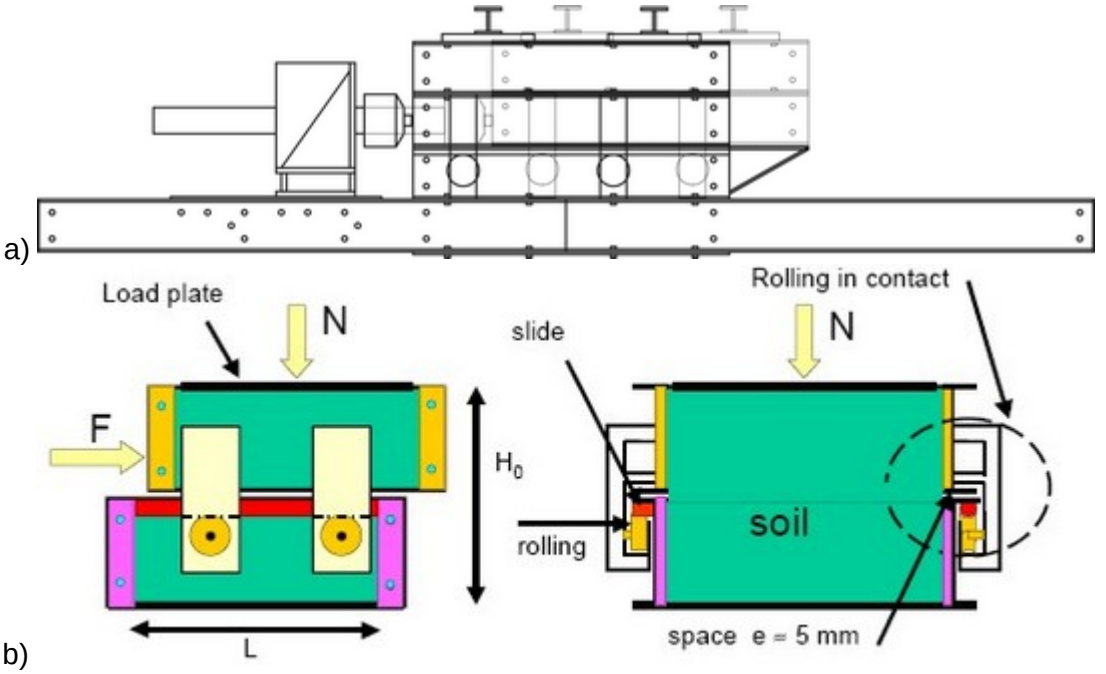

Figure 3-8 a) Schematic of the large shear device with movable upper box and fixed lower box; b) Details of top and bottom frame (Gotteland *et al.*, 2000)

Another, but not preferable, possibility would be an examination of downscaled engineered waste. In laboratory centrifuge tests (for example Jessberger & Kockel, 1993) a downscaled model waste was examined and the findings from the laboratory scale were converted and projected to full-scale conditions. For examining the influence of reinforcing components in a 300*300mm shear device, a model waste with a maximum particle size <100mm would mean that the maximum displacement of 100mm could be utilised. However, the large shear device (l/w/h = 1.0/1.0/0.8m) used in the laboratory tests and shown in Figure 3-8 is a development of the LIRIGM-Polytech'G, Joseph-Fourier-University in Grenoble, France, and has been utilised before for research on real waste (Gotteland *et al.*, 1995, 2000, 2001 and Thomas *et al.*, 1999). It consists of a fixed bottom frame and a horizontally moveable upper frame, which is supported by two rollers on the left and right side of the box. In an unloaded state the upper frame lies directly on top of the bottom frame; after normal loading it lifts up and the rollers touch a guide rail attached to the bottom frame. The lifting induces an approximately 5-10mm wide gap. Thus only the friction of the rollers has an effect on the shear results. An electrical jack pushes the

upper frame generating a shear force between the top and the bottom boxes. The shear rate is adjusted manually and is thus subject to differ. A load cell is located in front of the driving jack. Three displacement transducers are installed, two linear variable displacement transducers are used to measure the vertical displacement of the sample in the front and back of the box during shearing and a magnetostrictive transducer, which is fixed to the upper frame, is used to record the horizontal displacement of the upper box. Prior to setting up the first sample, all the equipment such as displacement transducers and load cell, need to be calibrated. Internal friction tests have to be conducted prior to setting up the first test (i.e. running the box forwards to measure the friction on the linear bearings). The results from these tests are used to correct the values obtained from all subsequent shear tests.

3.6.3 Sample Preparation

Materials like plastic foils and textiles were cut to equivalent sizes in accordance with the chosen composition. They were thoroughly mixed with the remaining components in an additional compartment (as already shown in Figure 3-6) placed next to the large shear box to minimise the distance between the working steps mixing and filling. Granular materials, i.e. sand, were evenly added during the filling process of the box. Including the sand in the mixing process would result in an agglomeration of the sand at the bottom of the compartment. For large sample amounts the mixing/filling process had to be repeated due to a limited volume of the mixing compartment.

3.6.4 Large Shear Test Setup

The upper frame was set to start position matching the bottom frame. For an efficient load transmission a plate with ribs mounted transversal to shear direction was placed inside the bottom box (Figure 3-9a). Thereafter, the component mixture was evenly placed into the shear box and compacted by placing the load plate (Figure 3-9b) on top of the sample and applying the desired pre-compaction stress by means of the horizontal jacks provided with the shear box. The load plate was also equipped with ribs, which were orientated transverse to the shear direction. If the material was placed in layers, it had to be made sure that the interface of two layers did not correspond to the interface between the upper and lower box (i.e. the forming of a preferential shear plane had to be avoided).

a)  b) 

Figure 3-9 a) Bottom load transmission plate; b) Top load plate

The amount of material put into the shear box was approximately calculated by means of the results of the compression test, i.e. the results indicated the amount of compression (vertical strain) of the examined material composition, which was related to the applied vertical stress. From this the expected reduction of the sample height in the shear box at a given pre-compaction and normal stress, respectively, could be estimated. This was necessary to retain a minimum sample height during the shear test.

a)  b) 

Figure 3-10 a) Jacks for normal stress application; b) Hydraulic hand pump

For the pre-compaction procedure and the application of the normal stress four jacks were to be placed on top of the load plate. Two metal beams mounted on top of the shear box acted as a counter bearing (Figure 3-10a). The hydraulic jacks were connected to a hydraulic hand pump, with which the normal stress was applied (Figure 3-10b).

Displacement transducers were placed for measuring the vertical displacement at the front and the back at the box. As a last step, transducers and load cell had to be connected to a data-logger (i.e. PC) and the software had to be set up, before starting the test procedure.

3.6.5 Test Procedure

The shear tests comprised 8 different stages:

1. Filling
2. Pre-compaction
3. Application of the normal stress
4. Shearing 1
5. Unload
    a. Stop shear stress
    b. Unload normal stress
6. Re-load
    a. Re-applying normal stress
    b. Re-applying shear stress
7. Shearing 2
8. Unload
    a. Stop shear stress
    b. Unload normal stress

After setting up the large shear box and starting the software to log the displacement and load data (measurement are recorded in 5 second intervals, additionally, manual control measurements of shear stress were recorded in 2 minute intervals and the vertical displacement was measured at each stage of the shear test), the sample was pre-compacted. The desired pre-compaction stress was manually applied to the sample and re-adjusted until a constant normal stress was established.

As waste always has a certain stress history when delivered to site and placed, pre-compaction was conducted prior to applying the normal stress under which the test was done. The stress history relates to different states between the actual intact product (e.g. intact plastic packaging) and the depositing on site. There are in-between stages like manual compression of the component before disposing in a dust bin, manual compression of the waste bags (and their contents) in a wheelie bin for the purpose of volume reduction, compaction of the waste after being emptied into the collection vehicle, a subsequent relaxation of the material after being delivered to and dumped on site and a re-compaction due to distributing and applying the waste on the landfill by the compaction vehicle. Especially the final compaction has a large influence on the material, as the compaction is primarily done for a laminar and thin distribution (i.e. layering of the deposited waste). On this account a pre-compaction was conducted. The pre-compacting stress was 75kPa at maximum. The values chosen represented a waste height equivalent to maximum 5-10m, as this was thought to be an approximate but appropriate value for the applied compaction effort during depositing processes. Thereafter, the sample was unloaded and the desired normal stress was applied (25, 50, 75/100kPa). For the highest normal stress a distinction was made, which was based on material characteristics. High compressible compositions were only loaded up to 75kPa to reduce the amount of sample material needed, whilst low compressible/incompressible compositions were loaded up to 100kPa. The upper part of the shear box was automatically raised 5-10mm, after vertical stress was applied. This was necessary to avoid the frictional effects between the upper and lower frame and to establish a connection between the rollers of the upper frame and the guide rail of the bottom frame (Figure 3-11a)

a) 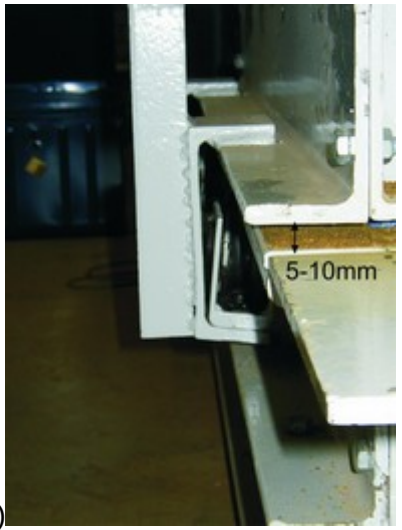

b) 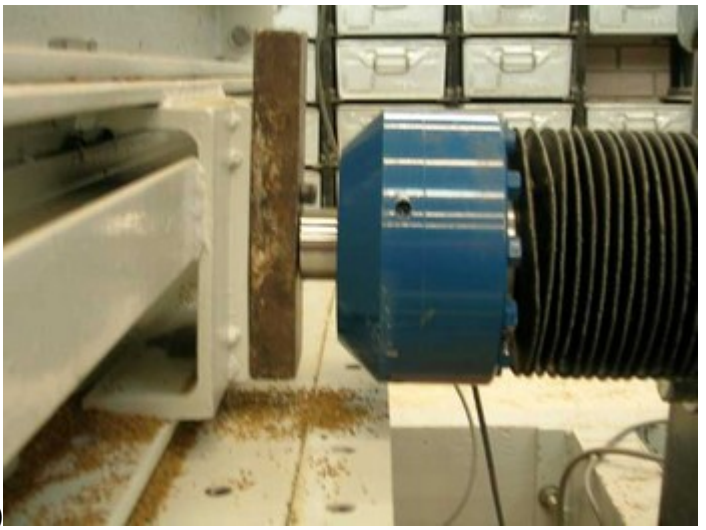

Figure 3-11 a) Normal stress induced gap between upper and lower box; b) Horizontal jack including load cell

After establishing a constant normal stress, shearing was started by applying a horizontal load to the upper part of the shear box (Figure 3-11b). A shear rate of 6mm/min was chosen after a series of tests with higher and lower shear rates. From shear tests on sand with different shear rates (section 6.2.2), the chosen shear rate was found to be

appropriate for the examined material. An unload-reload-cycle was used to investigate elastic properties of the sample (shear modulus) shearing is stopped after 120mm and the jack was driven back. The normal stress was reduced to zero and the rebound of the upper frame of the box was logged. When a constant value for the horizontal displacement was reached, the normal stress was re-applied to the sample. Shearing was continued after establishing a constant normal stress up to a displacement of 250mm. Then the jack was driven back to the start position.

The normal stress had to be monitored constantly, as it was manually controlled and fluctuations were not automatically compensated. As required, the normal stress was re-adjusted to grant a constant normal stress throughout the test.

At the end of a test the jacks and the load plate were removed. The sample in the upper frame was examined and carefully removed. Thereafter, the upper frame was manually pulled/pushed back to establish a better access to the bottom sample fraction. As before it was examined before it was carefully taken out of the box. Sample components were examined for signs of damage, stretching and so forth. Sheared samples were stored properly for reuse.

3.6.6 Analysis and Presentation of Shear Data

The voltage output of the LVDTs and load cell was converted by means of the equipment calibrations in appendix 11.1 into horizontal shear force, horizontal and vertical displacement. These values were demonstrated in Chapter 6 as follows. Shear stress was derived from the logged shear force and the shear area. An area correction (i.e. consideration of a decreasing shear plane) was not taken into account.

$$\tau_t = \frac{F_{h,t}}{A_{Sample}} \qquad \text{Equation 3-5}$$

The vertical displacement was related to the sample height after compaction and normal stress application, i.e. sample height at shear start h_2:

$$\varepsilon_{v,t} = \frac{h_2 - h_t}{h_2} \qquad \text{Equation 3-6}$$

The shear modulus was calculated according to Equation 2-4. It was related to the beginning of reload and it was determined for three strain levels (1, 2 and 3% strain). The figures in Chapter 6 depict shear stress against horizontal displacement and vertical strain against horizontal displacement. For each test set the Mohr-Coulomb failure envelope is shown for two states during the test. As a true peak value was not expected, an envelope at 110mm displacement (just before the unload-reload loop) was demonstrated and the envelope for maximum displacement and thus maximum shear stress is also shown.

Additionally, examinations of the shear material were conducted. Like the analysis for the compression tests, the material was sorted after shearing into shape-related subdivisions, material groups and sizes ranges, in order to be able to relate the effect of shearing/compressing on the components to the geotechnical classification. At the end of

the tests SW_02 (section 6.3.2.1) one side of the shear box was dismantled to examine the effect shearing has on the structure.

3.7 Data Output and Conversion

The linear variable displacement transducers and load cells used have a voltage output. A change in load or displacement results in a voltage change. The voltage signals had to be converted in millimetre and kilonewton, respectively. The output voltages were saved in text files, which were imported into Microsoft® Excel-files for further processing.

For further processing of the output and the data conversion, calibrations of the test equipment were necessary. The results for the calibrations are attached in appendix 11.1. Regression statistics are presented, as well as the coefficients for the conversion. Moreover, standard error and upper and lower 95% quantil were also identified.

3.8 Sorting Analysis of the Examined Material

The sample material of selected compositions was manually sorted after conducting compression and shear tests. Therewith, changes in shape-related subdivisions and size ranges of input and output sample material were analysed. The results are compared to be able to make statements about the component behaviour after loading and to visualise the shifting of components within shape-related subdivisions, i.e. the altering of mechanical function of components.

4 Waste Classification and Synthetic Waste

4.1 General Introduction

In this chapter a framework for a geotechnical classification is presented. It is based on the findings from the literature stated in section 2.4.2. The elements necessary to classify waste are demonstrated and explained and a data set from literature is applied. The second part of this chapter describes the derivation of a family of synthetic wastes. Based on the results of an in-situ waste sorting analysis, the main components of the examined waste sample are identified and synthetic replacement components are proposed. Finally, the synthetic compositions tested in this work are introduced.

4.2 Geotechnical Classification of Municipal Solid Waste

Whitlow (1983) justifies the need for a classification system and describes the principles for classifying soil as follows.

“The system adopted needs to be sufficiently comprehensive to include all […] deposits, while still being reasonable, systematic and concise. […]. Without the use of a classification system, published information or recommendations on design and construction based on the type of material are misleading, and it will be difficult to apply experience gained to future design. Furthermore, unless a system of conventional nomenclature is adopted, conflicting interpretations of the terms used may lead to confusion. […] A classification system must satisfy a number of conditions:

a) It must incorporate definitive terms that are brief and yet meaningful […].

b) Its classes and sub-classes must be defined by parameters that are reasonably easy to measure quantitatively.

c) Its classes and sub-classes must group together soils having characteristics that will imply similar engineering properties.”

All of these issues are also important for a waste classification system. In proposing a framework for classification and description of waste materials it is appropriate to follow those developed for soils, although additional properties will also have to be considered.

4.2.1 Elements of a Classification System

The findings of the literature review in chapter 2.4 form the basis for developing a first-step geotechnical classification. In the following, the chosen elements of the classification are demonstrated and a data set is applied to give an example.

4.2.1.1 Description of the Components

The starting point for a classification system is identification of the main waste components by material type. Due to the large variety of materials present in waste, a practical approach is to identify major groups of materials. For example, an American waste composition survey done by the Department of Environmental Quality (1998) used the following ten main groups: organic, paper, wood, polymer/plastics, metal (Fe/non-Fe),

soil-like, ceramic, glass, inerts and rubber. Waste composition is defined by measuring the mass percentage of each material group present in a sample. A significant barrier to the sharing of information on waste behaviour is the use of different groups of materials by those classifying samples used in experimental programmes. In many instances the reasoning behind selection of specific groupings is not explained, and hence the factors influencing measured behaviour cannot be fully understood. Figure 4-1 shows an American waste composition survey done by Department of Environmental Quality (1998) and an average UK waste composition. The latter is derived from a literature review of composition of UK waste and is based upon the following eight different datasets: Department of the Environment, 1994a; Department of the Environment, 1994b; Dunn, 2002; Green and Jamnejad, 1997; Jotisankasa, 2001; University of Newcastle upon Tyne, 1999; NWET, 2002; University College Northampton, 2000.

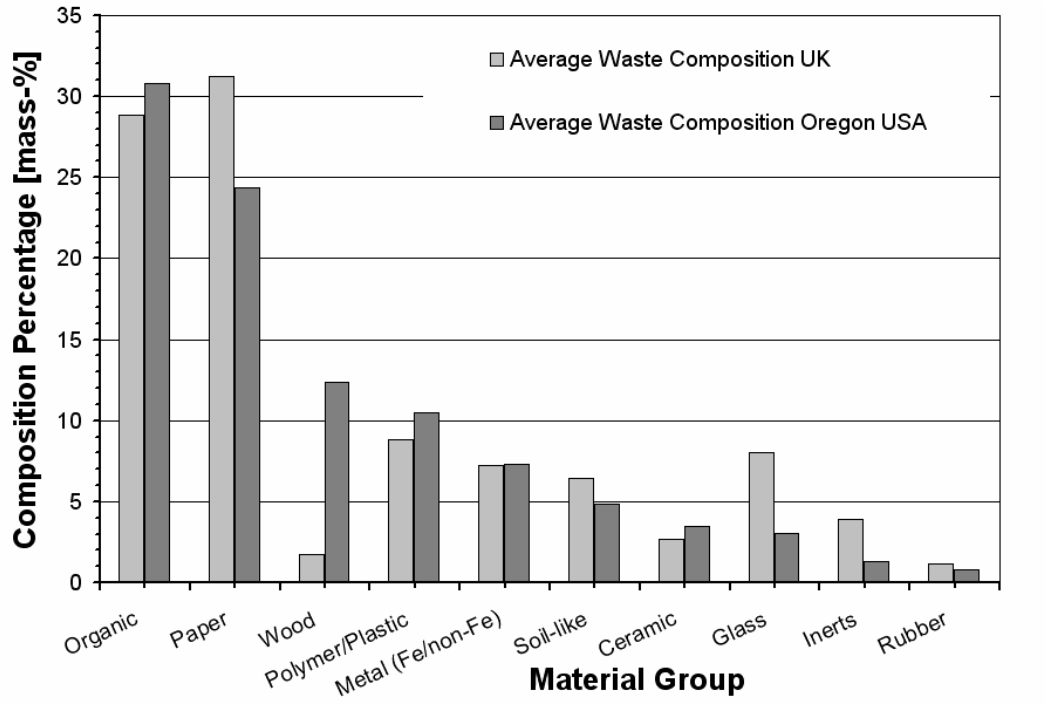

Figure 4-1 Waste compositions from the USA (Oregon Department of Environmental Quality, 1998) and the UK (from various authors, sources in Figure 1-3)

4.2.1.2 Mechanical Properties of Components in Material Groups

Selection of appropriate groups requires consideration of component mechanical properties. It is proposed that components are considered in the condition they have on delivery to the landfill site. Definition of this initial state is required because mechanical properties, shape and size of components will change as a result of placement conditions (i.e. compaction) and stresses due to burial, due to the deformability of some particles, and in the long-term due to degradation processes. The classification system must provide the possibility for components to change group as a result of these processes. Moreover, the groups should be appropriate for every type of waste. The following mechanical properties are considered as a basis for producing component material groups:

- Shear strength
- Tensile strength
- Compressive strength
- Elongation at break (at given strain)
- Modulus of elasticity

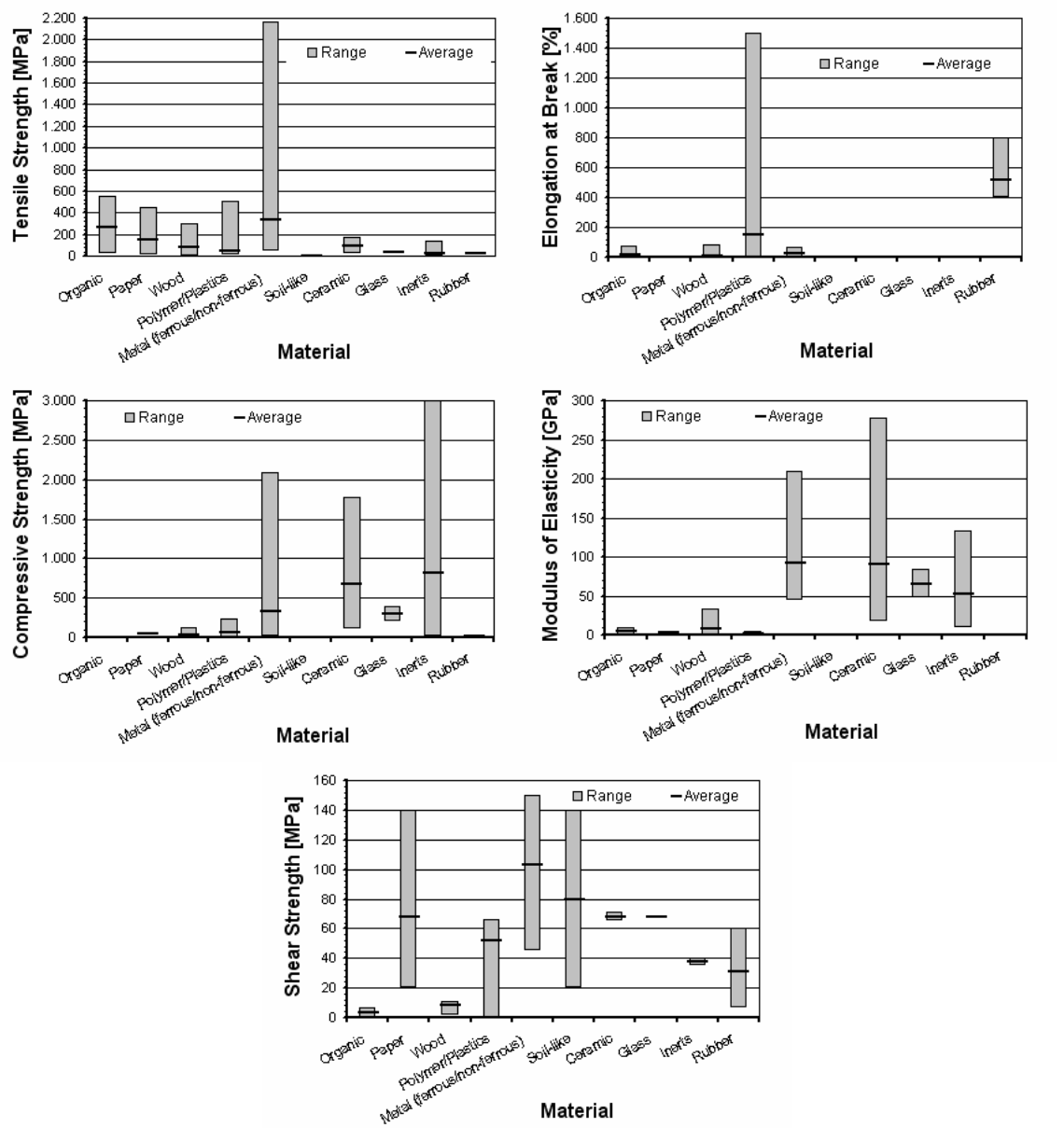

Figure 4-2 Minimum-maximum range and average values of mechanical properties for components in selected material groups from sources listed in the text

For the material groups initially defined by Department of Environmental Quality (1998), Figure 4-2 shows indicative shear and tensile strengths, elongation at break, compressive strength and modulus of elasticity. The data for mechanical properties are derived from various published sources and databases (Cambridge Engineering Selector; Carderelli,

1966; IdeMat, 2002; MatWeb, 2004; Schneider, 1996). These show significant variability. In addition to the average values for components in each material group, the range of values is presented to emphasise variability. It is not intended to use the information in these diagrams to define materials by specific material values, but to highlight the state of variability within groups, and stress similarities and differences of the material groups. This information can be used to identify those groups of materials that can be amalgamated to simplify the classification. In addition, it provides an indication of the groups that could influence specific aspects of waste body mechanical behaviour (e.g. compressibility, shear strength). However, it should be noted that waste body behaviour is also dependant on the overall composition of the waste body and on the in-situ density, structure and stress state.

For tensile strength, organic matter and paper are the dominant materials (Figure 4-2). The high tensile strength of metals has only limited influence due to the low percentage present in this sample of waste. Considering compressive strength, possible groupings of materials could be: ceramics and inerts with a very high compressive strength; glass and metals with a high to medium compressive strength; and paper, wood and polymers/plastics with a low compressive strength. Figure 4-2 indicates that the organic and soil-like material possess almost no compressive strength. In the case of soil this is misleading as individual soil grains (i.e. waste components) have a relatively high compressive strength. It is important that the properties of only the components are considered in a classification and not of assemblages of components (i.e. a quantity of soil). The information summarised in Figure 4-2 has been used to select the material groups for use in the proposed classification.

Table 4-1 Comparison of material groups

Oregon Department of Environmental Quality (1998)	**Kölsch (1996)**
Organic	Putrescible Organics
Paper	Paper/Cardboard
Wood	Wood/Leather/Textiles
Rubber	
Polymer/Plastics	Rigid Plastic (incl. Tyres)
	Flexible Plastic
Metal (Fe/non-Fe)	Metals
Soil-like	Miscellaneous
Ceramic	Minerals
Glass	
Inerts	

The material groups utilised in subsequent analyses and tests are derived from Kölsch (1996) and based on eight material groups. There are some differences in the groups defined as shown in Table 4-1. The amount of material groups is reduced from ten to eight, which also decreases the number of unconfident parameters. The decreased number results from the aggregation of the groups of ceramics, glass and inerts, which exhibit similar characteristics, to a single group of minerals.

4.2.1.3 Shape-related Subdivision of Components

In addition to the material groups, the shape of components has to be considered in a classification, as the shape is a potential characteristic for its mechanical function. The following distinction is based on observations of waste components and consideration of mechanical properties of components (e.g. how easily they can be compressed). Assessments have been made about the role material groups could play in mechanical behaviour of the waste body. It is proposed that the shape of waste components could be characterised by one of two basic groups based on shape-related properties, in conjunction with associated subdivisions:

- One-, two-dimensional components
    - Reinforcing components (e.g. plastic bags, sheets of paper)
- Three-dimensional components
    - Compressible components
        a) High compressibility (e.g. putrescible materials, plastic packaging)
        b) Low compressibility (e.g. beverage cans)
    - Incompressible components (e.g. bricks, pieces of metal)

The subdivision of compressible components is necessary for assessing changes resulting from placement activities (i.e. depositing and compacting the waste) and overburden stresses from additional waste layers. Stressing high compressibility components could lead to shearing and crushing of components, while low compressibility components could remain unaffected during deposition. The simplified distinction between high and low compressibility components provides a solution for consideration of short-term behaviour due to placement and compaction, and long-term behaviour of components in response to increasing overburden stress and creep. However, at present there is insufficient experimental data to enable such a subdivision to be quantified (i.e. to define the threshold stress between high and low compressibility). The threshold should be related to the maximum stress imposed during waste placement and compaction. Further work is required to develop an appropriate simple test for assessing the compressibility of each component and to provide relevant threshold values. Incompressible components are those that will not compress if subjected to the maximum overburden stress in a specific landfill (i.e. in a 50 metre deep landfill the maximum overburden stress will be approximately 500 kPa).

Definition of a component as reinforcing is based on an assessment of the size of reinforcing components (e.g. fibre or foil) in relation to the size of surrounding regular shaped 3-D components (i.e. those particles tending to spherical in shape). Theoretically, reinforcing can result when fibre/foil length exceeds the nominal diameter of the regularly shaped particles. If bonding of reinforcing components between regularly shaped 3-D particles does not occur, tensile forces in the mixture cannot be generated. Figure 4-3 schematically shows the correlation between reinforcing and surrounding element. For example, Michalowski and Zhao (1996) suggest that the length of the reinforcement must be at least one order of magnitude larger than the diameter (d_{50}) of sand grains for fibre-reinforced soils. The relationship between fibre/foil dimensions and size of regular particles for reinforcing behaviour was also investigated through the study on shear and compression behaviour using controlled synthetic MSW and is discussed in chapter 7.

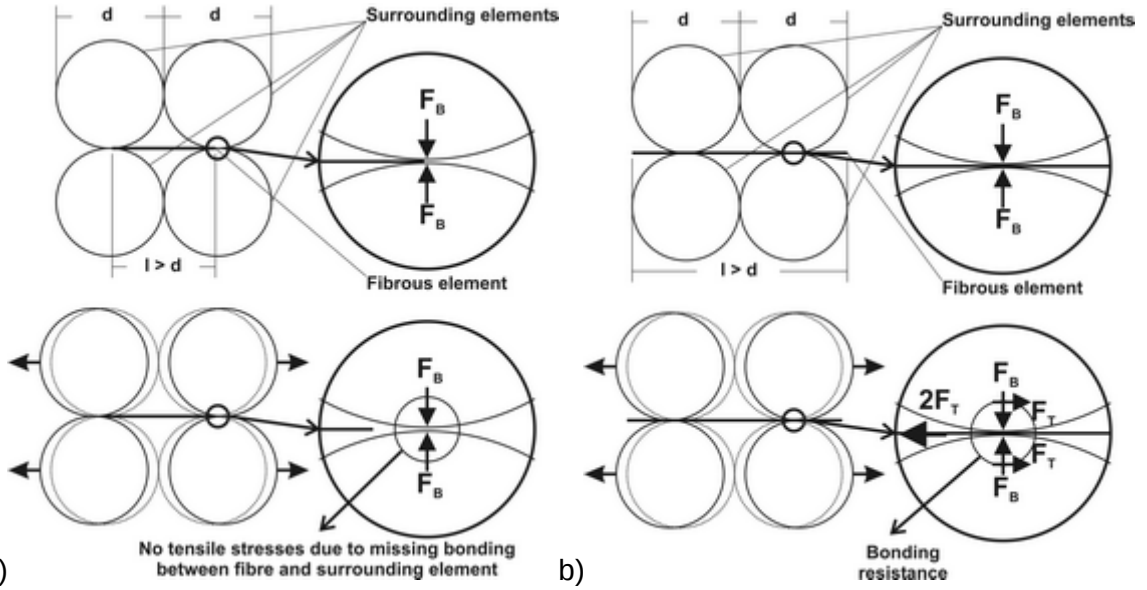

Figure 4-3 Idealised scheme of the reinforcing effect a) missing bonding resistance and b) with bonding resistance

With a shape-related subdivision of waste constituents, a grouping of components with similar general mechanical behaviour (i.e. (in-)compressible and reinforcing properties) can be given. This meets the requirements of a geotechnical classification system.

4.2.1.4 Grading of Waste - Size of Components

A key element of a classification is information on grading. Data from Kölsch (1996) is used to demonstrate a dry mass distribution for waste components including grading. The data shown in Figure 4-4 is for a fresh domestic refuse from an urban district. As a result of a separate bio-waste collection the organic content was reduced prior to grading. The waste components were sorted using three different criteria: material type, shape and size. The material groups used were: paper/cardboard; flexible plastics; rigid plastics; metals; minerals; wood/leather; organics and miscellaneous <40mm. Although there are some similarities with the groups used by Department of Environmental Quality (1998), there are also significant differences that make it difficult to compare waste types.

The data was re-sorted to adapt it to the new classification framework. Each material group was subdivided based on shape-related properties (i.e. compressible, incompressible and reinforcing components). The final step was to grade components into the following size ranges: <8mm, 8-40mm, 40-120mm, 120-500mm, 500-1000mm, >1000mm. From Figure 4-4, it can be seen that the components forming the largest proportion by weight in this sample are those with sizes in the range 40-120mm. These are heavy components such as broken glass, stones, etc. and also components defined as reinforcing (e.g. paper and plastic). The fine fraction, <40mm, would be higher in areas without pre-treatment to reduce organic materials (i.e. due to the presence of coffee grounds, tea bags, food residues, etc.).

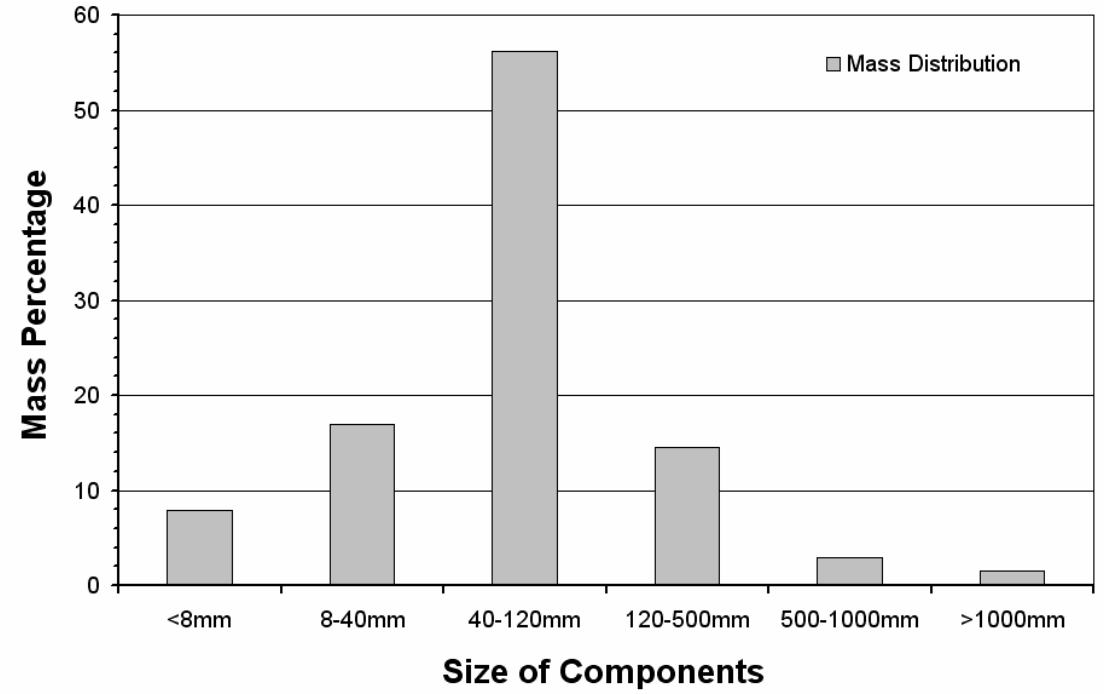

Figure 4-4 Mass distribution based on size of the components (after Kölsch, 1996)

An example of subdivision of material groups based on component shapes is shown in Figure 4-5 to Figure 4-7 for the shape-related subdivision of compressible (30.6% dry mass), reinforcing (43.4% dry mass) and incompressible components (26.0% dry mass), respectively. It has been assumed that the miscellaneous material group initially defined by Kölsch (1996) is composed of compressible and incompressible components in equal shares. This is justified by the observation that this material mixture contains compressible organic material and incompressible soil-like material, stones, fractions of bricks etc. For incompressible components a clear concentration is visible for the groups of metals, minerals and wood/leather in the size range of 8-500mm and for the miscellaneous material with a size less than 40mm (Figure 4-5).

Reinforcing components show their highest peak for paper/cardboard and flexible plastics between 40mm and 500mm; but reinforcing element also exist in rigid plastics, metals, minerals and wood/leather up to a size >1000mm (Figure 4-6). Clear peaks for flexible plastics and miscellaneous material are shown in Figure 4-7 for compressive components within the range of 40-120mm and 8-40mm. After applying load, a percentage of these

components will change group within the shape-related subdivision from compressible to reinforcing components (i.e. as they are flattened). It should be noted that this data is for the waste in its initial, pre-placement, condition. The figures demonstrate how detailed information on material group, size, and shape of components can be presented.

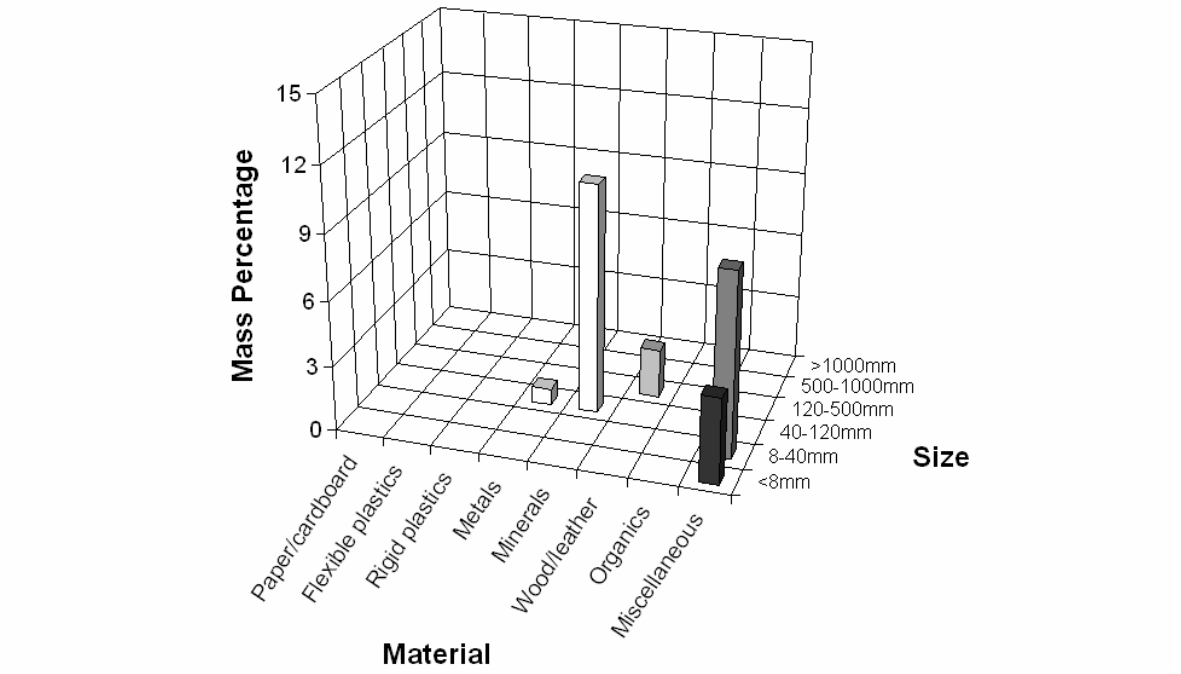

Figure 4-5 Mass distribution for incompressible components (data from Kölsch, 1996; with estimated data for miscellaneous material)

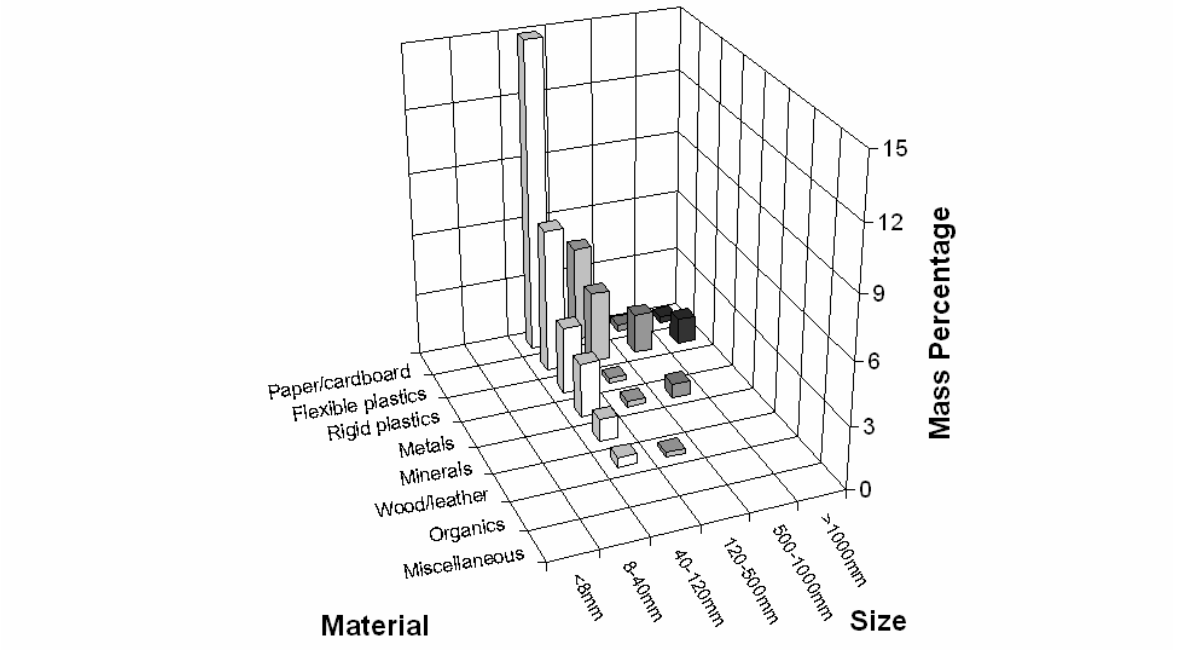

Figure 4-6 Mass distribution for reinforcing components (data from Kölsch, 1996)

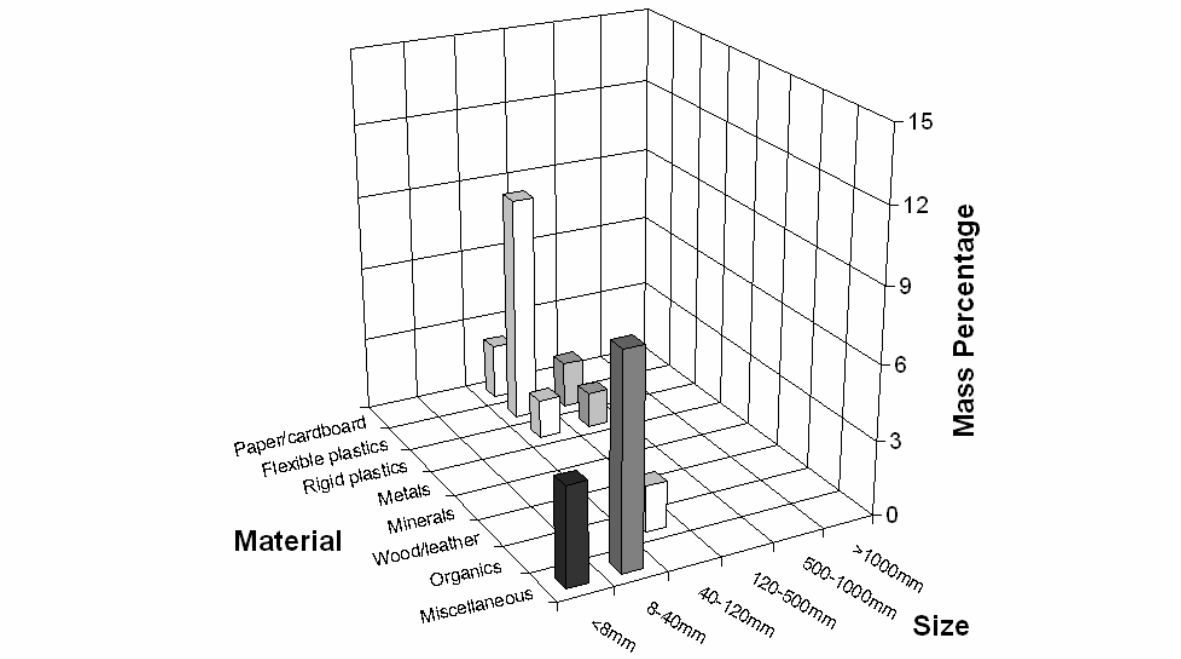

Figure 4-7 Mass distribution for compressible components (data from Kölsch, 1996; with estimated data for miscellaneous material)

4.2.1.5 Degradation Potential

In order to be able to represent changes in classification that occur due to degradation of components, it is necessary to provide information on degradation potential. The subdivisions proposed by Landva and Clark (1990), and discussed above, are considered to provide an appropriate framework. For assessment of degradation potential, it is important to distinguish between short-term, medium-term and long-term degradation rates. Paar (2000) specifies the hierarchy of biodegradable substances (Table 4-2). As the largest degradation alteration of waste components occurs by bio-degradation, the framework introduced here only considers this. Other degradation processes like corrosion and dissolution or other chemical reactions depend on the surrounding milieu. For physical decay or weathering processes, temperature, water content and water and solids movement play important roles. There is inadequate information in the literature to develop this aspect of waste behaviour further at the present time.

Table 4-2 Degradation hierarchy of substances after Paar (2000)

Substance	**Degradability**
Sugar, starch, protein, fat	Easy
Hemicelluloses, celluloses, wax, synthetic oil	Medium difficult
Lignin, resin	Difficult
Leather, rubber, plastics	Very difficult to non-degradable

The distinction of the different stages of degradation can also be linked to different materials. For example, kitchen waste (for the most part vegetable residue or the like)

degrades more rapidly than paper. A comprehensive classification system should include these factors. There are various methods available to assess the organic content. Methods such as the loss of ignition and the Total Organic Content (TOC) only provide information on the general organic fraction and the amount of organic carbon, respectively, and not on the degradable organic fraction and carbon, which is required if using the Paar (2000) subdivision. However, in conjunction with the Biological Oxygen Demand, conclusions can be made about the biological activity of the waste.

4.2.2 Proposed Classification Framework

A framework of waste classification is shown in Figure 4-8 and Figure 4-9. The procedure of classifying waste components is presented in Figure 4-8; Figure 4-9 demonstrates the application of the framework. The application considers the state of waste components at three stages during landfilling: as delivered to site, following placement and in the long-term following degradation. Components of a waste sample are examined to obtain information on: material type, shape and size. This would typically be achieved through a combination of visual assessment of material type and properties, measurement (e.g. size and shape) and estimation of degradation potential (i.e. related to material type. Based on the material property information, components can be grouped in order to minimise the number of material categories. Information about material properties and shape of components is used to group them according to whether they are compressible, incompressible or reinforcing. An overall grading for each material group in each of the shape-related subdivisions is then obtained. The subdivisions are then reviewed and modified, if required, by taking into considering the relative size of reinforcing components to regular shaped components as discussed above. Finally, the degradation potential of components in each shape-related material group is defined.

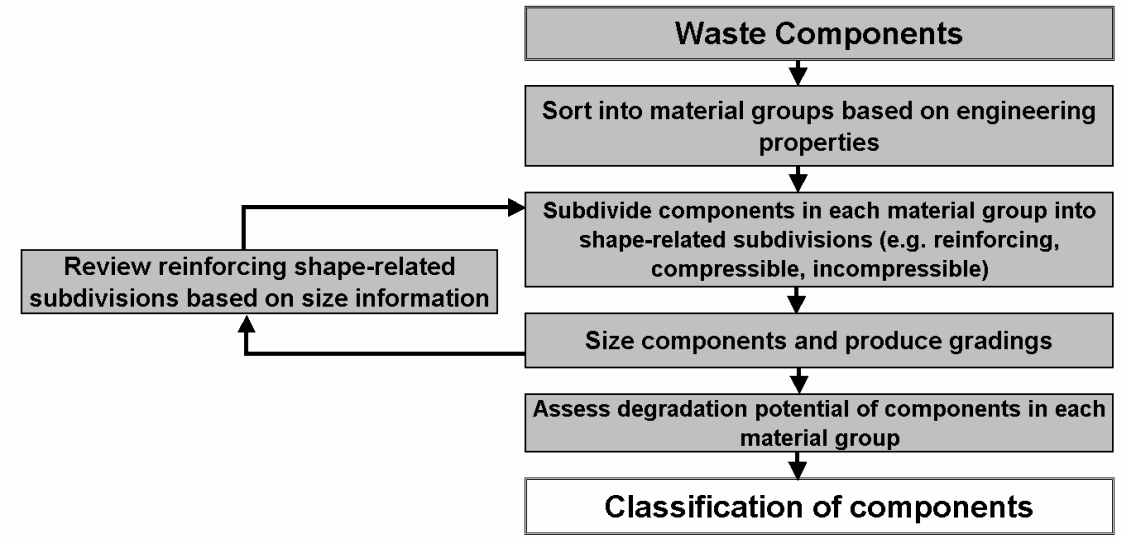

Figure 4-8 Procedure of the proposed classification framework

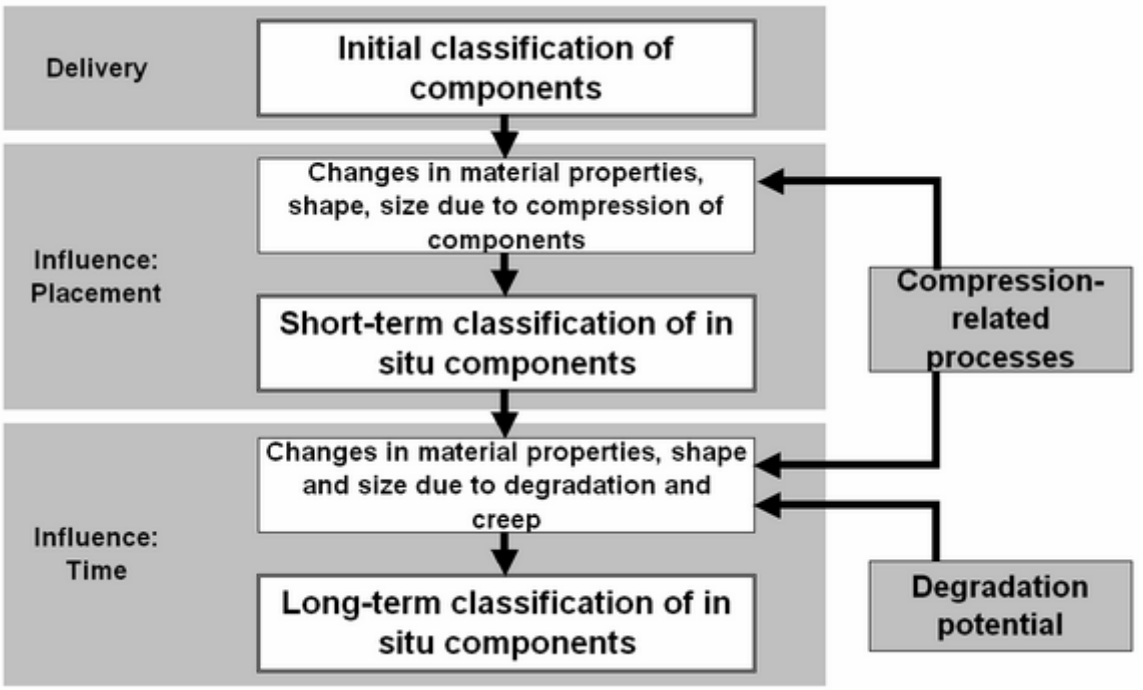

Figure 4-9 Application of the proposed classification framework

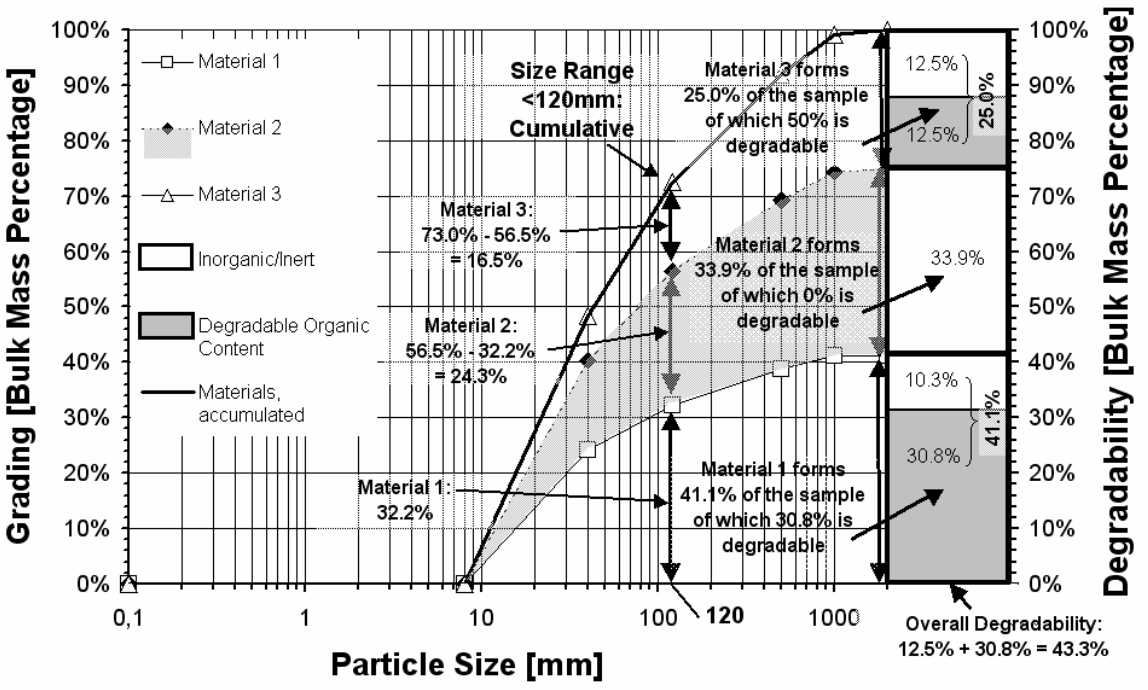

Figure 4-10 Example graph demonstrating presentation of size, shape and degradation data relevant for classification

Unlike soil, waste consists of components with a wide range of material properties and this complicates the conventional presentation of data. In addition, the issue of bio-degradation is crucial for waste. Therefore, a revised format for presenting information on component material type, shape, size, grading and degradation potential is proposed. Figure 4-10 shows an example, fictitious, diagram for a shape-related subdivision of the

waste, to demonstrate and explain the format used to present real data in subsequent figures (Figure 4-11 to Figure 4-13).

Figure 4-10 shows grading curves for the three different material groups (material 1, 2, and 3). The upper curve, denoted by a thick black line, gives the cumulative grading for the combined material groups forming the shape-related subdivision. The grading lines below this can be used to calculate the cumulative gradings for each material group. For example as shown in Figure 4-10, the size range of >120mm represents 73% of the overall material mass and is composed of 32.2% material 1, 24.3% (56.5% minus 32.2%) of material 2 and 16.5% (73% minus 56.5%) of material 3. The cumulative dry mass percentage of a material group for a given component size is simply the difference between the cumulative values of the material groups plotted immediately above and below. In this manner, computed values are related to the shape-related subdivision mass percentage of 100%.

Information on degradability potential is provided in the column on the right hand side of Figure 4-10, where the percentage of degradable and non-degradable content for each material group is related to the total mass of waste in this shape related subdivision. Sections of the column are used to represent each material group, with the height based on the percentage of that group as a proportion of the total sample (i.e. the three material groups in this example add up to 100% of the sample, with material 1 forming 41.1%, material 2 forming 33.9% and material 3 forming 25% of the total). If there is biologically degradable material present in a group, the information is represented by a grey section of the column with the percentage shown by the height (i.e. in relation to the overall mass of the shape related sample), and the white section represents the inert percentage. The total percentage of degradable material present in a shape-related subdivision is obtained from the sum of the grey sections of the column. For example, in Figure 4-10 the total degradable material in this subdivision is 43.3% (30.8% from material 1, 0% from material 2 and 12.5% from material 3). The information on degradation potential enables an assessment of possible mass reduction of materials due to degradation, and thus the reduction in proportion of the entire waste sample composed of the shape-related subgroups. This information can be used to revise the classification of the waste for the long-term condition when degradation is complete.

The data produced by Kölsch (1996) is used to demonstrate data analysis and classification of an initial state before waste placement. Information for components in the incompressible, reinforcing and compressible shape-related subdivisions is presented in Figure 4-11 to Figure 4-13 respectively. These figures show the selected material groups, an overall grading of components in the particular shape-related subdivision, gradings for components in each material group and degradation potential for components forming each material group, as discussed above.

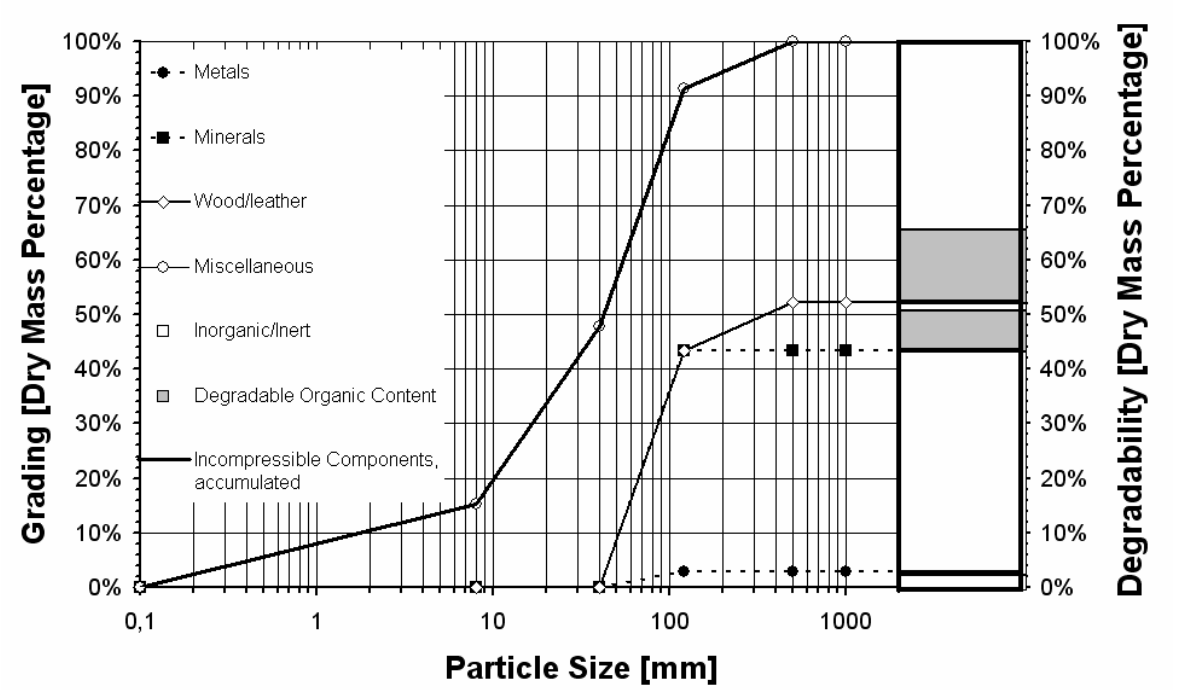

Figure 4-11 Incompressible components: Material groups, gradings, organic content of the material groups related to 100% of the overall sample mass (data from Kölsch, 1996; data for miscellaneous material modified by the Authors)

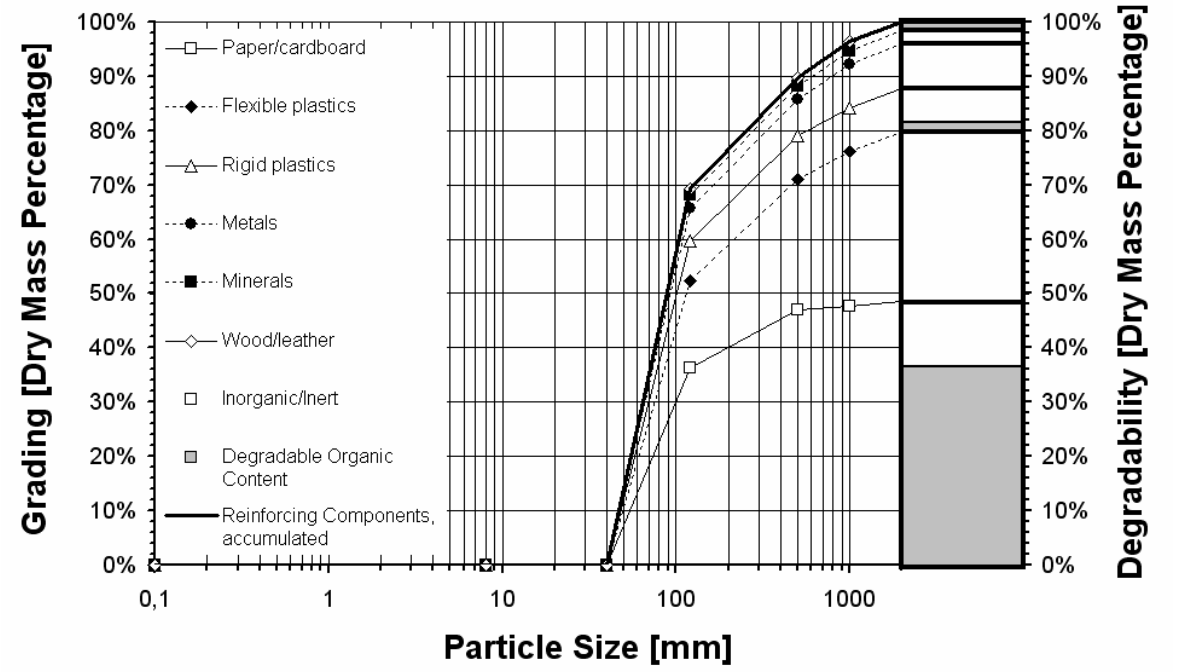

Figure 4-12 Reinforcing components: Material groups, gradings and organic content of the involved material groups related to 100% of the overall sample mass (data from Kölsch, 1996)

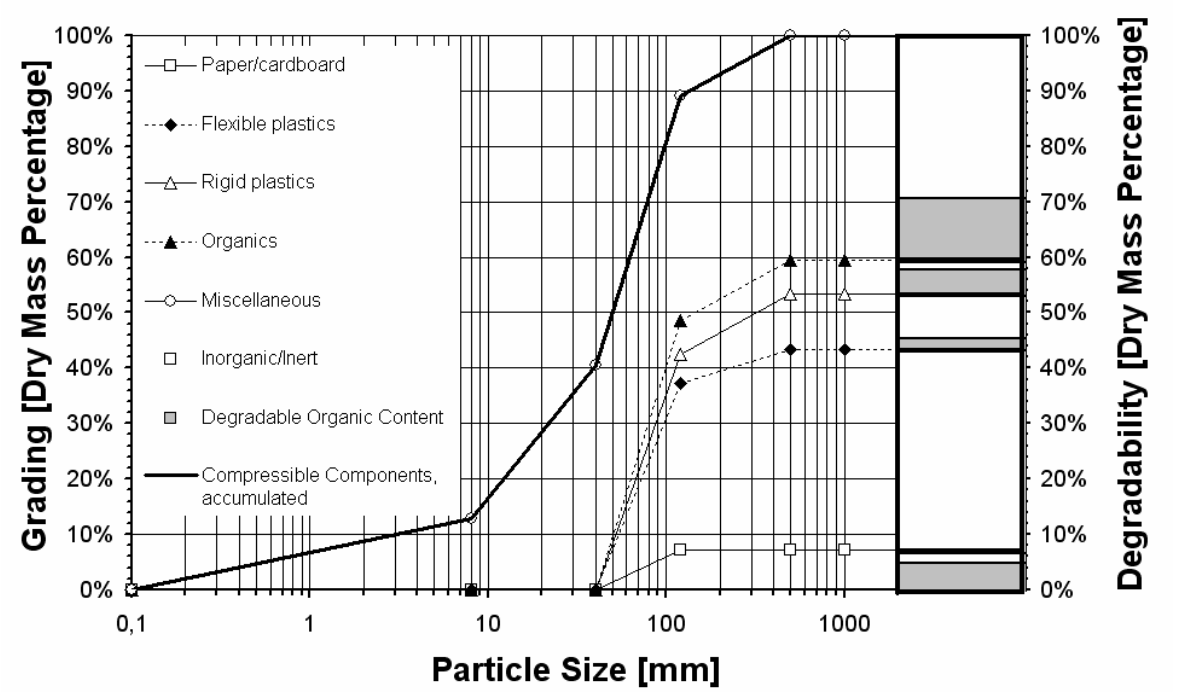

Figure 4-13 Compressible components: Material groups, gradings, organic content of the material groups related to 100% of the overall sample mass (data from Kölsch, 1996; data for miscellaneous material modified by the Authors)

The data produced by Kölsch (1996) and re-analysed above can be used to classify the waste components in their initial state (i.e. as delivered to site) based on percentages of the shape-related subdivisions, as shown in Table 4-3 and Figure 4-14. In addition, this diagram can be used to demonstrate changes in classification resulting from waste placement, which causes compression of some components, and in the long-term following degradation of some components.

Table 4-3 Percentages of shape-related subdivisions used to define initial, post placement and final states on the ternary classification diagram

	Shape-related Subdivisions by Dry Mass			
	Reinforcing	**Incompressible**	**Compressible**	**Sum**
State	**[%]**	**[%]**	**[%]**	**[%]**
Initial State	43.4	26.0	30.6	100
Potential State after Placement	56.3	28.2	15.5	100
Potential Final State relative	52.9	37.1	0.0	90[3]
Potential Final State absolute	58.7	41.3	0.0	100

[3] Mass loss due to biodegradation

In Figure 4-14 the initial state is derived directly from the original shape and material properties data. For the potential state after placement, it has been assumed that the percentage of the reinforcing and incompressible components both increase due to the compression of highly compressible components such as paper, flexible plastic packaging and organic materials. A distinction was made between material sizes <40mm and >40mm, and the smaller sized components were assumed to have an insignificant effect on reinforcement (i.e. based on the ratio between the size of reinforcing and regular-shaped components as discussed above); consequently they were reassigned to compressible and incompressible components. Degradation was not taken into account for the waste state following placement due to the fact that placement is by definition a short-term event. Stronger materials such as rigid plastics, wood/leather, and the defined part of the miscellaneous material were assumed to remain in their initial state.

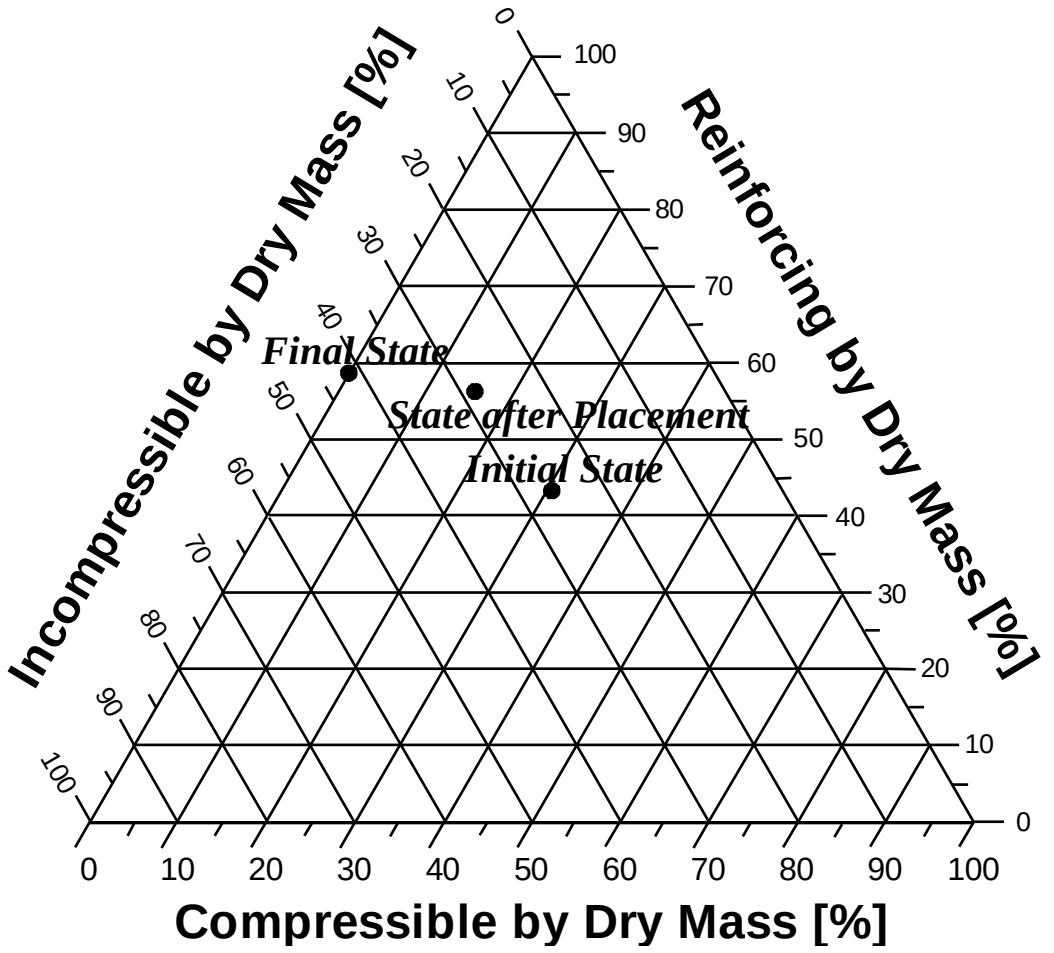

Figure 4-14 Potential use of shape-related subdivisions to aid evaluation of changes in waste mechanical behaviour resulting from placement and final state after long-term degradation.

The final state of the waste has been calculated based on the percentage of materials in each shape-related subdivision with potential to degrade. A loss of mass due to methane and carbon dioxide generation and the alteration of organic into mineral matter was calculated using values for the degradation potential of components (Table 4-4, after Fricke *et al.*, 1999). The remaining compressible components in particular material groups

(e.g. rigid plastic, wood/leather and miscellaneous) were assumed to become incompressible (sized <40mm) and reinforcing (sized >40mm) due to overburden stress. It is assumed that the overburden stress exceeds the maximum compressive strength of these components and that this therefore causes flattening. Due to the material characteristics of metals and minerals, these groups stayed in their initial state. The use of the ternary diagram requires the presentation of the shape-related subdivisions as percentages as shown in Table 4-3, which means that the loss of mass is not shown, due to the fact that the sum of the shape-related subgroups always has to equal 100%. In fact there is a loss of mass in each of the three groups due to degradation.

Table 4-4 Specific material values for the biodegradable part of waste components (after Fricke *et al.*, 1999)

Material Groups	Degradation Potential by Dry Mass [%]
Paper/cardboard	76
Flexible plastics	0
Rigid plastics	23
Metals	0
Minerals	0
Wood/leather	85
Organics	76
Miscellaneous	28

4.3 Development of a Family of Synthetic Wastes

4.3.1 Waste Sorting Analysis

The waste sorting analysis was conducted on Narborough landfill (Leicestershire, UK), which is operated by SITA. For the sorting fresh waste was examined, which was originated from the region around Narborough. After the content of a collecting vehicle was deposited on site approximately $3m^3$ of fresh waste material was delivered to the sorting area.

4.3.1.1 Description of the Sample

Figure 4-15 shows the amount of the waste sample. The volume was assumed to be about $3m^3$ (the sample was put on a plastic sheet with an area of 2*3m; the height was at an average of approximate 0.5-0.6m). The sample contained a majority of black waste bags, which were mostly half to fully filled. The average dimension of a bag was about 0.6*0.25*0.3m (approx. 50 litres), while the weight varied significantly. About 1/3 of the overall sample amount was examined and sorted (approximately $1m^3$). With an overall wet sample mass of 126.2kg the non-compacted bulk unit weight for the fresh waste results in $1.26kN/m^3$.

Figure 4-15 Waste sample mass before sorting

An example for the individual content of a waste bag is shown in Figure 4-16. Often smaller, filled bags (shopping bags) were found within the big waste bags. From the first impression it was concluded that the waste comprises with high amounts of paper, plastic sheets, plastic beverage bottles and organic material (kitchen and garden waste like vegetables, bread, meat, flowers and plants). Progress of degradation was not obvious, although from the odour level of the waste, especially from the organic fraction, it could be inferred that degradation was actively ongoing. Another indication for initial degradation was the soft structure of the organic components like fruits and vegetables. Paper and cardboard (packaging, newspaper, magazines, letters) were partially moist, providing good boundary conditions for degradation. However, major parts were in a dry state. Plastic foils, bags and plastic packaging, which could be compressed one-handed without much effort, were defined as flexible plastics. The main part of this group was represented by plastic bags. Rigid plastics were components like beverage bottles, stable plastic packaging and the remaining plastic (boxes, cans, rubber shoes). The majority of the plastic bottles were closed; some of them contained residual fluids (about 200ml in an 1.5-2l bottle). The metal fraction largely consisted of food cans, some with food residue, and empty aluminium beverage cans. Regarding the progress of compression of rigid plastics and metals, it was observed that these components were in their original undamaged state or hardly compressed. The group of glass and minerals was primarily composed of intact bottles and glass jars. There was a small amount of mineral soil-like cat litter and a minor amount of ceramic and stoneware plates was also found. In terms of wood, leather and textile, only a very small amount was found. It consisted of clothing, curtains and shoes. The fraction of miscellaneous material is defined by fine-grained materials (<40mm), which could not be sorted. A large amount of this group was organic and

mineral material, but also paper, plastic and metal crown caps. Another distinctive feature was the observation, that the waste contained a lot of products, which were still in their original packaged state, as there was food in plastic packaging, beverages in bottles or unopened cans.

Figure 4-16 Content of waste bags during sorting

4.3.1.2 Waste Composition

With assumed water content values (appendix 11.2) for the different materials, the dry mass could be calculated. About 1/3 of the dry sample mass (32%) is represented by organic material. Reinforcing components like paper and flexible plastic form another third of the dry mass (36%). Minerals, metals, rigid plastics, wood/leather and miscellaneous material form the remaining part of the dry sample mass (32%). A similar result applies for the wet mass composition. The masses are slightly shifted in advantage of organic material and paper/cardboard (37%, 37%, 26%), but that does hardly affect the general result. Figure 4-17 shows the waste composition representing the examined fresh waste.

Considering the amount of paper/cardboard and the organic fraction, it can be concluded that this waste sample consists of about 50% medium-slow to readily degradable material. That leads to the conclusion of a very reactive and compressible material. There are two reasons for the assumption of a compressible waste, which is the physical properties of the organic material (soft, easily compressible) and on the other hand the high degradation potential of the organic material (i.e. degradation leads to loss of volume and mass).

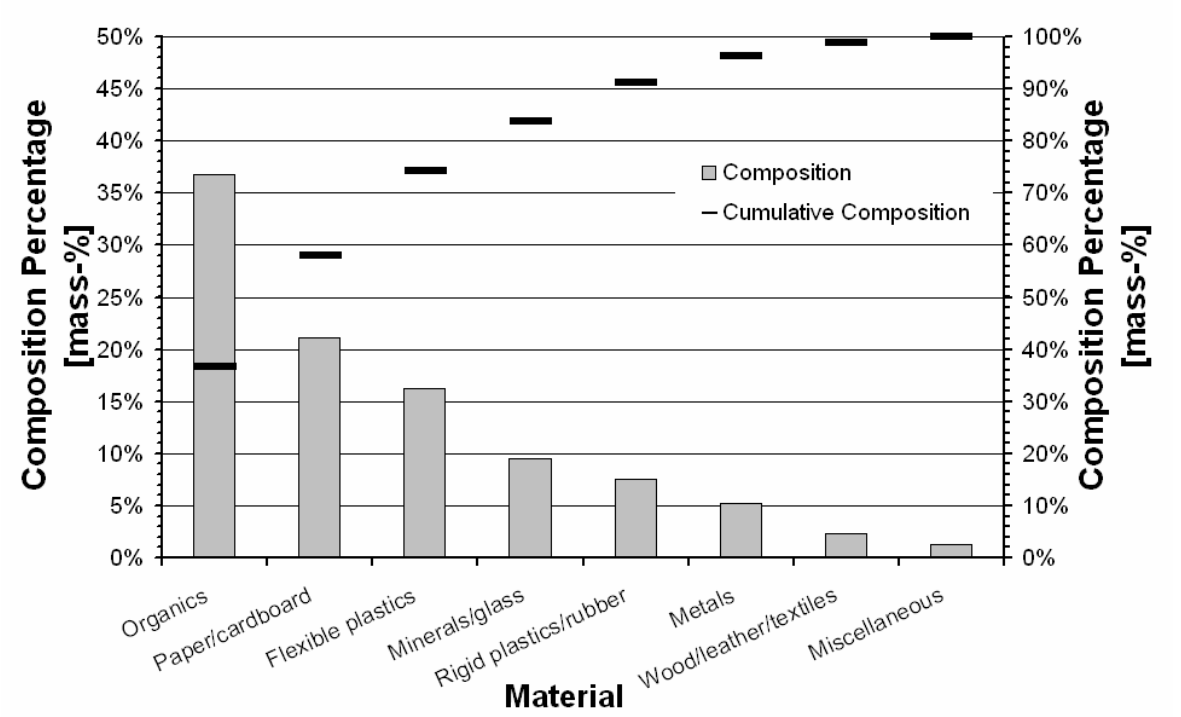

Figure 4-17 Wet weight waste composition

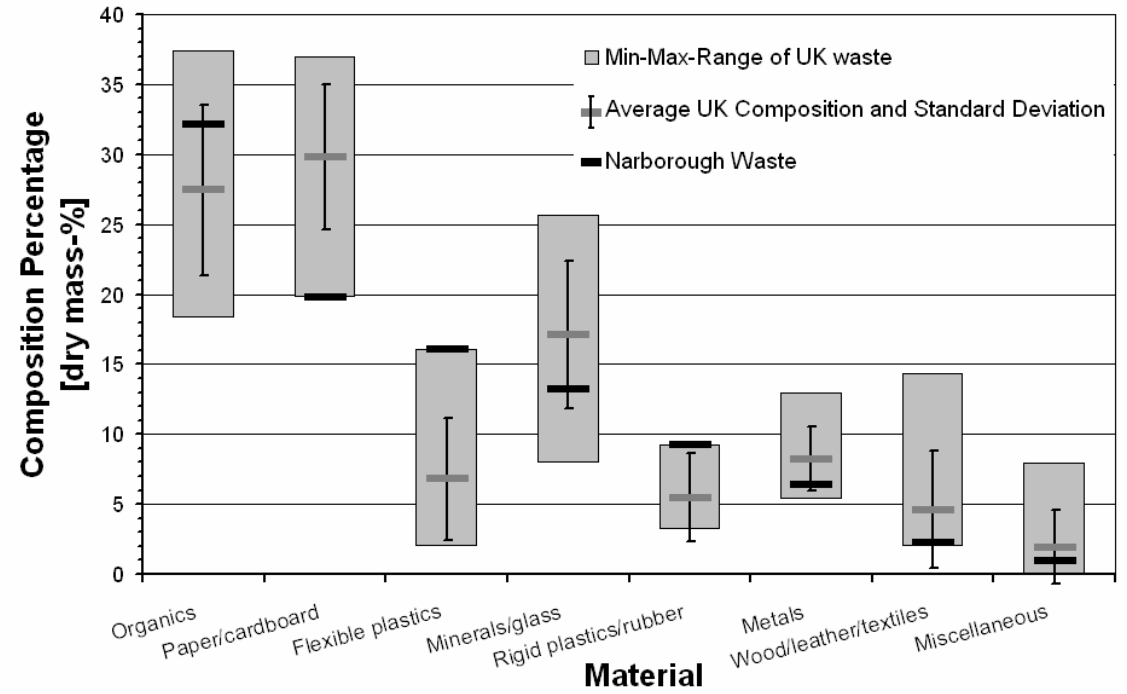

Figure 4-18 Narborough waste composition compared with average UK composition

Figure 4-18 shows a comparison of the Narborough waste to an average UK waste composition, which is derived from 8 datasets found in literature. Additionally, the figure shows the minimum-maximum-range and the standard deviation of the datasets used for this comparison. The largest difference is visible in the groups of paper/cardboard and flexible plastics. In both groups the Narborough waste differs considerably from the UK

average. It is on the outer limit of the minimum-maximum-range and it exceeds the standard deviation of the data sets. The amount of organic material and rigid plastic is just within the range of the standard deviation, while the remaining material groups are on a similar level as the average UK composition. It is concluded that the Narborough waste sample shows an exceptional low amount paper and wood/leather/textiles but a high amount of flexible and rigid plastics.

4.3.1.3 Shape-related Subdivision

A shape related subdivision is necessary to assess the role material groups could play in waste body mechanical behaviour in regard to their mechanical properties. It is proposed that the shape of waste components could be characterised by one of the basic groups based on shape-related properties and mentioned in chapter 4.2.

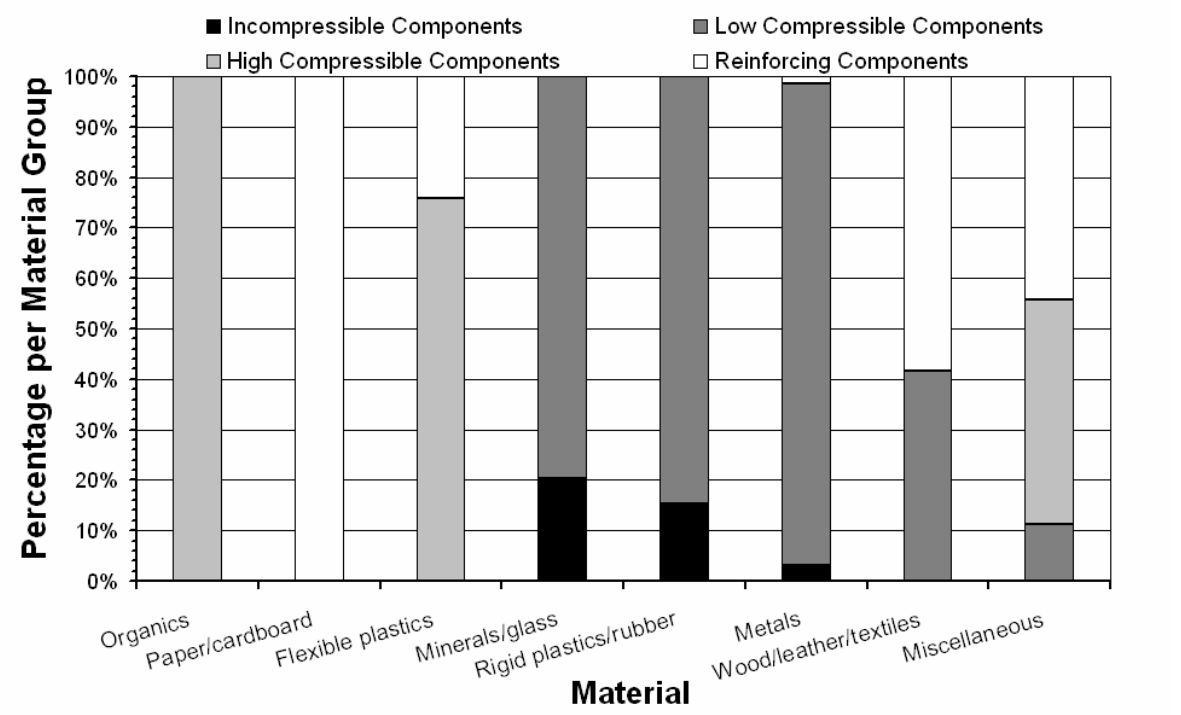

Figure 4-19 Shape-related subdivisions (in-, compressible and reinforcing components) within the material groups

Figure 4-19 demonstrates the shape-related subdivisions in every material group. It is striking that almost every material group is dominated by a certain shape-related subdivision except for miscellaneous materials. For example, the group of paper and cardboard only consists of reinforcing components, organic components only seem to have highly compressible properties, while metals and minerals exhibit low compressibility and a small amount of incompressible components. Rigid plastic components show more low compressibility components than incompressible, flexible plastic contents mostly high compressible components and a smaller amount of reinforcing components.

At this stage of the examination, each material group with two exceptions is clearly dominated by one of the three shape-related subdivisions[4], as there are:

1. Incompressible components: No domination
2. Compressible components
    a. High compressible: Flexible Plastic (76%), Organics (100%)
    b. Low compressible: Rigid Plastic (85%), Metals (95%) and Minerals (80%)
3. Reinforcing components: Paper/Cardboard (100%)

The first exception (Wood/Leather/Textiles) is at this stage slightly dominated by reinforcing components (58%); the second exception (Miscellaneous material) exhibits a marginal domination of compressible (high and low) components (55%).

4.3.1.4 Available Size Ranges

The size of the components or the grading of waste is a crucial characteristic, when it comes to assess the mechanical function of components. In conjunction with the shape-related properties, it is possible to distinguish between e.g. reinforcing components and surrounding matrix. Considering small-sized reinforcing components (i.e. one- or two-dimensional) surrounded by relatively large non soil-like components, the reinforcing effect does not occur due to missing bonding of the reinforcing components to the soil-like material.

Figure 4-20 shows the mass distribution of the examined waste for the selected size ranges. This largest mass concentration is situated in the size range of 120-500mm. Organic components, glass components and the large amount of plastic and paper of this sample account for this mass concentration. The range 40-120mm is also dominant and largely consists of organic materials and small amounts of metal and minerals. Sizes less than 40mm occurred only in minor amounts; miscellaneous materials exhibit sizes between 10mm and 40mm and a fraction of the minerals feature a size less than 10mm. The low amount of components greater than 500mm is derived from textiles. Due to the fact that the degradation progress was not advanced, exceptional high masses within the small size ranges were not expected.

Figure 4-21 to Figure 4-23 show the size ranges and material groups within each shape-related subdivision. Figure 4-21 demonstrates incompressible components. Only metals in the range of 40-120mm, rigid plastic within 120-500mm and minerals sized <10mm are represented. Compressible components in Figure 4-22 are represented in the size range between 40mm and 500mm for the most part by organic and mineral material and rigid and flexible plastic, especially with a size of 120-500mm. Components of paper/cardboard stand for reinforcing components in Figure 4-23 with a size of 120-500mm.

[4] All values in dry mass percentage

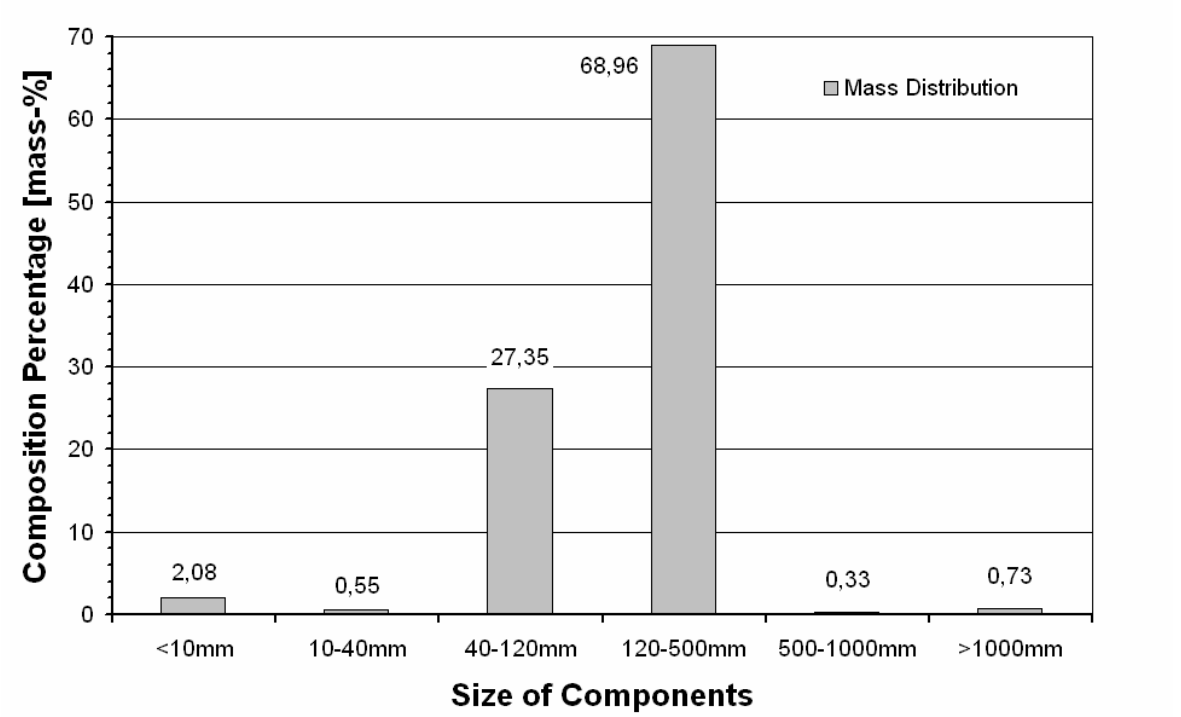

Figure 4-20 Mass distribution within the size ranges

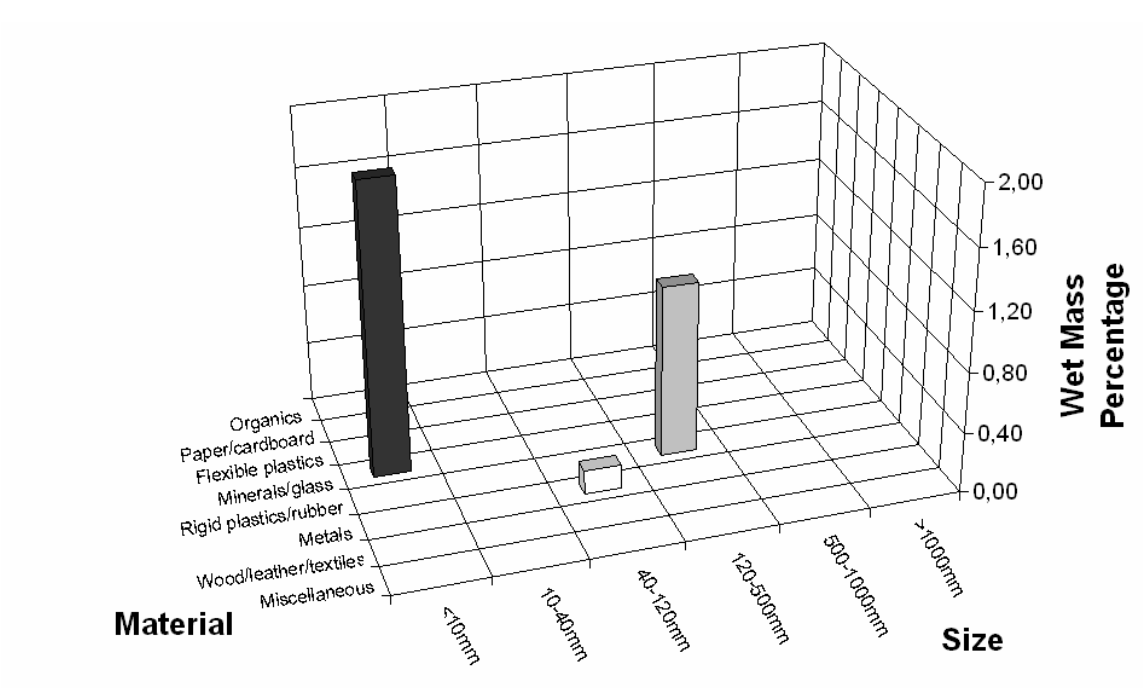

Figure 4-21 Size range and material groups for incompressible components

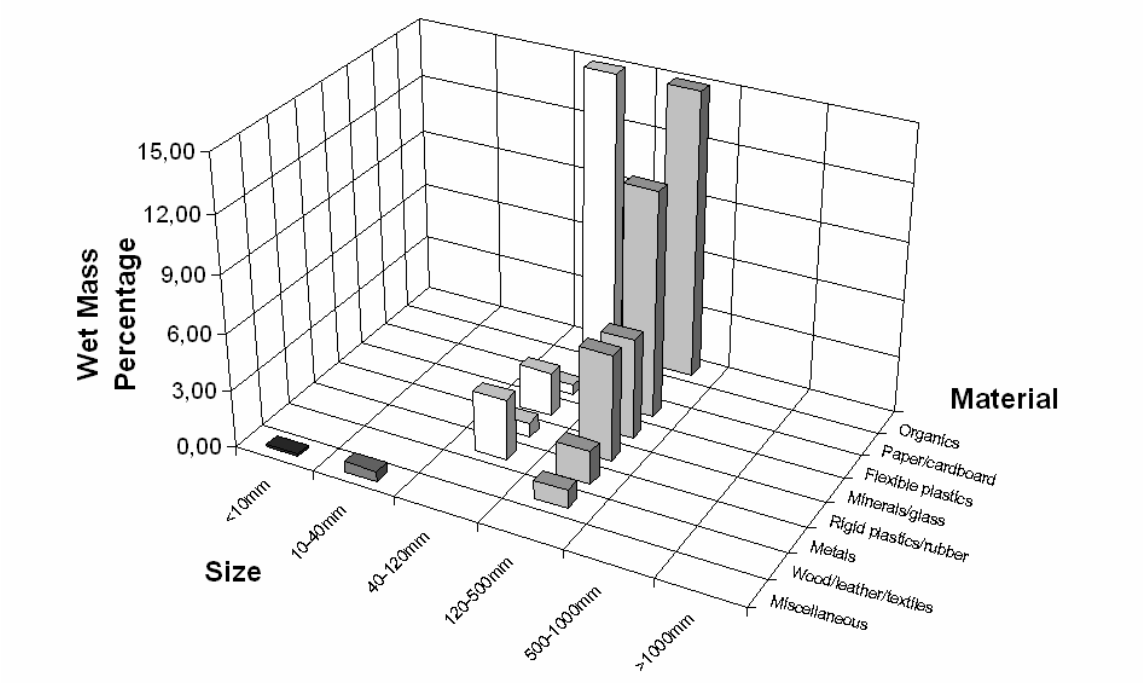

Figure 4-22 Size range and material groups for compressible components

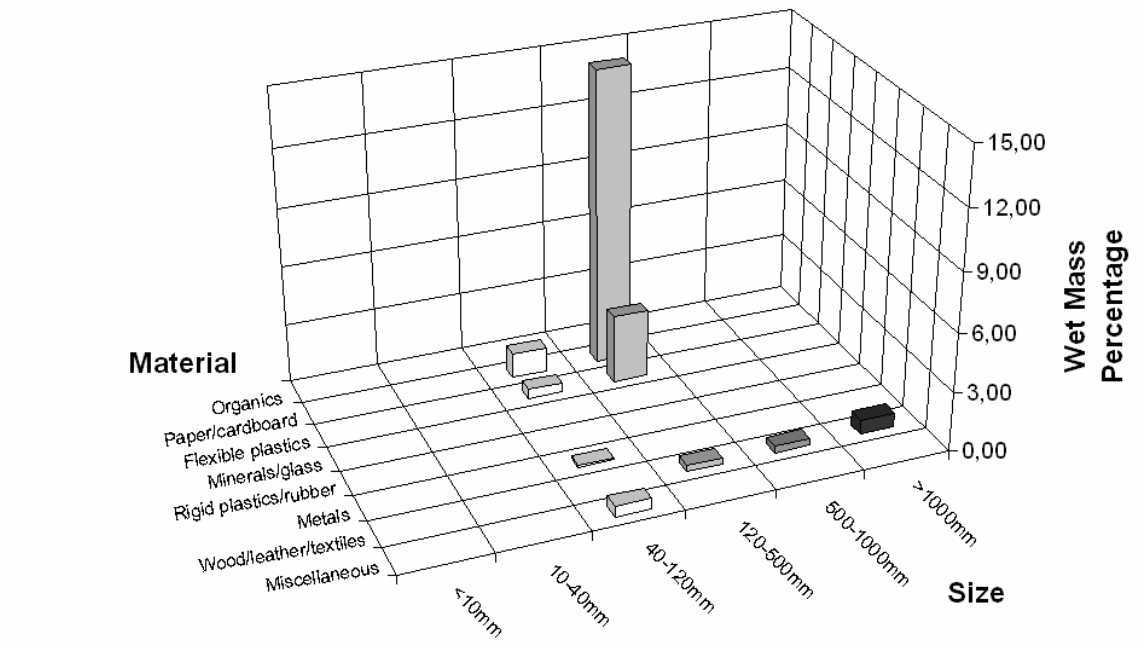

Figure 4-23 Size range and material groups for reinforcing components

4.3.1.5 Classification of Components by Means of Material Properties, Degradability, Size Ranges and Consideration of Different Landfill Stages

Figure 4-24 to Figure 4-26 show the application of the classification framework to the data acquired from the waste sorting analysis. The shape-related subdivisions are shown including the grading and the degradability of the components.

The shown amount of incompressible components is not expected to decrease to a high extent, as the materials involved (metals, minerals) do not possess degradation potential (column on the right-hand side in Figure 4-24) and materials like rigid plastics and rubber are very slowly degrading. In further stages of the depositing process the amount of incompressible components will increase as the compression potential of these components will be fully tapped. In terms of degradability for the compressive components important changes are expected to occur. They are characterised by organic components (>50%). The degradability of these organic components accounts for about 40% of the overall dry mass within this size range. Organic components as defined in this project (kitchen and green waste) are expected to degrade rapidly. In consequence, this means a reduction of the compressible components and an increase of incompressible components due to an alteration to soil-like (mineral) sub-products. The degradation potential of paper reflects about 46% of the overall dry mass for reinforcing components and is due to change provided that a sufficient water content allows degradation. Additionally, wood/leather/textiles show a degradable potential of about 5% of the overall dry mass.

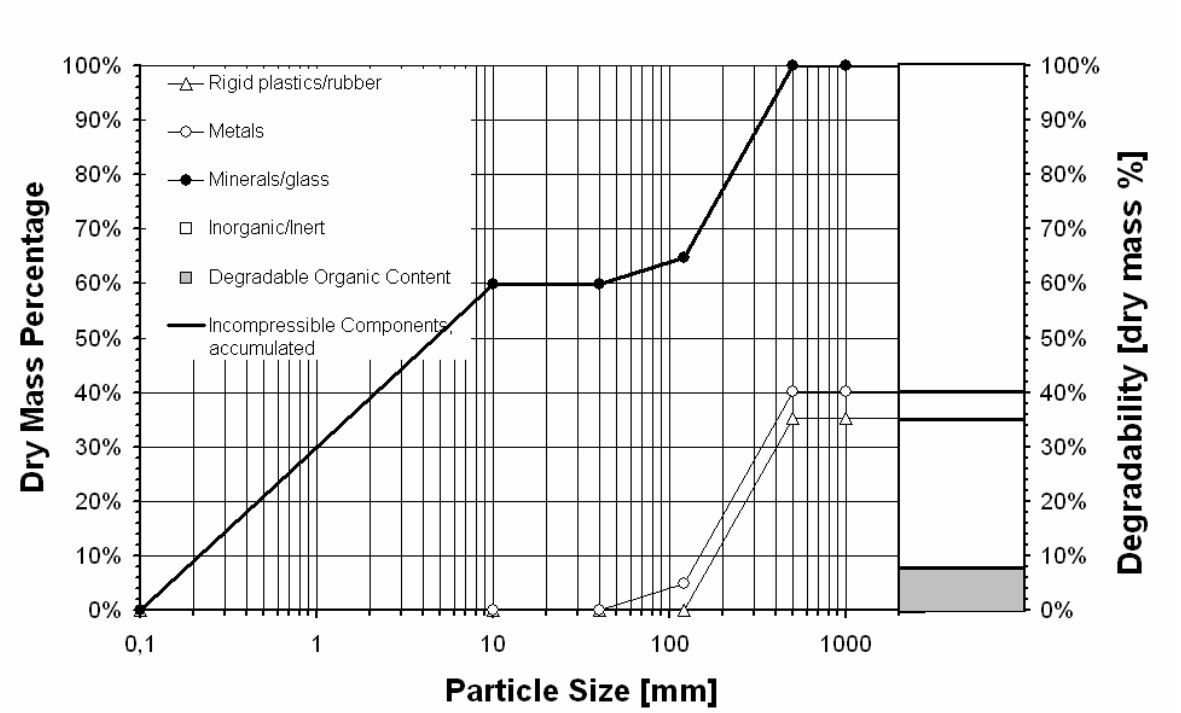

Figure 4-24 Incompressible components: material groups, gradings, organic content (waste from SITA landfill, Narborough)

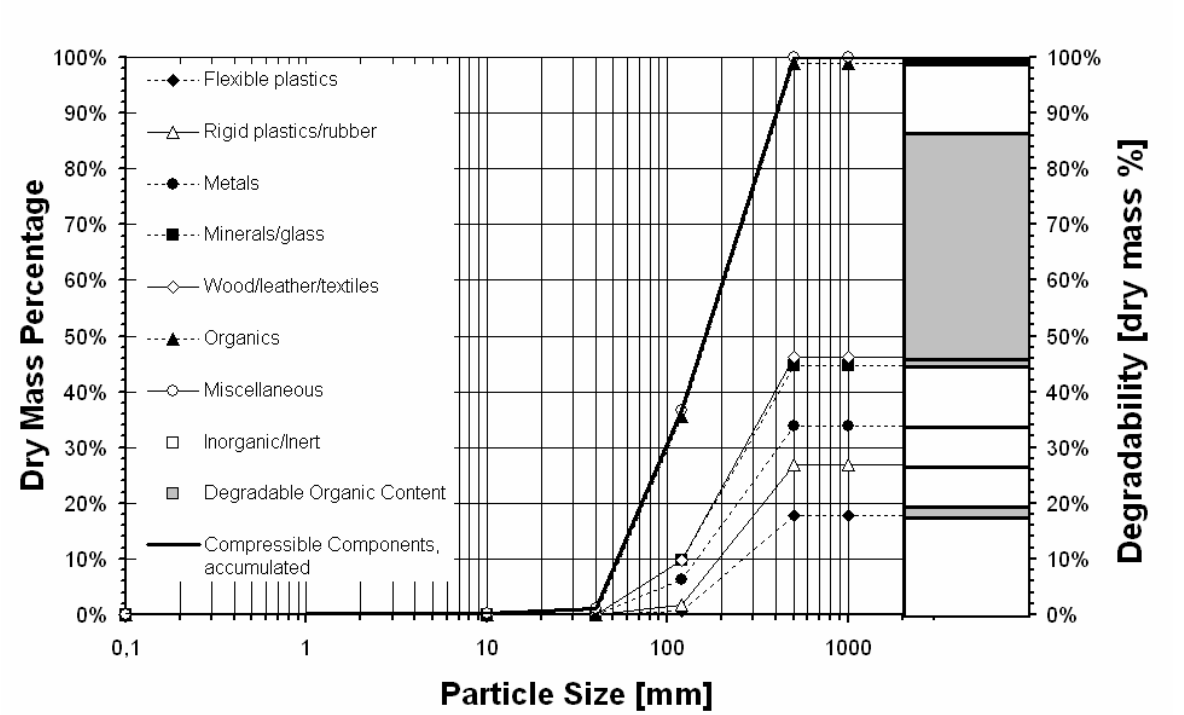

Figure 4-25 Compressible components: material groups, gradings, organic content (waste from SITA landfill, Narborough)

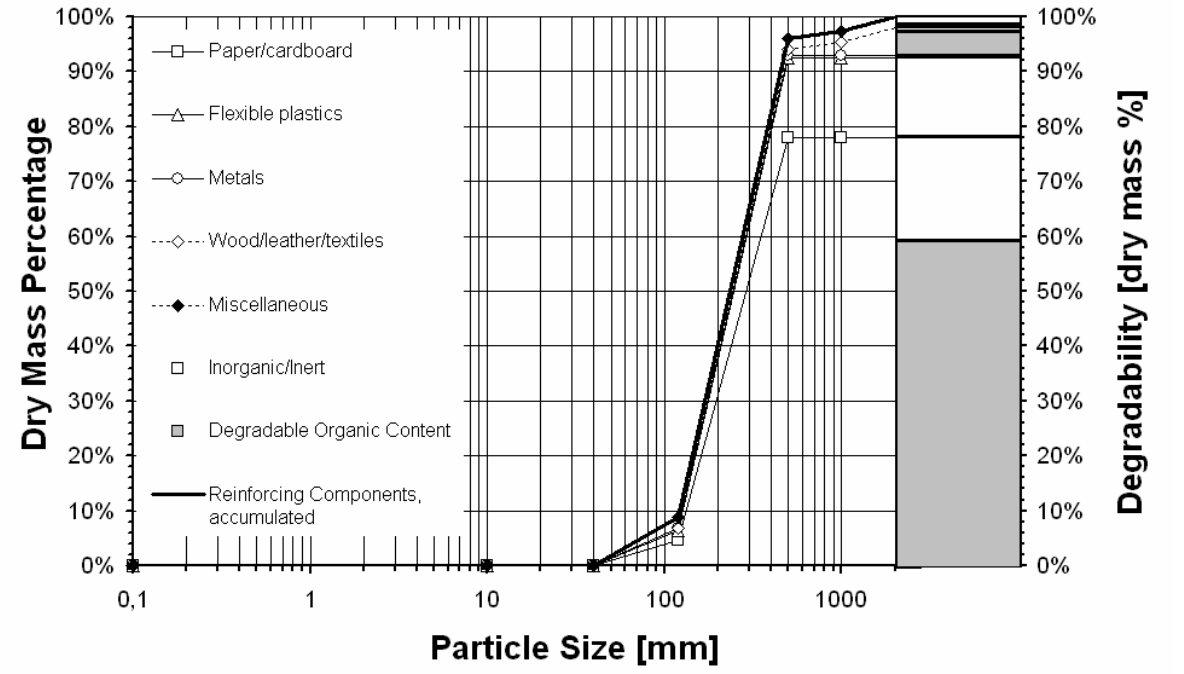

Figure 4-26 Reinforcing components: material groups, gradings, organic content (waste from SITA landfill, Narborough)

4.3.1.6 Consideration of Three Different Stages During Landfilling

Figure 4-24 to Figure 4-26 show the initial stage of the components as delivered to site. The data surveyed in the sorting analysis could be used without the need of any changes or additional considerations. For the subsequent states (post-placement and final state), some assumptions have to be made, which are based on considerations regarding the shape-related material properties and the components size. Table 4-5 shows the basic assumptions, which are made for the definition of the state after placement and the final state.

Table 4-5 Assumptions for defining the states

		State		
Group	**Materials**	**Initial**	**After Placement**	**Final**
I	Paper/Cardboard, Flexible Plastic, Rigid Plastic	C_I	$C_P=C_{L,\,I}$	$C_F=0$
		I_I	$I_P=I_I$	$I_F=I_P$
		R_I	$R_P=R_I+C_{H,\,I}$	$R_F=R_P+C_P$
II	Metals, Minerals/Glass, Wood/Leather/Textiles	C_I	$C_P=C_{L,\,I}$	$C_F=0$
		I_I	$I_P=I_I+C_{H,\,I}$	$I_F=I_P+C_P$
		R_I	$R_P=R_I$	$R_F=R_P$
III	Organics	C_I	$C_P=C_{L,\,I}$	$C_F=0$
		I_I	$I_P=I_I$	$I_F=I_P+0.5*(R_P+C_P)$
		R_I	$R_P=R_I+C_{H,\,I}$	$R_F=0.5*(R_P+C_P)$
IV	Miscellaneous	C_I	$C_P=C_{L,\,I}$	$C_F=0$
		I_I	$I_P=I_I+C_{H,\,I}$	$I_F=I_P+0.5*(R_P+C_P)$
		R_I	$R_P=R_I$	$R_F=0.5*(R_P+C_P)$

Where

C = Compressible components
I = Incompressible components
R = Reinforcing components

Indices

I =Initial state
P =State after placement
F =Final state
H =High
L =Low

Another general assumption concerns size and reinforcing function of the component. Generally, it is assumed that components with a size <40mm do not exhibit a reinforcing function, and ideally compressible components do not exist in the final state.

Compressible components from the prior states are transformed into either incompressible or reinforcing components due to compression.

As any changes were not necessary for the initial state, the material is shown as it appeared during sorting. The compressible components of each material group in the state after placement are those with a low compressibility in the initial state. For group I and III incompressible components remain as initially and the reinforcing components are represented by initial reinforcing and high compressible components, while for group II and IV the high compressible components add up to the incompressible and the reinforcing components remain the same.

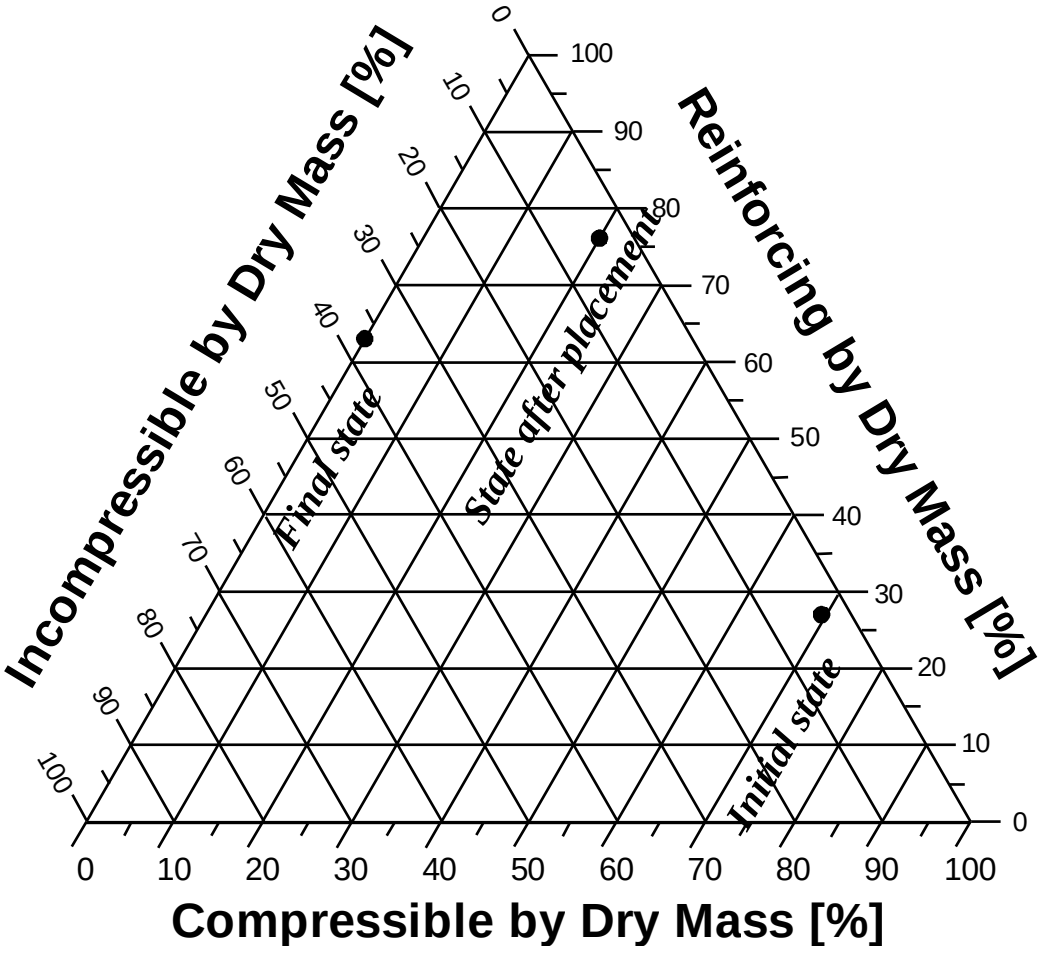

Figure 4-27 Classification based on ratios of the shape-related subdivisions (waste from Narborough landfill of SITA)

As compressible components are non-existent in the final state, all compressible components are assumed to become either incompressible or reinforcing due to compression processes. The incompressible components of group I still remain in their initial state. Group II shows incompressible components represented by incompressible and former compressible components of the state after placement. The incompressible components of groups III and IV contain the incompressible components of the earlier state and 50% of the compressible and reinforcing components. This is due to the alteration and decrease of the shape by degradation. The remaining 50% account for the reinforcing components in the final state.

These assumptions result in the shifting of the shape-related subdivisions shown in Figure 4-27. From a very compressible waste with reinforcement in the initial state, it turns into highly reinforced waste in the state after placement and to a reinforced and incompressible waste in the final state. Due to the high amount of compressible components the waste shows big potential for variation within the shape-related subdivisions. Compressible components are transformed into reinforcing and incompressible components.

4.3.2 Synthetic Waste

4.3.2.1 Statements Derived from the Waste Sorting Analysis

From Figure 4-21 to Figure 4-23 first conclusions about possible synthetic waste components and their properties can be deduced. It is obvious that the shape-related subdivisions show clearly defined material groups and size ranges. For the design of synthetic waste, these graphs clearly limit the amount and size of materials per shape-related subdivision.

Incompressible material groups are minerals, rigid plastics and metals. The amount of these materials is in this case in very low percentages of below 2% dry mass. Compressible components accounting for the mass majority of the sample (with amounts up to 15% dry mass) are represented in almost all material groups. The size is limited to an overall range of 40-500mm, with the main materials being organics, flexible and rigid plastics, and minerals. In the group of reinforcing materials, paper and cardboard account for the biggest part. Additionally, there are small amounts of flexible plastic.

4.3.2.2 First Approach Towards a Comprehensive Amount of Material Fractions

For an initial approach, the initial size ranges and the material groups of the waste sorting analysis are reconsidered. The size ranges within the shape-related subdivisions are examined in order to identify the most dominant size range. The second step involves the identification of the predominant materials in the particular size range. Herewith, the most outstanding materials within the examined sample will be identified, which have to be represented in the synthetic waste.

Table 4-6 provides an overview about the dominant materials within the shape-related subdivisions. 60% of the incompressible components is represented by minerals and glass, rigid plastic and rubber amount for another 35% of this subdivision. In approximately equal shares of about one third of the mass, rigid plastics and rubber, minerals and glass, and metals define the group of low compressibility components. Almost three quarter of the high compressibility components is represented by organic material; another quarter is flexible plastic. The main reinforcing material is paper and cardboard; flexible plastic is with 15% a reasonably large amount.

Table 4-6 Dominant materials in the shape-related subdivisions

Material (wet)	In-compressible	Low compressible	High compressible	Reinforcing
Of 100% mass:	**3.2%**	**20.1%**	**49.6%**	**27.1%**
Paper, cardboard	0%	0%	0%	**78%**
Flexible plastics	0%	0%	**25%**	**15%**
Rigid plastics, rubber	**35%**	**32%**	0%	0%
Metals	5%	**25%**	0%	0%
Minerals, glass	**60%**	**38%**	0%	0%
Wood, leather, textiles	0%	5%	0%	5%
Organics	0%	0%	**74%**	0%
Miscellaneous	0%	1%	1%	2%

Table 4-7 Dominant materials in the size range

Material (wet)	<10	10-40	40-120	120-500	500-1000	>1000
				[mm]		
Of 100% mass:	**2.1%**	**0.6%**	**27.3%**	**69.0%**	**0.3%**	**0.7%**
Paper, cardboard	0%	0%	5%	**29%**	0%	0%
Flexible plastics	0%	0%	4%	**22%**	0%	0%
Rigid plastics, rubber	0%	0%	3%	10%	0%	0%
Metals	0%	0%	13%	3%	0%	0%
Minerals, glass	**93%**	0%	8%	8%	0%	0%
Wood, leather, textiles	0%	0%	0%	2%	**100%**	**100%**
Organics	0%	0%	**66%**	**27%**	0%	0%
Miscellaneous	7%	**100%**	2%	0%	0%	0%

Table 4-7 shows the distribution of the materials within the size ranges. Fines (<10mm) are clearly dominated by the material groups of minerals and glass. Soil-like materials also account for this material group. The range of 10-40mm is defined by miscellaneous material, which was not sortable. Metals and organic material in particular account for the range of 40-120mm. Due to 120-500mm being the range with the biggest mass percentage almost every material group is represented. Paper, cardboard, organic material and flexible plastics form the greatest part of this size range. The size ranges 500-1000mm and >1000m are visibly dominated by wood leather and textiles.

Table 4-8 Reduced mass distribution within the relevant size ranges of the shape-related subdivisions

Shape-related division	Sub-division	Incompressible			Low Compressible		High Compressible		Reinforcing			Sum
Size [mm]	Range	<10	40-120	120-500	<10	40-120	10-40	40-120	120-500	40-120	120-500	500-1000	>1000	
Material		[dry mass-%]												
Paper/ Cardboard										1.27	19.89			21.16
Flexible Plastics								0.49	11.84	0.49	3.45			16.27
Rigid Plastics, Rubber				1.14		0.76	5.58							7.48
Metals			0.16			3.19	1.76			0.08				5.19
Minerals, Glass		1.94				2.29	5.28							9.51
Wood, leather, textiles							0.99				0.33	0.33	0.73	2.38
Organics								18.07	18.70					36.77
Miscell-aneous					0.14		0.55			0.55				1.24
Sum		1.94	0.16	1.14	0.14	6.24	13.61	0.55	18.56	30.54	2.39	23.67	0.33	0.73	100

From the findings of the waste sorting analysis the following can be stated. As dominant material groups can be found in each size range and in each shape-related subdivision, it does not seem necessary to involve every size range of each material group in the shape-related subdivision for an initial synthetic waste. On the other hand it seems necessary to consider the materials involved in the size ranges present, e.g. wood, leather and textiles and miscellaneous materials do not dominate any of the shape-related subdivisions, but they account for three size ranges, which have to be covered in order to reflect the grading of the real waste.

Dominant material groups within the shape-related subdivisions are shown in Table 4-6. There are three dominant material groups as maximum involved in these subdivisions. Table 4-7 demonstrates that in the smallest and largest size ranges (<40mm and >500mm) only one material group is dominant. In size ranges with a big mass concentration (40-120mm and especially 120-500mm) the percentage of the materials involved is distributed to up to four prominent material groups. As a consequence, Table 4-8 is the reduced set of material groups and size ranges in the shape-related subdivision. The size ranges of incompressible and low-compressible components could be reduced to two size ranges each. A very small amount of components are available in the 40-120mm range of incompressible components and the <10mm size range for low-compressibility components. The statement, which can be derived from the conducted waste sorting, is only valid for the fresh waste examined and not for subsequent states of the depositing process. A different mass distribution of the material groups within the shape-related subdivisions and size ranges has to be considered in order to find an appropriate reflection of following realistic waste conditions.

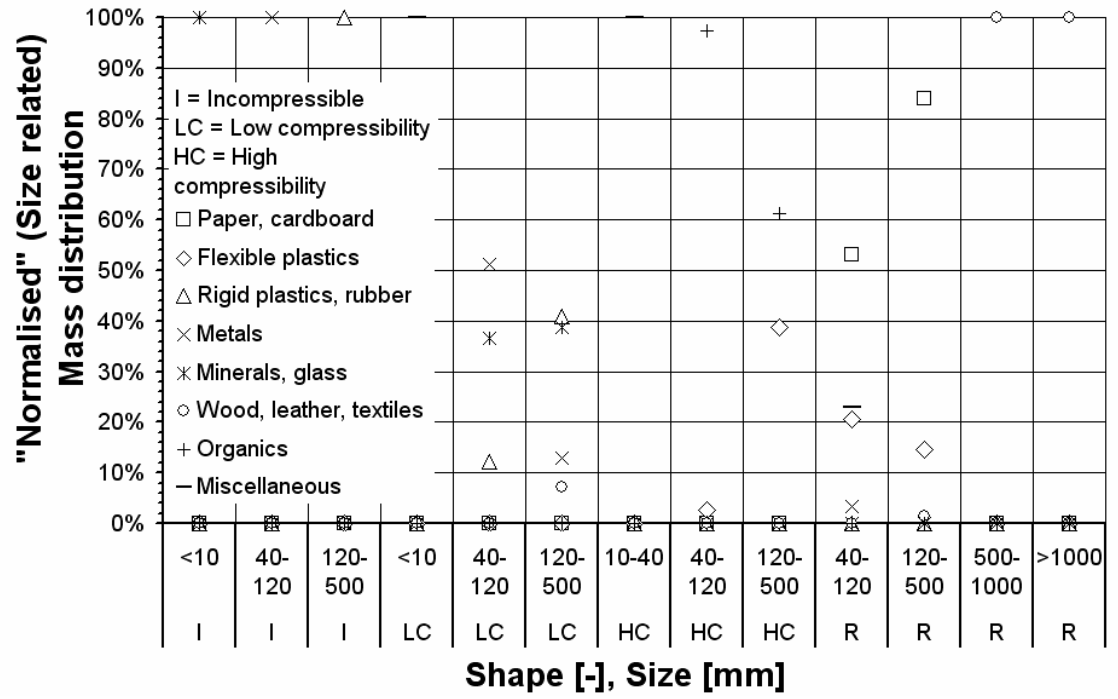

Figure 4-28 Size-related mass distribution

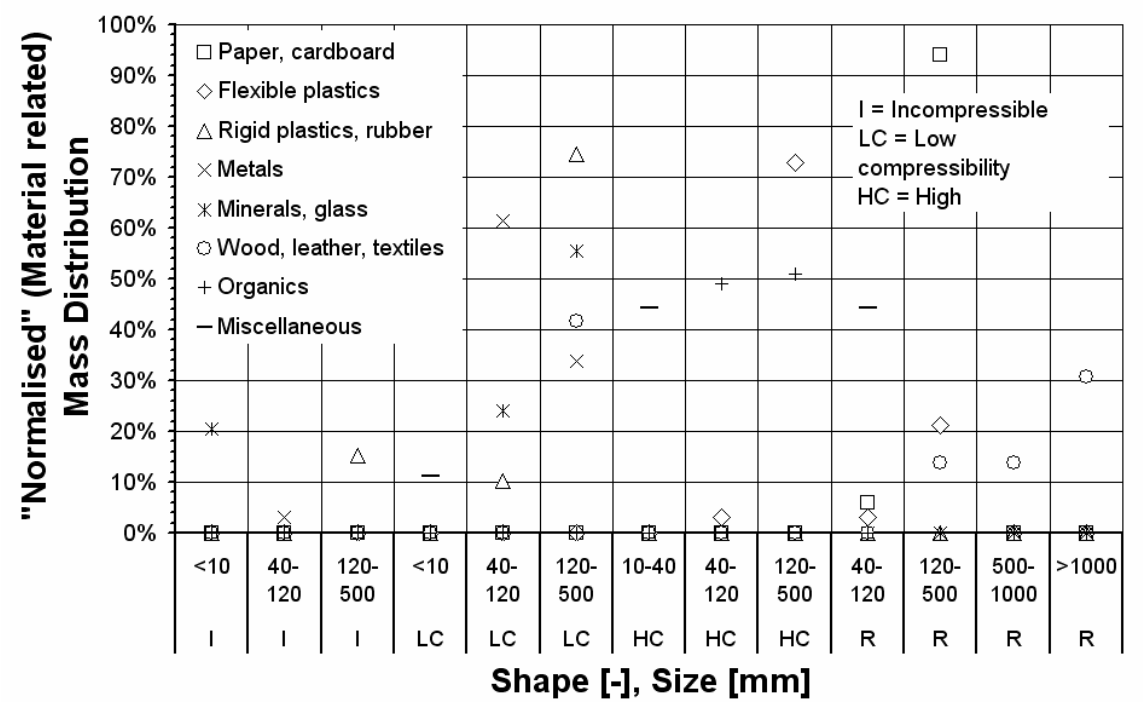

Figure 4-29 Material-related mass distribution

To decide which fractions of a specific material group are dispensable two considerations were combined. On the one hand the mass distribution within a size range (Figure 4-28) was examined, and on the other hand the distribution within one material group (Figure 4-29) was reconsidered. For each material group and size range the percentage distribution of the masses was calculated, i.e. each material group and each size range was considered separately from the overall mass. The distribution of the waste composition in regard to the material groups and the size ranges, respectively, is described by the matrix:

$$\begin{matrix} a_{11} & a_{21} & a_{31} & \cdots & a_{i1} \\ a_{12} & \ddots & & & \vdots \\ a_{13} & & \ddots & & \vdots \\ \vdots & & & \ddots & \vdots \\ a_{1j} & \cdots & \cdots & \cdots & a_{ij} \end{matrix}$$

$$m_{ij} = \frac{a_{ij}}{\sum_{j=1}^{8} a_{ij}}, \qquad j = 8 \text{ material groups} \qquad \text{Equation 4-1}$$

$$s_{ij} = \frac{a_{ij}}{\sum_{i=1}^{13} a_{ij}}, \qquad i = 13 \text{ size ranges} \qquad \text{Equation 4-2}$$

where the index “j” describes the material group and “i” the size range. m_{ij} is the ratio between individual material group and material sum within the size range i. s_{ij} is the ratio between the individual size range and the sum of the particular size range within the material group.

In a further step both values of each material and size fraction consideration were multiplied to result in a “distribution of relevant fractions” in order to emphasis the most dominant material and size range fraction.

$$\begin{matrix} ms_{11} & ms_{21} & ms_{31} & \cdots & ms_{i1} \\ ms_{12} & \ddots & & & \vdots \\ ms_{13} & & \ddots & & \vdots \\ \vdots & & & \ddots & \vdots \\ ms_{1j} & \cdots & \cdots & \cdots & ms_{ij} \end{matrix}$$

$$ms_{ij} = m_{ij} * s_{ij} = \frac{a_{ij}}{\sum_{j=1}^{8} a_{ij}} * \frac{a_{ij}}{\sum_{i=1}^{13} a_{ij}}$$ Equation 4-3

With that, dominant values of both considerations are included with the result of a general statement about dominant values. After normalising the sum of the fractions to 100%, values less than or equal to 1% were eliminated in a next step (Figure 4-30). At last, the sum of the fraction were set back to 100% to assess the new mass distribution:

$$\begin{matrix} a'_{11} & a'_{21} & a'_{31} & \cdots & a'_{i1} \\ a'_{12} & \ddots & & & \vdots \\ a'_{13} & & \ddots & & \vdots \\ \vdots & & & \ddots & \vdots \\ a'_{1j} & \cdots & \cdots & \cdots & a'_{ij} \end{matrix}$$

$$a'_{ij} = a_{ij} * \frac{1}{1 - \sum_{i} \sum_{j} a_{ij}\left(ms_{ij} < 0.01\right)}$$ Equation 4-4

Ten fractions with a value of less than or equal to 1% relevance (i.e. they range between 0.01% and 1%) were taken out of the further considerations (Figure 4-30). Figure 4-31 shows the mass distribution of the waste sorting. The neglected fractions are visible as dark columns. A maximum of 3.45% dry mass (flexible plastics, reinforcing materials 120-500mm) is disregarded. With this approach, approximately 10% dry mass from the overall sample mass are eliminated leading to a new modified mass distribution (Figure 4-32), which comprises all fractions with a relevance of more than 1%.

With this method a relation between the dominant values in the size ranges and material groups was built, and calculative irrelevant values were purged in order to minimise the amount of variables for the synthetic waste. The remaining values are important for the material groups and size ranges. It has to be examined if there is a disturbing effect on the behaviour of the synthetic waste compared to real waste. This method considers the dominant fractions within the size ranges and within the material groups, but it neglects the volumes of the materials.

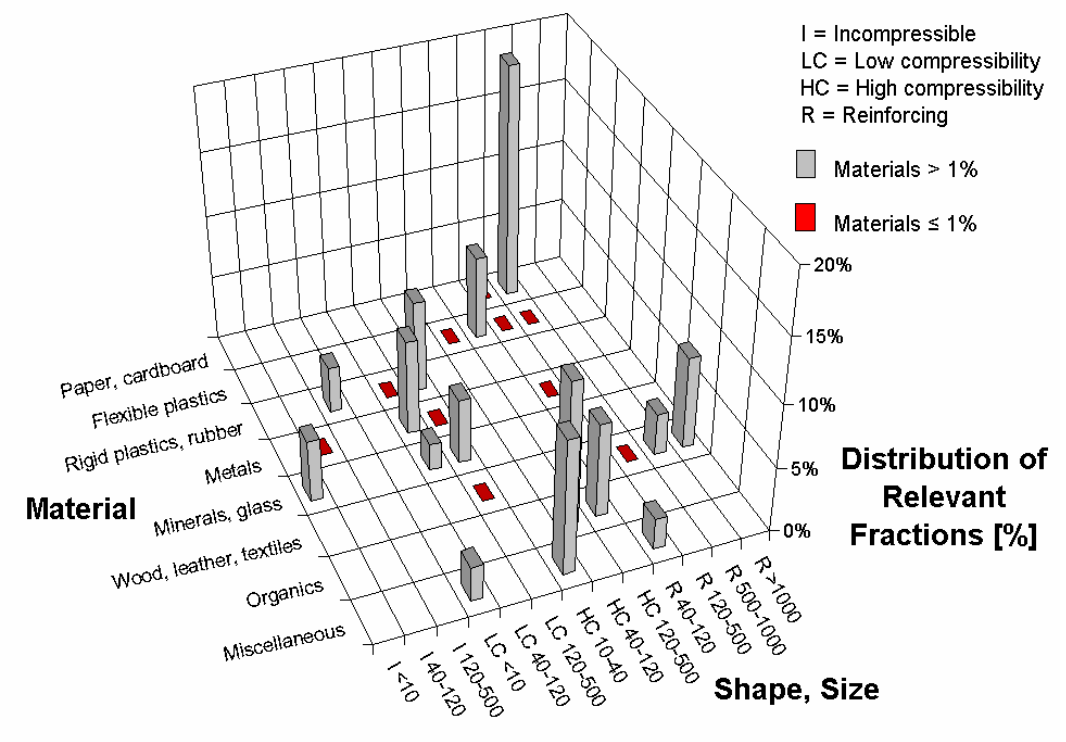

Figure 4-30 Distribution of relevant fractions without fractions <1%, set to 100%

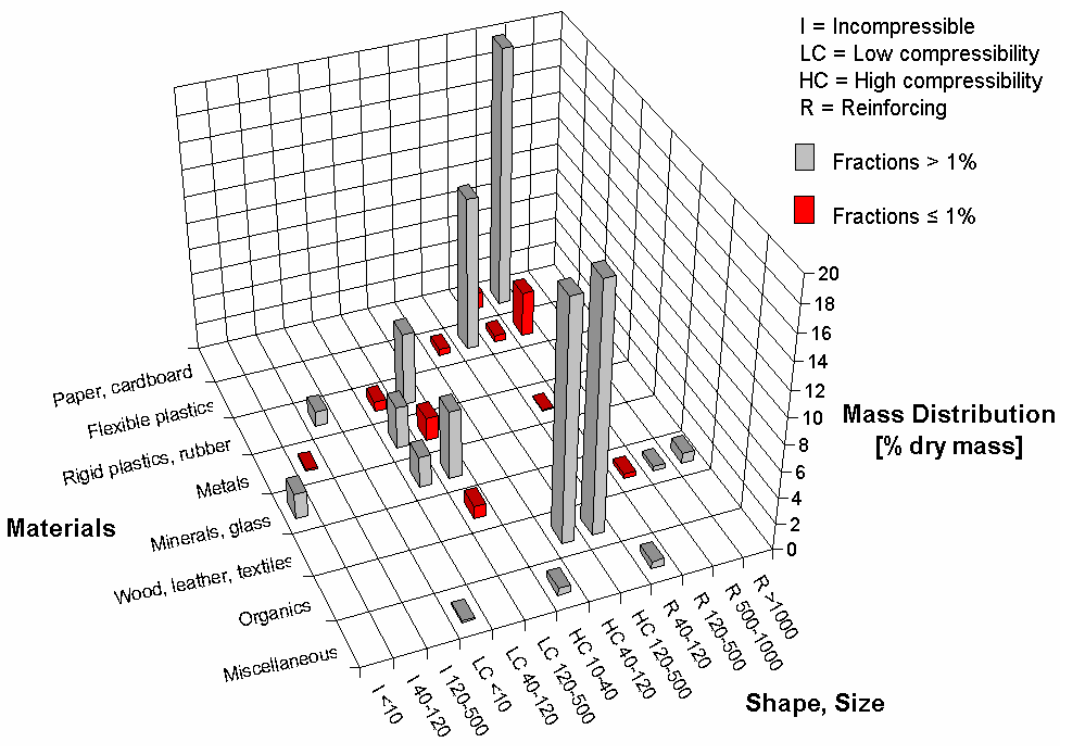

Figure 4-31 Old mass distribution with negligible fraction

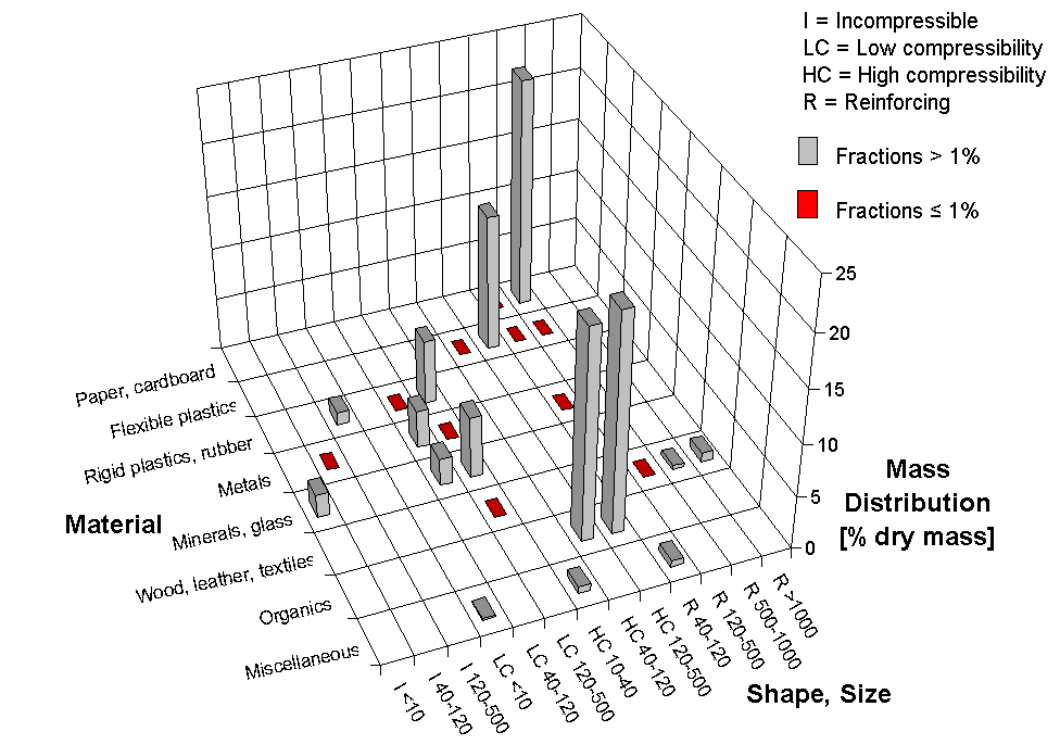

Figure 4-32 New modified mass distribution

4.3.2.3 Second Approach Towards a Comprehensive Amount of Material Fractions

To incorporate the volume of the materials the following consideration were made. The volume of a waste bag used in this survey was related to the mass of the material inside. An average value for mass per bag was calculated and from that a volume per 1000g was derived (mrv). Due to the fact that the bags used in this analysis were identical, the dimensions of the bag were not necessary for the calculation. In this way relation between the materials groups were generated. From these relations volumetric factors vf_j (Table 4-9) could be calculated, which are the ratios of the values to the lowest $mrv_{min}(j)$ (highest density). The amount of bags per material group is defined as n.

$$mrv_j = \frac{n}{\sum_{k=1}^{n} m_{jk}}$$ Equation 4-5

$$vf_j = \frac{mrv_j}{mrv_{min}(j)}$$ Equation 4-6

When considering the size ranges within the material groups, a common base was assumed being equal material properties throughout the size ranges. To be able to compare different materials within a size range a different approach has to be found. The basis, which was chosen, is the relation of a volume-indicating value to a constant mass.

Table 4-9 Volumetric factors

Material j	Mass-related Volume mrv_j [Volume-% of the bag]	Volumetric Factor vf_j [-]
Paper, cardboard	21.5	2.0
Flexible plastics	30.3	2.9
Rigid plastics, rubber	38.3	3.6
Metals	28.8	2.7
Minerals, glass	16.1	1.5
Wood, leather, textiles	23.1	2.2
Organics	10.5	1.0
Miscellaneous	25.6	2.4

The procedure of choosing the dominant material fraction is generally the same as mentioned in chapter 4.3.2.2. Within the material groups the dominant size range is calculated. For the size ranges the mass percentages of the survey are multiplied with the volumetric factors and set to 100%. Afterwards the values of the material groups and size ranges are multiplied and a distribution of relevant fraction is generated (Figure 4-33). Values below 1% relevance are eliminated from the new mass distribution (Figure 4-34).

$$\begin{matrix} ms_{11} & ms_{21} & ms_{31} & \cdots & ms_{i1} \\ ms_{12} & \ddots & & & \vdots \\ ms_{13} & & \ddots & & \vdots \\ \vdots & & & \ddots & \vdots \\ ms_{1j} & \cdots & \cdots & \cdots & ms_{ij\ j} \end{matrix}$$

$$ms_{ij} = m_{ij} * s_{ij} * vf_j = \frac{a_{ij}}{\sum_{j=1}^{8} a_{ij}} * \frac{a_{ij}}{\sum_{i=1}^{13} a_{ij}} * vf_j \qquad \text{Equation 4-7}$$

The new alternative mass distribution is:

$$\begin{matrix} a''_{11} & a''_{21} & a''_{31} & \cdots & a''_{i1} \\ a''_{12} & \ddots & & & \vdots \\ a''_{13} & & \ddots & & \vdots \\ \vdots & & & \ddots & \vdots \\ a''_{1j} & \cdots & \cdots & \cdots & a''_{ij} \end{matrix}$$

$$a''_{ij} = a_{ij} * \frac{1}{1 - \sum_i \sum_j a_{ij}\left(ms_{ij} < 0.01\right)} \qquad \text{Equation 4-8}$$

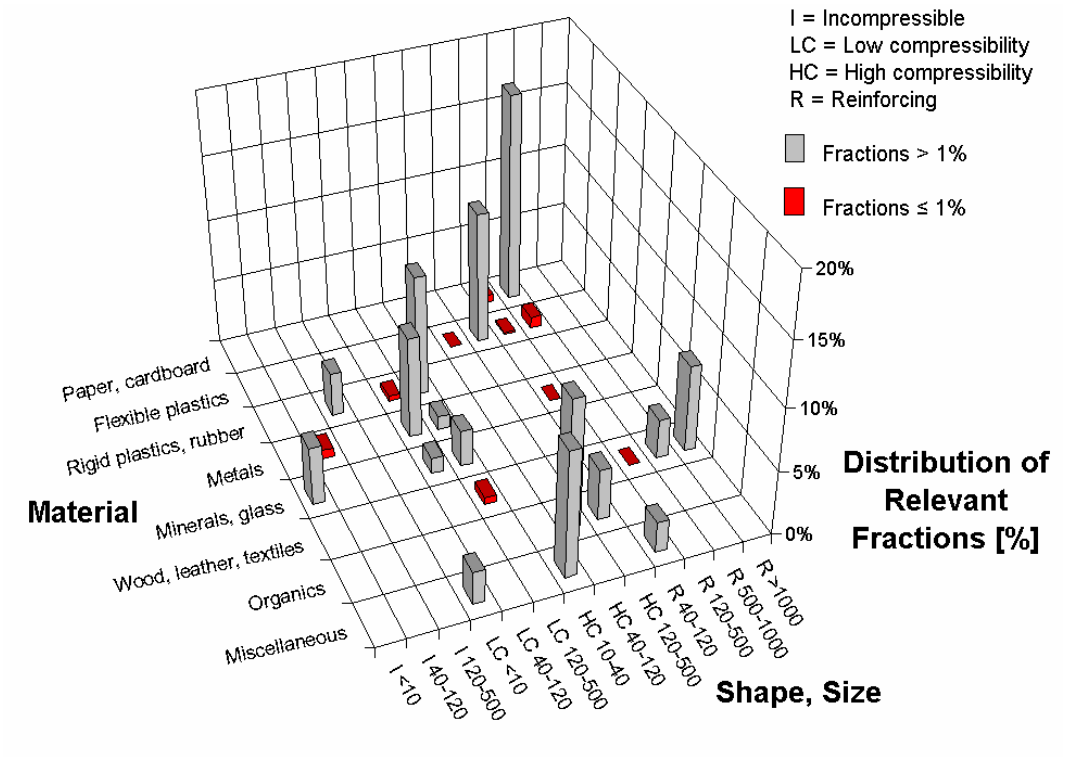

Figure 4-33 Alternative distribution of relevant fractions

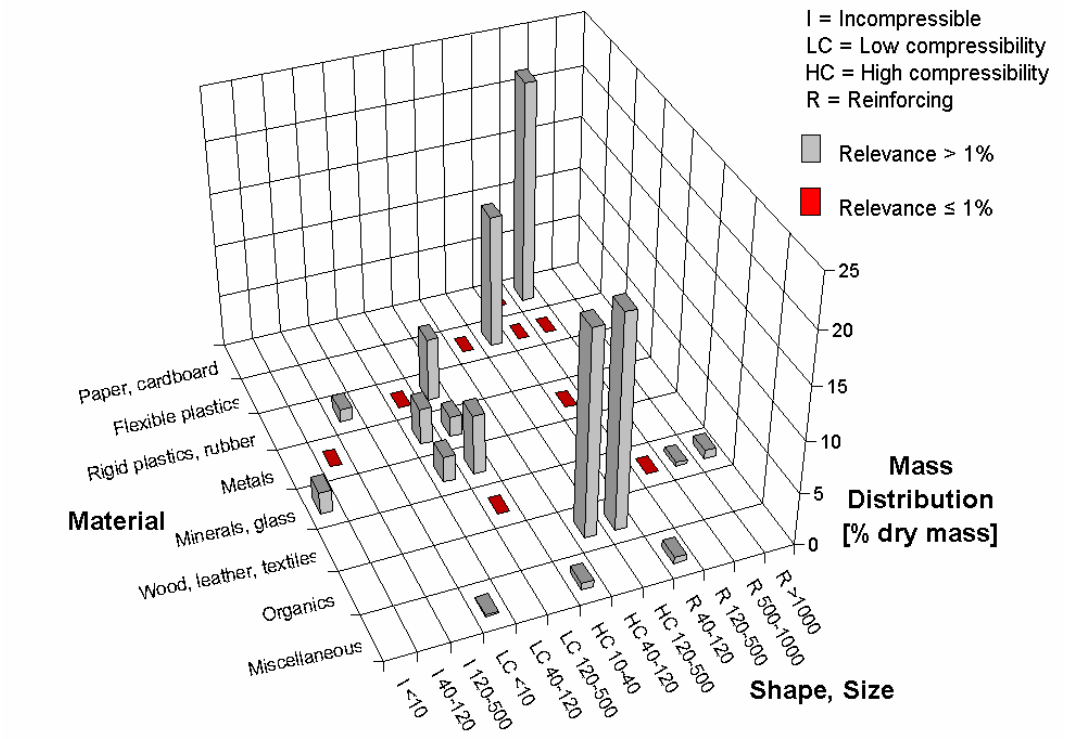

Figure 4-34 Alternative distribution of relevant fractions

Table 4-10 Reduced waste component fraction

Shape-related division	Sub-division	Incompressible		Low Compressible		High Compressible		Reinforcing			Sum
Size [mm]	Range	<10	120-500	<10	40-120	10-40	40-120	120-500	40-120	120-500	500-1000	>1000	
Material		[dry mass-%]											
Paper/ Cardboard									21.62				21.62
Flexible Plastics							12.87						12.87
Rigid Plastics, Rubber			1.24			6.07							7.31
Metals					3.47	1.91							5.38
Minerals, Glass		2.11			2.49	5.74							10.34
Wood, leather, textiles											0.36	0.79	1.15
Organics							19.65	20.33					39.98
Miscell-aneous				0.15		0.60			0.60				1.35
Sum		2.11	1.24	0.15	5.96	13.72	0.60	19.65	33.20	0.60	21.62	0.36	0.79	100

Compared to the first method, materials with a large volume, but a small mass are considered in a more appropriate way. The relevance for materials like paper, flexible and rigid plastics increase due to the volumetric factor. Nevertheless, the only material

fraction, which is additionally considered with the second method, is the fraction 120-500mm of metals (low compressibility). The other fractions remain essentially the same.

The second method is therefore the more appropriate and eliminates a factor of uncertainty related to the volume of the components due to including the volume into the process of minimising the fractions found in the waste sorting analysis. The final mass distribution is shown in Table 4-10.

4.3.2.4 Preliminary Choice of Synthetic Components

For the choice of appropriate synthetic waste components some crucial issues have to be taken into account.

1. Mass relation of components
2. Volume relation of components
3. Shape (shape-related properties) of components
4. Size relation components (Table 4-10)

Table 4-10 contains the size relations within the shape-related subdivisions. Table 4-11 shows the general component inter-relation of the sample. These relations have to be reflected by the synthetic waste to build an initial waste in its state before placement. To reflect these properties in synthetic waste appropriate components have to be found. With these components the relations have to be validated and adjusted.

Table 4-11 Inter-component relations of the synthetic waste

	General Relations		Shape-related Subdivision			
Material	**Dry Mass**	**Volume**	**Incom-pressible**	**Low com-pressible**	**High com-pressible**	**Re-inforcing**
Paper, cardboard	21.62%	11.07%	0.00%	0.00%	0.00%	21.62%
Flexible plastics	12.87%	15.60%	0.00%	0.00%	12.87%	0.00%
Rigid plastics, rubber	7.31%	19.70%	1.24%	6.07%	0.00%	0.00%
Metals	5.38%	14.81%	0.00%	5.38%	0.00%	0.00%
Minerals, glass	10.34%	8.30%	2.11%	8.23%	0.00%	0.00%
Wood, leather, textiles	1.15%	11.90%	0.00%	0.00%	0.00%	1.15%
Organics	39.98%	5.43%	0.00%	0.00%	39.98%	0.00%
Miscellaneous	1.35%	13.20%	0.00%	0.15%	0.60%	0.60%
Sub-total			3.3%	19.8%	53.4%	23.4%
Sum	100%	100%		100%		

In regard to the size fraction of the materials in Table 4-10 the following possible replacement components are chosen, as shown in Table 4-12. It has to be considered that the original or “natural” state of the components differs from the depositing state, e.g. most plastic bags or cling film for example, which were sheet-like in their original state, are often creased or crumpled. In that condition and for the consideration of the initial state they may have different shape-related mechanical functions, i.e. rather high compressible than reinforcing.

Most of the present material groups do not have to be replaced. Putrescible organic material has to be synthesised by clay having also a soft and weak character. To prevent the clay from contaminating the remaining materials, it could be wrapped in flexible plastic. Miscellaneous material could be, as in reality, a mixture of different material group components, as there are plastics and paper, clay, soil and stone.

Table 4-12 Preliminary replacement components for an initial synthetic waste

Material group	**Replacement**	**Shape-related Subdivision**	**Size [mm]**
Paper/Cardboard	A4 paper	Reinforcing	120-500
Flexible plastics	Waste bags	High compressible	120-500
Rigid plastics, rubber	Tyre shreds	Incompressible	120-500
	Packaging Beverage bottles	Low compressible	120-500
Metals	Aluminium beverage cans	Low compressible	120-500
Minerals, glass	Leighton Buzzard Sand	Low Compressible	<10
	Brick Fractions	Incompressible	40-120 120-500
Wood, leather, textiles	Textiles	Reinforcing	500-1000 >1000
Organics	Lumps of clay	High compressible	40-120 120-500
Miscellaneous	Soil, clay	Low compressible	<10
	Plastic, paper, clay	High compressible	10-40
	Plastic, paper	Reinforcing	40-120

The paper/cardboard material group can easily be produced by using paper sheets. Flexible plastic is simulated by plastic waste bags. Low compressible rigid plastic are taken from rigid plastic packaging and beverage bottles and the incompressible part is represented by solid chunks tyres shreds. Aluminium beverage cans simulate the group of

metals, while sand and brick fractions cover minerals and glass. Textiles in this waste survey only represent the group of wood, leather and textiles. For the reason of representing this waste, only textiles should be used to reflect this group.

Table 4-13 Properties of the synthetic waste components

	Dimensions (l or ∅/w/h)			Mass	Density	Unit weight[5]
	[mm]	[mm]	[mm]	[g]	[kg/m³]	[kN/m³]
Aluminium cans	66	-	188	17	2720	0.14
Paper[6]	297	210	80	5000	1000	10.00
Flexible plastic bags[7]	430	380	-	9	920	0.12
Rigid plastic packaging[8]	125	53	-	18	940	0.17
Rigid plastic packaging[9]	86/100	53/70	113/134	11/25	940	0.18/0.19
Rigid plastic bottles[10]	85	85	300	41	1380	0.14
Textiles	1000	500	10	165	1540[11]	0.33
Tyre shreds[12]	150	100	10	230	2650	4.68
Brick[13]	225	70	100	2400	2190	14.84
Leighton-Buzzard sand[14]	-	-	-	-	1650	16.50
Clay lumps	50-100	-	50-100	100-1000	1900	19.00

1. Aluminium cans
2. a) - c) Rigid plastic packaging
3. Leighton-Buzzard sand
4. Textiles
5. Paper
6. Flexible plastic bags
7. Brick fractions
8. Tyres shreds
9. Clay lumps wrapped in plastic foil

The properties of the synthetic waste components chosen for the subsequent tests are shown in Table 4-13. The components are visualised in Figure 4-35:

[5] Uncompressed
[6] 1000 sheets A4 paper, 80g/m², piled, sheet thickness d = 72µm
[7] LDPE (low density polyethylene), foil thickness d = 50µm
[8] PP (polypropylene), round tub including lid
[9] PP (polypropylene), square small and large tub, large tub including lid
[10] PETP (polyethyleneterephthalat)
[11] Density of cotton fibres
[12] Approximate values
[13] Approximate values
[14] The grading is shown in chapter 11.3

Figure 4-35 Synthetic waste components used in subsequent tests

4.3.3 Synthetic Waste Compositions

For subsequent shear and compression tests, nine waste compositions basing on the synthetic waste components introduced above were chosen. Composition SW_01 is an initial simple composition, consisting to a majority of Leighton-Buzzard-sand and of a relatively small amount of paper. Due to its high amount of sand it is regarded as an incompressible composition. SW_02 is a random waste composition with a high amount of compressible and reinforcing materials, like aluminium cans and paper. From this composition a highly compressible behaviour is expected. Incompressible material (tyre shreds and brick fractions) account for the highest mass in composition SW_03. Though a high amount of incompressible components are involved, SW_03 is also regarded to have a very compressible character, as the compressible components exhibit a very volume. SW_04 and SW_05 contain a large amount of flattened aluminium cans, and therefore represent a composition with a distinctive component dominating the composition. In SW_05 the impact of changing the component ratio is investigated. In SW_06 to SW_08 plastic packaging and flattened cans were tested in a sand matrix. The sand matrix increases the unit weight and moreover, the impact of a small component size is examined. SW_09 finalises the test series with a composition, which is based on the Narborough real waste composition.

Table 4-14 Synthetic Waste Compositions

Components		SW_01	SW_02	SW_03	SW_04	SW_05	SW_06	SW_07	SW_08	SW_09
Aluminium cans	[mass-%]	0%	20,0%	15,0%	49,9%	70,0%	0,3%	2,6%	4,2%	5,1%
Paper	[mass-%]	1,1%	40,2%	18,1%	0%	0%	0%	0%	0%	21,2%
Textiles	[mass-%]	0%	14,1%	7,2%	0%	0%	0%	0%	0%	2,4%
Flexible plastic bags	[mass-%]	0,1%	7,7%	0%	0%	0%	0%	0%	0%	16,8%
Rigid plastic packaging	[mass-%]	0%	10,2%	0%	5,0%	15,0%	0,3%	2,6%	4,2%	4,0%
Rigid plastic bottles	[mass-%]	0%	7,7%	0%	0%	0%	0%	0%	0%	3,1%
Tyre shreds	[mass-%]	0%	0%	29,9%	24,9%	15,0%	0%	0%	0%	1,2%
Brick fractions	[mass-%]	0%	0%	29,9%	20,2%	0%	0%	0%	0%	2,0%
Leighton-Buzzard Sand	[mass-%]	98,8%	0%	0%	0%	0%	99,4%	94,9%	91,5%	7,5%
Clay	[mass-%]	0%	0%	0%	0%	0%	0%	0%	0%	36,7%
Sum	[mass-%]	100%	100%	100%	100%	100%	100%	100%	100%	100%

All nine compositions were tested for shear behaviour. Due to the fact that only slight changes were expected to occur between SW_04 and SW_05, and between SW_6 to SW_08, only SW_04 and SW_07 was tested for their compression behaviour. Additionally, SW_01 was tested with two different sample heights in the shear box and SW_02 was tested for repeatability in the compression cell (two tests using identical compositions and an additional test with a doubling of the unit weight of the precedent tests).

Figure 4-36 reflects the location of the synthetic waste compositions within the ternary diagram. The initial states are shown.

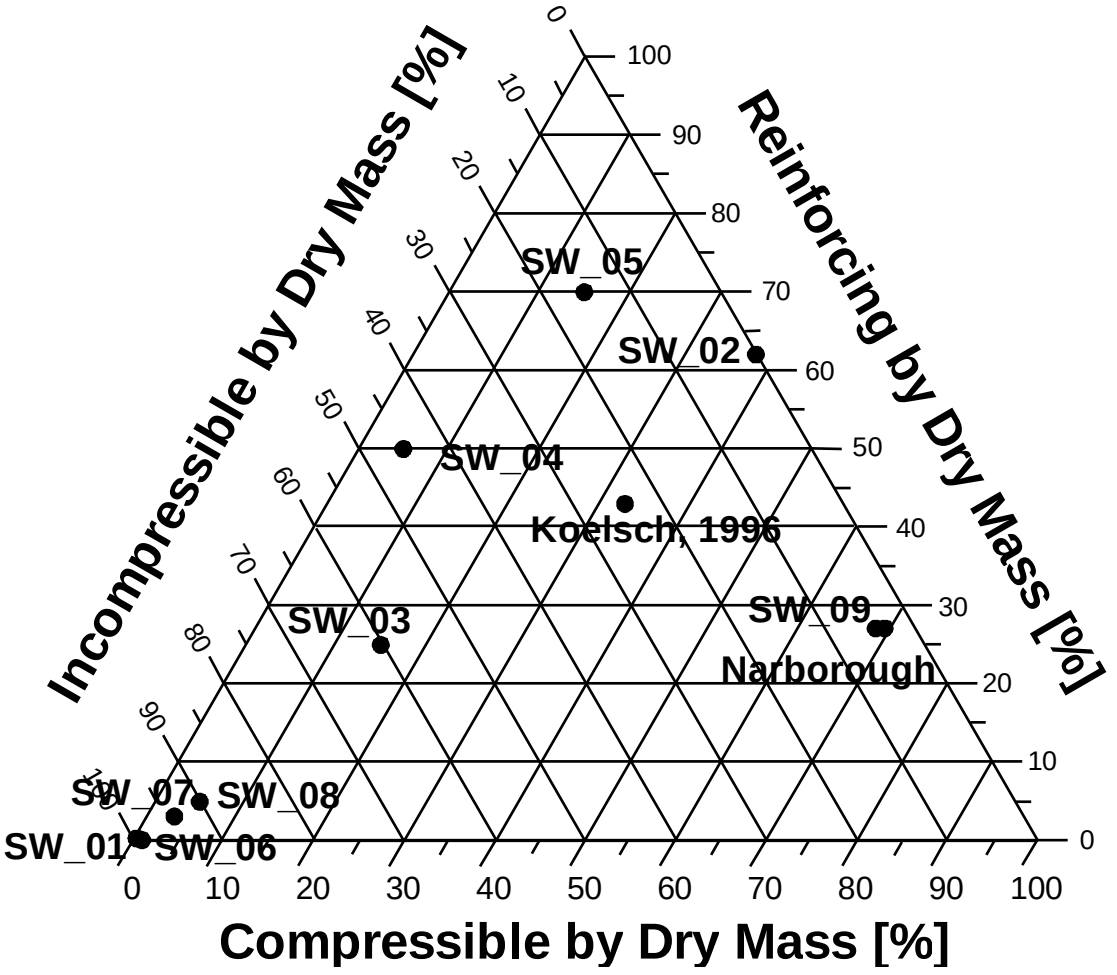

Figure 4-36 Ternary diagram with synthetic waste compositions

4.4 Summary of Waste Classification and Synthetic Waste

A uniform framework for classifying waste components has been introduced, which complies with the requirements for a comprehensive geotechnical waste classification. Its classification elements are material groups, which are based upon similar mechanical properties like shear, tensile and compressive strength, elongation at break and elastic modulus, components size (>10mm, 10-40mm, 40-120mm, 120-500mm, 500-1000mm and >1000mm) and shape (i.e. shape-related subdivision of reinforcing, compressible and incompressible components) and degradation potential. A way of presenting and

comparing data from different sources is demonstrated and a data set from literature is applied to the framework.

From an in-situ waste sorting analysis conducted on a SITA landfill, Narborough, the main component groups, size ranges and shape-related subdivisions were identified and related to the geotechnical classification framework. The material and size distribution of the waste components was used to generate a synthetic waste by eliminating insignificant waste fraction after consideration of their mutual significance in size and material distributions. Replacement components used in the synthetic waste were identified and demonstrated. A family of synthetic waste including the compositions, which were tested in shear and compression tests, was introduced.

5 Compression Behaviour

5.1 General Introduction

In the following, the results from compression tests conducted on six synthetic waste composition are presented (SW_01; two repeatability tests of SW_02 and one tests on approximately double unit weight of SW_02; SW_03; SW_04; SW_07; SW_09). As the composition SW_05 was very similar to SW_04, and SW_06 and SW_08 were comparable to SW_07, the compression behaviour of SW_05, SW_06 and SW_08 was not tested. Due to the expected characteristic of the compositions and their components, the results of the compression tests were split into four different sub-categories being incompressible, compressible and mono-component compositions and a simulation of a real waste composition. Alongside with compression test photographs, constrained modulus and compression index, the component shifting of four compositions (SW_02_2 and SW_02_3, SW_04, SW_09) within the shape-related subdivisions due to the compression process is demonstrated.

5.2 Incompressible Compositions

5.2.1 Composition SW_01

Table 5-1 summarises the boundary conditions for the compression tests on composition SW_01. Due to the large Leighton-Buzzard sand fraction present in the composition a high initial unit weight of 11kN/m^3 was achieved. The visual result for the sand-paper-plastic composition is shown in Figure 5-1. As small-sized incompressible and large-sized high compressible components were involved, major material migration, i.e. filling of voids, was noticeable. Paper deformed even at the lowest low normal stress.

Table 5-1 Boundary conditions for SW_01

Max. normal stress σ	Input mass	Compression rate	h_0	h_e	ε_{max}	Unit weight γ_0	Unit weight γ_e
[kPa]	[kg]	[mm/min]	[mm]	[mm]	[%h_0]	[kN/m^3]	[kN/m^3]
254	158	3.6	560	423	24	11.38	14.91

The corresponding stress levels and displacements for Figure 5-1 are denoted in Table 5-2. A relatively small displacement of 136mm was necessary to result in a normal stress of 253kPa. The initial normal stress of 0.6kPa was due to the test setup. Mounting the jack in its initial position on top of the compression cell at the beginning of the test resulted in a normal load as the jack directly touched the load cell not leaving a gap. Figure 5-2 demonstrates constrained modulus and compression index at the appropriate normal stress levels. A decrease of the constrained modulus is identifiable up to a normal stress of 25kPa. The fluctuation of the constrained modulus at 90kPa is due to the load plate jamming on a welding seam of the side wall of the compression cell. The compression index fluctuated between 0.005 and 0.05, without reaching a constant value.

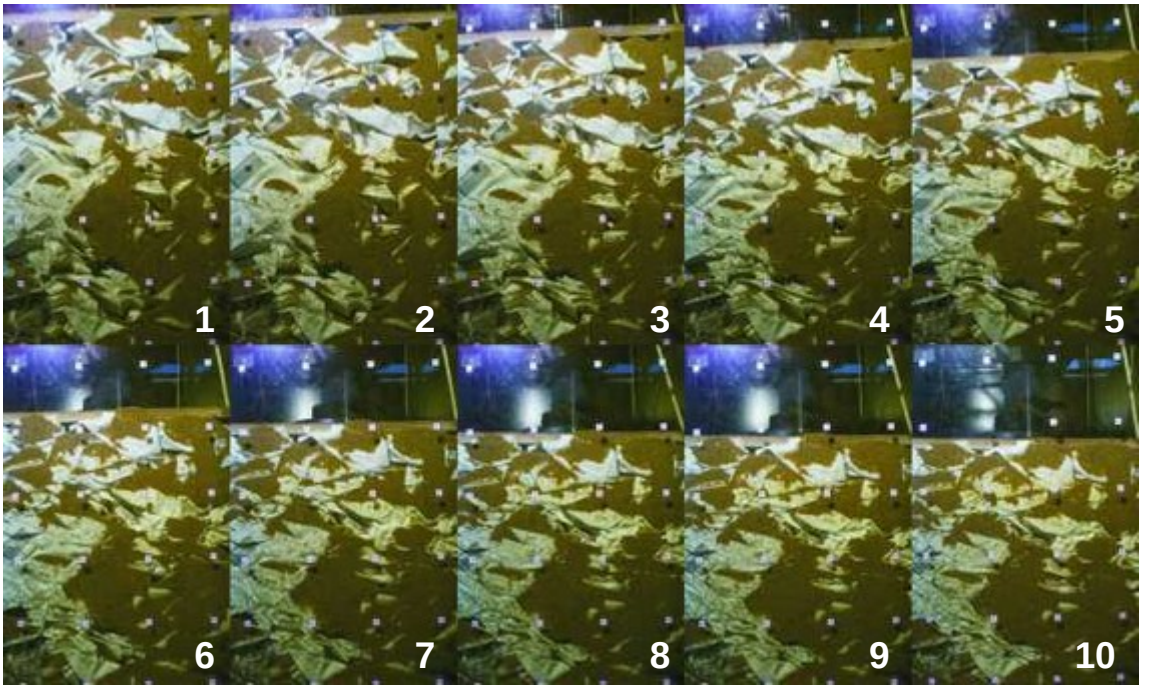

Figure 5-1 Compression behaviour of composition SW_01[15]

Table 5-2 Stress states shown in Figure 5-1

Picture		1	2	3	4	5	6	7	8	9	10
σ	[kPa]	0.6	17.7	39.1	71.0	113.7	148.0	194.3	251.3	250.4	253.0
s	[mm]	0.0	13.5	32.1	51.0	69.8	88.1	105.4	122.5	126.2	136.6

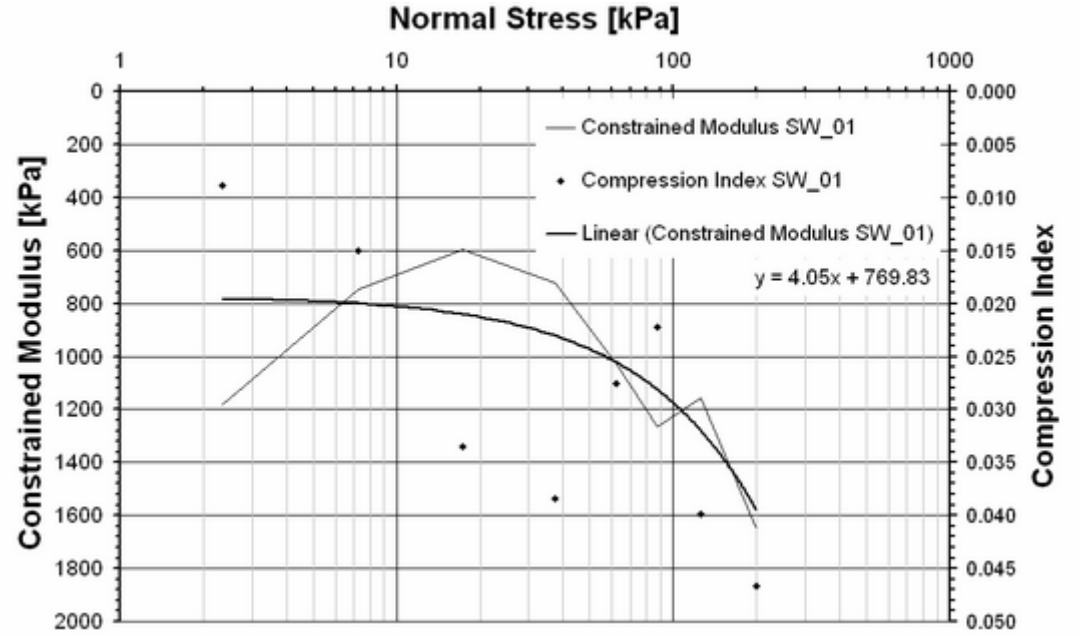

Figure 5-2 Constrained modulus and compression index for SW_01

[15] Fiducial markers in 100mm vertical and horizontal distance

5.2.2 Composition SW_07

Table 5-3 summarises the boundary conditions for the compression tests on composition SW_07. During the test preparation sand segregation was noticeable, which might be due to the sand pouring height, which was approximately 0.8m. The Leighton-Buzzard sand fraction present in this composition led to an initial unit weight of 7.3kN/m^3. Figure 5-3 visually depicts the compression behaviour of SW_07. The first four pictures show materials re-arranging. From the fifth picture onwards material deformation is clearly visible, especially perceivable at the tub on the peak of sand. The material at the bottom of the sand started deforming at a high normal stress level.

Table 5-3 Boundary conditions for SW_07

Max. normal stress σ	Input mass	Compression rate	h_0	h_e	ε_{max}	Unit weight γ_0	Unit weight γ_e
[kPa]	[kg]	[mm/min]	[mm]	[mm]	[%h_0]	[kN/m^3]	[kN/m^3]
188	114	4.1	625	379	39	7.29	12.03

Table 5-4 describes the stress levels shown in the precedent figure. It is very obvious that a demixing during test setup has occurred. Nevertheless, the test was conducted with plausible results. A stress level of 183kPa was reached at a displacement of 246mm. Constrained modulus and compression index in Figure 5-4 show a similar character as already seen before, though the compression index tended to flatten near the end of the test and reached a values similar to the initial value of SW_01.

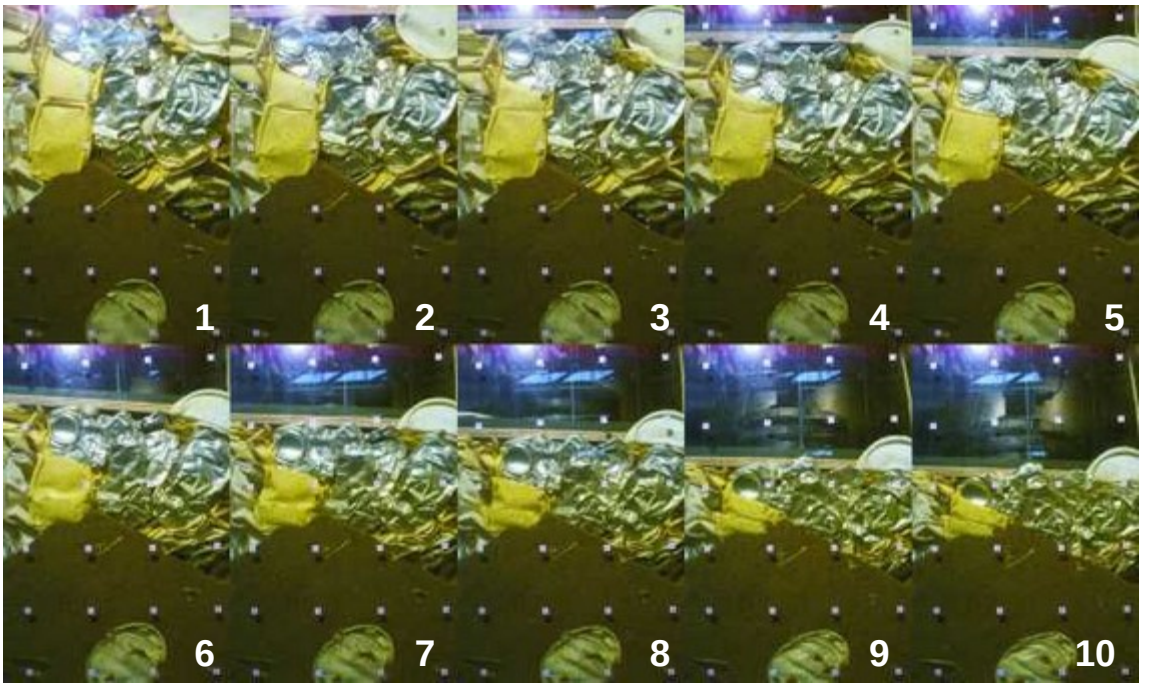

Figure 5-3 Compression behaviour of composition SW_07

Table 5-4 Stress states shown in Figure 5-3

		1	2	3	4	5	6	7	8	9	10
σ	[kPa]	2.8	11.8	15.6	20.5	**27.3**	36.1	45.9	64.2	134.5	183.1
s	[mm]	0.0	41.5	63.2	84.5	105.2	122.5	143.7	163.9	224.6	245.9

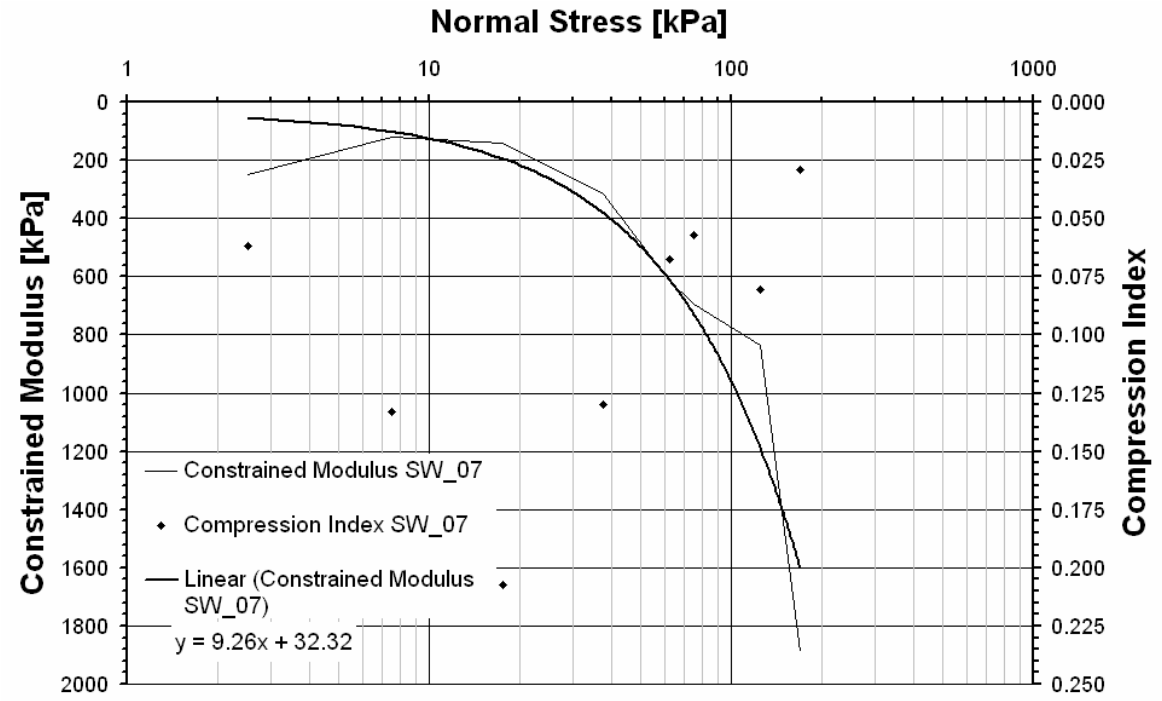

Figure 5-4 Constrained modulus and compression index for SW_07

5.3 Compressible Compositions

5.3.1 Composition SW_02_1

The boundary conditions for SW_02_1 are shown in Table 5-5. Only a very low unit weight of 0.27kN/m^3 was achieved. This waste composition was expected to be very compressible as a large amount of compressible and lightweight components were involved.

Table 5-5 Boundary conditions for SW_02_1

Max. normal stress σ	Input mass	Compression rate	h_0	h_e	ε_{max}	Unit weight γ_0	Unit weight γ_e
[kPa]	[kg]	[mm/min]	[mm]	[mm]	[%h_0]	[kN/m^3]	[kN/m^3]
40	4.1	10.1	620	181	71	0.27	0.91

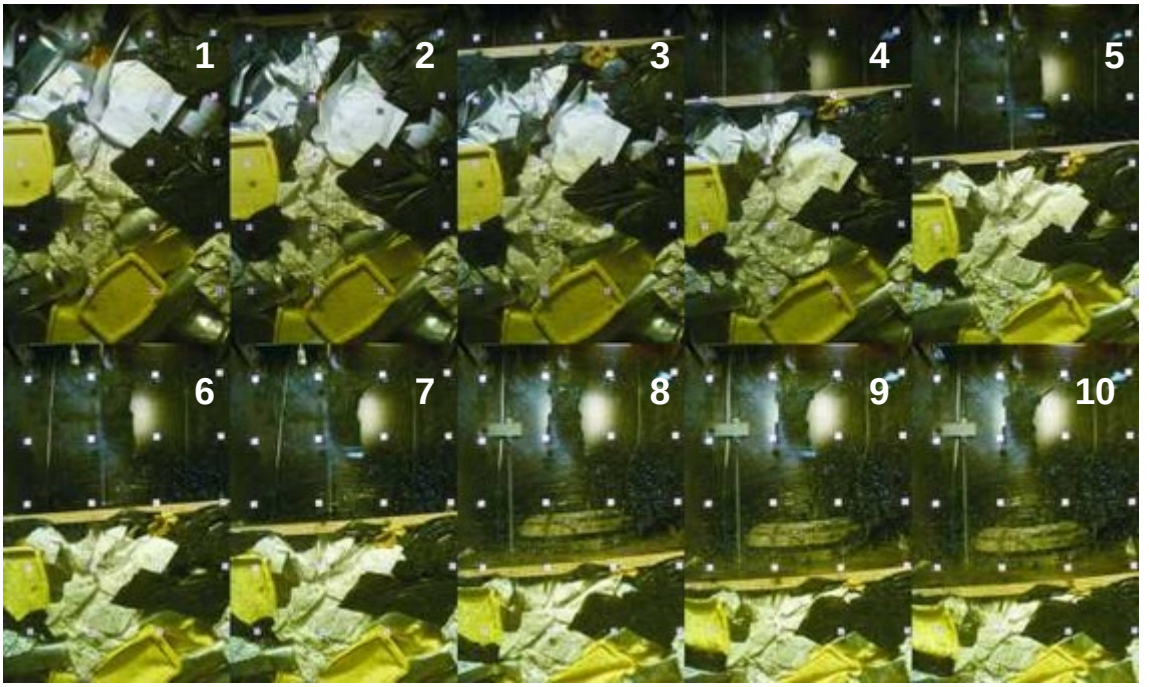

Figure 5-5 Compression behaviour of composition SW_02_1

Table 5-6 Stress states shown in Figure 5-5

		1	2	3	4	5	6	7	8	9	10
σ	[kPa]	0.0	3.4	5.6	10.4	14.3	17.6	21.0	24.2	29.6	36.0
s	[mm]	0.0	99.3	144.2	232.3	271.8	305.0	337.9	375.0	408.8	430.2

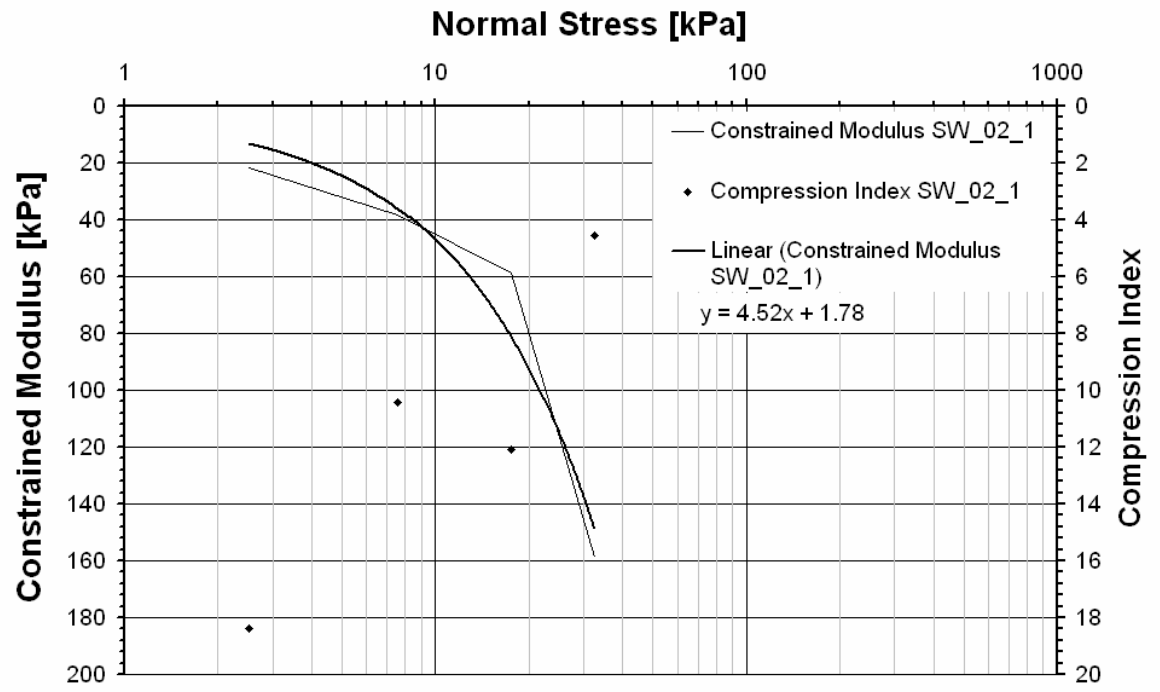

Figure 5-6 Constrained modulus and compression index for SW_02_1

From Figure 5-5 and Table 5-6 the expectations of the compressible behaviour are confirmed. A large displacement of more than 2/3 of the initial sample height resulted in a low normal stress of 36kPa. High compressible components started deforming at a low normal stress level. Up to 10kPa normal stress component rearrangement occurred mostly. From pictures 5 onwards (14kPa) component deformation is obvious. The compression index in Figure 5-6 turned out to be significantly larger (4-19) than in tests SW_01 and SW_07, but it generally decreased.

5.3.2 Composition SW_02_2

SW_02_2 consists of the same composition as SW_02_1. This test was conducted to check the repeatability of this kind of test, i.e. the boundary conditions in Table 5-7 are the same as in the test before.

Table 5-7 Boundary conditions for SW_02_2

Max. normal stress σ	Input mass	Compression rate	h_0	h_e	ε_{max}	Unit weight γ_0	Unit weight γ_e
[kPa]	[kg]	[mm/min]	[mm]	[mm]	[%h_0]	[kN/m^3]	[kN/m^3]
42	4.1	10.2	620	211	66	0.27	0.78

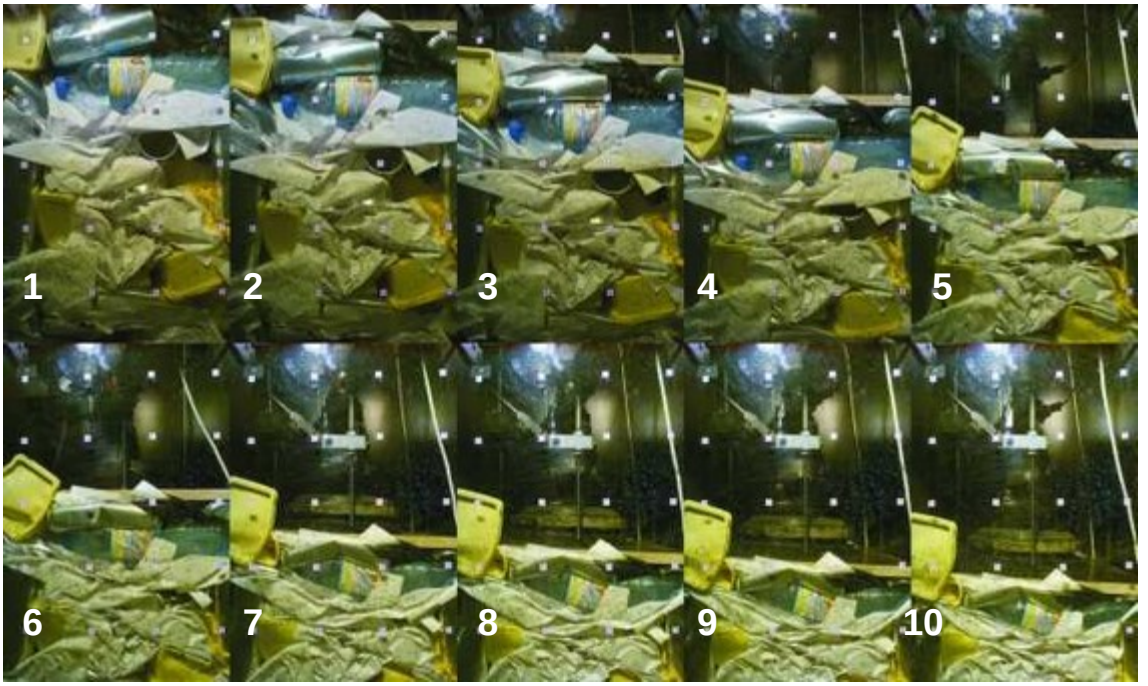

Figure 5-7 Compression behaviour of composition SW_02_2

As observed before, high compressible components like paper and flexible plastic started deforming at low normal stresses (pictures 1 to 4). At relatively high normal stresses low compressible components like the yellow tub bottom right or the plastic bottle just below the load plate in picture 5 showed considerable deformations.

Table 5-8 Stress states shown in Figure 5-7

		1	2	3	4	5	6	7	8	9	10
σ	[kPa]	1.0	4.0	5.5	8.2	13.3	18.6	24.8	29.7	33.5	42.5
s	[mm]	0.0	47.7	91.5	175.2	243.7	279.7	333.4	355.0	376.6	408.7

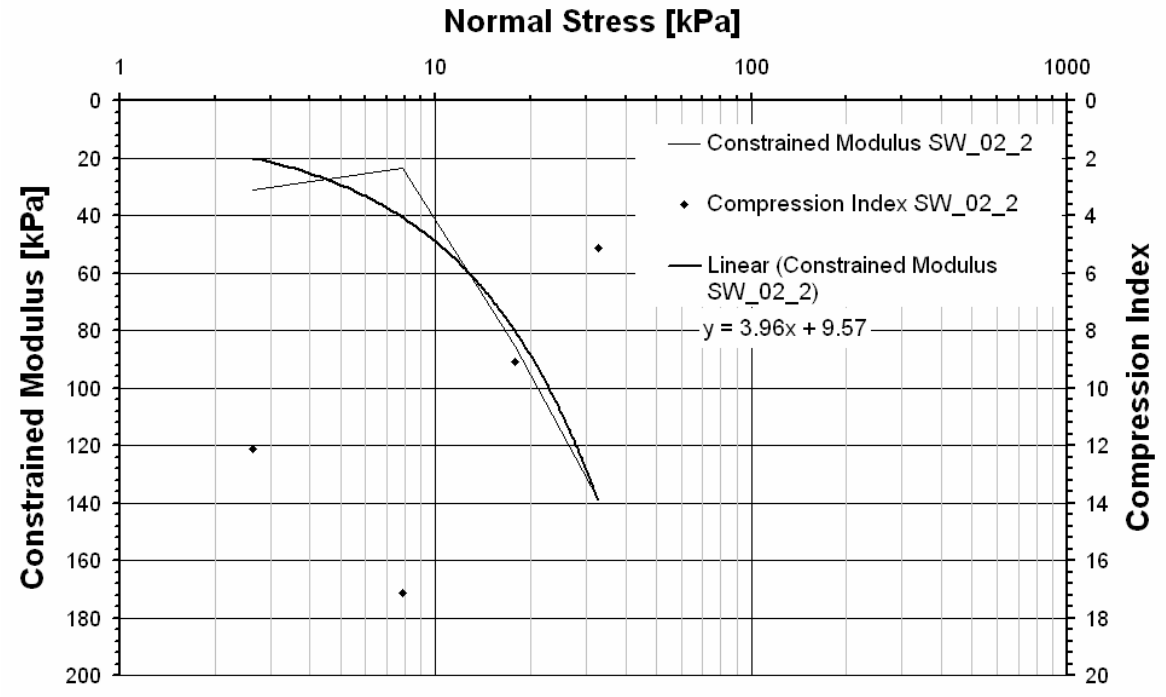

Figure 5-8 Constrained modulus and compression index for SW_02_2

Figure 5-8 demonstrates constrained modulus and compression index for SW_02_2. The trend line for constrained modulus results in similar values as SW_02_1. The compression index exhibited high values (4-17) and decreased through the course of the test.

5.3.3 Composition SW_02_3

Composition SW_02_3 comprised the same material ratios used in the two preceding tests, but the amount and thus the unit weight was doubled as demonstrated in Table 5-9. This test was conducted with two different compression rates. The slower rate was necessary after a motor failure on the jack.

Table 5-9 Boundary conditions for SW_02_3

Max. normal stress σ	Input mass	Compression rate	h_0	h_e	ε_{max}	Unit weight γ_0	Unit weight γ_e
[kPa]	[kg]	[mm/min]	[mm]	[mm]	[%h_0]	[kN/m^3]	[kN/m^3]
55[16]/122	8.2	10.3[17]/3.9	650	159	76	0.49	2.02

[16] Pictures were taken up to 55kPa

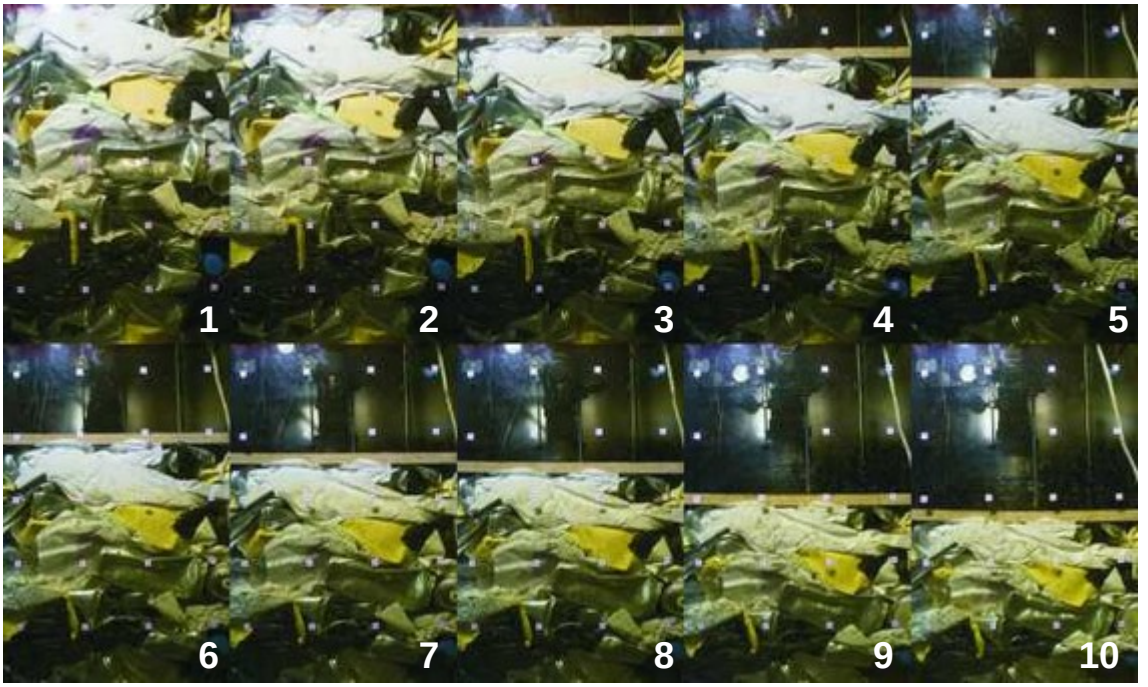

Figure 5-9 Compression behaviour of composition SW_02_3

The components of the composition SW_02_3 possessed the stress histories of the preceding tests SW_02_1 and SW_02_2. For this reason, the components were pre-deformed as visible from Figure 5-9 (first picture). Further deformation is recognisable for the aluminium can in the middle of picture 4 (σ = 19kPa) and also from the upright tub in the bottom left corner. High compressible components like flexible plastic bags (visible at the bottom of each picture) altered their shape from the beginning of the test.

Table 5-10 Stress states shown in Figure 5-9

		1	2	3	4	5	6	7	8	9	10
σ	[kPa]	0.3	10.1	16.8	18.8	25.3	27.0	32.5	34.7	48.7	55.6
s	[mm]	0.0	47.2	101.7	136.7	191.0	211.7	243.7	263.2	301.3	329.1

The normal stress for the compression behaviour is shown in Table 5-10. Constrained modulus and compression index in Figure 5-10 could be related to the preceding tests. The gradient of the constrained modulus occurred in the same range as before, but the intercept (expressed in the trend line equation) was considerably higher. The compression index, which ranged between 5.5 and 0.9 approached a value at 32.5kPa normal stress of about 4, which could be related to the values observed in tests SW_02_1 and SW_02_2, respectively.

[17] Motorised jack defect, after repair compression rate was reduced

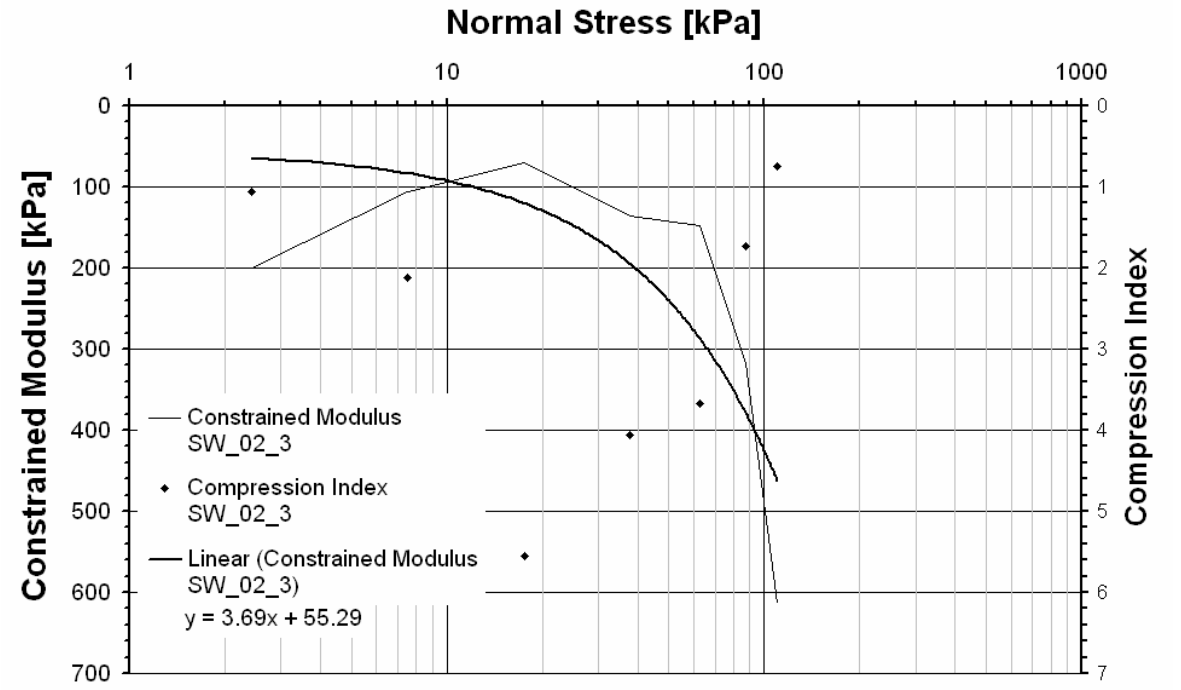

Figure 5-10 Constrained modulus and compression index for SW_02_3

5.3.4 Composition SW_03

According to its mass ratio, SW_03 seemed to be an incompressible composition with approximately 60% of incompressible, heavy components. But nevertheless, the initial unit of 0.71kN/m^3 was still very low (Table 5-11). But as the compressible components represented the largest volume in this composition, they dominated the behaviour in terms of compressibility (ε = 76%).

The compression behaviour of this composition was characterised by aluminium cans as they accounted for the largest volume. The cans seemed essentially intact until picture 4 of Figure 5-11. Only adjacent cans and such cans that were located above each other showed traces of deformation even earlier, especially at contact points between the rigid edge of one can end and the deformable body of another can, e.g. top right or bottom middle of the compression cell, as visible from picture 1 to 3. A re-arrangement of components is noticeable from picture 1 and 2. The components appeared to be non-deformed, but the sample height decreased. From Picture 5 onwards, deformation of all visible components is apparent.

Table 5-11 Boundary conditions for SW_03

Max. normal stress σ	Input mass	Compression rate	h_0	h_e	ε_{max}	Unit weight γ_0	Unit weight γ_e
[kPa]	[kg]	[mm/min]	[mm]	[mm]	[%h_0]	[kN/m^3]	[kN/m^3]
151	9.7	4.2	550	133	76	0.71	2.92

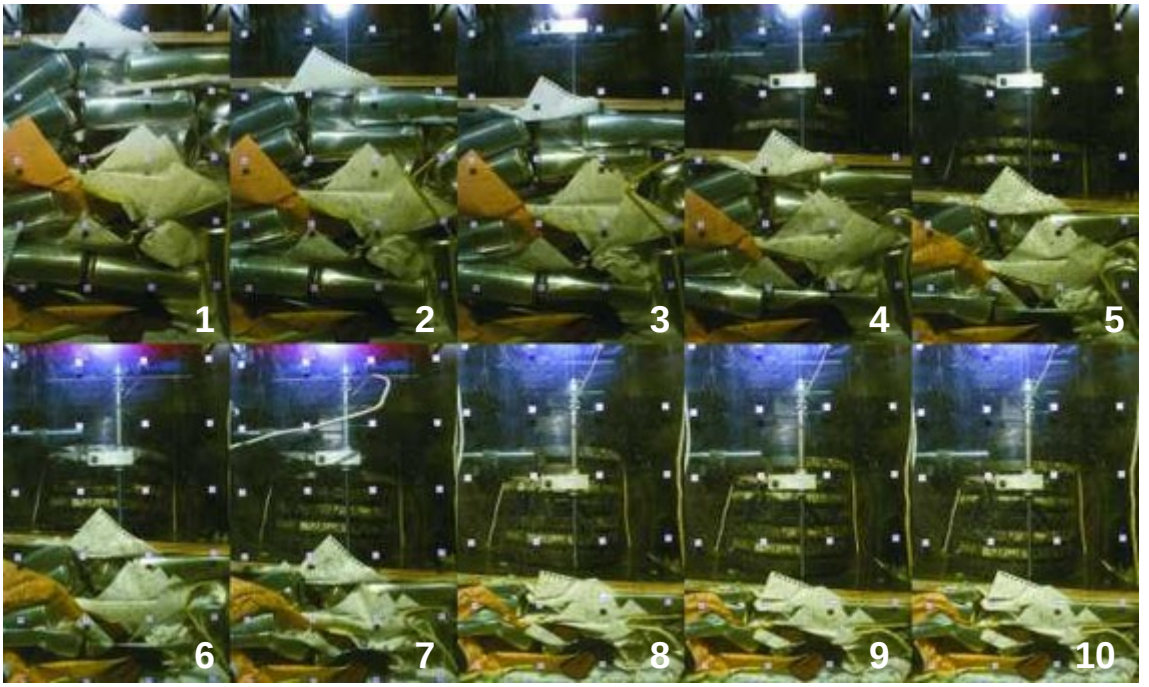

Figure 5-11 Compression Behaviour of composition SW_03

Table 5-12 Stress states shown in Figure 5-11

		1	2	3	4	5	6	7	8	9	10
σ	[kPa]	0.5	3.0	5.0	11.8	22.5	27.9	48.5	104.2	138.1	150.9
s	[mm]	0.0	73.8	110.5	205.8	281.1	297.2	345.8	397.2	411.1	416.9

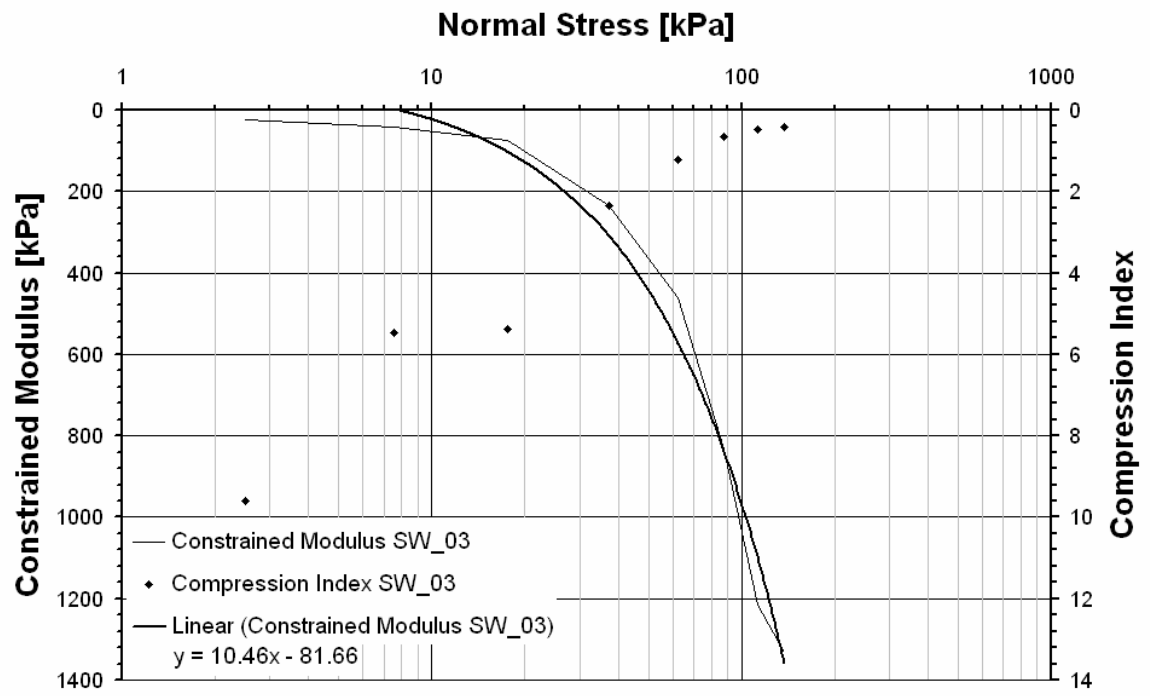

Figure 5-12 Constrained modulus and compression index for SW_03

The constrained modulus resembled values similar to those of the incompressible composition SW_07, while on the other hand the compression index was similar to the compressible composition of SW_02_3. A distinct feature for the compression index was a constant value of 5.4 at 7.5kPa and 17.5kPa normal stress.

5.4 Mono-Component Composition SW_04

Compositions dominated by a single component were defined as mono-component compositions. SW_04 was dominated by aluminium cans, not only in terms of mass ratio (approximately 50% of the overall sample mass), but also in volumetric terms as qualitatively noticeable from Figure 5-13. From the first and the second picture component compression is not obvious. Picture 3 exhibits a deformed plastic tub (middle right). A plastic tub at the bottom was essentially unaffected until the normal stress is doubled (picture 5).

Table 5-13 Boundary conditions for SW_04

Max. normal stress σ	Input mass	Compression rate	h_0	h_e	ε_{max}	Unit weight γ_0	Unit weight γ_e
[kPa]	[kg]	[mm/min]	[mm]	[mm]	[%h_0]	[kN/m^3]	[kN/m^3]
110	12.0	2.1	625	285	54	0.77	1.69

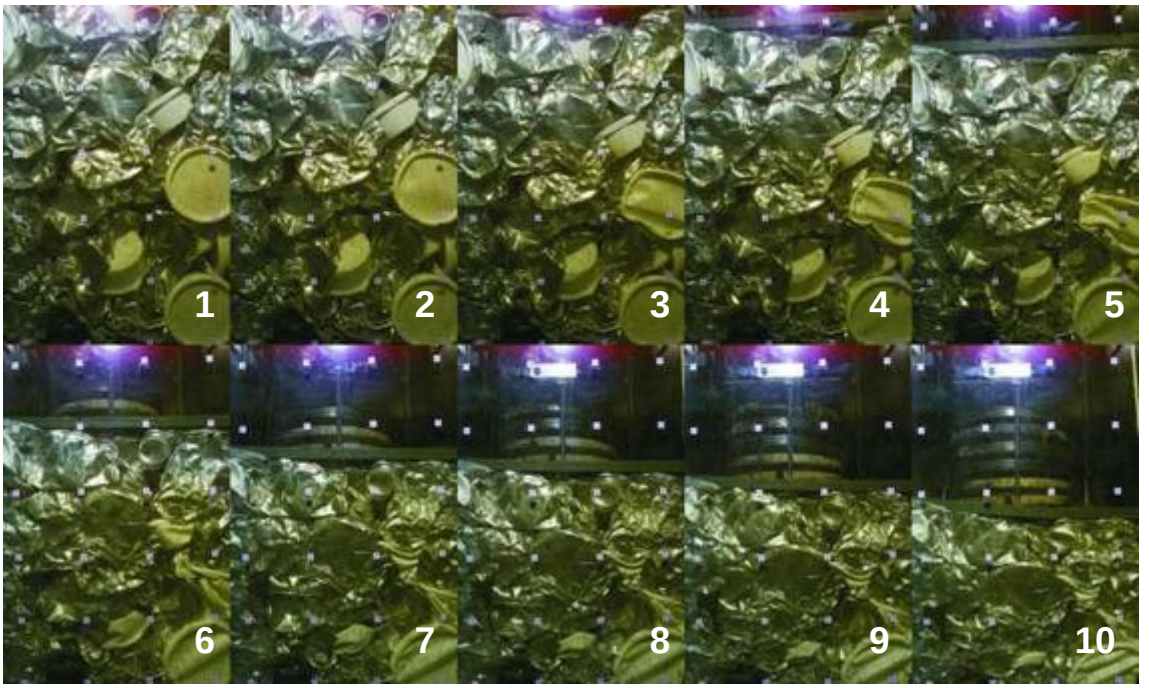

Figure 5-13 Compression behaviour of composition SW_04

Due to the high amount of low-weight components, the initial unit weight was 0.77kN/m^3 (Table 5-13). The constrained modulus in Figure 5-14 produces similar values to SW_02_3, while the compression index values are slightly lower than those for SW_03.

Table 5-14 Stress states shown in Figure 5-13

		1	2	3	4	5	6	7	8	9	10
σ	[kPa]	0.8	6.0	11.1	14.1	20.3	34.6	51.0	65.9	82.3	103.8
s	[mm]	0.0	11.7	61.5	82.1	123.3	192.2	244.8	266.0	298.0	341.3

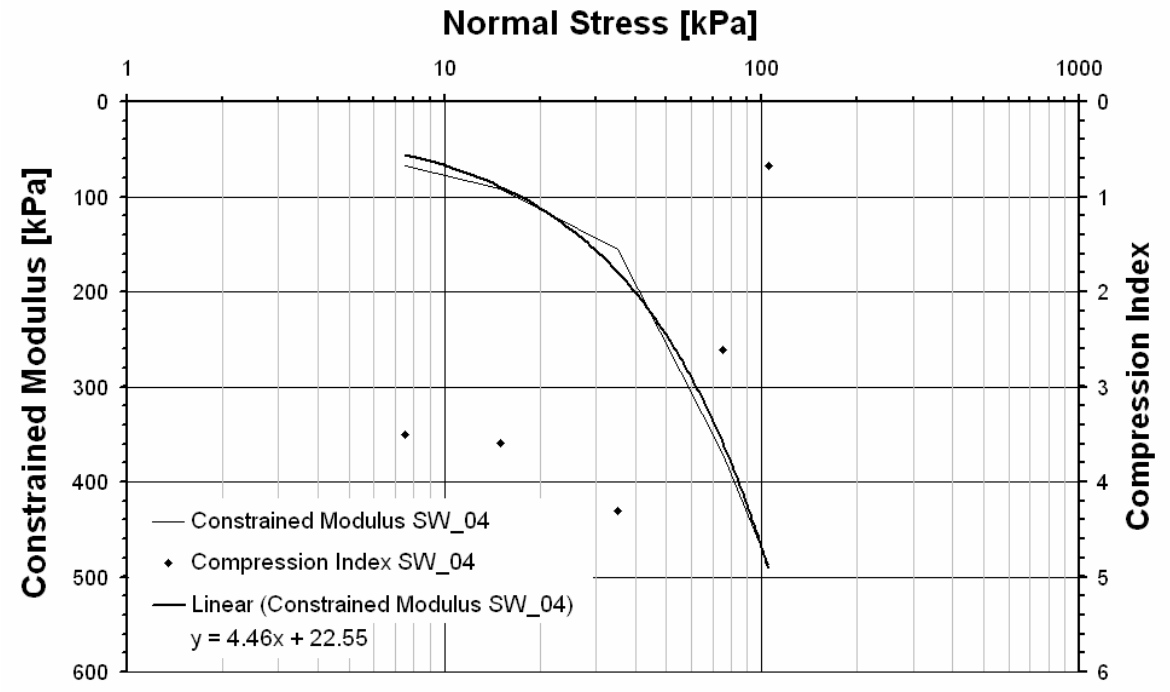

Figure 5-14 Constrained modulus and compression index for SW_04

5.5 Simulation of a Real Waste Composition SW_09

SW_09 was based on the findings from the waste sorting analysis conducted on Narborough landfill (chapter 4.3.1). The input of this test was about 16kg of material resulting in a low unit weight of 1.04kN/m^3 (Table 5-15). With a vertical strain of ε = 73% the composition showed similar characteristics to the compressible compositions SW_02_1, SW_02_2 and SW_03, and resulted in a final unit weight comparable to SW_03.

Table 5-15 Boundary conditions for SW_09

Max. normal stress σ	Input mass	Compression rate	h_0	h_e	ε_{max}	Unit weight γ_0	Unit weight γ_e
[kPa]	[kg]	[mm/min]	[mm]	[mm]	[%h_0]	[kN/m^3]	[kN/m^3]
102	16.3	4.2	625	166	73	1.04	3.91

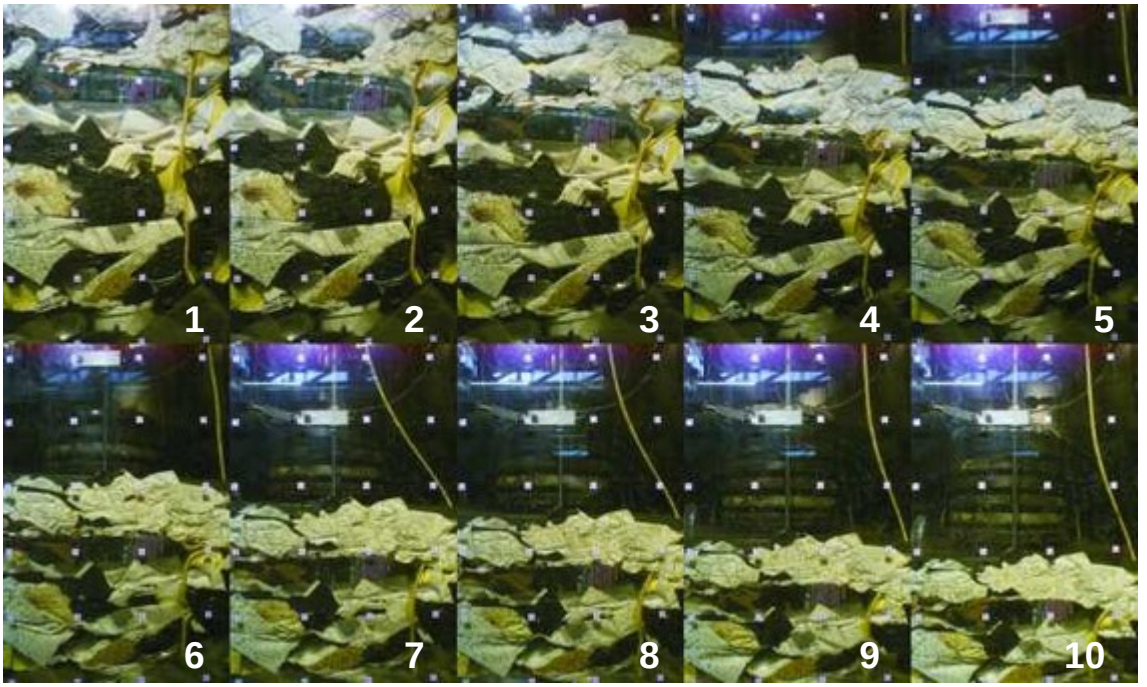

Figure 5-15 Compression behaviour of composition SW_09

Table 5-16 Stress states shown in Figure 5-15

		1	2	3	4	5	6	7	8	9	10
σ	[kPa]	0.0	5.6	10.6	15.0	24.6	31.2	44.0	52.3	75.7	100.4
s	[mm]	0.0	40.4	123.2	191.5	294.2	335.5	378.7	398.7	439.0	458.7

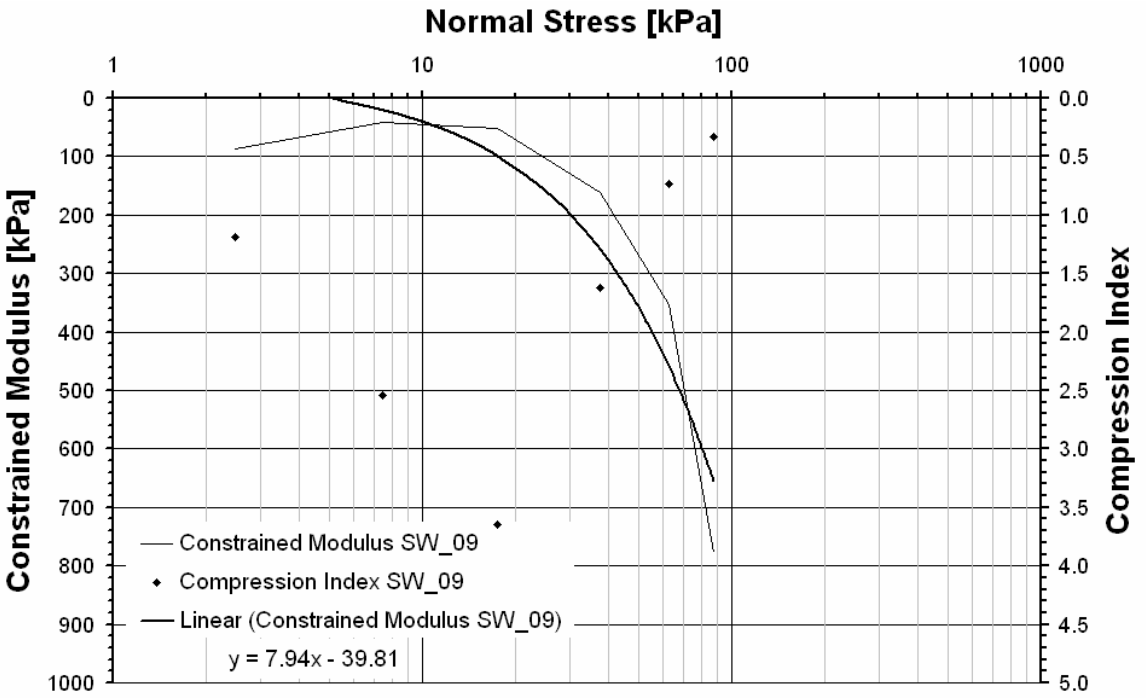

Figure 5-16 Constrained modulus and compression index for SW_09

From the pictures in Figure 5-15 a threshold value for low compressible components is not visible. High compressible components were deformed from the beginning. There might be a “cushion-effect” as high compressible components surrounded the low compressible components of rigid plastics and aluminium cans. With a compression index between 0.3 and 3.7 it reached a value in the range of SW_04. The constrained modulus at 100kPa normal stress is near the value for SW_03.

5.6 Shifting of Components within Shape-Related Subgroups after Compression

For the tests on compositions SW_02_2, SW_02_3, SW_04 and SW_09 a sorting analysis was conducted to compare the material output with the initial material. The sample was examined in accordance to the proposed classification system into material groups, size ranges and shape-related subdivisions.

Figure 5-17 shows the result for the composition SW_02_2. With a low compressive normal stress of 42kPa (Table 5-7) the majority of the aluminium cans remained low compressible and due to flattening a percentage were shifted to the reinforcing subdivision. In terms of paper a shifting from high compressible towards reinforcing components was visible. While flexible plastic and rigid plastic packaging remained essentially the same, plastic bottles changed their shape from being low compressible to reinforcing. Textiles did not change their shape-related subdivision of reinforcing components.

a)

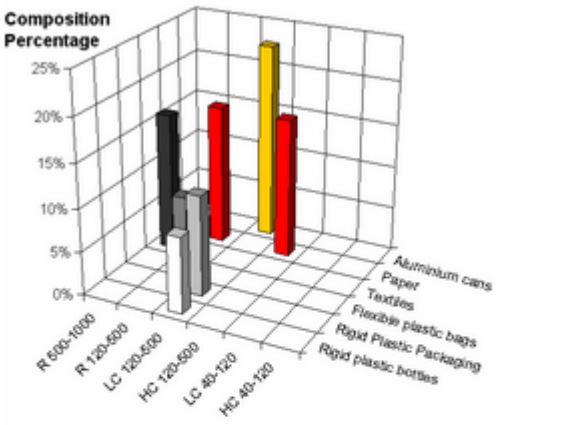

	HC 40-120	LC 40-120	HC 120-500	LC 120-500	R 120-500	R 500-1000
Aluminium cans				22.7%		
Paper			16.2%		16.2%	
Textiles						16.0%
Flexible plastic bags					8.7%	
Rigid Plastic Packaging				11.5%		
Rigid plastic bottles				8.7%		

b)

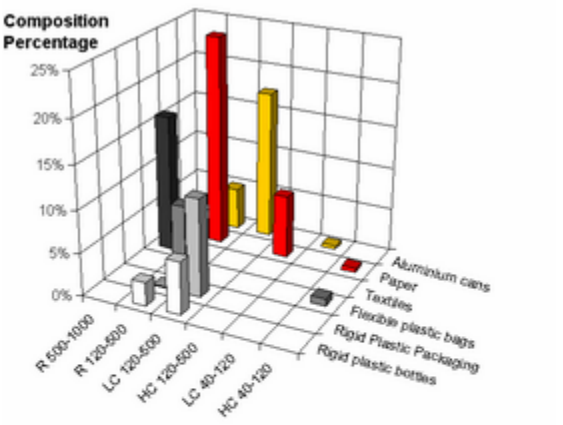

	HC 40-120	LC 40-120	HC 120-500	LC 120-500	R 120-500	R 500-1000
Aluminium cans		0.4%		17.4%	4.9%	
Paper	0.5%		7.3%		24.5%	
Textiles						16.0%
Flexible plastic bags	0.9%				7.9%	
Rigid Plastic Packaging				11.4%	0.2%	
Rigid plastic bottles				6.1%	2.7%	

Figure 5-17 a) Input and b) output SW_02_2

The Input of SW_02_3 was the output of SW_02_1 and SW_02_2. As a sorting analysis was only conducted for SW_02_2, it was assumed that the output of SW_02_1 did not differ largely from SW_02_2. Thus the same output material distribution in the shape-

related subdivisions and size ranges was estimated. For this reason the input distribution of SW_02_3 complied with the output distribution of SW_02_2.

a)

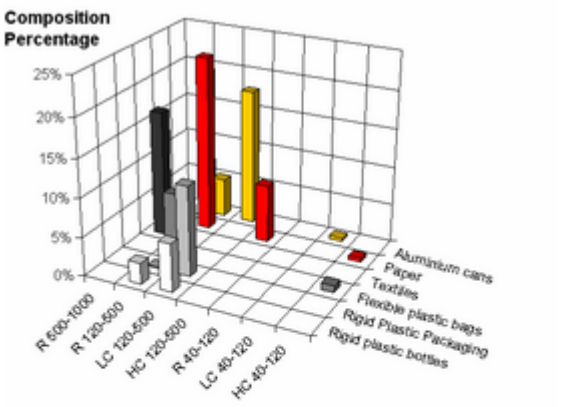

	HC 40-120	LC 40-120	R 40-120	HC 120-500	LC 120-500	R 120-500	R 500-1000
Aluminium cans		0.4%			17.8%	5.0%	
Paper	0.5%			7.5%		22.8%	
Textiles							16.4%
Flexible plastic bags	0.9%					8.0%	
Rigid Plastic Packaging					11.6%	0.2%	
Rigid plastic bottles					6.2%	2.7%	

b)

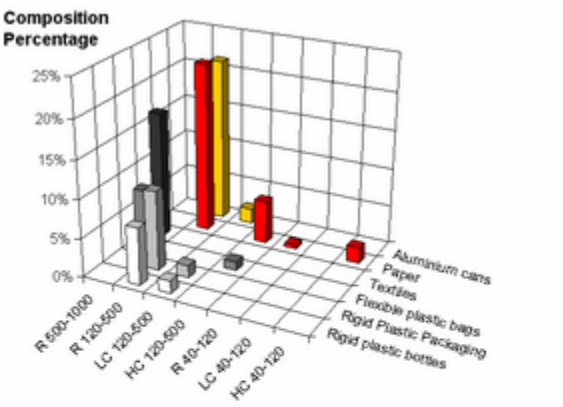

	HC 40-120	LC 40-120	R 40-120	HC 120-500	LC 120-500	R 120-500	R 500-1000
Aluminium cans					1.9%	21.4%	
Paper	2.1%		0.6%	5.5%		22.2%	
Textiles							16.5%
Flexible plastic bags				1.1%			7.9%
Rigid Plastic Packaging					1.6%	10.3%	
Rigid plastic bottles					1.6%	7.4%	

Figure 5-18 a) Input and b) output SW_02_3

The material already exhibited a stress history of approximately 40kPa from previous tests. Thus the components were not in their original state when the sample was placed into the compression apparatus. A maximum normal stress of 122kPa was applied on composition SW_02_3. From Figure 5-18, it is apparent that for the input the majority of aluminium cans were low compressible. During compression the majority were shifted to the subdivision of reinforcing components and only a small percentage of low compressible aluminium cans remained. For paper only a slight shift toward a decreased component size was visible. The amount of high compressible components in the size range 120-500mm was decreased. For flexible plastics only a change in the size range was observed as high compressible components in the size range 40-120mm disappeared and high compressible components sized 120-500mm were found. In terms of rigid plastic packaging (and also bottles) a clear altering of the low compressible to reinforcing components is visible.

The aluminium can-dominated composition SW_04 only exhibited slight changes despite a relatively high normal stress level of 110kPa. For cans, the amount of reinforcing components was increased, while the amount of low compressible components in the size range of 120-500mm decreased. Rigid plastic packaging altered its mechanical function only by a very small percentage from low compressible to reinforcing. Due to the mechanical forces, brick parts showed signs of failure, which explained the appearance of brick parts sized 10-40mm.

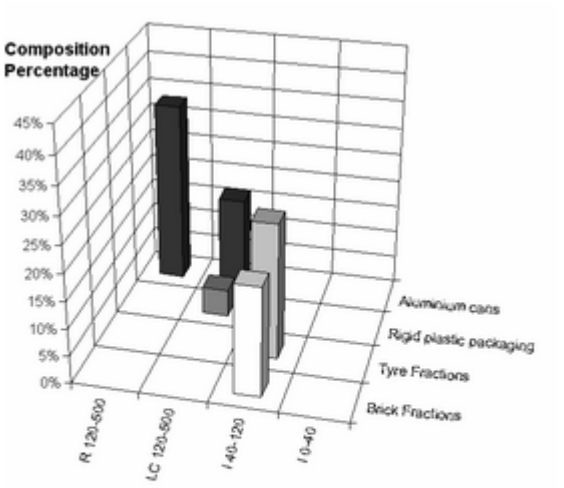

a)

	I 0-40	I 40-120	LC 120-500	R 120-500
Aluminium cans			16.7%	33.3%
Rigid plastic packaging			5.0%	
Tyre Fractions		25.0%		
Brick Fractions		20.0%		

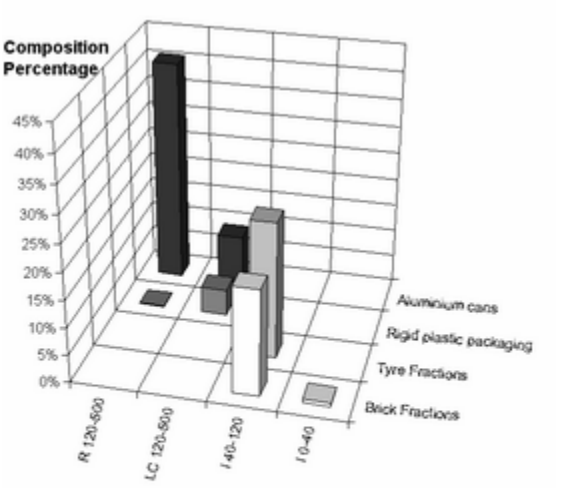

b)

	I 0-40	I 40-120	LC 120-500	R 120-500
Aluminium cans			9.2%	40.8%
Rigid plastic packaging			4.8%	0.2%
Tyre Fractions		25.0%		
Brick Fractions	0.7%	19.3%		

Figure 5-19 a) Input and b) output SW_04

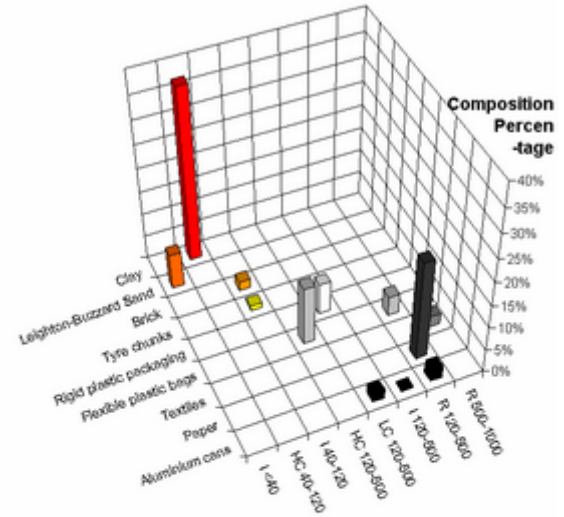

a)

	I <40	HC 40-120	I 40-120	HC 120-500	LC 120-500	I 120-500	R 120-500	R 500-1000
Aluminium cans					2.1%	0.2%	2.9%	
Paper							21.4%	
Textiles								2.4%
Flexible plastic bags				12.6%			4.2%	
Rigid plastic packaging					6.5%			
Tyre chunks			1.2%					
Brick			1.9%					
Leighton-Buzzard Sand	7.6%							
Clay		37.0%						

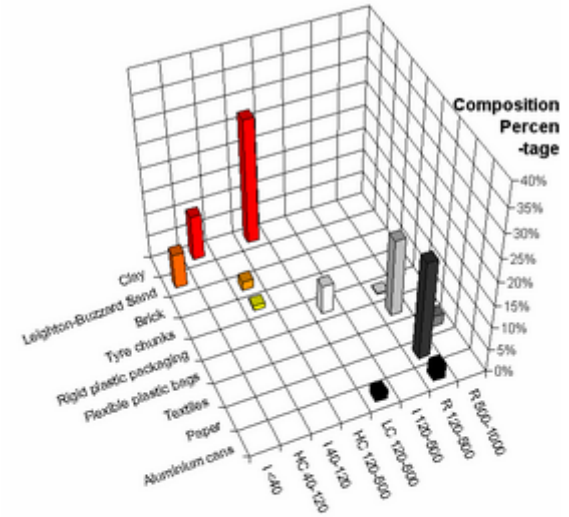

b)

	I <40	HC 40-120	I 40-120	HC 120-500	LC 120-500	I 120-500	R 120-500	R 500-1000
Aluminium cans					1.8%		3.3%	
Paper							21.4%	
Textiles								2.4%
Flexible plastic bags							16.9%	
Rigid plastic packaging					6.2%		0.3%	
Tyre chunks			1.2%					
Brick			1.9%					
Leighton-Buzzard Sand	7.6%							
Clay		9.8%		27.2%				

Figure 5-20 a) Input and b) output SW_09

In composition SW_09 bricks, tyre chunks, textiles and paper did not alter their mechanical function. Clay lumps were distributed over two size ranges (40-120mm and 120-500mm). The explanation for the size increase is the flattening of the lumps. Flexible plastic bags shifted from being high compressible to being reinforcing.

5.7 Summary of Compression Behaviour

Compression tests on six different compositions were conducted. The tests were divided into tests on incompressible compositions (SW_01, SW_07), compressible compositions (variations of SW_02: SW_02_1, SW_02_2, SW_02_3, and SW_03), a mono-component composition (SW_04), and a composition simulating a real waste composition (SW_09). For these compositions the results from compression tests were presented. These comprised the general boundary conditions of the test, visualisations of the component behaviour during the test (i.e. photographs at different normal stress levels of the test) and constrained modulus and compression index for each test.

The compositions exhibited expected behaviour, i.e. incompressible compositions with a high portion of Leighton-Buzzard sand (SW_01 and SW_07) resulted in high constrained moduli and low compression indices, while compressible compositions (SW_02 series and SW_03) showed low constrained moduli and high compression indices, due to their highly compressible character caused by the amount of aluminium cans and plastic packaging. The mono-component composition SW_04 and the real waste simulation SW_09 exhibited characteristics similar to the compressible compositions, as a large amount of compressible components like plastic tubs, paper sheets and aluminium cans were involved (SW_09) and due to the amount of aluminium cans involved (SW_04). Two different groups of compression (incompressible compositions exhibiting stiff behaviour and compressible showing low constrained moduli) behaviour could be clearly identified.

Additionally, an input-output comparison of the components in the tests SW_02_2, SW_02_3, SW_04 and SW_09 was accomplished. For this, the components were sorted according to the classification system into the material groups, size ranges and shape-related subdivisions. Subsequently, input and output were compared.

A detailed discussion of the compression behaviour and a comparison to values from the literature is provided in chapter 7.4.

6 Shear Behaviour

6.1 General Introduction

The following chapter presents the results of the laboratory work on shear behaviour. It generally consists of two shear box calibrations, large- and small-scale tests on Leighton-Buzzard sand and the results of the testing programme on all compositions introduced in section 4.3.3. Shear stress and horizontal displacement curves, Mohr-Coulomb envelopes and shear moduli G are presented. The final analysis displayed in this chapter is the component shifting within the shape-related subdivisions.

6.2 Calibration of the Shear Box

To calibrate the shear apparatus, the internal friction values, i.e. the rolling resistance of the device bearings were determined in a first step. Secondly, results from large-scale shear tests on Leighton-Buzzard sand were compared to results from small-scale direct shear tests in order to validate performance of the large shear box.

6.2.1 First Calibration

To investigate the values for the rolling resistance of the shear box, a set of five tests on the empty box at low normal stresses was accomplished. For the set-up, the height of the upper frame was reduced to a single layer of beams and two rollers were placed inside the box serving as horizontal free-moving bearing in the shear direction. The hydraulic jacks applied the normal stress onto a stiff spreader load plate placed on top of the rollers. The shear process ended in the range of 100 to 120mm displacement.

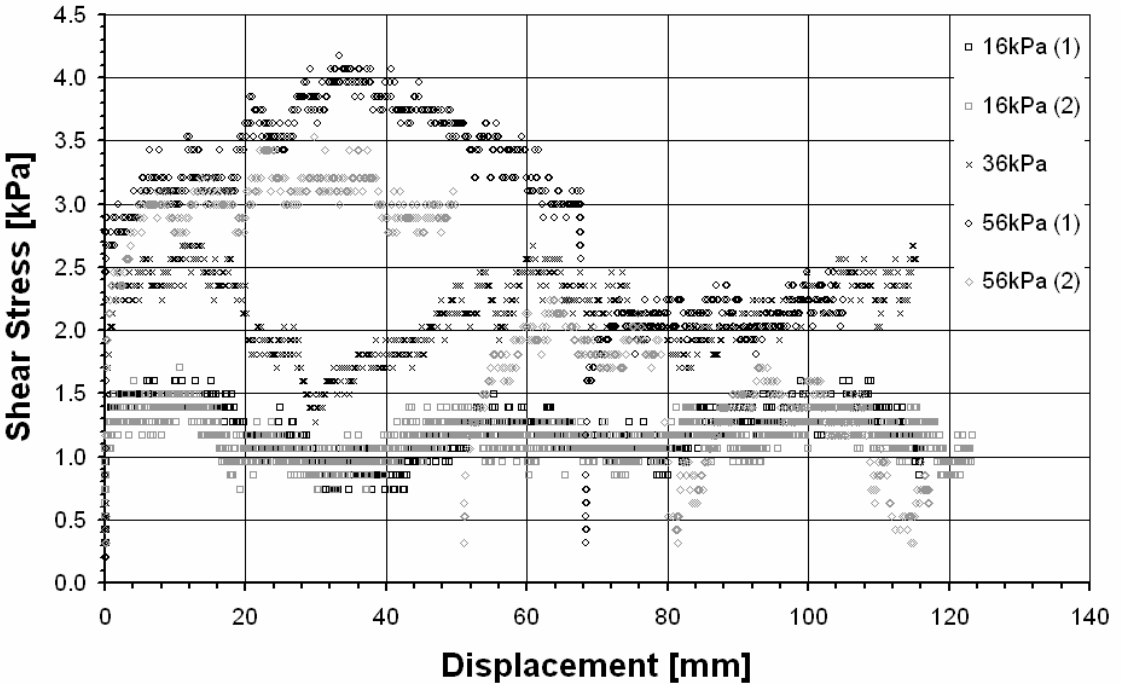

Figure 6-1 Shear stress-displacement curves of the first calibration

Figure 6-1 shows the shear stress-displacement curves for the first calibration. The repetition of the 16kPa-test resulted in good accordance, while the second test on 56kPa normal stress exceeded the shear stress of its predecessor by 30% at its maximum, but it matched a similar value after 60mm displacement. The differences were probably due to impurities on the shear box bottom causing rolling resistances, which resulted in increasing shear stresses to a maximum value and decreasing values after overcoming this resistance.

The straight line of shear stress-normal stress is plotted in Figure 6-2. Amongst the results from the calibration tests, extrapolated values for higher normal stresses (i.e. 100kPa and 150kPa) and a maximum and average line for the test results are shown. The values found in these tests were taken into account for the subsequent shear tests on sand.

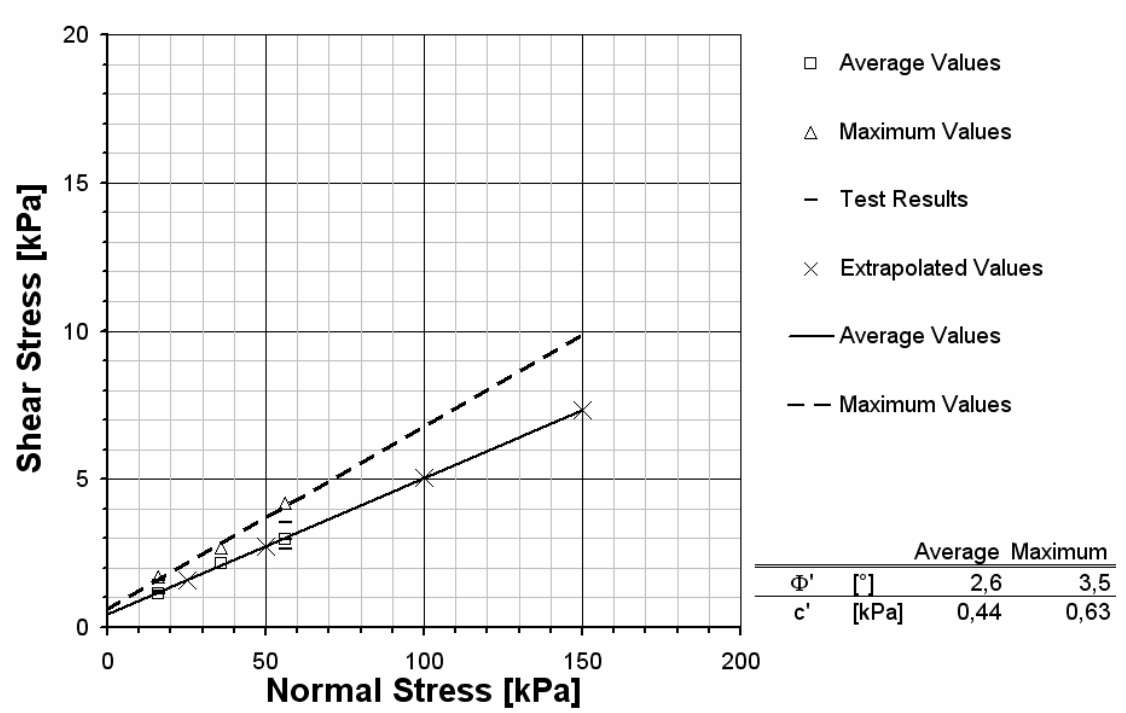

Figure 6-2 Shear stress-normal stress lines of the first calibration

6.2.2 Shear Tests on Leighton-Buzzard-Sand

For a validation of the large shear box operation, tests on Leighton-Buzzard sand were conducted on both small- and large-scale devices. The small-scale tests were accomplished in a 100mm*100mm direct shear device. The results were subsequently compared.

6.2.2.1 Large-Scale Shear Tests on Leighton-Buzzard-Sand

Three different sets of shear tests were conducted in the large shear device. These differed from each other in terms of sample height and shear rate. Additionally, tests were repeated to confirm or disapprove results. The normal stress levels represented 25/50/100/150kPa. The input of test sets 1 and 2 amounted for approximately 700kg, in set 3 round about 950kg of sand was sheared.

Table 6-1 Boundary conditions for the tests

		Set 1_1, 1_2	Set 2	Set 3
Sample height	[mm]	429/436	439	572
Shear rate	[mm/min]	10.2/10.5	1.9	1.9
Initial unit weight	[kN/m^3]	16.5/16.5	16.5	16.5
Final unit weight	[kN/m^3]	n.d.	16.7	16.9

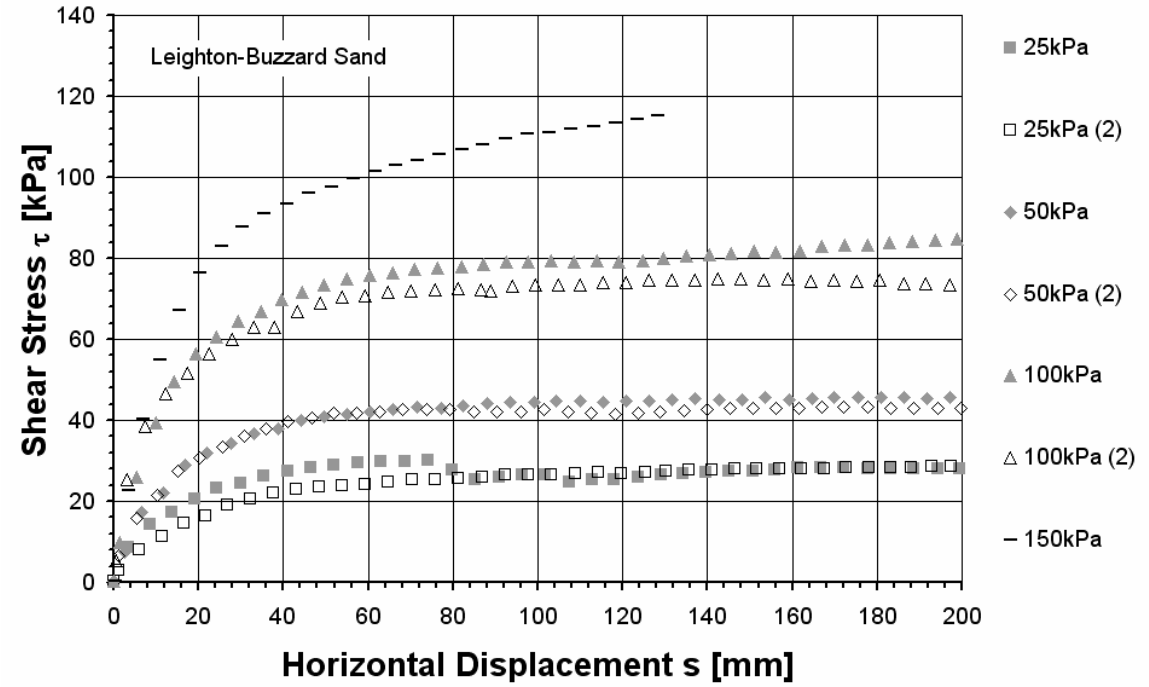

Figure 6-3 Shear stress-displacement curves of set 1_1 and set 1_2 with a shear rate of approximately 10mm/min

Shear stress in relation to the displacement is plotted in Figure 6-3. The results of set 1_1 and set 1_2 were in good accordance especially in the lower normal stress ranges of 25kPa and 50kPa. A slight difference was noticeable at 100kPa.

Decreasing the shear rate from around 10mm/min to approximately 2mm/min resulted in a consistent flattening of the shear curve, especially for 150kPa, as depicted in Figure 6-4. As before, it was observed that repeating a test (25kPa in this case) resulted in similar values for the shear stress. Compared to set 1_1 and 1_2 the peak (or ultimate) shear stress values were not affected by decreasing the shear rate. Decreasing the sample height apparently resulted in slightly higher shear stress values as visible from Figure 6-5. Also a tendency to increase further seemed to be more present than in preceding test sets. Figure 6-6 summarises the test results and provides a direct comparison of the test sets. Especially for the high normal stresses (100kPa and 150kPa) a tendency of strain hardening is observed with one exception (150kPa and slow shear rate).

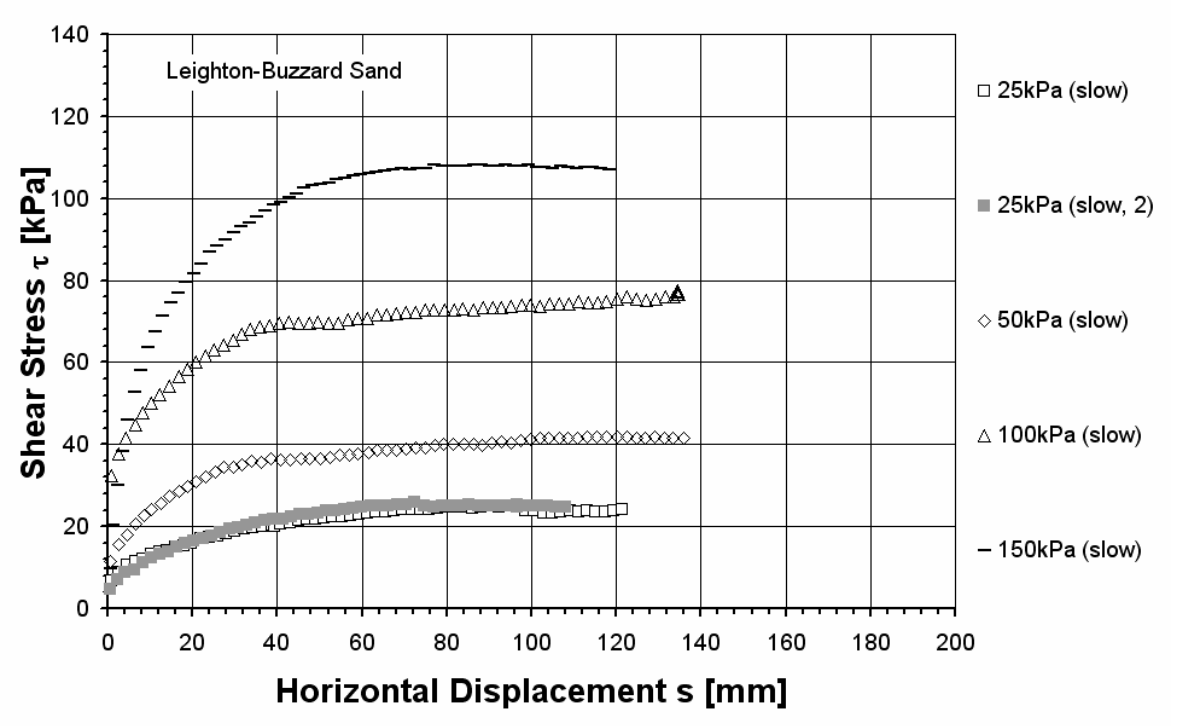

Figure 6-4 Shear stress-displacement curves of set 2 with a shear rate of approximately 2mm/min

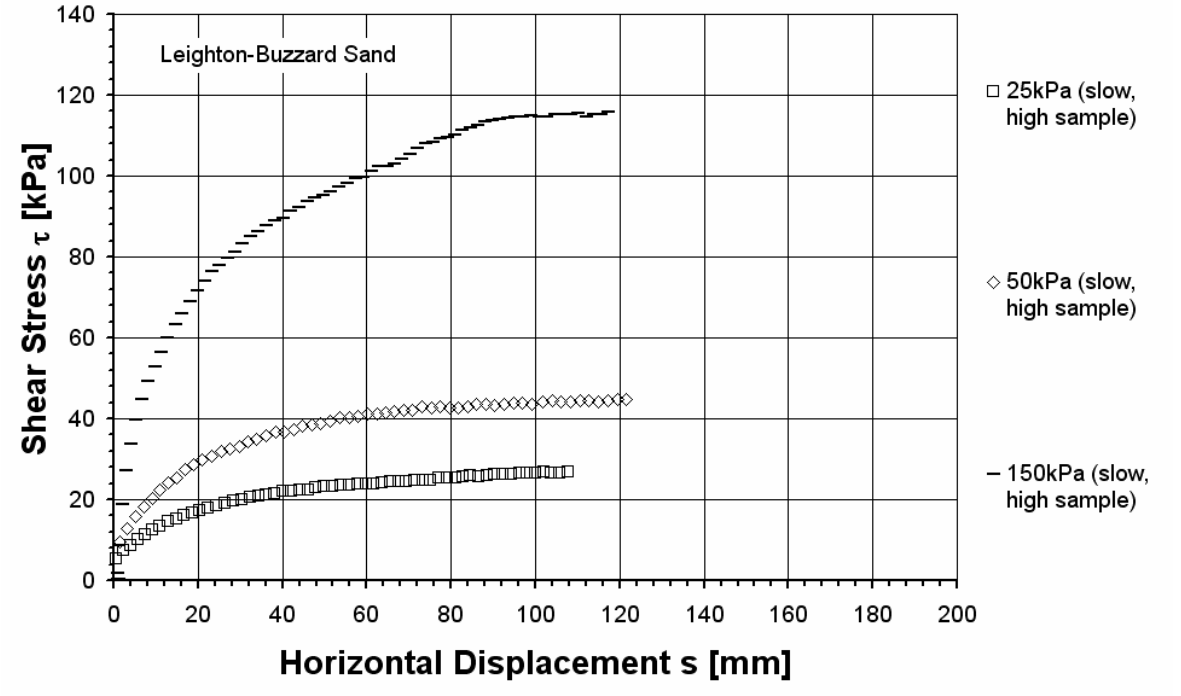

Figure 6-5 Shear stress-displacement curves of set 3 (high sample) with a shear rate of approximately 2mm/min

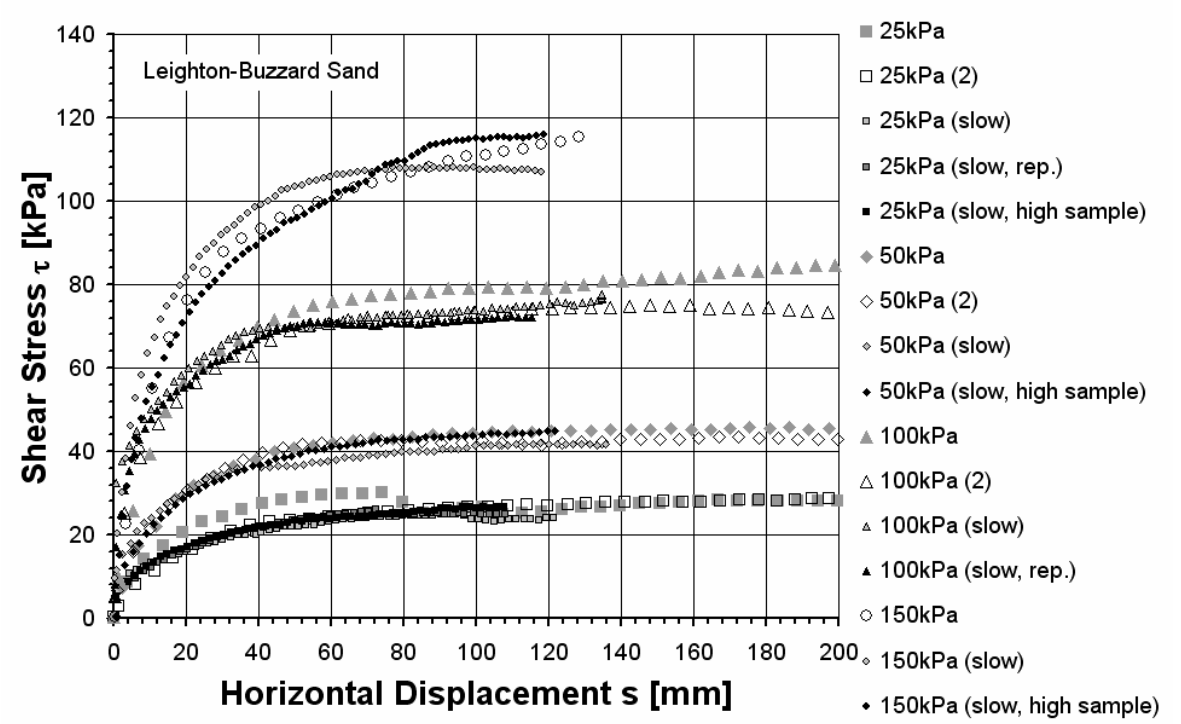

Figure 6-6 Shear stress-displacement curves of all large-scale sets

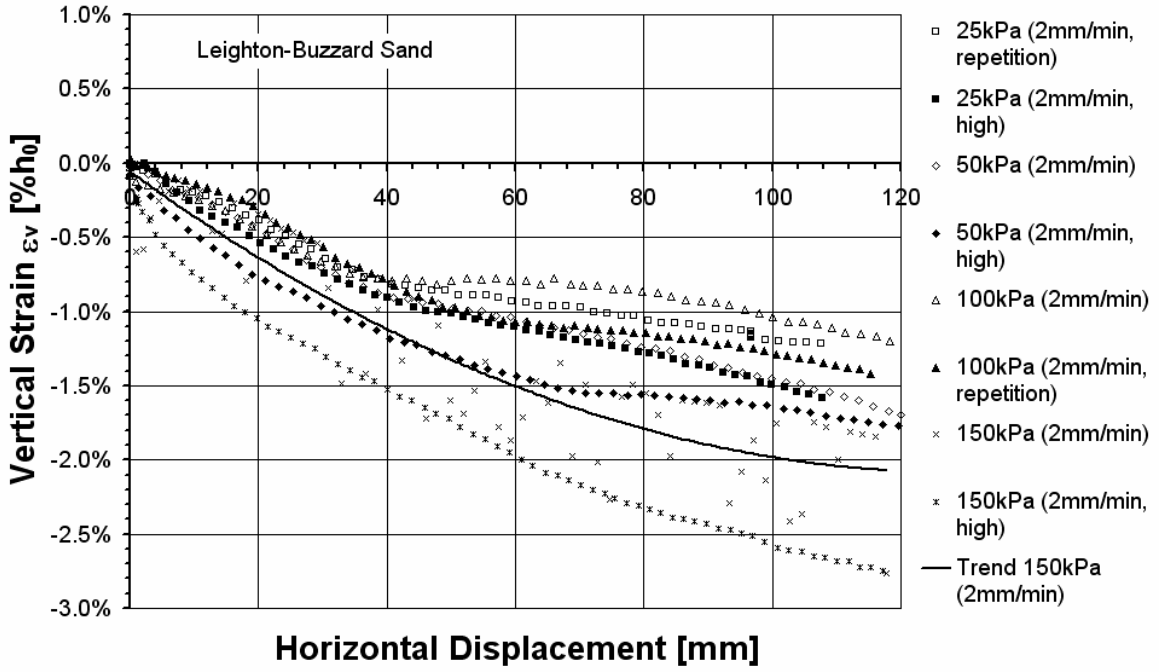

Figure 6-7 Vertical and horizontal displacement curves of large shear tests on Leighton-Buzzard sand[18]

Figure 6-7 summarise the volume change behaviour of the tests conducted with a shear rate of 2mm/min. For the test 150kPa (slow) a second-degree polynomial trend line is

[18] Settlement describes the decrease of an initial sample height, thus it is subsequently shown using negative values

additionally shown, as the logged data fluctuated considerably. Contractant behaviour of a loose material was observed for all tests.

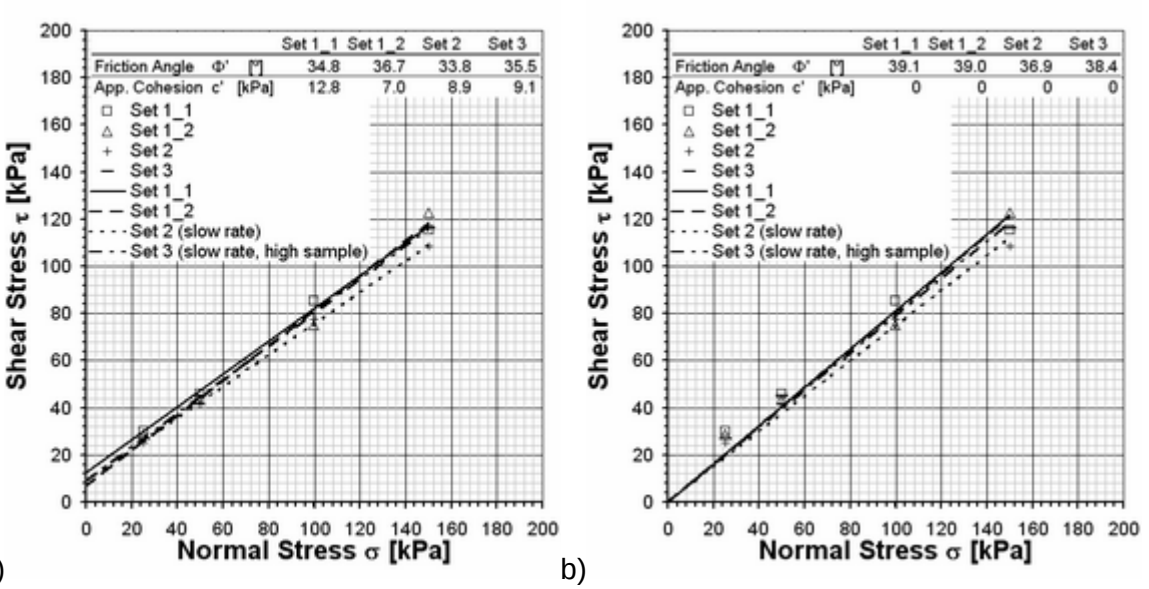

a) b)

Figure 6-8 Mohr-Coulomb failure envelope for large-scale shear tests on sand: a) with apparent cohesion; b) Apparent cohesion = 0

The Mohr-Coulomb failure envelope is shown in Figure 6-5; in a) the apparent cohesion is shown. As Leighton-Buzzard sand is by definition a cohesionless soil (i.e. consisting of rounded or angular particles) the friction angle without a cohesion intercept is shown in b) resulting in an increase of about 4°. The shear stress values are the ultimate values observed in the tests, as a true peak strength value was not detected.

6.2.2.2 Small-Scale Shear Tests on Leighton-Buzzard-Sand

The shear device with a shear area of 100mm*100mm (Figure 6-9) used for the small-scale tests consisted of a fixed upper frame held in position by horizontal bolts, and a moveable bottom frame. A load plate was placed on top of the sample, onto which the normal load was applied by means of a mechanical lever with a ratio 1:10, i.e. a weight of 1kg equals 10kPa. The lever was loaded with the appropriate amount of weights. Two adjusting screws driven through the upper frame induced a shear gap. Both, vertical and horizontal displacement as well as shear load is measured with dial gauges and was manually logged. Approximately 600g of Leighton-Buzzard sand were installed per test. With an average measured sample height of 34mm, the initial unit weight resulted in 17.7kN/m^3, and the final unit weight amounted for about 17.6kN/m^3.

Figure 6-10 shows the displacement curves for three sets, which showed reasonable conformance in each normal load stage, especially at 25kPa and 50kPa. A peak value was distinctive for the high normal stresses, but also the lower normal stresses exhibited a peak value. As an example, Figure 6-11 shows the dilatant behaviour of set 3 being a characteristic of dense sand.

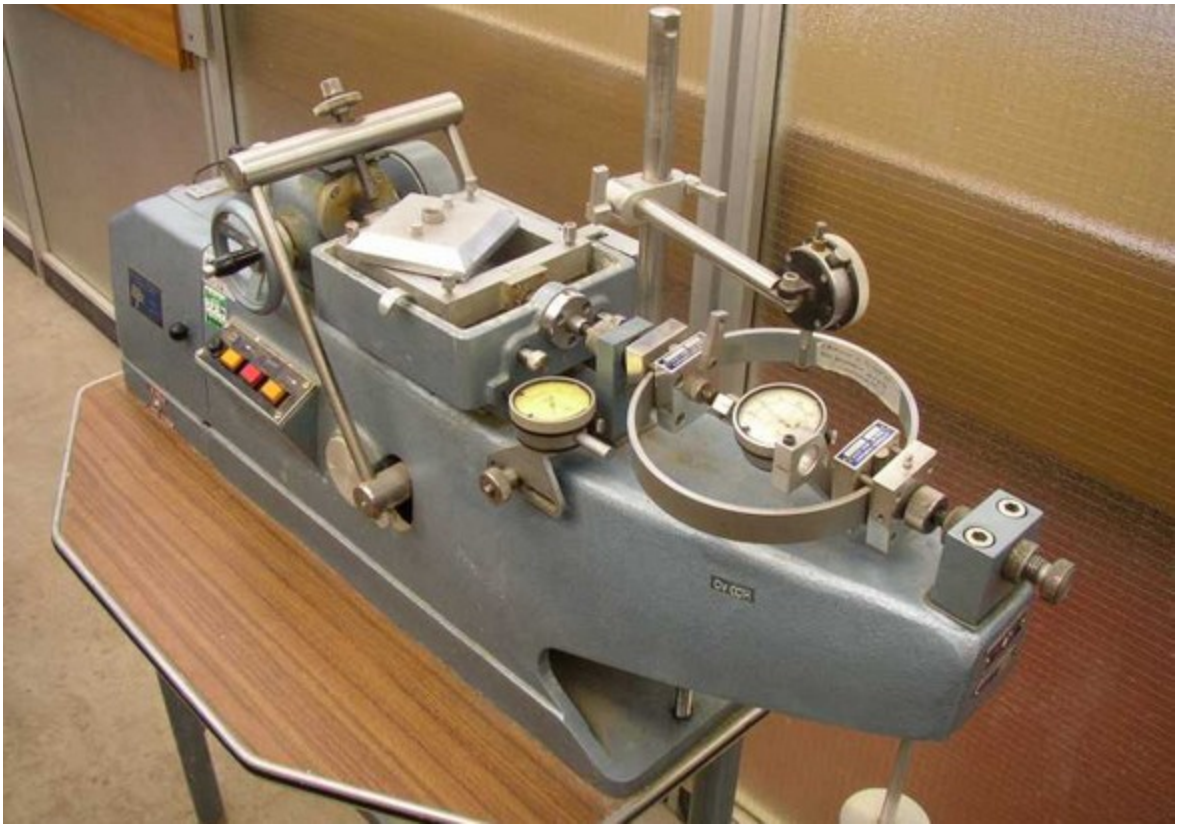

Figure 6-9 Small-scale direct shear device

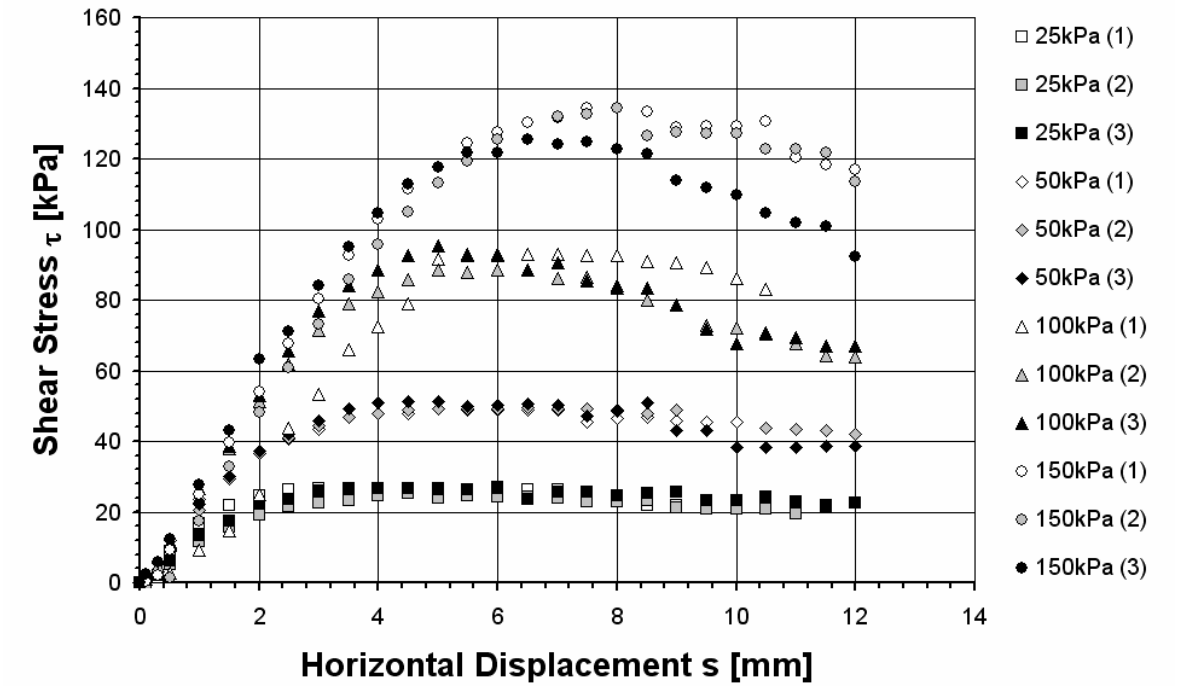

Figure 6-10 Shear stress – displacement curves of three small-scale test sets on Leighton-Buzzard sand

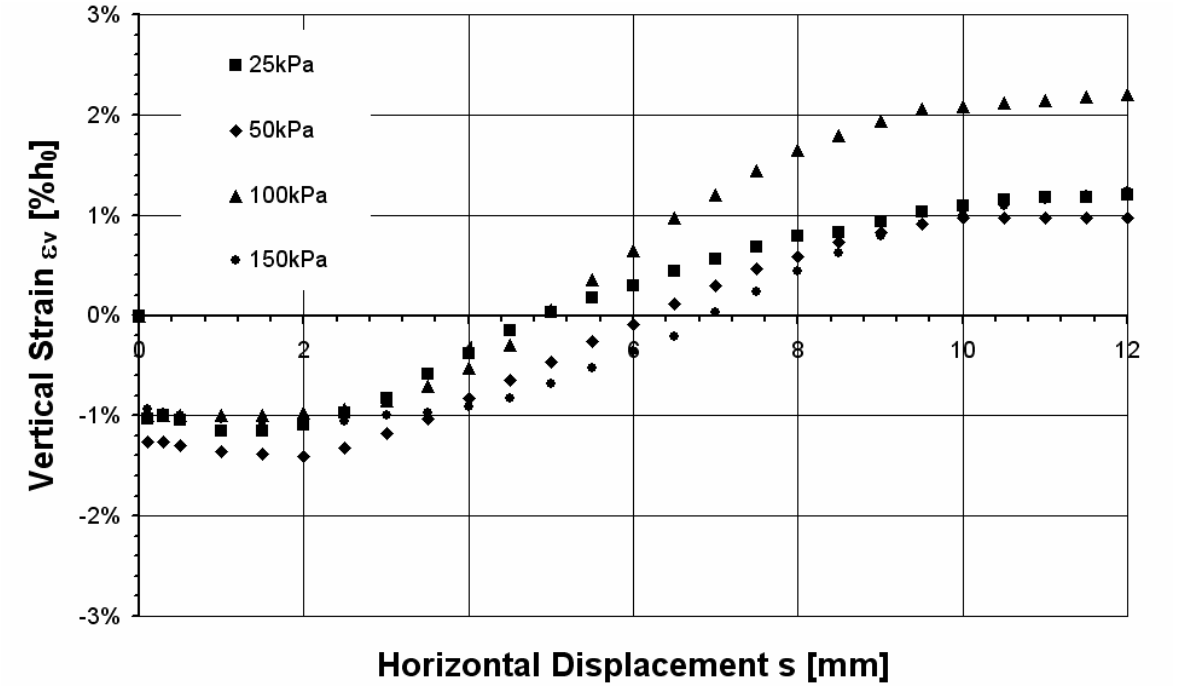

Figure 6-11 Vertical and horizontal displacement curves of set 3

Figure 6-12 demonstrates the Mohr-Coulomb envelope for the small-scale shear tests using the observed peak shear strength values. The apparent cohesion is half the amount of the value found in the large-scale shear test. Thus the friction angles calculated with the assumption of zero cohesion increase to about 105% of their initial values.

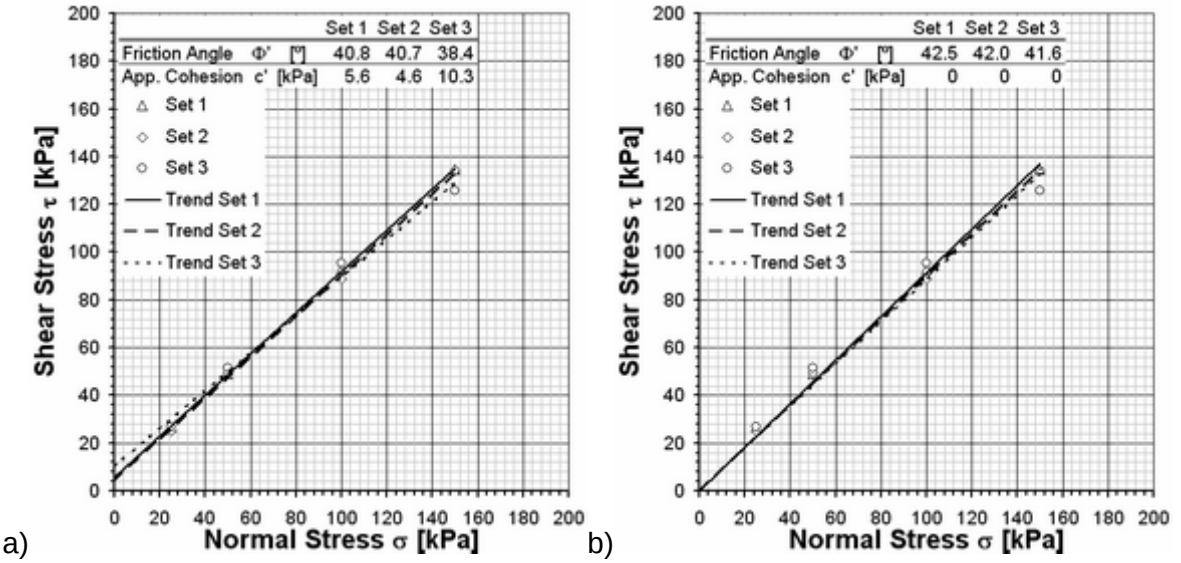

a) b)

Figure 6-12 Mohr-Coulomb failure envelope for small-scale shear tests on sand: a) with apparent cohesion; b) Apparent cohesion = 0

6.2.2.3 Comparison of Small-Scale and Large-Scale Tests

From the shear tests conducted on Leighton-Buzzard sand it was observed that the large-scale shear device exhibited lower values for the friction angle than the small-scale one. Moreover, an apparent cohesion was found, which was approximately twice the amount of the data from the small shear device. The friction angles for both tests were within the

range of a medium dense sample type of Leighton-Buzzard sand with 36° to 46°, as mentioned in Talby (1997), and 38° to 42°, as stated by Lings and Dietz (2004). The values from the small-scale device with an average of 42° tended to reflect a more dense behaviour, while the values from the large device with an average of 38° tended towards the lower limit for a medium sample type. The differences could be due to slightly different sample densities for small- (γ_0 = 17.6kN/m^3) and large-scale tests (γ_0 = 16.5kN/m^3).

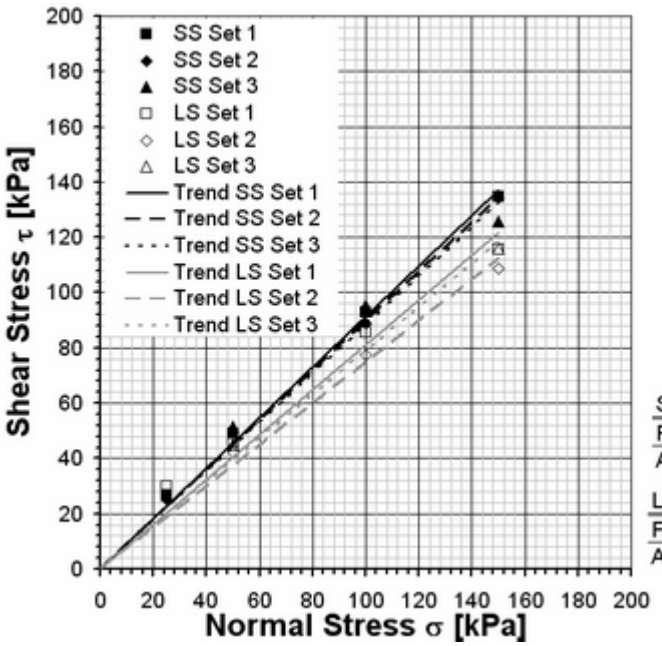

Small Scale Tests (SS)		Set 1	Set 2	Set 3
Friction Angle	Φ' [°]	42.5	42.0	41.6
App. Cohesion	c' [kPa]	0	0	0

Large Scale Tests (LS)		Set 1	Set 2	Set 3
Friction Angle	Φ' [°]	39.1	36.9	38.4
App. Cohesion	c' [kPa]	0	0	0

Figure 6-13 Mohr-Coulomb envelopes for the small- and large-scale shear tests

Due to the size of the large-scale shear device, there is a risk of imprecision. For example, even though the normal stress-induced gap was covered with plastic foil to prevent sand from accessing it and thus increasing the friction, an absolute protection was not possible as the plastic foil bended and shifted during the tests. Moreover, with the size of the device some disadvantages are involved. The load plate left a gap at all four sides inside the box, with the effect that sand could migrate through those gaps and thus the normal stress did not stay constant. At high normal stresses and resulting high shear stresses, the steel frame anchoring the horizontal jack started to bend, with the result that the shear load diverged from its horizontal alignment. The normal stress was applied manually and needed to be adjusted, as volume changed. This also led to slight inconsistencies. As the shear rate also was set manually, another inconsistency was present. For example, the first large-scale test set had an average shear rate of 10.2mm/min. The rate varied between 9.8mm/min and 10.7mm/min, resulting in a deviation of 0.25 from the average. These issues had to be born in mind during the analysis of data resulting from the large shear device.

6.2.3 Second Calibration

Due to a material failure of the upper frame near the roller bearings of the shear box (welding seam in Figure 3-11a), it was necessary to dismantle and fix the device, and thus conduct a new calibration. The test set-up slightly differed from the first calibration, as

three steel beams were placed in the shear direction into the bottom part of the box. For stabilisation, sand was filled into the spaces between the beams (Figure 6-14a).

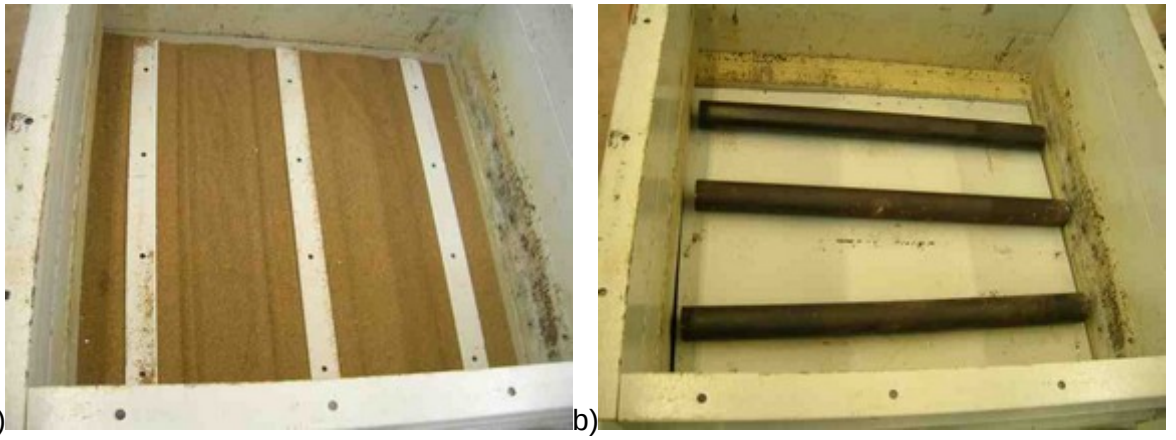

Figure 6-14 a) Bottom box filled with sand and steel beams in shear direction; b) Bottom box with rollers on steel plate

A steel plate was placed on top of the sand, on which three rollers could act as horizontally mobile bearings. As for the first calibration, load plate and jacks for the vertical load application were arranged onto the bearings. The arrangement of the second calibration resulted in a more stable test procedure, as the underlying material, on which the test was conducted, seemed to be stiffer in comparison to the set-up of the first calibration, where the calibration directly took place on the bottom plate of the shear box. Furthermore, as the rollers were almost level with shear plane, a further displacement could have been possible. Three tests with σ = 25/50/100kPa were conducted.

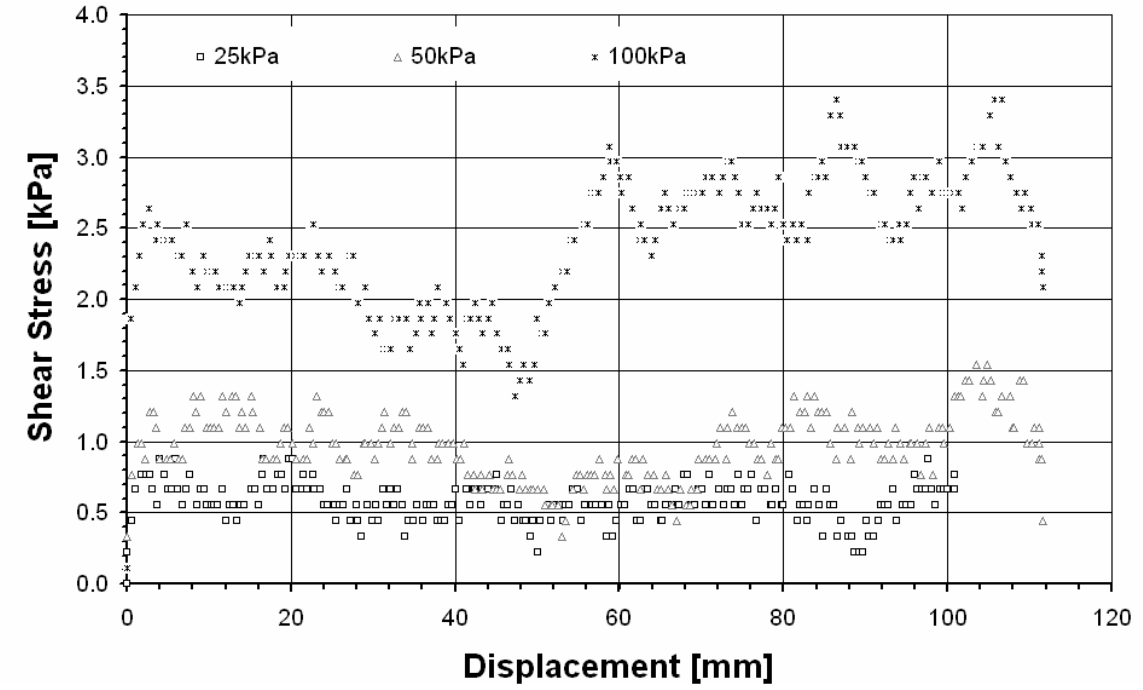

Figure 6-15 Shear stress – displacement curves of the second calibration

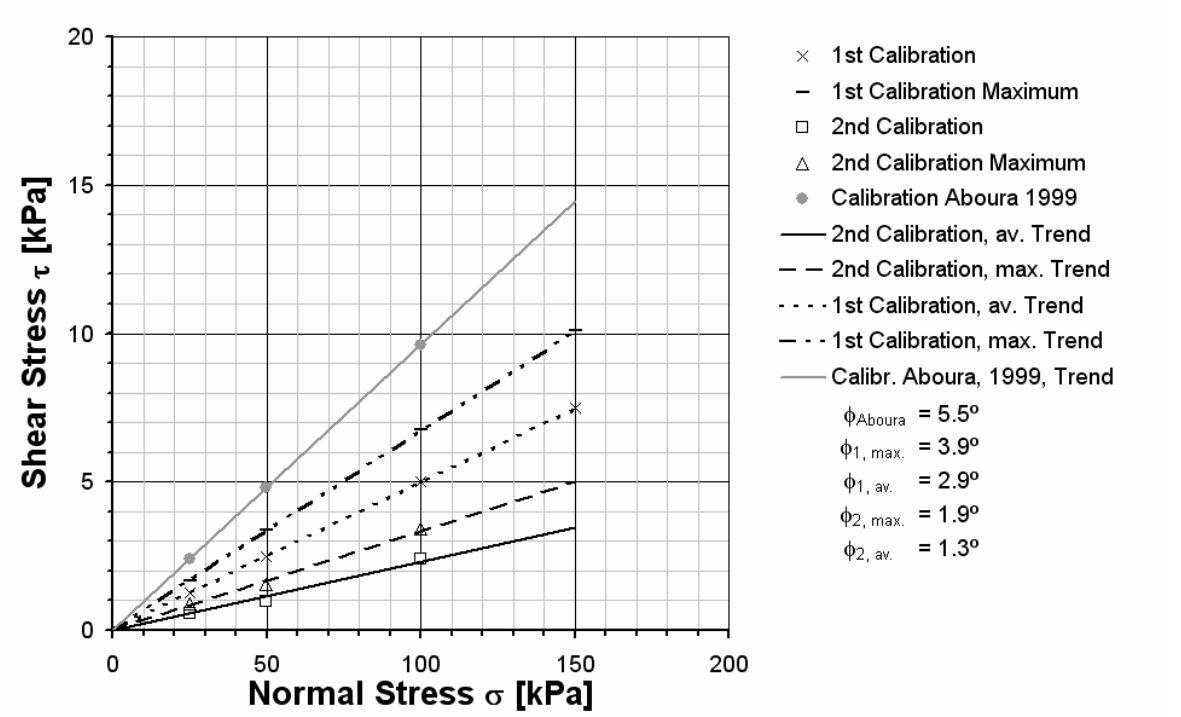

Figure 6-16 Shear stress – normal stress lines of the second calibration

Figure 6-15 shows the shear stress-displacement curves for the second calibration. The increase in shear stress was striking at about 50mm displacement for the 100kPa-test, which was due to a stress adjustment after the normal stress decreased. Figure 6-16 shows the result of the second calibration in comparison to the result of the first and values derived from a calibration done by Aboura (1999), who utilised the same device for testing. As a cohesive effect should not occur, all calculated intercepts were set to zero resulting in apparent friction angles between 1.3° and 5.5°. For all further calculations a correction factor based on the second calibration's average values in relation to the respective normal stress was considered in the results. Table 6-2 summarises the correction values for the normal stresses used in shear testing.

Table 6-2 Shear stress correction values for different normal stress levels

Normal Stress	[kPa]	25	50	75	100
Shear Stress Correction	[kPa]	-0,58	-1,15	-1,73	-2,30

6.3 Large-Scale Shear Tests on Synthetic Waste

6.3.1 Incompressible Compositions

6.3.1.1 Composition SW_01_1

Composition SW_01_1 was one of two identical composition initially tested. Compared to SW_01_2, it was sheared with a low sample height. All boundary conditions are shown in Table 6-3. The heights stated in the table relate to the initial sample height (h_0), the

sample height after pre-compaction (h_1), the sample height at shear start (h_2) and the sample height at shear end (h_e). The shear rate ranged between 4.2 and 5.2mm/min as a matter of manual adjustment. For the test the depth of the bottom box was reduced by placing steel beams orientated in the shear direction gaps filled with sand, similar to the setup of the second calibration. This was done in order to reduce the overall volume, which otherwise would have to be filled with sample material. On top of this layer, the bottom load transmission plate was put, and on that the sample was placed.

Table 6-3 Boundary conditions for SW_01_1

Normal Stress σ [kPa]	Input Mass [kg]	Shear rate [mm/min]	h_0 [mm]	h_1 [mm]	h_2 [mm]	h_e [mm]	Unit weight γ_0 [kN/m^3]	Unit weight γ_e [kN/m^3]
25	484	4,2	444	374	384	390	12.61	12.43
50	484	5,2	444	364	379	369	12.78	13.13
100	484	4,7	444	359	399	377	12.14	12.83

The test with 100kPa was disrupted at 25mm displacement due to a rapid normal stress decrease. After noticing the failure, the boundary conditions were recovered and the test continued. As visible from Figure 6-17 the shear stress build-up after the failure complied with the precedent course of the initial shear stress. The fluctuations, which were especially visible at a displacement larger than 100mm, were a result of normal stress increase during the test and the manual adjustment, i.e. decreasing the normal stress.

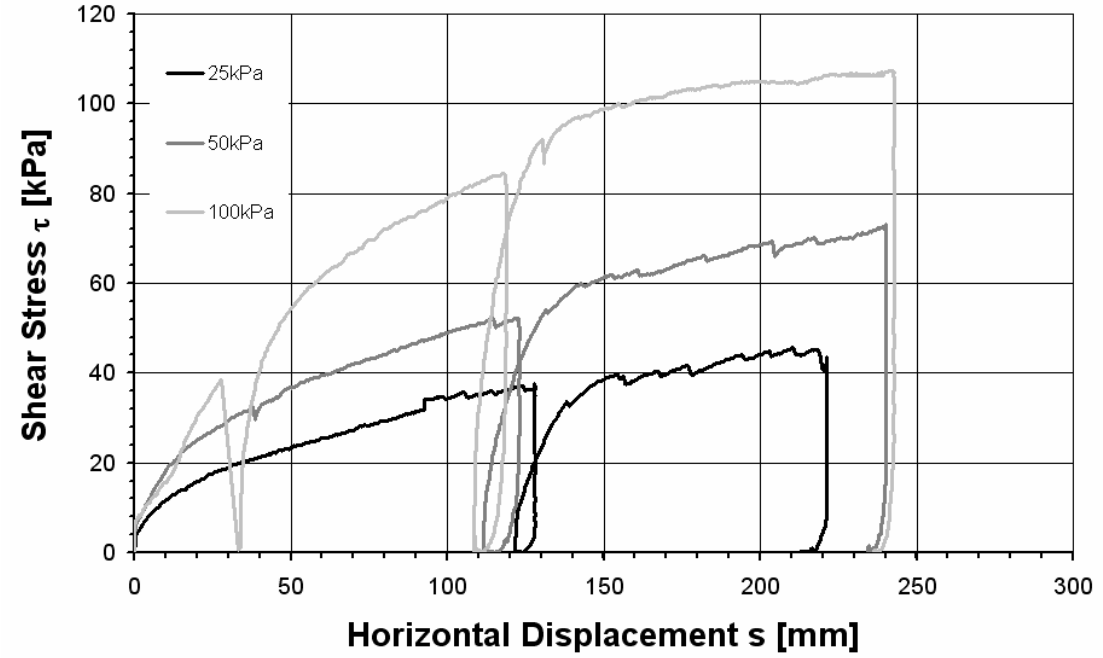

Figure 6-17 Shear-displacement curves for SW_01_1

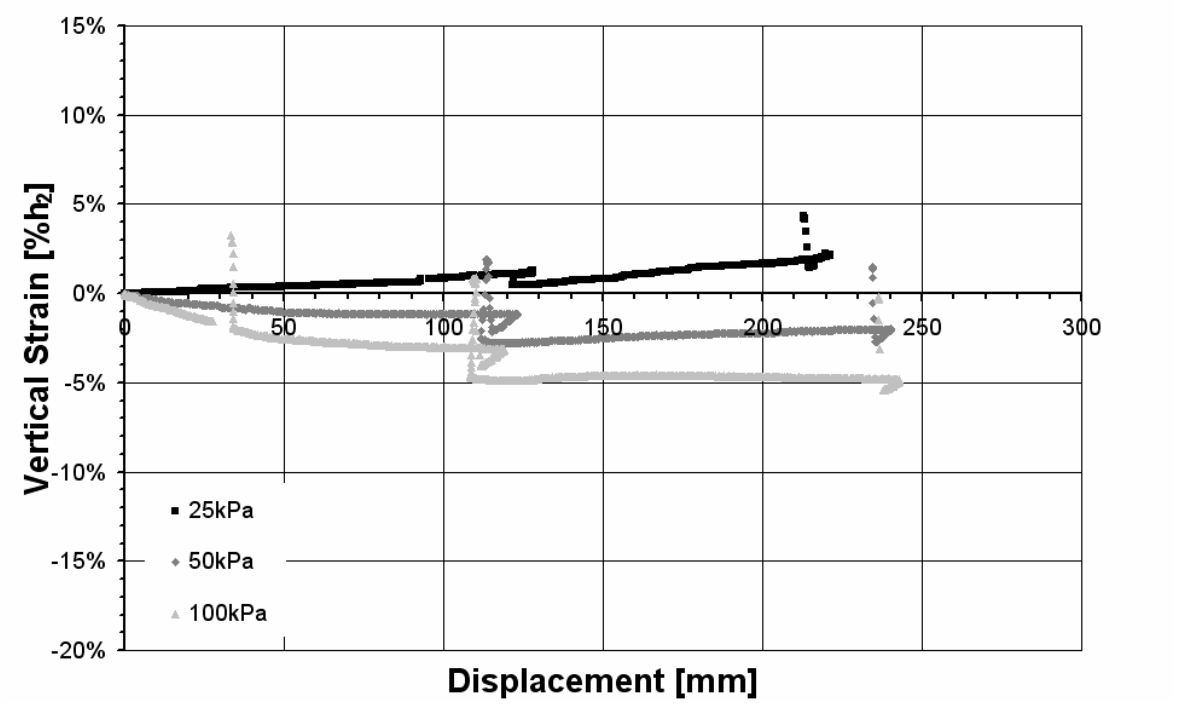

Figure 6-18 Vertical Strain over displacement of SW_01_1

A peak value is not noticeable from Figure 6-17. The shear stress of the sand-plastic-paper mixture was constantly increasing. At the highest normal stress of 100kPa the stress curve flattened after a displacement of 150mm.

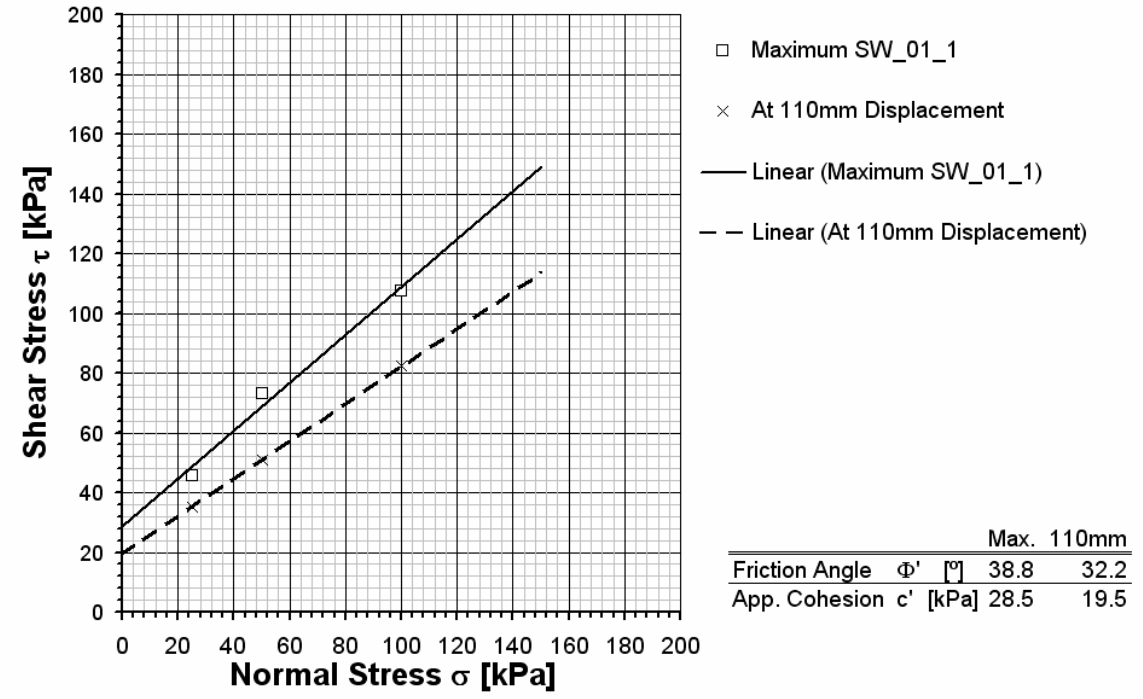

Figure 6-19 Mohr-Coulomb envelope for SW_01_1

The vertical strain in Figure 6-18 confirms the contractant behaviour of a loose medium, with the exception of the lowest stress level of 25kPa, which exhibited a slight dilatant behaviour. The disruption of the test on 100kPa is clearly visible as a vertical strain

increase in Figure 6-18. Also, the effect of the unload-reload loop in this figure (and in all subsequent figures showing the vertical strain from shear tests) is noticeable as a rebound in the horizontal displacement and an increase of the vertical strain, followed by rapid decrease. The Mohr-Coulomb envelope for composition SW_01_1 is shown in Figure 6-19. A friction angle of 38.8° and an apparent cohesion of 28.5kPa was found for the maximum shear stress values (i.e. maximum displacement). A comparative value for mobilised friction angle and mobilised cohesion was chosen at a displacement of 110mm for all tests, as this value describes the shear parameter before the unload-reload loop, while the maximum values occurred afterwards. At 110mm displacement the friction angle was reduced to 32.2° and the apparent cohesion represented 19.5kPa. Table 6-4 indicates values for secant shear moduli, which were determined after reloading at three strain levels.

Table 6-4 Shear moduli for SW_01_1

Normal Stress σ [kPa]	G at 1% strain [kPa]	G at 2% strain [kPa]	G at 3% strain [kPa]
25	2701	1718	1299
50	3914	2708	1980
100	7022	4520	3192

6.3.1.2 Composition SW_01_2

For the second test set on composition SW_01 the spacer at the bottom of the shear box was removed and a larger sample amount was tested to investigate the effects different sample heights have on the result. After this test set the spacer used in SW_01_1 was re-placed into the bottom box and remained there for all subsequent tests.

Table 6-5 Boundary conditions for SW_01_2

Normal Stress σ [kPa]	Input Mass [kg]	Shear rate [mm/min]	h_0 [mm]	h_1 [mm]	h_2 [mm]	h_e [mm]	Unit weight γ_0 [kN/m^3]	Unit weight γ_e [kN/m^3]
25	674	5.7	599	539	539	527	12.50	12.79
25	674	6.0	574	514	524	525	12.73	13.13
50	674	5.8	594	529	529	513	12.98	13.57
50	674	5.9	574	509	514	501	12.86	12.83
100	674	5.9	594	519	519	496	13.11	13.45

As stated in Table 6-5, the shear rate differed between 5.7 and 6.0mm/min. Due to the volume increase the sample mass equalled 674kg and the initial uncompressed sample heights were between 574 and 599mm.

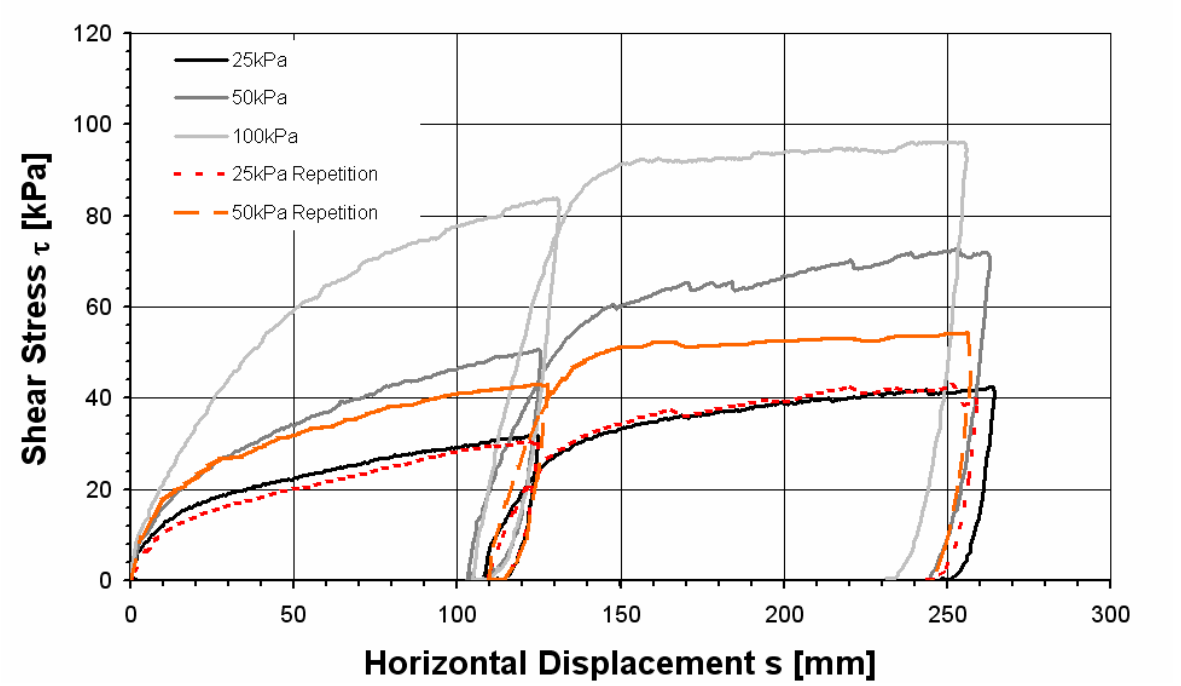

Figure 6-20 Shear-displacement curves for SW_01_2

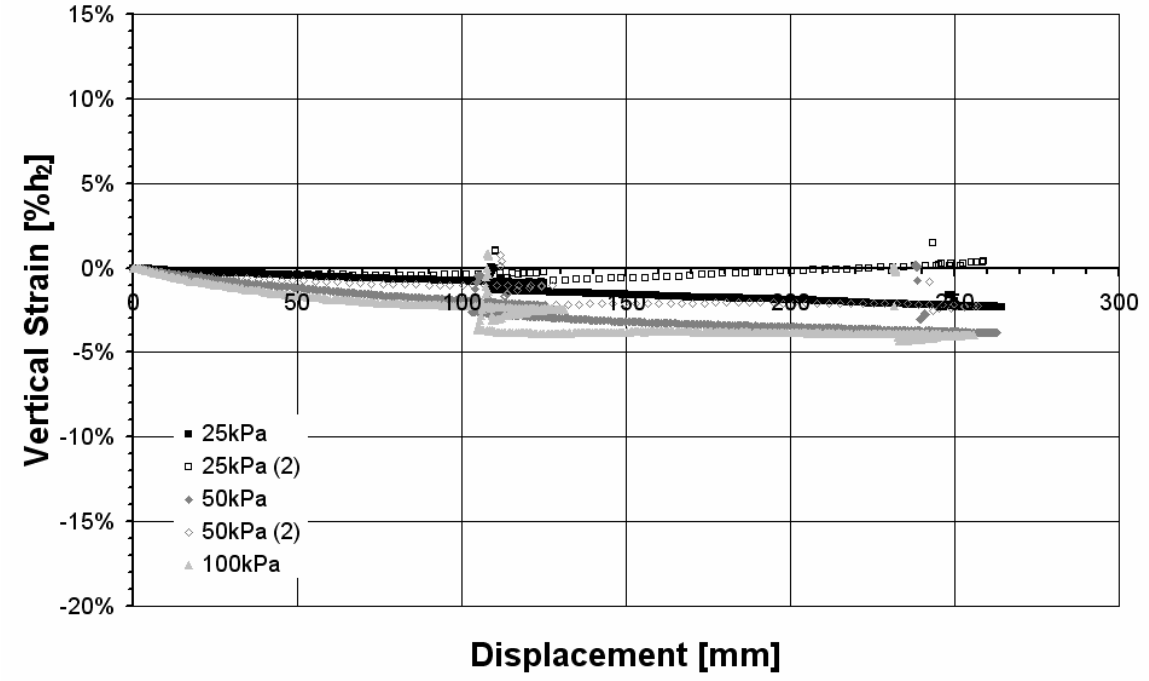

Figure 6-21 Vertical Strain over displacement of SW_01_2

The repetitions of 25kPa and 50kPa were conducted after the complete set was finished. As the components were reused for each test, paper and plastic exhibited symptoms of fatigue, i.e. the strength of the particular material was weakened, which probably resulted in a reduced initial sample height. Also, the curves of the 50kPa repetition in Figure 6-20

show a similar effect as it resulted in considerably lower shear stress values. The 25kPa repetition led to good accordance in shear stress. As before, the contractant behaviour of the material is visible from Figure 6-21. The 25kPa repetition tended to dilate as already observed in SW_01.

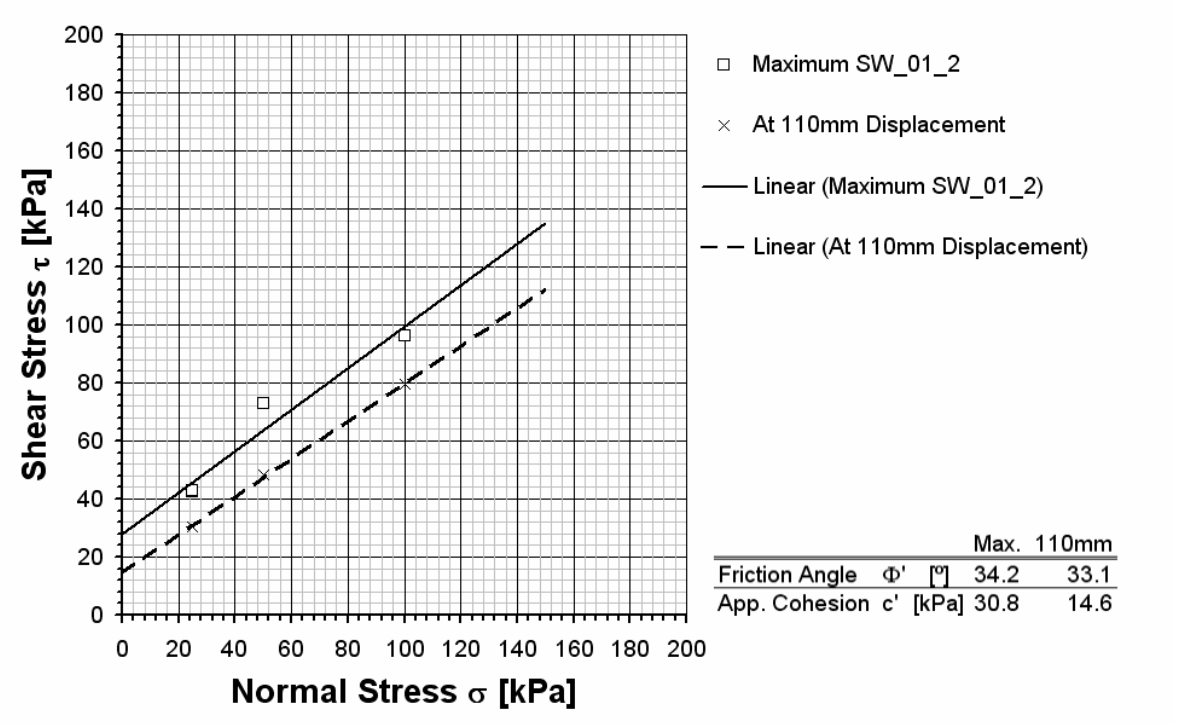

Figure 6-22 Mohr-Coulomb envelope for SW_01_2

The Mohr-Coulomb envelope in Figure 6-22 is defined by a friction angle of 34.2° and an apparent cohesion of 30.8kPa for the maximum values and a friction angle of 33.1° and an apparent cohesion of 14.6kPa, respectively. Table 6-6 present secant shear moduli determined for SW_01_2. The repetitions for 25kPa and 50kPa exhibited results similar to the first examination.

Table 6-6 Shear moduli for SW_01_2

Normal Stress σ [kPa]	G at 1% strain [kPa]	G at 2% strain [kPa]	G at 3% strain [kPa]
25	1677	1011	1017
50	2582	2063	1751
100	3747	3264	2741
25 rep.	1763	1391	1063
50 rep.	2657	2112	1608

6.3.1.3 Composition SW_06

SW_06 consisted of a Leighton-Buzzard-sand matrix composition, in which aluminium cans and plastic packaging were arranged (arrangement pictures in appendix 11.4). The shear rate was constant at about 5.9mm/min. The initial sample height varied between 532 and 554mm. With the high amount of sand in this composition the initial unit weight accounted for 13.72kN/m^3 to 14.32 kN/m^3 (Table 6-7).

Table 6-7 Boundary conditions for SW_06

Normal Stress σ [kPa]	Input Mass [kg]	Shear rate [mm/min]	h_0 [mm]	h_1 [mm]	h_2 [mm]	h_e [mm]	Unit weight γ_0 [kN/m^3]	Unit weight γ_e [kN/m^3]
25	746	5.9	554	544	544	522	13.72	14.29
50	746	5.9	540	531	525	499	14.21	14.94
100	746	5.8	532	529	521	488	14.32	15.27

The shear stress curves in Figure 6-23 were divided by the unload-reload-loop into two parts with different shape. For 50kPa and 100kPa, the part before the loop was characterised by a gradually increasing shear stress, the second part featured a rapid increase of the shear stress, which exceeded the preceding stress before the loop and approached a constant value. In this case, the 100kPa test reached a peak shear stress at 160mm displacement.

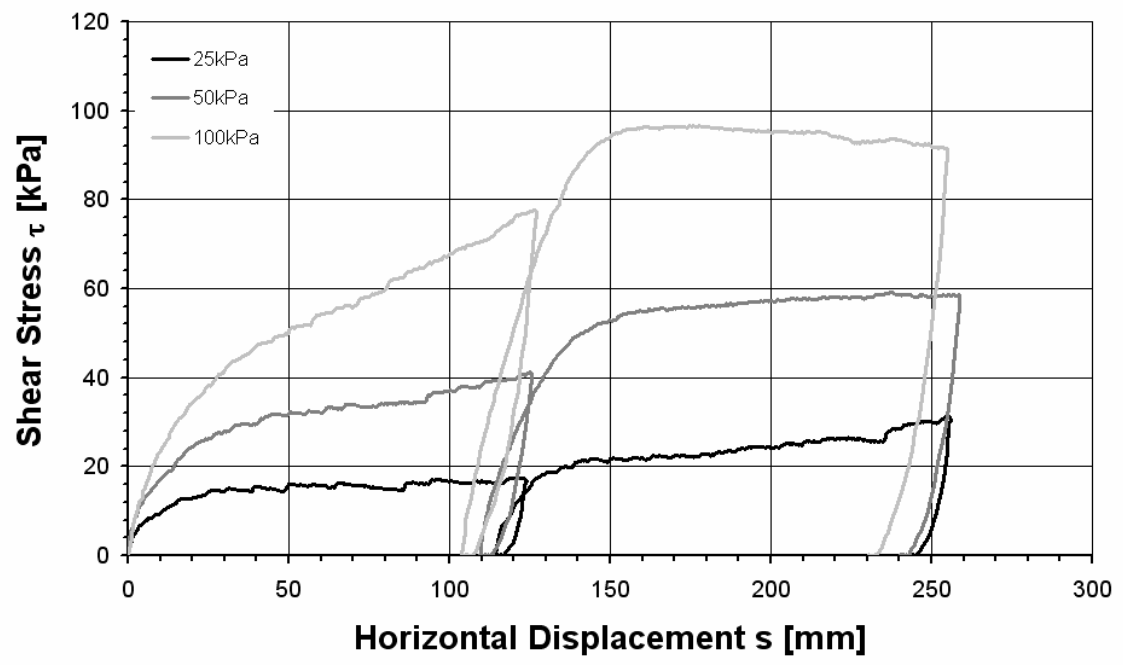

Figure 6-23 Shear-displacement curves for SW_06

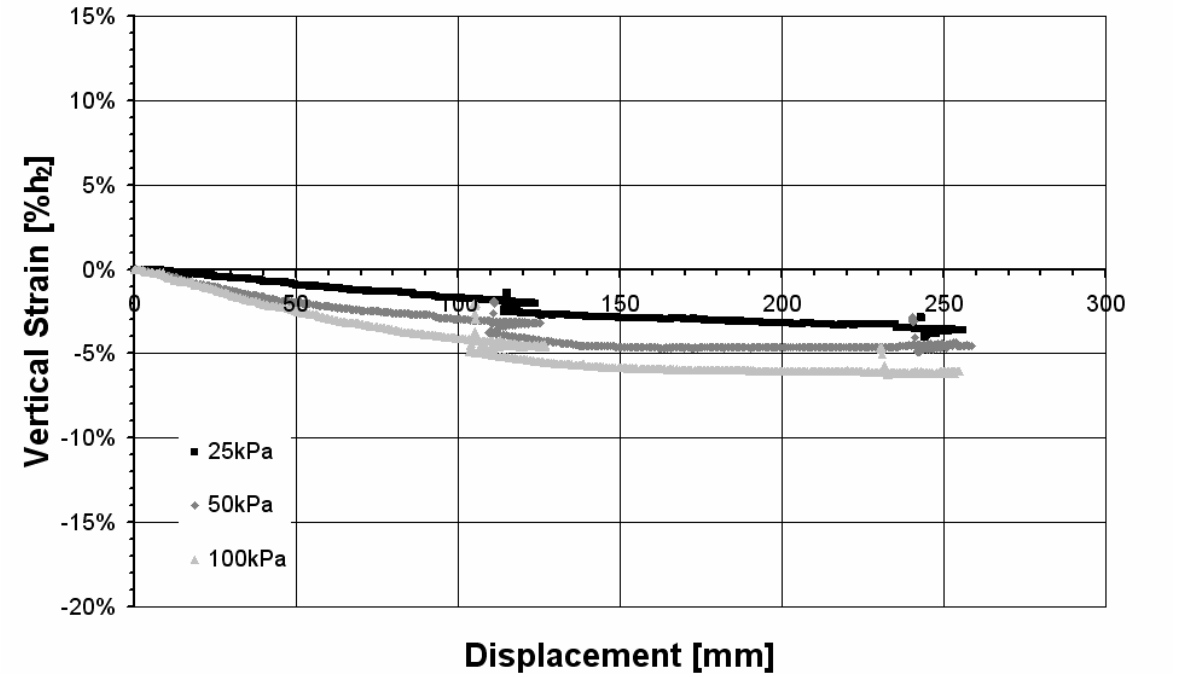

Figure 6-24 Vertical Strain over displacement of SW_06

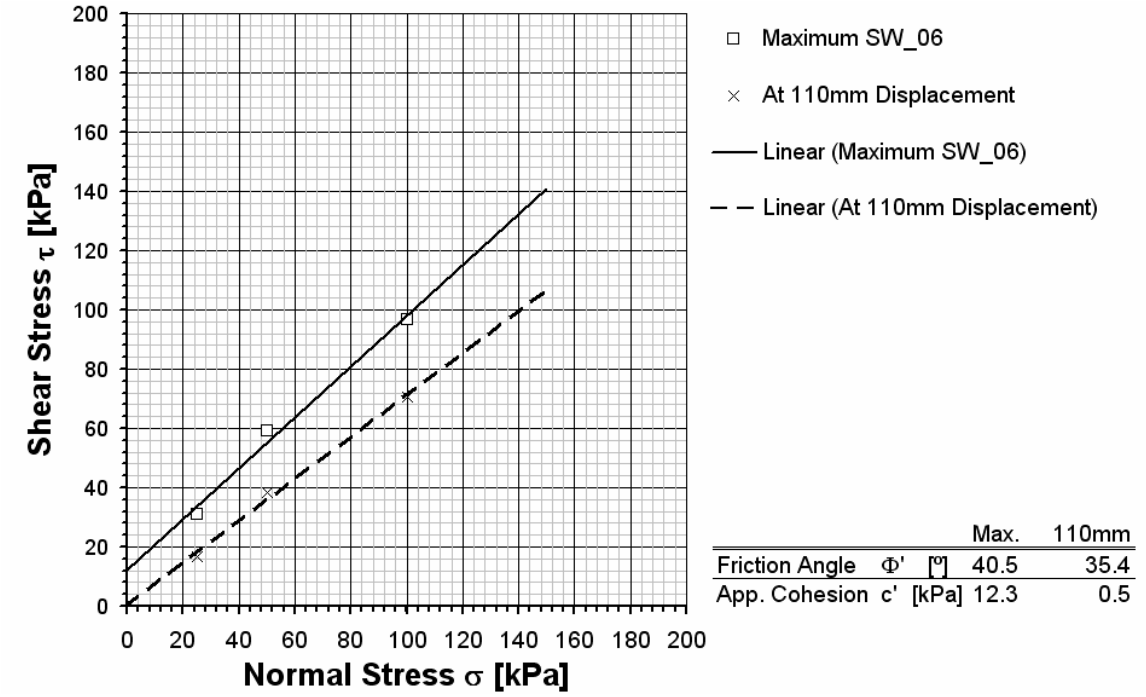

Figure 6-25 Mohr-Coulomb envelope for SW_06

Table 6-8 Shear moduli for SW_06

Normal Stress σ [kPa]	G at 1% strain [kPa]	G at 2% strain [kPa]	G at 3% strain [kPa]
25	1445	975	721
50	2579	2020	1640
100	3495	2993	2603

The test with a low normal stress revealed similar characteristics, after the loop the shear stress continued its increase. As in all tests before, the sample behaviour was contractant, as obvious from Figure 6-24, with vertical strains during the tests of 6-7% of the initial height at maximum. The maximum shear stress values produced a friction angle of 40.5° and 12.3kPa apparent cohesion. At 110mm the apparent cohesion was decreased to 0.5kPa and the friction angle drops to 35.4°. The secant shear moduli for SW_06 are presented in Table 6-6.

6.3.1.4 Composition SW_07

SW_07 also comprised a Leighton-Buzzard-sand matrix, but a higher fraction of aluminium cans and plastic packaging than SW_06. Additionally, these components were randomly placed. The initial height per test was 587mm, the input mass varied slightly. The initial unit weight ranged from 9.39kN/m^3 to 9.76kN/m^3 at 100kPa (Table 6-9).

Table 6-9 Boundary conditions for SW_07

Normal Stress σ	Input Mass	Shear rate	h_0	h_1	h_2	h_e	Unit weight γ_0	Unit weight γ_e
[kPa]	[kg]	[mm/min]	[mm]	[mm]	[mm]	[mm]	[kN/m^3]	[kN/m^3]
25	430	6.0	587	485	458	436	9.39	9.86
50	430	5.9	587	496	449	427	9.57	10.08
100	429	5.9	587	500	440	394	9.76	10.90

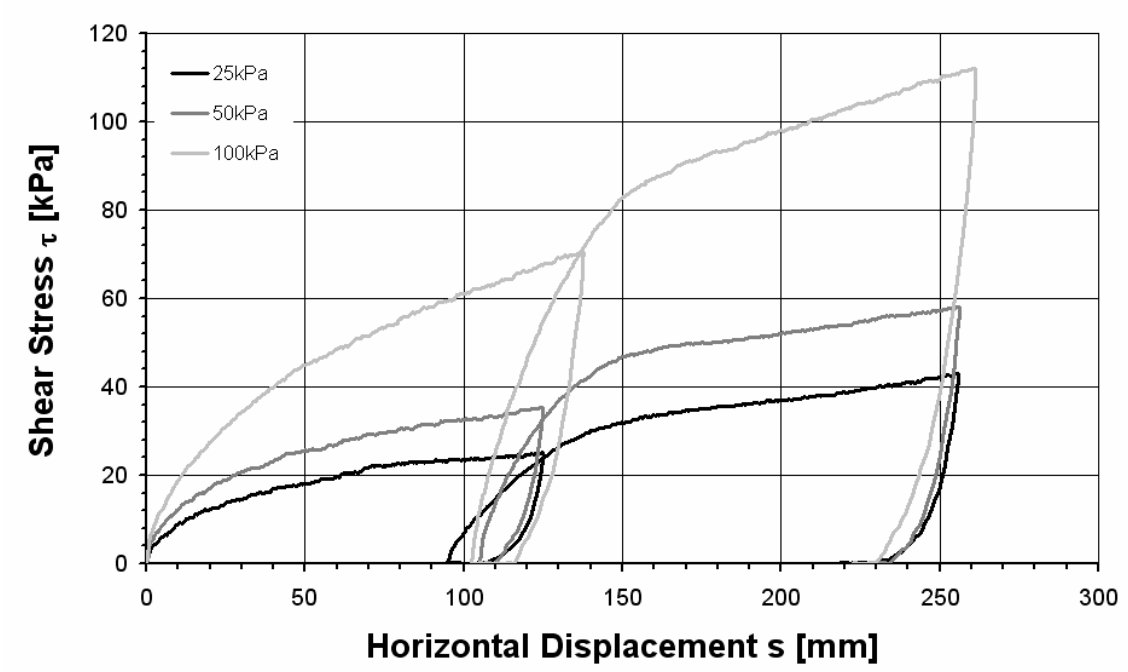

Figure 6-26 Shear – displacement curves for SW_07

Figure 6-26 demonstrates the increase of the shear stress for all three normal stresses. The curves of all three tests have a similar shape. A peak value was not observed and a

tendency towards a constant value was not noticeable either. Figure 6-27 demonstrates contractant behaviour as in all tests.

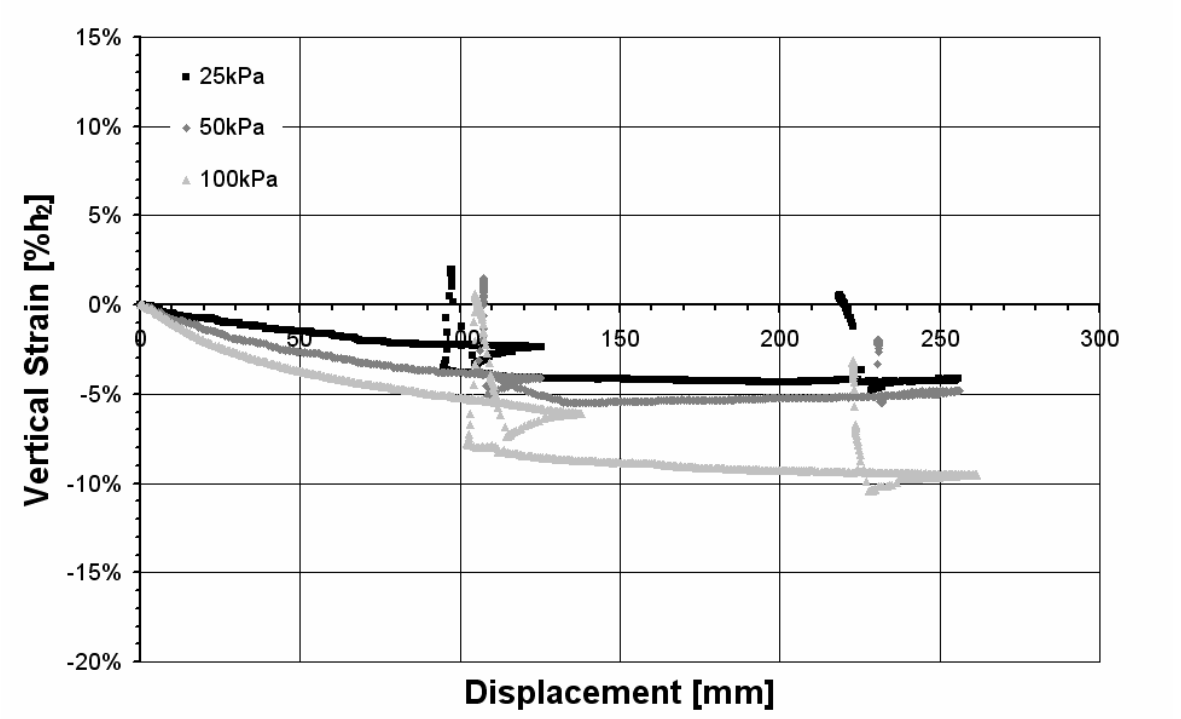

Figure 6-27 Vertical Strain over displacement of SW_07

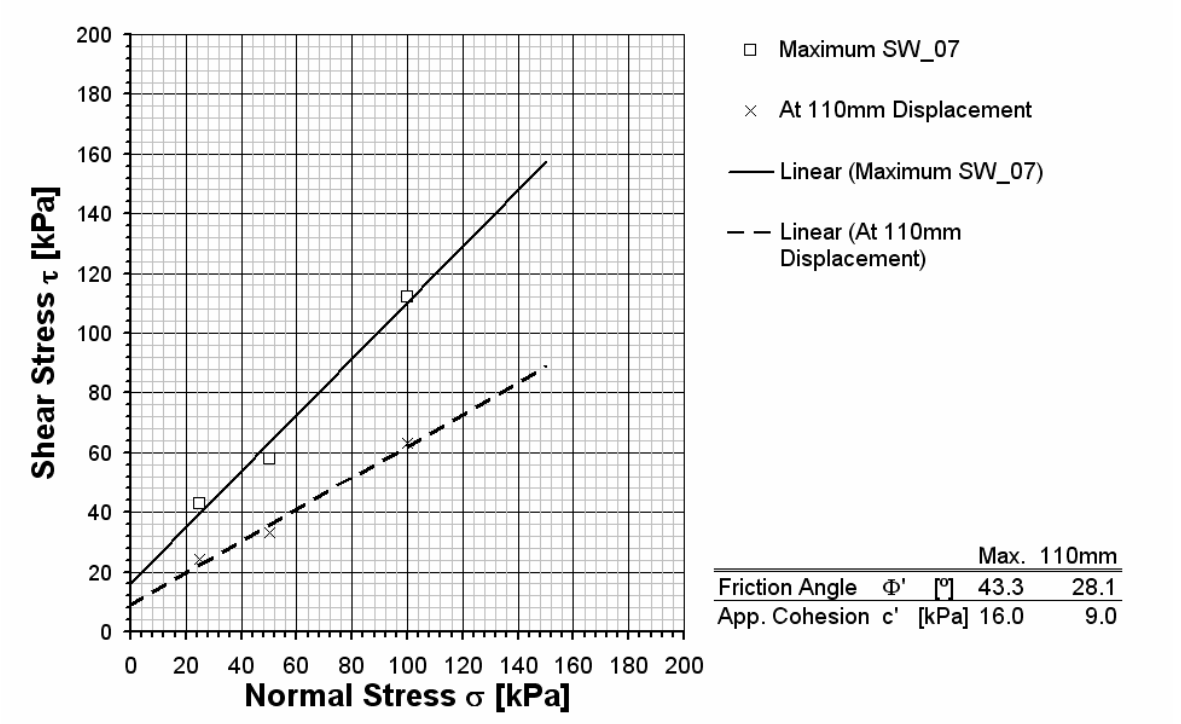

Figure 6-28 Mohr-Coulomb envelope for SW_07

The high constant increase of the shear stress led to large differences between the mobilised friction angles (Figure 6-28). For the maximum displacement the mobilised

friction angle was 43.3°. For 110mm displacement only 28.1° was reached. The mobilised apparent cohesion diverged from 16kPa at maximum to 9kPa at 110mm. The secant shear moduli for SW_07 are displayed in Table 6-13.

Table 6-10 Shear moduli for SW_07

Normal Stress σ [kPa]	G at 1% strain [kPa]	G at 2% strain [kPa]	G at 3% strain [kPa]
25	1102	900	800
50	2139	1628	1361
100	3087	2531	2210

6.3.1.5 Composition SW_08

For SW_08 the amount of plastic packaging and aluminium cans was again increased. With a lower amount of sand, the input decreased to 351kg-355kg. As a consequence, the initial unit weight only amounted for 7.02 kN/m^3 and 7.82kN/m^3, respectively. The sample height before normal stress application was in the range 715mm to 784mm.

Table 6-11 Boundary conditions for SW_08

Normal Stress σ [kPa]	Input Mass [kg]	Shear rate [mm/min]	h_0 [mm]	h_1 [mm]	h_2 [mm]	h_e [mm]	Unit weight γ_0 [kN/m^3]	Unit weight γ_e [kN/m^3]
25	351	5.8	718	458	501	483	7.02	7.07
50	355	5.9	784	519	506	482	7.02	7.36
100	354	6.0	715	497	452	406	7.82	8.71

Similar to SW_07, the curves in Figure 6-29 show that the shear stress gradually increased with increasing displacement. A peak value was not observed. In comparison to SW_07 the gradient of the curves was lower. The low normal stress curve tended to flatten at the end of the observation. This test showed also a contractant behaviour (Figure 6-30).

The Mohr-Coulomb envelope in Figure 6-31 exhibited considerably lower values than SW_07. For the maximum displacement, a friction angle of 36.4° and an apparent cohesion of 15kPa were gained. A similar apparent cohesion c' (14.4kPa) for 110mm displacement was found. The friction angle of 20.3° resulted in a considerably lower value. Secant shear moduli calculated from the unload-reload loop at three strain levels are displayed in Table 6-10. The shear moduli for the normal stress levels are shown in Table 6-12.

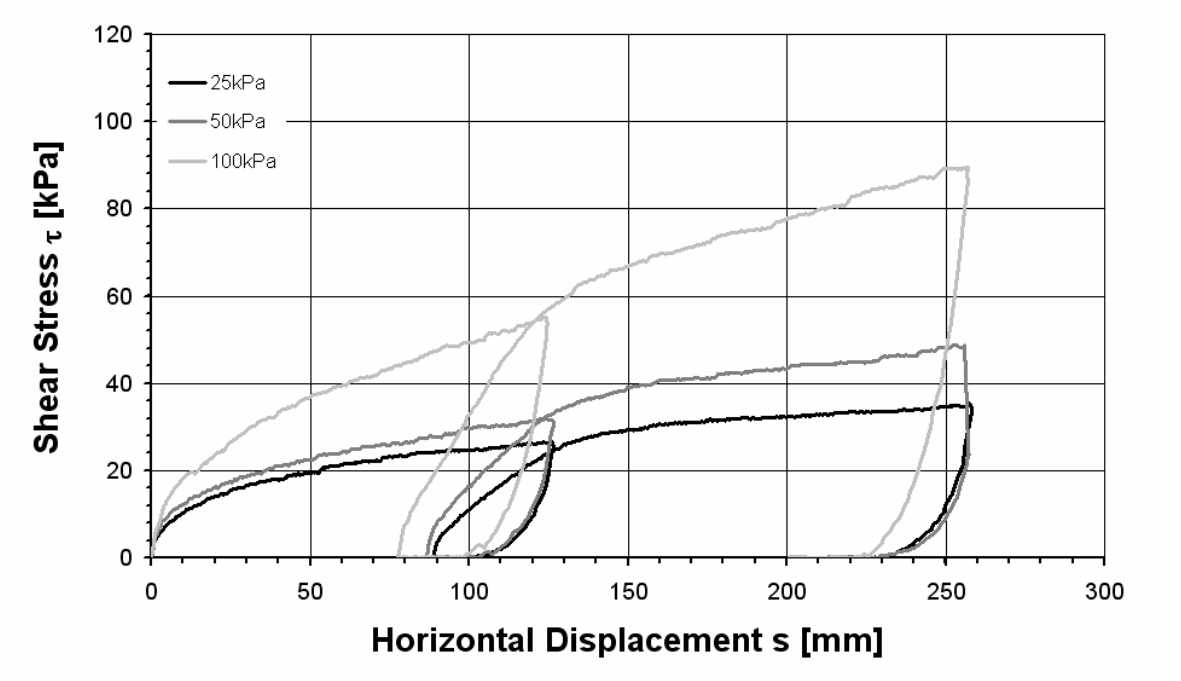

Figure 6-29 Shear – displacement curves for SW_08

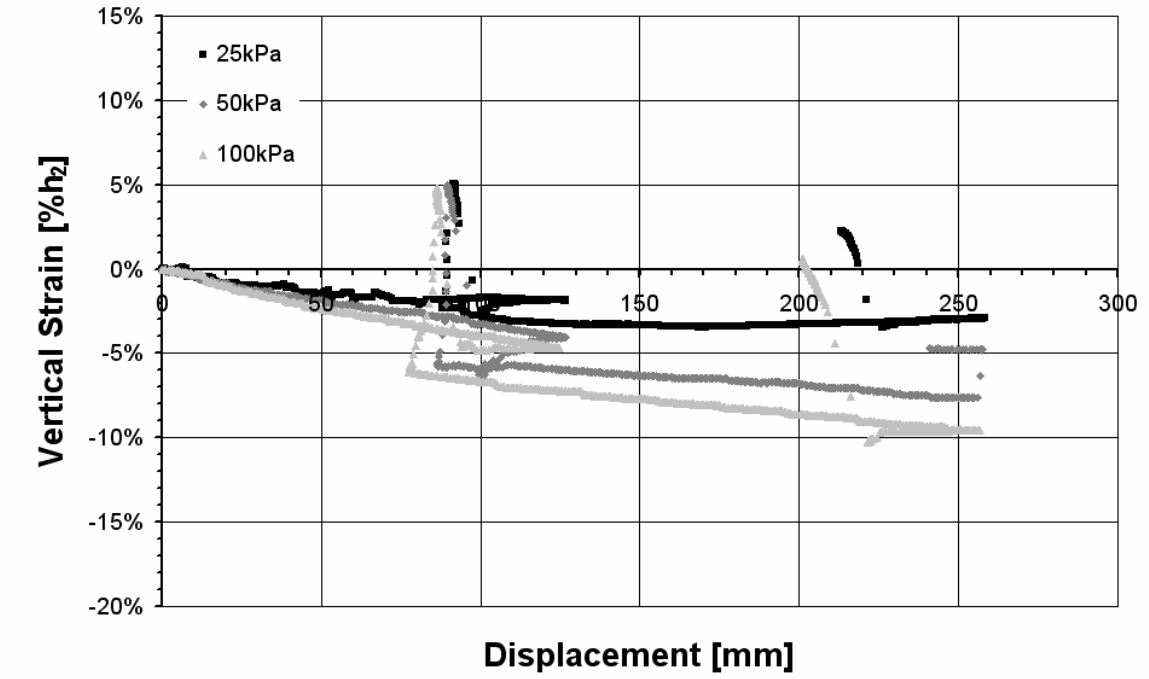

Figure 6-30 Vertical Strain over displacement of SW_08

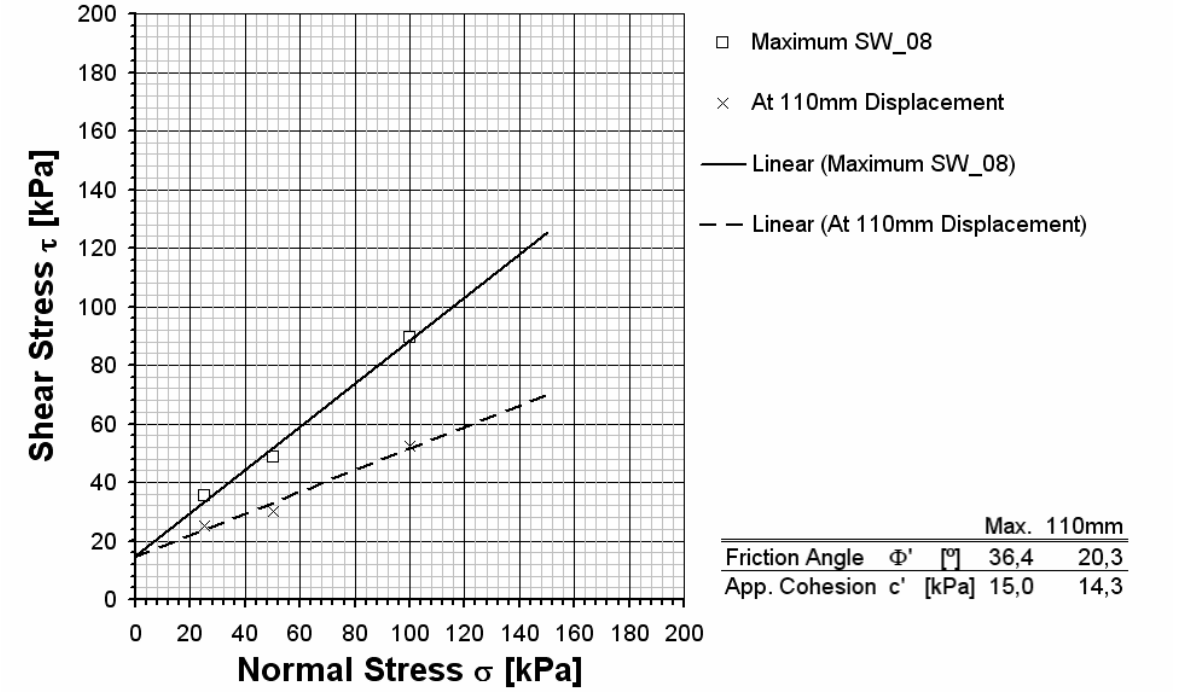

Figure 6-31 Mohr-Coulomb envelope for SW_08

Table 6-12 Shear moduli for SW_08

Normal Stress σ [kPa]	G at 1% strain [kPa]	G at 2% strain [kPa]	G at 3% strain [kPa]
25	1016	803	707
50	1377	1059	910
100	1734	1501	1412

6.3.2 Compressible Compositions

6.3.2.1 Composition SW_02

Table 6-13 Boundary conditions for SW_02

Normal Stress σ [kPa]	Input Mass [kg]	Shear rate [mm/min]	h_0 [mm]	h_1 [mm]	h_2 [mm]	h_e [mm]	Unit weight γ_0 [kN/m^3]	Unit weight γ_e [kN/m^3]
25	29	5.8	1244	209	394	381	0.74	0.76
50	38	5.9	737	342	344	311	0.85	1.21
75	38	6.0	544	319	267	236	1.41	1.51

The compressible compositions generally consisted of large amounts of paper, rigid and flexible plastic packaging and aluminium cans. With these components, a large volume

but a low mass was involved, as stated in Table 6-13. The input was 29kg and 38kg, respectively, and the initial (theoretical) height of the uncompacted sample exceeded 1000mm. As the shear box has a maximum height of 800mm, which was also reduced to 700mm by a spacer, it should be mentioned that the sample was placed in layers and compacted, as described in chapter 3.6.4.

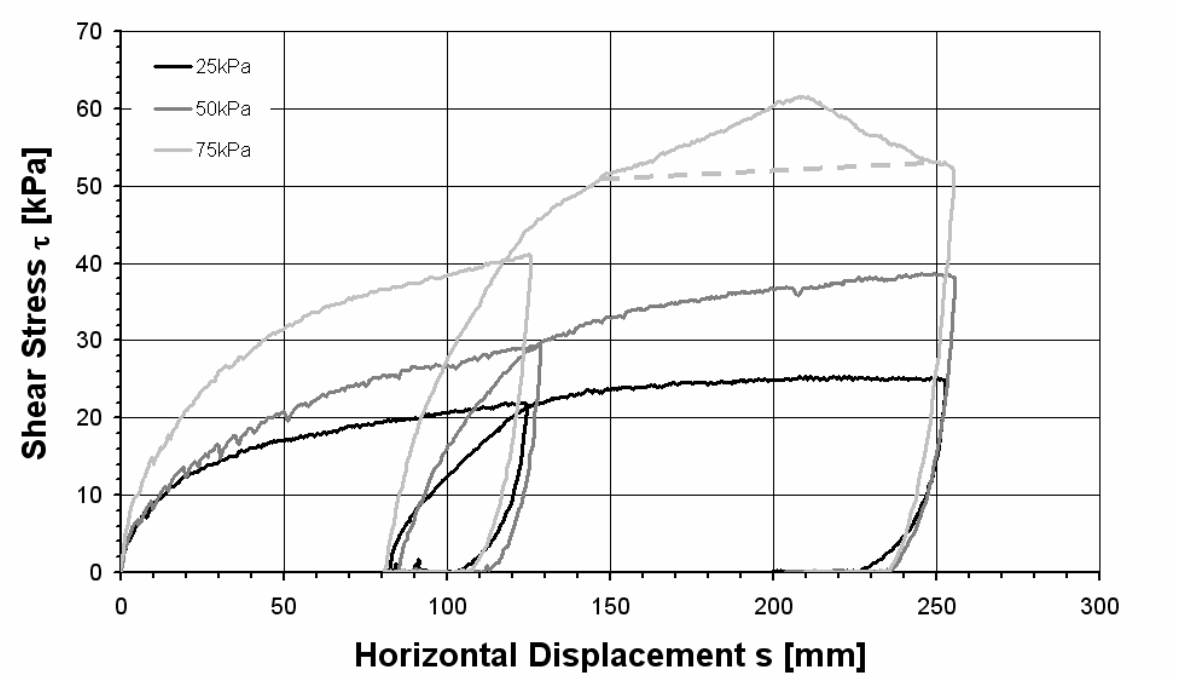

Figure 6-32 Shear – displacement curves for SW_02

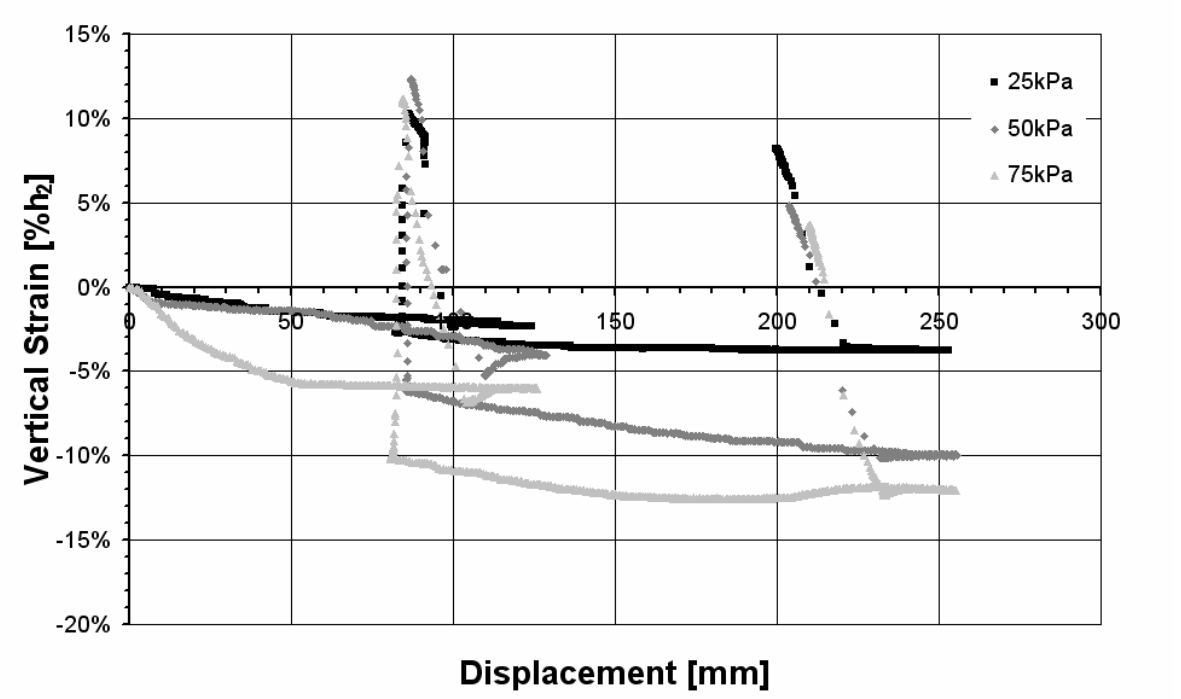

Figure 6-33 Vertical Strain over displacement of SW_02

Figure 6-32 shows the shear stress curves for SW_02. The shapes of these curves differ from those seen before. A high increase of the shear stress in the first 25-50mm displacement was visible, which was then reduced to a lower rate of increase. An actual peak value was not observed. The peak the 75kPa test exhibited was a result of components jammed between a rib of the load transmission plate and the edge of the bottom box. The ribs were welded to the load transmission plate at 200mm spacings and ran perpendicular to the direction of shearing. As the displacement for the peak for 75kPa corresponded to 200mm, and the sample height was low, a component could be easily jammed, this was assumed to be the reason and it was also confirmed by the observation of the sample after shearing (Figure 11-6). Consequently, for the Mohr-Coulomb envelope at maximum shear stress a value at maximum displacement was considered. Figure 6-33 demonstrates the contractant behaviour of SW_02 with large vertical strains of up to 13%h_2.

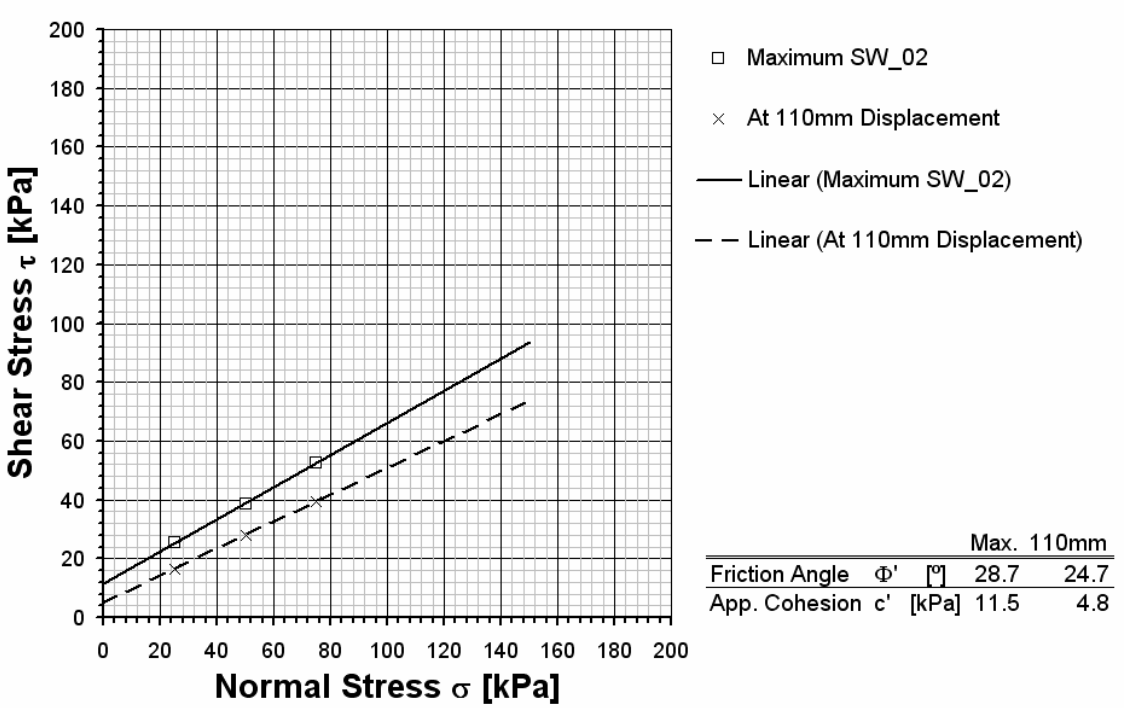

Figure 6-34 Mohr-Coulomb envelope for SW_02

Table 6-14 Shear moduli for SW_02

Normal Stress σ [kPa]	G at 1% strain [kPa]	G at 2% strain [kPa]	G at 3% strain [kPa]
25	973	647	575
50	1302	957	827
75	1824	1406	1191

The Mohr-Coulomb envelope provided low friction angles in comparison to the tests conducted on low compressible materials. At maximum displacement the mobilised

friction angle amounted for 28.7°, at 110mm displacement the mobilised friction angle is 24.7°. The mobilised apparent cohesion represented 11.5kPa (maximum) and 4.8kPa, respectively at 110mm. The secant shear moduli of SW_02 presented in Table 6-14 resulted in considerably lower values as observed before.

6.3.2.2 Composition SW_03

Table 6-15 Boundary conditions for SW_03

Normal Stress σ [kPa]	Input Mass [kg]	Shear rate [mm/min]	h_0 [mm]	h_1 [mm]	h_2 [mm]	h_e [mm]	Unit weight γ_0 [kN/m^3]	Unit weight γ_e [kN/m^3]
25	67	5.9	654	351	376	353	1.77	1.89
50	67	5.9	489	328	326	295	2.04	2.26
75	79	6.0	662	366	311	267	2.54	2.96

SW_03 possessed a high mass ratio of incompressible components. The volume was dominated by compressible components like cans and paper, leading to a low initial unit weight of 1.77kN/m^3 to 2.54kN/m^3. As more material was put into the 75kPa test, the input mass was accordingly higher (Table 6-15).

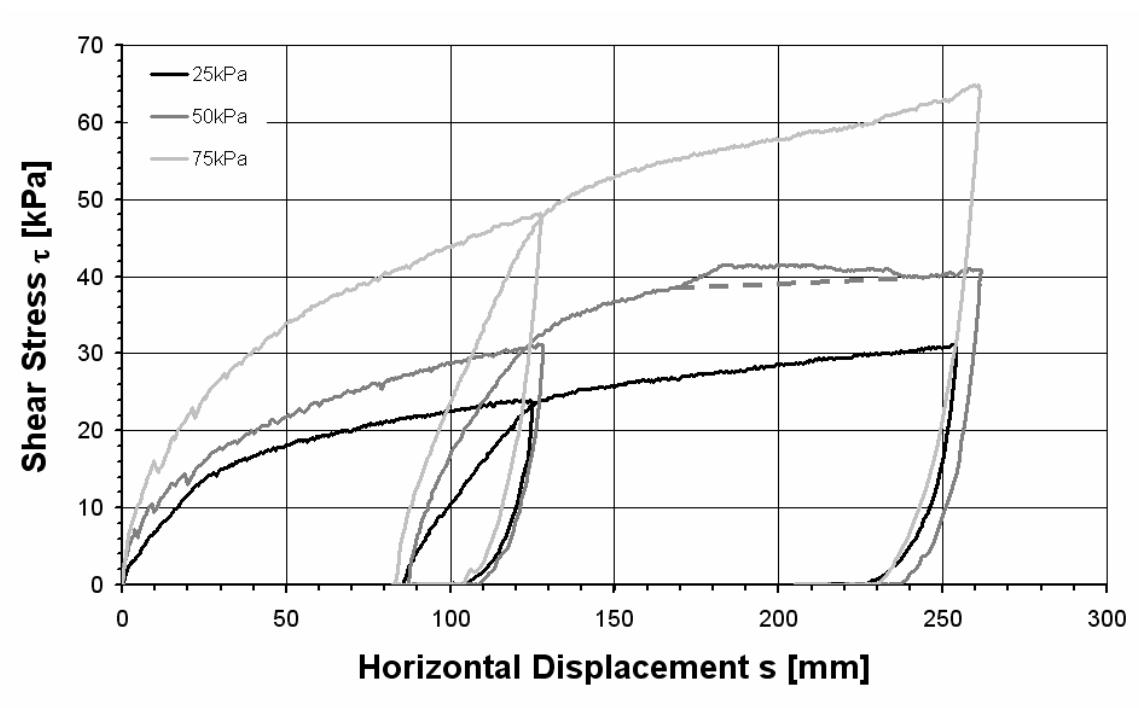

Figure 6-35 Shear – displacement curves for SW_03

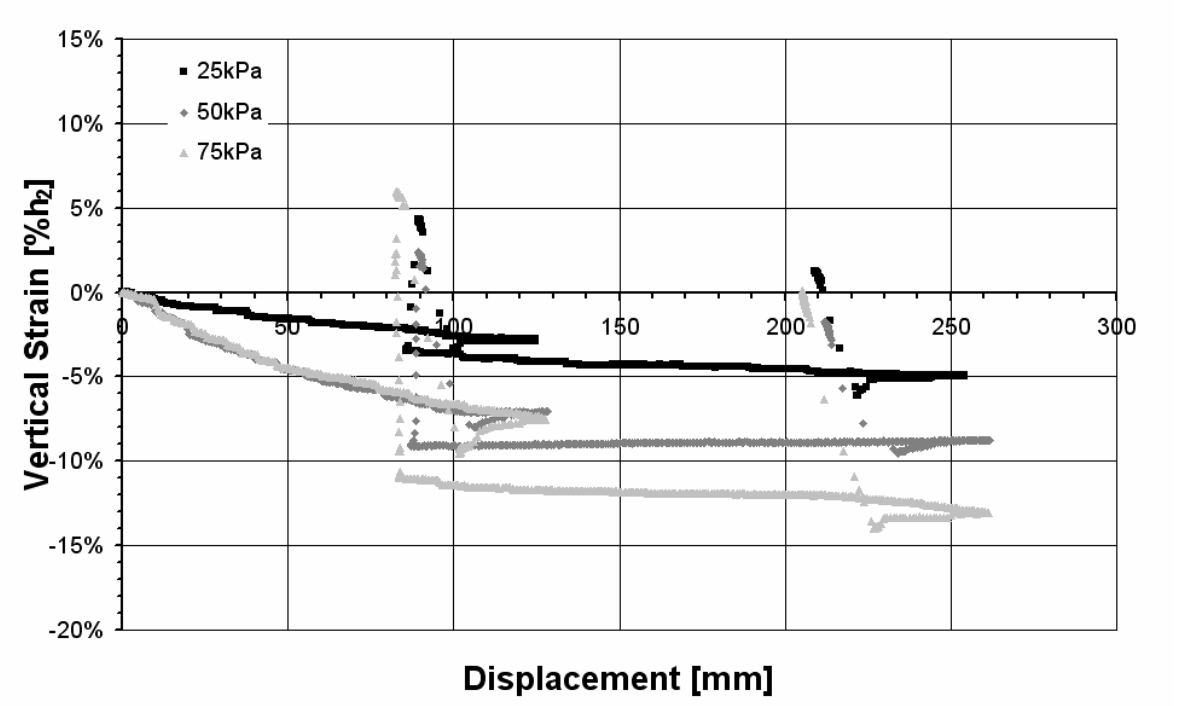

Figure 6-36 Vertical Strain over displacement of SW_03

The shear stress curves in Figure 6-35 exhibit a smooth increase of shear stress with displacement with the exception of the 50kPa test, where it was assumed that components were again jammed between load transmission rib and bottom box edge. Peak values were not observed.

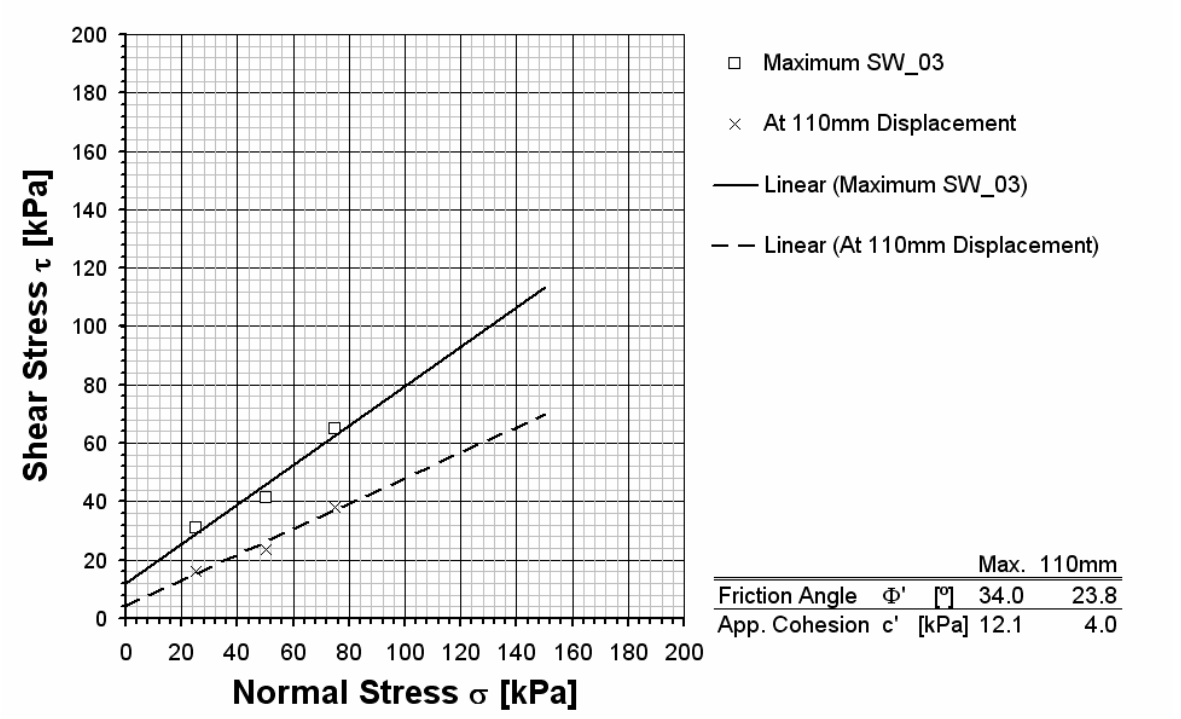

Figure 6-37 Mohr-Coulomb envelope for SW_03

Mobilised friction angle and apparent cohesion for maximum displacement in Figure 6-37 were slightly higher, while these values at 110mm displacement were somewhat smaller than in composition SW_02. For both displacements the test on 50kPa normal stress resulted in low values, which did not exactly fit to the assumed linear Mohr-Coulomb envelope. Table 6-16 shows the secant shear moduli calculated for SW_03.

Table 6-16 Shear moduli for SW_03

Normal Stress σ [kPa]	G at 1% strain [kPa]	G at 2% strain [kPa]	G at 3% strain [kPa]
25	839	685	643
50	1452	1091	928
75	1695	1358	1220

6.3.3 Mono-Component Compositions

6.3.3.1 Composition SW_04

Composition SW_04 consisted of a large amount (approximately 50mass-%) of aluminium cans resulting in an initial unit weight of 1.03kN/m^3 to 1.49kN/m^3 at sample heights ranging from 572mm to 602mm. The sample mass for the last test of the set increased from 42kg to 46kg.

Table 6-17 Boundary conditions for SW_04

Normal Stress σ [kPa]	Input Mass [kg]	Shear rate [mm/min]	h_0 [mm]	h_1 [mm]	h_2 [mm]	h_e [mm]	Unit weight γ_0 [kN/m^3]	Unit weight γ_e [kN/m^3]
25	42	5.8	604	407	407	382	1.03	1.10
50	42	5.9	572	347	347	311	1.21	1.35
75	46	6.0	604	359	309	270	1.49	1.70

The shape of the shear stress-displacement curves in Figure 6-38 exhibits a rapid increase for a normal stress of 25kPa and 50kPa and a subsequent slowly increasing straight linear relationship. The shear stress after the unload-reload loop showed good accordance to the final stress level before the loop. For 75kPa normal stress, it was difficult to maintain a constant normal stress. It had to be re-adjusted considerably during the test, as obvious from Figure 6-38. The curve is correspondingly characterised by fluctuations.

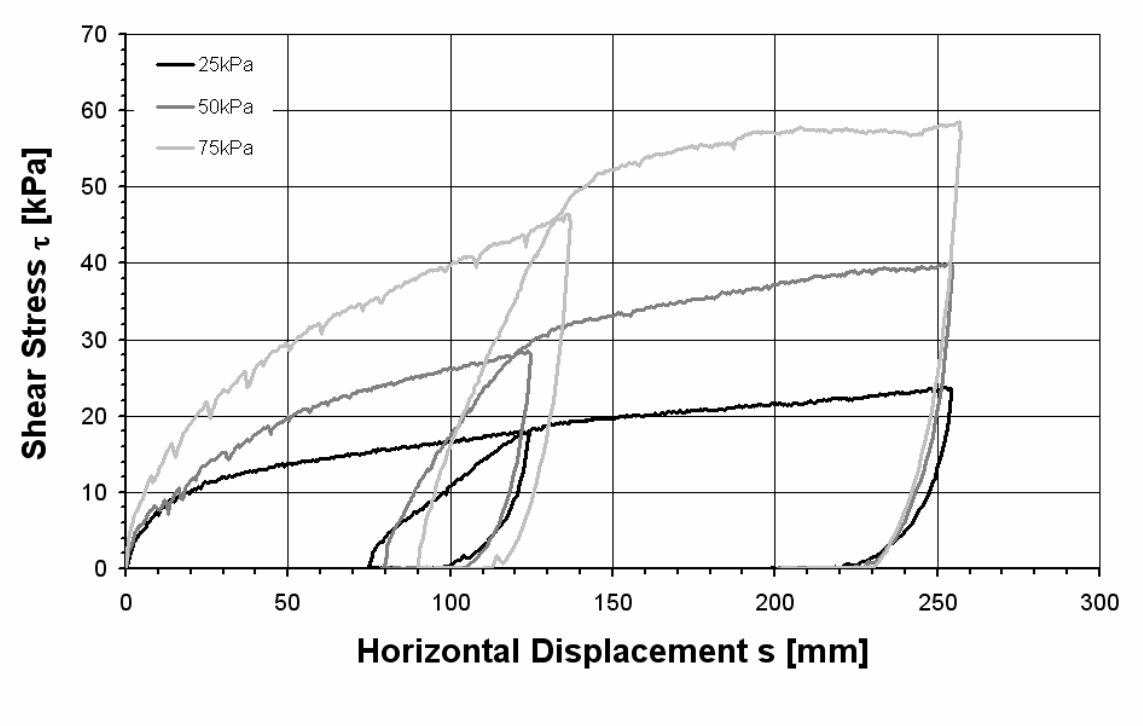

Figure 6-38 Shear-displacement curves for SW_04

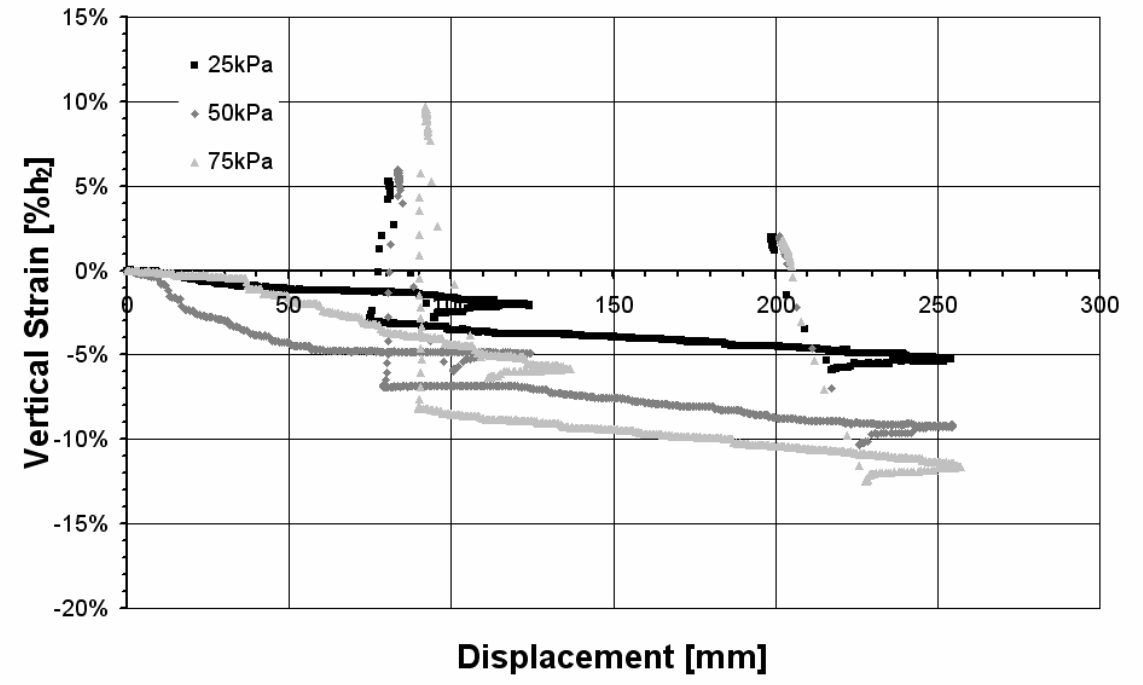

Figure 6-39 Vertical strain over displacement of SW_04

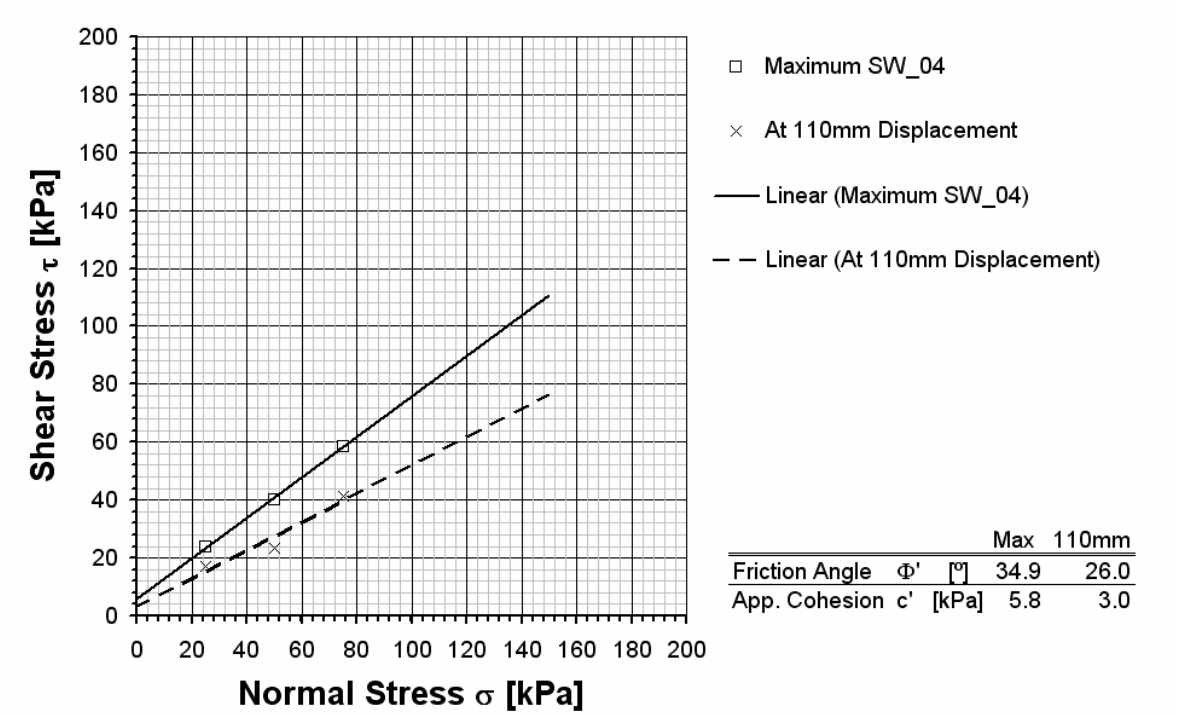

Figure 6-40 Mohr-Coulomb envelope for SW_04

This composition provided low mobilised apparent cohesion values (5.8kPa for the maximum and 3.0 for 110mm displacement). The mobilised friction angle varied between 34.9° at maximum and 26.0°. The strain-dependent secant shear moduli are presented in Table 6-18.

Table 6-18 Shear moduli for SW_04

Normal Stress σ [kPa]	G at 1% strain [kPa]	G at 2% strain [kPa]	G at 3% strain [kPa]
25	624	449	414
50	1023	855	767
75	1620	1309	1173

6.3.3.2 Composition SW_05

Table 6-19 Boundary conditions for SW_05

Normal Stress σ [kPa]	Input Mass [kg]	Shear rate [mm/min]	h_0 [mm]	h_1 [mm]	h_2 [mm]	h_e [mm]	Unit weight γ_0 [kN/m^3]	Unit weight γ_e [kN/m^3]
25	35	5.9	757	419	413	387	0.85	0.90
50	35	5.9	604	422	349	298	1.00	1.18
75	37	5.9	609	425	312	269	1.18	1.38

Increasing the amount of aluminium cans in comparison to SW_04 and taking out incompressible components like the brick fraction resulted in large sample heights of 604-757mm and low unit weights of 0.85-1.18kN/m^3. The input mass was increased for the highest normal stress (Table 6-19).

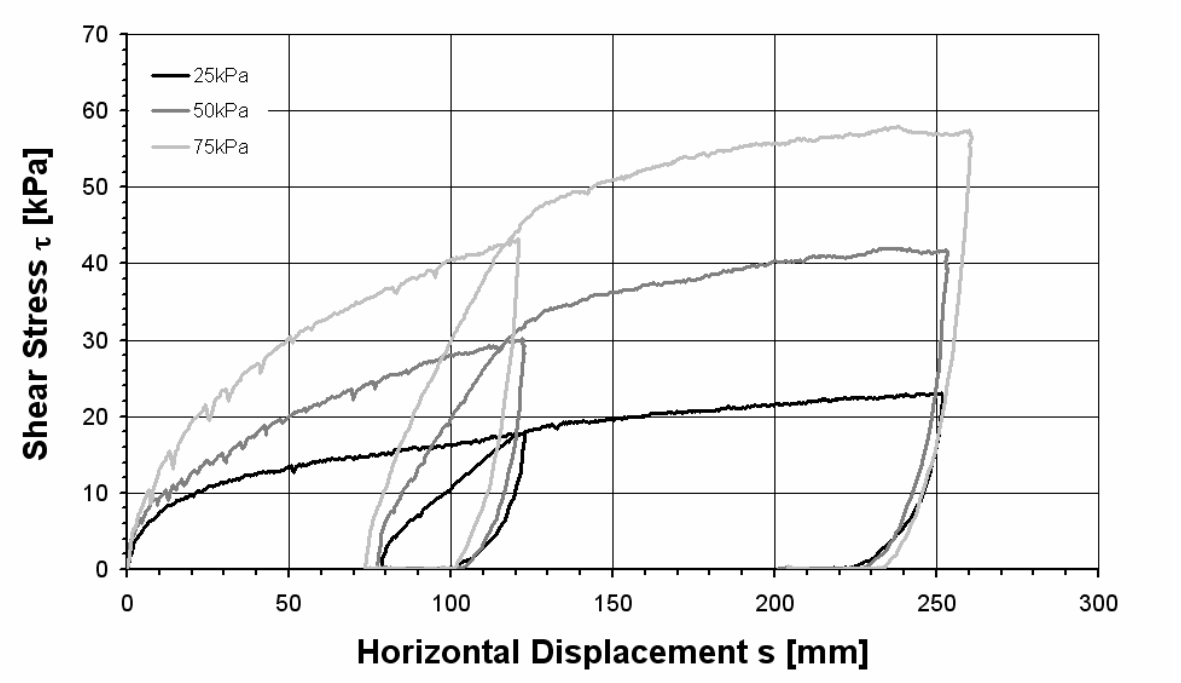

Figure 6-41 Shear – displacement curves for SW_05

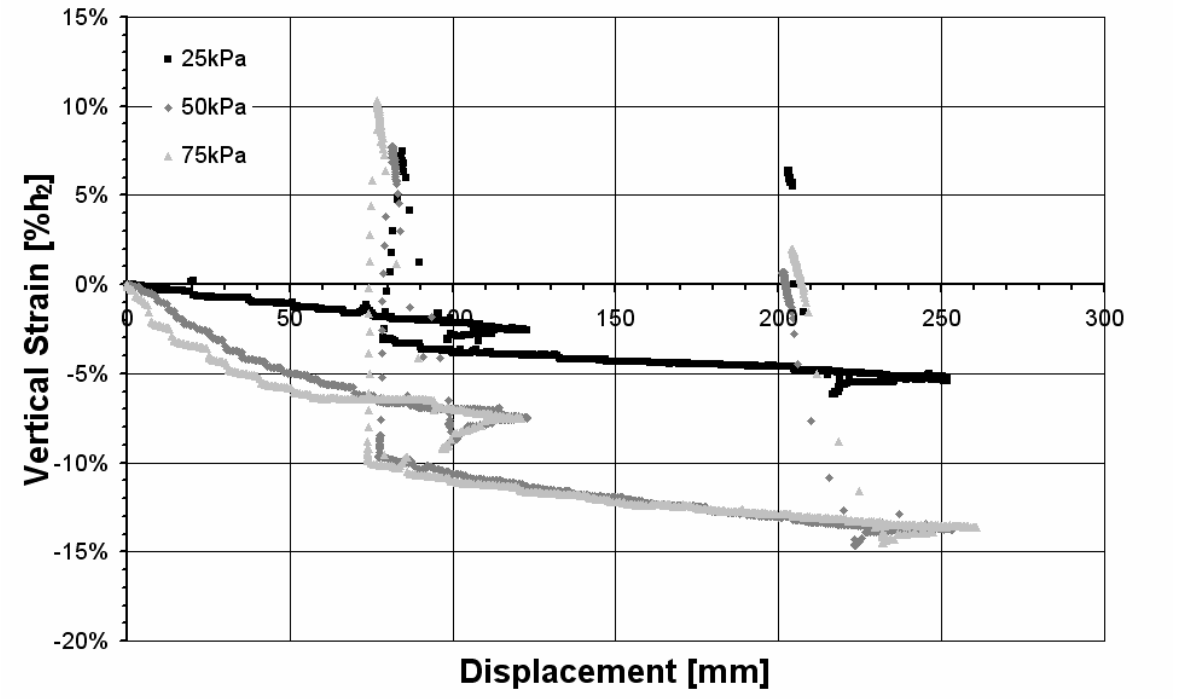

Figure 6-42 Vertical Strain over displacement of SW_05

SW_05 resulted in similar values for shear stress as SW_04. Also, the shape of the test on 25kPa normal stress was almost identical (e.g. considering shear stress of 20kPa at 150mm displacement and the shape of the unload-reload loop). Additionally, the tests on 50 and 75kPa normal stress resulted in values similar to SW_04 (Figure 6-41).

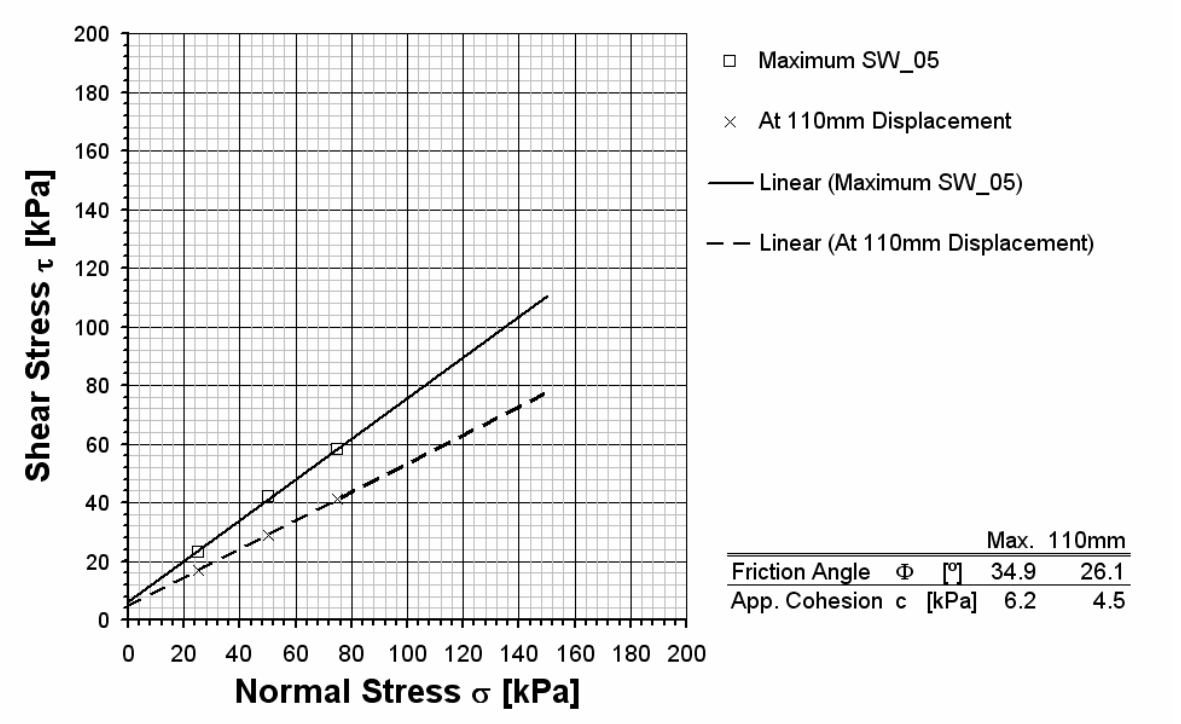

Figure 6-43 Mohr-Coulomb envelope for SW_05

The vertical strain in Figure 6-42 shows contractant behaviour. Generally, a higher vertical strain is obvious for SW_05 in comparison to SW_04. In this test set, vertical strain for 50kPa and 75kPa normal stresses was very alike with a maximum strain of 13%h_2. The friction angles depicted in Figure 6-43 were nearly identical to those of composition SW_04 for both maximum and 110mm displacement. Apparent cohesion was fractionally smaller than those of the precedent composition. Table 6-20 indicates the secant shear moduli for this test. The moduli are slightly smaller than those for the preceding test with less aluminium cans.

Table 6-20 Shear moduli for SW_05

Normal Stress σ [kPa]	G at 1% strain [kPa]	G at 2% strain [kPa]	G at 3% strain [kPa]
25	683	508	460
50	1151	914	813
75	1545	1239	1091

6.3.4 Simulation of a Real Waste Composition

Composition SW_09 was formed by a large amount of compressible material and thus a similar result to the compressible composition presented above was expected. With input masses of 65kg for 25kPa, 87kg for 50kPa and 108kg for 75kPa normal stress and initial shear heights of approximately 300mm, the initial unit weights were 2.20, 2.88 and 3.58kN/m^3.

Table 6-21 Boundary conditions for SW_09

Normal Stress σ [kPa]	Input Mass [kg]	Shear rate [mm/min]	h_0 [mm]	h_1 [mm]	h_2 [mm]	h_e [mm]	Unit weight γ_0 [kN/m^3]	Unit weight γ_e [kN/m^3]
25	65	6.0	578	264	296	291	2.20	2.23
50	87	6.0	594	306	301	274	2.88	3.16
75	108	6.0	595	347	303	272	3.58	3.99

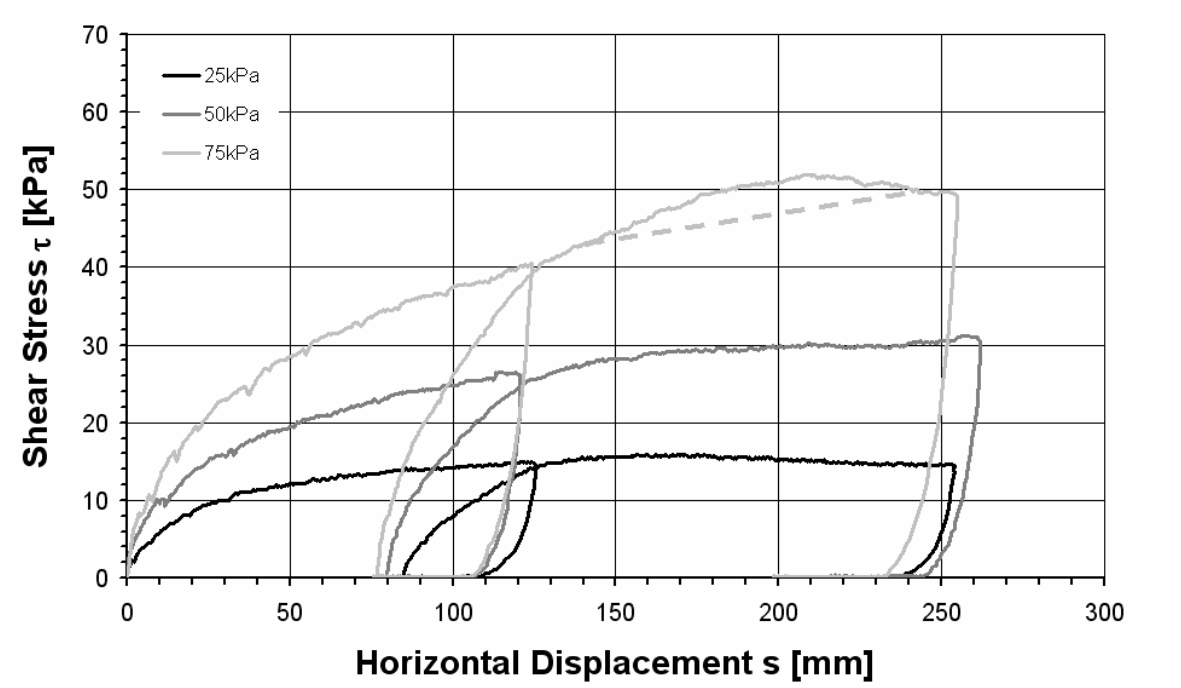

Figure 6-44 Shear – displacement curves for SW_09

Figure 6-44 demonstrates low shear stress values. The curves tended to flatten off at the end of the test. The test with the lowest normal stress exhibited a flattening and a “peak” values was observed. Nevertheless, this value should be interpreted as a constant value. This was again confirmed by the contractant behaviour shown in Figure 6-45. For a normal stress of 75kPa a peak was visible, but as it was again located in the area of 200mm displacement, it was not found to be a “true” peak, but to be a result from jammed components due to a low sample height.

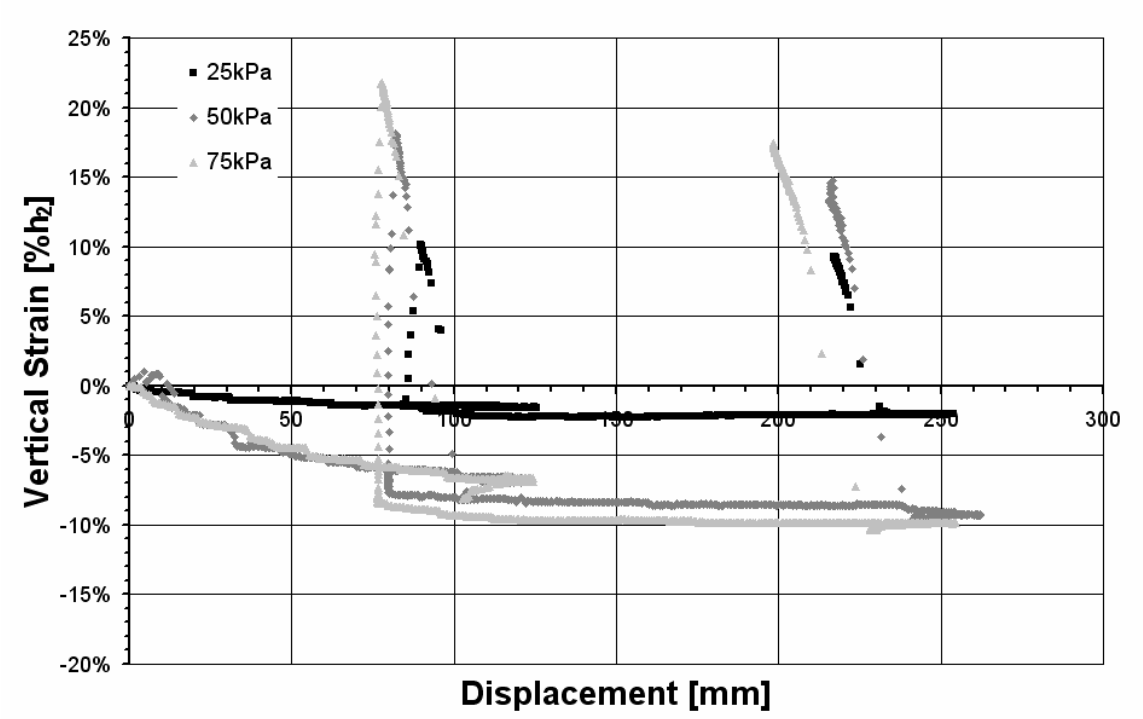

Figure 6-45 Vertical Strain over displacement of SW_09

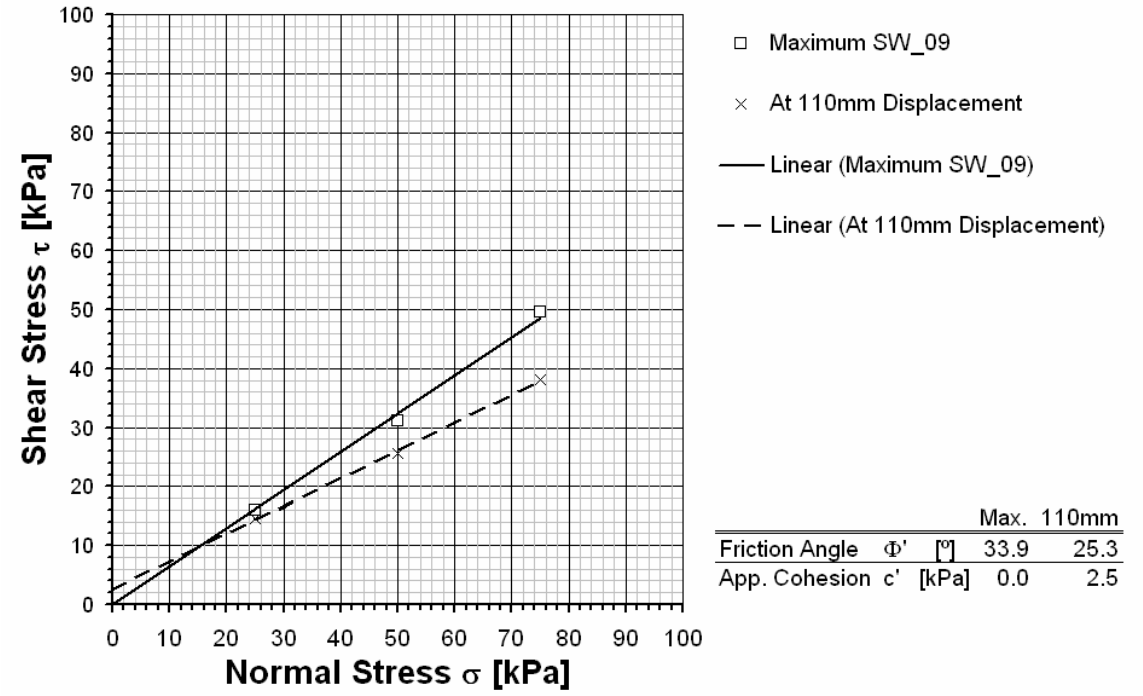

Figure 6-46 Mohr-Coulomb envelope for SW_09

For maximum displacement, the Mohr-Coulomb envelope in Figure 6-46 resulted in a friction angle of 33.9° and as the apparent cohesion resulted in a negative value it was assumed to be zero. At 110mm displacement, the friction angle decreased to 25.3° and the apparent cohesion resulted in 2.5kPa. The secant shear moduli for SW_09 are shown in Table 6-22.

Table 6-22 Shear moduli for SW_09

Normal Stress σ [kPa]	G at 1% strain [kPa]	G at 2% strain [kPa]	G at 3% strain [kPa]
25	657	465	403
50	1108	833	691
75	1620	1191	1005

6.4 Shifting of Components within Shape-Related Subgroups after Shearing

After shearing compositions SW_02, SW_03, SW_04, SW_05 and SW_09, the sample material used in the test was examined and sorted. The results from the sorting analysis are shown in the following figures.

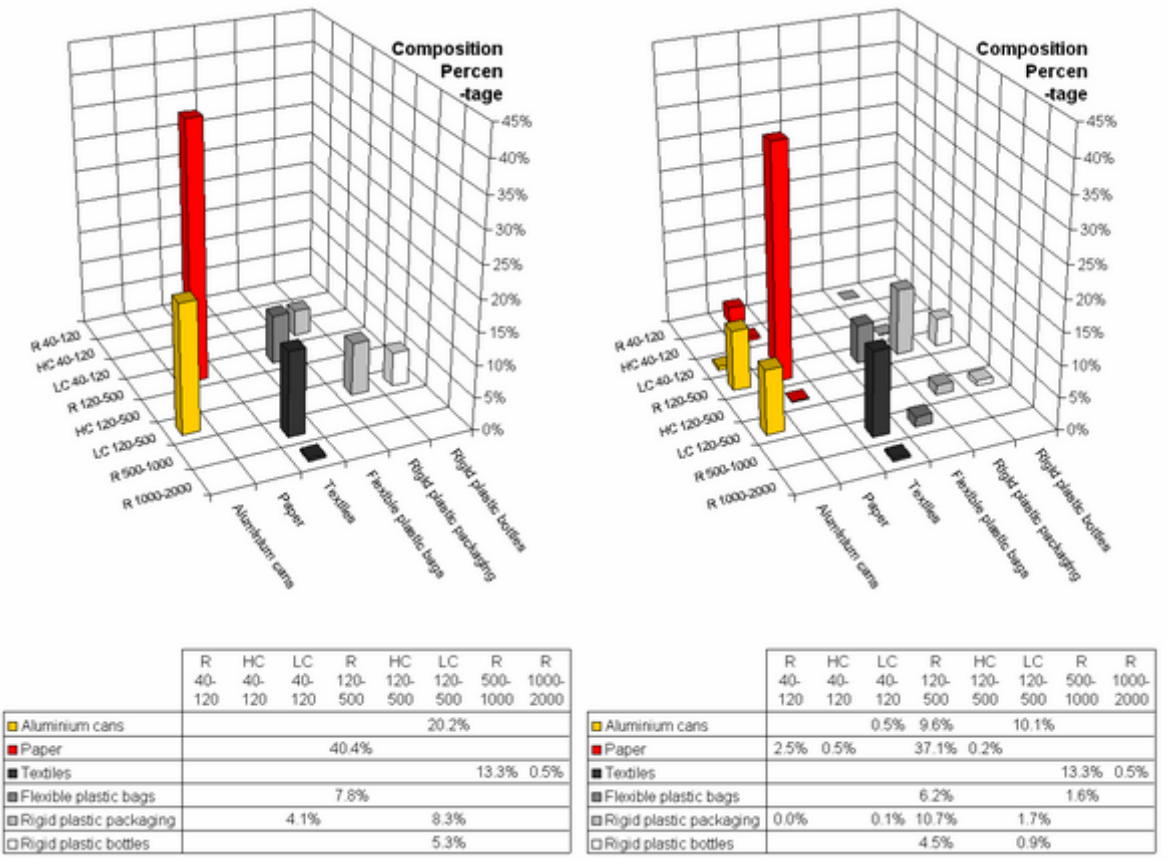

	R 40-120	HC 40-120	LC 40-120	R 120-500	HC 120-500	LC 120-500	R 500-1000	R 1000-2000
Aluminium cans						20.2%		
Paper				40.4%				
Textiles							13.3%	0.5%
Flexible plastic bags				7.8%				
Rigid plastic packaging			4.1%			8.3%		
Rigid plastic bottles						5.3%		

	R 40-120	HC 40-120	LC 40-120	R 120-500	HC 120-500	LC 120-500	R 500-1000	R 1000-2000
Aluminium cans			0.5%	9.6%		10.1%		
Paper	2.5%	0.5%		37.1%	0.2%			
Textiles							13.3%	0.5%
Flexible plastic bags				6.2%			1.6%	
Rigid plastic packaging	0.0%		0.1%	10.7%		1.7%		
Rigid plastic bottles				4.5%		0.9%		

Figure 6-47 Input and output of shear test SW_02

In Figure 6-47 the input and output distributions for SW_02 are demonstrated. The majority of plastic bottles were flattened, so that they shifted from low compressible to reinforcing. A similar behaviour was observed for rigid plastic packaging. Additionally, plastic packaging altered into low compressible and reinforcing components within the size range 40-120mm. Reinforcing flexible plastics were apparently stretched and “unfolded” through shearing and thus reached a size range of 500-1000mm. The paper

input was initially only present in the size range 120-500mm and had a reinforcing function. In the output, low compressible paper in the size range of 40-120mm was present and for both size ranges parts of the paper had also a high compressible character. Textiles remained in its size range and did not alter shape-related subdivision. Originally low compressible aluminium cans were approximately halved into reinforcing and low compressible. A small percentage was shifted to 40-120mm although keeping the low compressible character.

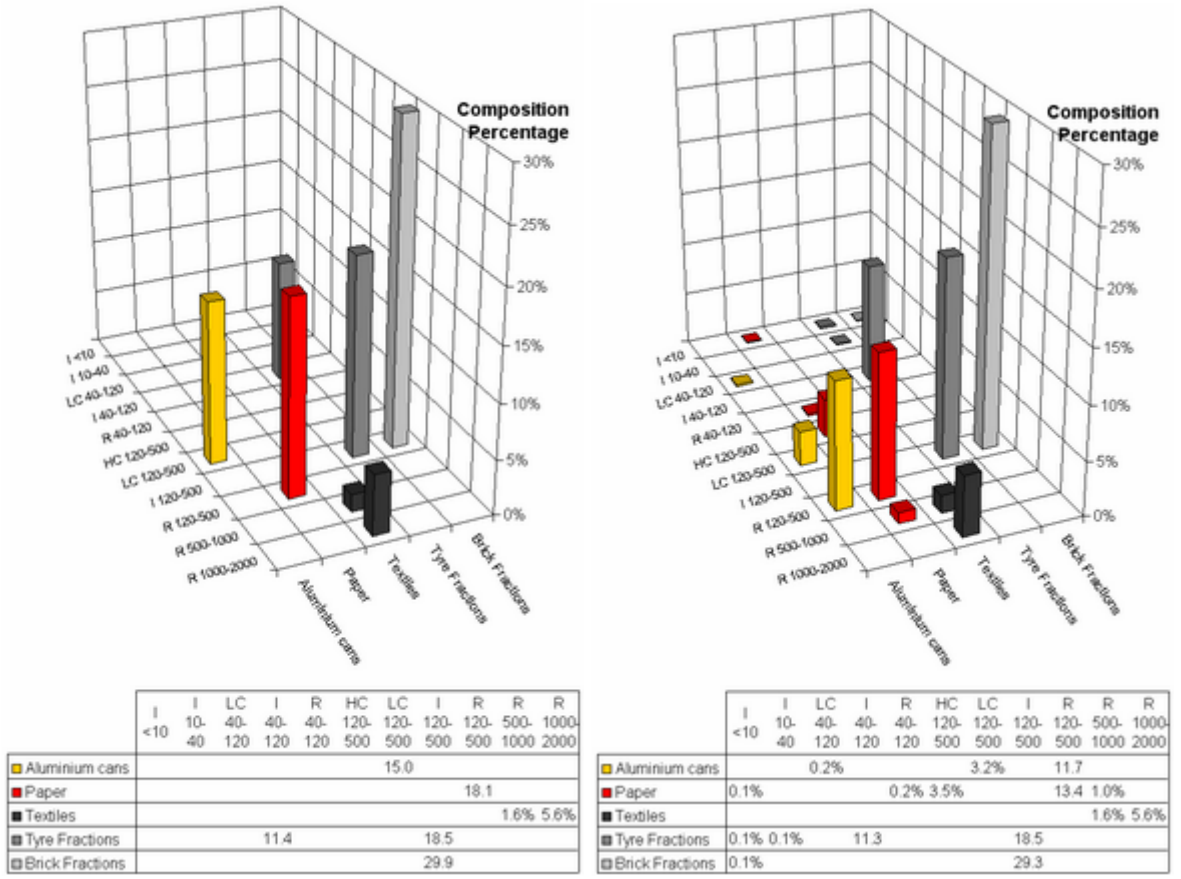

	I <10	I 10-40	LC 40-120	I 40-120	R 40-120	HC 120-500	LC 120-500	I 120-500	R 120-500	R 500-1000	R 1000-2000
Aluminium cans							15.0				
Paper									18.1		
Textiles										1.6%	5.6%
Tyre Fractions				11.4				18.5			
Brick Fractions								29.9			

	I <10	I 10-40	LC 40-120	I 40-120	R 40-120	HC 120-500	LC 120-500	I 120-500	R 120-500	R 500-1000	R 1000-2000
Aluminium cans			0.2%				3.2%		11.7		
Paper	0.1%				0.2%	3.5%			13.4	1.0%	
Textiles										1.6%	5.6%
Tyre Fractions	0.1%	0.1%		11.3				18.5			
Brick Fractions	0.1%							29.3			

Figure 6-48 Input and output of shear test SW_03

Figure 6-48 demonstrates the input and output component distribution of SW_03. As before, textiles remained in their initial state. Incompressible components like brick fractions and tyre shreds only exhibited a small variation in size due to material failure during shearing. Paper was pressed to a sheet-like agglomeration and thus achieved a size of 500-1000mm. Also, high compressible paper components in the size range 120-500mm were found. Small amounts of reinforcing paper were in the size range of 40-120mm and fines, and therefore incompressible paper components were generated during the shearing process. Aluminium cans were divided into reinforcing and low compressible components with 120-500mm and a small amount of low compressible components in the size range of 40-120mm were also present.

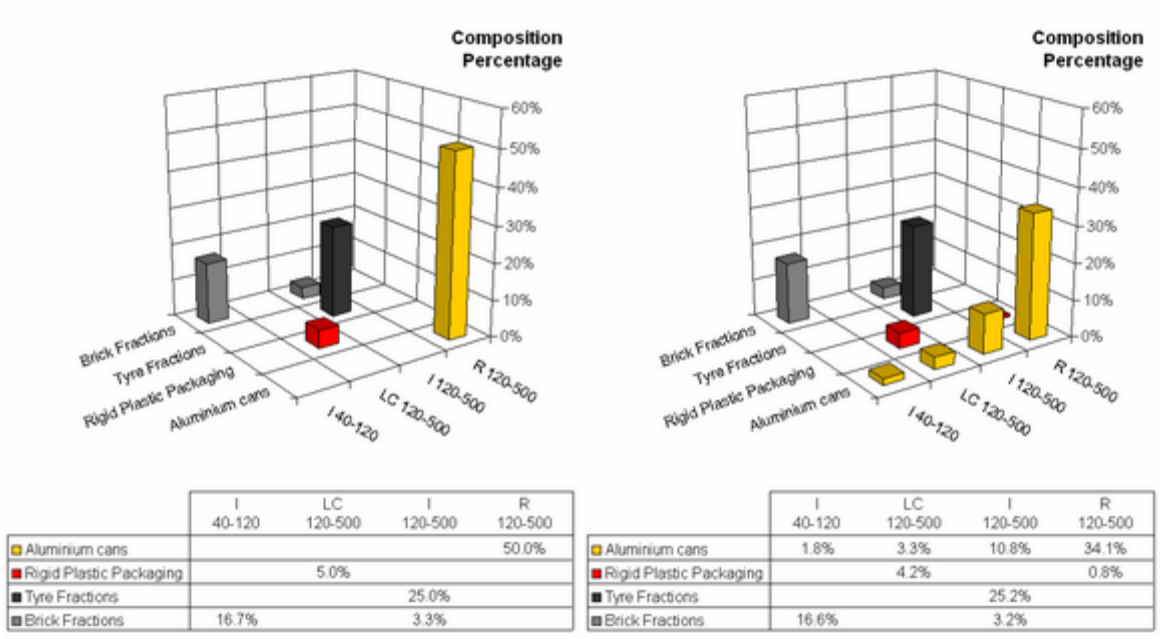

	I 40-120	LC 120-500	I 120-500	R 120-500
Aluminium cans				50.0%
Rigid Plastic Packaging		5.0%		
Tyre Fractions			25.0%	
Brick Fractions	16.7%		3.3%	

	I 40-120	LC 120-500	I 120-500	R 120-500
Aluminium cans	1.8%	3.3%	10.8%	34.1%
Rigid Plastic Packaging		4.2%		0.8%
Tyre Fractions			25.2%	
Brick Fractions	16.6%		3.2%	

Figure 6-49 Input and output of shear test SW_04

SW_04 was dominated by aluminium cans. Incompressible components of bricks and tyre fractions were not modified and stayed in the size range of 40-120mm and 120-500mm, respectively. The majority of rigid plastic packaging also remained in its initial shape-related subdivision and size range, though a small part became reinforcing. The largest alteration is visible for aluminium cans. They started being fully reinforcing (i.e. flattened) in the size range 120-500mm, but the output material was distributed over the two size ranges involved (40-120mm and 120-500mm) and exhibited also low and incompressible characteristics. This could be due to compressing and shearing cans into smaller sections.

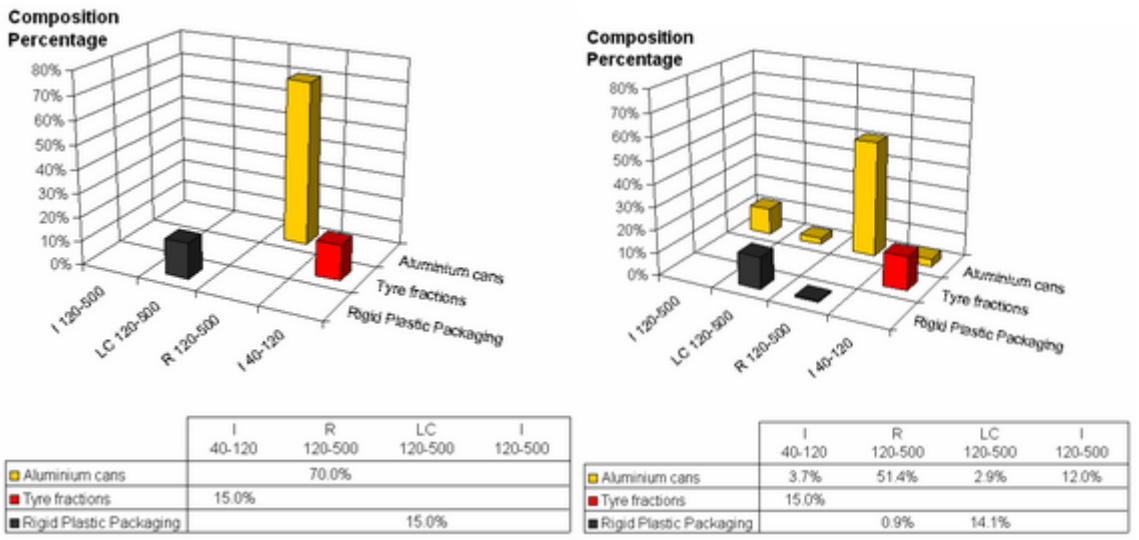

	I 40-120	R 120-500	LC 120-500	I 120-500
Aluminium cans		70.0%		
Tyre fractions	15.0%			
Rigid Plastic Packaging			15.0%	

	I 40-120	R 120-500	LC 120-500	I 120-500
Aluminium cans	3.7%	51.4%	2.9%	12.0%
Tyre fractions	15.0%			
Rigid Plastic Packaging		0.9%	14.1%	

Figure 6-50 Input and output of shear test SW_05

SW_05 in Figure 6-50 shows results similar to SW_04. A small amount of rigid plastic packaging changed from low compressible components to reinforcing components. Tyre

shreds kept their initial size and shape. Cans partly changed from being reinforcing and sized 120-500mm to being low and incompressible in the same size range and incompressible in the size range 40-120mm.

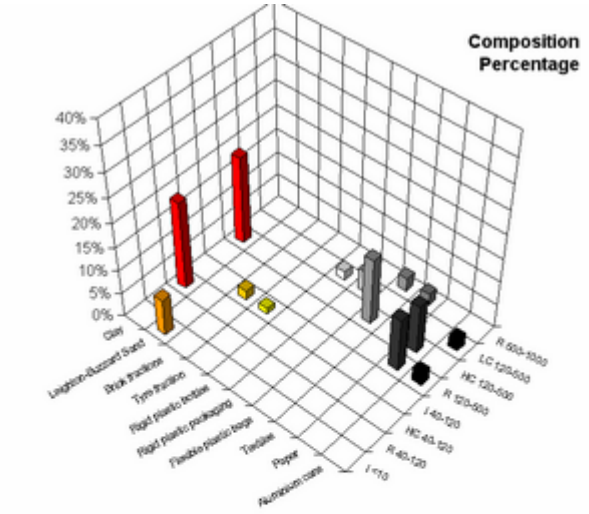

	I <10	R 40-120	HC 40-120	I 40-120	R 120-500	HC 120-500	LC 120-500	R 500-1000
Aluminium cans					2.7%		2.5%	
Paper					11.1%	10.2%		
Textiles								2.5%
Flexible plastic bags						14.0%		2.9%
Rigid plastic packaging							4.6%	
Rigid plastic bottles							1.9%	
Tyre fraction				1.2%				
Brick fractions				2.0%				
Leighton-Buzzard Sand	7.6%							
Clay			18.5%			18.5%		

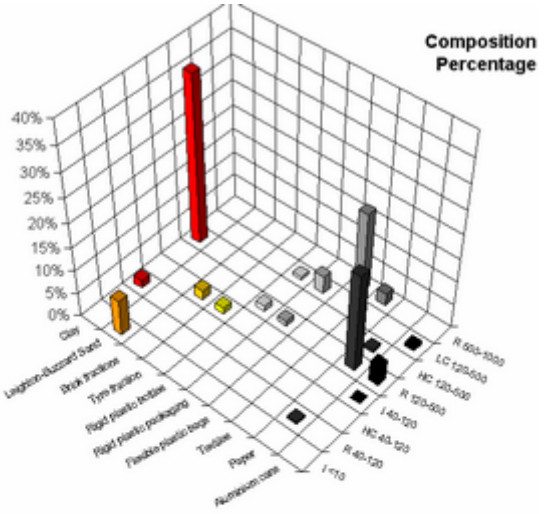

	I <10	R 40-120	HC 40-120	I 40-120	R 120-500	HC 120-500	LC 120-500	R 500-1000
Aluminium cans				0.1%	4.2%		0.8%	
Paper		0.5%			20.4%	0.6%		
Textiles								2.5%
Flexible plastic bags								16.8%
Rigid plastic packaging					0.9%		3.7%	
Rigid plastic bottles					1.2%		0.7%	
Tyre fraction				1.2%				
Brick fractions				2.0%				
Leighton-Buzzard Sand	7.5%							
Clay			1.7%			35.1%		

Figure 6-51 Input and output of shear test SW_09

The input and output for SW_09 is shown in Figure 6-51. Clay distinctively changed from being high compressible in the size range 40-120mm to high compressible within the size range 120-500mm. Again, textiles, brick and tyre fractions remained in their initial state. Rigid plastic bottles were largely altered to being reinforcing. In opposite to the plastic bottles, the rigid plastic packaging was only slightly altered into reinforcing components. The initial high compressible part of paper totally disappeared and was shifted towards a large percentage of reinforcing components. Small fractions of paper were found in the size range 40-120mm (reinforcing) and <40mm. Flexible plastic bags were only found to be reinforcing and sized 500-1000mm in the output material. For aluminium cans the part of low compressible components decreased and the reinforcing components increased. A small fraction of incompressible cans size 40-120mm were also found.

6.5 Summary of Shear Behaviour

To investigate shear behaviour of MSW, ten synthetic waste compositions were tested. Similar to the compositions used for the investigation of compression behaviour, the compositions were divided into incompressible (SW_01, SW_06, SW_07, SW_08), compressible (SW_02, SW_03), mono-component compositions (SW_04, SW_05) and a real waste composition (SW_09). Also, two variations of SW_01 with different sample

heights were examined. Boundary conditions of the tests, shear stress-displacement graphs, vertical strain, secant shear moduli, and Mohr-Coulomb failure envelopes were presented. The Mohr-Coulomb failure envelopes show values for mobilised friction and cohesion at 110mm before the unload-reload loop and maximum displacement, as peak values and thus failure was not apparent.

As for the compression behaviour, the tested compositions showed different behaviour in accordance to their outlined character, i.e. incompressible compositions SW_01, SW_06, SW_07 and SW_08 exhibited high shear stress with resulting high friction angles, the compressible compositions (SW_02 and SW_03) resulted in similar low values as the mono-component compositions (SW_04 and SW_05). The lowest shear stress was observed for the real waste simulation SW_09. Values for shear stiffness reflected a behaviour analogous to precedent observation of shear stress, i.e. incompressible compositions resulted in high shear moduli and compressible, mono-component compositions and the real-waste simulation resulted in relatively low shear moduli. The shear tests confirmed expected differences between the compositions in shear behaviour

In addition, input-output analyses of the shear tests SW_02, SW_03, SW_04, SW_05 and SW_09 were conducted. The results were compared. A detailed discussion of the shear behaviour and a comparison to values from the literature is provided in chapter 7.5.

7 Discussion

7.1 General Introduction

In this chapter the findings from the geotechnical classification, synthetic waste compositions, compression and shear behaviour are summarised, discussed and assessed. Shear and compression data are compared to data from the literature and analysed to validate the use synthetic wastes for the assessment of mechanical behaviour.

7.2 Geotechnical Classification

The geotechnical classification framework presented in chapter 4.2 uses the description of waste components to identify the mechanical characteristic of waste. The classification elements material groups, grading, degradation potential and shape-related subdivisions (high/low compressible, incompressible, and reinforcing) seem to sufficiently describe a waste sample in order to classify it qualitatively.

The chosen material groups introduced by Kölsch (1996) and used in this work are based on similar material properties and should therefore satisfactorily cover the variability of materials involved. Similar material groups have been used before (e.g. DEQ, 1998) to summarise the large amount of materials found in MSW. In a direct comparison of the two sets of groupings it was decided to use the set with fewer material groups. It was not deemed necessary to subdivide minerals into ceramic, glass and inerts (Table 4-1), as they display similar mechanical material properties. On the other hand, polymer and plastics were subdivided into rigid and flexible plastics, as the mechanical behaviour was expected to differ considerably.

For the waste sorting analysis conducted on Narborough landfill, the chosen material groups could be easily related to the waste components of the sample with one exception. As the material groups do not allow any overlap, a problem arose from material combinations. For example, cans or plastic packaging were found, which still contained organic material, or bottles with beverage residues were identified. In these cases a clear allocation of the components to one material groups was not possible, the material of the repository was defined to be the decisive one. Nevertheless, the specific mechanical properties used for the justification of the material grouping may have to be re-considered, as these properties reflect the material of the particular component but not the particular component, which could result in different mechanical behaviour (e.g. aluminium foil has similar material properties but different component properties than a aluminium beverage can).

The shape-related subdivisions take the component shape into account. The chosen subdivisions were reinforcing, compressible (high and low) and incompressible components (section 4.2.1.3). The definition for the reinforcing components, i.e. relating the size of the potentially reinforcing components to the size of the surrounding components, is derived from work on reinforced soils. Incompressible components were easily identified, as they do not exhibit deformation when subjected to load, which is

equivalent to the compaction and overburden stress in a landfill (i.e. the components, which did not alter their shape after completion of the filling). The subdivision of compressible components was also unproblematic to identify. Nevertheless, a difficulty was found to be the differentiation of high and low compressible components, as a threshold could not be quantified. This led to an individual decision whether a component was high or low compressible. A rough distinction could be made by a visual assessment of the materials, i.e. originally thin packaging material like plastic foil and paper, which was not present as a “two-dimensional” foil-like element, but rather a “three-dimensional” element, which was manually compressible without much effort, was assigned to the group of high compressible components.

High compressible component could be defined to be compressed during the compaction stage, while low compressible components are flattened due to overburden. This means that the boundary of high and low compressible components is site-specific, which could lead to misconceptions. Results from the compression test conducted in this work will be used to ascertain, whether a threshold value could be found. This value would be dependent on the component properties defined as high and low compressible.

A similar problem as mentioned for the material groups was found for the shape-related subdivisions. Combined components could not clearly be sorted to one shape-related subdivision. For example, a combination of aluminium can and food residues consisted of high and low compressible components. But as the majority of these combined components were found in the in the groups of high and low compressible components, the decisive element was the more rigid one, as this would dominate the behaviour of the combined component, when subjected to load.

For the grading of waste components, the size ranges from Kölsch (1996) were used, but slightly modified for the sorting analysis, as <10mm instead of <8mm were defined as being the finest size range. They were deemed to provide a good profile of the sizes represented in waste. Bearing in mind the mass distribution for waste from Narborough landfill in Figure 4-20, it might be useful to reconsider the size range 120-500mm. As the largest amount of waste mass is located in this range, a further examination of the size distribution and a possible subdivision of the size range 120-500mm could be advisable. On the one hand, the large amount in this size range is due to heavy materials, such as organic waste and soaked materials, on the other hand most of the disposable packaging products, mainly lightweight reinforcing and compressible components of various sizes in the limit of 120-500mm, fall into this range. The resolution of the remaining size ranges (<10mm, 10-40mm, 40-120mm, 500-1000mm and >1000mm) does seemingly not need further changes.

So far, data for the degradation potential of waste components is based on data from the literature. Furthermore, the data used does not distinguish between readily, medium and slow biodegradable, as demonstrated in Table 4-2. Such a distinction would contribute to the overall assessment of waste mechanical behaviour, as the application of the framework (Figure 4-9), and in particular the long-term stage, could be refined. Moreover, only biodegradability is taken into consideration. Simple assumptions were made about

the alteration of component size and shape in regard to their component properties, but size and shape alteration due to physical processes like shearing processes due to placement and chemical degradation were not considered.

As the water content was not measured for the components of the waste sorting analysis due to the large sample amount, which would have been necessary to achieve representative results, assumptions for the water contents were made (appendix 11.2). Nevertheless, in a comparison between the wet and the dry masses, it was concluded that the mass ratio differences between wet and dry components were not crucial. The discrepancies were marginal, i.e. a minor mass shifting from the usually on site wet materials (e.g. organics) to the dry materials (e.g. plastic packaging) was observed (Figure 11-2).

The classification procedure is laborious but considering the heterogeneity and variability of waste and the amount of information acquired, the procedure is deemed appropriate. The practicability of the classification procedure in a large scale is questionable. As for the assessment of biological and chemical properties of MSW, representative sampling and sorting seems to be a solution for describing and classifying municipal solid waste.

The data presentation, as demonstrated in Figure 4-10, summarises all information necessary for a more detailed material characterisation. For each of the three main groups of shape-related subdivision (compressible, incompressible and reinforcing components) the material groups involved including their grading and degradability is combined in one graph and provides a way of comparing data. For a direct comparison Figure 7-1[19] depicts the already presented data from Kölsch (1996) and from the waste sorting analysis on Narborough landfill. The percentages shown describe the ratio of the subdivision on the overall sample mass.

Generally, the appearance of the shape-related subdivisions of Braunschweig and Narborough fresh waste was very different. Narborough waste possessed a high percentage of compressible components and Braunschweig was evenly distributed but exhibited a majority of reinforcing components. While the Braunschweig waste from Kölsch (1996) exhibited a component distribution with most components in the size range of 40-120mm, the Narborough waste from the waste sorting comprised most components in the size range of 120-500mm. This is also visible from Figure 4-4 and Figure 4-20. The largest variety of materials could be found within reinforcing components for Braunschweig waste and within compressible components for Narborough waste.

Minerals and miscellaneous material was dominant within the shape-related subdivision of Braunschweig. Most components ranged in the size of 40-120mm, except for miscellaneous material, which was located in <40mm. An overall degradability of approximately 25% for both, incompressible and compressible components was calculated. Compressible components were dominated by flexible plastics. The predominant size was between 40 and 500mm. Miscellaneous materials were located in <40mm, as observed before. Reinforcing components were dominated by paper and

[19] Also: section 4.2.2 (Kölsch, 1996) and 4.3.1.5 (SITA landfill, Narborough)

flexible plastic for the most part. The observed size range included all sizes above 40mm and 40% overall degradability was estimated.

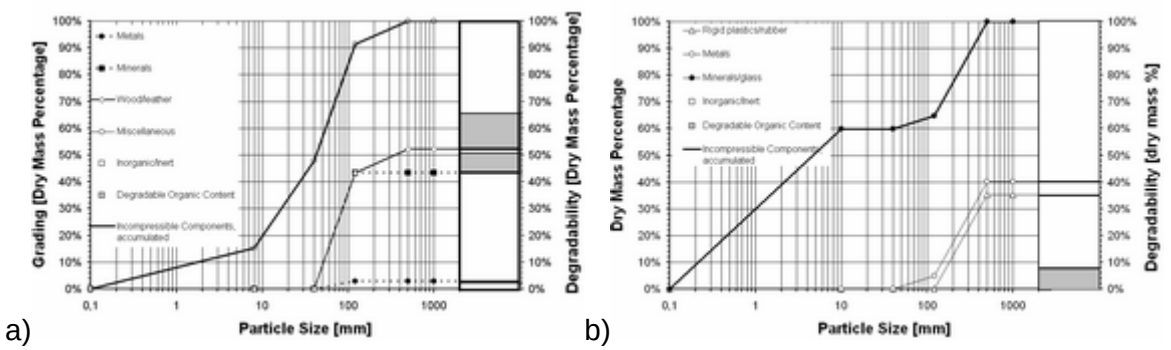

a) b)

Incompressible components a) 23.7% b) 3.3%

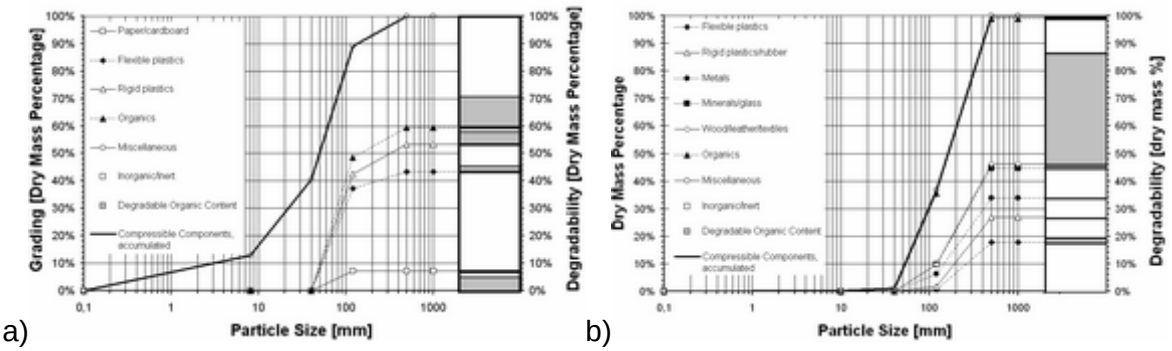

a) b)

Compressible components a) 32.9% b) 69.6%

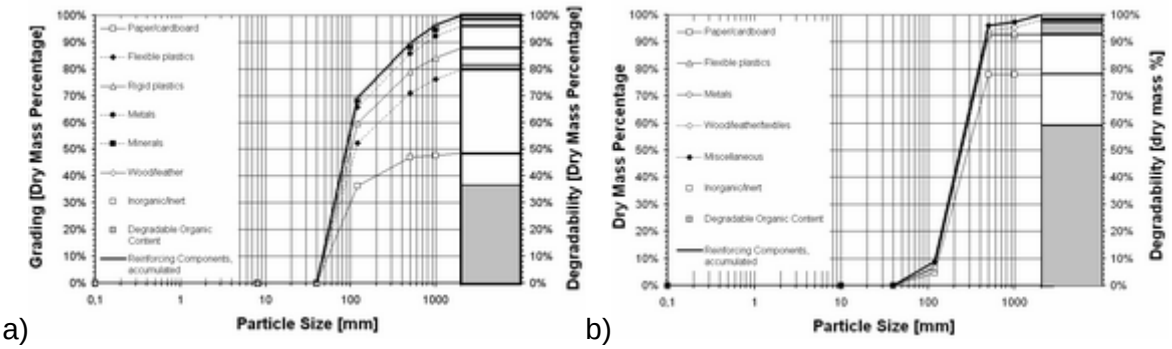

a) b)

Reinforcing components a) 43.4% b) 27.1%

Figure 7-1 Comparison of the shape-related subdivisions with data from a) waste from Braunschweig (Kölsch, 1996) and b) SITA landfill, Narborough

Narborough waste showed a lot of minerals and rigid plastics within the subdivision of incompressible components. The dominant size range was 120-500mm and for the high amount of minerals, a size ranges <10mm was observed. A very low degradability of <10% was calculated. Compressible components were mainly composed of putrescible organics and flexible plastics between 120mm and 500mm. The degradability was estimated to be approximately 45%. Reinforcing components were dominated by paper and flexible plastics. Most components were found with the size range 120-500mm. With 65% the degradability was estimated to be very high.

From the description of the waste compositions and their components, it is concluded that the initial state of Narborough appeared to be highly compressible, while the waste from

Braunschweig showed a high amount of reinforcing materials. Additionally, the amount of incompressible components was considerably higher in opposite to Narborough waste. As the further development of the shape-related subdivisions is highly dependant on compressible components (they are altered into reinforcing and incompressible components) the Narborough waste exhibits a higher variety of shape-shifting. But as most of the compressible components were found within a size range >120mm, a shifting towards the reinforcing components for the next stage (post-placement) could be expected. In comparison to Braunschweig waste, the changes within the Narborough waste can generally be expected to be more extreme.

Finally, the results for the mass ratios of the shape-related subdivisions from both Kölsch (1996) and the waste sorting analysis are depicted in Figure 7-2. Different initial and post-placement locations are obvious, but a general trend is also visible. While the Narborough waste exhibits a very compressible character (with about 70% compressible components), the waste examined by Kölsch (1996) has reasonably balanced mass ratios. A slight predominance of reinforcing components (45%) is apparent. After placement, the amount of reinforcing components increases, compressible components decrease as the high compressible components change into incompressible or reinforcing and the incompressible components derived from Kölsch (1996) slightly increase. The final state is very similar for both data sets. In the final state all compressible components are assumed to be altered to either reinforcing or incompressible components. Thus, only these components are found within the compositions to different percentages (40% incompressible and 60% reinforcing for Kölsch (1996) and 37% and 63% for Narborough). The trend obvious from Figure 7-2 is thus a decrease of compressible and an increase of reinforcing components after placement, and an additional decrease of compressible and reinforcing components with a resulting increase of incompressible components in the final state. It was also assumed that biodegradable components degrade and thus a loss of mass was considered, which is not apparent from the ternary diagram. It is apparent from Table 4-3 for the waste from Braunschweig, and Table 7-1 shows the values for Narborough waste.

Table 7-1 Percentages of shape-related subdivisions from Narborough waste used to define initial, post placement and final states

	Shape-related Subdivisions by Dry Mass			
	Reinforcing	**Incompressible**	**Compressible**	**Sum**
State	**[%]**	**[%]**	**[%]**	**[%]**
Initial State	27.12	3.24	69.64	100
Potential State after Placement	76.22	3.79	19.99	100
Potential Final State relative	52.96	30.96	0.00	84[20]
Potential Final State absolute	63.11	36.89	0.00	100

[20] Mass loss due to biodegradation

The values for the state after placement and for the final state are based on assumption (as stated in Table 4-5). These assumptions could be substantiated and refined by conducting sorting analyses on site at different stages of the landfill, i.e. analysing waste components after placement and sorting already deposited waste from different burial depths. This could also be coupled with a analysis of the degradability of the components. Compression tests could be another sources for determining the shapes, sizes of components. However, stress levels would have to be pre-defined, which should be related to the applied stress at deposition and to one or more stress levels due to overburden from additional waste layers and daily covers. The discussion about the compression behaviour of the synthetic waste in chapter 7.4 also deals with this problem.

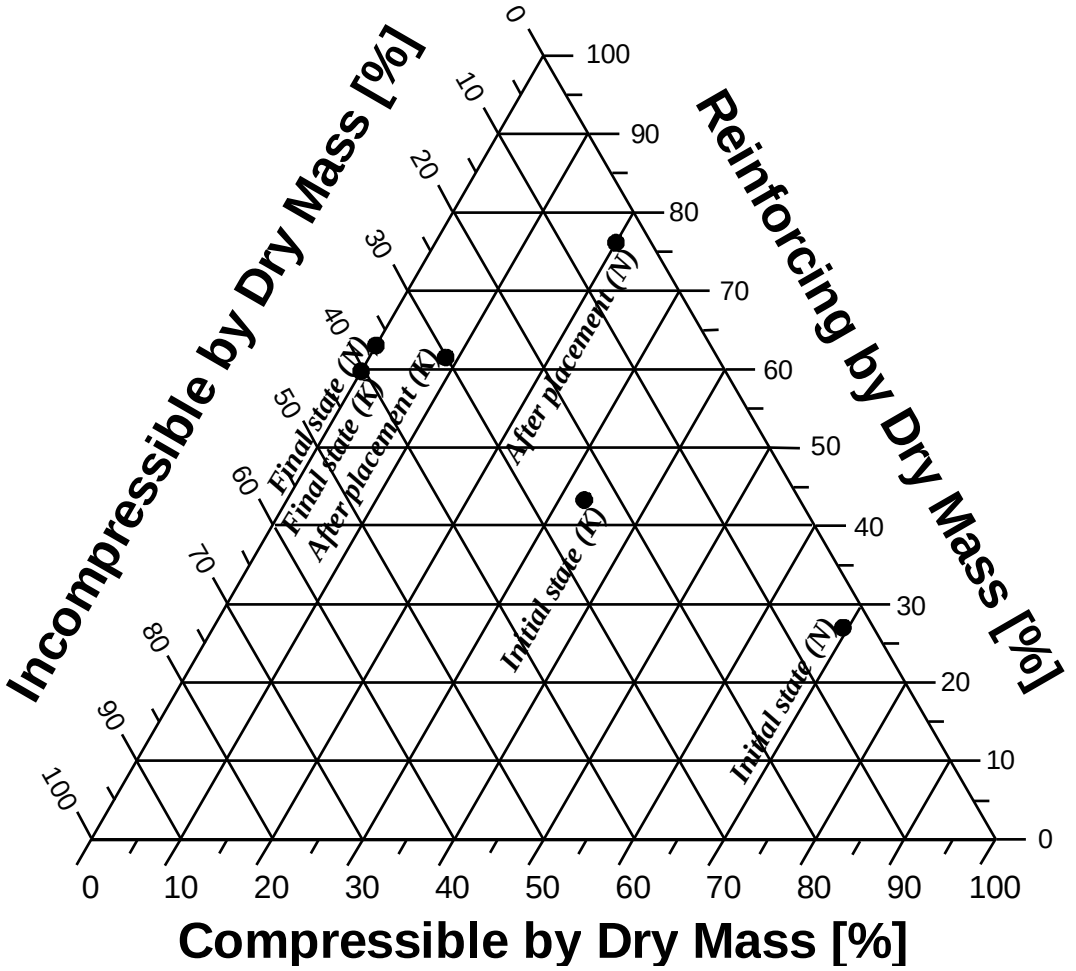

Figure 7-2 Comparison of data from Kölsch (1996) and the waste sorting on SITA landfill, Narborough

The proposed classification can be used to describe general mechanical behaviour of MSW, provided that data required by the frame work is present. Under the same premise, it is qualified to compare data from different sources and gives a first impression of a potential mechanical character, as demonstrated above.

7.3 Synthetic Waste

At present, the synthetic waste engineered and presented in this work is derived from the results of a single waste sorting analysis. The examined waste composition from

Narborough landfill falls within the minimum-maximum range of an average UK composition, which resulted from information in the literature as shown in Figure 4-18. The sorted waste sample defined only a random fresh waste composition and even though it ranged within the borders of literature values, it does not represent an overall initial waste composition. For further refinement, it would be advantageous to examine a range of initial waste compositions. Even though a range would contribute to the knowledge about the variety of waste components and its properties, it would not represent an overall initial UK waste composition due to e.g. constantly changing waste streams, consumer behaviour and legislative actions, i.e. it is not possible to determine an overall initial waste composition, but it is possible to define composition ranges for it. Nevertheless, as this composition represents a random initial waste composition it was suited for a first-step derivation of synthetic waste. On its components, size ranges and shape-related subdivision, the basis for a synthetic waste could be founded. The main components and sizes were identified by minimising the size and material fractions of the real waste component distribution. For a further development and refinement of the synthetic waste, it could be helpful to investigate the material groups, sizes and shapes of a set of initial compositions.

An objective of the synthetic waste was the simplicity of its components in regard to size and shape. Eight material groups used in the classification framework were also identified to resemble the main components of real waste. For the synthetic waste these eight material groups were retained to represent real waste. The material groups were putrescible organics, paper, wood/leather/textiles, flexible and rigid plastic, metal, minerals, and miscellaneous material. Only putrescible organics were replaced by clay lumps wrapped in plastic foil, and miscellaneous material was shared between plastic, paper and minerals. Rigid plastic had to provide compressible and incompressible components. Thus rigid plastics were composed of the three components plastic tubs, plastic bottles and incompressible tyre shreds. Flexible plastic component were easily replaced by flexible plastic bags, which reflected reinforcing (straight) and compressible components, depending on their pre-defined state. The incompressible group of minerals had to provide three different size ranges, resulting in two kinds of components being brick fractions (40-120mm and 120-500mm) and Leighton-Buzzard sand for the fines <10mm. Paper did not have to be replaced, A4 sheets were used to represent this material. For textiles, blankets were cut in appropriate sizes (500-1000mm and >1000mm) and metal was resembled by aluminium cans.

The amount of components for the synthetic waste seems manageable, as eleven waste components of eight material groups define the range of the synthetic waste. Considering the amount of different materials, component sizes and shapes within the real waste (e.g. visualised in Figure 4-16) the simplicity of the engineered waste is obvious. Nevertheless, it covers the main material groups, sizes and shapes, which were necessary to reflect a real waste composition, as the derivation considered material groups, sizes and shape-related subdivisions. The derivation comprised two approaches. The first approach was the minimisation of components by identifying the most important dominant size ranges within each material group, but also the most important material groups within the size ranges had to be taken into account. As the fraction in size and material groups were

given as percentage related to the overall sample mass, the mass distribution was incorporated. Especially in respect to compressibility of waste, the volumetric distribution plays an important role. Thus a volumetric factor had to be defined and incorporated in the second approach towards a comprehensive amount of material fractions. As this approach was based on observations rather than on measurements, an optimisation is obvious. The volumetric factor vf_j (Equation 4-6) was derived from assumed volumes observed from the sorting compartment, as a volume measurement was not conducted. Therefore, uncertainties are likely to be involved. With a thorough volume measurement the volumetric factors could be refined and their accuracy in regard to the description of the volumetric impact of components could be improved. For an initial definition of the synthetic components a loose volume should be measured.

The mechanical behaviour of the synthetic waste is assessed in the following sections, which are dealing with the results of laboratory compression and shear tests. Subsequently, the results are included in the ternary diagram.

7.4 Compression Behaviour

7.4.1 Assessment of the Compression Test Sets

For assessing compression behaviour of the synthetic waste, it was continued to distinguish between incompressible, compressible, mono-component composition and a simulation of a real waste composition. The latter exhibited properties, which were similar to the compressible compositions. Therefore the discussion of the real waste simulation will be mainly related to the results of the compressible compositions.

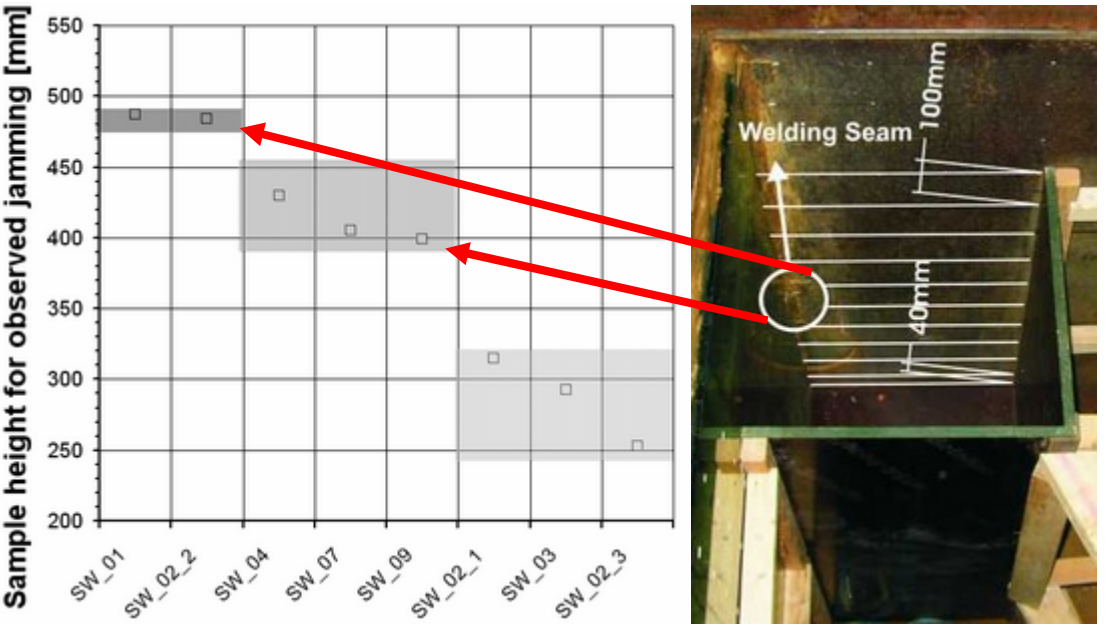

Figure 7-3 Compression Tests: Jamming heights and welding seam in the compression cell

Generally, it was often observed that the constrained modulus started as a high value and decreased over the next one or two values before starting to increase (0-27.5kPa at maximum). This could be due to two factors. The first factor involves the unstable material bridges built by components, when place into the compression cell. Up to a certain normal stress value, which ranged between 2.5kPa and 7.5kPa (in case of SW_01 up to approximately 30kPa), the constrained moduli decreased as a matter of component rearrangement and collapse of unstable material bridges. The second factor could be due to overcoming the friction between side wall and load plate (possibly 290mm) or due to a jamming of the load plate at the side wall. Also, there were observations (e.g. SW_01 and SW_02_2), where the constrained modulus decreased during the tests, which could be attributed to a welding seam (410-490mm) on the test chamber wall, on which the load plate and also components became jammed leading to an increase and a subsequent decrease after deblocking of the components and load plate, respectively.

7.4.1.1 Compressible Compositions

Figure 7-4 is an overview of constrained modulus and compression index for the compressible compositions SW_02_1, SW_02_2, SW_02_3 and SW_03. Generally, similarities of the moduli for compressible compositions were visible. The constrained moduli reached in the tests were comparatively low, when compared to the remaining results or to values from the literature. The compression indices of the SW_02 series and SW_03 showed large differences, which is due to the dissimilar compositions.

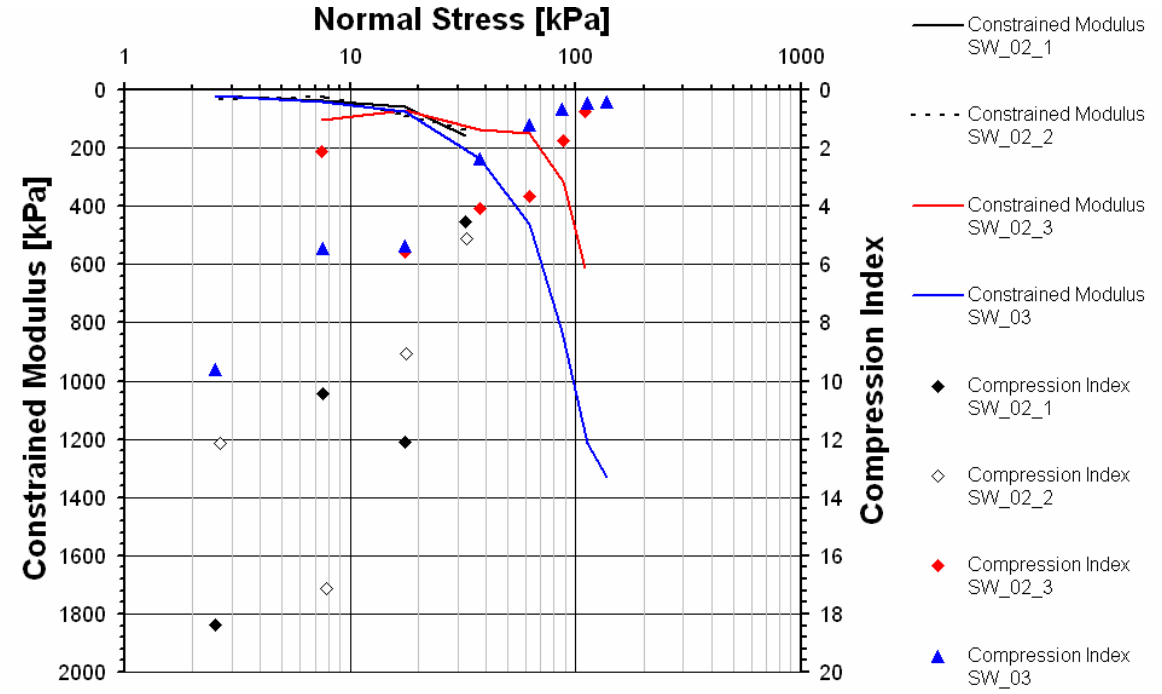

Figure 7-4 Constrained modulus and compression index for the compressible compositions SW_02 series and SW_03

In the following, constrained modulus and compression index are compared and discussed. As the tests on compressible compositions also comprised repeatability tests, the issue of repeatability is discussed in the next section. Additionally, the influence of altering the unit weight is addressed in the following.

Constrained Modulus

SW_02_1 and SW_02_2 showed very similar results for the constrained modulus. Both tests were conducted on the same composition with an initial unit weight of 0.27kN/m^3. The constrained moduli for both tests ranged between 22kPa and 159kPa, whereas SW_02_2 exhibited a slightly lower value (D = 139kPa) for the highest normal stress level of 40kPa. This was also visible from the final unit weight, which was with 0.76kN/m^3 lower than that of SW_02_1 (0.91kN/m^3). Nevertheless, both tests were in good agreement. The linear best-fit lines for the tests did not show large discrepancies, although SW_02_2 resulted in a slightly smaller increase of the constrained modulus.

For SW_02_3, the components used in the preceding tests SW_02_1 and SW_02_2 were utilised in one test to produce a higher initial unit weight of 0.49kN/m^3. The components had a certain stress history, as a normal stress of 40kPa was applied in the earlier tests. Thus the first three values (except for the very first) for the constrained modulus illustrated similar values to the first two tests. From a normal stress of 40kPa to approximately 60kPa a very low increase of the constrained modulus was visible, which might be due to collapses of unstable component bridges and therefore rearrangement of components. From 60kPa onwards a high increase of the modulus was obvious. Looking at the data from this and the two preceding tests a general picture could be drawn. Combining the data showed that approximately twice as much normal stress (62.5kPa) than on the preceding tests (32.5kPa on average) has to be applied on SW_02_3 to reach a similar constrained modulus as SW_02_1 or SW_02_2 (Figure 7-6).

Table 7-2 Normal stress range, unit weight and constrained modulus for the compressible SW_02 series

	SW_02_1		SW_02_2		SW_02_3	
Normal Stress Range [kPa]	Constrained Modulus [kPa]	Unit weight [kN/m^3]	Constrained Modulus [kPa]	Unit weight [kN/m^3]	Constrained Modulus [kPa]	Unit weight [kN/m^3]
0-5	22	0.27	31	0.27	200	0.49
5-10	38	0.38	24	0.36	106	0.52
10-25	59	0.55	86	0.50	70	0.61
25-40	159	0.91	139	0.76	135	0.81
50-75	-	-	-	-	148	1.15
75-100	-	-	-	-	317	1.56
100-120	-	-	-	-	613	1.87

The values for normal stress, constrained modulus and unit weight of the SW_02 series are shown in Table 7-2. These values were used in Figure 7-6 and also, for the unit weight correlation in Figure 7-7. This figure depicts the linear relation ship of an average

unit weight value (SW_02_1 and SW_02_2) with the applied normal stress level and the unit weight of SW_02_3 at high stress levels.

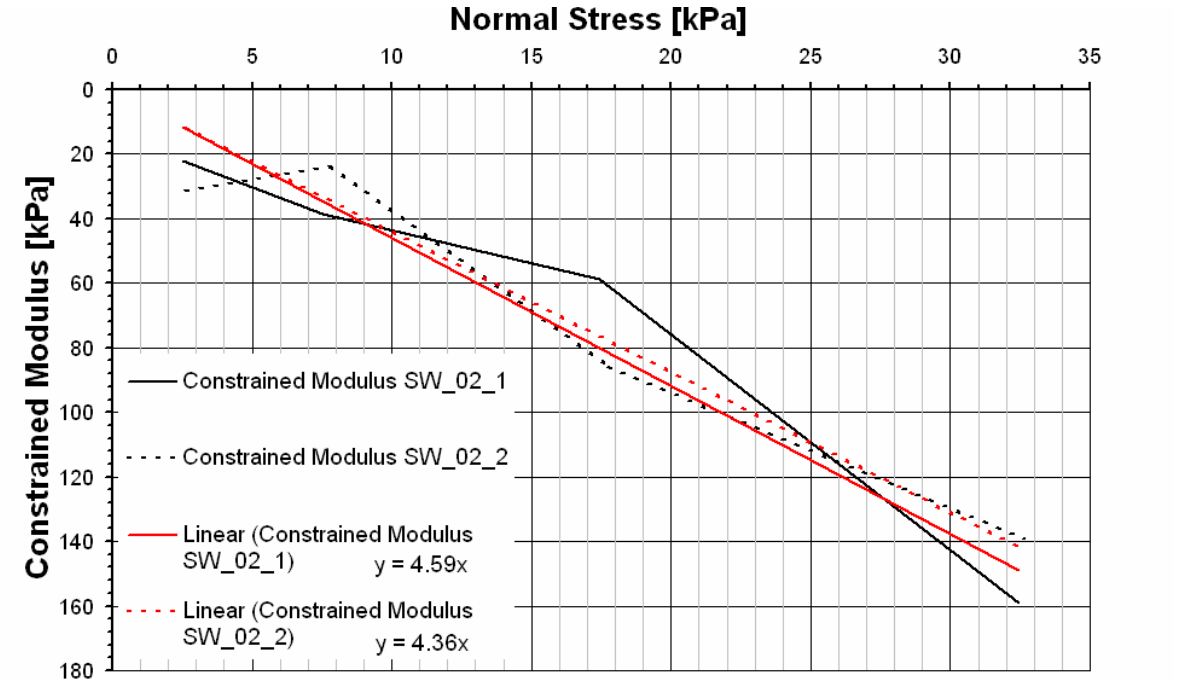

Figure 7-5 Repeatability of compression tests: Results for constrained moduli of composition SW_02_1 and 2

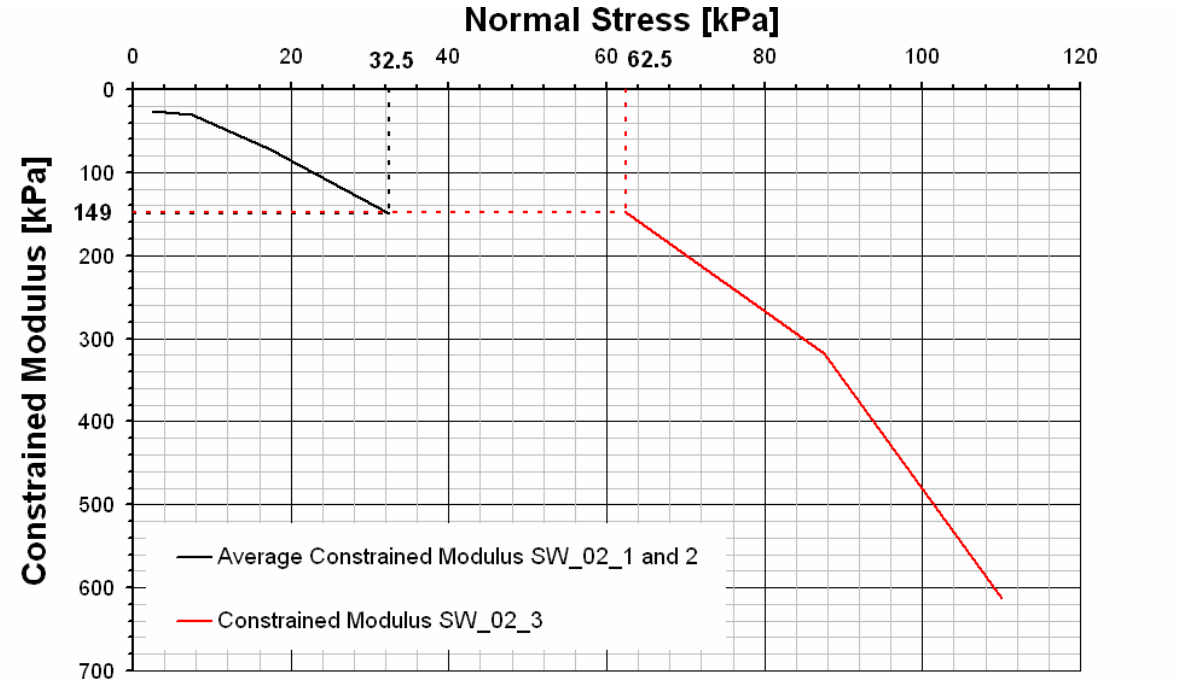

Figure 7-6 Influence of the unit weight: Correlation of the constrained moduli for an average out of SW_02_1 and 2, and for SW_02_3

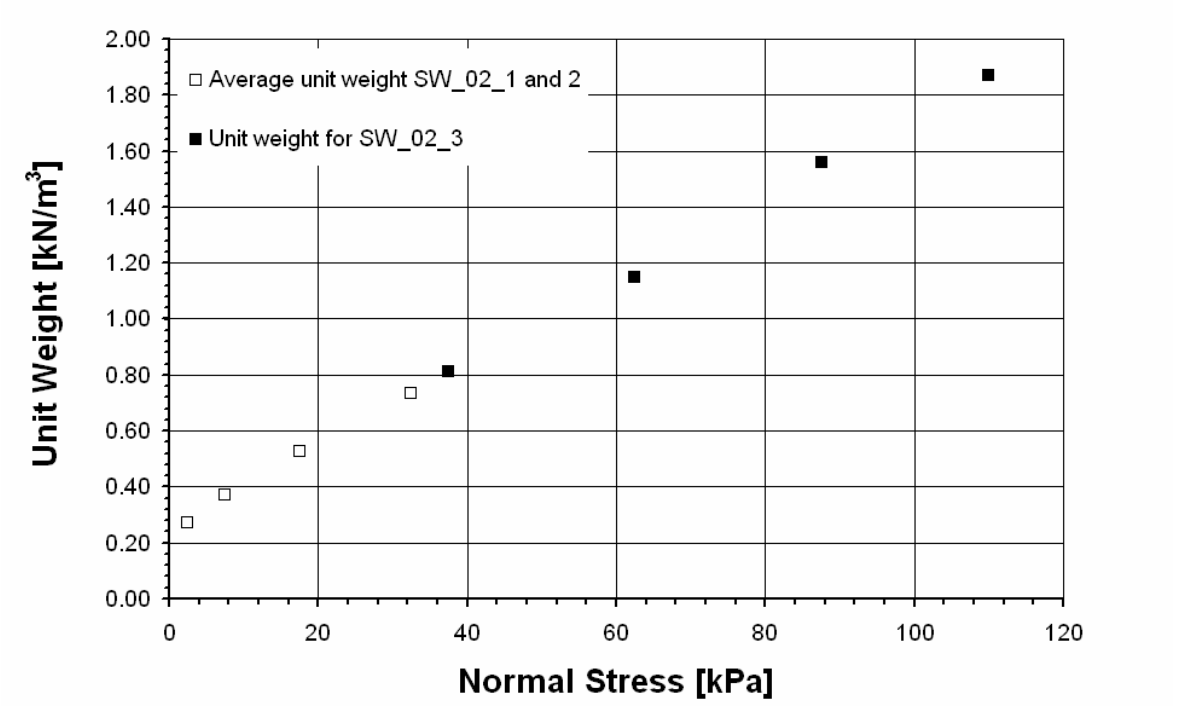

Figure 7-7 Correlation between unit weight and normal stress for the SW_02 series

Composition SW_03 showed a similar compression behaviour in comparison to the preceding tests SW_02_1 and 2. Especially in the low normal stress up to 17.5kPa, comparable constrained moduli were found as shown in Table 7-3 and Figure 7-8.

Table 7-3 Normal stress range, unit weight and constrained moduli for an average value for SW_02_1 and 2, and SW_02_3 and SW_03

	Av. SW_02_1 and 2		SW_02_3		SW_03	
Normal Stress Range	Constrained Modulus	Unit weight	Constrained Modulus	Unit weight	Constrained Modulus	Unit weight
[kPa]	[kPa]	[kN/m³]	[kPa]	[kN/m³]	[kPa]	[kN/m³]
0-5	22	0.27	200	0.49	22	0.71
5-10	38	0.37	106	0.52	41	0.97
10-25	59	0.53	70	0.61	74	1.27
25-40/50[21]	159	0.91	135	0.81	236	1.71
50-75	-	-	148	1.37	460	2.10
75-100	-	-	317	1.56	834	2.38
100-120/125	-	-	613	1.87	1215	2.60
125-150	-	-	-	-	1333	2.81

[21] Second value for SW_03

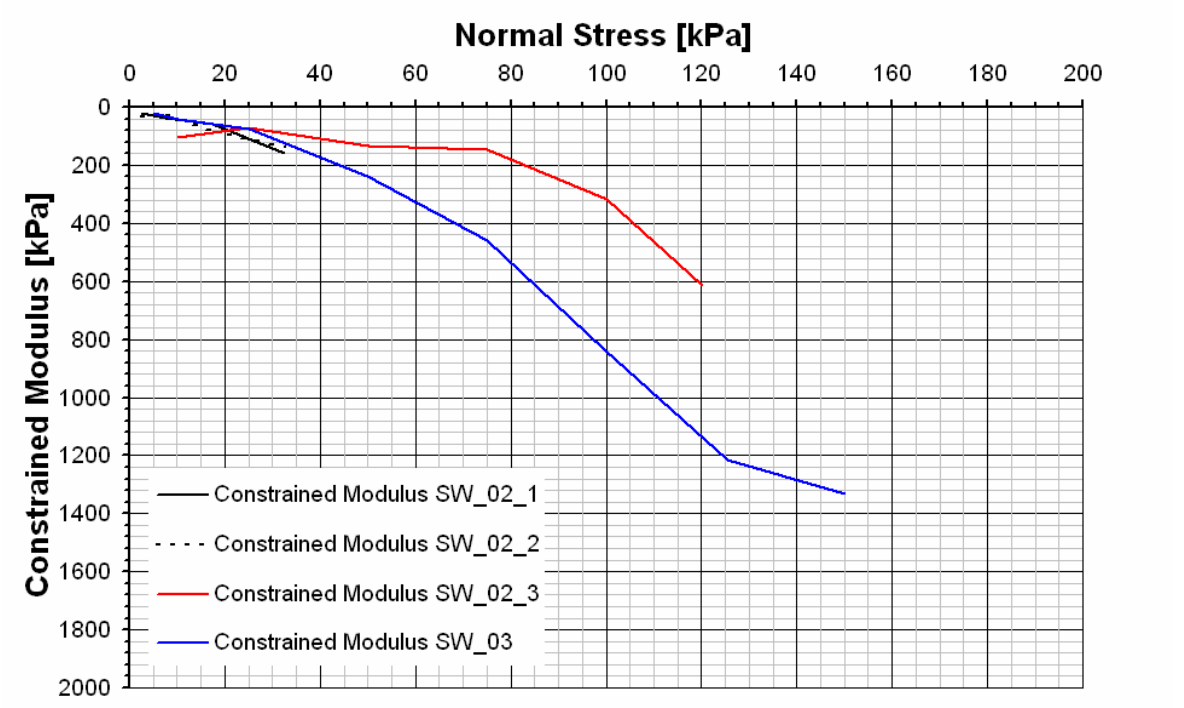

Figure 7-8 Constrained modulus for SW_02_1 and 2, and SW_03

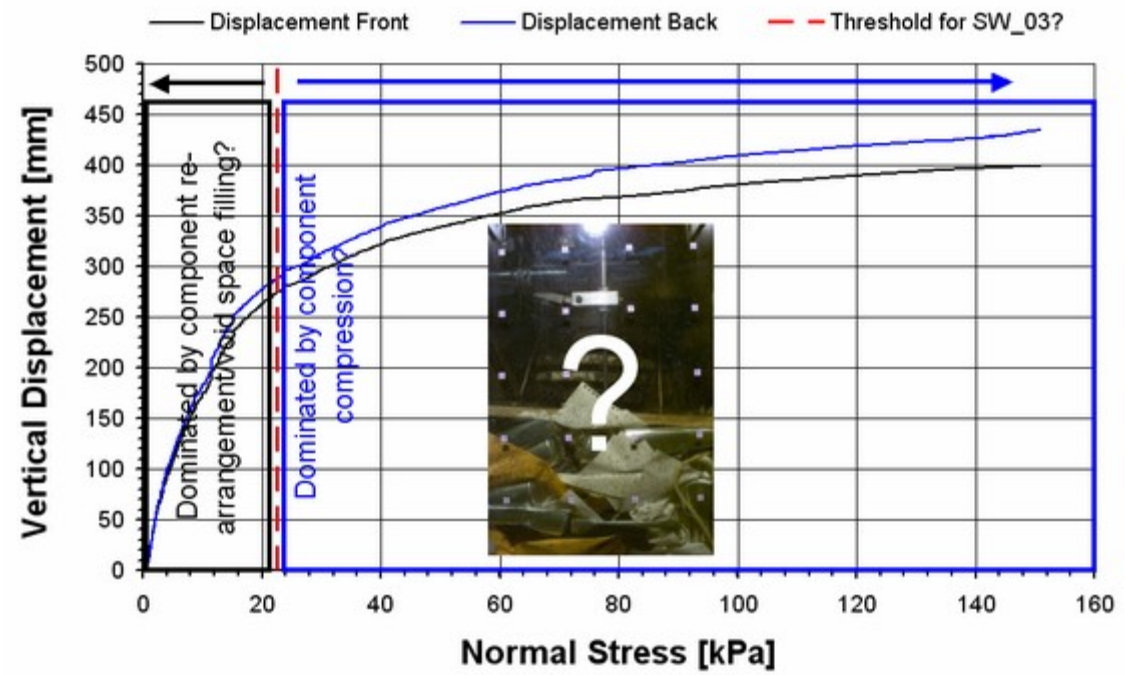

Figure 7-9 Qualitative threshold value for void space and component compression for the compressible composition SW_03

A maximum normal stress of 150kPa was applied to SW_03 resulting in values of up to 1.33MPa for the constrained modulus. This composition comprised a large amount (in terms of mass) of incompressible components like brick fractions and tyre shreds. Nevertheless, up to 25kPa normal stress, SW_03 exhibited values similar to SW_02_1 and 2. Thereafter, the constrained modulus increased far more than SW_02_3 in

comparison. It is imaginable that the influence of the incompressible components started at a stress level of 22.5kPa, after most voids were filled and a large amount of component compression had already taken place. Figure 5-11 shows the state of the components. It is obvious that after that stage the amount of settlement of the sample gradually decreased, which could mean that the void space were mostly filled and the majority of the settlement was due to component compression. It is visible from Figure 7-9 that the amount of settlement was decreasing, but it still has to be examined, whether a normal stress threshold value for void space filling and component compression can be quantified. This value would be dependant on the composition in terms of size, shape and material properties of the components.

Compression Index

Figure 7-10 depicts the compression indices for SW_02_1, 2 and 3, and for SW_03 including two exponential best-fit lines for the SW_02 series and SW_03. Two pairs of similar values are identifiable. SW_02_1 and 2 showed comparable values as the same composition was tested. C_c resulted in a range of 4.5 to 18.5 for the identical tests. SW_02_3 exhibited C_c values in higher normal stress levels (>32.5kPa), which fitted into the course of SW_02_1 and 2. SW_03 reached slightly lower values than SW_02_3, but showed reasonable similarity. It exhibited a more consistent decreasing trend of values than SW_02_3, with one exception at a normal stress of 7.5kPa.

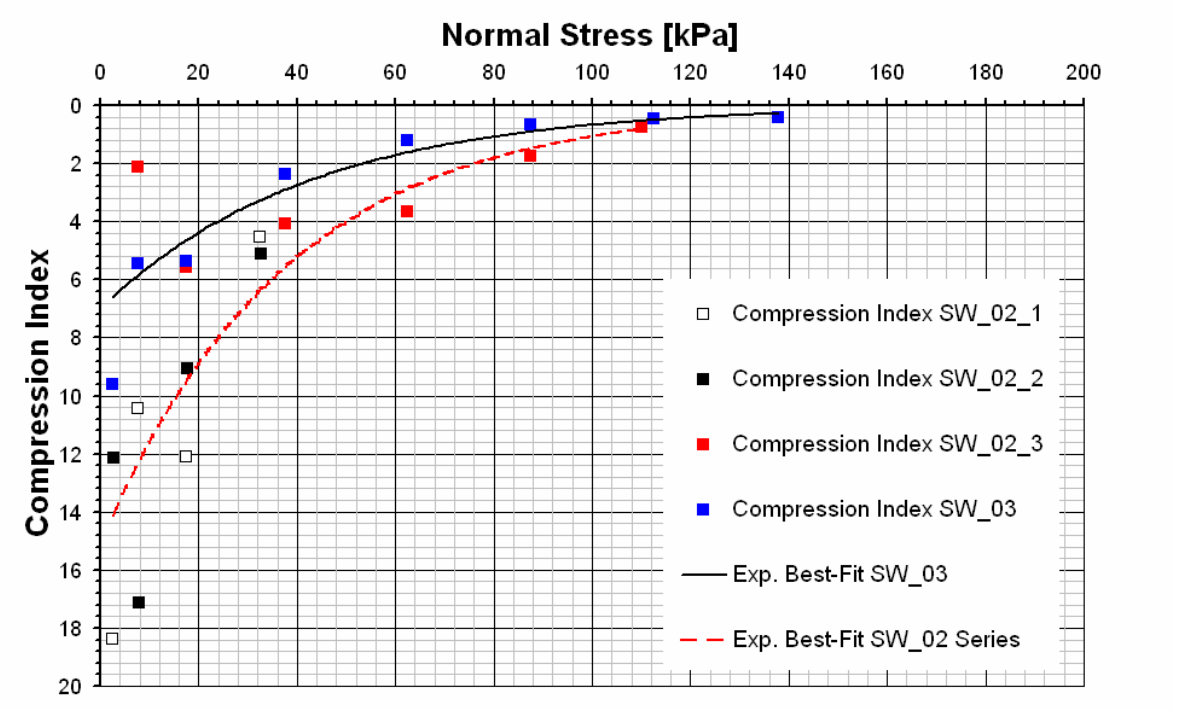

Figure 7-10 Compression indices for the compressible compositions SW_02_1 SW_02_2, SW_02_3 and SW_03

7.4.1.2 Incompressible Compositions

Figure 7-11 shows constrained moduli and compression indices of the two incompressible compositions SW_01 and SW_07. Both compositions comprised large amounts of Leighton-Buzzard sand in terms of both volume and thus also mass (Table 5-1 and Table 5-3). In addition to Leighton-Buzzard sand, SW_01 contained also paper and flexible plastic bags, SW_07 additional components were rigid plastic tubs and aluminium cans. Thus the difference of the additional components was constituted in their rigidity.

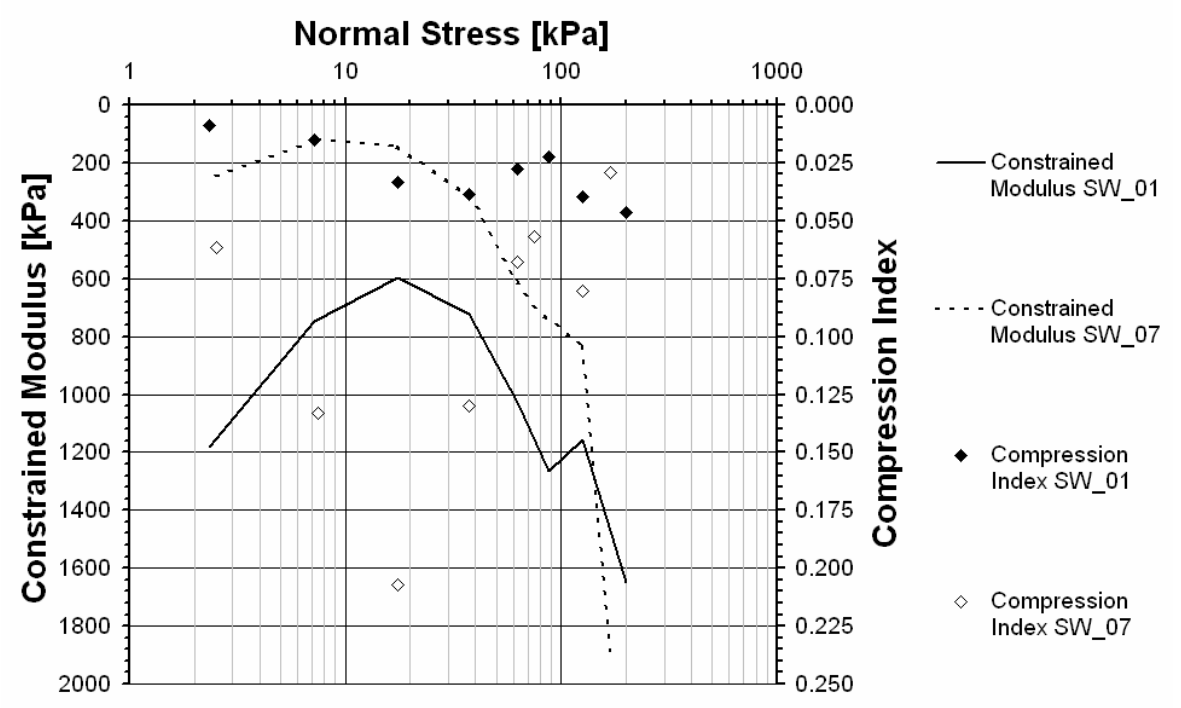

Figure 7-11 Constrained modulus and compression index for incompressible compositions SW_01 and SW_07

Constrained Modulus

Figure 7-12 depicts the constrained moduli for the incompressible compositions. For SW_01 higher constrained moduli were calculated than for SW_07. At a normal stress level of 17.5kPa SW_01 already exhibited a constrained modulus of 600kPa, while SW_07 was in the range of 150kPa. There are two reasons for the difference. SW_01 contained more sand then SW_07 and thus less voids, which is also visible from the lower compression index. Paper and flexible plastic sheets are high compressible material, thus void space was already decreased during filling, as the flexible components were compressed by the self-weight of the sand, while the components like plastic tubs and aluminium cans in SW_07 provided compression resistance due to component rigidity. Moreover, the segregation of sand at the bottom of the box aggravated this effect, as the self weight of the Leighton-Buzzard sand did not pre-act on the low compressible components.

Table 7-4 Normal stress range, unit weight and constrained modulus for the incompressible compositions SW_01 and SW_07

	SW_01		SW_07	
Normal Stress Range [kPa]	Constrained Modulus [kPa]	Unit weight [kN/m^3]	Constrained Modulus [kPa]	Unit weight [kN/m^3]
0-5	1180	10.56	248	7.36
5-10	749	10.59	122	7.52
10-25	599	10.77	141	8.16
25-50	721	11.11	314	9.10
50-75	1028	11.47	614	9.84
75-100	1265	11.75	694	10.37
100-150	1155	12.19	836	11.13
150-250/188[22]	1649	12.97	1183	11.83

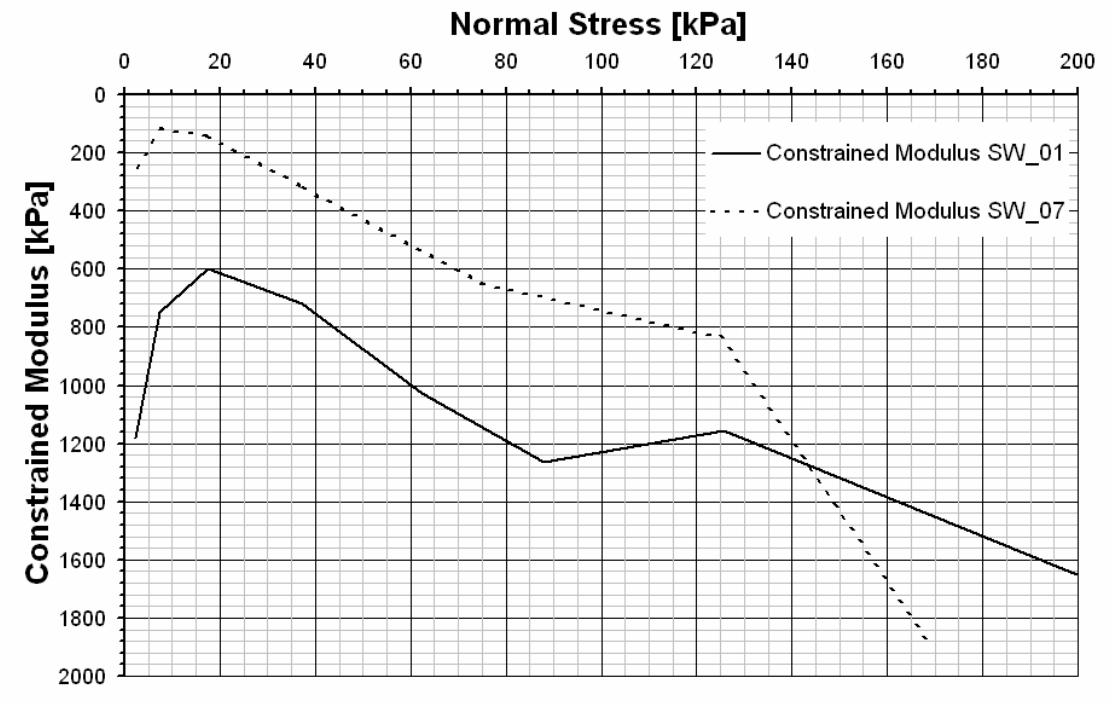

Figure 7-12 Constrained modulus for SW_01, and SW_07

A component-specific threshold value for the end of components compression of SW_07 is questionable. It was observed that the constrained modulus increased at about 125kPa and at a displacement, which ranged in the area of the bottom end of the welding seam at

[22] SW_07 was stopped at 188kPa

the compression cell side wall. Thus it could be suspected that the sudden increase of the constrained modulus was due to the jammed load plate.

Compression Index

The compression indices for both compositions in Figure 7-13 were very low in comparison to the compressible compositions (section 7.4.1). While the compressible compositions exhibited a C_c of 11-25, an average value of 0.025 was obtained for SW_01 and a value between 0.21 and 0.03 for SW_07 was found. The C_c gradient of SW_01 appeared to fluctuate around the average valued of 0.02, while SW_07 decreased from 0.21 to 0.03 after an initial increase possibly caused by component (bridge) collapse. This indicated, that for SW_07 there was large potential to decrease void space as a constant value was not reached, which is plausible considering the amount of compressible components in this composition.

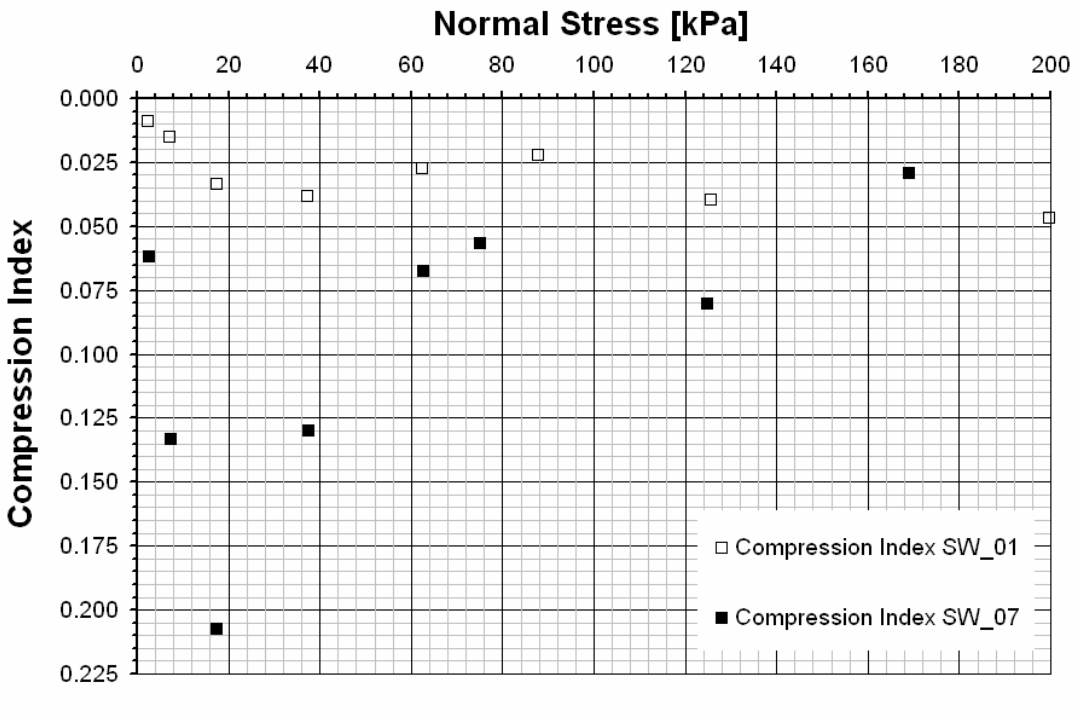

Figure 7-13 Compression indices for incompressible compositions SW_01, SW_07

The values for the compression index did not feature a constant decrease or a constant value towards the end of the test. As already mentioned, SW_01 showed values, which were fluctuating around 0.025. SW_07 exhibited a sudden increase up to about 25kPa normal stress, which is was also visible in the constrained modulus shown in Figure 7-12. As mentioned above, this phenomenon was observed regularly and was attributed to initial component bridge failure. It is also visible in composition SW_01, but at a much smaller scale, which could confirm the theory of bridge failure, as high compressible components were involved, which did not provide a resistance as the rigid components in SW_07 could.

7.4.1.3 Real Waste Simulation

In the following, results of the real waste simulation SW_09 are discussed. They are compared to the findings of the compressible composition SW_03, as this composition showed similar results (Figure 7-14). Judging from the compositions, SW_09 should illustrate similar behaviour to SW_03, as in both compositions a large amount of compressible components (in this case especially paper) is involved. Additionally, SW_09 comprised a large percentage of heavy but deformable components like clay lumps, which contributed to the comparatively high initial unit weight. Throughout the test, the unit weight stayed higher than in SW_03, even though SW_03 exhibited higher constrained moduli.

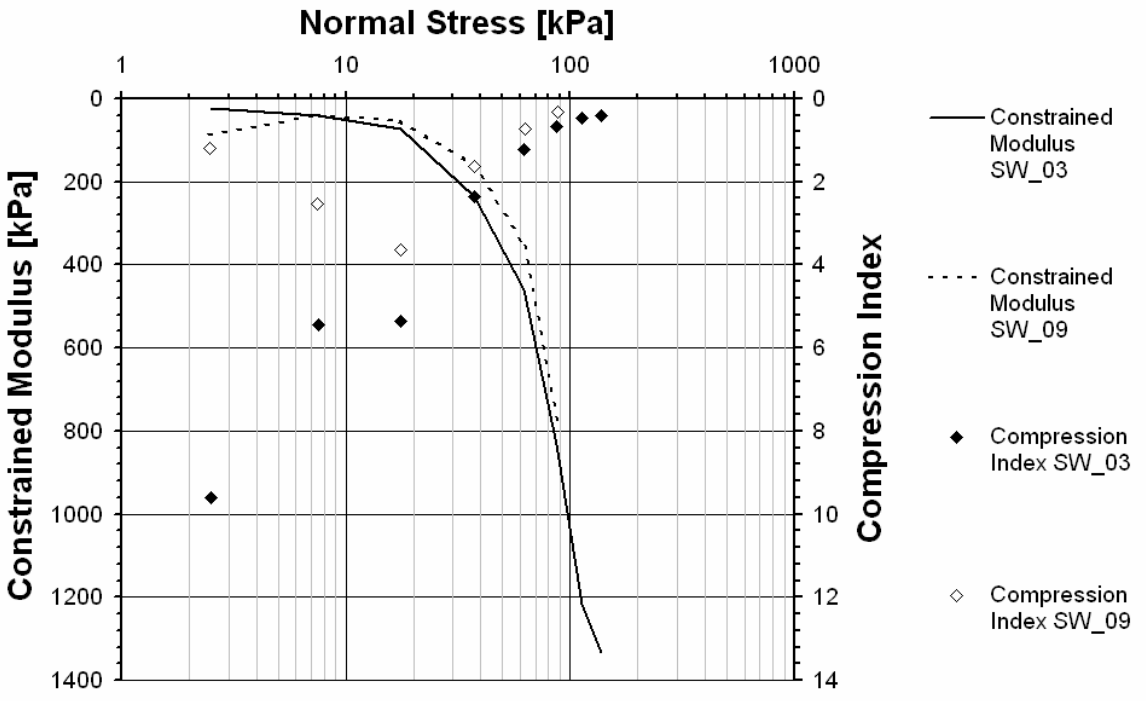

Figure 7-14 Constrained modulus and compression index for the compressible composition SW_03 and the real waste simulation SW_09

Constrained Modulus

Composition SW_09 compression behaviour was very similar to the compressible compositions, as it also featured large amounts of compressible components. The constrained moduli for SW_03 and SW_09 are shown in Table 7-5 and Figure 7-15. SW_09 exhibited continuously lower values than SW_03. SW_03 possessed a higher amount of brick fractions and tyre shreds, i.e. a high amount of incompressible components were present in SW_03. Additionally, the amount of aluminium cans in SW_03 exceeded the amount used in SW_09. It was observed that these cans could build stable material bridges (Figure 5-11), i.e. lightweight components could result in relatively high constrained moduli, as it is indicated by the comparison of the unit weight in Table 7-5.

Table 7-5 Normal stress range, unit weight and constrained modulus for the incompressible compositions SW_01 and SW_07

	SW_03		SW_09	
Normal Stress Range [kPa]	Constrained Modulus [kPa]	Unit weight [kN/m^3]	Constrained Modulus [kPa]	Unit weight [kN/m^3]
0-5	22	0.71	87	1.10
5-10	41	0.97	41	1.19
10-25	74	1.27	51	1.62
25-50	236	1.71	161	2.40
50-75	460	2.10	354	3.15
75-100	834	2.38	778	3.69
100-125	1215	2.60	-	-
125-150	1333	2.81	-	-

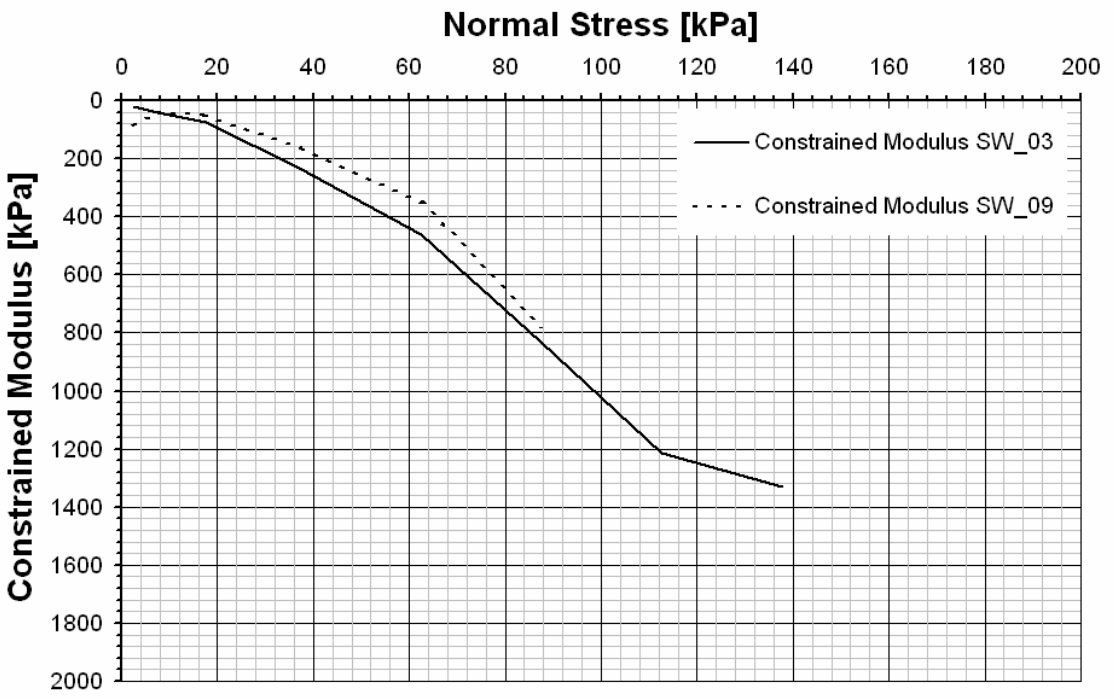

Figure 7-15 Constrained modulus for SW_03 and SW_09

Compression Index

Figure 7-16 presents the compression indices of SW_03 and SW_09. The real waste simulation reached values, which were lower than SW_03 and thus lower than values of the SW_02 series. After a short stage in the range of <17.5kPa normal stress with C_c

values increasing from initially 1.2 to 3.6, SW_09 continued decreasing to compression index values of 0.3.

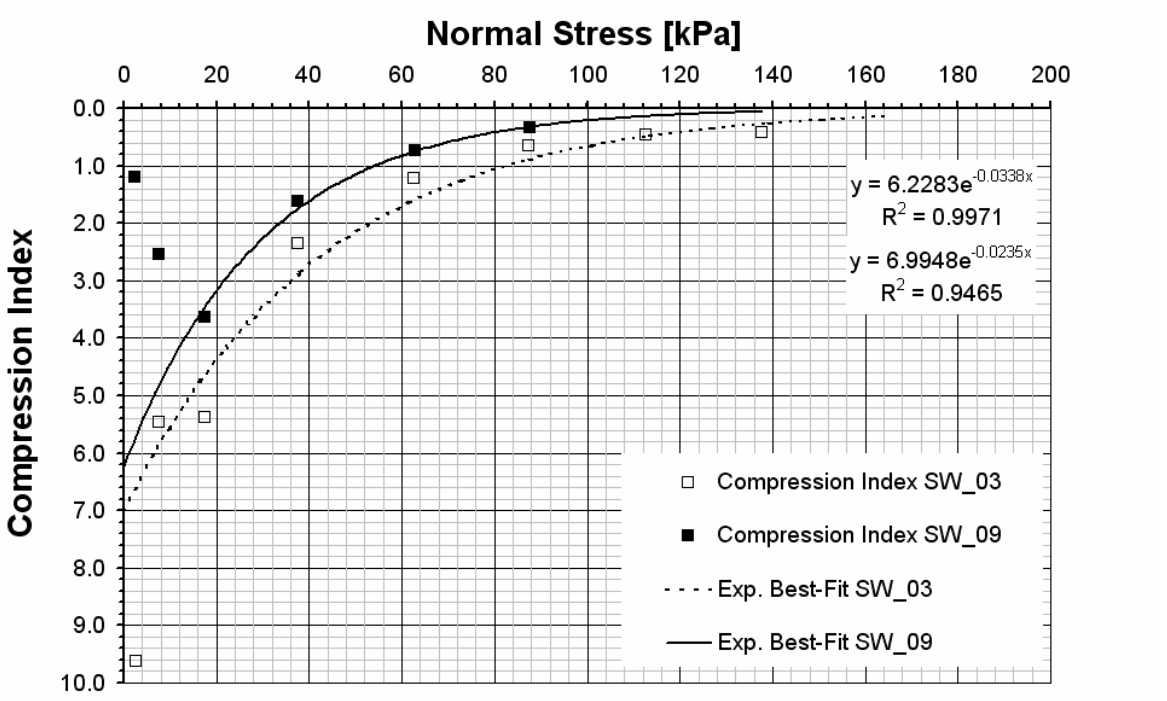

Figure 7-16 Compression indices for the compressible composition SW_03 and for the real waste simulation SW_09

As already shown for the SW_02 series and SW_09 in Figure 7-10, the starting phase (excluding the initial values, which showed increasing values) of the compression index could be described by an exponential best-fit line. This was also observed for SW_09. The exponential best-fit trend line in Figure 7-16 shows similar course similar to SW_03.

7.4.1.4 Mono-Component Composition

To examine the influence of a single dominant component, the mono-component composition SW_04 was tested in the compression device. The results from SW_04 are discussed and compared with the compressible composition SW_02_3, as these compositions show similar behaviour. SW_04 comprised a large amount of already compressed (flattened) aluminium cans and a small amount of rigid plastic packaging. Additionally, a tyre shreds and brick fraction were incorporated to this composition, which accounted for approximately half of the sample mass. Unlike SW_04, SW_02_3 did not possess any incompressible materials like bricks or tyre shred but a similar amount of low compressible components as in SW_04 was included. Figure 7-17 shows constrained moduli and compression indices for SW_02_3 and SW_04. A striking observation is the similarity between the compression indices of both compositions.

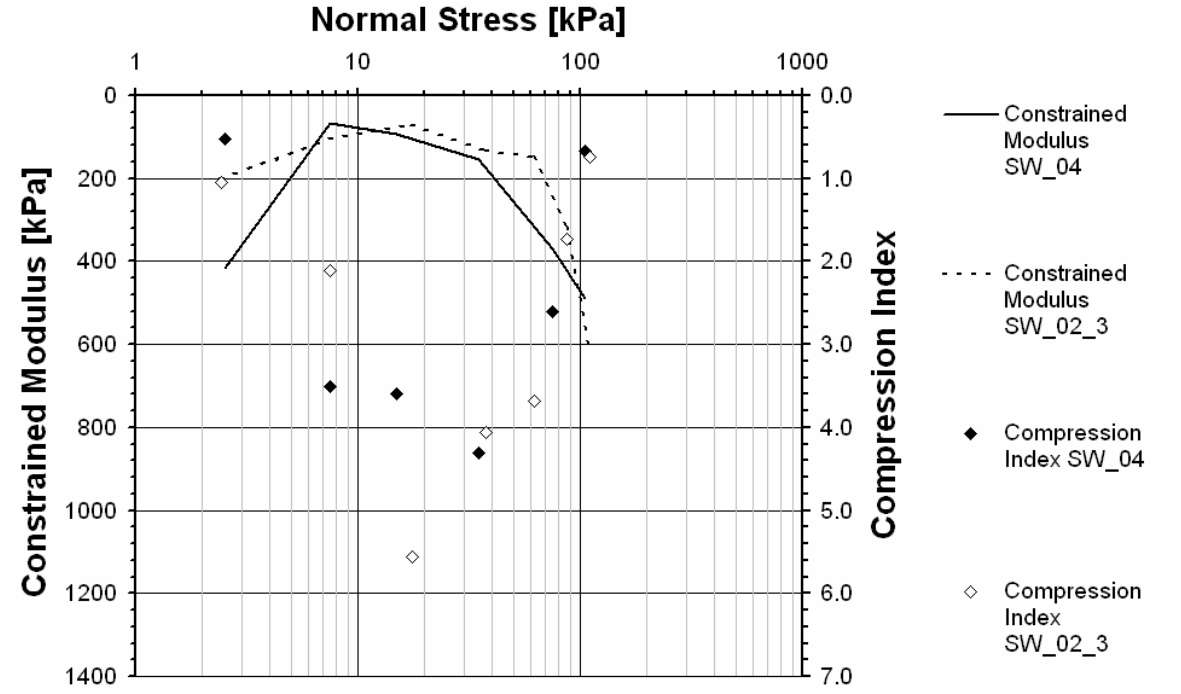

Figure 7-17 Constrained modulus and compression index for the mono-component composition SW_04 and for the incompressible composition SW_07

Constrained Modulus

The constrained modulus for SW_04 in Figure 7-19 shows an constant relationship, which was possibly due to aluminium cans dominating the composition. This is obvious from Figure 5-13, where a small amount of rigid plastic packaging is surrounded by a large (volumetric) amount of aluminium cans. The high mass content of tyre shreds and brick fractions is barely visible. It is suspected that the high volumetric amount of cans dominated the compression behaviour of SW_04. Even though the aluminium cans used in SW_04 were flattened, constrained moduli similar to those from SW_02_3 were found. This might be due to the structure that was built up during filling. As the cans were not fully flattened (Figure 7-18), a waste body structure could develop, which was interspersed with large void spaces.

Figure 7-18 Typical flattened aluminium can

Table 7-6 and Figure 7-19 show a constant increase of the constrained modulus of SW_04. The gradient was slightly changed between 35 and 75kPa normal stress, but continued evenly thereafter. Between 7.5kPa and 35kPa the SW_04 showed a similar gradient as SW_02_3, but shifted down by 20kPa. Both lines meet at 98kPa normal

stress, which was due to SW_02_3 exhibiting a high increasing constrained modulus. At normal stresses between 15kPa and 98kPa SW_04 provided higher moduli than SW_02_3 due to the large amount of aluminium cans and incompressible component. At normal stresses >98kPa SW_04, it showed lower stiffness values than SW_02_3. It must be mentioned that towards the end of tests SW_04 cracking noises of the load plate were audible. Of course, this must have resulted in a qualitative and quantitative reduction of the load transfer, which caused lower stiffness values of SW_04.

Table 7-6 Normal stress range, unit weight and constrained modulus for SW_02_3 and the mono-component composition SW_04

	SW_02_3		SW_04	
Normal Stress Range [kPa]	Constrained Modulus [kPa]	Unit weight [kN/m^3]	Constrained Modulus [kPa]	Unit weight [kN/m^3]
0-5	200	0.49	416	0.78
5-10	106	0.52	67	0.81
10-25	70	0.61	169	0.92
25-50	135	0.81	367	1.13
50-75	148	1.37	373	1.51
75-100	317	1.56	488	1.64

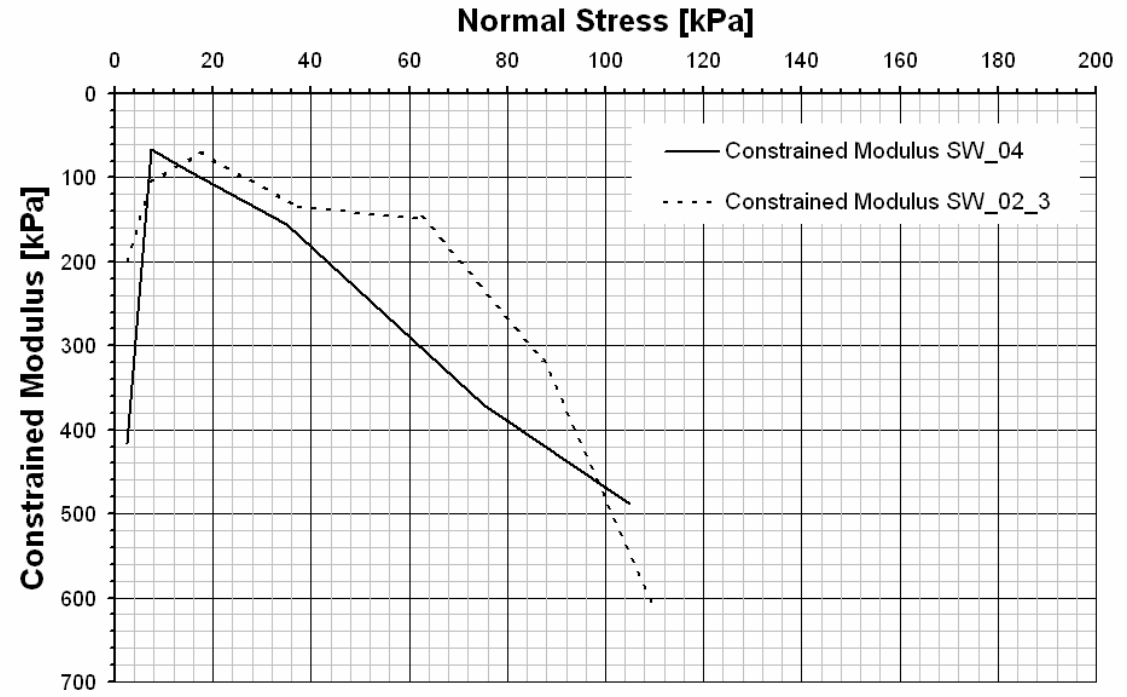

Figure 7-19 Constrained modulus for the mono-component composition SW_04 and the compressible composition SW_02_3

Compression Index

The compression indices for both compositions similarly ranged between 0.7 and 5.6 as shown in Figure 7-20. SW_02_3 possessed slightly higher values as a lot of compressible components were involved as already described before. They also exhibited a similar course, i.e. an increase up to 17.5kPa normal stress and a decrease from 17.5kPa onwards, reaching a value of 0.7 at their highest normal stress.

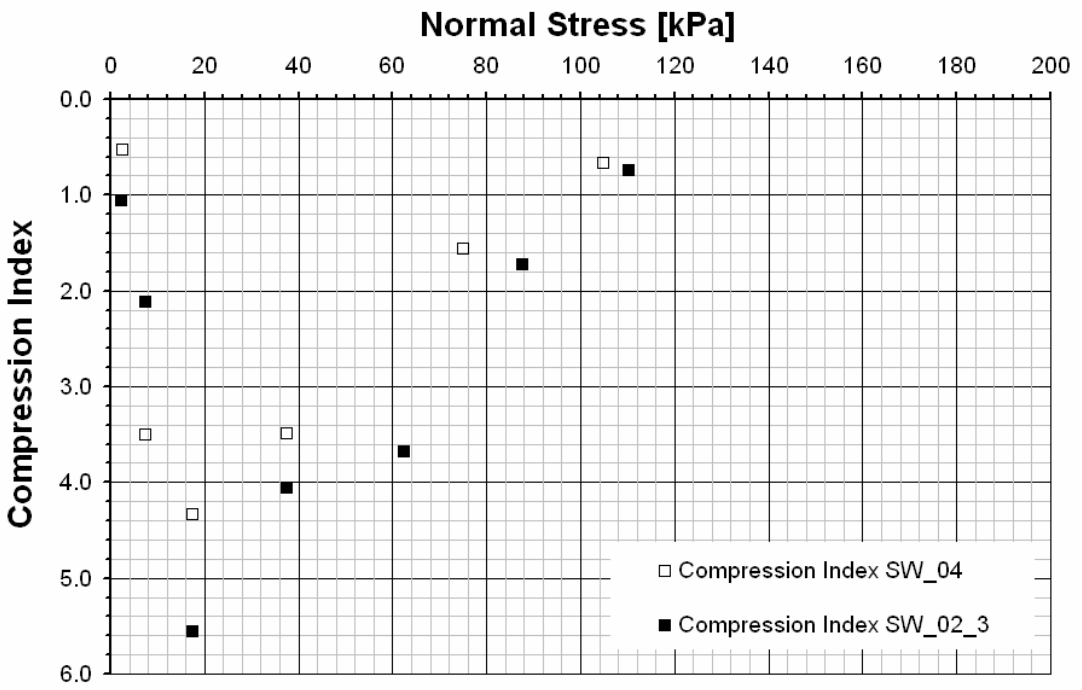

Figure 7-20 Compression indices for the compressible composition SW_02_3 and for the mono-component composition SW_04

7.4.2 Assessment of the Compositions Based on Similar Stress Levels and on Similar Sample Heights

Table 7-7 demonstrates a comparison of the compression tests on basis of similar normal stress levels (33.5kPa<σ<39.1kPa, average 35.7kPa) and similar sample heights (433mm<h<445mm, average 439mm) to visualise the differences and similarities of the chosen compositions. In addition to the two parameters mentioned above, the unit weight at the particular stage of each compression test is also given. It has to be borne in mind that the sample heights given in Table 7-7 are averaged out of two measured values (front and back of the load plate). Moreover, possible discrepancies between sample heights and pictures are derived from the limited view, one has on the sample, as only the front part, but not the back of the sample is visible from the pictures shown.

As expected and implied in chapter 5, the compressible compositions (SW_02_1 and 2, SW_03) possessed the lowest sample heights at the comparison of similar stress levels due to its high compressibility. SW_02_3 showed a comparable unit weight to SW_02_1 at almost twice the sample height, which was plausible considering the double amount of sample of SW_02_1 incorporated in SW_02_3.

Table 7-7 Compression tests at similar normal stress levels and sample heights

	SW_01	SW_02_1	SW_02_2	SW_02_3	SW_03	SW_04	SW_07	SW_09
33.5kPa<σ<39.1kPa								
σ [kPa]	39.1	36.0	33.5	34.7	36.1	34.6	36.1	35.9
h [mm]	528	190	243	387	229	433	503	269
γ [kN/m³]	11.96	0.87	0.68	0.85	1.70	1.11	9.06	2.42
433mm<h<445mm								
σ [kPa]	251.3	6.7	8.2	27.0	5.0	34.6	85.4	15.0
h [mm]	438	444	445	438	439	433	442	434
γ [kN/m³]	14.43	0.37	0.37	0.75	0.88	1.11	10.33	1.50

SW_02_2 showed slightly lower normal stress values and thus a higher sample height than SW_02_1. SW_03 and SW_09 resembled a similar character. SW_09 had 40mm less settlement at a higher unit weight. The mono-component composition SW_04 exhibited a sample height, which was comparable to the incompressible compositions due to its high volumetric amount of aluminium cans. The incompressible compositions SW_01 and SW_07 exhibited high sample heights, i.e. the lowest compression at this stress level.

Similar results derive from the comparison at similar sample heights. The lowest normal stress was found at the high compressible compositions SW_02_1 and 2, and SW_03. SW_02_3 exhibited at double unit weight more than three times higher stress than SW_02_1 and 2. Compared to the mono-component composition SW_04, the real waste simulation SW_09 displayed a much lower stress at the same sample height. As the unit weight of SW_09 was higher than SW_04, it confirmed the rigidity of the aluminium can composition. As expected, SW_01 and SW_07 exhibited the highest normal stresses.

7.4.3 Comparison of the Synthetic Waste's Compression Behaviour to Data from the Literature

Figure 7-21 depicts the results from the compression test with data from literature. The values Burntstump 1 and 2 are derived from field test analysis stated in Dixon *et al.* (2004). Landva et al. (2000), Beaven and Powrie (1995), Jessberger and Kockel (1993), Powrie and Beaven (1999) and Watts and Charles (1999) are also illustrated in Dixon et al. (2004). The values from Beaven and Powrie (1995) and Powrie and Beaven (1999) were results from large compression tests on real waste on the Pitsea compression cell. The red straight line is a recommendation value for fresh waste from the DGGT (1997).

It is obvious that most results from the laboratory compression tests range in normal stresses <150kPa, with the exception of SW_01 and SW_07. These were the compositions with a high Leighton-Buzzard sand ratio, which easily reached high stress levels. It is also obvious that the compression test results are distributed over a small range in the low normal stress levels and also fall within the range of the data provided in the literature. The sand composition SW_01 describes in stress levels <100kPa an upper bound for the synthetic waste (lower dashed red line), while the compressible composition SW_02_3 describe the lower bound (upper dashed red line). For the stress level <100kPa, all other synthetic waste composition fall within this bound. The GDA recommendation line is found in the middle of these bounds. The majority of the data from the literature, e.g. the data provided Jessberger and Kockel (1993) and Watts and Charles (1999) settles between the recommendation line and the upper bound, i.e. it expresses a higher stiffness, while most of the data from Landva et al., (2000), Beaven and Powrie (1995) and Powrie and Beaven (1999) is found near the recommendation line and above, respectively, i.e. the lower bound, and thus displays a less stiff waste. The Burntstump data stated in Dixon et al. (2004) is ranged in the area with high stiffness and exhibits values similar to Watts and Charles and Jessberger and Kockel (1993). For both, the Burntstump data and for the combination of the data from Landva et al. (2000), Beaven

and Powrie (1995) and Powrie and Beaven (1999) a trend line is depicted in the data collection.

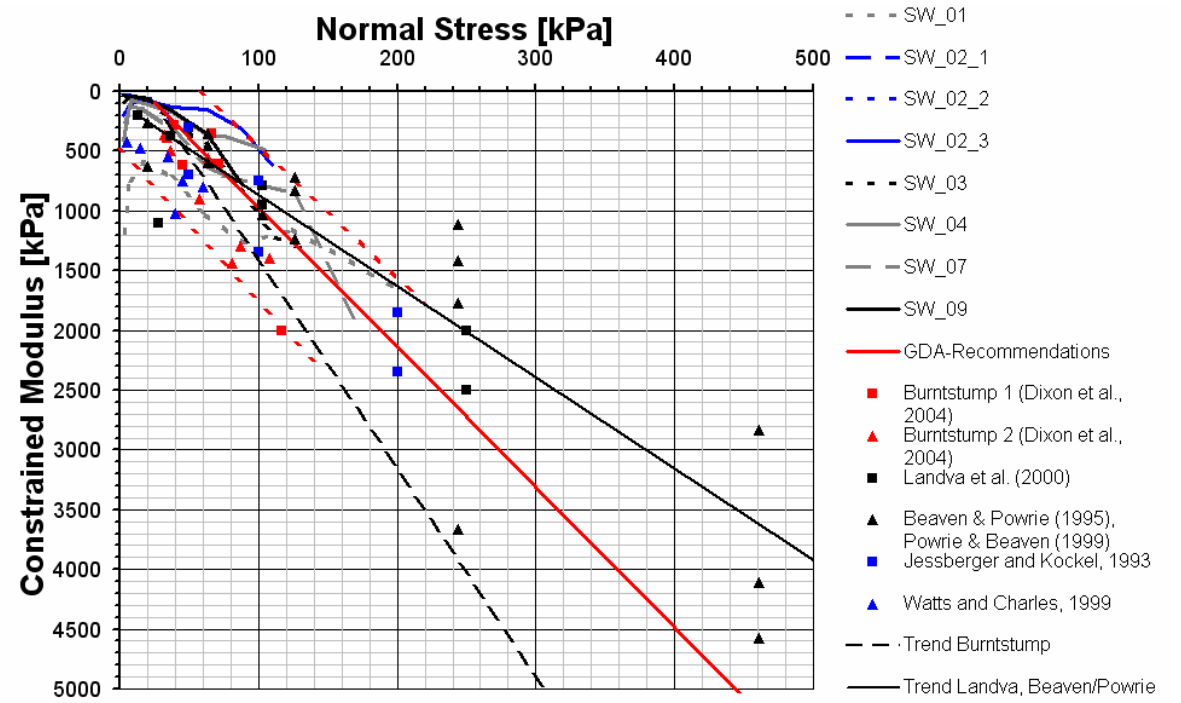

Figure 7-21 Linear best-fit line of the constrained modulus: Comparison of test results and data from the literature

7.4.4 Component Shifting within the Shape-related Subdivisions

The compositions SW_02_2, SW_02_3, SW_04 and SW_09 were analysed for examining the component shifting as stated in chapter 5.6. The results are shown in Figure 7-22. The initial component ratio is shown as an “A”, the final mass ratios are marked with a “B” in front of the composition name in the ternary diagram.

Generally, a shifting from compressible components towards reinforcing components was visible for all compositions. The percentage of incompressible components was barely changed. With the definition of reinforcing components as stated in section 4.2.1.3, a decision was made, whether a component is reinforcing (i.e. at least twice as large as the majority of the surrounding components) or incompressible. In the present tests most of the flattened components were therefore defined as being reinforcing. Thus the component ratios were altered towards reinforcing components.

It has to be borne in mind that most of the waste compositions were not only composed of a mixture of spherical and sheet-like components as shown in the scheme in Figure 4-3, but of components with similar sizes and shapes. For example, 80% of the sample mass of the compressible composition SW_02_2 comprised components in the size range 120-500mm in the reinforcing and high and low compressible shape-related subdivision. Nevertheless, the waste was highly reinforced as shown in Figure 7-23. This figure depicts two separate parts of a horizontal layer (red frame) found in SW_02_2 during the examination of the sample after compression. Both parts represent a tight connection of

reinforcing components due to component interlocking and overlap. Horizontal layering is also visible from Figure 2-15 by Kölsch (1996).

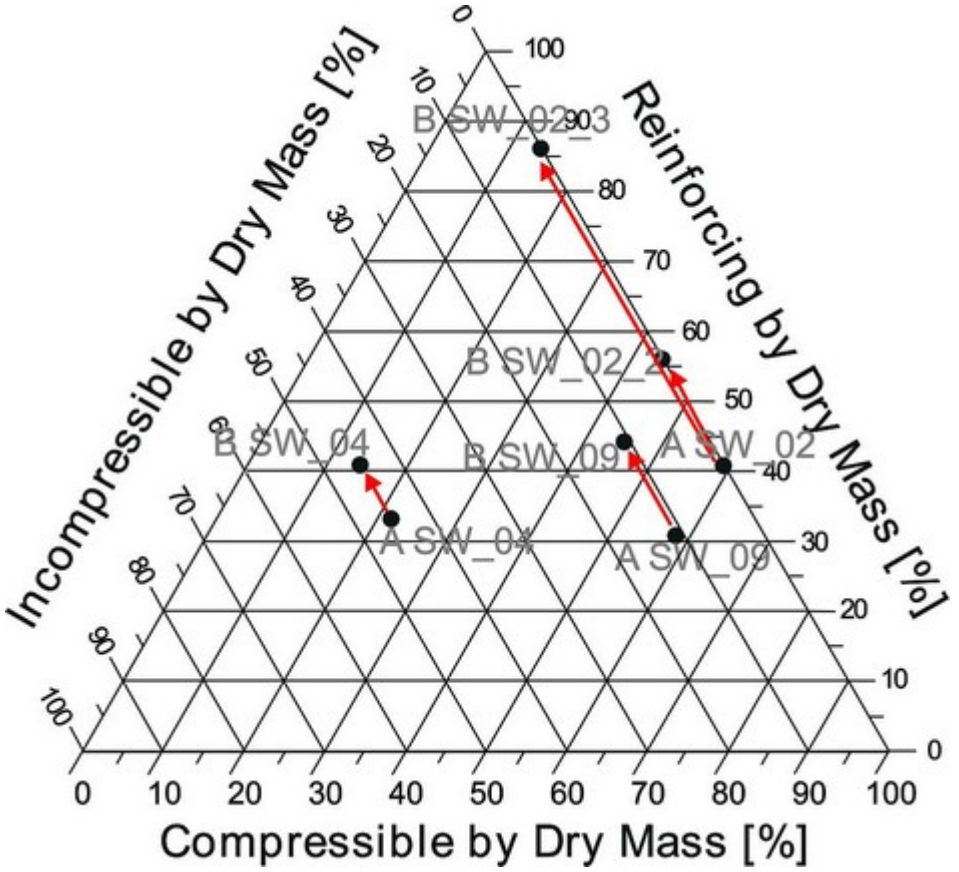

Figure 7-22 Shifting of the shape-related subdivisions of the synthetic waste compositions before and after compression

Figure 7-23 Composition SW_02_2: Visual analysis of horizontal component agglomerations after compression

From this observation it could be concluded that the definition of reinforcing components has to be widened, as MSW components comprise not a majority of homogeneous spherical interspersed by sheet-like reinforcing components, but there is also the possibility of a large amount of reinforcing components, which build up a relatively stable bond. Therefore, the definition of reinforced components not only comprises the distinction

of spherical and sheet-like components, but also has to be related to an interlocking of the potentially reinforcing components. In this case, the relative position of the components regarding other components is crucial, i.e. the overlap of components, and also the interaction of components, i.e. the interlocking and bending (e.g. it is visible in the left part of Figure 7-23 that paper bent around a flexible plastic bag and the opening of a aluminium beverage can deformed and clamped paper sheets, the right part shows interlocking of different components like cans and rigid plastic with paper and textiles).

7.4.5 Findings of Compression Behaviour

The compression behaviour of the family of synthetic waste compositions for normal stresses of up to 200kPa ranged within boundaries obtained from the literature. Compositions dominated by Leighton-Buzzard sand with high unit weights (SW_01 and SW_07) exhibited expectedly high values for the constrained modulus, while compositions with a high ratio of lightweight and compressible components (SW_2 series, SW_03, SW_09) showed low values for the constrained modulus. Higher normal stresses could not be reached due to the limitations of the compression device.

The boundaries for the constrained modulus from the literature were derived from data published by Dixon *et al.* (2004) for the upper bound, and from Landva *et al.* (2000), Beaven and Powrie (1995) and Powrie and Beaven (1999) for the lower bound. A good approximation for an average trend of these boundaries was provided by the DGGT (1997).

Considerable differences were found in comparing the compression behaviour of the examined synthetic waste compositions. SW_01 and SW_07 resulted in high constrained moduli and low compression indices due to a high amount of sand and thus relatively low void spaces. While the SW_02 series and SW_03 exhibited similar low constrained moduli and high compression indices due to the large amount of voids caused by high compressible components (e.g. compartments like tubs and cans with high intraparticular voids. The mono-component composition SW_04 showed similar behaviour to SW_02_3, though the material involved (aluminium cans) in SW_04 appeared to be more rigid than SW_02_3. Both resulted in similar C_c values. The behaviour of the real waste composition was comparable to the compressible composition SW_03, with similar constrained moduli and compression indices.

The test results could generally be divided into high compressible behaviour and low unit weight (SW_02 series, SW_03, SW_04 and SW_09) and low compressible behaviour and high unit weight (SW_01 and SW_07). Further refining of the synthetic waste compositions is necessary to access the behaviour for compositions in between these test results.

7.5 Shear Behaviour

7.5.1 Performance Validation of the Large Shear Box

The performance validation of the shear box comprised two stages. One stage was the assessment of the rolling resistance, the second stage was a test set on Leighton-

Buzzard sand, which was subsequently compared to a test set performed in a small-scale shear box to assess potential differences in the results of small- and large-scale shearing. Moreover, repeatability of test results was examined.

Large- and Small-Scale Shear Tests on Leighton-Buzzard Sand

Figure 7-24 depicts the stress-strain curves for small- and large-scale shear tests. The displacement was converted to strain for comparison of both test types. The differences between the tests are clearly visible. The small-scale tests resulted in higher shear stresses. Especially for high normal stress levels (σ' > 50kPa), higher values were reached in the small-scale device. The reason might be a difference in the unit weight, as the unit weight for the small scale was 17.7 kN/m^3 and the unit weight of the tests in the large shear device resulted in 16.5kN/m^3, i.e. the comparably dense sample in he small shear device resulted in a higher shear stresses than in the large shear device.

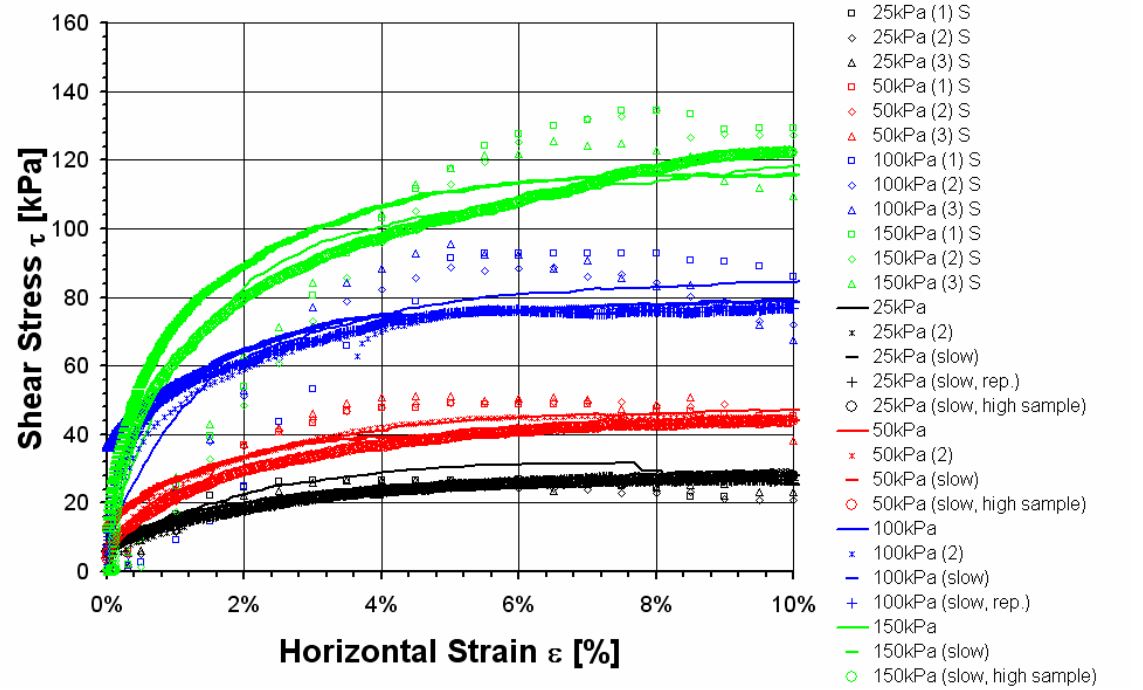

Figure 7-24 Shear stress-strain curves for the small- and large-scale shear tests on Leighton-Buzzard sand

Though the difference in the unit weight appeared to be relatively small, it was reflected in the shear behaviour. From Figure 6-7 for the large-scale tests and from Figure 6-11 for the small-scale tests, it is also obvious, that the shear behaviour was different. The small-scale tests displayed a dilatant behaviour (typical for a dense material), while sample of the large scale test contracted (typical for a loose material). Another reason could be found within the scale and thus the device-specific conditions. As the large device was built out of steel segments, which were bolted together, there was a high possibility that the bolts slightly loosen during the course of the test, which was confirmed by the observation that bolts had to be tightened after testing. This implied that the large-scale shear device could also move vertically to a very limited extent. It was also observed that the roller bearing started to bend, especially at high normal stresses. As one of the roller

bearings was running on a curved guide rail, this could aggravate a lifting effect of the upper box during shearing, which would result in a decrease of the sample height, as the vertical displacement transducers were attached to the upper box. Nevertheless, it must be mentioned that these effects would produce a very small range of vertical displacement, but they would amplify the observation of contractant behaviour of a sample in the large shear device.

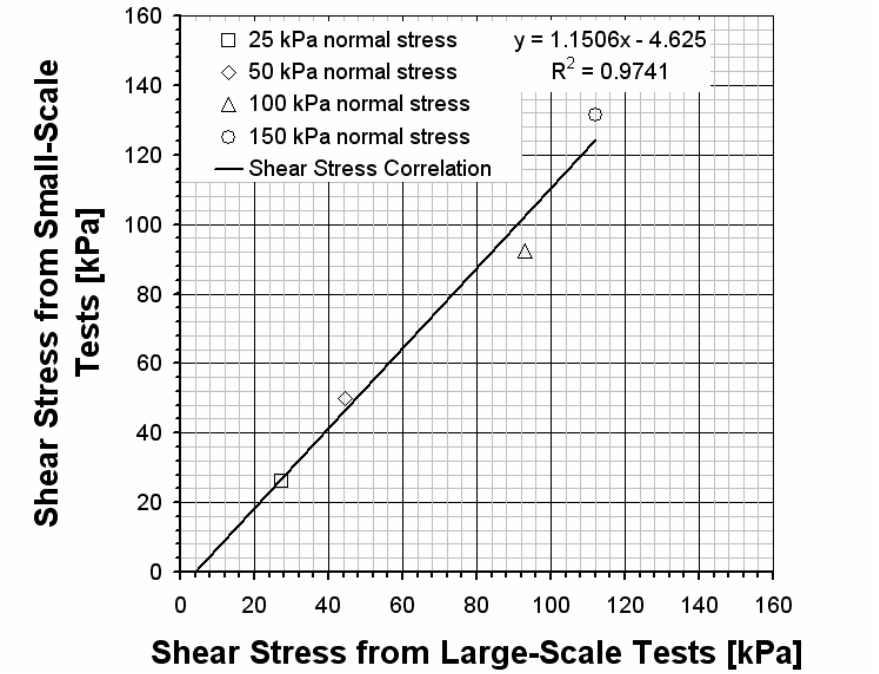

Figure 7-25 Correlation between the shear stress of large- and small-scale shear tests on Leighton-Buzzard sand

The Mohr-Coulomb envelopes in Figure 6-13 provide a direct comparison of the large- and the small scale tests. As the small-scale tests resulted in generally higher shear stresses than the tests in the large shear box, the friction angle exceeded the values from the large-scale tests. The friction angle, which was derived from the average shear stresses for each normal stress level of the small-scale tests resulted in 42.0°, and the tests in the large-scale device produced an average friction angle of 39.2°. This meant a difference of 2.8°. Figure 7-25 demonstrates the correlation between the shear stresses recorded for the tests. The difference between the two test types is obvious, as the large shear device resulted in lower values. The gradient of 1.15 implies that the shear stress difference between small- and large-scale test increases, as the normal stress level raises.

Repeatability

The repeatability of test results was examined by repeating tests in the large shear device. Figure 6-3 shows the results for a high shear rate of approximately 10mm/min. The repetitions of the tests at a normal stress of 25kPa, 50kPa and 100kPa exhibited good accordance. The tests on a normal stress of 25 did not differ with a small exception at the beginning of the test, but the higher shear stress at set 1_2 resulted from a slightly higher

normal stress than test set 1_1. After re-adjusting of the normal stress, the shear stress values also decreased to values that matched the preceding test set. The tests on 50kPa showed only a marginal difference of less than 5kPa shear stress after 80mm displacement. It has to be borne in mind that the shear stress increased for almost all tests with increasing displacement. From Figure 6-4 a threshold is visible. At a normal stress of 50 and 100kPa the shear stress levelled at approximately 40mm displacement and started increasing from displacement of 55mm onwards. Moreover, Figure 6-4 shows matching values for a repetition of two tests on a normal stress of 25kPa.

The results for repeatability of test yielded satisfactory results, as there were no significant differences between tests with identical boundary conditions on low normal stresses (test set 1_1 and 1_2 on 25 and 50kPa). At high normal stresses (test set 1_1 on 100kPa) the differences had an acceptable range.

Rolling Resistance of the Large Shear Device

The impact rolling resistance on the shear stress values had to be assessed twice, as after a material failure of the upper frame, the shear device had to be repaired. After that, a new calibration of the device was required. Generally, the rolling resistance resulted in low values, as shown in Figure 6-16. Table 7-8 summarises the data for three different calibrations conducted on the large shear device. The calibration done by Aboura (1999) is shown for comparative reasons. Since the calibration was conducted, changes were applied to the shear device, such as a new horizontal jack and a new coating. The first and second calibration reflects the rolling resistance directly before and after the necessary reparation during this project. It is obvious that for the second calibration, the rolling resistance could be reduced to half the value of the first calibration.

Table 7-8 Overview of the calibrations of the large shear device (normal stress, and shear stress values for correction)

	Aboura (1999)	1st Calibration	2nd Calibration
Normal Stress	Shear Stress	Shear Stress	Shear Stress
[kPa]	[kPa]	[kPa]	[kPa]
25	2.41	1.25	0.58
50	4.81	2.50	1.15
100	9.63	5.00	2.30
150	n.d.	7.50	n.d.

7.5.2 Assessment of the Shear Test Sets

In the following sections, the results from the large shear tests on the synthetic waste compositions SW_01 to SW_09 are discussed. As for the compression tests, similar waste compositions are compared being compressible, incompressible, mono-component

compositions and the real waste composition. The shear stress-displacement curves at a normal stress of 50kPa are shown for each composition in order to compare the shape of the curves and thus the shear behaviour.

7.5.2.1 Compressible Compositions

Figure 7-26 shows the shear curves for the compressible compositions SW_02 and SW_03. The curves exhibit a similar shape. SW_03 reached a higher value for the mobilised shear strength and also featured a peak potentially caused by components jammed between load plate and the edge of the bottom box. For both tests, the shear moduli at the initial part of the curve and for the reload loop at 50kPa normal stress were relatively close, as shown in the subsequent table:

Table 7-9 Shear moduli for SW_02 and SW_03 at 20% horizontal strain (equal to 200mm displacement)

		SW_02	SW_03
$G_{Initial}$	[kPa]	619	651
G_{Reload}	[kPa]	957	1091

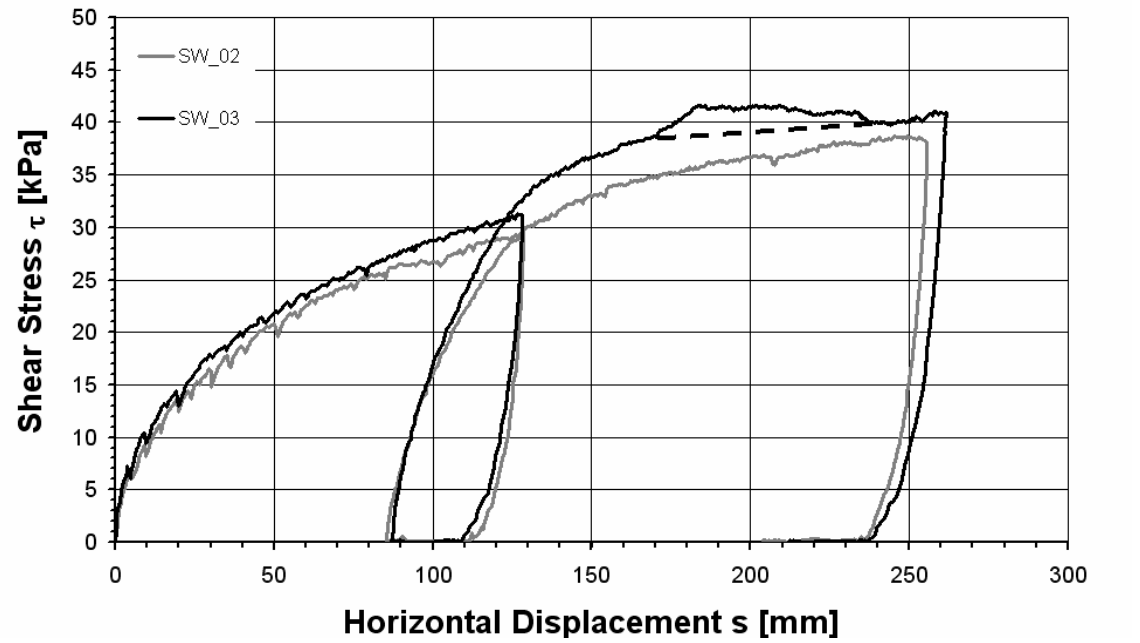

Figure 7-26 Comparison of the shear curve for the compressible compositions SW_02 and SW_03 at a normal stress of 50kPa

SW_03 comprised a large amount of incompressible materials (tyre shreds and brick fractions) and less compressible material (no rigid plastic packaging) than SW_02 making the composition less compressible and resulting in a higher unit weight, the shear stress expectedly resulted in higher shear stresses and also higher shear moduli than SW_02. Generally, the final part, i.e. the part of the shear curve after the reload loop, differed considerably, as a higher shear stress was reached with the composition SW_03 than

with the composition SW_02. The initial part showed a parallel shear stress increase and the comparison of the reload loops resulted in a steeper shear stress increase of SW_03.

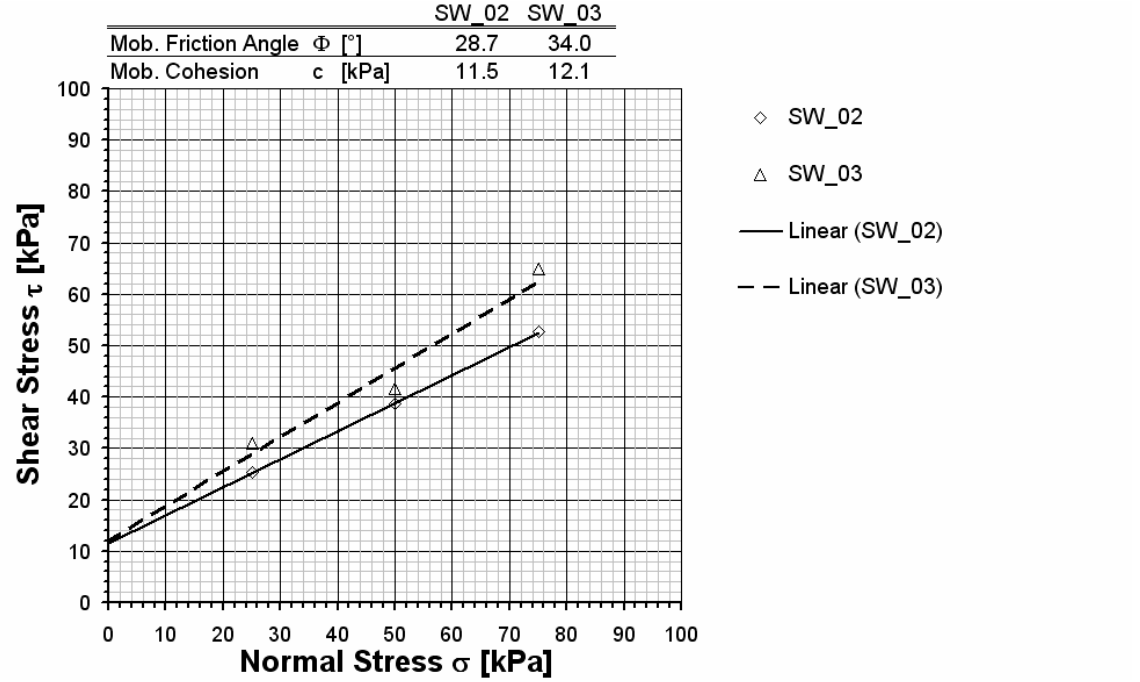

Figure 7-27 Mohr-Coulomb envelope for SW_02 and SW_03

The differences in shear stress are also reflected by the Mohr-Coulomb envelope shown in Figure 7-27. Both compositions exhibited a similar mobilised apparent cohesion, but SW_03 resulted in a higher mobilised friction angle than SW_02.

7.5.2.2 Incompressible Compositions

The shear stress-displacement curves for incompressible composition SW_01_1, SW_01_2, SW_06, SW_07 and SW_08 are shown in Figure 7-28. All samples were composed of a sand matrix. Additionally, the SW_01 series contained paper and flexible plastic, while SW_06 to SW_08 comprised amounts of aluminium cans and rigid plastic packaging. With one exception (SW_06), all compositions with Leighton-Buzzard sand matrix exhibited a constant and almost parallel increase of shear stress over the displacement. A flattening of the curves was not visible.

As SW_01_1 and SW_01_2 consisted of identical compositions (but different sample heights), the shear curves differed only slightly, as SW_01_1 resulted in higher shear stress in the initial stage of the shearing (before unloading). In comparison to the remaining compositions, the SW_01 series resulted in higher shear stresses. This might be a result of the reinforcing materials (flexible plastic and paper), which were mixed with the sand. In the compositions SW_06, SW_07 and SW_08 the amount of sand decreased and the amount of rigid plastic packaging and aluminium cans increased. This led to a higher compressibility (section 7.6). The elasticity visible from the rebound effect of the unload-reload-loop also increased with increasing amount of aluminium cans and plastic packaging. The shear moduli in For the SW_01 a large discrepancy of the shear moduli after unloading was observed. The test with a low sample height exhibited shear moduli,

which were higher than the shear tests on a large sample height. The large sample height could have resulted in a higher potential of particle rearrangement, which led to a shallower increase of the shear strength values and thus the shear moduli for SW_01_2.

Table 7-10 reflect this observation. The composition with the lowest ratio of compressible components (SW_06) exhibited the highest shear modulus for both, initial shear stress increase and increase after unloading, and composition SW_08 containing the highest amount of aluminium cans and rigid plastic packaging resulted in the lowest shear moduli.

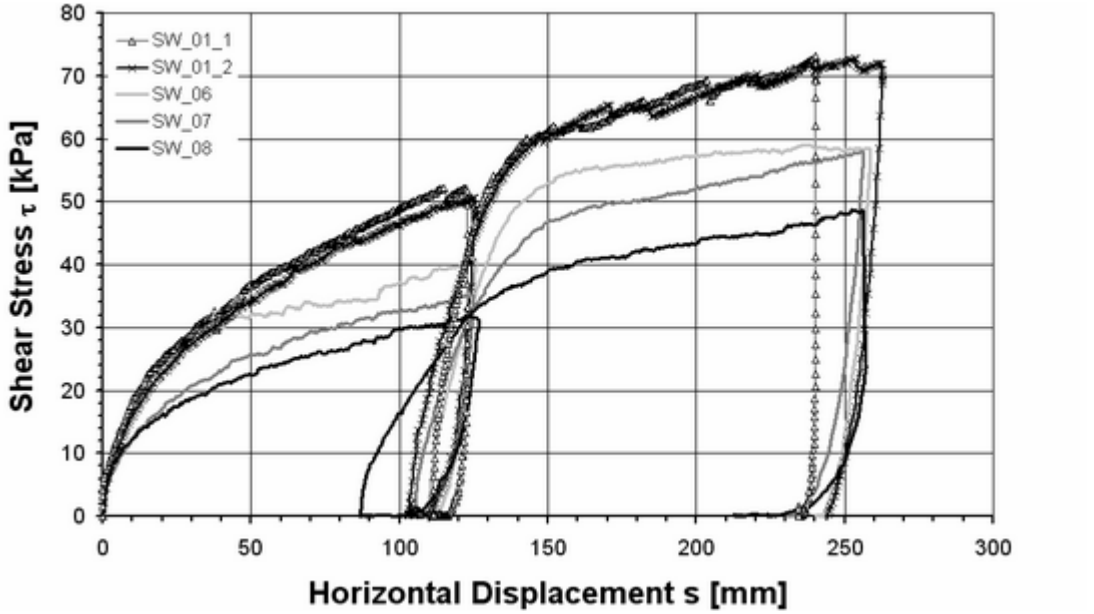

Figure 7-28 Comparison of the shear curve for the incompressible compositions SW_01 series, SW_06, SW_07 and SW_08 at 50kPa normal stress

For the SW_01 a large discrepancy of the shear moduli after unloading was observed. The test with a low sample height exhibited shear moduli, which were higher than the shear tests on a large sample height. The large sample height could have resulted in a higher potential of particle rearrangement, which led to a shallower increase of the shear strength values and thus the shear moduli for SW_01_2.

Table 7-10 Shear moduli for SW_01_1, SW_01_2, SW_06, SW_07 and SW_08 at 20% horizontal strain (equal to 200mm displacement)

		SW_01_1	SW_01_2	SW_06	SW_07	SW_08
$G_{Initial}$	[kPa]	1253	1151	1225	849	801
G_{Reload}	[kPa]	2708	2063	2020	1628	1051

Considering the intercepts of the linear trend lines of the Mohr-Coulomb envelopes in Figure 7-29, two groupings are visible. One group features the SW_01 series, the second groups consists of the sand matrix compositions with low compressible components (SW_06, SW_07, and SW_08). The mobilised friction angles varied between 34.2° and 43.3°. The SW_01 series featured the lowest mobilised friction angles, but the highest

apparent cohesion in the group of incompressible compositions, and the sand matrix compositions with low compressible components exhibited comparatively high mobilised friction angles, but low apparent cohesion.

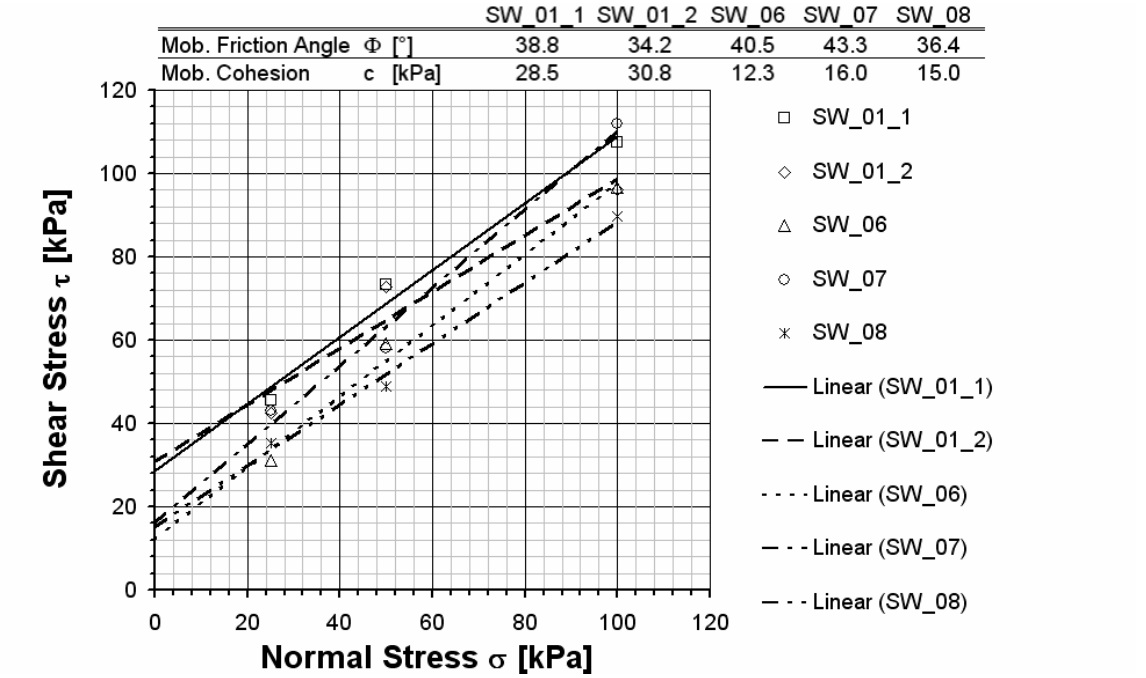

Figure 7-29 Mohr-Coulomb envelope for the compositions SW_01_1, SW_01_2, SW_06, SW_07 and SW_08

7.5.2.3 Mono-Component Compositions

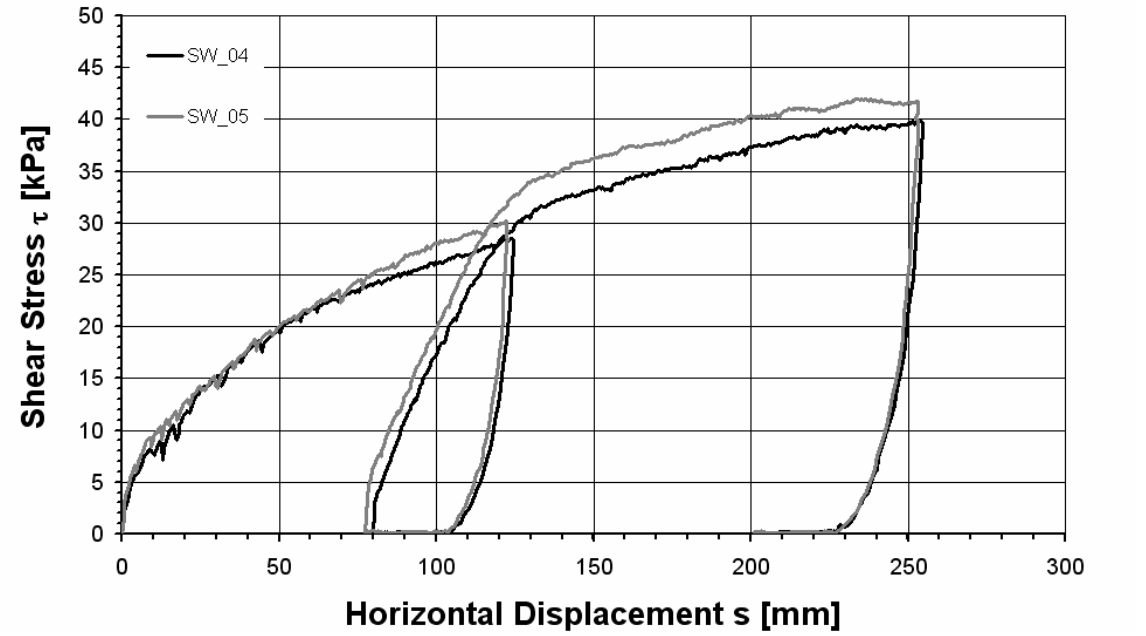

Figure 7-30 Comparison of the shear curve for the mono-component compositions SW_04 and SW_05 at a normal stress of 50kPa

Compositions SW_04 and SW_05 were dominated by aluminium cans. SW_04 also possessed a large percentage of incompressible components (tyre shreds and brick fractions), which amounted to 45% of the overall sample mass, but only for a very small percentage of volume. As a result, the volume of the incompressible components “disappeared” in the large volume of aluminium cans. This was also observed for the compression tests on the same composition (Figure 5-13).

Up to a displacement of 70mm, the shear curves were nearly identical. Thereafter, the shear stress for SW_05 increased. The unload-reload loop looked basically similar. The loop of SW_05 was shifted as a result of a shorter displacement before unloading.

Table 7-11 Shear moduli for SW_04 and SW_05 at 20% horizontal strain (equal to 200mm displacement)

		SW_04	SW_05
$G_{Initial}$	[kPa]	576	635
G_{Reload}	[kPa]	855	914

The shear moduli had a constant difference of approximately 60kPa between the two samples at the beginning of the test and after reload. The rebound effect differed insignificantly for the two tests either.

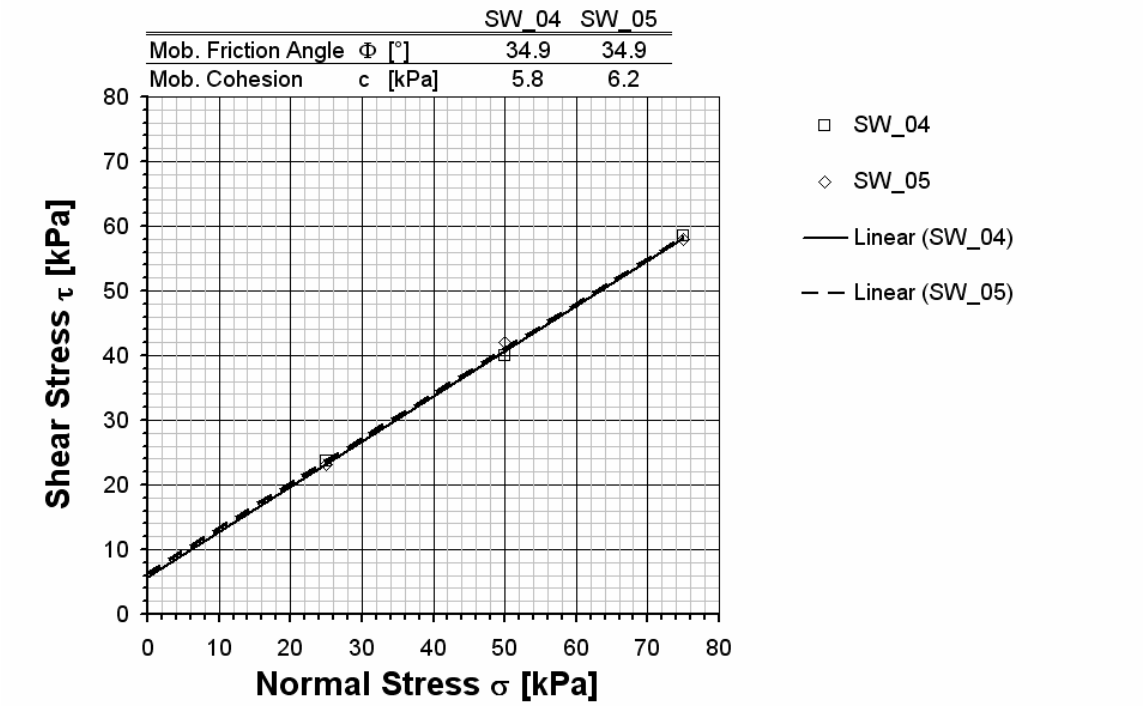

Figure 7-31 Mohr-Coulomb envelope for SW_04 and SW_05

Considering Figure 7-31, the biggest difference in these test sets occurred at 50kPa normal stress. At 25kPa and 75kPa, the maximum mobilised shear stress was almost identical. Thus the mobilised friction angles resulted in equal values (34.9°) and similar

apparent cohesion (5.8 and 6.2kPa). Different shear behaviour due to this kind of component variation (i.e. decrease of incompressible components and increase of compressible/reinforcing components) could not be detected.

7.5.2.4 Real Waste Simulation

In Figure 7-32, the real waste simulation SW_09 is compared to a compressible composition (SW_03), as a large percentage of compressible materials were involved in SW_09, and to a mono-component composition (SW_04), as a similar elastic behaviour was observed.

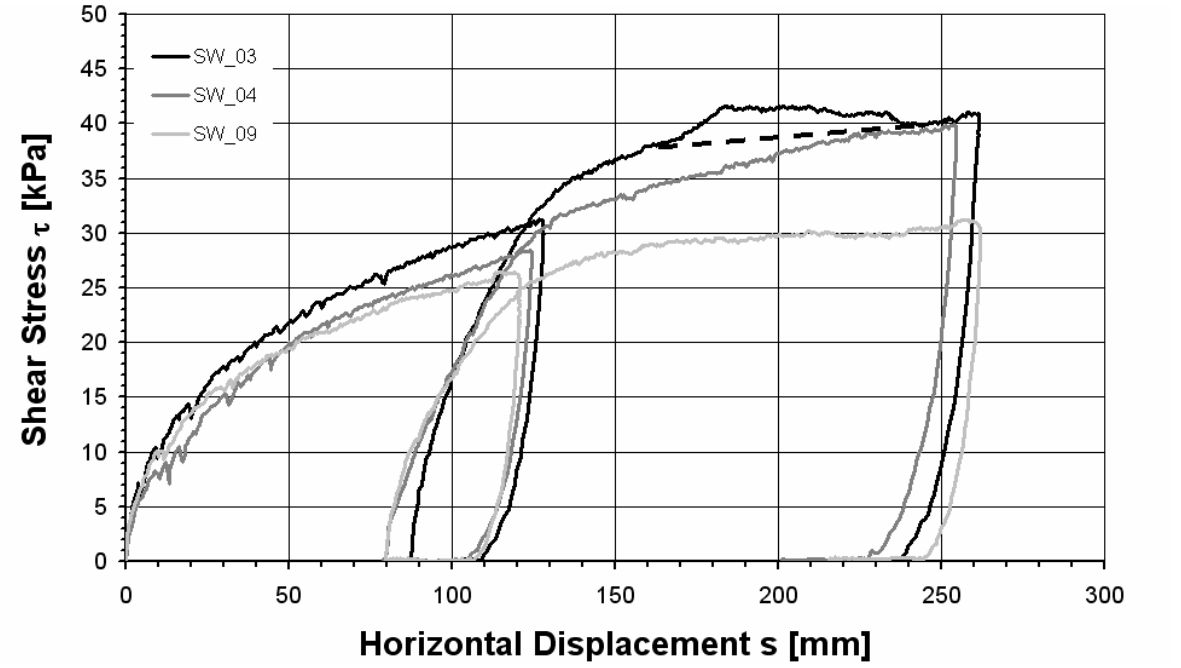

Figure 7-32 Comparison of the shear curve for the real-waste simulation SW_09, and SW_03 and SW_04 and at a normal stress of 50kPa

The compressible composition SW_03 resulted in the highest shear stress from the three compositions compared in Figure 7-32. It comprised the highest amount of incompressible materials and a higher unit weight than SW_04. The sample mass of SW_09 exceeded the mass of SW_03, but did not contain as many incompressible materials as SW_03. Clay made up for approximately 36% of the overall sample mass. But as it had a deformable character, it could not provide a high shear resistance. Moreover, as for the incompressible materials in SW_04, clay exhibited a high mass but a low volume and thus "vanished" between the reinforcing and compressible components like paper and plastic packaging (which was also visible from the compression test in Figure 5-15 and in Figure 7-33).

SW_09 and SW_04 showed a similar increase at the initial part of the test. Up to 50mm displacement, the shear stress increase of SW_09 was slightly higher than the increase of SW_04, after the displacement of 50mm, it flattened and the increase was less than the one of SW_04. Nevertheless, the shear stress of SW_03 and SW_09 was in a similar range up to 20mm displacement, which was also reflected by the shear modulus in Figure 7-12. The unload-reload loop of SW_09 resembled SW_04. SW_04 exhibited a marginally

bigger rebound, probably as a result of higher a shear stress. The shear modulus of the reload loop for SW_04 and SW_09 only differed by 22kPa. It has to be mentioned that they would differ at a strain after reload, which is larger than 25%, as obvious from Figure 7-32.

Figure 7-33 Synthetic waste composition SW_09

Table 7-12 Shear moduli for SW_03, SW_04 and SW_09 at 20% horizontal strain (20mm displacement)

		SW_03	SW_04	SW_09
$G_{Initial}$	[kPa]	651	576	678
G_{Reload}	[kPa]	1091	855	833

From the Mohr-Coulomb envelopes in Figure 7-34 similar mobilised friction angles of the three compositions in the range of 34° are recognisable. The mobilised apparent cohesion varied between zero (it was set to zero as the linear trend resulted in a negative intercept) for the real waste simulation and 12.1kPa for the compressible composition SW_03.

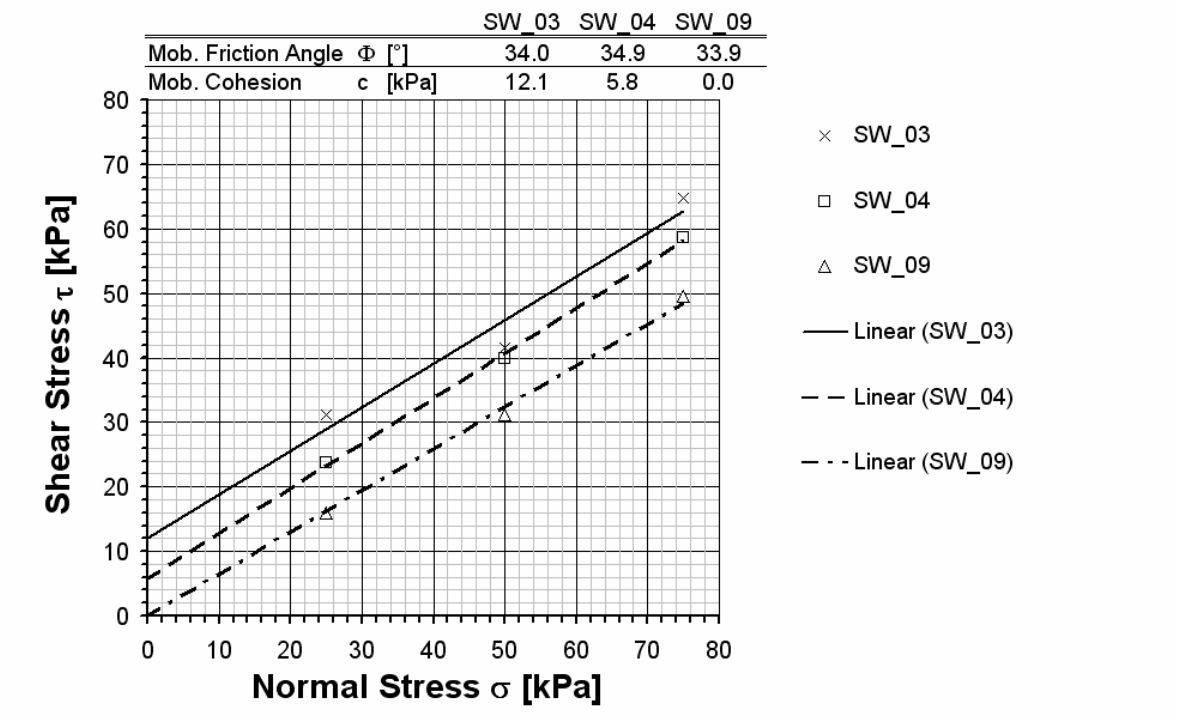

Figure 7-34 Mohr-Coulomb envelope for SW_03, SW_04 and SW_09

7.5.3 Qualitative Influence of the Unit Weight on the Shear Parameters

Figure 7-35 is an expansion of shear parameters from the literature (Figure 2-14). The results from the shear tests on synthetic waste conducted during this project were added.

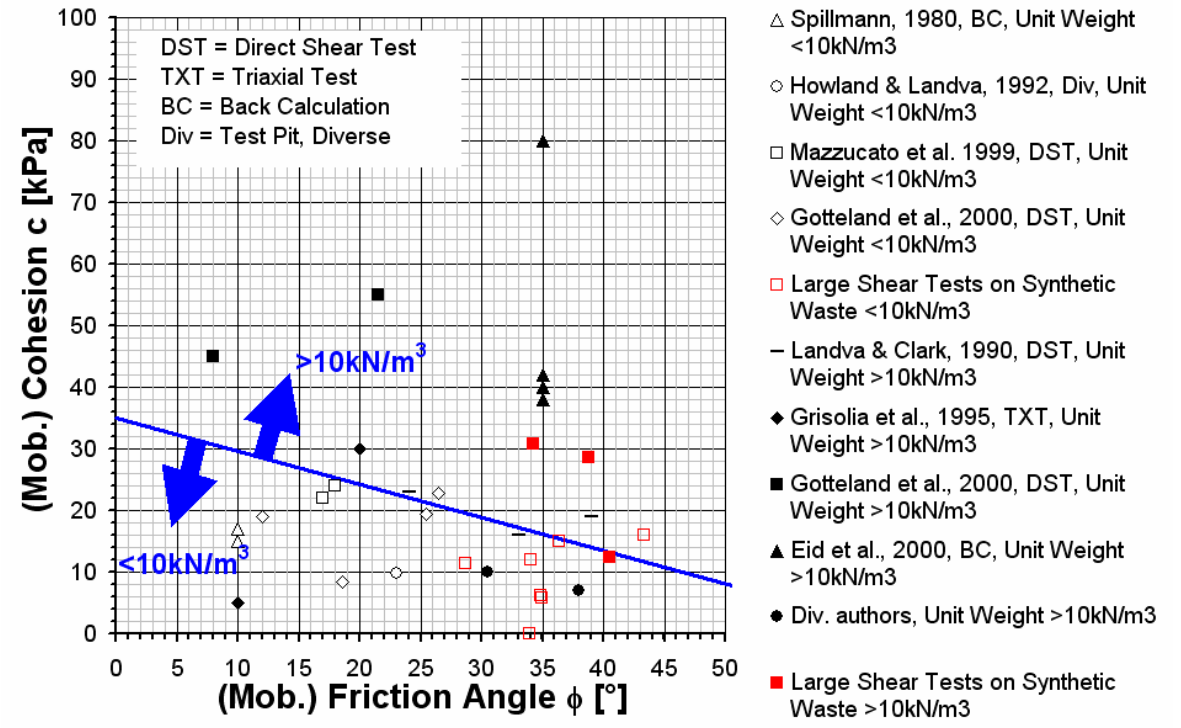

Figure 7-35 Qualitative influence of the unit weight on the shear parameters

The blue line in the figure depicts a rough threshold for unit weigh larger and smaller than 10kN/m^3. Below this line a concentration of pairs of friction angle and cohesion of sample with a low unit weight (<10kN/m^3) is visible, above cohesion and friction angles with a high unit weight (>10kN/m^3) are found. As this is a qualitative analysis and no further influences on the shear parameters were taken into account, only a trend is pointed out. A scatter of data beyond the boundary line is also obvious, as shear parameters resulting from sample with high unit weight are found in the area of the low unit weigh data concentration and vice versa. Generally, a definite influence of the cohesion is visible, i.e. a high unit weight apparently leads to high cohesion. The friction angle does not show a clear trend. A scatter of the data points is obvious and thus a data concentration or a trend regarding the friction angle is not identifiable.

For the quantification of the impact unit weight has on the shear parameters, further tests are necessary. Preferably, tests on an identical composition with different unit weights could be conducted to assess the influence of different unit weights on the shear behaviour of municipal solid waste.

7.5.4 Comparison of Synthetic Waste's Shear Behaviour to Design Data and Recommendations from the Literature

In the following, results from shear tests on synthetic waste are compared to shear parameters for MSW recommended for design and to general shear testing results on waste from the literature to assess and validate the representativeness of the synthetic waste. The design parameters and the shear test results in the literature were presented in different ways, i.e. in normal and shear stress diagrams (Mohr-Coulomb envelope) and in pairs of cohesion and friction angles.

As mentioned in chapter 2.2, Manassero *et al.* (1997) divided the Mohr-Coulomb envelope into four different areas. Zones A, B, and C (0kPa < σ <250kPa) are explained in Figure 7-36. An unknown zone in a high normal stress range (σ > 250kPa) could not be covered by the large shear tests conducted in the course of this work, as the normal stress only ranged between zero and 100kPa due to the structural limitations of the shear device.

The values for the shear strength observed in the laboratory tests on synthetic waste ranged above and below the correlation suggested by Manassero *et al.*, (1997). To be more specific, the compositions dominated by the Leighton-Buzzard sand were found above the line, the compressible compositions (SW_02 and SW_09) were located below the line. The mono-component compositions and the compressible compositions SW_03 met the line. As 25kPa was the minimum applied normal stress, a friction angle of zero could not be observed below 20kPa normal stress (zone A). Also, the shear behaviour of zone B and C could not be fully reflected. It was found that some tests exhibited a decreasing friction angle, when the straight line of the three values was divided into two sections (Figure 7-37). Three of the sand matrix tests resulted in high friction angles for the first section (25kPa and 50kPa normal stress, approximately zone B), while a consideration of the second section (50kPa and 100kPa, approximately zone C) led to a decreased friction angle.

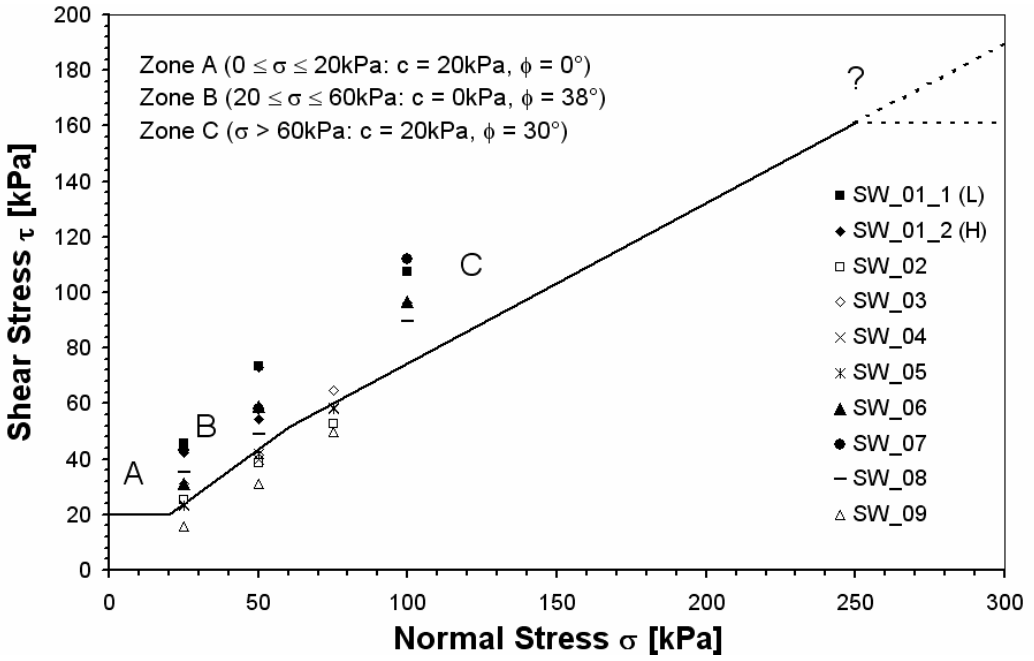

Figure 7-36 Shear- normal-stress diagram after Manassero *et al.* (1997) including large shear test results

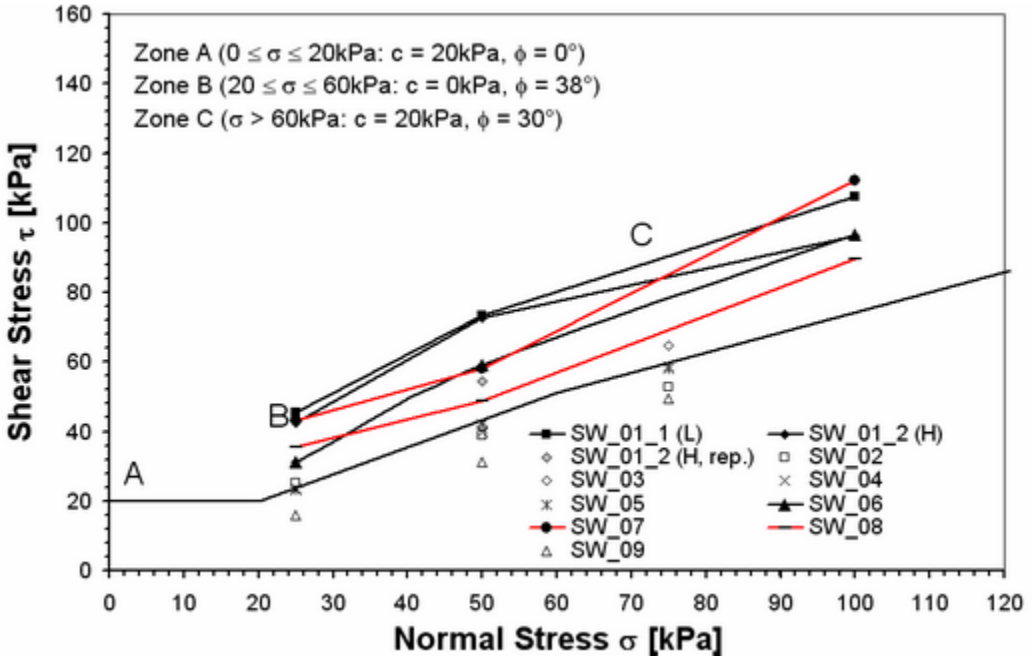

Figure 7-37 Detail of the shear- normal-stress diagram after Manassero *et al.* (1997) including large shear test results

The SW_01 series (sand, paper and flexible plastic) and the compositions with the lowest amount of compressible and reinforcing components (SW_06) confirmed the shear behaviour suggested by Manassero *et al.*, (1997). These compositions could also be considered as reinforced samples, as the SW_01 series exhibited a composition similar to reinforced sand (Figure 11-4), and SW_06 could also be regarded as a composition with a low amount of reinforcement (Figure 11-5). As municipal solid waste is also considered as a reinforced medium and with the theory of the activation of reinforcement in waste (Kölsch, 1996) mentioned in section 2.2.2.4 and demonstrated in Figure 2-5, the

suggested bilinear envelope could be confirmed. On the other hand, two of the sand matrix tests resulted in low friction angle for the first section and high friction angle for the second. As the majority of the remaining tests did not result in a bilinear envelope, the suggestions of Manassero *et al.*, (1997) could not be fully confirmed. Further research is necessary on the influence of the reinforcing effect components like paper and plastic have on the shear behaviour.

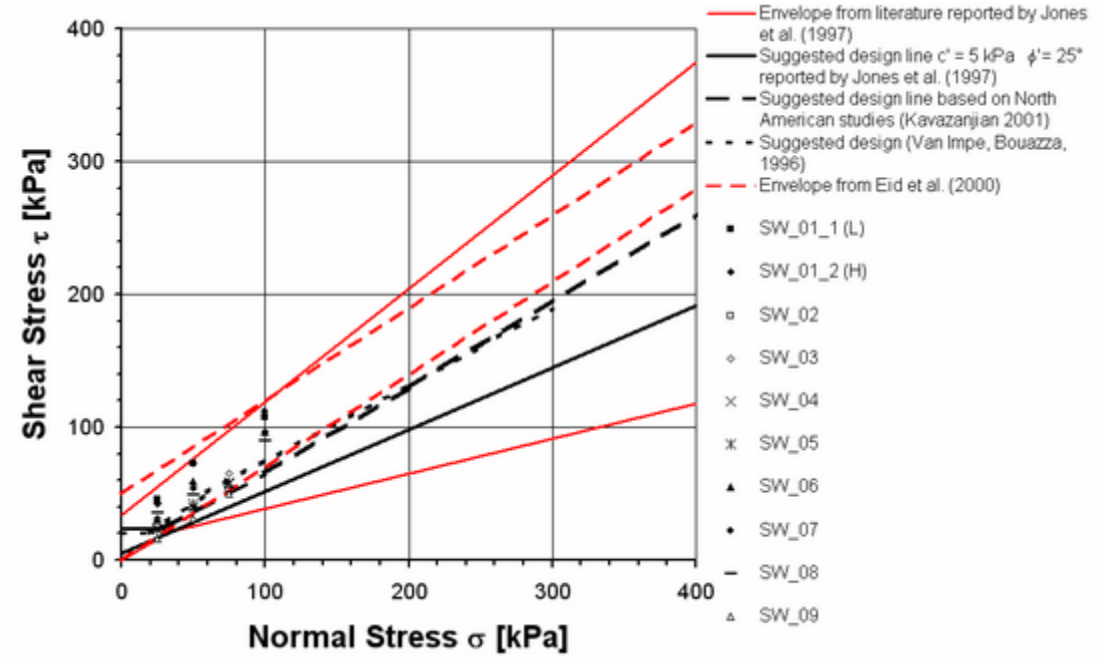

Figure 7-38 Shear- normal-stress diagram after Jones *et al.* (1997) including envelope from Eid *et al.* (2000) and large shear test results

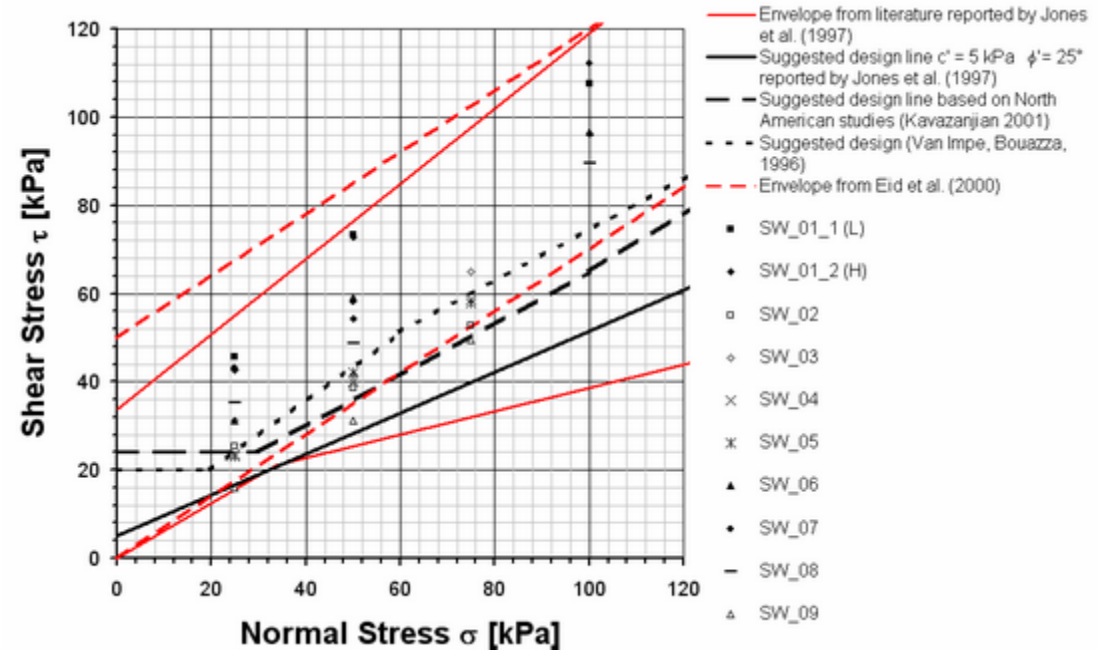

Figure 7-39 Detail of the shear- normal-stress diagram after Jones *et al.* (1997) including envelope from Eid *et al.* (2000) and large shear test results

Figure 7-38 shows a summary of suggested design lines and a design envelope proposed by Jones *et al.* (1997). Additionally, the envelope from Eid *et al.* (2000) and the shear test results on the synthetic waste are demonstrated. It is an extended summary of design values for shear parameter similar to the suggestion from Manassero *et al.* (1997). It is visible that the synthetic waste results are located within the upper and lower bound of the proposed envelope from Jones *et al.* (1997) and from Eid *et al.* (2000). The two distinctive groups within the synthetic waste compositions (sand-matrix and compressible) are found near the upper and lower bound of the envelopes respectively (Figure 7-39).

Sánchez-Alciturri *et al.* (1993) suggested design shear parameter by means of zoning the diagram in Figure 2-42 with pairs of cohesion and friction angle. The graph was extended with values from the literature after 1993 and the results from shear testing on the synthetic waste compositions were also added and demonstrated in Figure 7-40. It is clearly visible that the suggested boundaries for laboratory test results and field test analyses do not fully comprise the data from the last 12 years. Nevertheless, two issues should be mentioned. The shear parameters recommended by diverse authors range near the design area suggested by Sánchez-Alciturri *et al.* (1993). The results from the shear tests on synthetic waste ranged without exception within the zone of laboratory tests.

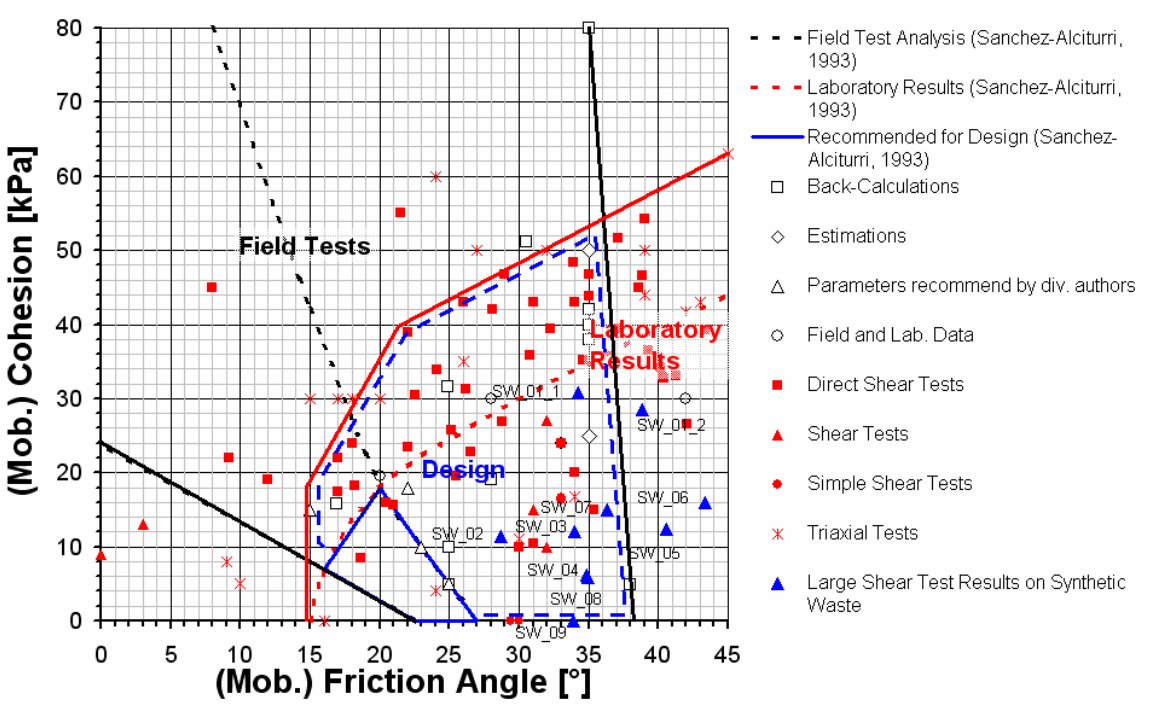

Figure 7-40 Modified graph with recommended design shear parameters from Sánchez-Alciturri *et al.* (1993)

The zones for laboratory tests and field test analyses were expanded. Following the example of Sánchez-Alciturri *et al.* (1993), who recommended the overlapping area of laboratory tests and field tests analyses as the area for design values, the new design area comprises a large part of the diagram and thus diffuses the values recommended for design. From these results it can be stated that a fixation of a design area or even a design line is not sensible considering the variability of waste. As for different soils, it

would be a sensible and comprehensive approach to set design areas/lines for waste, which are describing the individual properties of a waste types, i.e. describing individual waste types according to their mechanical properties, which are controlled by their components.

7.5.5 Influence of the Displacement on the Shear Strength Parameters

Figure 7-41 shows pairs of cohesion and friction angle, which were determined at different displacement during shear tests. Additionally, the maximum particle size is given. In particular, the data from Scheelhaase *et al.*, (2001) on mechanically and biologically pre-treated (MBP) waste shows that a displacement of at least 60-80% of the maximum particle size has to be applied to result in the maximum mobilised cohesion. It cannot be stated if a maximum friction angle was mobilised for the present data. The data from Scheelhaase *et al.*, (2001) continued to increase, but it is obvious that the increase is flattening with displacement.

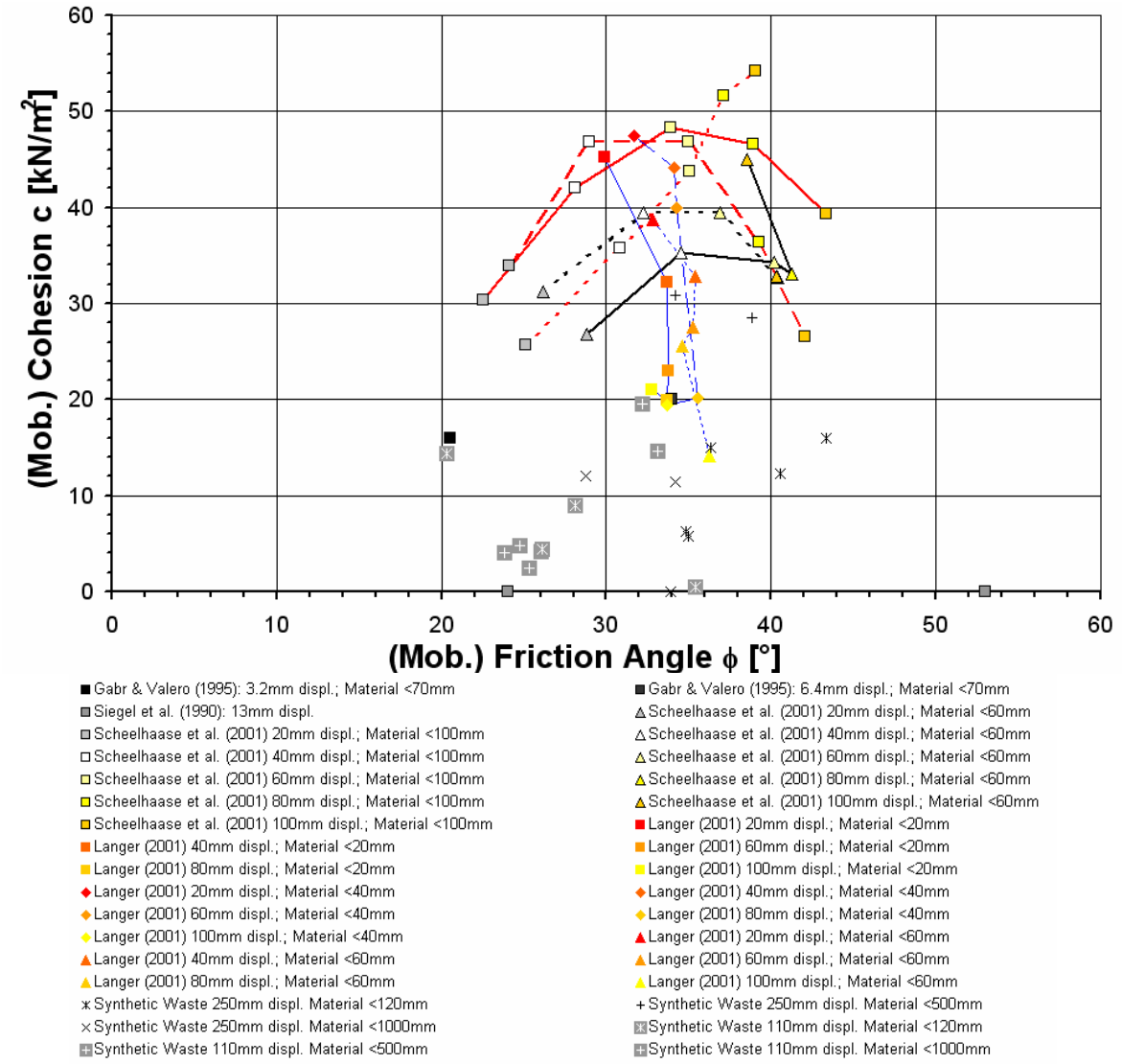

Figure 7-41 The effect of displacement and component size on shear parameters

Additional data on MBP waste from Langer (2001) shows a maximum mobilised cohesion at a displacement that was 33% to 100% of the maximum component size. The maximum mobilised friction angles for MBP waste were essentially constant after a displacement that amounted to 66 to 200% of the maximum component size. The synthetic waste tested in the large shear device exhibited a similar behaviour. As a peak value for the shear stress was not reached, the mobilised friction angle increased with increasing displacement. The same behaviour was found for the cohesion. As most of the synthetic waste compositions comprised components, which were larger than the maximum displacement of the box, peak values could not be reached. It is therefore crucial to take the component size into account, when interpreting shear data, provided that the displacement is also given. Also, tests should be conducted in devices, which are able to apply a displacement, which is large enough to activate tensile forces of the reinforcement to increase the potential of reaching a peak value.

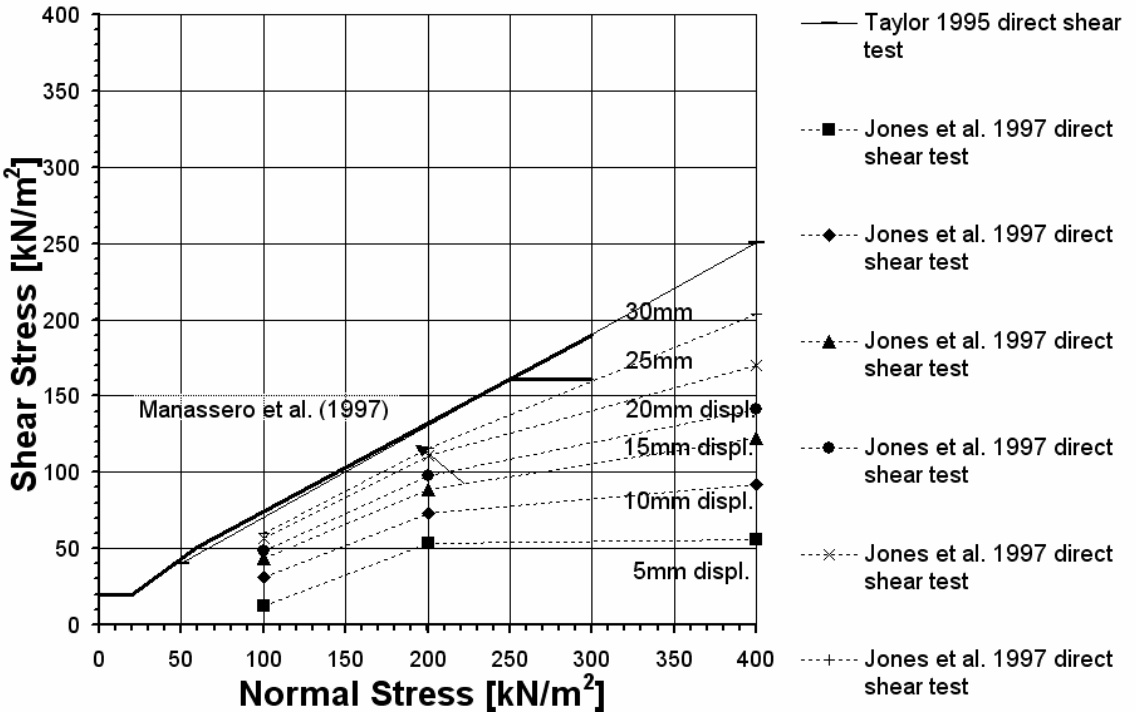

Figure 7-42 Mohr-Coulomb envelopes for different displacements

Figure 7-42 depicts different Mohr-Coulomb envelopes. To help interpretation, the suggestion from Manassero (1997) is also shown. Envelopes of shear and normal stress at different displacement are demonstrated in the graph. The mobilised shear stress increases with increasing displacement. A statement can be made from this figure. It was mentioned by many authors (e.g. Jessberger, 2001) that the Mohr-Coulomb envelope is only limited to values derived from failure conditions. Thus, the use of the Mohr-Coulomb envelope with mobilised values is misleading for design purposes, if a limit state is not reached. The use of mobilised values may result in a calculation “on the safe side”, but is probably not efficient and economic. The comparison of mobilised shear parameters is only meaningful, if a similar displacement for the mobilised shear parameters is chosen.

A further refinement and development of the determination of shear parameters and behaviour is needed. The boundary conditions of the devices, which test the mechanical properties of municipal solid waste, have to be adjusted to the circumstances the waste and its components dictate. Limitations by the devices are not satisfactory and acceptable for sustainable landfill design and management.

7.5.6 Comparison with Real Waste Tests Conducted in the Same Device

The LIRIGM-Polytech'G of the Joseph-Fourier University in Grenoble, France, conducted various shear tests on municipal solid waste using the same large shear device, which was used for the synthetic waste. In the following section, the results from both, tests on real waste and tests on synthetic waste will be briefly compared and discussed.

7.5.6.1 Comparison of the Shear Data with Real Waste Results Conducted in the Same Device

Figure 7-43 is a comparison of Mohr-Coulomb envelopes derived from large shear tests on synthetic waste, and on real waste conducted by Gotteland *et al.* (2000), who tested non-hazardous industrial waste (NHIW) and domestic waste (DW). The compositions for the real waste were already shown in Table 2-4. The envelopes are based on mobilised shear parameters determined at 100mm displacement. Table 7-13 summarises the mobilised shear parameters for the test results demonstrated in Figure 7-43.

Table 7-13 Mobilised shear parameters at 100mm displ.; b) Gotteland *et al.* (2000)

a)	**SW_**	**01_1**	**01_2**	**02**	**03**	**04**	**05**	**06**	**07**	**08**	**09**
Mob. Friction Angle Φ	[°]	30.7	33.9	19.6	23.1	24.7	26.0	34.0	27.1	18.6	25.0
Mob. app. Cohesion c	[kPa]	19.5	9.8	10.8	10.4	4.5	3.9	1.3	9.2	15.0	2.1

b)	**Real Waste**	**NHIW_1**	**NHIW_2**	**DW_1**	**DW_2**	**DW_3**
Mob. Friction Angle Φ	[°]	13.9	25.8	19.5	25.5	26.6
Mob. Cohesion c	[kPa]	29.2	42.8	50.7	19.6	14.4

It is clearly visible that the high compressible synthetic waste and the real waste simulation exhibited the lowest values. The compositions with high shear stress values (SW_01_1 and SW_01_2) were found near the values for DW_1 of the real waste tests. Only the reinforced sand compositions (SW_01 series) could be fully found in the range of the real waste, two of the sand matrix compositions (SW_06 and SW_07) reach the real waste range at high normal stresses of >50kPa. At 75kPa the high compressible composition SW_03 could be found near the bottom limit of the real waste range.

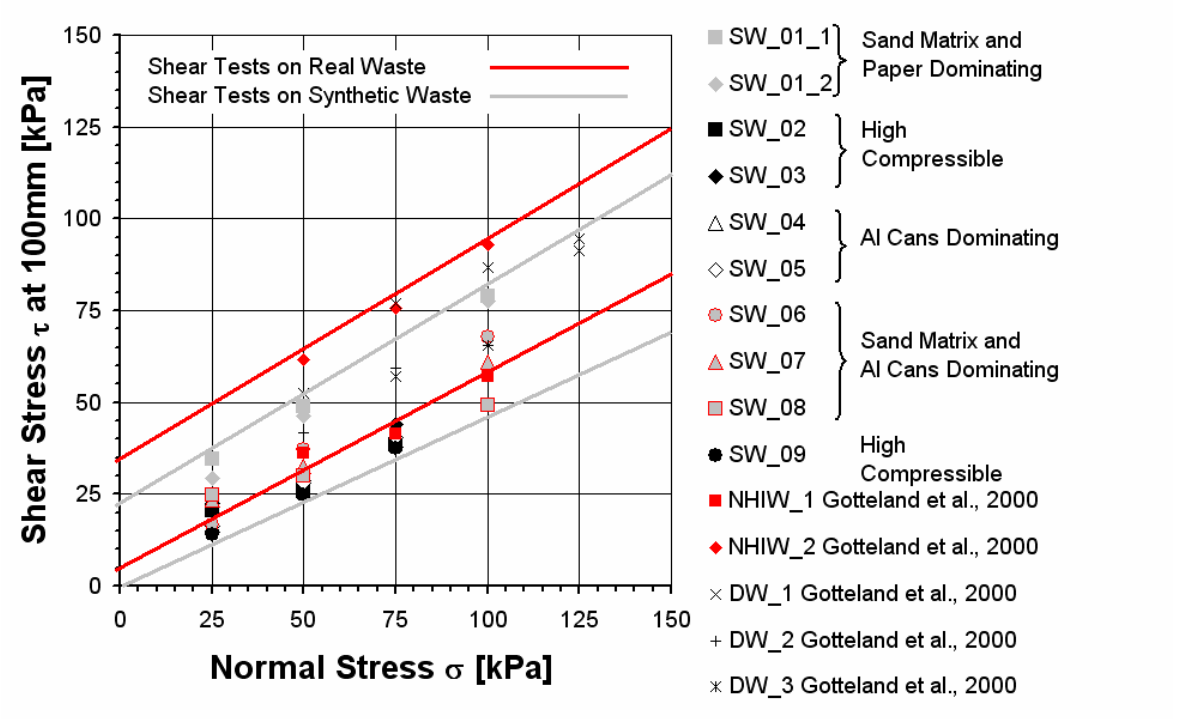

Figure 7-43 Comparison of shear test results with values from the literature

Nevertheless, the mobilised friction angles found for the synthetic waste were generally in the range of or higher than the friction angles of the real waste. On the other hand, the real waste exhibited higher mobilised cohesion than the synthetic waste compositions. The difference in cohesion can be explained by two effects. The real waste sample contained a larger amount of fines. Especially, the TII series shown in Table 2-4 (NHIW_2) contained about 66% of fine material (Figure 7-45b) leading to a soil-like character. As the tests were done on wet samples, there is also the possibility of capillary forces increasing the cohesive effect.

7.5.6.2 Comparison of the Shear Curves

Figure 7-44 is a direct comparison of composition SW_07 and SW_08 (Leighton-Buzzard sand matrix with aluminium cans and plastic packaging) to a real waste shear curve from Aboura (1999). The unit weight for SW_07 was 9.6kN/m^3 and SW_08 amounted to 7.3kN/m^3. Similar values were given by Aboura (1999). The unit weights of the real waste samples range from 7.9 to 9.7 kN/m^3. For an example of the composition, the Montech waste comprised 40% plastic, 10% textiles, 10% paper, 15% green waste and 20% diverse material.

Both curves show a constant increase of the shear stress. But the French waste exhibited a steeper gradient than the synthetic waste. The shear curve of the real waste had also an initially rapid shear stress increase, while the shear stress of tests on synthetic waste slowly and evenly increased. As a general statement, the similarity between the shape of the curves has to be mentioned. A detailed comparison is not possible as different media were tested.

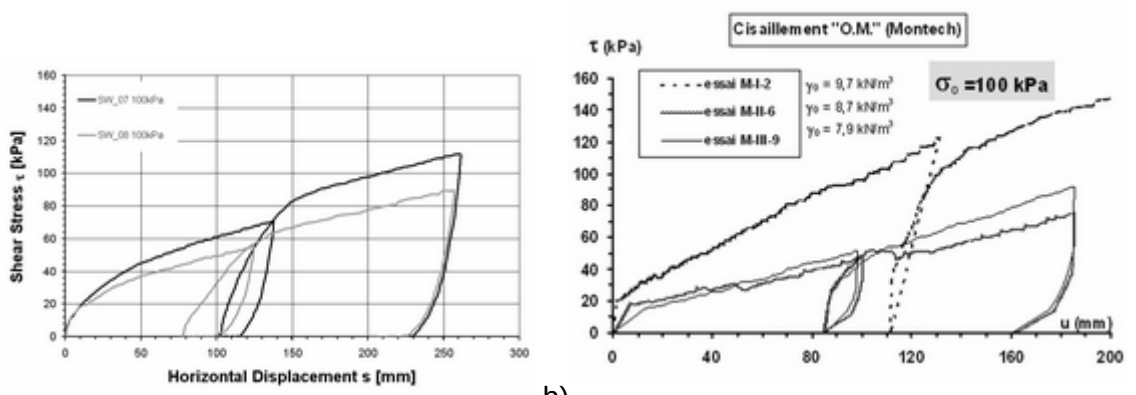

a) b)

Figure 7-44 Shear curves at 100kPa normal stress a) SW_07 and SW_08, b) Real waste from Aboura, (1999)

7.5.6.3 Analysis of the Shear Plane

After finishing the test set of SW_02, the side beams of the upper and lower box were removed in order to assess the structure build-up and component deformation, respectively. Composition SW_02 was chosen for this purpose, as it contained a large amount of compressible components. It was expected that these components would have the largest impact on the built-up of the structure, as the components were easily compressible and deformable. Figure 7-45 depicts a side view for both, synthetic and real waste.

A shear plane was visible for the real waste (shown by the red dashed line). The synthetic waste did not clearly exhibit a shear plane, but it was roughly indicated (red dashed line). While the shear plane for the real waste occurred horizontally, a more diagonal shear plane was found for the synthetic waste, as directly at the edge of the bottom box a rigid plastic bottle was jammed, which did apparently not move further during shearing. Also, the bottle was obviously not sheared but bent around the edge of the bottom box. Other materials (plastic packaging, paper and aluminium cans) were pushed over the bottle leading to a diagonal movement of the components.

Regarding the structure a horizontal alignment of especially high compressible components like paper and flexible plastic was recognisable. But also low compressible components like rigid plastic packaging were orientated horizontally. Interlocking of components was often found. Aluminium cans and rigid plastic were flattened and jammed other components (paper, flexible plastic). This resulted in flat compounds of different components.

The real waste looks like a soil-like and heavy material. A horizontal alignment of components with the sample is not recognisable. This was probably prevented by the soil-like material. It is assumed that component bridge were built up in the synthetic waste (e.g. due to packaging material) and thus a moving of components was possible with increasing displacement. As the unit weight was 10.7kN/m^3 and thus almost seven times larger than the unit weight of the synthetic waste, the possibility for components to move was limited, which might be indicated by the horizontal shear plane.

a)

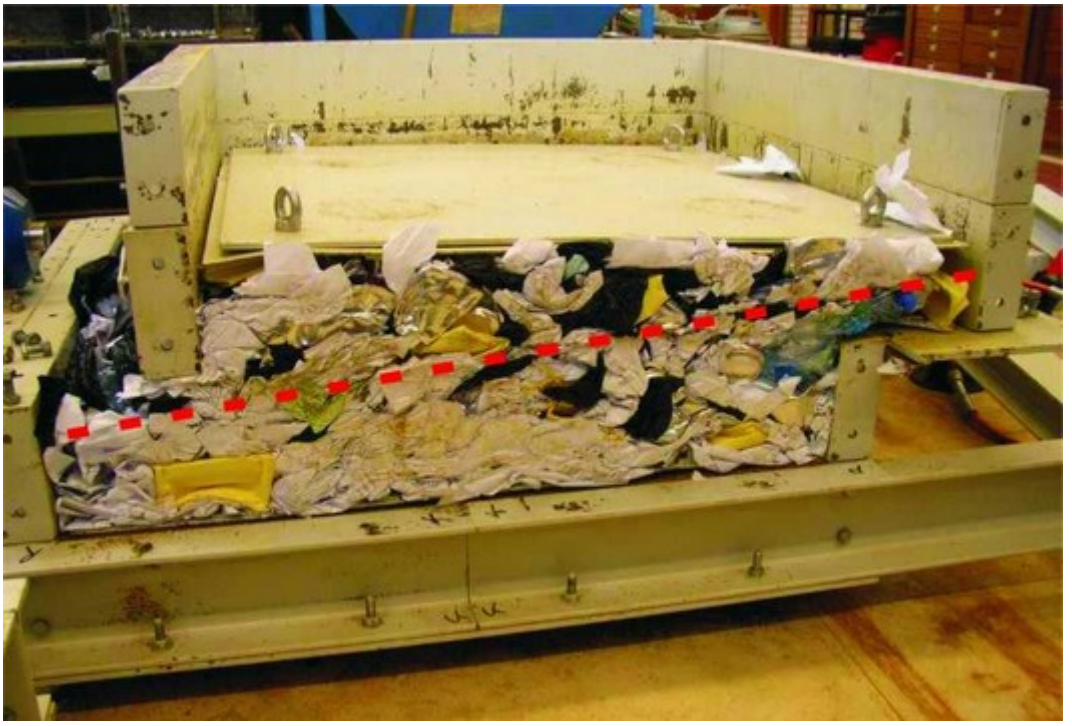

b)

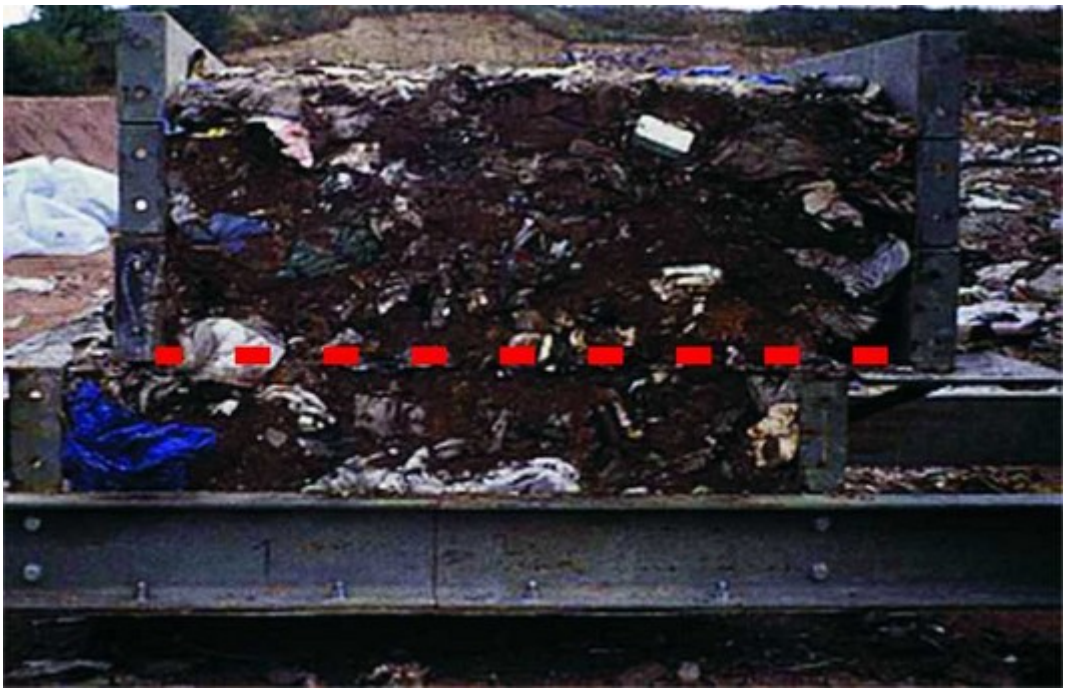

Figure 7-45 a) Shear plane of SW_02 at 75kPa normal stress; b) Shear plane of real waste (Aboura, 1999)

7.5.7 Comparison of Compression Data Obtained from Pre-compaction with Data from Compression Tests

From the pre-compaction of samples before shearing, constrained moduli could be calculated. All tests were pre-compacted with 50kPa normal stress, except for the SW_01 series, which could be compacted with 100kPa normal stress. After having reached 50(100)kPa a constrained modulus could be determined by measuring the strain. These moduli were compared to the constrained moduli derived from the compression tests.

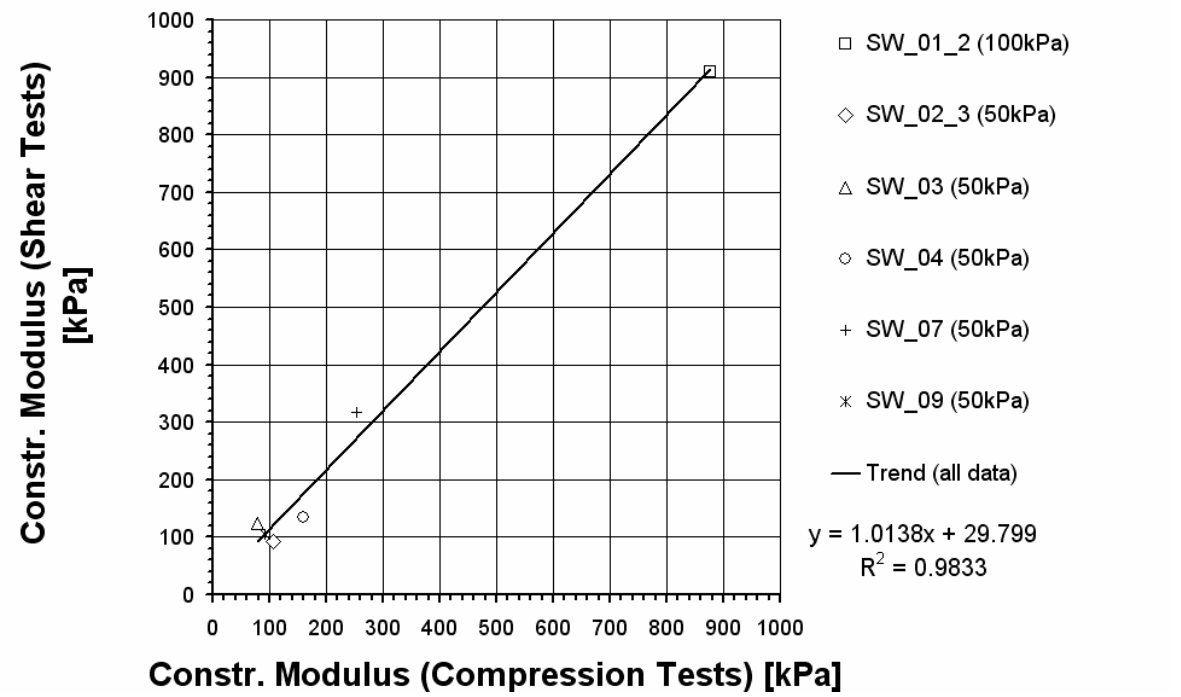

Figure 7-46 Comparison of the constrained moduli from compression and shear test

Figure 7-46 illustrates the results for the constrained moduli from the shear and compression tests. For the SW_02 series, the test with the highest unit weight (SW_02_3) was chosen for the comparison, for the SW_01 series the test on the high sample (SW_01_2) seemed to be most appropriate. A general linear relationship is recognisable.

The constrained moduli calculated from the shear device data exhibited higher values than from the compression box. This is probably due to the following factors. The wall friction of the compression box was estimated to be lower than the wall friction of the shear box, as two partition side walls compression cell were covered with a low friction plastic coating and the glass front had low friction. As the wall of the shear box were built from metal beams, small edges caused by adjacent beams were inevitable. Moreover, these metal beams were rough despite being covered in paint. Also, the paint was removed in the course of the tests, as a result of components scratching the surface of the box.

The values obtained from pre-compaction of the synthetic waste in the shear device could be used to complete the information derived from the set of compression test. They were used in the final characterisation and classification in section 7.6.

7.5.8 Component Shifting within the Shape-related Subdivisions

The compositions SW_02, SW_03, SW_04, SW_05 and SW_09 were analysed to examine the component shifting as stated in chapter 6.4. Changes for the components of the SW_01 series, SW_06, SW_07 and SW_08 were not experienced. It was observed that the shape of the components in the sand-matrix compositions SW_06, SW_07 and SW_08 were altered, but the alteration did not affect their general shape, i.e. even though compressible components showed signs of deformation, they still kept their compressible

character. The results are shown in Figure 7-47. As for the compression tests, the initial component ratio is shown as an “A”, the final mass ratios are marked with a “B” in front of the composition name in the ternary diagram.

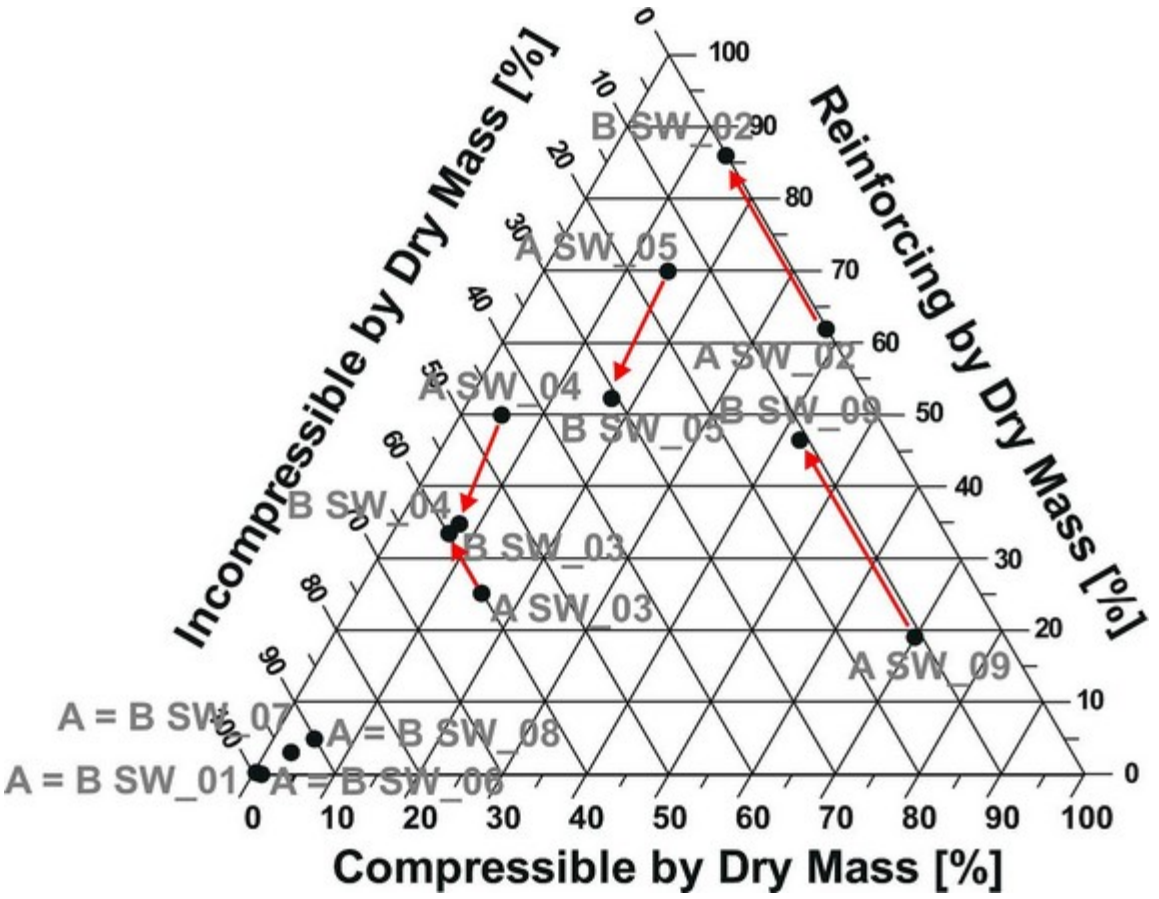

Figure 7-47 Shifting of shape-related subdivisions of the synthetic waste compositions in the ternary diagram after shearing

The shape-shifting after shearing exhibited similarities to the shifting after compression discussed in section 7.4.4. Again, a shifting from compressible components towards reinforcing components was visible for all compositions. A change for the shape-related subdivisions of the incompressible components was not observed. As a consequence, they remained in their initial state. A general shifting from reinforcing components towards incompressible components was also visible (SW_04 and SW_05). Thus the component shifting occurred anti-clockwise in the ternary diagram. SW_03 is the only exception. This composition contained a large mass percentage of incompressible components, but its behaviour was characterised by high compressibility.

The compressible compositions SW_02 and the real-waste composition SW_09 showed results similar to the compression tests. The amount of compressible components decreased and reinforcing components increased. The amount of incompressible components remained essentially constant. Both of the mono-component compositions had a decrease in the reinforcing components and increase in the amount of incompressible components. A slight increase of compressible components is apparent for composition SW_04, which could be due to a deformation (and thus building of “three-

dimensional components and not further flattening) of aluminium cans initially classed as reinforcing components.

Considering the discrepancy between the behaviour of SW_03 (dominated by compressible components) and its mass composition (dominated by incompressible components), the use of mass percentage should be reconsidered. Bearing in mind that the compressible components in SW_03 accounted for the majority of the volume, it might be more meaningful to describe the waste composition by volume percentages. This has to be examined in further compression and shear tests. A volumetric analysis of the components should also be conducted.

7.5.9 Findings of Shear Behaviour

In general, three different sets of waste compositions were tested: incompressible (SW_01 series, SW_06, SW_07 and SW_08) with high unit weights, compressible (SW_02, SW_03 and SW_09) and mono-component compositions (SW_04 and SW_05) with comparably low unit weights, as already indicated in Figure 7-43. Thus the shear parameters resulted in similar ranges. In a direct comparison of mobilised shear parameters at identical displacement, incompressible compositions resulted in values similar to those from real waste samples that were tested in the same device. The incompressible compositions exhibited the highest shear parameter of the synthetic waste compositions. Compressible and mono-component compositions produced the lowest shear strength values and were located below the range for real waste.

The incompressible composition resulted in the highest mobilised friction angles and apparent cohesion, which can be assigned to the high unit weights and the high portion of small-sized material (Leighton-Buzzard sand). In particular, the sand-matrix compositions with a high fraction of aluminium cans exhibited the highest mobilised friction angles. The reinforced sand compositions resulted in the highest apparent cohesion. The lowest mobilised friction angle was found for the compressible composition SW_02 with the lowest unit weight. The real waste simulation (and compressible composition) SW_09 surprisingly exhibited the lowest mobilised apparent cohesion. The mono-component compositions produced similar values for both, mobilised friction angle and mobilised apparent cohesion.

Nevertheless, the shear behaviour of the family of synthetic waste compositions for normal stresses of up to 100kPa ranged within boundaries obtained from the literature (e.g. Sánchez-Alciturri *et al.* (1993), Jones *et al.* (1997), Manassero *et al.* (1997) and Eid *et al.* (2000)). The comparison to values from the literature must be handled with caution. As often, mobilised values are published and boundary conditions like displacement and component size have to be taken into account to avoid misleading interpretations.

As a result from these shear tests and from the literature review on shear behaviour, it can be stated, that peak values were rarely found when testing waste shear behaviour. It has to be examined, if a sufficient displacement in relation to the maximum component size could lead to peak values. From tests on processed waste a possibility a reaching a failure state for waste is indicated.

Generally, the use of design areas (e.g. pairs of c and ϕ) and lines (e.g. Mohr-Coulomb envelopes) is dangerous and also misleading in regard to the variability of waste. Such reference values have to be differentiated according to the properties of different kinds of waste. To satisfy the largely variable waste composition and thus properties a classification of waste is necessary as a basis.

The data from pre-compaction of the sample used for shear tests could be used to complete the analysis of the compression behaviour of the tested synthetic waste composition. A linear relationship was found between the constrained moduli derived from compression tests and pre-compaction. The latter produced slightly higher values than the compression tests due to different test boundary conditions.

The synthetic waste could be used to demonstrate waste mechanical behaviour. To complete and refine the investigation, a further examination of compositions with high unit weights would be advantageous. In particular, compressible compositions with high unit weight would complete the analysis. Also, the influence of water would be interesting to examine.

7.6 Characterisation and Classification of the Synthetic Waste by Its Compression and Shear Behaviour

Compression Behaviour

From Figure 7-46, a correlation between the compression test data and the data acquired from pre-compaction of the shear box is obvious. The trend line shows a linear relationship between the compression and shear data. The latter had constrained moduli approximately 30kPa higher than the data from the compression tests. The uneven and rough surface of the shear box could be one reason for the higher values.

Therefore, the constrained moduli from the compression tests were completed with the results from the shear tests for SW_05, SW_06 and SW_08. The data collection is shown in the ternary diagram in Figure 7-48. As the data shows neither a satisfactory trend nor a sufficient differentiation of the synthetic waste composition within the diagram in Figure 7-48a, which shows mass relations of the shape-related subdivisions. SW_01, SW_06, SW_07 and SW_08 were all found within a small range in the ternary diagram, even though there were large differences in the compositions. As a result, some new assumptions were introduced regarding the volume of the components. The bulk volume for the synthetic waste was measured and assumptions about their deformability behaviour were made. It was assumed that components like Leighton-Buzzard sand, tyre shreds, brick fractions and also clay lumps did not show any deformation when placed into the compression and shear device. Rigid plastic packaging exhibited minor deformation, aluminium cans showed a medium deformation and paper, textiles and flexible plastic packaging showed major deformation, when placed. This was considered for the volume calculation. With these assumptions and measurements a volume for each synthetic waste component was approximated, which was then related to the overall sample volume. Thereafter, the volume for the shape-related subdivisions was calculated. It should be stated that the assumptions made are subjected to potential errors. Therefore,

Figure 7-48b is only meant to show trends, but it is not reflecting an exact overall behaviour. For a thorough quantification, the deformation behaviour of the synthetic waste components has to be examined and put into relation to unit weights and pre-compaction stress.

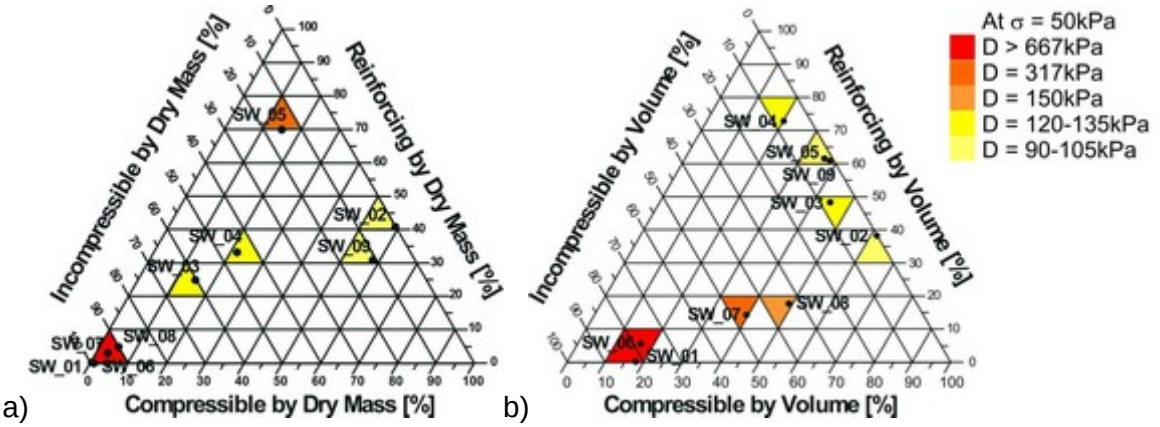

Figure 7-48 Compression behaviour of the synthetic waste compositions in relation to their position in the ternary diagram a) mass related, b) volume related

With these assumption a better differentiation of the compositions was possible and a compression trend within the compositions was visible. As expected, a large volume of incompressible materials led to a high constrained modulus. A high amount of compressible and reinforcing components resulted in a low constrained modulus. An exception in this consideration is solely composition SW_05 (with D = 147.8kPa), which reached a constrained modulus similar to SW_08 (D = 150kPa), but its shape-related subdivision ratio was found very close to SW_09, which resulted in a value for D of 105kPa.

Shear Behaviour

The same approach was used to depict shear behaviour. The shear moduli are demonstrated in Figure 7-49. As for the compression data a distinct trend is not obvious from Figure 7-49a. With the use of volumetric data, the differences between the compositions are better visualised than with mass related compositions and a clear trend is visible. The shear moduli demonstrated were determined at 2% strain (20mm displacement) after the unload-reload loop. There is a trend to decrease shear stiffness towards the upper corner of the ternary diagram. It is apparent from the ternary diagram that the shear modulus decreased anti-clockwise. A large volume of compressible and reinforcing material led to a low shear modulus, while a high of incompressible material produced a high shear modulus.

As mentioned in the section before, the data depicted in Figure 7-49 is potentially subjected to errors, as assumptions about the volume were made. Generally, it seems to be meaningful to use a volumetric relation of the shape-related subdivisions rather than a mass-related relation to describe mechanical behaviour of the synthetic waste and thus of real waste.

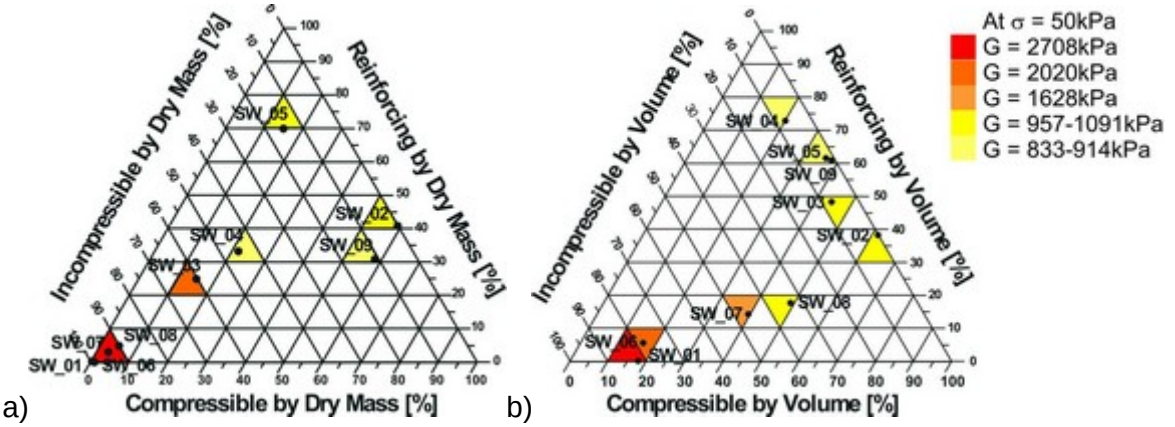

Figure 7-49 Shear behaviour of the synthetic waste compositions in relation to their position in the ternary diagram a) mass related, b) volume related

7.7 General Findings from the Geotechnical Classification, Synthetic Waste and Waste Mechanical Behaviour

Waste mechanical behaviour is inconsistent due to the variability of waste compositions and other influencing factors. In the course of this work, the necessity for a uniform basis for comparing and sharing waste mechanical data was stressed. The waste geotechnical classification framework introduced and demonstrated in this work provides a consistent method to classify waste by considering the most important properties of its components (material mechanical properties, component size and shape, degradability). Classifying the shape-related subdivisions in a ternary diagram on a volumetric basis offers the possibility of allocating mechanical properties to individual waste compositions. It is also important to consider the unit weight and stress state of the waste, as they influence the component behaviour. So far, neither is directly incorporated. The stress state is indirectly reflected by the shape-related subdivisions, i.e. the higher the previously applied stress, the lower the percentage of compressible components and the higher the percentage of the subdivisions of incompressible and reinforcing components. High unit weight was caused by a high portion of fine material (in this case Leighton-Buzzard sand) in the present set of composition. Considering fine organic material, which is reasonably wet on site and thus contributes to a high unit weight, the unit weight cannot be allocated to the incompressible components only. Further work is required to incorporate unit weight and stress state of waste.

The classification could be refined in terms of size ranges (further subdivision of 120-500mm), as stated in section 7.2. Moreover, only biodegradation is taken into account for the alteration of waste components. Physical and chemical changes were not considered. The classification procedure is laborious at the moment, as sorting analyses have to be conducted in order to describe the properties of waste components. Nevertheless, it provides a uniform basis for comparing waste mechanical behaviour from different sources.

Replacing the real waste with synthetic components resulted in a simple system of nine components. The compositions could be engineered without much effort. A systematic

alteration of the waste composition was also easily possible. So far, the synthetic waste family is based on dry components, the influence of water has still to be examined.

The examination of mechanical behaviour of the synthetic waste compositions produced results comparable to those from real waste. The unit weight represented a large influence on the results. The components of the synthetic waste were linked to the unit weight. Most of the components exhibited a low bulk unit weight, with the exception of sand, clay. tyre chips and bricks. For further examination of waste mechanical behaviour, it might be useful to replace existing synthetic waste components or add components, which have a large volume and mass to increase the unit weight and also to increase the volumetric portion of those components.

The use of synthetic waste for a systematic study of waste mechanical behaviour was feasible. The structured exchange of waste components and thus the systematic change of waste compositions led to different results. The results of shear and compression tests on the synthetic waste could be related to values from the literature, i.e. to design and recommendation values and areas.

Shear tests on synthetic waste compositions led to the result that compositions with a high portion of fine materials, which generally led to a relatively high unit weight, produced high apparent cohesions. As these compositions comprised reinforcing components like paper and flexible plastics, the mobilised friction angles were also considerably higher. The highest mobilised friction angle was produced from a mixture of mainly angular, compressed aluminium cans and Leighton-Buzzard sand. As the compressible compositions exhibited a low unit weight, they resulted in the lowest shear strengths. Altering the amount of a dominating component (i.e. a component, which is dominating the volume) did not change the shear behaviour. A simulation of a real waste composition resulted in a reasonable mobilised friction angle but zero cohesion.

The compression tests on the synthetic waste composition resulted in constrained moduli, which could be compared to values from the literature and put into similar ranges. Again, the unit weight had a crucial influence on the results. Compositions with a large sand portion achieved higher constrained moduli than compressible compositions with lightweight components. As only a small range of composition was covered by the tests, there is a need for conducting additional tests with compositions, which range between the high unit weight of the incompressible compositions and the low unit weight of the compressible compositions.

To confirm the trend of the mechanical behaviour and to complete the data shown in the ternary diagram, it would be advantageous to test compositions, which exhibit the ratio of shape-related subdivisions and which were not covered by the testing program. In terms of volume, these compositions are found in the middle area of the ternary diagram, i.e. compositions exhibiting a balanced ratio of compressible, incompressible and reinforcing components, and also very compressible compositions with remaining equal parts of reinforcing and incompressible components would contribute to the completion of the investigation of the mechanical behaviour. It would be very interesting to test a synthetic

waste composition, which is base on a real waste composition with known mechanical properties for further validation of the synthetic waste and of the classification.

Most of the tested composition did not reflect a particular real waste composition except for the real waste simulation. Nevertheless, certain results can be transferred to real waste and the implication of the likely change of the waste composition. As mentioned in the literature review, the waste stream is constantly changing. Recycling and waste minimisation actions influence the waste composition. Consequently, components like plastic, paper, biodegradable organic, glass and metal are reduced. This could result in a waste composition, which is dominated by a few, in particular inert and small-sized components (e.g. soil-like material, minerals). Also, mechanical and biological pre-treatment and waste incineration is leading to relatively inert and fine components. Obviously, it is not avoidable to maintain a certain percentage of recyclable and reusable components within the waste. It is therefore possible that future waste compositions are similar to the sand-matrix compositions tested in this project, though the waste is not expected to be as stiff and “incompressible”, as the fine or small-sized material would comprise a mixture of materials with different properties. In terms of shear behaviour, this would mean that the parameter would approximate reinforced soils. The mobilised friction angles of the tested compositions resulted in values that were reasonably high. This behaviour is related to the size and material type of reinforcement. As the influence of water would also have to be taken into account, an increase of the (mobilised) cohesion would have to be expected.

8 Conclusions and Recommendations for Further Work

In the following, the results from the preceding chapters and thus the objectives of this work are summarised and reviewed. Finally, the future prospects including suggestion for further work on this research topic are given.

8.1 Geotechnical Classification of MSW

A framework for classifying components of waste has been developed and presented. It is proposed that it can be used to provide information on the state of components as delivered to site, following placement and in the long-term following degradation. The presented framework proposes classifying waste components based on (1) their material type and hence engineering properties, (2) the component shape, (3) the size of the components and (4) the degradation potential. The method is likely to be of use to researchers involved in sharing and interpreting experimental data on mechanical properties of waste. This will aid the development of a consistent understanding of waste mechanics. This field of study is currently dominated by varying interpretations leading to inconsistent conclusions.

It was shown that the classification is also useful to describe mechanical properties in relation to the MSW composition, if the volumetric ratio of the three shape-related subdivisions of compressible, incompressible and reinforcing components is used. A first trend was demonstrated by linking the results from compression and shear tests to the ternary diagram of the classification system.

8.2 Family of Synthetic Waste

The family of synthetic waste was designed on the basis of the results of an in-situ real waste sorting analysis. The examined waste was freshly deposited uncompacted material and represented waste in its initial state as delivered to site. It did not reflect an overall initial waste composition, but a random initial UK waste composition and thus served as a orientation to identify typical materials, sizes and shapes of waste components.

With the information derived from the waste sorting analysis, the main materials, size ranges and shapes for the synthetic waste components were assessed by minimising the size and material fractions to be relevant and representative, but still manageable amounts. Nine different component types were used for the synthetic waste compositions (aluminium cans, rigid plastic packaging, flexible plastic packaging, Leighton-Buzzard sand, textiles, paper, brick fractions, tyre shreds and clay lumps). Water was not included in these compositions.

Twelve different waste composition variations were designed, which could initially be distinguished in the four general groups of incompressible, compressible, mono-component compositions and a real waste simulation. The mechanical behaviour of these synthetic waste compositions led to the conclusion that the synthetic waste is suited for simulating real MSW properties in a first step.

8.3 Shear Behaviour of MSW

Before determining the shear behaviour of MSW, the large shear device (1.0m/1.0m/0.8m) of the LIRIGM, Joseph-Fourier-University, Grenoble, France, underwent a performance check. For this, the device was calibrated by analysing the rolling resistance of the shear box, and subsequently, correction values for the shear strength were derived from this data. Thereafter, Leighton-Buzzard sand was sheared in a small-scale direct shear device and also in the large-scale device. The data was subsequently compared. It could be stated that the large shear device generally resulted in lower values than the small-scale direct shear device. While the small-scale data exhibited a dilatant behaviour, the large-scale shear tests resulted in contractant behaviour. The possible reason for the discrepancy was a slightly lower unit weight of the Leighton-Buzzard sand in the large shear test than in the small-scale shear test. Also, irregularities such as a minimum lateral tilting of the box linked to the large scale test could have had impact on the results. Repeatability tests on both Leighton-Buzzard sand and synthetic waste led to satisfactorily results with small variability.

To assess the shear behaviour ten synthetic waste compositions (including a variation of a composition) were tested in the large shear device. A peak failure state was not observed during the tests. The peak values found were due to components being jammed between a load plate rib and edge of the bottom box. A shear plane within the sample body was indicated but not fully developed. It has to be mentioned that development of a shear area was modified by development of a relatively large gap between upper and bottom elements of the large shear device induced by applying a normal load. Also, the composition of the test analysed for a shear plane exhibited a very low unit weight and moreover, the normal stress was relatively low (75kPa). Additionally, all tests contained components with a size, which exceeded the maximum displacement (e.g. plastic sheets). Considering the theory of activation of reinforcement, the possibility of a failure state was thus decreased.

Nevertheless, the mobilised shear parameters derived from the shear tests ranged in zones found in the literature. Incompressible compositions with a high unit weight and a large portion of small-sized components produced high shear strength parameters comparable to real waste, while compressible compositions resulted in low shear strength parameters, which were found at the limit of design ranges found in the literature. Altering the amount of components (in this case less than 10% of the overall component weight), in a sample already dominated by this component type in terms of volume, did not result in a change of the shear parameters. Only if alteration of the ratio is large enough, is it assumed that the shear behaviour would change significantly. Compositions with a high portion of small-sized components resulted in the highest mobilised apparent cohesion values. The highest mobilised friction angles were observed for compositions with a large amount of angular, already compressed cans in a sand matrix.

Reload shear modulus values measured at 50kPa normal stress and 20mm displacement were presented in the ternary diagram in relation to the shape-related subdivisions of the compositions. From this, a trend was apparent, which could be described as a anti-

clockwise decrease of the shear modulus from a volumetric dominance of incompressible components to a dominance of compressible/reinforcing components.

Comparing data to the literature, especially to design lines or areas has to be done with caution. It is often reported that a failure is not reached during direct shear tests (also in triaxial tests). Consequently, mobilised shear parameter are usually given. The comparison of the mobilised data is misleading, if the grading of the sample and the displacement of the test are unknown. As mentioned above, the probability of fully activating tensile forces and thus the occurrence of a reinforcing effect is decreased, if the component size exceeds the maximum displacement. Thus, the potential activation of the reinforcing effect cannot be estimated without knowing sample grading and displacement.

8.4 Compression Behaviour of MSW

To assess the compression behaviour of the MSW, eight synthetic waste composition (including two variations of a composition) were tested in a large compression cell (0.50m/0.50m/0.75m). The applied normal stress was limited to the capacity of the electric jack of about 2tonnes. The tests were displacement-controlled. The compositions tested were grouped as incompressible and compressible compositions, a mono-component composition and a real waste simulation.

The constrained moduli calculated from the test data were comparable to values from the literature. Most of the test results from the compressible, the mono-component composition and the real waste simulation gave moduli lower than recommendation line, i.e. the values were slightly lower than recommended in the literature. The incompressible compositions exhibited a stiff compression behaviour (high values for the constrained modulus), and were therefore found to be higher than recommended in the literature. This was valid for a normal stress up to 200kPa. Single values for the constrained modulus of real waste from the literature were also found above and below the recommendation line and thus exhibited appropriate values for low and high stiffness. The stiffness values for the synthetic waste were found in the range of the literature values.

The compression indices could generally be described by exponential functions, which did not include values that increased at the beginning of the test, as a matter of component-bridge collapse.

Considering a common basis to compare the constrained moduli, i.e. the constrained modulus at a uniform normal stress of 50kPa for all tests, the constrained moduli exhibited a trend within the volumetric ternary diagram. The constrained moduli decreased anti-clockwise from compositions dominated by incompressible components to compositions being dominated by compressible and/or reinforcing components. A similar result was found for the shear moduli.

Generally, it can be concluded that the synthetic waste could describe waste mechanical behaviour, but could also be refined for a further and more realistic approach to gradually assess waste mechanical properties. The classification system showed that it is possible to classify different waste compositions by means of their component properties and that it is also possible to allocate mechanical behaviour to these compositions and thus define

waste mechanical behaviour in the classification system. Further research is necessary for a more detailed definition. Synthetic waste mechanical behaviour (i.e. shear and compression behaviour) could be assigned to ranges of values from the literature.

The waste stream is constantly changing due to legislative changes and consumers' behaviour. Therefore, designers of landfill facilities must be aware of potential changes in waste mechanical properties. Past experience is a poor guide to assess future waste behaviour. Applying old experience to new boundary conditions could lead to misjudgement of waste mechanical behaviour and therefore to economical mismanagement, and it could even endanger human health. It is therefore necessary to assess waste mechanical properties based on its component properties. Further gradual examination of synthetic waste could eliminate uncertainties derived from various influences on mechanical behaviour of MSW. This would complete the classification system. Further development of the waste geotechnical classification would contribute to the process of waste properties assessment and thus to a sustainable waste management.

8.5 Recommendations for Further Work

Further work is required to relate classification of waste components to mechanical behaviour of waste bodies (e.g. in relation to shear strength, compressibility, stiffness) and in respect to their degradability. This includes the need to develop protocols for describing the structure of waste bodies (i.e. orientation of components and particle packing arrangements). In addition, the influence of water should be incorporated into the classification system. The influence of water on mechanical properties of components (e.g. shear strength of paper) and hence mechanical behaviour of waste bodies is rarely considered, except for effective stresses. Such research is required urgently.

A differentiation of the component degradation is also necessary, in order to develop a classification system, which is able to describe the change of the waste components and thus the waste body with time. It is suggested to differentiate between readily degradable, degradable on medium-term, and slow to non-degradable. A reconsideration of the size ranges, in particular of the size range 120-500mm could be helpful to distinguish and identify further dominating materials and components.

In terms of the classification system's demonstration, it has to be examined, if the assumption can be confirmed that a volumetric relationship results in a more meaningful trend than the use of the mass-relationship. This would involve an investigation about the volumetric behaviour of waste components, i.e. the deformation and compression behaviour of (synthetic) waste components, which would be necessary to assess the compression/deformation of the components at different stages and thus normal stress levels of the depositing process, e.g. the three stages of the classification application being initial, post-placement and long-term stages.

The synthetic waste engineered from a waste sorting analysis and used in this project for the investigation of MSW shear and compression behaviour reflected MSW properties and its mechanical behaviour. But the result for the mechanical behaviour is limited to normal

stresses of up to 100kPa only for shear tests and to 200kPa for compression tests. Further research is necessary to complete the behaviour for higher normal stresses and thus to contribute to the general understanding of waste mechanical behaviour.

An additional disadvantage of the synthetic waste family is the fact that generally two ranges of unit weight were tested, being a low unit weight range (of compressible compositions) and a high unit weight range (of incompressible compositions). This was due to the low ratio of mass and volume of certain components. Finding additional or new components with a high mass/volume ratio, which ranges between the extremes of the used components (i.e. Leighton-Buzzard sand and lightweight components like paper and plastic packaging) would contribute to a better reflection of MSW properties. So far, the synthetic waste was only tested without the influence of water. Introducing water to the synthetic waste would also mean an increase in the bulk unit weight. Moreover, the influence of the moisture content on MSW mechanical behaviour could be investigated.

A further validation of the synthetic waste could be accomplished, if the mechanical properties of a known real waste composition are determined and compared to the properties of a synthetic waste composition based on the real waste. The use of identical shear/compression devices would simplify the comparison and minimise errors by having the same boundary conditions for the tests.

For the determination of waste shear behaviour, the accomplishment of the shear tests could be optimised by the use of load cells for the application of the normal stress. This would result in compression data, which could be compared fully to the data from the compression tests. This could also mean that the compression tests would be unnecessary, if an optical monitoring of the components is not required. An automatic normal stress adjustment would simplify the test procedure (it would also save a labour force) and would result in a constant normal stress and more even shear stress behaviour.

To assess the influence of reinforcing components on waste shear behaviour, it would be interesting to accomplish tests, either on a composition including reinforcing components with a size that does not exceed the maximum displacement of the device, or in a device which is capable of applying a shear displacement that could activate tensile forces of reinforcing components. With this, the activation of the reinforcing effect could be gradually examined.

The compression test could be optimised by real-time normal stress monitoring to be able to take pictures at identical normal stress levels and thereafter compare the component compression behaviour. The compression behaviour of waste could also be refined by assessing the compression behaviour of waste components first. With information of the component compression behaviour, it could be possible to detect a normal stress value for the threshold between void decrease and component compression. In this work, a threshold value or range for this could not be determined.

Contact: Ulrich Langer shearing@online.ms

9 References

Aboura, A., 1999 “Etude expérimentale du comportement mécanique de matériaux granulaires non conventionnels”. Ph.D. Thesis, Laboratoire Lirigm, University of Grenoble, France (in French)

Andersland, O.B., Khattak, A.S. and Al-Khafaji, A.W.N., 1981. "Effect of Organic Material on Soil Shear Strength." Laboratory shear strength of soil, ASTM STP 740, Yong, R.N. and Townsend, F.C., eds., American Society for Testing and Materials, 226-242.

Barriera, A.J., Overmann, L.K., Wong, D.K.H. and King, A.C., 2001. "Settlement Monitoring at Shuen Wan Landfill, Hong Kong, During Restoration and Ongoing Aftercare and Afteruse." *8th International Waste Management and Landfill Symposium*, S. Margherita di Pula, Cagliari, Italy, 525-534.

Beaven, R. P., 1993. "Geotechnical and Hydrogeological Properties of Wastes." *Engineering Geology of Waste Storage and Disposal*. Special publication of Geological Society.

Beaven, R. P. and Powrie, W., 1995. “Hydrogeological and Geotechnical Properties of Refuse Using a Large Scale Compression Cell”. *5th International Landfill Symposium*, S. Margherita di Pula, Cagliari, Italy, CISA. 745-760

Bouazza, A., Van Impe, W.F. and Heageman W., 1996. “Quality control of dynamic compaction in municipal solid waste fills.” Proc. 2nd International Congress on Environmental Geotechnics, Osaka, Vol. 2, pp. 635-640.

Bowders, J., Bouazza, M., Loehr, E. and Russell, M., 2000. "Settlement of Municipal Solid Waste Landfills." *4th Kansai International Geotechnical Forum*, Kyoto, Japan.

Brink, D., Day, P.W. and Du Preez, L., 1999. "Failure and Remediation of Bulbul Drive Landfill: Kwazulu-Natal, South Africa." *7th International Landfill Symposium*, S. Margherita di Pula, Cagliari, Italy, 555-562.

Cambridge Engineering Selector (CES) [CD-Rom], Cambridge: Granta Design

Cardarelli, F., 1966, “Materials handbook: a concise desktop reference”. Springer, London c2000.

Charles, J. A. and Burland, J. B., 1982. "Geotechnical Considerations in the Design of Foundations for Buildings on Deep Deposits of Waste Material." *The Structural Engineer*, 60A(No. 1): 8-14.

Collins, H.-J., 2001. "Compaction of Municipal Solid Waste After Mechanical and Biological Treatment." *8th International Waste Management and Landfill Symposium*, S. Margherita di Pula, Cagliari, Italy, 455-464.

Coumoulos, D.G., Koryalos, T.P., Metaxas, I.L., and Gioka, D.A., 1995. "Geotechnical Investigation at the Main Landfill of Athens." *5th International Landfill Symposium, S. Margherita di Pula*, Cagliari, Italy, 885-895.

Coumoulos, D. G. and T. P. Koryalos, 1999. “Prediction of Long-Term Settlement Behaviour of Landfill Covers After Closure”. *7th International Landfill Symposium*, S. Margherita di Pula, Cagliari, Italy, CISA.

Cowland, J.W., Tang, K.Y. and Gabay, J., 1993. “Density and Strength of Hong Kong Refuse”. *4th International Landfill Symposium*, Sardinia, Italy, CISA. 1433-1446

CSR [online], 2002. Interim WDO Reports. Available at: http://www.csr.org/archives/iwdo_reports.htm [Accessed February 2003]

DEFRA [online], 2003. “Landfill Directive Briefing Paper”, Department for Environment Food and Rural Affairs, London, United Kingdom. Available at http://www.defra.gov.uk/environment/waste/topics/landfill-dir/landfilldir.pdf [Accessed December 2003]

Del Greco, O., and Oggeri, C., 1997. "Shear Strength Characteristics at Geosynthetic Interfaces." *6th International Landfill Symposium*, S. Margherita di Pula, Cagliari, Italy, 443-451.

Department of Environmental Quality [online], 1998. “Oregon Solid Waste Characterization and Composition 1998”. Oregon; available at: http://www.deq.state.or.us/wmc/solwaste/wcrep1998 [accessed: February 17th, 2004].

Department of the Environment, 1994a. “The Technical Aspects of Controlled Waste Management - National Household Waste Analysis Project - Phase 2 - Report on Further Composition and Weight Data”. Waste Technical Division, London, CWM 086/94.

Department of the Environment, 1994b. “The Technical Aspects of Controlled Waste Management - National Household Waste Analysis Project - Phase 2 Volume 1 - Report on Composition and Weight Data”. Waste Technical Division, London, CWM 082/94.

De Poli, F., Fabrizi, F. and Rinaldi, L., 1999. "Modelling Landfill Settlement for the Design of Biogas Plant and Top Cover." *7th International Landfill Symposium*, S. Margherita di Pula, Cagliari, Italy, 513-519.

Deutsche Gesellschaft für Geotechnik (DGGT), 1997. "Geotechnik der Deponien der Deponien und Altlasten." GDA-Empfehlungen E2-24, Deutsche Gesellschaft für Geotechnik e.V. (German Society for Geotechnics), Ernst & Sohn Verlag, Berlin (in German).

Dixon, N., 2003. "Design and Regulation of Geosynthetics in Landfill Engineering: European Legislation and UK Practise." *Forum on Geosynthetics 2003*, Toronto, Ontario, Canada.

Dixon, N. and Jones, D.R.V., 1998. "Stress States in, and Stiffness of, Landfill Waste." *Geotechnical Engineering of Landfills*, Dixon, N., Murray, E.J., and Jones, D.R.V., eds., Thomas Telford, London, 19-34.

Dixon, N., Langer, U., Gourc, J.P. and Gotteland, P., 2004a "Factors Influencing Shear Behaviour of MSW." *Waste 2004*, Stratford-Upon-Avon, UK, 591-600.

Dixon, N., Ng'Ambi, S. and Jones, D.R.V., 2004b. "Structural Performance of a Steep Slope Landfill Lining System." *Geotechnical Engineering*, 157(GE3), 115-125.

Dunn, R., 2002. “Pilot Study on the Composition of Municipal Solid Waste in Wales”. *Waste 2002, Integrated Waste Management and Pollution Control: Research, Policy and Practice*, Stratford-upon-Avon, UK. 221-227.

Edil, T.B., Ranguette, V.J., and Wuellner, W.W., 1990. "Settlement of Municipal Waste." *Geotechnics of Waste Fills - Theory and Practise, ASTM STP 1070*, Landva, A.O. and Knowles, G.D., eds., American Society for Testing and Materials, Philadelphia, USA, 225-239

Eid, H.T., Stark, T.D., Evans, W.D. and Sherry, P.E., 2000. “MSW Slope Failure; I: Waste and Foundation Properties”. *Journal of Geotechnical and Geoenvironmental Engineering* 126(5): 397-407.

El-Fadel, M., Sadek, S. and Khoury, R., 1999. "Simulation of Solid Waste Settlement in Laboratory Columns." *7th International Landfill Symposium*, S. Margherita di Pula, Cagliari, Italy, 521-528.

Environment Agency, 2002. “Landfill Directive Regulatory Guidance Note 6.0.”

European Community, 1999. Council Directive of 26 April 1999 on the Landfill of Waste (1999/31/EC). Official Journal of the European Communities; Council of the European Community L182(1).

Fassett, J.B., Leonards, G.A. and Repetto, P.C., 1994. "Geotechnical Properties of MSW and Their Use in Landfill Design." *WasteTech '94 - Landfill Technology Conference*, Charleston, South Carolina, USA.

Fricke, K., Müller, W., Bartetzko, C., Einzmann, U., Franke, J., Heckenkamp, G., Kellner-Aschenbrenner, K., Kölbl, R., Mellies, R., Niesar, M., Wallmann, R., and Zipfel, H., 1999. "Biologische Vorbehandlung von zu deponierenden Abfällen: Stabilisierung von Restmüll durch mechanischbiologische Behandlung und Auswirkungen auf die Deponierung (Biological Pre-treatment of Waste for Landfills: Stabilisation of Residual Waste by Mechanical and Biological Pre-treatment and Effects on Landfilling)." 1480945, German Federal Ministry of Education and Research (BMBF), Witzenhausen, Germany.

Gabr, M.A. and Valero, S.N., 1995. “Geotechnical Properties of Municipal Solid Waste”. *ASTM Geotechnical Testing Journal*, GTJODJ 18 (No. 2): 241-251.

Gasparini, P.A., Saetti, G.F. and Marastoni, M., 1995. "Experimental Research on MSW Compaction Degree and its Change with Time." *5th International Landfill Symposium*, S. Margherita di Pula, Cagliari, Italy, 833-842.

Ghaly, A.M., 2000. "Discussions: Large Shear Tests on Compacted Bales of Municipal Solid Waste." *Soils and Foundation; Japanese Geotechnical Society*, 40(No. 3), 127.

Gilbert, R.B., Wright, S.G. and Liedtke, E., 1998. “Uncertainty in Back Analysis of Slopes: Kettleman Hills Case History”. *Journal of Geotechnical and Geoenvironmental Engineering* 124(12): 1167-1176.

Gotteland, P., Lemarechal, D., and Richard, P., 1995. "Analysis and Monitoring of the Stability of a Domestic Waste Landfill." *5th International Landfill Symposium*, S. Margherita di Pula, Cagliari, Italy, 777-787.

Gotteland, P., Gourc, J.P., Aboura and A., Thomas, S., 2000. “On Site Determination of Geomechanical Characteristics of Waste”. *International Conference on Geotechnical and Geological Engineering*, Melbourne, Australia, ICMS, (CD).

Gotteland, P., Gachet, C., and Vuillemin, M., 2001. "Mechanical Study of Municipal Solid Waste Landfill." *8th International Waste Management and Landfill Symposium*, S. Margherita di Pula, Cagliari, Italy, 425-433.

Green, D.C. and Jamnejad, G., 1997. Settlement Characteristics of Domestic Waste. *Conference on Contaminated Ground*, Cardiff, Wales, British Geotechnical Society. 319-324.

Grisolia, M., Napoleoni, Q. and Tancredi, G., 1995. “Contribution to a Technical Classification of MSW”. *5th International Landfill Symposium*, S. Margherita di Pula, Cagliari, Italy, CISA. 703-710.

Howland, J.D. and Landva, A.O., 1992. “Stability Analysis of a Municipal Solid Waste Landfill”. Stability and Performance of Slopes and Embankments, II: *Proceedings of a Specialty Conference*, Berkeley, California, USA, American Society of Civil Engineers. 2 1216-1231.

Hull, R.M., Krogmann, U., and Strom, P.F., 2001. "Characterisation of Municipal Solid Waste (MSW) Reclaimed from a Landfill." *8th International Waste Management and Landfill Symposium*, S. Margherita di Pula, Cagliari, Italy, 567-576.

IdeMat [online], 2002. Delft, The Netherlands: University of Technology; Faculty of Design, Engineering and Production, available at: http://www.io.tudelft.nl/research/dfs/idemat/Onl_db/od_frame.htm [accessed: October 27th, 2004].

INGUT [online], 2003. Results of waste analyses. Independent office of environmental technology. Available at: http://www.ingut.de/English/indexstart.htm [accessed: January 2003]

Jessberger H.L., Kockel, R. and Graßl, P., 1990. “Abschlussbericht zur Untersuchung der Zusammendrückbarkeit und Scherfestigkeit von Hausmüll”. Forschungsbericht 90-2, Lehrstuhl für Grundbau und Bodenmechanik, Ruhr-Universität, Bochum, Germany. (in German).

Jessberger, H.L. and Kockel, R., 1993. “Determination and Assessment of the Mechanical Properties of Waste Materials”. *4th International Landfill Symposium*, Sardinia, Italy, CISA. 167-177.

Jessberger, H.L., Sylwasschy, O. and Kockel, R., 1995. “Investigation of Waste-Body-Behaviour and Waste-Structure-Interaction”. *5th International Landfill Symposium, Sardinia*, Italy, CISA. 731-743.

Jessberger, H. L., 2001. „Geotechnical Parameters of MSW“. Grundbau und Bodenmechanik; Ruhr-Universität Bochum; http://www.gub.ruhr-uni-bochum.de/tc5/SC303.htm. 2001.

Jones, R., Taylor, D. and Dixon, N., 1997. “Shear Strength of Waste and Its Use in Landfill Stability Analyses”. British Geoenvironmental Engineering Conference, Cardiff, UK, British Geotechnical Society, 343-350.

Jones, D.R.V. and Dixon, N., 2003. “Stability of Landfill Lining Systems: Report I, Literature Review”. Environment Agency, P1-385. R&D Technical report.

Jones, D.R.V. and Dixon, N., 2005. "Landfill Lining Stability and Integrity: The Role of Waste Settlement." *Geotextiles and Geomembranes*, 23 (1), 27-53.

Jotisankasa, A., 2001. “Evaluating the Parameters that Control the Stability of Landfills”. M.Sc. Thesis, Department of Civil and Environmental Engineering, Imperial College of Science, Technology and Medicine, London (unpublished).

Kavazanjian, E.J., Matasovic, N., and Bachus, R.C., 1999. "Large-Diameter Static and Cyclic Laboratory Testing of Municipal Solid Waste." *7th International Landfill Symposium*, S. Margherita di Pula, Cagliari, Italy, 437-444.

Kavazanjian, E., 2001. "Mechanical Properties of MSW." *8th International Waste Management and Landfill Symposium*, S. Margherita di Pula, Cagliari, Italy, 415-424.

Kockel R., and Jessberger, H.L., 1995. “Stability Evaluation of Municipal Solid Waste Slope”. *Proceedings XI ECSMFE*, Copenhagen, Bulletin 11, Vol. 2

Kölsch, F., 1993. "The Bearing Behaviour of Domestic Waste and Related Consequences for Stability." *4th International Landfill Symposium*, S. Margherita di Pula, Cagliari, Italy, 1393-1410.

Kölsch, F., 1996. "Der Einfluss der Faserbestandteile auf die Scherfestigkeit von Siedlungsabfall (The Influence of Fibrous Constituents on Shear Strength of Municipal Solid Waste)," Ph.D. Thesis, Technische Universität Braunschweig, Brauschweig, Germany (in German).

Koerner, R.M. and Soong, T.-Y., 2000. “Leachate in Landfills: The Stability Issues”. *Geotextiles and Geomembranes* 18: 293-309.

Landva, A.O. and Clark, J.I., 1990. “Geotechnics of Waste Fill - Theory and Practice”. ASTM STP 1070; Geotechnics of Waste Fill - Theory and Practice. Landva, A.O. and Knowles, G.D. Philadelphia, USA, American Society for Testing and Materials: 86-103.

Landva, A.O., Valsangkar, A.J., and Pelkey, S.G., 2000. "Lateral Earth Pressure at Rest and Compressability of Municipal Solid Waste." *Canadian Geotechnical Journal*, 37(No. 6), 1157-1165.

Langer, U. 2001. “Untersuchung der Scherfestigkeit, Kompressibilität und Durchlässigkeit von mechanisch-biologisch vorbehandeltem Abfall“. Student Research Project at the IGBE, Hanover, University (unpublished, in German)

Langer, U. and Dixon, N., 2004. “Mechanical Properties of MSW: Development of a Classification System”. *4th British Geotechnical Association Geoenvironmental Engineering Conference; Integrated Management of Groundwater and Contaminated Land*, Stratford-upon-Avon, UK, Thomas Telford, London. 267-274.

Langer, U., Dixon, N., Gotteland, P., and Gourc, J.P., 2005. "Waste Mechanics: Investigations Using Synthetic MSW." *10th International Waste Management and Landfill Symposium*, S. Margherita di Pula, Cagliari, Italy. (on CD)

Lings, M. L. and Dietz, M. S., 2004. “An Improved Direct Shear Apparatus for Sand”. *Geotechnique* 54, No. 4, 245–256

Machado, S.L., Carvalho, M.F. and Vilar, O.M., 2002. “Constitutive Model for MSW”. *Journal of Geotechnical and Geoenvironmental Engineering* 128(11): 940-951.

Manassero, M., Van Impe, W.F. and Bouazza, A., 1997. “Waste Disposal and Containment”. *Environmental Geotechnics*. Kamon, M. Rotterdam, Balkema, A.A.: 1425-1474.

MatWeb [online], 2004. MatWeb – The Online Materials Information Resource. Christiansburg, VA USA: Automation Creations, Inc., http://www.matweb.com or http://www.matls.com.

Mazzucato, A., Simonini, P. and Colombo, S., 1999. “Analysis of Block Slide in a MSW Landfill”. *7th International Landfill Symposium*, Sardinia, Italy, CISA. 537-544.

McDougall, J. R. and Pyrah, I. C., 2001. “Settlement in Landfilled Waste: Extending the Geotechnical Approach”. *8th International Waste Management and Landfill Symposium*, S. Margherita di Pula, Cagliari, Italy, CISA.

Michalowski, R.L. and Zhao, A., 1996. “Failure of Fiber-Reinforced Granular Soils”. *Journal of Geotechnical Engineering* 122 (3): ASCE, 226-234.

MoE [online], 2000. Environmental Indicator 2000: Domestic Waste in British Columbia. Ministry of Environment, Government of British Columbia. Available at: http://www.env.gov.bc.ca/soerpt/files_to_link/2000tecdocs/03-domestic-techdoc.pdf [accessed: February 2003]

MVRHH [online], 2003. Input Waste Utilisation Plant Rugenberger Damm. Müllverwertungsanlage Hamburg. Available at: http://www.mvr-hh.de/eng/start.htm [accessed: January 2003]

NSO [online], 2002. Domestic waste composition survey 2nd Quarter. National Statistic Office, Malta. Available at: http://www.nso.gov.mt/statdoc/document_file.aspx?id=705 [accessed: February 2003]

NWET, 2002. “Waste Characterisation Study Results”. Northwest Environmental Trust, Ltd, Trust News 2(1): 11-14.

Oweis, I.S. and Khera, R.P., 1990. “Geotechnology of Waste Management”. Butterworth-Heinemann, 2nd edition.

Oweis, I.S., 1993. "Stability of Landfills." *Geotechnical Practice for Waste Disposal*, Daniel, D.E., ed., Chapman & Hall, London.

Paar, S., 2000. "Das Dombelüftungsverfahren - Ein Verfahren zur Belüftung offener Rottemieten unter Nutzung des thermischen Auftriebs (The Chimney Aeration Technique - A Technique for Ventilation of Open Rotting Heaps Utilising the Thermal Lift)," Ph.D. Thesis, Technische Universität Dresden, Dresden, Germany (in German).

Pelkey, S.G., Valsangkar, A.J. and Landva, A.O., 2001. „Shear Displacement Dependent Strength of MSW and Its Major Constituents”. ASTM GTJODJ 24 (No. 4): 381-390.

Powrie, W., and Beaven, R.P., 1999. “Hydraulic Properties of Household Waste and Implication for Landfills”. Proceedings of the Institution of Civil Engineers; Geotechnical Engineering, 137, 235-247.

Powrie, W., Richards, D.J., and Beaven, R.P., 1998. "Compression of Waste and Implications for Practice." *Geotechnical Engineering of Landfills*, Dixon, N., Murray, E.J., and Jones, D.R.V., eds., Thomas Telford, London, 3-18.

Reuter, E. and Nolte, H.C., 1995. “Conception of a Stability Analysis for Large Landfills: Case Study in Hannover”. *5th International Landfill Symposium*, Sardinia, Italy, CISA. 801-812.

Richard, P., Gotteland, P., Lemarechal, D., and Gachet, C., 2001. “Evaluation of Stability and Settlements for the Design of a MSW Landfill”. *8th International Waste Management and Landfill Symposium*, S. Margherita di Pula, Cagliari, Italy, CISA.

Salomo, K.P., Krüger, D. and Fischer, D., 2001. “Großrahmenscherversuche auf der Deponie Wernsdorf”. *Müll und Abfall*; Erich Schmidt Verlag GmbH & Co., Berlin 10(587) (In German)

Sánchez-Alciturri, J.M., Palma, J., Sagaseta, C., and Canizal, J., 1993. "Mechanical Properties of Waste in a Sanitary Landfill." *Waste Disposal by Landfill; Symposium entitled "Geotechnics related to the environment" (GREEN'93)*, 193-199.

Scheelhaase, T., Bidlingmaier, W., Klümper, A., Maile, A. and Rechberger, M., 2001. “Geotechnical Behaviour of Mechanically-Biologically Pretreated Residual Waste”. *8th International Waste Management and Landfill Symposium*, Sardinia, Italy, CISA. 445-453.

Schneider, K.-J., 1996. Bautabellen für Ingenieure mit europäischen und internationalen Vorschriften. Werner-Verlag, Düsseldorf, Germany (In German).

Sharma, H.D., Fowler, W.L., and Cochrane, D.A., 1999. "Evaluation and Remediation of Ground Cracking Associated With Refuse Settlements." *7th International Landfill Symposium*, S. Margherita di Pula, Cagliari, Italy, 495-503.

Siegel, R.A., Robertson, R.J. and Anderson, D.G., 1990. “Slope Stability Investigations at a Landill in Southern California”. ASTM STP 1070; Geotechnics of Waste Fill - Theory and Practice. Landva, A.O. and Knowles, G.D. Philadelphia, USA, American Society for Testing and Materials: 259-284.

Singh, S. and Murphy, B.J., 1990. “Evaluation of the Stability of Sanitary Landfills”. ASTM STP 1070; Geotechnics of Waste Fill - Theory and Practice. Landva, A.O. and Knowles, G.D. Philadelphia, USA, American Society for Testing and Materials: 240-258.

Sowers, G.F., 1973. “Settlement of Waste Disposal fills”. *Proceedings 8th International Conference on Soil Mechanics and Foundation Engineering*, Moscow, 22, pp. 207-210.

Talby, R., 1997. “Behaviour of Buried Pipes and Bored Tunnels in Sand”. Ph.D. Thesis, Loughborough University, Loughborough, UK

Thomas, S., Aboura, A.A., Gourc, J.P., Gotteland, P., Billard, H., Delineau, T., Gisbert, T., Ouvry, J.F. and Vuillemin, M., 1999. “An In Situ Waste Mechanical Experimentation on a French Landfill”. *7th International Landfill Symposium*, S. Margherita di Pula, Cagliari, Italy, CISA. 445-452.

Turczynski, U., 1988. "Geotechnische Aspekte beim Aufbau von Mehrkomponentendeponien (Geotechnical Aspects of Building Multicomponent-Landfills)“, Ph.D. Thesis, Freiberg (Sachsen), Germany (In German).

University College Northampton [online], 2000. Forward to the Future: Issues for Domestic Waste Minimisation; Examples from Northamptonshire; available at: http://oldweb.northampton.ac.uk/aps/env/waste_min_guide/shanksproject.html [accessed: February 17th, 2004].

University of Newcastle upon Tyne [online], 1999. Workshop about the Case Study of the Byker Incinerator. School of Chemical Engineering and Advanced Materials; available at: http://www.ncl.ac.uk/sustain/case/bykercase/byker.htm [accessed: February 17th, 2004].

University of New South Wales [online], 2003. Waste Survey for the City of Tea Tree Gully; available at http://www.civeng.unsw.edu.au/water/awdb/compostn/sa/Teatreeg.htm [accessed: January 2003]

Van Impe, W.F. and Bouazza, A., 1998. “Large Shear Tests on Compacted Bales of MSW”. *Soils and Foundation*; *Japanese Geotechnical Society* 38 (No. 3): 199-200.

Van Impe, W.F., and Bouazza, A., 2000. "Large Shear Tests on Compacted Bales of Municipal Solid Wastes; Closure." *Soils and Foundation; Japanese Geotechnical Society*, 40(No. 3), 128.

Wallace, R.B., Ochiltree, C.R., and Jones, M.A., 2001. "Waste Characteristics and Their Impact on Landfill Closure and Future Land Use." *8th International Waste Management and Landfill Symposium*, S. Margherita di Pula, Cagliari, Italy, 361-370.

Watts, K. S. and Charles, J. A., 1990. "Settlement of Recently Placed Domestic Refuse Fills." Proceedings of the Institution of Civil Engineers; *Geotechnical Engineering* 88: 971-993.

Watts, K. S. and Charles, J. A. 1999. “Settlement characteristics of landfill wastes”. Proceedings of the Institution of Civil Engineers, *Geotechnical Engineering*, October 1999, 137, 225-233.

Watts, K.S., Charles, J.A. and Blaken, N.J.R., 2002. “Settlement of Landfills: Measurements and Their Significance”. *Waste 2002*, Integrated Waste Management and Pollution Control: Research, Policy and Practice, Stratford-upon-Avon, UK, 673-682.

Whitlow, R., 1983. Basic Soil Mechanics, Pearson Education Limited. 4th Edition, 2001

Yen, B.C., and Scanlon, B., 1975. “Sanitary Landfill Settlement Rates,” *Journal of the Geotechnical Engineering Division*, ASCE, May, pp. 475–487.

10 Chronological List of Publications

Langer, U., and Dixon, N., 2004 "Mechanische Eigenschaften von Siedlungsabfall: Entwicklung eines Klassifikationssystems." *Abfallforschungstage*, Hannover, Germany, 78-93 (in German).

Langer, U., and Dixon, N., 2004 "Mechanical Properties of MSW: Development of a Classification System." *4th BGA Geoenvironmental Engineering Conference; Integrated Management of Groundwater and Contaminated Land*, Stratford-upon-Avon, UK, 267-274.

Dixon, N., Langer, U., Gourc, J.P., and Gotteland, P., 2004 "Factors Influencing Shear Behaviour of MSW." *Waste 2004*, Stratford-Upon-Avon, UK, 591-600.

Dixon, N., and Langer, U. "Development of a MSW Classification System for the Evaluation of Mechanical Properties." *Waste Management*, Accepted for publication 2005.

Langer, U., Dixon, N., Gotteland, P., and Gourc, J.P., 2005 "Waste Mechanics: Investigations Using Synthetic MSW." *10th International Waste Management and Landfill Symposium*, S. Margherita di Pula, Cagliari, Italy.

11 Appendix

11.1 Calibration of the Technical Equipment Used during Compression and Shear Testing

Linear Variable Displacement Transducer 150mm

Table 11-1 LVDT 795 specification

Date	11/05/2005
Device	LVDT 150mm
Type	Ether 6''
Serial no	795
Amplifier	RDP S7DC, 58409
Bridge Volts	10v

Table 11-2 Calibration run LVDT 795

Regression Statistics	
Multiple R	0.999999
R^2	0.999998
Adjusted R^2	0.999998
Standard Error	0.068292
Observations	6

	Coefficients	Standard Error	Lower 95%	Upper 95%
Intercept	-0.061253	0.063612	-0.237868	0.115363
X Variable 1	**20.022391**	0.013075	19.986090	20.058692

Table 11-3 LVDT 632 specification

Date	11/05/2005
Device	LVDT 150mm
Type	Ether 6''
Serial no	632
Amplifier	RDP S7DC, 58407
Bridge Volts	10v

Table 11-4 Calibration run LVDT 632

Regression Statistics	
Multiple R	0.999998
R^2	0.999997
Adjusted R^2	0.999996
Standard Error	0.093562
Observations	6

	Coefficients	Standard Error	Lower 95%	Upper 95%
Intercept	0.013607	0.087091	-0.228195	0.255410
X Variable 1	**19.990797**	0.017884	19.941143	20.040452

Linear Variable Displacement Transducer 50mm

Table 11-5 LVDT 76391 specification

Date	04/11/2005
Device	LVDT 50mm
Type	ACT1000A
Serial no	76391
Amplifier	RDP S7AC, 59297
Bridge Volts	5v

Table 11-6 Calibration run LVDT 76391

Regression Statistics	
Multiple R	0.999972
R^2	0.999945
Adjusted R^2	0.999939
Standard Error	0.129657
Observations	11

	Coefficients	Standard Error	Lower 95%	Upper 95%
Intercept	32.788630	0.039696	32.698830	32.878429
X Variable 1	-16.370437	0.040476	-16.462001	-16.278873

Magnetostrictive Transducer

Table 11-7 EPs0500md601vo specification

Date	29/06/2005
Device	Temposonic 500mm
Type	EPs0500md601vo
Serial no	0525 1079
Amplifier	
Bridge Volts	10v

Table 11-8 Calibration run EPs0500md601vo

Regression Statistics	
Multiple R	1.000000
R^2	1.000000
Adjusted R^2	1.000000
Standard Error	0.001384
Observations	9

	Coefficients	Standard Error	Lower 95%	Upper 95%
Intercept	-0.369663	0.000719	-0.371364	-0.367962
X Variable 1	0.019994	0.000003	0.019987	0.020001

Load Cell Used in Compression Tests

Table 11-9 Mayes load cell specification

Date	12/04/2005
Device	Mayes Load Cell
Type	5 ton
Serial no	1404
Amplifier	RDP S7DC,58402
Bridge Volts	10v

Table 11-10 Calibration run 1 Mayes load cell

Regression Statistics	
Multiple R	0.999954
R^2	0.999909
Adjusted R^2	0.999900
Standard Error	0.174176
Observations	12

	Coefficients	Standard Error	Lower 95%	Upper 95%
Intercept	0.115823	0.085288	-0.074210	0.305856
X Variable 1	4.939342	0.014925	4.906087	4.972596

Table 11-11 Calibration run 2 Mayes load cell

Regression Statistics	
Multiple R	0.999886
R^2	0.999771
Adjusted R^2	0.999746
Standard Error	0.263848
Observations	11

	Coefficients	Standard Error	Lower 95%	Upper 95%
Intercept	0.037640	0.148832	-0.299042	0.374321
X Variable 1	4.967698	0.025053	4.911025	5.024371

Load Cell Used in Shear Tests

250kN load cell model 1220AF (sn174886A) with tracker model 220

Table 11-12 Load cell 1220AF specification

Date	24/05/2005
Device	250kN Load Cell
Type	1220AF
Serial no	174886A
Amplifier	tracker model 220
Bridge Volts	10v

Table 11-13 Calibration run 1 load cell 1220AF

Regression Statistics	
Multiple R	0.999988
R^2	0.999976
Adjusted R^2	0.999972
Standard Error	0.010355
Observations	8

	Coefficients	Standard Error	Lower 95%	Upper 95%
Intercept	-0.027241	0.006978	-0.044316	-0.010165
X Variable 1	0.041184	0.000083	0.040982	0.041386

Table 11-14 Calibration run 2 load cell 1220AF

Regression Statistics	
Multiple R	0.999996
R^2	0.999991
Adjusted R^2	0.999990
Standard Error	0.006755
Observations	9

	Coefficients	Standard Error	Lower 95%	Upper 95%
Intercept	-0.000520	0.003813	-0.009536	0.008495
X Variable 1	0.040821	0.000045	0.040714	0.040929

11.2 Assumed Values for Water Content

The values for the water content are derived from waste survey data conducted by Kölsch (1996). Amongst other, he examined three different samples of fresh waste. Kölsch analysed the water content of the different material groups represented in the waste samples.

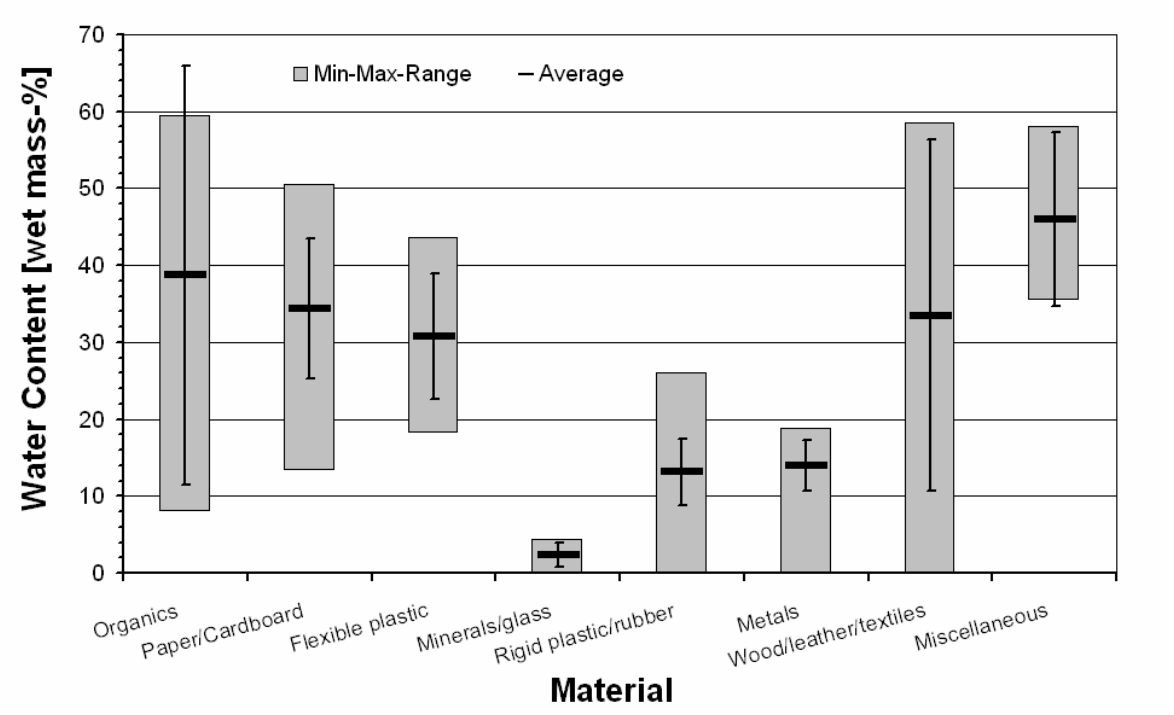

Figure 11-1 Water contents (average, minimum-maximum-range and standard deviation) of materials (after Kölsch, personal correspondence 2004)

From the results a minimum-maximum-range, an average value and the standard deviation were generated (Figure 11-1). The average values for the water content were applied to the measured wet masses to calculate the dry weight of the sample and the different sorted fractions. There was no differentiation between the size ranges. It was assumed that the water content does not differ considerably within the size ranges.

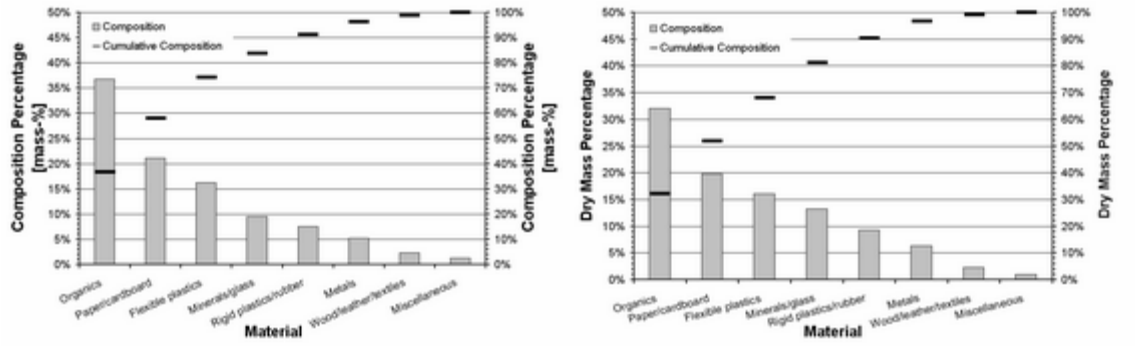

Figure 11-2 Wet and Dry weight Narborough waste composition

11.3 Grading of Leighton-Buzzard-Sand

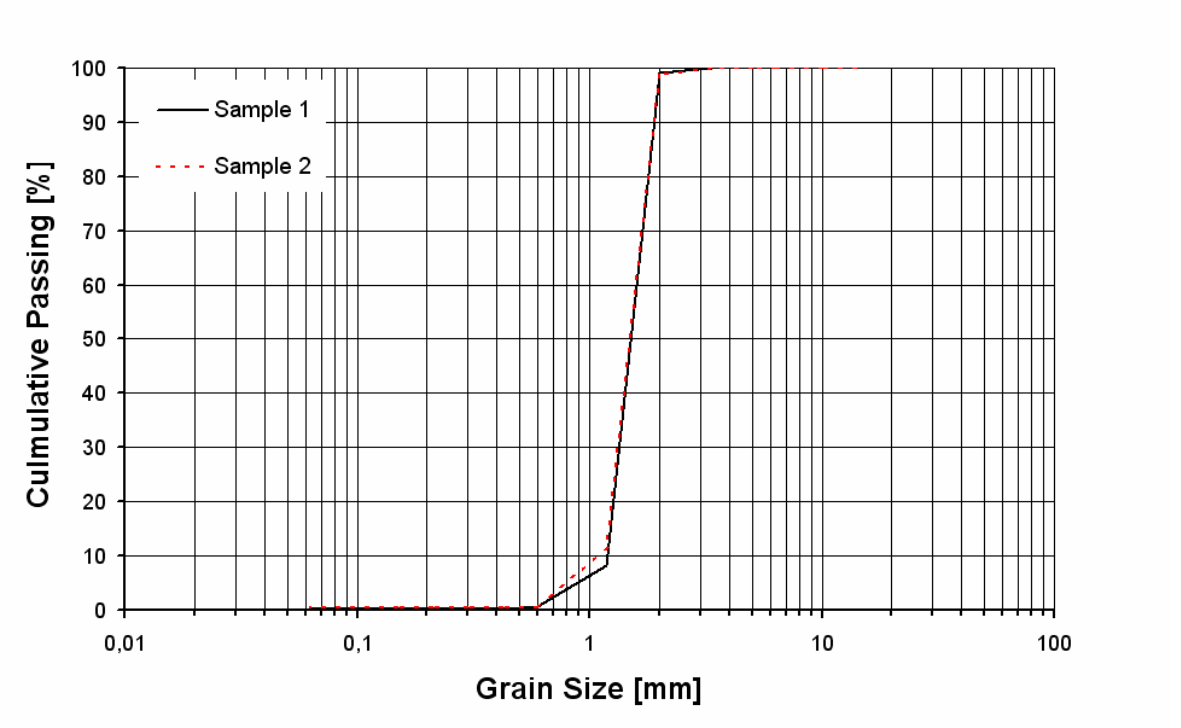

Figure 11-3 Grading of Leighton-Buzzard-sand

Grading of two dry samples was conducted. The net weight of sample 1 is 884g and 974g, respectively for sample 2.

11.4 Compression Tests

Table 11-15 Component masses for the compositions tested in compression tests

Components	SW_	01	02_1	02_2	02_3	03	04	07	09
Aluminium cans	[kg]	0	0.94	0.94	1.87	1.46	6.00	2.93	0.84
Paper	[kg]	1.71	1.33	1.33	2.67	1.46	0	0	3.48
Textiles	[kg]	0	0.66	0.66	1.52	0.97	0	0	0.39
Flexible plastic bags	[kg]	0.15	0.36	0.36	0.72	0	0	0	2.74
Rigid plastic packaging	[kg]	0	0.48	0.48	0.95	0	0.60	2.93	0.54
Rigid plastic bottles	[kg]	0	0.36	0.36	0.72	0	0	0	0.52
Tyre shreds	[kg]	0	0	0	0	2.92	3.00	0	0.19
Brick fractions	[kg]	0	0	0	0	2.89	2.40	0	0.31
Leighton-Buzzard Sand	[kg]	155.94	0	0	0	0	0	108.00	1.23
Clay	[kg]	0	0	0	0	0	0	0	6.02
Sum	[kg]	157.8	4.12	4.12	8.25	9.70	12.00	113.86	16.26

11.5 Shear Tests

Table 11-16 Component masses for the compositions tested in shear tests

Components	SW_	01_L	01_H	02	03	04	05	06	07	08	09
Aluminium cans	[kg]	0	0	7.57	11.87	22.97	24.51	2.35	11.06	15.00	5.61
Paper	[kg]	5.24	7.29	15.12	14.32	0	0	0	0	0	23.07
Textiles	[kg]	0	0	5.16	5.69	0	0	0	0	0	2.67
Flexible plastic bags	[kg]	0.47	0.65	2.92	0	0	0	0	0	0	18.33
Rigid plastic packaging	[kg]	0	0	3.82	0	2.29	5.25	2.46	11.06	15.00	4.31
Rigid plastic bottles	[kg]	0	0	2.95	0	0	0	0	0	0	3.42
Tyre shreds	[kg]	0	0	0	23.70	11.48	5.25	0	0	0	1.26
Brick fractions	[kg]	0	0	0	23.70	9.29	0	0	0	0	2.18
Leighton-Buzzard Sand	[kg]	478.50	665.74	0	0	0	0	741.12	408.29	323.30	8.20
Clay	[kg]	0	0	0	0	0	0	0	0	0	40.02
Sum	[kg]	484.21	673.68	37.54	79.28	46.03	35.01	745.93	430.41	352.30	109.07

11.5.1 Sample Setup for Shear Test SW_01

Figure 11-4 Composition SW_01

11.5.2 Sample Setup for Shear Test SW_06

Figure 11-5 Sample structure of SW_06

The sample was set up in a structured way. On a layer of sand plastic packaging and aluminium cans were placed and covered with sand. On top of that layer, a new layer was placed. Seven of such layers were subsequently placed in the box.

11.5.3 Dismantling the Shear Box with Composition SW_02

Figure 11-6 Sample analysis SW_02: Components jammed between bend around the edge of the bottom shear box

11.5.4 Examination of Composition SW_03 after the 50kPa Test

Figure 11-7 Sample analysis SW_03: Component failure of a brick fraction at the edge of the bottom shear box